NOTE TO USERS

This reproduction is the best copy available

UMI

University of Alberta

Geotechnical Characteristics of Penticton Silt

by

Said Iravani ©

A thesis submitted to the Faculty of Graduate Studies and Research in partial
fulfillment of the requirements for the degree of Doctor of Philosophy

Department of Civil and Environmental Engineering

Edmonton, Alberta

Spring 1999

National Library
of Canada

Acquisitions and
Bibliographic Services

395 Wellington Street
Ottawa ON K1A 0N4
Canada

Bibliothèque nationale
du Canada

Acquisitions et
services bibliographiques

395, rue Wellington
Ottawa ON K1A 0N4
Canada

Your file Votre référence

Our file Notre référence

The author has granted a non-exclusive licence allowing the National Library of Canada to reproduce, loan, distribute or sell copies of this thesis in microform, paper or electronic formats.

L'auteur a accordé une licence non exclusive permettant à la Bibliothèque nationale du Canada de reproduire, prêter, distribuer ou vendre des copies de cette thèse sous la forme de microfiche/film, de reproduction sur papier ou sur format électronique.

The author retains ownership of the copyright in this thesis. Neither the thesis nor substantial extracts from it may be printed or otherwise reproduced without the author's permission.

L'auteur conserve la propriété du droit d'auteur qui protège cette thèse. Ni la thèse ni des extraits substantiels de celle-ci ne doivent être imprimés ou autrement reproduits sans son autorisation.

0-612-39544-8

Canada

University of Alberta

Library Release Form

Name of Author: Said Iravani

Title of Thesis: Geotechnical Characteristics of Penticton Silt

Degree: Doctor of Philosophy

Year This Degree Granted: 1999

Permission is hereby granted to the University of Alberta Library to reproduce single copies of this thesis and to lend or sell such copies for private or scientific research purposes only.

The author reserves all other publication and other rights in association with the copyright in the thesis, and except as hereinbefore provided, neither the thesis nor any substantial portion thereof may be printed or otherwise reproduced in any material form whatever without the author's prior written permission.

Said Iravani

Said Iravani
8-10620-83 Ave.
Edmonton, AB
Canada T6E 2E2

Date: April 16, 1999

"I don't answer the question: Do you believe in god?"

"If I say yes, people think I believe in their image of god; and if I say no, I am condemned as some materialist without spiritual dimensions."

Stephen Hawking *

---

* Source: The interview with the National Magazine, the Canadian Broadcasting Corporation (CBC), spring 1998.

To:

The Origin.

The Destiny.

Whom existed before anything else.

Whom will continue to exist after everything else ceases to exist.

Whom is beyond matter.

Whom is beyond time.

Whom I worship not because I am fearful and scared of His hell.

Whom I worship not because I am greedy and desire His heaven.

Whom I worship because I love Him.

To:

God

Said Iravani

April 1999

University of Alberta

Faculty of Graduate Studies and Research

The undersigned certify that they have read, and recommend to the Faculty of Graduate Studies and Research for acceptance, a thesis entitled Geotechnical Characteristics of Penticton Silt submitted by Said Iravani in partial fulfillment of the requirements for the degree of Doctor of Philosophy.

Dr. P. K. Robertson

Dr. N. R. Morgenstern

Dr. D. M. Cruden

M. J. Dudas
Dr. M. J. Dudas

Dr. Z. Xu

DG Fredlund
Dr. D. G. Fredlund

S Leroueil
Dr. S. Leroueil

Date: April 16, 1999

Abstract

The behavior of structured soils can be different from the behavior of ideal soils. Soils are generally structured and may also be unsaturated. The influence of soil structure on soil behavior may be as important as the effect of void ratio and stress history.

The glaciolacustrine silt sediments in the southern interior of British Columbia, known as Penticton silt, have been chosen as the primary material to study the behavior of structured soils. These silt sediments appear to be cemented and unsaturated.

Background information, geology of the Okanagan Valley, site selection, sampling, in-situ testing, basic soil properties, compressibility, shear strength, and soil structure were reviewed and discussed.

It was found that Penticton silt is a normally consolidated highly anisotropic silt size non-active low-plasticity soil with mica (muscovite) and chlorite as the dominant minerals. Penticton silt is found to be a structured soil with moisture sensitive inter-particle physicochemical bonding. Bonding agents include amorphous silica acid gel, carbonate and sulfate precipitates of Na^+, Mg^{++}, and Ca^{++}, and iron oxides. Silica acid gel present in the silica surfaces was found to be the primary bonding agent. It is also found that the magnitude of structural bonding controls the compressibility and strength of the Penticton silt rather than excess pore pressure generation. Results of seismic cone penetration testing (SCPT) were promising. In addition, based on the physicochemical state of soil, a conceptual critical state soil mechanics model is proposed for the behavior of structured soils.

Acknowledgement

The author would like to express sincere gratitude and appreciation to his Ph.D. supervisor, Dr. Peter K. Robertson, for his consistent guidance, comments, suggestions, interest, support and encouragement throughout this study. I have no doubt in my mind that your never ending attention to my professional, social, and personal growth will have significant influence in my future endeavors and achievements.

I would like to appreciate the contribution and valuable ideas of Dr. Norbert R. Morgenstern to this study. In addition, I would like to acknowledge your continuing support, and attention to my professional and personal progress and achievements.

I would like to thank Dr. David M. Cruden for his valuable inputs to this study, through discussions on the geological aspects. Also, I like to appreciate your interest in my professional and personal progress.

I would like to express my sincere appreciation for the high quality collaboration and in kind support of the Geotechnical and Materials Engineering Division, the Thompson-Okanagan Region, B. C. Ministry of Transportation and Highways. Special appreciation is extended to my colleague Mr. Joe Valentinuzzi for his unconditional support and dedication throughout the study.

Special thanks to Dr. William J. Lown from the Department of Chemistry for those valuable discussions on the chemical aspects of my research and your interest in my progress. Your encouragement and advice are highly appreciated.

I would also like to thank Dr. Marvin J. Dudas, Department of Renewable Resources, and Dr. Zhenghe Xu, Department of Chemical and Materials Engineering, for their valuable inputs through our many and interesting discussions.

I wish to make special mention to the technical staff that were involved with the experimental program, in particular Mr. Gerry Cyre and Mr. Steve Gamble. Gerry's assistance in the experimental program, especially field activities, is appreciated. Special thanks to Steve for his assistance and advice throughout the laboratory program.

I would also like to acknowledge the contribution of Dr. D. G. Fredlund from University of Saskatchewan. I would like to thank you for accepting to be member of my supervisory committee and for your valuable comments. Also, I would like to acknowledge the collaboration of the Unsaturated Soil Group (USG) of the University of Saskatchewan during the experimental program for soil-water characteristics curve determinations.

I would like to thank Dr. Serge Leroueil from Laval University for accepting to be the external examiner and reviewer of this thesis and for your valuable comments and inputs.

I would also like to thank Dr. D. C. Sego for his inputs through discussions at early stages of this study.

Special thanks to my colleague, Mr. Doug Dewar, for his assistance in the geological aspects of this study and supply of the local geological information.

The in kind contribution of ConeTec investigation Ltd. to this study for conducting three seismic cone penetration tests adjacent to the Okanagan Lake Park Slide is appreciated.

The assistance and collaboration of the local community, local authorities, and local engineers are highly appreciated. Particular appreciation is extended to the following: Dr. Jeff. Harries, owner of the Paradise Ranch Vineyards which covers the Koosi Creek Slide area for assistance and collaboration; Okanagan District of the B. C. Ministry of Environment, Lands, and Parks, that have jurisdiction over the Okanagan Lake Park Slide area; Mr. Robert. G. Wilson, Wilson Associates Geotechnical, and Mr. Norm. Williiams, Interior Testing Services Ltd.

I would like to thank my M.Sc. degree supervisor Dr. James G. MacGregor for his continuing interest in my progress and for his support.

I would also like to acknowledge the support and continuing interest in my progress, expressed by Dr. D. J. Laurie Kennedy and Dr. David W. Murray from the Structural Engineering Group.

Special thanks to Professor Art E. Peterson from the Canadian Society for Civil Engineering for his attention to my progress and his continuing support.

It cannot be a proper acknowledgment without a reference to my colleagues, graduate students that I worked with throughout the coursework and the research. Their contribution, encouragement and assistance are highly appreciated.

I would also like to thank all those friends and acquaintances that been helpful through these years of university life. You are very much appreciated, however space limitations prevent me from thanking each of you by name.

The financial support for this study, provided by the Federal Government of Canada through Natural Science and Engineering Research Council (NSERC), is highly appreciated by the author.

I would like to use this opportunity to commemorate the memory of Late Dr. Bruce C. Bain from the Department of Educational Psychology for his encouragement and attention to my progress.

At last, but definitely not the least, I shall express my deepest appreciation for all that my mother, Iran Keshavarzi, and my father Mehdi Iravani have done for me throughout my life. Growing up and satisfying the high expectations of my parents was not easy, but greatest gift they gave me is a never-ending thirst for learning.

Table of Contents

CHAPTER ONE: Introduction

1.1 General 1
1.2 Research Significance 2
1.3 Background Information 3
1.4 Site Selection 14
1.5 Objective and Scope 15
1.6 Thesis Arrangement 15

CHAPTER TWO: Geology of the Okanagan Valley

2.1 Introduction 24
2.2 Literature Review 25
2.3 Bedrock Geology 29
2.4 Late Pleistocene History of the Okanagan Valley 30
2.5 Formation of the Glaciolacustrine Silt Sediment 38
2.6 Colluvial Silts 52
2.7 Geological Hazards 53
2.7.1 Toppling 54
2.7.2 Sinkhole Formation and Piping Processes 54
2.7.3 Slides 55
2.7.3.1 Shallow Planner Slides 56
2.7.3.2 Deep Seated Rotational Slides 56
2.8 Summary 57

CHAPTER THREE: Site Selection and Sampling

3.1 Introduction 62
3.2 Meteorological Records of Okanagan Valley 63

3.3 Review of Slides 65
3.4 Koosi Creek Slide 69
3.4.1 Documentation of the Records 69
3.4.1.1 General 69
3.4.1.2 Topography 72
3.4.1.3 Geology Maps 72
3.4.1.4 Aerial Photographs 77
3.4.1.4.1 Pre-Slide Aerial Photographs 77
3.4.1.4.2 Post-Slide Aerial Photographs 78
3.4.2 Field Reconnaissance 80
3.4.3 Geometry of Slide 82
3.5 Okanagan Lake Park Slide 82
3.5.1 Documentation of the Records 82
3.5.1.1 General 82
3.5.1.2 Topography 84
3.5.1.3 Geological Maps 84
3.5.1.4 Aerial Photographs 88
3.5.1.4.1 Pre-Slide Aerial Photographs 88
3.5.1.4.2 Post-Slide Aerial Photographs 88
3.5.2 Field Reconnaissance 89
3.5.3 Geometry of Slide 90
3.6 Sampling 90
3.6.1 General 90
3.6.2 Koosi Creek Slide Site 91
3.6.3 Okanagan Lake Park Slide Site 92
3.7 Summary 92

CHAPTER FOUR: Cone Penetration Testing (CPT)

4.1 Introduction 130
4.2 General 131

4.3 Soil Behavior Type 131
4.4 Assessment of Soil Structure 133
4.5 Soil Parameters Interpretation 136
4.5.1 Undrained Shear Strength 136
4.5.2 Sensitivity 137
4.5.3 Estimation of Yield Stress Ratio 138
4.5.4 Friction Angle 139
4.6 Summary 140

CHAPTER FIVE: Basic Properties of Penticton Silt

5.1 Introduction 154
5.2 Grain Size Distribution 154
5.3 Specific Gravity, Density, and Insitu Void Ratio 155
5.4 In-Situ Water Content and Atterberg Limits 156
5.5 Soil-Water Characteristic Curve 157
5.6 Mineralogy 160
5.7 Fabric and Scanning Electron Microscopy (SEM) 164
5.8 Soil and Pore Fluid Chemistry 169
5.9 Summary 173

CHAPTER SIX: One Dimensional Consolidation Testing

6.1 Introduction 209
6.2 Literature Review 209
6.2.1 Compressibility of Structured Soils 209
6.2.2 Compressibilty of Glaciolacustrine Silts in the Southern Interior of B. C. 214
6.3 Experimental Program 218
6.3.1 General 218
6.3.2 Testing Apparatus 219

6.3.3 Test Procedure 219
6.3.4 Material, Specimen Preparation, and Test Results 220
6.4 Discussion of Results 222
6.5 Summary 229

CHAPTER SEVEN: Triaxial Testing

7.1 Introduction 251
7.2 Literature Review 251
7.2.1 Shear Strength of Structured Soils 251
7.2.2 Shear Strength of Glaciolacustrine Silts in the Southern Interior of B. C. 258
7.3 Experimental Program 259
7.3.1 General 259
7.3.2 Testing Apparatus 260
7.3.3 Material and Specimen Preparation 260
7.3.4 Test Procedure 261
7.4 Test Results and Discussions 263
7.4.1 General 263
7.4.2 Reconstituted Specimens 263
7.4.3 Undisturbed Specimens 264
7.4.3.1 Specimens at 36% to 38% In-Situ Water Content 264
7.4.3.2 Specimens at 23% to 28% In-Situ Water Content 266
7.4.3.3 Air-Dried Water Saturated Specimens 267
7.4.3.4 Air-Dried Kerosene Saturated Specimens 270
7.4.4 General Discussion 271
7.5 Summary 274

CHAPTER EIGHT: Soil Structure of Penticton Silt

8.1 Introduction 310

8.2 Literature Review 312
8.2.1 Soil Structure 312
8.2.2 Soil at Unsaturated State 320
8.3 Experimental Program 331
8.3.1 Relevant Test Results Presented from the Previous Chapters 331
8.3.2 Observational Experiments 333
8.4 Discussion 338
8.4.1 Role of Suction 338
8.4.2 Nature of Bonding and Destructuring 340
8.4.3 Swelling 343
8.4.4 General Discussion 345
8.5 Summary 348

CHAPTER NINE: Summary, Conclusions, Practical Implications, and Recommendations

9.1 Summary 372
9.2 General Conclusions and Practical Implications 373
9.2.1 General Conclusions 373
9.2.2 Practical Implications 376
9.3 Recommendations for Further Studies 380

References 382

APPENDIX A: Maps of the Surficial Deposits of Late Glacial and Recent Age of the Okanagan Valley 400

APPENDIX B: One Dimensional Consolidation Test Results 401

List of Tables

CHAPTER THREE: Site Selection and Sampling

3.2-A Meteorological Records of Penticton Station 94

3.2-B Meteorological Records of Summerland Station 96

CHAPTER FIVE: Basic Properties of Penticton Silt

5.2 Summary of the Grain Size Analyses, Carried out as Part of the Other Studies 175

5.3 Summary of the Specific Gravity, Density, and In-Situ Void Ratio Determination, Carried out as Part of the Other Studies 177

5.4 Summary of the In-Situ Water Content and Atterberg Limits Determinations, Carried out as Part of the Other Studies 178

5.6-A(a) Summary of the Reported Mineralogical Analyses (Bulk Silt Samples) 179

5.6-A(b) Summary of the Reported Mineralogical Analyses (Clay Fraction Samples) 179

5.6-B(a) Results of the X-Ray Diffraction Analyses of the Bulk Samples 180

5.6-B(b) Results of the X-Ray Diffraction Analyses of the Clay Fraction 180

5.8-A Summary of Soil Chemistry Analyses by Quigley (1976) 181

5.8-B Summary of the Results of Soil Chemistry Analyses, Courtesy of the B. C. Ministry of Transportation and Highways (1977) 182

5.8-C Summary of the Results of Soil and Ground Water Chemistry Analyses 183

CHAPTER SIX: One Dimensional Consolidation Testing

6.3.1 Properties of Kerosene Used 230

6.3.4-A Basic Properties of Series A Specimens 231

6.3.4-B Basic Properties of Series B Specimens 231
6.3.4-C Basic Properties of Series C Specimens 232
6.3.4-D Basic Properties of Series D Specimens 232
6.3.4-E Basic Properties of Series E Specimens 233
6.3.4-F Basic Properties of Series F Specimens 233

CHAPTER EIGHT: Soil Structure of Penticton Silt

8.3.2 Summary of the Results (Observational Test Five (OT-5)) 350
8.4 Characteristics of Pore Fluid Used in Observational Tests 351

List of Figures

CHAPTER ONE: Introduction

1.3-A Structure Determining Factors and Processes 17

1.3-B Failure Envelope for Reconstituted Clays 18

1.3-C The Intrinsic Compression Line (ICL) in (a) e-log σ'_v and (b) I_v-log σ'_v 19

1.3-D Summary of State Transformations 20

1.3-E Compressibility of an Intact Specimen Relative to the ICL 21

1.3-F Compression and Shear Yield of Structured Soils 22

1.3-G Yield Surface for Unsaturated Soil in $(p-u_a)$-q Space 23

CHAPTER TWO: Geology of the Okanagan Valley

2.1-A Locality of the Okanagan Valley Area Relative to Continental North America 59

2.1-B Locality of the Okanagan Lake Area Relative to the Southern Interior of B. C. 60

2.1-C Position of the Okanagan Valley in the Interior System 61

CHAPTER THREE: Site Selection and Sampling

3.3-A Koosi Creek Slide (1942) 97

3.3-B Okanagan Lake Park Slide (1975) 98

3.3-C Position of Koosi Creek and Okanagan Lake Park Slides in the Southern Okanagan Lake Area 99

3.4.1.2 Topography Map of the Koosi Creek Slide Area 100

3.4.1.3 Surficial Materials of the Vicinity of Koosi Creek 101

3.4.1.4.1-A Pre-Slide Aerial Photograph (1938) (Koosi Creek Slide Area) 102

3.4.1.4.1-B Magnified Pre-Slide Aerial Photograph of Koosi Creek Slide Area 103
3.4.1.4.2-A Post-Slide Aerial Photograph (1963) (Koosi Creek Slide Area) 104
3.4.1.4.2-B Magnified Post-Slide Aerial Photograph of Koosi Creek Slide Area 105
3.4.1.4.2-C Post-Slide Aerial Photograph (1974) (Koosi Creek Slide Area) 106
3.4.1.4.2-D Post-Slide Aerial Photograph (1985) (Koosi Creek Slide Area) 107
3.4.2-A Bedrock Exposure in Koosi Creek Slide Area 108
3.4.2-B General View of Koosi Creek Slide 108
3.4.2-C Groundwater Discharge Zone (Koosi Creek Slide) 109
3.4.2-D White Precipitates in Groundwater Discharge Zone (Koosi Creek Slide) 109
3.4.2-E Rapidly Draining Strata in Groundwater Exit Zone (Koosi Creek Slide) 110
3.4.2-F Sand Lenses in Groudwater Exit Zone (Koosi Creek Slide) 110
3.4.2-G Northwest Wall of Koosi Creek Slide Area 111
3.4.2-H Southeast Wall of Koosi Creek Slide 111
3.4.3-A Topography Plan of Koosi Creek Slide 112
3.4.3-B The Cross Section of the Axis of the Koosi Creek Slide 113
3.5.1.1-A Okanagan Lake Park Slide (May 1975) 114
3.5.1.1-B Reworked Shape of the Okanagan Lake Park Slide 114
3.5.1.2 Topography of the Okanagan Lake Park Slide Area 115
3.5.1.3 Surficial Materials of the Okanagan Lake Park 116
3.5.1.4.1-A Pre-Slide Aerial Photograph (1974) (Okanagan Lake Park Slide Area) 117
3.5.1.4.1-B Magnified Pre-Slide Aerial Photograph of Okanagan Lake Park Slide Area 118
3.5.1.4.2-A Post-Slide Aerial Photograph (1985) (Okanagan Lake Park Slide Area) 119
3.5.1.4.2-B Magnified Post-Slide Aerial Photograph of Okanagan Lake Park Slide Area 120
3.5.2-A Okanagan Lake Park Slide (1997) 121

3.5.2-B South Wall of the Okanagan Lake Park Slide (1996) 121
3.5.2-C Top Part of the South Wall (Okanagan Lake Park Slide) 122
3.5.2-D Bottom Part of the South Wall (Okanagan Lake Park Slide) 122
3.5.3-A Plan Geometry of Okanagan Lake Park Slide 123
3.5.3-B The Cross Section of the Axis of the Okanagan Lake Park Slide 124
3.6.2-A Locality of Sampling Zone in Koosi Creek Slide Site 125
3.6.2-B Closer Look at the Sampling Area (Koosi Creek Slide Site) 126
3.6.2-C Sampling Area above Groundwater Exit (Koosi Creek Slide Site) 127
3.6.2-D Sampling Area below Groundwater Exit (Koosi Creek Slide Site) 127
3.6.3-A Locality of Sampling Zone in Okanagan Lake Park Slide Site 128
3.6.3-B Sampling Area in the South Wall of Okanagan Lake Park Slide 129
3.6.3-C Closer Look at the Sampling Zone (Okanagan Lake Park Slide Site) 129

CHAPTER FOUR: Cone Penetration Testing (CPT)

4.2-A The Location of the SCPTU Tests in the Vicinity of the Okanagan Lake Park Slide 141
4.2-B Summary of the Results for SCPTU-1 142
4.2-C Summary of the Results for SCPTU-2 143
4.2-D Summary of the Results for SCPTU-3 144
4.3-A Soil Behavior Chart Based on Normalized CPT and CPTU 145
4.3-B Soil Behavior Type Classification (SCPTU-1) 146
4.3-C Soil Behavior Type Classification (SCPTU-2) 147
4.3-D Soil Behavior Type Classification (SCPTU-3) 148
4.4-A Use of Unusual Soil Identification Chart for Penticton Silt 149
4.4-B Use of Cementation Assessment Chart for Penticton Silt 150
4.5.1 CPT Evaluation of S_u for Penticton Silt 151
4.5.2 CPT Evaluation of S_t for Penticton Silt 152
4.5.3 CPT Evaluation of YSR (OCR) for Penticton Silt 153

CHAPTER FIVE: Basic Properties of Penticton Silt

5.2 Grain Size Distribution for Penticton Silt 184

5.5-A Soil-Water Characteristic Curve for Penticton Silt 185

5.5-B Typical Soil-Water Characteristic Curves for a Sandy Soil, a Silty Soil, and a Clayey Soil 186

5.5-C Typical Desorption and Adsorption Soil-Water Characteristic Curves for a Silty Soil 186

5.7-A(a) Horizontal Surface of an Undisturbed Specimen from Koosi Creek Slide Site at its In-Situ Moisture Content 187

5.7-A(b) Vertical Surface of an Undisturbed Specimen from Koosi Creek Slide Site at its In-Situ Moisture Content 188

5.7-B(a) Horizontal Surface of an Undisturbed Specimen from Okanagan Lake Park Slide Site at its In-Situ Moisture Content 189

5.7-B(b) Vertical Surface of an Undisturbed Specimen from Okanagan Lake Park Slide Site at its In-Situ Moisture Content 190

5.7-C(a) Horizontal Surface of an Undisturbed Air-Dried Specimen from Okanagan Lake Park Slide Site 191

5.7-C(b) Horizontal Surface of an Undisturbed Air-Dried Specimen from Okanagan Lake Park Slide Site 192

5.7-D(a) Horizontal Surface of a Saturated Slurry Specimen of Penticton Silt 193

5.7-D(b) Vertical Surface of a Saturated Slurry Specimen of Penticton Silt 194

5.7-E(a) Horizontal Surface of an Undisturbed Initially Air-Dried Specimen from Okanagan Lake Park Slide Site after Gradual Saturation 195

5.7-E(b) Horizontal Surface of the Specimen Shown in Figure 5.7-E(a) after Re-Air-Drying 196

5.7-F(a) Vertical Surface of an Undisturbed Initially Air-Dried Specimen from Okanagan Lake Park Slide Site after Gradual Saturation 197

5.7-F(b) Vertical Surface of the Specimen Shown in Figure 5.7-F(a) after Re-Air-Drying 198

5.7-G Crack Formation, Swelling, and Destructuring upon Gradual Moistening under Unconfined Condition 199
5.7-H Crack Formation, Swelling, and Destructuring upon Flooding under Unconfined Condition 200
5.7-I Open and Flexible Structure of Platy Particles Such as Muscovite and Chlorite in Soil Structure of Penticton Silt 201
5.7-J Illite Formation from Mica (Muscovite) Disintegration 202
5.7-K Calcite Particle Present in Penticton Silt Soil Structure 203
5.7-L Silica Over-Growth and Structural Bonding between Two Muscovite Particles 203
5.7-M(a) $Mg(OH)_2$ Precipitates on a Quartz Surface 204
5.7-M(b) Unknown Precipitates on the Surface of Particles 204
5.7-N Precipitate Bridge between Two Muscovite Particles 205
5.7-O Formation of Mg Precipitates on Plagioclase Surface 206
5.7-P Aggregation of Particles with Iron Oxides 207
5.7-Q Aggregated Deformed Muscovite Particle 208

CHAPTER SIX: One Dimensional Consolidation Testing

6.2.1-A The Intrinsic Compression Line (ICL) in (a) e-log σ'_v and (b) I_v-log σ'_v 234
6.2.1-B Summary of State Transformations 235
6.2.1-C Compressibility of an Intact Specimen Relative to the ICL 236
6.2.2-A Summary of Load Controlled Consolidation Tests (Carried Out by Lum (1977)) 237
6.2.2-B Summary of Strain Controlled Consolidation Tests (Carried Out by Lum (1977)) 237
6.3-A(a) Summary of One-Dimensional Consolidation Tests for Specimens from Okanagan Lake Park Site with Air as Pore Fluid 238
6.3-A(b) Summary of One-Dimensional Consolidation Tests for Specimens from Koosi Creek Site with Air as Pore Fluid 238

6.3-B(a) Summary of One-Dimensional Consolidation Tests for Specimens from Okanagan Lake Park Site with Water as Pore Fluid 239

6.3-B(b) Summary of One-Dimensional Consolidation Tests for Specimens from Koosi Creek Site with Water as Pore Fluid 239

6.3-C(a) Summary of One-Dimensional Consolidation Tests for Specimens from Okanagan Lake Park Site with Kerosene as Pore Fluid 240

6.3-C(b) Summary of One-Dimensional Consolidation Tests for Specimens from Koosi Creek Site with Kerosene as Pore Fluid 240

6.4-A(a) Normalized One Dimensional Consolidation Test Results, Series A, Okanagan Lake Park Slide Site Specimens 241

6.4-A(b) Normalized One Dimensional Consolidation Test Results, Series A, Koosi Creek Slide Site Specimens 241

6.4-B(a) Normalized One Dimensional Consolidation Test Results, Series B, Okanagan Lake Park Slide Site Specimens 242

6.4-B(b) Normalized One Dimensional Consolidation Test Results, Series B, Koosi Creek Slide Site Specimens 242

6.4-C(a) Normalized One Dimensional Consolidation Test Results, Series C, Okanagan Lake Park Slide Site Specimens 243

6.4-C(b) Normalized One Dimensional Consolidation Test Results, Series C, Koosi Creek Slide Site Specimens 243

6.4-D(a) Normalized One Dimensional Consolidation Test Results, Series D, Okanagan Lake Park Slide Site Specimens 244

6.4-D(b) Normalized One Dimensional Consolidation Test Results, Series D, Koosi Creek Slide Site Specimens 244

6.4-E(a) Normalized One Dimensional Consolidation Test Results, Series E, Okanagan Lake Park Slide Site Specimens 245

6.4-E(b) Normalized One Dimensional Consolidation Test Results, Series E, Koosi Creek Slide Site Specimens 245

6.4-F(a) Normalized One Dimensional Consolidation Test Results, Series F, Okanagan Lake Park Slide Site Specimens 246

6.4-F(b) Normalized One Dimensional Consolidation Test Results, Series

F, Koosi Creek Slide Site Specimens 246
6.4-G State of OL and KC Relative to the ICL and the SCL 247
6.4-H(a) Summary of Normalized 1-Dimensional Consolidation Tests for Specimens from Okanagan Lake Park Site with Air as Pore Fluid 248
6.4-H(b) Summary of Normalized 1-Dimensional Consolidation Tests for Specimens from Koosi Creek Site with Air as Pore Fluid 249
6.4-I(a) Summary of Normalized 1-Dimensional Consolidation Tests for Specimens from Okanagan Lake Park Site with Water as Pore Fluid 249
6.4-I(b) Summary of Normalized 1-Dimensional Consolidation Tests for Specimens from Koosi Creek Site with Water as Pore Fluid 250
6.4-J(a) Summary of Normalized 1-Dimensional Consolidation Tests for Specimens from Okanagan Lake Park Site with Kerosene as Pore Fluid 250
6.4-J(b) Summary of Normalized 1-Dimensional Consolidation Tests for Specimens from Koosi Creek Site with Kerosene as Pore Fluid 250

CHAPTER SEVEN: Triaxial Testing

7.2.1-A Failure Envelope for Reconstituted Saturated Soils 276
7.2.1-B Different Type of Yielding 277
7.2.1-C Compression and Shear Yield of Structured Soils 278
7.2.1-D Typical Test Results for Structured Intact Calcarenite 279
7.3.2 Automated Triaxial Testing System 280
7.4.2-A Summary of Test Results (Specimen RA-K-CIU300) 281
7.4.2-B Summary of Test Results (Specimen RA-K-CIU400) 282
7.4.2-C Summary of Test Results (Specimen RA-K-CIU500) 283
7.4.2-D Normalized Summary Results for Reconstituted CIU Tests 284
7.4.2-E Summary of Test Results (Specimen RA-K-CAU372) 285
7.4.2-F Summary of Test Results (Specimen RA-K-CAD372) 286
7.4.2-G Summary of Test Results (Specimen RA-K-EAU190) 287

7.4.3.1-A Summary Results for Specimens from Koosi Creek Slide Site with In-Situ Water Content of 36%-38% 288
7.4.3.1-B Summary of Test Results (Specimen UI(KC)-W-CAU372) 289
7.4.3.1-C Summary of Test Results (Specimen UI(KC)-W-CAD372) 290
7.4.3.1-D Summary of Test Results (Specimen UI(KC)-W-qcte372) 291
7.4.3.2-A Summary Results for Specimens from Okanagan Lake Park Slide Site with In-Situ Water Content of 23%-28% 292
7.4.3.2-B Summary of Test Results (Specimen UI(OL)-K-CAU372) 293
7.4.3.2-C Summary of Test Results (Specimen UI(OL)-K-CAD372) 294
7.4.3.3-A Summary Results for Air-Dried Water Saturated Specimens 295
7.4.3.3-B Summary of Test Results (Specimen UA-W-CAU372(a)) 296
7.4.3.3-C Summary of Test Results (Specimen UA-W-CAU372(b)) 297
7.4.3.3-D Summary of Test Results (Specimen UA-W-CAD372(a)) 298
7.4.3.3-E Summary of Test Results (Specimen UA-W-CAD372(b)) 299
7.4.3.4-A Summary of Test Results (Specimen UA-K-CAU372) 300
7.4.3.4-B Pore Pressure Generation in Speciment UA-K-CAU372 301
7.4.3.4-C Summary of Test Results (Specimen UA-K-CAD372) 302
7.4.3.4-D Summary of Test Results (Specimen UA-K-CAD1680) 303
7.4.4-A Stress Paths of Reconstituted Specimens 304
7.4.4-B Stress-Strain Curves of Undrained Compression Tests 305
7.4.4-C Stress Paths of Undisturbed Specimens (Series UI-(KC)-W, UI(OL)-K, and UA-W) 306
7.4.4-D Stress Paths of Undisturbed Specimens (Series UA-K) 307
7.4.4-E Contours of the State Boundary for Compacted Jossigny Silt at Various Suctions 308
7.4.4-F State Boundary Surface in q-(p-u_a)-s Space 309

CHAPTER EIGHT: Soil Structure of Penticton Silt

8.2.1-A Structure Determining Factors and Processes 352
8.2.1-B Relationship between Swelling Index and Mica Content for

Coarse-Grained Mixtures 353
8.2.1-C Main Chemical Groups of Silica Surface 354
8.2.1-D Bonding (Sintering) of Silica Groups 355
8.2.1-E Swelling of the Silica Surfaces 356
8.2.1-F Bi-Axial Ultimate Strength Envelope of Concrete 357
8.2.1-G Results of Triaxial Tests on Concrete 358
8.2.2-A Soils Classification Using Pore Water Pressure (U_w) 359
8.2.2-B State Boundary Surface in q-(p-u_a)-s 360
8.2.2-C Triaxial Test Results at Various Suctions 361
8.2.2-D Critical State Line (CSL) at Various Suctions 362
8.2.2-E Contours of the State Boundary for Compacted Jossigny Silt at Various Suctions 363
8.3.1-A One Dimensional Consolidation Testing for Structure Determination (Results of Undisturbed Specimens) 365
8.3.1-B One Dimensional Consolidation Testing for Structure Determination (Results of Reconstituted Specimens) 364
8.3.1-C Summary of Triaxial Test Results for Structure Determination 365
8.3.2-A Response of Penticton Silt to Moistening 366
8.3.2-B Soil Fabric of the Athabasca Locked Sand 367
8.3.2-C Contact Point of Two Sand Grains 367
8.3.2-D Presence of Fine Grains Around the Contact Points 368
8.3.2-E Texture of the Fine Grains Around the Contact Points 368

APPENDIX A: Maps of the Surficial Deposits of Late Glacial and Recent Age of the Okanagan Valley

A-2.5-A Surficial Deposits of Late Glacial and Recent Age (Southern Okanagan Valley) – (The Pocket on the Back Cover of the Thesis)
A-2.5-B Surficial Deposits of Late Glacial and Recent Age (Northern Okanagan Valley) – (The Pocket on the Back Cover of the Thesis)

APPENDIX B: One Dimensional Consolidation Test Results

B-6.3-A(a) One Dimension Consolidation Test Results, Series A, Okanagan Lake Park Slide Site Specimens 402

B-6.3-A(b) One Dimension Consolidation Test Results, Series A, Koosi Creek Slide Site Specimens 402

B-6.3-B(a) One Dimension Consolidation Test Results, Series B, Okanagan Lake Park Slide Site Specimens 403

B-6.3-B(b) One Dimension Consolidation Test Results, Series B, Koosi Creek Slide Site Specimens 403

B-6.3-C(a) One Dimension Consolidation Test Results, Series C, Okanagan Lake Park Slide Site Specimens 404

B-6.3-C(b) One Dimension Consolidation Test Results, Series C, Koosi Creek Slide Site Specimens 404

B-6.3-D(a) One Dimension Consolidation Test Results, Series D, Okanagan Lake Park Slide Site Specimens 405

B-6.3-D(b) One Dimension Consolidation Test Results, Series D, Koosi Creek Slide Site Specimens 405

B-6.3-E(a) One Dimension Consolidation Test Results, Series E, Okanagan Lake Park Slide Site Specimens 406

B-6.3-E(b) One Dimension Consolidation Test Results, Series E, Koosi Creek Slide Site Specimens 406

B-6.3-F(a) One Dimension Consolidation Test Results, Series F, Okanagan Lake Park Slide Site Specimens 407

B-6.3-F(b) One Dimension Consolidation Test Results, Series F, Koosi Creek Slide Site Specimens 407

List of Symbols, Nomenclature, or Abbreviations

a'_p	attraction intercept
B. C.	British Columbia
c'	effective cohesion
C^*	strength parameter at unsaturated state
C_U	coefficient of uniformity
C.E.C.	cation exchange capacity
CPT	cone penetration Test
CPTU	cone penetration test with pore pressure measurement
CS	critical state
CSL	critical state line
CSSM	critical state soil mechanics
e	void ratio
e_c	void ratio after consolidation in triaxial tests
e_f	final void ratio in triaxial tests
e_i	initial void ratio in triaxial tests
e_{in}	initial void ratio in one dimensional consolidation tests
e_o	void ratio at the start of one dimensional consolidation tests
e_s	void ratio after swelling in triaxial tests
e_{sw}	void ratio after swelling in one dimensional consolidation tests
e^*_{100}	void ratio on ICL at $\sigma'_v = 100$ kPa
e^*_{1000}	void ratio on ICL at $\sigma'_v = 1000$ kPa
E.C.	electric conductivity
EDXA	elemental dispersive x-ray analysis
EPA	environmental protection agency
F	normalized friction ratio
f'_c	specified compressive strength of concrete
f_s	sleeve friction

g	gravitational acceleration
G_o	small strain shear modulus
$h_{c(a\text{-}o)}$	maximum capillary height for air-oil system
$h_{c(a\text{-}K)}$	maximum capillary height for air-Kerosene system
$h_{c(a\text{-}w)}$	maximum capillary height for air-water system
$h_{c(K\text{-}w)}$	maximum capillary height for Kerosene-water system
$h_{c(o\text{-}w)}$	maximum capillary height for oil-water system
HIV	hydroxy-interlayered vermiculite
I_v	void index
ICL	intrinsic Compression line
ICP	inductively coupled plasma
K	$= \sigma'_3 / \sigma'_1$
K_o	coefficient of earth pressure at rest
KC	specimen from Koosi Creek Slide site soil sample
M	Molar (moles/L)
M	slope of critical state line
M(s)	slope of CSL (suction dependent)
M^*	strength parameter at critical state in unsaturated state
M_a	total stress ratio at the critical state
M_b	strength parameter for unsaturated soil at critical state
M_C	slope of critical state line in compression
M_E	slope of critical state line in extension
M_s	structured strength parameter at the critical state
M_w	suction ratio at the critical state
M.C.	moisture content
N_K	an empirical cone factor
NCL	normal compression line
OCR	over-consolidation ratio
OL	specimen from Okanagan Lake Park Slide site soil sample
OT	observational test
p	net mean normal stress

P_a	reference pressure of 100 kPa
p'	effective mean normal stress
p'_{cs}	effective mean normal stress at critical state
P_a	reference pressure of 100 kPa
$p-u_a$	net mean normal stress at unsaturated state
P.I.	plasticity index
q	deviator stress
Q	normalized cone resistance
q_c	cone penetration resistance
r	pore radius
R_f	friction ratio
s	suction
S_r	degree of saturation
$S_{residual}$	residual degree of saturation
S_t	sensitivity
S_u	undrained shear strength
SBS	state boundary surface
SCL	sedimentation compression line
SCPTU	seismic cone penetration test with pore pressure measurement
SEM	scanning electron microscopy
$T_{S(a\text{-}K)}$	surface tension of air-Kerosene interface
$T_{S(a\text{-}w)}$	surface tension of air-water interface
$T_{S(K\text{-}w)}$	surface tension of Kerosene-water interface
u	pore pressure
u_a	pore air pressure
u_a-u_w	matric suction
$(u_a-u_w)_f$	matric suction on the failure plane at failure
$u_{c(a\text{-}w)}$	capillary pressure for air-water interface
u_{eff}	effective matric suction
u_w	pore water pressure
v	specific volume

v_s	shear wave velocity
w	water content
W_L	liquid limit
W_P	plastic limit
YSR	yield stress ratio
α_K	contact angle of Kerosene
α_w	contact angle of water
χ	Bishop's unsaturated soil parameter
ϕ'	effective angle of internal friction
ϕ'_{cs}	intrinsic critical state friction angle
ϕ'_{pr}	post rupture friction angle
ϕ'_r	residual friction angle
ϕ^b	angle indicating the rate of increase in shear strength relative to matric suction, $(u_a-u_w)_f$
$\mu(s)$	intercept of CSL with q axis at a given value of suction
π	osmotic suction
ρ	mass density
ρ_K	density of Kerosene
ρ_w	density of water
σ	total stress
σ_1	major principal stress or axial stress
σ_3	minor principal stress, or lateral stress
σ'_1	major principal effective stress
σ'_2	intermediate principal effective stress
σ'_3	minor principal effective stress
$(\sigma_f-u_a)_f$	net normal stress state on the failure plane at failure
$(\sigma_f-u_w)_f$	effective normal stress on the failure plane at failure
σ'_p	maximum past effective consolidation stress
σ'_v	effective vertical stress

σ_{vo}	overburden stress
σ'_{vo}	effective overburden stress
σ'_{vy}	vertical yield stress
τ	shear stress
τ_{ff}	shear stress on the failure plane at failure
ω	intercept of CSL with q axis at a given value of structural bonding
Ω	intercept of CSL with q axis for structured soils
ψ	total suction

CHAPTER ONE

Introduction

1.1 General

Soil is an important engineering material. Construction of most structures involves soil. Soil can be used as construction material for earth structures such as earth dams or embankments. Soils can also be used as foundation or support for other structures. Most civil engineering activities are dependent on the behavior of soils.

In Geotechnical Engineering, soils can be classified based on their grain size. Soils can be fine-grained (i.e., clays) or coarse-grained (i.e., sands and gravels). Soils can also be divided into cohesive soils (clays) and cohesionless soils (sands).

In classical soil mechanics, the behavior and state of a soil is expressed as a function of its void ratio and stress history. Critical state soil mechanics, developed using reconstituted isotropically consolidated saturated soil specimens, utilized the concepts of yielding and critical state. According to critical state soil mechanics the behavior and state of an ideal saturated soil can be uniquely expressed in terms of the deviator stress (q), effective mean normal stress (p'), and void ratio (e).

Soils are generally structured. The behavior of structured soils can be influenced by many parameters. Their behavior can be different from the behavior of ideal soils. Structure of a soil is a function of fabric and chemical and physical processes.

Structured soils may also be unsaturated. An unsaturated soil may have other fluids such as air in the voids. In unsaturated soil mechanics, the behavior of a soil can be expressed in terms of the total stress, σ, the pore water pressure, u_w, and the pore air pressure, u_a.

The behavior of structured soils is not well known. During the last two decades, several studies have been carried out to improve our understanding of the behavior of structured soils. However, there are many factors of the behavior of structured soils that still require further study.

The glaciolacustrine silt sediments in the interior of British Columbia have been chosen as the material to study the behavior of structured soils. These silt sediments appear to be cemented and unsaturated.

1.2 Research Significance

In general, the study of the behavior of cohesionless soils has mainly been carried out using uncemented, unaged, clean sands. Cohesive soils have been studied using both reconstituted and undisturbed specimens. The difference in the behavior of reconstituted and undisturbed cohesive soils has generally been expressed in terms of "over-consolidation ratio" or "sensitivity". The origin or source of structure has been the topic of some research in geotechnical engineering. Some studies have emphasized the significance of physical processes such as particle interlocking due to aging. Results of other studies have shown the importance of chemical processes such as calcium carbonate cementation at particle contacts. There have been some studies using sands especially carbonated sands; but, the majority of research on structure has been carried out using cohesive soils. In some research, the effect of structure has been studied using the concept of yielding and critical state soil mechanics (CSSM). These studies have been carried out using clays, weak rocks, or carbonated sands.

The glaciolacustrine silt sediments in the interior of British Columbia are mainly composed of silt size cohesionless mica and chlorite minerals. The carbonate content is relatively low. Their mineralogy and physical and chemical characteristics make them an interesting natural soil on which to study the cause and effect of structure. These soils provide the opportunity to study the links between structured, fine-grained cohesionless silt and cohesionless coarse-grained materials such as sands and cohesive fine-grained materials such as clays.

1.3 Background Information

Some concepts, definitions, and theories from the literature have been used frequently in this study. They are briefly discussed here to provide the reader with the required background. Detailed literature reviews are presented in the appropriate sections of the following chapters.

Mitchell (1993) discussed the structure of soils and defined the structure of a soil as a composition of its fabric and inter-particle force system. He also defined fabric as "the arrangement of particles, particle groups, and pore spaces in a soil". Figure 1.3-A, adopted from Mitchell (1993) summarizes the factors and processes controlling soil structure. This inter-particle force system is the result of factors such as soil composition, history, present state, and environment. In structured soils, the present state is generally different from the initial state because of chemical and physical processes, which have altered the state and have caused changes in the fabric and inter-particle force system. These processes can be both physical and chemical and can influence the structure of both cohesive and cohesionless soils.

Many studies have been carried out to investigate the physical processes that influence soil structure. According to Mitchell (1993), consolidation, especially under pressure, causes structural improvement, which increases the strength of the soil by decreasing the porosity and forming stronger inter-particle contacts. Confining pressure, especially as a function of time, is considered to induce structural improvements to soil as mentioned by Afifi and Richart (1973), Lee (1977), Anderson and Stokoe (1978), Dusseault and Morgenstern (1979), and Mesri et al. (1990). Schmertmann (1991) and Mesri et al. (1990) reported that structural improvements could occur because of particle rearrangements. Structural improvements are also considered to cause an increase in horizontal stresses by Whitman et al. (1964) and Schmertmann (1987 and 1991). Based on a comparison of undisturbed and reconstituted specimens, an increase in the cyclic strength of the soils as a result of over-consolidation was reported by Ishihara et al. (1978). Temperature can also influence physical processes that can change the soil structure. According to Mitchell (1993), changes in structure as a result of pressure increase occur faster at high temperatures than at low temperatures. As can be seen in Figure 1.3-A, wetting and drying and freezing and thawing can lead to structural changes in soil through physical processes. Wetting can lead to elimination of mechanical forces in the form of capillary tension. Mitchell (1993) wrote that cycles of wetting and drying or freezing and thawing can change the particle assemblages. Drying can cause shrinkage, which can lead to structural collapse and tension cracks in some soils. Mitchell (1993) stated that drying could transfer clay particles to the contact points of adjacent silt and sand particles. Concentration of clay particles at contact points of silt and sand grains can cause structural improvements. According to Mitchell (1993), shearing and unloading are among the physical processes that can change soil structure. Shearing can cause structural collapse in homogeneous isotropic normally consolidated soils or the formation of shear bands and structural changes in the vicinity of the shear bands in over-consolidated soils. Mitchell (1993) stated that seepage could cause erosion through particle movements and consolidation as the result of seepage force. Physical weathering can also be in the form of mechanical disintegration resulting in reduction of particle size. Fanning et al. (1989) reported cases of the formation of clay minerals like illitic clays correspond quantitatively to mechanical disintegration of mica minerals in the sand and silt grain sizes.

Chemical processes, as summarized in Figure 1.3-A, are also involved in processes that change and influence the structure of soils. According to Mitchell (1993), diffusional processes and chemical reactions are time, temperature, and pressure dependent. According to Mitchell (1993), seepage can remove or introduce chemicals, colloids, and microorganisms. Cementation and aggregation can occur as the result of precipitation of materials onto particle surfaces or at particle contacts. Several researchers including Dupas and Pecker (1979), Clough et al. (1981), Rad (1982 and 1984), Rad and Tumay (1986), Acar et al. (1986), and Acar (1987) considered cementation or some kind of welding at the particle contacts as a source of structural improvement in soil. Seed (1979) stated that improvement in the cyclic resistance of sand can be due to cementation or welding at particle contacts. Many other studies including Denisov and Reltov (1961), Henderson et al. (1970), Miura and Yamanouchi (1973 and 1978), Lee (1977), Dusseault and Morgenstern (1979), Mitchell and Solymar (1984), and Mitchell (1986) not only considered cementation as the source of structural improvements but also speculated that cementation in some soils is due to mechanisms involving the dissolution and re-precipitation of amorphous or crystalline silica and formation of silica acid gel on particle surfaces. According to Mitchell (1993) and Fanning et al. (1989), chemical weathering and mineralogical transformations are processes that can change the soil structure. For example, chemical weathering can cause mineral transformation of a potassium (K) bearing mica like biotite to an expansible 2:1 mineral like Vermiculite by replacement of potassium (K) with hydrated cations or water (H_2O). Structural changes due to chemical processes involving inter-particle forces can happen in the soil environment as the result of changes in the pore fluid chemistry. Hight et al. (1994) also mentioned that clay content, mineralogy of clay, and chemistry of pore fluid can influence the structure of the soil.

Critical state soil mechanics has proven to be a strong tool for studying soil behavior. According to Leroueil (1997), its fundamentals are based on works of Terzaghi, Casagrande, and Hvorslev. Roscoe et al. (1958) unified the works by Rendulic (1937) and Hvorslev (1937) and developed the basic framework of critical state soil mechanics using reconstituted and isotropically consolidated saturated clay specimens. The failure envelope for a reconstituted clay is shown in Figure 1.3-B. The failure envelope consists of Roscoe-Rendulic surface, Hvorslev surface, and a no-tension cut-off line. The Roscoe-Rendulic surface is also known as "limit state", "yield", or "state boundary" surface. The boundaries of the Roscoe-Rendulic surface are "normal compression line" (NCL) and "critical state line" (CSL). The normal compression line (NCL) is defined as the line formed by isotropic consolidation of a reconstituted clayey soil with initial water content close to its liquid limit. At large shear strains, an ideal saturated soil moves towards a unique state in the space formed by the deviator stress (q), effective mean normal stress (p'), and void ratio (e). The assembly of these ultimate states forms "critical state line" (CSL). The projection of critical state line (CSL) in the q-p' plane is a straight line, defined as:

$q = M\,p'$ (Equation 1.3-A)

in which:

$q = \sigma'_1 - \sigma'_3$,

$p' = \dfrac{\sigma'_1 + \sigma'_2 + \sigma'_3}{3}$, and

M is the strength parameter at the critical state, which is equal to $\dfrac{6\sin\phi'}{3-\sin\phi'}$ in triaxial compression.

Interested readers are referred to Atkinson and Bransby (1978) for detailed study of concepts of the critical states soil mechanics.

Many researchers including Airey (1993), Burland (1990), Burland et al. (1996), Coop (1990), Coop and Atkinson (1993), Coop and Lee (1993 and 1995), Coop et al. (1995), Cuccovillo and Coop (1993), Kavvadas (1995), Lee and Coop (1995), Leroueil and Vaughan (1990), and Leroueil (1992 and 1997) have studied the behavior and response of structured soils and weak rocks utilizing the concepts of yielding and critical state soil mechanics (CSSM). Using the framework of critical state soil mechanics, the influence of structure on the mechanical behavior of soils can be addressed by comparing the behavior of structured and de-structured soils. These studies are briefly reviewed in the following.

According to Burland (1990), Skempton studied the consolidation of twenty normally consolidated clay deposits under gravitational compaction. Skempton used the relationship between the in-situ void ratio (e_o) and the effective overburden pressure (σ_{vo}'); and referred to the resulting curve as the "sedimentation compression curve" (SCL). As reported by Burland (1990), Skempton concluded that the sedimentation compression curves are essentially linear and converging.

A reconstituted soil specimen can be obtained in many ways. It is necessary to have a standard procedure to make reconstituted specimens in order to be able to compare the behavior of structured soils with a de-structured reference state. Burland (1990) proposed a set of characteristics for a reconstituted clay specimen that can represent the "intrinsic properties" of that soil. A clay specimen should be "reconstituted at a water content of W_L to $1.5W_L$ (preferably $1.25W_L$) without air-drying or oven drying, and then consolidated – preferably under one-dimensional conditions", where W_L is liquid limit. Burland (1990) recommended that the pore fluid chemistry of the slurry should be similar to the chemistry of the pore fluid in the natural state of the clay. The properties of such specimens are independent of the natural and in-situ state of soil and such properties are representative of its inherent nature. Different soils have different void ratios at their W_L. The consolidation curves of the intrinsic state of different soils are different, if they are plotted in e-log σ_v' space; but they have the same shape. In an attempt to create a unique reference line, which represents the intrinsic state of all soils, Burland (1990) normalized the intrinsic compression curves (ICL) using the intrinsic void ratios at effective vertical stresses (σ_v') equal to 100 kPa and 1000 kPa (e^*_{100} and e^*_{1000}). "void index" (I_v) is defined as:

$$I_v = \frac{e - e^*_{100}}{e^*_{100} - e^*_{1000}} \qquad \text{(Equation 1.3-B)}$$

Figure 1.3-C, adopted from Burland (1990), shows the intrinsic compression curve in e-log σ_v' space and the transformed intrinsic compression line (ICL) in the normalized I_v-log σ_v' space. According to Burland (1990), the intrinsic compression line (ICL) is reasonably unique, which can be represented with the following equation:

$$I_v = 2.45 - 1.285 \log\sigma_v' + 0.015 \log\sigma_v'^3 \qquad \text{(Equation 1.3-C)}$$

Referring to experimental data from the study by Leonards and Ramiah (1959), Burland (1990) showed that aging influence the compressibility of reconstituted soils. Experimental evidence was presented indicating the resistance to compression would increase during aging without dependency on volume change due to creep.

Structured soils show increased resistance to compression compared to the intrinsic state of soils. Burland (1990) criticized the use of terms "pre-consolidation pressure" and "over-consolidation ratio" to refer to this increased resistance due to the presence of structure. Burland (1990) proposed the term "vertical yield stress" (σ_{vy}') to refer to the critical pressure that represents the increased resistance to compression. He said, "the term pre-consolidation pressure should be reserved for situations in which the magnitude of such pressure can be established by geological means". Burland (1990) also said, "the term over-consolidation ratio should be reserved for describing a known stress history". He proposed the use of the term "yield stress ratio" (YSR), which is defined as the ratio of the vertical yield stress to effective overburden pressure ($YSR = \sigma_{vy}'/\sigma_{vo}'$). The terminology proposed by Burland (1990) has been followed throughout this study.

The in-situ natural state of a soil may not be on the ICL. Some of the potential states are summarized in Figure 1.3-D. The intrinsic state of a soil is presented by the "intrinsic compression line", ICL (line D-I-F). One or several of the following processes may transform the state of a soil from its initial state (i.e., I on ICL Line in Figure 1.3-D):

- Partial removal of overburden causes decrease in effective overburden pressure (σ_{vo}') and some increase in void ratio. This process leads the soil to the "over-consolidation" state (transformation along I-O in Figure 1.3-D). For a given value of σ_{vo}', the soil is at a lower value of void ratio in the over-consolidated state compared to its intrinsic state. In other words, a soil is at a more stable state.

- Drained creep causes a decrease in void ratio at a constant effective overburden pressure (σ_{vo}') (transformation along I-A in Figure 1.3-D). Such processes lead the soil to a denser and more stable state.

- If physicochemical bonding develops, the compressibility of soil decreases. Any further increase of the effective overburden pressure (σ_{vo}') smaller than the vertical yield stress (σ_{vy}') causes little change in void ratio (transformation along I-C in Figure 1.3-D). The physicochemical bonding in the soil structure carries extra effective overburden pressure. For a given value of effective overburden pressure (σ_{vo}'), the soil exists at a void ratio higher than those for its intrinsic state. Such processes lead the soil to a "meta-stable" state on the right side of the "intrinsic compression line" (ICL).

- At constant effective overburden pressure (σ_{vo}'), disintegration of solid phases by processes like diagenesis of organic material or dissolution of soluble minerals like calcium carbonate can cause an increase in void ratio (transformation along I-B in Figure 1.3-D). Such processes lead the soil to values of void ratio that are higher than those for its intrinsic state and the soil is transferred to a meta-stable state.

Leroueil and Vaughan (1990) and Coop et al. (1995) discussed compressibility and strength characteristics of structured soils, using the framework of critical state soil mechanics. A schematic presentation of the response of an intact structured soil relative to the intrinsic compression line (ICL) is shown in Figure 1.3-E. The presence of structure allows the intact specimen to exist in the meta-stable state on the right side of the ICL. Upon reaching the effective yield stress (σ_{vy}'), the compressibility of soil increases and large plastic deformations occur. Finally, at large deformations and after total de-structuring, the soil approaches its intrinsic behavior. According to Coop et al. (1995), the distance that an intact structured specimen can travel beyond the intrinsic compression line prior to yielding, is a function of the degree of bonding.

Leroueil and Vaughan (1990) defined yield as a discontinuity in the stress-strain behavior under monotonic stress changes. "An irreversible post yield change in the stiffness and strength of the material" is an indicator of yielding of the soil structure. Bonded structured soils may yield as the result of de-structuring caused by swelling pressure. Swelling yield occurs at low effective stresses. According to Leroueil and Vaughan (1990) and Coop et al. (1995), yielding of the structure may also occur in either compression or shear. A schematic presentation of compression and shear yield of structured soils is shown in Figures 1.3-F(a) and (b), respectively. The intrinsic state boundary surface (SBS), obtained using a reconstituted specimen is also shown. Structured soils can reach states outside the intrinsic state boundary surface. If a structured soil specimen consolidates beyond its effective yield stress, de-structuring occurs prior to shearing. The stress path for the specimen that yielded in compression is similar to that for a reconstituted specimen. For a specimen that yielded during undrained shearing, three stages can be recognized. During the first stage of shearing, no significant change in mean effective normal stress (p') occurs. The induced external forces are balanced with internal structural forces. The second stage is characterized by yielding of the soil structure. At this stage, the de-structuring of the soil occurs. Finally, at third stage, the state of soil travels towards the critical state for a reconstituted specimen.

The effect of structure on soil behavior is as important as void ratio and stress history. Norwegian and Canadian sensitive clays are well known cases of structured soils in which landslides can occur due to soil structural failure and changes in physicochemical bonding. Karlsrud et al. (1984) and Tavenas (1984) reviewed the behavior of these deposits. Both of these deposits are silty marine deposits, with mica and chlorite as the dominant minerals. According to Karlsrud et al. (1984), leaching of the salt water pore fluids caused the structural changes in Norwegian marine clays and increased their sensitivity from 3-6 to values larger than 20. Karlsrud et al. (1984) showed that Norwegian sensitive clays have extremely brittle behavior in undrained triaxial tests. These soils reach their peak strength at small axial strains of 0.3% and their post peak strength is about 50% of the peak strength. Karlsrud et al. (1984) also stated that the post peak strength loss in undrained triaxial testing of Norwegian sensitive clays was entirely due to pore pressure increase and hence, decrease in effective stress. They also concluded that the undrained shear strength of Norwegian sensitive clays is highly anisotropic.

Karlsrud et al. (1984) also commented on the behavior of Eastern Canadian sensitive clays. The Canadian structured clay deposits showed strain softening behavior in undrained shearing and had effective stress envelopes and post-peak effective shear strengths, which were above the envelope for the unstructured soil. The post peak strain softening for these materials during undrained shearing occurred by breakage of cementation bonds with small pore pressure generation. The stress-strain curves of the undrained shearing tests of Eastern Canadian sensitive clays showed a post peak plateau with a distinct value for post peak shear strength. This behavior is in contrast with the post peak behavior of Norwegian sensitive clays.

Tavenas (1984) and Karlsrud et al. (1984) linked the occurrence of flow-slides to the plasticity of the soils. According to Tavenas (1984), marine clays with plasticity index less than 20% and salinity less than 3 g/l are susceptible to occurrence of flow-slides. It should be mentioned that Karlsrud et al. (1984) reported the salinity of Norwegian sensitive clays to be 1 g/l.

Structured soils may also be unsaturated. A change in the degree of saturation is considered to be responsible for expansion of swelling clays and collapse of some loose silty soils. Fredlund and Rahardjo (1993) used that the terms "saturated soil mechanics" and "unsaturated soil mechanics" to distinguish the zones where positive and negative pore pressures exist, respectively. A saturated soil is a two phase material consisting of water and solid phases while an unsaturated soil is a composition of several phases. According to Fredlund and Rahardjo (1993), "a portion of a mixture is called an independent phase if it has differing properties from the contiguous materials and definite bounding surfaces". An unsaturated soil can have air in the voids. An unsaturated soil has at least four phases, which are solid, air, water, and the air-water interface that can be referred to as the contractile skin. Air and water mixtures can be immiscible or miscible. In an immiscible mixture, there is no interaction between air and water. It is a mixture of free water and air, separated by the contractile skin. The miscible mixture of air and water can be in the form of dissolved air in water or water vapor in the air.

In saturated soil mechanics, the behavior of a soil can be expressed in terms of the total stress, σ, and the pore water pressure, u_w. The behavior of saturated soils, which are composed of two phases, can be described using effective stress (σ-u_w) as the stress state variable. The equilibrium of soil structure and contractile skin in unsaturated soils cannot be expressed entirely by the effective stress as the stress state variable. In unsaturated soil mechanics, the behavior of a soil is expressed in terms of the total stress, σ, the pore water pressure, u_w, and the pore air pressure, u_a. Fredlund and Morgenstern (1977) stated that $(\sigma-u_a)$ and matric suction (u_a-u_w) were the suitable stress state variables for unsaturated soils that control the equilibrium of soil structure and contractile skin.

The shear strength is one of the main mechanical characteristics of a soil. Mohr-Coulomb failure criteria can be used to express the shear strength of a saturated or an unsaturated soil. The shear strength of a saturated soil can be expressed in terms of effective stress parameters as follows:

$$\tau_{ff} = c' + (\sigma_f - u_w)_f \tan\phi' \qquad \text{(Equation 1.3-D)}$$

in which:

τ_{ff} = shear stress on the failure plane at failure,

c' = effective cohesion,

$(\sigma_f - u_w)_f$ = effective normal stress on the failure plane at failure,

ϕ' = effective angle of internal friction.

According to Fredlund et al. (1978), stress variables $(\sigma-u_a)$ and (u_a-u_w) can be used to express the shear strength of an unsaturated soil as follows:

$$\tau_{ff} = c' + (\sigma_f - u_a)_f \tan\phi' + (u_a - u_w)_f \tan\phi^b \qquad \text{(Equation 1.3-E)}$$

in which:

τ_{ff} = shear stress on the failure plane at failure,

c' = effective cohesion,

$(\sigma_f - u_a)_f$ = net normal stress state on the failure plane at failure,

ϕ' = angle of internal friction associated with the net normal stress state variable, $(\sigma_f - u_a)_f$,

$(u_a - u_w)_f$ = matric suction on the failure plane at failure,

ϕ^b = angle indicating the rate of increase in shear strength relative to matric suction, $(u_a - u_w)_f$.

Many attempts have been made to describe the state of an unsaturated soil using the concepts of critical state soil mechanics. The strength envelope of a saturated soil can be expressed as follow:

$$q = M p' \qquad \text{(Equation 1.3-A)}$$

in which, M is strength parameter at the critical state in saturated conditions. Different relationships has been proposed for unsaturated soils by several researchers including Fredlund et al. (1978), Escario and Saez (1986), Toll (1990), Wheeler and Sivakumar (1993 and 1995), Maatouk et al. (1995). Conceptually, all these relationships try to introduce strength parameters at the critical state in unsaturated conditions, using net mean normal stress (p-u_a), and matric suction (u_a-u_w). While some researchers like Fredlund et al. (1978) stated that these two stress state variables were independent, others like Maatouk et al. (1995) stated that they might be dependent.

Investigating the experimental results presented by Wheeler and Sivakumar (1993), an important observation can be made. The intrinsic compression line (ICL) and the critical state line (CSL) are not the same for saturated specimens and specimens under the condition of zero soil suction. In other words, elimination of soil suction does not necessarily transfer the soil to a saturated state.

Alonso et al. (1990) presented a constitutive model for unsaturated soils using (p-u_a), q, e, and suction (s). Details of the model are beyond the scope of this study but some key elements of the model are relevant to the current study. Alonso et al. (1990) stated that the volumetric response of partially saturated soil depends not only on the initial and final stress and suction values but also on the stress path. The proposed constitutive model is based on yield surfaces in $(p-u_a)$, q, and s space as shown in Figure 1.3-G. An interesting feature of the model is the introduction of the critical state line (CSL) for the condition of non-zero suction. As can be seen in Figure 1.3-G, CSL for unsaturated soil has been introduced by modeling the influence of suction as an intercept with the deviator stress axis (q) and drawing a line parallel to the CSL for saturated condition.

1.4 Site Selection

The glaciolacustrine silt sediments in the interior of British Columbia have been chosen as the material to study the behavior of a structured soil. These sediments are located in the South Thompson River Valley and the Okanagan Lake Valley. Silt bluffs, which have slope angles as high as 70 degrees, are in generally stable conditions in their natural state. These materials generally have less than 10% clay size fraction and are mainly composed of silica grains. They are also dominantly silt size (approximately 90%).

More than twenty landslides have been reported in these sediments by Nasmith (1962), Nyland and Miller (1977), Buchanan (1977), Lum (1977), Wilson (1985), and Klohn Leonoff (1992). There were block falls from the vertical silt bluffs, shallow planar slides in sloping colluvial silts, and complex rotational slides. Deep-seated rotational slides created the greatest hazard to human life and property. Their volume and zone of accumulations were large and their occurrences were sudden.

In a search for deep-seated rotational slides, all reported landslides were reviewed and visited by a team consisting of author, representatives from the Geotechnical Engineering Group of the Department of Civil and Environmental Engineering of the University of Alberta, authorities from local office of B. C. Ministry of Transportation and Highways, and a group of local engineers. Koosi Creek Slide (also known as Chute Creek Slide), Okanagan Lake Park Slide, Randolph Creek Slide, and Harper Ranch Road Slide were found to be deep-seated rotational slides. Taking into account the size, geometry and documentation, the Koosi Creek Slide and Okanagan Lake Park Slide were chosen as the sites for sampling and studying the behavior of these materials. The Koosi Creek Slide occurred in the summer of 1942 on the east shore of Okanagan Lake. Approximately

500,000 m^3 of material moved. The Okanagan Lake Park Slide, on the west shore of Okanagan Lake, occurred in the spring of 1975 when 50,000 m^3 moved. Details of the geology, site selection, and sampling are presented in Chapters 2 and 3.

1.5 Objectives and Scope

The main objective of this research is to study the nature and cause of the behavior of the Okanagan Lake Valley silt sediments (geologically also known as Penticton silt). Explaining the geotechnical and geological hazards of the silt bluffs in the southern interior of British Columbia and revisiting and discussing the Koosi Creek Slide and the Okanagan Lake Park Slide are considered as the other objectives of the current study. Concepts from soil mechanics, soil chemistry, mineralogy, geology, and surface chemistry are implemented in this study.

1.6 Thesis Arrangement

A literature review for each topic under investigation is presented in the chapter or section corresponding to that topic. The geology of Okanagan Valley is presented in Chapter 2. This chapter covers the geological history, the surficial geology, and the geological hazards in the area. Site selection and sampling is explained in Chapter 3. The Koosi Creek Slide and the Okanagan Lake Park Slide are also reviewed in this chapter. Chapter 4 describes the cone penetration testing (CPT) carried out in these sediments. Chapter 5 summarizes the data and discussion of the basic soil properties including specific gravity, grain size distribution, Atterberg limits, soil-water characteristic curve, mineralogy, scanning electron microscopy (SEM), and soil and pore fluid chemistry. Stress-controlled, one-dimensional consolidation tests are utilized in Chapter 6 to study the compressibility of these materials. Non-traditional techniques are used to find the conceptual answers for the behavior and response of these soils using the change in their compressibility. The details of drained and undrained triaxial compression testing are presented in Chapter 7. A unified conceptual model for the behavior of structured soils is discussed in Chapter 8 based on the physicochemical state of these soils, using results of this study and previous studies. A summary, practical implications, conclusions, and recommendations for further studies are presented in Chapter 9.

Maps of the surficial deposits of late glacial and Recent age of the Okanagan Valley and detailed results of one-dimensional consolidation tests are presented in Appendix A and B, respectively.

Figure 1.3-A – Structure Determining Factors and Processes

(after Mitchell (1993))

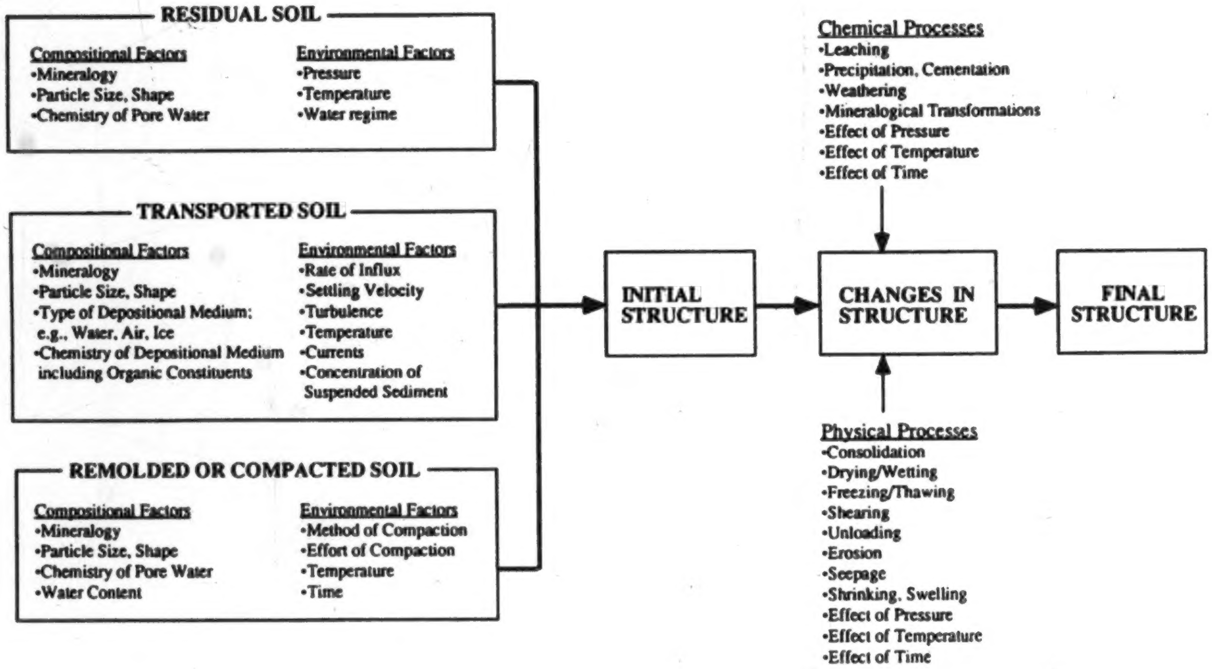
RESIDUAL SOIL
Compositional Factors
•Mineralogy
•Particle Size, Shape
•Chemistry of Pore Water
Environmental Factors
•Pressure
•Temperature
•Water regime
TRANSPORTED SOIL
Compositional Factors
•Mineralogy
•Particle Size, Shape
•Type of Depositional Medium: e.g., Water, Air, Ice
•Chemistry of Depositional Medium including Organic Constituents
Environmental Factors
•Rate of Influx
•Settling Velocity
•Turbulence
•Temperature
•Currents
•Concentration of Suspended Sediment
REMOLDED OR COMPACTED SOIL
Compositional Factors
•Mineralogy
•Particle Size, Shape
•Chemistry of Pore Water
•Water Content
Environmental Factors
•Method of Compaction
•Effort of Compaction
•Temperature
•Time
INITIAL STRUCTURE
Chemical Processes
•Leaching
•Precipitation, Cementation
•Weathering
•Mineralogical Transformations
•Effect of Pressure
•Effect of Temperature
•Effect of Time
CHANGES IN STRUCTURE
Physical Processes
•Consolidation
•Drying/Wetting
•Freezing/Thawing
•Shearing
•Unloading
•Erosion
•Seepage
•Shrinking, Swelling
•Effect of Pressure
•Effect of Temperature
•Effect of Time
FINAL STRUCTURE

Figure 1.3-B – Failure Envelope for Reconstituted Clays

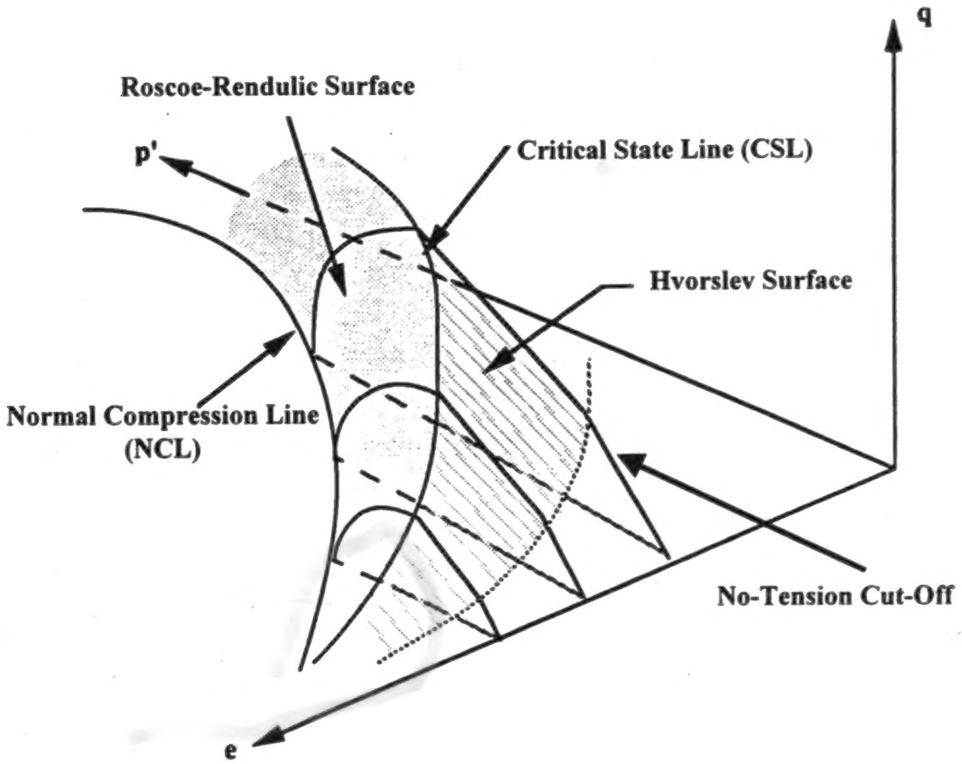
q
Roscoe-Rendulic Surface
p'
Critical State Line (CSL)
Hvorslev Surface
Normal Compression Line
(NCL)
No-Tension Cut-Off
e

Figure 1.3-C – The Intrinsic Compression Line (ICL) in
(a) e-log σ'_v and (b) I_v-log σ'_v
(after Burland (1990))

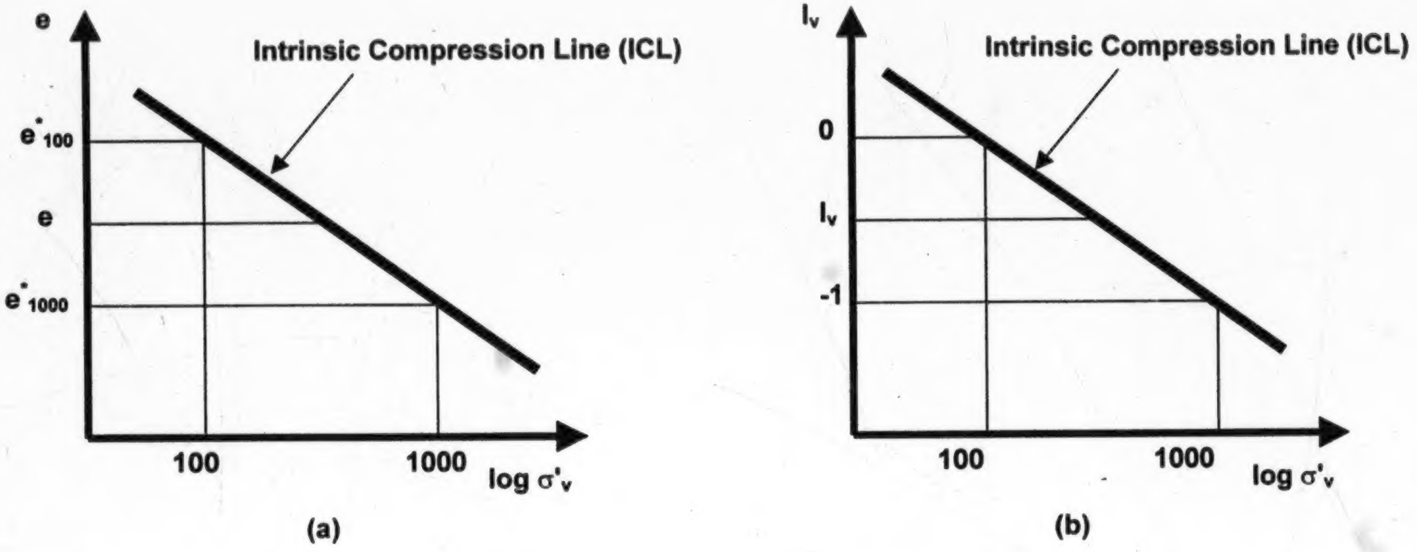
e
e^*_{100}
e
e^*_{1000}
Intrinsic Compression Line (ICL)
100
1000
log σ'_v
(a)
I_v
0
I_v
-1
Intrinsic Compression Line (ICL)
100
1000
log σ'_v
(b)

Figure 1.3-D – Summary of State Transformations

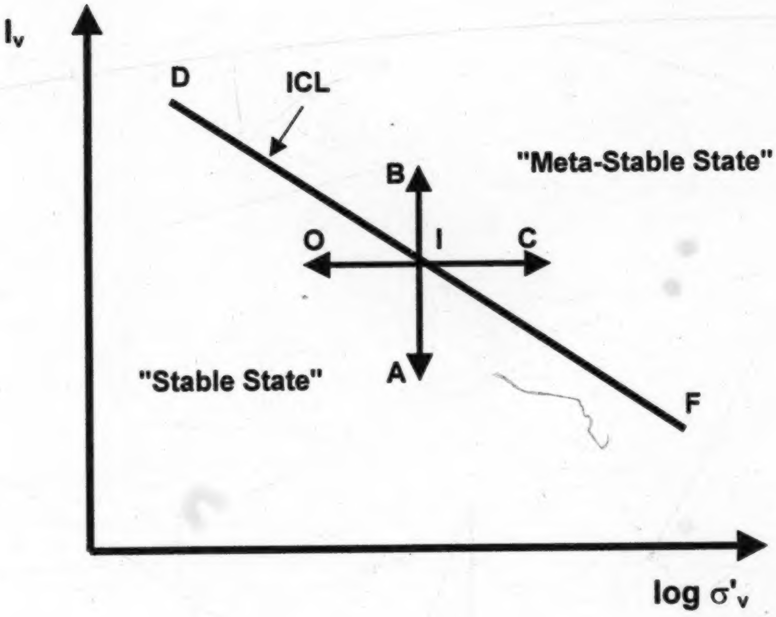

I_v
D
ICL
"Meta-Stable State"
B
O
I
C
A
"Stable State"
F
$\log \sigma'_v$

Figure 1.3-E – Compressibilty of an Intact Specimen Relative to the ICL

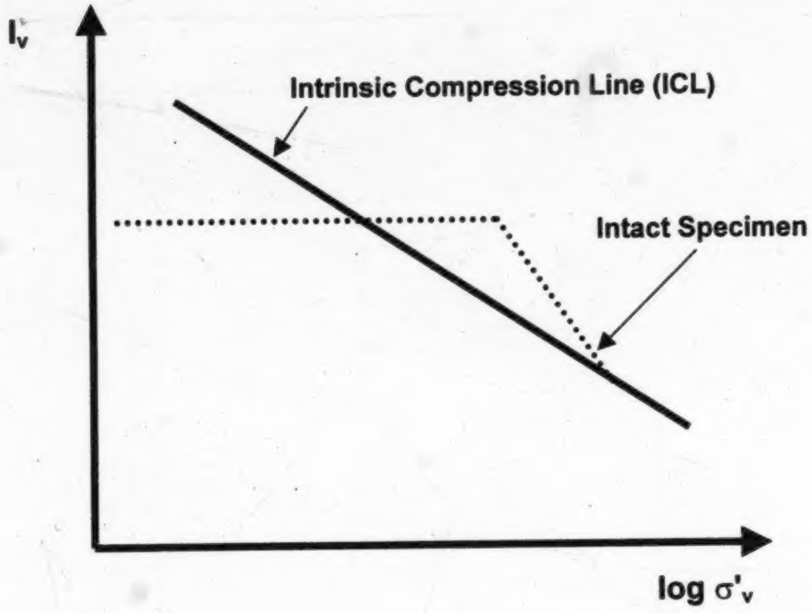
I_v
Intrinsic Compression Line (ICL)
Intact Specimen
$\log \sigma'_v$

Figure 1.3-F – Compression and Shear Yield of Structured Soils

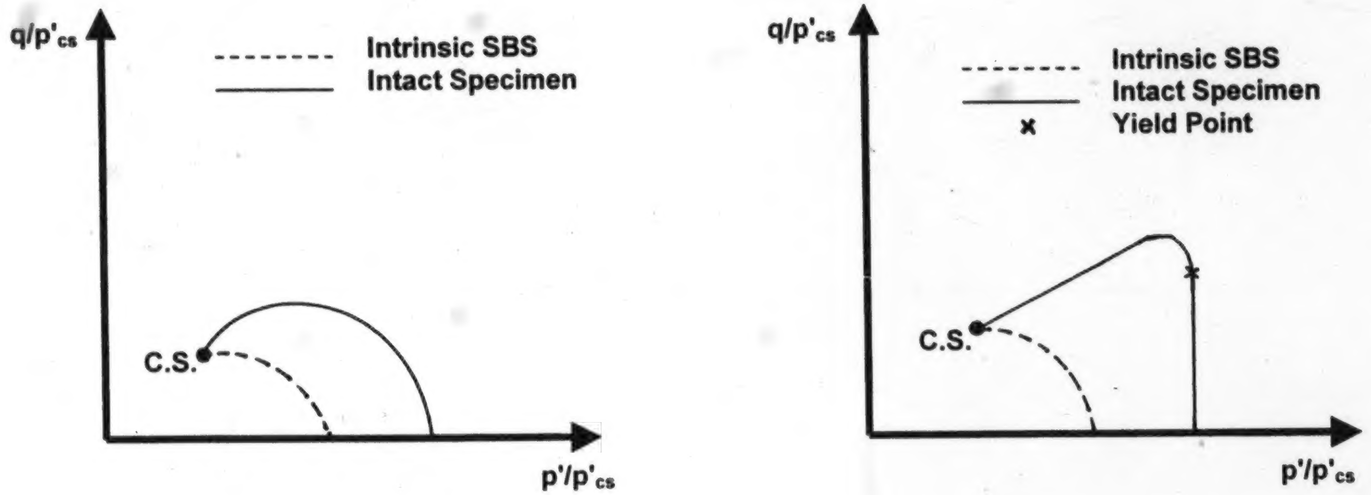
q/p'cs
Intrinsic SBS
Intact Specimen
C.S.
p'/p'cs
q/p'cs
Intrinsic SBS
Intact Specimen
×
Yield Point
C.S.
p'/p'cs

(a) Compression Yield

(b) Shear Yield

Figure 1.3-G – Yield Surface for Unsaturated Soil in $(p-u_a)$-q Space
(after Alonso et al. (1990))

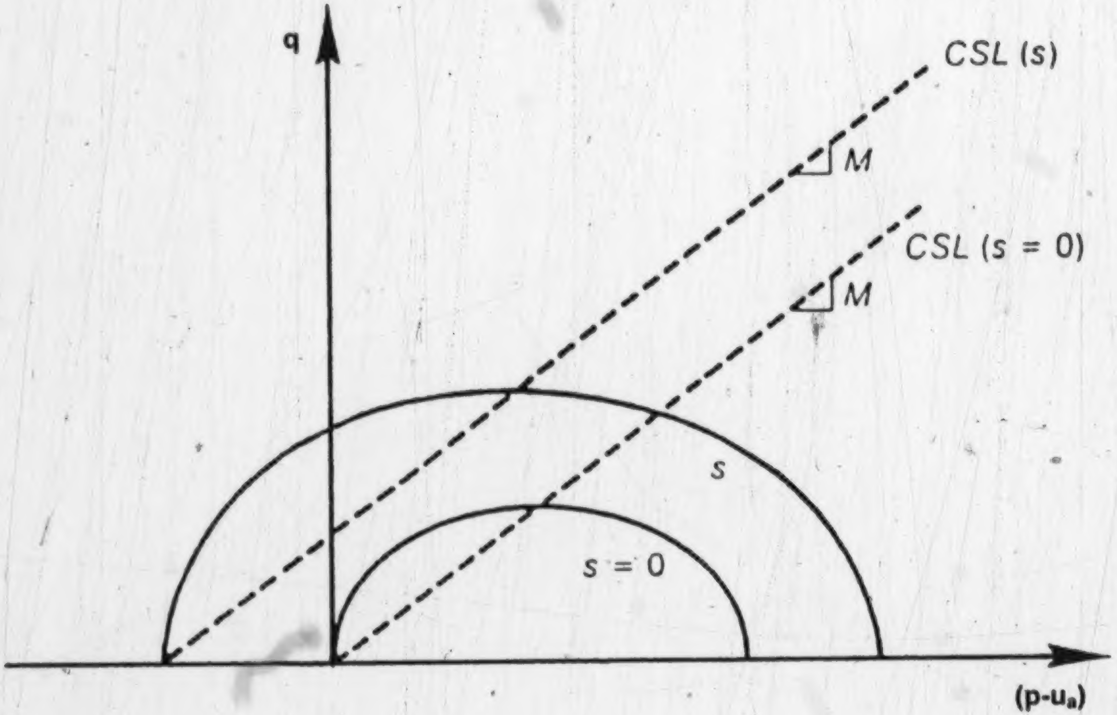
q
CSL (s)
M
CSL (s = 0)
M
s
s = 0
(p-u_a)

CHAPTER TWO

Geology of the Okanagan Valley

2.1 Introduction

The soil chosen as the material to study the behavior of structured soils is the glaciolacustrine varved laminated silt sediment located in the Okanagan Valley in the interior of British Columbia. Figure 2.1-A shows Okanagan Valley area relative to continental North America and Figure 2.1-B shows the study area and Okanagan Lake in southern British Columbia. Nasmith, (1962) has informally named the units and mapped their extents. These silt sediments, known as Lake Penticton silt (Nasmith, 1962, p. 34), are one of the geological features of the last glaciation in this area. It should be mentioned that there are several glaciolacustrine silt sediments in the Okanagan Valley; but all of them are not necessarily the glaciolacustrine, varved, laminated silt sediments that are the focus of the current study. Other glaciolacustrine silt sediments in the area may or may not share the same geotechnical characteristics.

As shown in Figure 2.1-C, which is adapted from Fulton (1971), the Okanagan Valley is part of the Interior System, confined by the Western System and the Alberta Eastern System in the west and east, respectively. It is a part of the Interior Plateau of British Columbia and the Columbia Plateau of Washington. From a geological standpoint, Okanagan Valley, which has a north-south trend, extends as far north as Enderby and as far south as Coulee City, approximately 150 km south of the international border at the forty ninth parallel. A major northeast-southwest divergence from the general north-south trend occurs between Peachland and Kelowna. Nasmith (1962) said the present form of Okanagan Valley is the result of intensive glacier erosion during the Pleistocene Epoch.

According to Nasmith (1962), the width of the Okanagan Valley bottom ranges from 3.2 km (2 miles) to 16 km (10 miles) and the bottom elevation varies from about 275 m (900 feet) above sea level at Osoyoos Lake, near the international border, to about 550 m (1,800 feet) above sea level west of Enderby, at the far north part of the valley. Nasmith

(1962) also said that the elevation of Okanagan Lake is 342 m (1,123 feet) with a maximum depth of 232 m (760 feet).

The bedrock geology, the geological history with emphasis on the formation of glaciolacustrine silt sediments, and geological hazards are reviewed in this chapter. Also, this chapter presents a brief review of studies of the geology of the Okanagan Valley and glaciolacustine sediments in the interior of British Columbia. Because the glaciolacustrine silt sediments under study, known as Penticton silt, are the result of the last glaciation and also because of the significant impact of the last glaciation (Fraser Glaciation) on the geology of the area under study, the late glaciation history of the Okanagan Valley is reviewed in a more detailed manner.

2.2 Literature Review

Fulton (1965, pp. 555-556) summarized the studies prior to 1965 of the geological origin of the glaciolacustrine silt sediments in the Interior Plateau as follows:

"Dawson (1878) described the silt bodies in the valleys of north central British Columbia and gave them the name White Silts. Dawson (1879) reported silt in the Okanagan and South Thompson Valleys and used the name White Silts to refer to all the silt deposits in British Columbia. A complete statement of his views on the White Silt formation is included in Dawson (1891). Pertinent points are:

1. silt was deposited in deep tranquil water;
2. silt was supplied by melting glaciers;
3. at the time of silt deposition ice occupied those parts of the valley that are free of silt today;
4. close correspondence of the upper limits of the various silt deposits and lack of morainic material or evidence of other dams indicate silt was deposited in fiords connected with Pacific Ocean."

"Daly (1915) agreed with Dawson on all points except the marine origin of the silt. Instead he proposed that the material was deposited in ice-dammed lakes. Daly gave the composition of the silt in the South Thompson Valley as: 49 percent albite, 15 percent orthoclase, 8.5 percent anorthite, and 18 percent quartz. It would appear, however that he arrived at this by means of a chemical analysis and analytical methods applicable only to igneous rocks."

"Flint (1935) descibed the silt of the Okanagan Valley as a glacial-lake deposit and presented a reasonable history of late glacial events in the area studied. He stated that the thickness of the deposit suggests a considerable time interval, and his description of the structure and distribution of the silt imply much of the material to be non-glacial in origin."

"Meyer and Yenne (1940) studied the texture and composition of samples of Okanagan silt. They concluded that the size distribution was similar to that of loess and that the composition of the Okanagan silt (about equal parts quartz and feldspar) differed markedly from that of the silt in the South Thompson Valley as given by Daly (1915)."

"Mathews (1944) concluded that, as silt in the South Thompson Valley did not extend above 1600 feet, it was deposited in a glacial lake that stood at this level."

"Nasmith (1962) described the Okanagan silt as glacial-lake sediment and presented a detailed picture of ice recession in the Okanagan Valley."

In his study of the silt sediments in the South Thompson Valley, Fulton (1965) concluded that silts were glacial lake sediments derived from erosion of till. He said that the deposits are horizontally stratified with some ripples. Like Flint (1935), Fulton (1965) also stated that the penecontemporaneous deformation, slumping because of melting of underlain buried ice, and the drag of floating ice influenced the structure of these glaciolacustrine silt sediments.

Fulton (1969) studied the glacial lake history of the Nicola, Thompson, Shuswap, and North Okanagan drainage basins. He wrote that one main lake, glacial Lake Penticton, occupied the North Okanagan Basin but a small separate lake occupied Coldstream Creek valley. He also stated that glacial Lake Shuswap was continuous with glacial Lake Penticton during several stages. He added that deglaciation of the Interior Plateau was advanced by 9750 BP and drainage of the glacial lakes were completed by 8900 BP.

Fulton (1971) agreed with Nasmith (1962) that ice tongues were in Okanagan Valley and Thompson Plateau at the same time that Okanagan Highlands were ice-free. He also commented that Columbia Mountains became ice free before the Okanagan Highlands.

Fulton (1975) made a comprehensive detailed study of the Quaternary geology and geomorphology of the Nicola-Vernon area. Based on reported results of a drill hole in Okanagan Valley, Fulton (1975) said that the thickness of glaciolacustrine silts can be as high as 120 m and these sediments can be found in any valley and large depression in the area. In many cases, it was found that the deposits are too small or too discontinuous to be mapped. He reported main extensive sediments to be located in the Nicola Valley at Merritt, the South Thompson Valley between Kamloops and Pritchard, Okanagan Valley between Okanagan Lake and Grindrod, north of Gardom Lake on the Gardom Midland, west and northeast of Enderby on the flanks of the Okanagan Valley, and southwest, northeast and east of Vernon on Vernon Midland.

Fulton and Smith (1978) divided the Pleistocene Epoch in the south central British Columbia into four periods. These four periods are a nonglacial period of deposition, Okanagan center glaciation, Olympia interglaciation, and Fraser glaciation. The nonglacial period of deposition ended more than 60000 years ago while the Okanagan center glaciation ended sometime between 43800 BP and 51000 BP. The Olympia interglaciation finished at about 19000 BP with the advance of Fraser glaciation, which ended at approximately 10000 BP. These periods correspond to the early Wisconsin Substage, early Wisconsin glacial period, the mid-Wisconsin Substage, and the late Wisconsin Substage, respectively. The corresponding lithologic units are Westwold

Sediments, Okanagan Center Drift, Bessette Sediments, and Kamloops Drift, respectively.

Fulton and Smith (1978) said that Okanagan Center Drift is a three unit geological feature composed of till and associated till driven deposits. The lower or upper unit of the Okanagan Center Drift may contain glaciolacustrine silt sediments. Fulton and Smith (1978) recorded 10.5 m of horizontally stratified laminated silt and clay with minor interbedded sand in the lower stratified unit of Okanagan Center Drift at about 1.5 km west of Westwold and 5.5 m of laminated dark grey glaciolacustrine silt in the upper unit of the drift 32 km south of Vernon.

Fulton and Smith (1978) said that Kamloops Drift is also a three unit geological feature that overlies Bessette Sediments and underlies postglacial deposits or the present erosion surface. Kamloops Drift, which is the lithologic unit for Fraser glaciation is divided into a lower stratified unit, nonstratified unit, and upper stratified unit. The lower and upper stratified units can be stratified silt, sand, and gravel. Layers of laminated rhythmically bedded silt and clay and fine grained ripple-laminated sand and pebbly sand and bouldery gravel are reported in the lower stratified unit. Fulton and Smith (1978) added that the lower stratified unit was deposited during the last major ice advance in impounded lakes.

According to Fulton and Smith (1978), glaciolacustrine silt sediments in South Thompson Valley east of Kamloops, Nicola River Valley at Merritt, Okanagan Valley north and south of Armstrong and in the vicinity of Penticton, and the Shuswap Lake area between Tappin and Blind Bay are stated to belong to the upper stratified unit of the Kamloops Lake Drift. Fulton and Smith (1978, p. 979) said, "upper stratified Kamloops Lake Drift is material that was deposited during deglaciation of the area. The finer-grained facies accumulated in the many glacial lakes that developed as the ice retreated. The gravel and sand were deposited in the form of glacial outwash and ice contact deposits and along spillways leading from one glacial lake to another."

In a review of slides in the urban areas of British Columbia, Evans (1982) recorded the spatial distribution of glaciolacustrine sediments and suggested that there is a spatial variation in the geological and geotechnical characteristics of these sediments. These sediments can be found in the vicinity of Fort Nelson, Fort St. John, Vanderloof, Prince George, Quesnel, Invermere, Sparwood, Fernie, Kamloops, Merritt, Vernon, Summerland, Kelowna, and Penticton. According to Evans (1982), the glaciolacustrine sediments in the Southern Interior and Columbia are dominantly varved silt sediments with sensitivity to moisture and loading conditions while the Northern Interior glaciolacustrine sediments are dominantly varved clay sediments.

2.3 Bedrock Geology

The information in the following section regarding the geological history of the bedrock in the area under study was obtained from Geological Survey of Canada (1982), Holland (1976), Kelowna Geology Committee (1995), Templemann-Kluit (1989), and Church (1980 and 1981).

The Monashee Gneiss represents the Precambrian Era in this area. The Monashee Gneiss, which is at least 2.0 billion years old, may be the oldest rock in British Columbia. The Monashee Gneiss is composed of metamorphic rocks of the Shuswap Terrane. The Shuswap Terrane was a deeply buried geological feature at depths between 10 to 40 km; however, these rocks reached the surface area in Okanagan valley as the result of tectonic activities. These rocks also experienced chemical changes in the mineralogical composition due to severe heat and pressure exposures.

Limestone and other rocks of Paleozoic Era are present in the far north and south areas of Okanagan Lake near Vernon and Penticton; however, they have been eroded in the central area of the lake.

Marine siltstone and shale of the Triassic Period and granite intrusive rocks of the Jurassic and Cretaceous Periods are representative rocks of the Mesozoic Era.

Cenozoic Era is the most recent era and there are many geological features in the study area that formed during this era. Cenozoic Era, which was started 66 million years ago, is divided into the Tertiary Period and Quaternary Period. During the Tertiary Period, the study area was a volcanically active zone. Rocks of this period are generally of volcanic origin and are widespread in the study area. Basalt lava, with a thickness up to 340 m, is the youngest material from this period.

On the east side of the Okanagan valley, the bedrock underlying the soil deposits is dominantly rocks of Shuswap Terrane which belongs to the Monashee Group. These rocks of Precambrian Era include granitoid gneiss, schist, quartzite, marble, slate, and phyllite. The underlying bedrock on the west side of the valley is dominantly rocks of upper Jurassic to mid Cretaceous Periods of the Mesozoic Era. These upper Jurassic to mid Cretaceous rocks are also present in the east side of the valley in Oliver, Skaha Lake, and Oyama. These rocks include acidic and intermediate rocks, mainly granodiorite, quartz diorite, granite, quartz monzonite, monzonite, syenite, diorite, gabbro. At Okanagan Falls, Summerland, Kelowna, West Bench, and Enderby, the underlying rocks are clastic sedimentary and volcanic rocks, which belong to Paleocene to Oligocene Epoch of the Tertiary Period of Cenozoic Era. The underlying bedrock in the west vicinity of Osoyoos, Vernon, Armstrong, and Enderby are clastic sedimentary and volcanic rocks of Pennsylvanian and Permian Periods of Paleozoic Era. Acidic rocks, mainly granite, syenite, and monzonite of the early Tertiary Period of Cenozoic Era are the underlying bedrock in a small area adjacent to Oaknagan Lake south of Peachland.

2.4 Late Pleistocene History of the Okanagan Valley

The Quaternary Period is the most recent period in geologic time and it includes Pleistocene Epoch (Ice Age) and Holocene Epoch, which is the last 10,000 years. Most surficial geological features in the study area, including the glaciolacustrine Penticton silt sediments formed during the Quaternary Period. Due to the significance of the Quaternary Period, especially late Pleistocene Epoch in the formation and nature of the glaciolacustrine Penticton silt sediments, this geologic time division is studied and reviewed in more detail.

There has not been enough geological research and study on the Interior System to provide a detailed comprehensive regional geological picture. However, fortunately, there has been a long time interest in the geological history and characteristics of the Okanagan Valley. Probably, the first geological study in this area was the work by Dawson (1878) for the Geological Survey of Canada; but the most comprehensive study in the late glacial history and surficial geology of the Okanagan Valley was done by Nasmith (1962).

Nasmith (1962) studied the late glacial history and surficial deposit of the Okanagan Valley. His study was focussed on the time when glaciers retreated and melted. Many of surficial deposits in the Okanagan Valley including glaciolacustrine Penticton silt sediments were formed during this time.

Nasmith (1962) stated that the late glacial lakes and meltwater channels in the interior of British Columbia were contemporaneous with the late glacial marine submergence features on the Pacific coast of British Columbia.

According to Nasmith (1962), the position of lake basins such as Kootenay Lake, Arrow Lakes, Okanagan Lake, Mabel Lake, Shuswap Lake, Adams Lake, Canim and Mahood Lakes, and Quesnel Lake relative to the Cariboo and Monashee Mountains are important in elaborating the origin of the Okanagan Valley. During the glacial period, these lake basins were the passageways for the flow of glacier ice. Nasmith (1962) stated that these basins, including Okanagan Valley, owe their narrow deep straight form to intensive erosion by valley glaciers passing through them.

Nasmith (1962) stated that the present form of the Okanagan Valley is the result of intensive deep glacier erosion during the Pleistocene Epoch, mainly prior to advance of the Fraser Glaciation. In support of his opinion, Nasmith (1962, pp. 44-45) referred to deep drilling near Enderby. He said, "a well drilled in search of oil near Enderby passed through approximately 700 feet (213 m) of silty clay, stated to be a glacial-lake deposit of Lake Penticton, and then through fine gravel and coarse sand containing a few fragments of wood to a depth of 1350 feet (411 m). It is stated that this sand and gravel was deposited either in front of the last glacier to advance into the Okanagan Valley or possibly earlier. The Okanagan Valley had therefore been eroded to approximately its present depth and form by some earlier glacier. It is of interest to note that the bedrock floor of the Okanagan Valley at this point is slightly lower than present sea-level". In addition, he also referred to the presence of a layer of unconsolidated and unweathered Pleistocene sediments under the Okanagan Lake that lies on the bedrock. The thickness of this deposit in a drilling test hole at the elevation of 372 m (1,220 feet) near Armstrong in the north part of the Okanagan Valley was more than 396 m (1,300 feet). According to Nasmith (1962), on the onset of last glacial period, the pre-glacial Okanagan Valley was an important passageway for flow of glacial ice from Monashee Mountains to Columbia Plateau in the south rather than being an accumulation point for the glacial ice. He added that the intensive deep glacial erosion of the Okanagan Valley occurred by the rapid flow of the glacier ice from Monashee Mountains through the valley before glacier ice from Coast Mountains reached the Okanagan Valley and ice sheet covered the southern part of the British Columbia to an elevation of 2134 m (7000 feet) or more.

Nasmith (1962) commented that transformation of a local mountain glacier to a continental glacier is different in a mountainous area like British Columbia from an area of low relief like eastern Canada. Nasmith (1962) stated that geologists working in relatively flat areas mainly developed the terminology and concepts of the mechanisms involved in the formation of geological features. Therefore, we should be cautious in using the terminology and applying the mechanisms to mountainous areas such as British Columbia. Nasmith (1962) said that unlike low relief areas, in mountainous areas like British Columbia, stagnation of ice does not need the reduction of ice thickness to approximately 30 m and subsequent breakage to isolated blocks of ice with no plastic flow of the ice. He said that in valleys like the Okanagan Valley an ice field fed by distant snowfields becomes stagnant when the surface of the ice has no gradient. He mentioned that in such geographical conditions, the ice lobe could be stagnated even if there is local plastic flow and the thickness is even as high as 300 meters.

For the conditions of the Okanagan Valley, Nasmith (1962, p. 9) said "stagnation of the ice lobe is inferred where there is evidence that it had insufficient gradient to produce kame terraces and meltwater channels with a significant down-valley slope. There could still be minor plastic flow of ice within the lobe itself. Active ice movement is inferred where evidences of meltwater channels and kame terraces clearly indicate a significant down-valley slope to the ice-lobe surface."

Nasmith (1962) said it was felt that during the Pleistocene Epoch, as in Europe and eastern North America, several advances and retreats of the continental glaciers, separated by periods of warm climates, occurred in British Columbia. Based on the similar degree of weathering of the glacier deposits, Nasmith (1962) concluded that the last glacial stage in British Columbia was correlated with the last glacial stage in eastern North America, known as Wisconsin stage.

Referring to the present day glaciers and ice-fields in British Columbia, which are in the Coast Mountains, the Columbia Mountains, and the Rocky Mountains, Nasmith (1962) strongly suggested that these current ice-fields were the ice accumulation centers during the Pleistocene Epoch. He added that glacier moved away from these gathering centers in the mountains onto the Interior Plateau and from the Interior Plateau southward across the forty-ninth parallel and northeastward into the Peace River area.

Nasmith (1962, p. 44) said "ice advanced onto the Interior Plateau from the Coast Mountains on the west, from the Skeena Mountains on the north, and from the Cariboo and Monashee Mountains on the east. The first ice to appear in the Okanagan Valley probably originated in the Monashee Mountains north and east of Mabel Lake, and formed valley glaciers that pushed south from Shuswap Lake and west along Coldstream Valley. While these glaciers were expanding, similar and probably more rapid expansion of glaciers from the Coast Mountains was taking place. Ultimately the coalescent piedmont glaciers on the eastern flank of the Coast Mountains covered the interior plateau and began to flow southward toward the forty-nine parallel and northeastward toward the Rocky Mountains."

Commenting on lack of significant glacial features in tributary valleys of the Okanagan Valley south of the Coldstream Valley (in Vernon area), Nasmith (1962) concluded that there was no contribution to the initial stages of the glaciation by the adjacent plateau and highlands. He added that in a later stage ice advanced, thickened, and filled the valley. Nasmith (1962) stated that at this stage the ice in the Okanagan Valley was joined by the southeast flow of ice from the Coast Mountains. Nasmith (1962) said increasing accumulation of ice in the Okanagan Valley caused climate change; and consequently, the highlands adjacent to Okanagan Valley became a gathering ground for the main ice sheet which later moved south and southeast to the Columbia Plateau south of the forty nine parallel in Washington State.

According to Nasmith (1962), at the maximum of the Wisconsin glaciation, the borders of the ice sheet were beyond the current borders of the Province of Brithish Columbia, on the west reaching off the coast of the British Columbia, on the east passing the Rocky Mountains and meeting the Keewatin ice-sheet, and on the north and south passing the borders of Yukon and international border (to about the forty eighth parallel), respectively. Nasmith (1962) said that because of continent wide nature of the climate changes during the Wisconsin glaciation, similar to Europe and eastern North America, there should be fluctuations and discontinuities in the process of ice retreat in British Columbia. He also mentioned that there is no clear evidence in the area to support these fluctuations and discontinuities during the Wisconsin glaciation.

Nasmith (1962) stated that the maximum advance of the glaciers was followed by a rapid and extreme change in climate. He concluded that as the result, the Wisconsin ice-sheet in British Columbia appears to have wasted away by down melting rather than by a retreat of the ice terminus along a well-defined front. He also mentioned that because of down melting, ground at higher elevations became ice-free before the ground at lower elevations.

Nasmith (1962) said there is no direct evidence in the Okanagan Valley regarding the state of ice at its maximum advance; but, based on terminal moraines south of the forty ninth parallel, he speculated that the maximum elevation of the ice surface in the Okanagan Valley near the forty ninth parallel was 2195 m (7200 feet). He implied that the Okanagan Valley and the adjacent highlands and plateau north of the forty nine parallel were completely buried under ice and the ice thickness over the valley axis was approximately as high as 1920 m (6300 feet).

Nasmith (1962) described the lowering of the ice surface, stagnation, and retreat of the ice as follows:

"After the maximum accumulation of ice had been reached, a climatic change occurred which brought about a decline and a retreat of the ice from its maximum position. Whether this climatic change resulted in a lessening of precipitation in the areas of ice accumulation or in an increase in the rate of melting is not known. The effect, however, was to cause a lowering of the ice surface and stagnation and retreat of the ice front." (Nasmith (1962), p. 39)

"No well-defined moraines are reported north of the terminal moraine near Coulee City, and it appears that retreat of the main ice front was accomplished largely by down-melting and stagnation of the ice mass as a whole, with no clearly defined halts or readvances. The down melting of the ice surface ultimately left the plateau and highland areas ice-free, and when the remaining glacial ice was confined to the valleys the surface area of the melting ice was greatly reduced. It seems likely that the effective withdrawal of the ice may have proceeded much more rapidly in the early stages of retreat than in the later stages because the sharp reduction of the ablation area may have been sufficient to bring down-melting into temporary equilibrium with ice accumulation. In other words, although the change to a milder climate may have been continuous, the rate of disappearance of the ice may not. When the ice was confined to the Okanagan Valley, there were times when sharp reduction of surface area could have brought about such a decrease in the accumulation rate of melting that melting was in temporary equilibrium with ice accumulation. Consequently a halt in the recession of the ice could have occurred that did not represent a reversal or halt in the rate of climatic change." (Nasmith (1962), p. 39)

"As the surface of the ice continued to melt down, it apparently had a flat cross-valley profile so that meltwater flowed on top of the ice instead of along the edge of the ice or in minor valleys parallel to the main valley. If the ice lobe had had a convex cross profile and an appreciable down-valley slope, meltwater would have been readily diverted into several minor valleys south of Oliver, but only one of these shows signs of meltwater activity in spite of the fact that all are favorably situated for diversion. From this evidence it is inferred that the ice lobe became essentially stagnant and was not reactivated south of Oliver, whereas to the north of Oliver it was." (Nasmith (1962), p. 39)

"Whereas the numerous minor valleys and notches paralleling the main valley south of Oliver show little or no evidence of meltwater deposits, similar features to the north show abundant evidence that they were occupied for short or long periods by meltwater flowing along the edge of the ice lobe. From this it is inferred that north of McIntyre Bluff the ice lobe had a convex cross profile and appreciable down-valley slope, in contrast to the stagnant ice lobe south of Oliver. This convex cross profiles and down valley slope is stated to indicate renewed activity of the ice lobe due to a temporary climate change. It is also possible that reduction of ablation area as the ice lobe melted down and the resistance to ice flow offered by the narrow section of the valley at McIntyre Bluff may have been factors which contributed to the change in character of the Okanagan ice lobe at Oliver." (Nasmith (1962), pp. 39-40)

"Following this minor readvance of the ice, the down-melting and retreat of the Okanagan ice lobe was resumed. All features of the Okanagan Valley appear to record that the subsequent decay of the ice lobe was continuous, uninterrupted by halts or readvances … ." (Nasmith (1962), p. 40)

"With continued melting of the Okanagan lobe, Lake Penticton came into being. Ponds first formed along the border of the ice, but these rapidly coalesced to form a body of water that filled the basin of Skaha Lake. The massive plug of outwash and stagnant ice that blocked the Okanagan Valley from near Okanagan Falls south to McIntyre Bluff governed the level of this early stage of Lake Penticton. ... Lake Penticton extended north past Penticton over stagnant ice, and at about this time the down cutting of the outlet of Lake Penticton must have been initiated. ... Lake Penticton reached its greatest extent, from Okanagan Falls north along the Okanagan Valley to beyond Enderby, possibly including much of Shuswap Lake and perhaps continuous with glacial lakes in the Thompson River valley. There is a difference in elevation between features which mark the apparent lake surface at the north end of the Okanagan Valley and the outlet at Okanagan Falls, that is largely due to a later upwarping of the north end of the valley relative to the south. There is little record of succeeding stages of Lake Penticton as the north end of the valley was uplifted and the lake was reduced in size." (Nasmith (1962), pp. 40-42)

"The drainage of the Shuswap River, Shuswap Lake, and possibly much of the lake system occupying the South Thompson Valley was probably to the south through Lake Penticton during much of the late glacial stage, but no well-defined channel existed until the level of Lake Penticton fell and glacial-lake silts were exposed. A prominent channel was then cut south from near Enderby to the north end of the Okanagan Lake in the glacial-lake sediments when the level of Lake Penticton stood only 50 feet (15.2 m) or so above the present level of Okanagan Lake near Vernon." (Nasmith (1962), p. 42)

"The abandonment of this channel and the diversion of the Shuswap drainage to the Thompson and Fraser Rivers may be regarded as marking the end of late glacial time in the Okanagan Valley. Near Armstrong, Fortune Creek built into this abandoned channel an alluvial fan which now forms the divide between Okanagan drainage to Columbia River and Shuswap drainage to the Fraser River." (Nasmith (1962), p. 42)

According to Nasmith (1962), stream erosion, the formation of deltas and alluvial fans, the accumulation of peat and swamp deposits in poorly drained locations, and lanslides have been the main post glacial geological features in the area since the current state of the Okanagan Lake and its drainage system was established. Sinkhole formation, piping, rock and silt block toppling can be added to post glacial geological features in the Okanagan Valley mentioned by Nasmith (1962).

2.5 Formation of the Glaciolacustrine Silt Sediments

The late glacial and deglaciation history of Okanagan Valley significantly influences the surficial geology of the Okanagan Valley and distribution of the glaciolacustrine silt sediments. Nasmith (1962) presented the surficial geology of the Okanagan Valley using the stages of glacier advance and retreat. The same methodology is adopted here and the surficial geology of the valley is presented in this section with emphasis on the distribution of the glaciolacustrine silt sediments. Information in this section is adapted directly or indirectly from Nasmith (1962, pp. 11-38) except as otherwise specified. The surficial geology of Okanagan Valley is shown in Map A-2.5-A and B in Appendix A, adapted from Nasmith (1962).

Nasmith (1962) commented that lithologic and time-stratigraphic units are not suitable for a report on glacial geology because of the short length of post-glacial time and limited distinctive marker events. Nasmith (1962) grouped the deposits in the Okanagan Valley in a loosely time related groups of Recent, Late Glacial, Stage of Glacial Retreat, Stage of Glacial Occupation, and Glacial Advance. While defining these groups, Nasmith (1962, pp. 11-12) mentioned "within the recent group are units which are forming now and have been formed within Recent time under climatic conditions essentially similar to those of the present day. Late Glacial contains units formed under climatic and hydrologic conditions distinctly different from the present, although deposition did not take place in contact with glacial ice. Units grouped under Stage of Glacial Retreat were formed in contact with or near stagnant glacial ice. Units grouped under Stage of Glacial Occupation were formed in contact with glacial ice, which was still active and was characterized by definite down-valley and cross-valley slopes. The oldest unit belongs to the stage of Glacial Advance and Earlier."

Because of the deep and narrow north-south nature of the Okanagan Valley and marked regular climate variation from south to north during the last stages of Wisconsin glaciation, while there is succession of deposits and events from older to younger in any given section of the valley, however, at any given time, there was a different geological environment along the valley from south to north. For example, geological units of the Stage of Glacial Occupation at the north end of the valley may have formed concurrent with Glacial retreat, Late Glacial, and even Recent units farther south. As the result, the geological groupings and units have dual time and spatial association with the glacial ice. Based on depositional mechanisms and environment, the deposits in the Okanagan Valley can be divided to the following geological units:

Recent:

1. Okanagan River Floodplain: There are three segments between Okanagan and Skaha Lakes, Skaha and Vaseux Lakes, and Vaseux and Osoyoos Lakes. These floodplain deposits consist of sand, silt, and swamp deposits.

2. Alluvial Fans and Deltas, and Associated Gullies and Stream Channels: These are the erosional and depositional features of the present day streams and their texture ranges from silty sand to coarse bouldery gravel.

3. Beaches, Spits, and Dunes: They are minor, recently formed deposits due to reworking of older deposit by wind and wave action.

Late Glacial:

4. River Terraces and Channels: These dominantly erosional are between Vaseux Lake and Osoyoos Lake, Enderby and Okanagan Lake, and a short segment in Marron

Valley. These features mark the courses of former streams carrying large flows of glacial melt-water. The channels are distinguished by being cut away from glacial ice and were abandoned because of lack of melt-water supply or drainage pattern changes. The areas categorized under this unit are not contemporaneous.

5. Raised Alluvial Fans and Deltas: These are geological features similar to alluvial fans and deltas that belong to "Recent" group but built by streams graded to a base level higher than at present. Lowering of the base level resulted in down-cutting and partial erosion in these features by the streams that built them. The basis of the distinction of these features from glacial outwash is the water supply of the stream that built them with precipitation rather than melt-water from the ice lobe in the valley.

Stage of Glacial Retreat:

6. Outwash Terraces: These deposits are defined as stratified drift that is built beyond the glacier itself, and they are different from kame terraces that are built in contact with the ice. It is necessary to distinguish between glacial drift and till. Glacial drift is all rock material in transport by glacier ice or deposited from meltwater streams or in meltwater lakes. It is a broader term than till, which it includes. Till is not stratified. The texture of the outwash terraces ranges from fine sand to coarse gravel. They are distinguished from alluvial fans and deltas by the source of the water, which is melt-water and its characteristics. The significance of outwash terraces is that they reflect down-valley conditions, including the level of glacial lakes, whereas kame terraces and ice contact features reflect the level of the ice in the area where they occur.

7. Kettled Outwash: These deposits are mainly stream deposited sand and gravel with possible silt and clay deposits in local ponds. These materials were deposited over and around stagnant blocks of ice, which by melting formed the kettle holes. The significance of kettled outwash is that their presence is the indication of the presence of stagnant ice.

8. Glacial Lake Sediments: Thick deposits of sand, silt, and clay accumulated in glacial lakes, formed by melting of the Okanagan ice lobe.

Stage of Glacial Occupation

9. Moraine Ridges: These constructional features mark the edge of the glacial ice at a time when it was active. These moraine ridges can be considered as lateral moraines because there was no formation of the true terminal moraines due to the topographic characteristics of the Okanagan Valley.

10. Kame Terraces and Meltwater Channels: Kame terraces are stratified drift deposits, which were deposited by meltwater streams flowing along the ice edge. The meltwater stream gradient was controlled with the adjacent ice. Meltwater channels are the meltwater stream channels that flowed along the ice lobe edge and are preserved as distinctive dry channels.

Glacial Advance and Earlier

11. Mixed Unconsolidated Deposits: This geological feature consists of ridges of advance glacial outwash and possibly earlier deposits.

The ice upper surface in the southern Okanagan was at an elevation of at least 2,134 m (7,000 feet). Meltwater channels on the east of the valley, just north of the forty ninth parallel, at elevations from 853 m (2,800 feet) to 1067 m (3500 feet) are the indicators of the earliest stages of retreat in the valley. Glacial meltwater was carried to a lake basin in the valley of the Nine Mile Creek, which was blocked just south of the forty nine parallel by the main Okanagan Valley ice lobe. The ice, which had a horizontal surface with possible slight south gradient, became stagnant and melted down. As the result, meltwater flow occurred in channels on the top surface of the ice. Lack of significant signs of carrying large, if any, meltwater flows in the valley that includes Inkaneep Indian village and the valley south of Myers Flat to near Fairview are considered as the reasons for the stagnation of the ice lobe in the Okanagan Valley south of the McIntyre and lack of down-valley slope or convex cross-valley profile. At this stage, ice probably remained active in northern half of the valley.

At a slightly later stage silts were deposited in a lake pounded in Wolfcub Creek valley and in the valley south of the Oliver. Glacial silt deposits in the Wolfcub Creek valley between elevation 460 m (1500 feet) and 610 m (2000 feet) were mainly cleared and only small portions of these glaciolacustrine silt sediments are left in this valley.

"As the ice surface became lower, ponds formed along the ice margin and rapidly coalesced over the stagnant ice. The resultant lake filled the valley south of Oliver, and is referred to as Lake Oliver. Into it were deposited glacial-lake silts very similar in a general character to the silts deposited later in the vicinity of Penticton and Summerland. The silt deposited in Lake Oliver were subsequently covered by sandy and gravelly outwash brought down from the melting ice lobe farther north in the Okanagan Valley, and the silts are now exposed only in road cuts and gullies." (Nasmith, 1962, p.16) Lake Oliver was not stable and did not have a constant water level. There is evidence of these silt sediments as far south as the forty ninth parallel on shores of Osoyoos Lake and as far north as north of Oliver. The upper limit of these glaciolacustrine silt sediments is at about elevation 366 m (1200 feet). These sediments are gray-white, horizontally-stratified silts with the strata thickness ranging from less than 25 mm to 150 mm. Following the drop of the lake level by down cutting of the outlet and by isostatic adjustment, glacial lake sediments were buried under massive sand and gravelly outwash. It was speculated that Osoyoos Lake was formed as a result of the melting of a massive piece of stagnant ice lobe.

In a later stage, a glacial lake was formed in Marron Valley, west of Skaha Lake, which was dammed between ice farther north in Marron Valley and a tongue of ice from Okanagan ice lobe near Kaleden. Sands and silts were deposited in this lake and later, were buried by sands and gravels of a terraced outwash. At a slightly later stage, because of flow of meltwater from Similkameen Valley, which had a thinner ice lobe than the

Okanagan ice lobe, a small glacial lake was formed between the Kaleden ice tongue and the spillway into the Yellow Lake channel and thin silt sediments were laid down in this area.

A glacial lake was formed at the junction of Shatford and Shingle Creeks by the blockage of an ice tongue extending up Shingle Creek from Okanagan lobe. The meltwater for this glacial lake was provided from the outlet of the Brent Lake – Farleigh Lake channel south along Marron Valley. Remnants of silt sediments of this glacial lake are exposed in steep banks near the junction of Shatford and Shingle Creeks. This glacial lake drained south through the Marron Creek channel.

Further melting of the Okanagan ice lobe caused the abandonment of the Marron Creek channel and initiation of the glacial Lake Penticton. Down-melting of the glacier ice in glacial Lake Penticton had a significant role in the formation of the glaciolacustrine silt sediments under study. "Marron Valley channel was probably abandoned when the ice tongue extending up Shingle Creek from the Okanagan lobe melted down to permit the draining of the glacial lake at the junction of Shingle Creek and Shatford Creek. This would have occurred when the ice surface at the mouth of Shingle Creek had melted down to an elevation of about 2000 feet (610 m), and meltwater that flowed south along Marron Valley would instead flow eastward to the Okanagan Valley through the valley of Shingle Creek below its junction with Shatford Creek. At about the same time, however, …, meltwater from ice at the north end of Marron Valley began to follow the course of Trout Creek and was diverted into the Trout Creek-Penticton channel, which joined the main Okanagan Valley on the west bench at Penticton. When this occurred the ice in the Okanagan Valley at the mouth of Shingle Creek had melted down to between 1800 and 1900 feet (549 m and 579 m). The drainage coming down the Shingle Creek valley was then no longer fed by meltwater from the melting Okanagan lobe but was derived from the watershed Shingle Creek and its tributaries. No doubt the climate was more severe than at present, due to proximity of the Okanagan ice lobe, and the runoff from the Shingle Creek watershed was higher than at a later period when the ice lobe had receded to the north." (Nasmith (1962), p. 21)

"At about the time the Marron Creek channel was abandoned by meltwater streams, the Okanagan ice lobe began to stagnate at the south end of Skaha Lake, and as the ice melted down stagnation of the lobe extended north past the present site of Penticton. As the ice stagnated, ponds formed on top of the ice and these coalesced to form the initial stage of glacial Lake Penticton. Glacial silts were deposited in this lake and remnants of these sediments form discontinuous terraces along the border of Skaha Lake up to elevations of about 1350 feet (411 m) in the vicinity of Kaleden. The lake level was controlled by the outlet stream which flowed across the outwash deposits and buried blocks of stagnant ice that filled the valley from Okanagan Falls to McIntyre to an elevation of about 1400 feet (427 m). The level of the outlet was lowered to the present level of Skaha Lake as the river flowing from Lake Penticton cut down through these deposits and as the ice blocks within them melted and allowed the outwash gravels to settle." (Nasmith (1962), p. 21)

"While the meltwater discharging from the Trout Creek-Penticton channel was building kame terraces and later depositing outwash sands and gravels along the western margin of the ice lobe, similar features were being built along the eastern side of the valley in conjunction with deposits from Penticton and Ellis Creeks. When the surface of the Okanagan lobe stood above about 2100 feet (640 m) at Penticton, meltwater flowing along the east side of the ice lobe was diverted east through channels north of Mount Campbell into the valley of Penticton Creek, and this meltwater, combined with the drainage of Penticton Creek, built outwash terraces along the east side of the Okanagan Valley east of Penticton. As the level of the ice fell, the meltwater flowed between the edge of the ice lobe and the valley wall and built kame terraces along the west slope of Mount Campbell. With further down-melting of the ice lobe, the ice became stagnant in the vicinity of Penticton, and glacial Lake Penticton was extended northward over the stagnating ice lobe. The Trout Creek-Penticton channel was abandoned when the level of the ice fell below about 1500 feet (457 m), which was approximately the level at which glacial Lake Penticton extended over the stagnant ice lobe in the vicinity of Penticton. The glacial lake silts, which are so prominent a feature of this part of the Okanagan

Valley, were deposited in this lake, and the maximum elevation of the silts in the vicinity of Penticton is approximately 1500 feet (457 m). The discrepancy between the apparent maximum elevation of the lake at Penticton and the elevation of the outwash south of the Okanagan Falls that served as a control on the lake is due to differential uplift of the Okanagan Valley as a result of the removal of the ice load." (Nasmith (1962), p. 21) Following the discharge of meltwater accumulated in glacial Lake Penticton to the south, Penticton, Shingle, Ellis, Shuttleworth, and Vaseux Creeks formed alluvial fans.

Melting of a small mass of stagnant ice formed a glacial lake west of Summerland, east of a rocky knoll, which divides Marron Valley at its junction with Trout Creek valley. Silts and fine sands were deposited in this glacial lake. The extent of glaciolacustrine silts is less than a square kilometer.

Due to extension of the main Okanagan ice lobe to the lower part of the Trout Creek in the vicinity of Summerland, there had been a meltwater channel to the south called the Trout Creek-Penticton diversion. Glacial silts were deposited in the northeastern part of the Trout Creek-Penticton division in a pond, which was formed against the Okanagan ice lobe. A drop in the elevation of this pond to elevation 549 m (1800 feet) caused the abandonment of the Trout Creek-Penticton diversion and east ward flow of meltwater approximately along the present course of Trout Creek.

In a later stage, the ice lobe south of Peachland at about Garnet Lake and further south in the vicinity of Summerland was confined to the main Okanagan Valley, which is now occupied by Okanagan Lake. Eneas Creek valley became mainly free of ice and a meltwater channel was formed.

"The main ice lobe had melted down to an elevation of 1500 feet (457 m) or less and had stagnated so that it no longer forced the meltwater drainage along the edge of the Okanagan Valley. The meltwater, which was still being deflected into the Eneas Creek valley by active ice in the neighborhood of Peachland now, discharged freely to the east into an early stage of Lake Penticton bordering and possibly partly covering the stagnant ice in the Okanagan Valley. The meltwater eroded the intermediate terrace to cut the lowest terrace ... and deposited fine silt in the lake bordering the ice lobe in the Okanagan Valley." (Nasmith (1962), p. 26)

Following this stage, the level of glacial Lake Penticton fell steadily and finally reached the present level of the Okanagan Lake. The large alluvial fan east of Summerland was built on top of the glaciolacustrine silts as a result of the considerable flow in Trout Creek. Okanagan Valley was still occupied by the massive ice lobe at the time that Interior Plateau became ice free at elevations of 1220 m (4000 feet) as the result of down melting.

The maximum elevation of glaciolacustrine silts northeast of Kelowna is approximately 472 m (1550 feet), which implied that the ice became stagnant with a flat surface when its elevation dropped to the 472 m (1550 feet) because of down melting. These geological activities in Kelowna area are concurrent with the formation of glacial lakes along the ice edge, the subsequent covering of the ice lobe front, and finally their extension across the Okanagan Valley to form glacial Lake Penticton.

Glaciolacustrine sediments in the valley between Winfield and Oyama are reported. "The lacustrine deposits in this area range in texture from silts to medium and coarse sand and are intermixed with sand and gravel outwash so that it is difficult to determine precisely the upper limit of glacial lake deposits." (Nasmith (1962), p. 30)

Morainal ridges were built in areas west of the current courses of Mission Creek, Hydraulic Creek, and Klo Creek. "These morainal ridges were cut by local channels, at the western ends of which kettled outwash was deposited. In places, depressions in the kettled outwash held local ponds in which silts accumulated, but for the most part the outwash consists of sand and gravel." (Nasmith (1962), p. 29)

The time interval when the level of glacial Lake Penticton dropped from its maximum at approximately 457 m (1500 feet) to the present elevation of the Okanagan Lake at 342 m

(1123 feet) is not known; but, it could have been a relatively short time period. The succession of events in glacial Lake Penticton is well recorded by geological features including glaciolacustrine silt sediments and alluvial fans in vicinity of Kelowna.

The highest of these alluvial fans is in the area of East Kelowna Bench. The presence of glaciolacustrine silt sediments in East Kelowna Bench region is more extensive than it appears in surficial geology maps. Based on a cross section presented by Nasmith (1962), it appears that glaciolacustrine silts are underlie raised alluvial fans, terraces, and deltas in East Kelowna Bench. "At the surface of East Kelowna Bench, 10 to 20 feet (3.0 m to 6.1 m) of coarse bouldery gravel is stratified parallel to the surface of the bench and represents sub-aerial stream deposits of Mission Creek. Foreset beds of a delta built into Lake Penticton underlie the coarse gravel and consist of sand and gravel, becoming more sandy at depth and at greater distances from the apex of the delta. The sandy foreset beds grade into varved silts and clays deposited in deeper water. At the front of the delta these varved silts are contorted by slumping over melting blocks of ice in the lake. As the level of Lake Penticton fell, Mission Creek cut down through the East Kelowna Bench, exposing till under the foreset sands and gravels. At one place the till is seen to overlie silts and river gravels which are probably sediments of Mission Creek laid down before the glacier which deposited the till overrode the area. In the course of cutting down to its present level, Mission Creek built a fan at an intermediate level, part of which was deposited on contorted silts at the west side of the East Kelowna Bench." (Nasmith (1962), p. 30)

The intermediate fan of Mission Creek is the Rutland fan. "As the lake fell from the level at which the Rutland fan was built, Mission Creek together with Kelowna Creek eroded a large part of the Rutland fan and the glacial-lake silts on which it was built, and redeposited them in Okanagan Lake to form the extensive delta which is the site of the city of Kelowna." (Nasmith (1962), p. 32)

Bellevue Creek also formed alluvial fans. "On Bellevue Creek, sections are exposed showing extensive deposits which were laid down before the advance of the latest ice-sheet. A little more than a mile (1.6 km) east of the mouth of the creek a thick gravel deposit is exposed on the north side of the creek. … In the space of half a mile (0.8 km) east of this gravel deposit, exposures reveal a thickness of 75 feet (22.9 m) or more of grey-white faintly stratified silt, very similar in general appearance to the Penticton silts. This silt underlies the gravels exposed to the west, however, and must have been deposited before the last advance of ice and cannot be correlated with the deposits of Lake Penticton. The bottom of the silts is not extensively exposed, but they appear to rest on a thin layer of till which is in turn underlain by stratified gravels and sands. No deposits of vegetation or other organic matter were seen in these exposures to suggest that they were deposited under interglacial conditions, and in general the deposits are fresh and unweathered." (Nasmith (1962), p. 33)

The state of lacustrine silt sediments in the Kelowna area can be summarized as follows:

"While the ice lobe was sufficiently thick to force the drainage of meltwater along the sides of the main valley, it pounded lakes in the tributary valleys. In the valley of Mission Creek, thick deposits of silt were laid down near the mouth of Hydraulic Creek. Subsequently these silts were eroded and partially buried under deposits of Mission Creek as it cut down to its present level. Locally small lakes formed in depressions in areas of kettled outwash, and in them small bodies of glacial silts accumulated. By far the largest part of the glacial-lake silts in the Kelowna area, however, was deposited in glacial Lake Penticton, which formed at an elevation of about 1500 feet (457 m), first along the margins of the ice lobe and then entirely covering the stagnating ice. The Largest area of silts is in the Glenmore Valley northeast of Kelowna, but other extensive areas occur in the valley north of Rutland and along the front of the bench south and west of East Kelowna. Alluvial deposits of local creeks overlie these glacial-lake silts in many places." (Nasmith (1962), p. 32)

In the Westbank area, the same sequence of late glacial and post glaciation events occurred as on the east of the lake; but because of the different topographical situation of the Westbank, the characteristics of the glacial features are different.

All glaciolacustrine silts in Westbank are not necessarily glacial Lake Penticton sediments. When down melting caused drop of the level of ice lobe to elevation 495 m (1625 feet), the ice in the depression northwest of Mount Boucherie became stagnant. Due to blockage of the depression north and south of Mount Boucherie by the ice in the Okanagan trench, a glacial lake called Lake Boucherie was formed. Taking into account the presence of a meltwater channel at elevation 495 m (1625 feet), "the level of Lake Boucherie was controlled by the spillway through the 1625-feet (495 m) channel at an elevation of about 1650 feet (503 m), or slightly higher. Powers Creek built an extensive fan at an elevation of 1675 feet (511 m) into Lake Boucherie, and glacial silts were deposited both north and south of Mount Boucherie. This lake remained as a separate entity with a level controlled by the level of the 1625-feet (495 m) channel. That channel, which initially may have been higher than 1625 feet (495 m), existed until the main ice lobe in the Okanagan Valley melted down to permit drainage across the surface of the ice, and the channel was abandoned. At an elevation of about 1500 feet (457 m), as indicated by features on the east side of the valley, the ice lobe became stagnant and Lake Boucherie merged with Lake Penticton, which filled the Okanagan Valley and covered the stagnant ice. Therefore, the Lake Penticton silts probably include all those exposed at the surface in the Westbank area below an elevation of 1500 feet (457 m), and only those exposed at the surface above this elevation can be referred to the earlier and smaller lake". (Nasmith (1962), p. 34) It should be mentioned that in spite of geological and depositional history differences between Lake Boucherie and Lake Penticton sediments, the author has not encountered any document that suggests geotechnical characteristics differ between these two glaciolacustrine silt sediments.

Further north, it is stated that glacial sediments and topographic features in Coldstream Valley, Vernon area, and the northern part of the Okanagan Valley were also related to stagnation of the Okanagan ice lobe and to successive stages of glacial Lake Penticton.

In later stage, glacial Lake Penticton was expanded to the Vernon area. "Areas of kame terraces and minor meltwater channels along the valley wall east of Vernon mark the stage at which the ice lobe diverted meltwater along the valley wall. The channels do not extend below about 1750 feet (533 m), and it was probably at this level that the ice lobe became stagnant and ponds formed on the surface and along the edge of the ice lobe. This was the initial stage of Lake Penticton in this area, although the lake already existed farther south in the valley. Lake Penticton formed a continous sheet of water extending from north of Vernon to Okanagan Falls. The fact that there is a difference in elevation between features which mark the lake levels at the north and south ends of the valley is accounted for by post-glacial uplift which was greater at the north end of the valley." (Nasmith (1962), p. 35)

Glacial lake sediments are deposited extensively in Vernon area. Nasmith (1962) did not elaborate the texture of the glacial lake sediments in Vernon area; but it can be inferred from his report that varved glaciolacustrine silt sediments are extensively present in this area. Deltaic deposits of sand and gravel and alluvial fans were deposited on top of the glacial lake sediment in many areas in the vicinity of Vernon.

Glacial lake sediments in the Armstrong area in the north end of the Okanagan Valley, which consist of silts and sands, are the highest extensive glacial lake sediments in the area covered by the study carried out by Nasmith (1962). The presence of these glacial lake sediments at such an elevation indicates that the level of glacial Lake Penticton north of Armstrong was at elevation 518 m (1700 feet) or higher. Glacial lake sediments in the vicinity of Armstrong are dominantly glaciolacustrine silt sediments with increasing thickness at lower elevations.

"When the level of Lake Penticton had fallen to between 30 and 50 feet (9.1 and 15.2 m) above the present level of Okanagan Lake, its outlines nearly coincided with those of the present lake, and the glacial-lake deposits were exposed from Okanagan Lake north to Enderby. At this stage the Shuswap River and probably the drainage of Shuswap Lake flowed south into the Okanagan system, cutting a prominent channel in the glacial-lake sediments from near Enderby to the north end of Okanagan Lake. The abandonment of this channel and the diversion of the Shuswap drainage into the South Thompson, together with the lowering of the lake to the present level, mark the close of glaciation in the Okanagan Valley area." (Nasmith (1962), p. 36)

"Finally, Fortune Creek built an alluvial fan into the Enderby-Okanagan channel, and from this fan drainage including Fortune Creek flows north to the Shuswap while Deep Creek flows south to the Okanagan. Vernon, Equesis, Naswhito, Hiteman, and other creeks built alluvial fans into Okanagan Lake, extending and concealing fans which were initiated during the late stages of Lake Penticton." (Nasmith (1962), p. 36)

Bedrock is shallow and exposed in many areas covered by silt bluffs that are formed by glaciolacustrine Penticton silt sediments. Due to deep extensive glacial erosion, it is possible that silt bluffs overlie the bedrock in many areas. Referring to a personal communication with Nasmith, Nyland and Miller (1977) stated that based on results of drilling tests in the Okanagan Valley, silt bluffs coincide with sharp drops in the bedrock surface.

It is also stated that silt bluffs had experienced slumping and differential settlement. Flint (1935) reported presence of broad synclinal sags and normal faults in silt bluffs. Commenting on observations by Flint, (1935), Nyland and Miller (1977) stated that glaciolacustrine silts, which were deposited in glacial Lake Penticton on isolated ice at the bottom of the lake, experienced slumping and differential settlement upon down-melting of the underlying ice. Nyland and Miller (1977) stated that sub-aqueous slides in glaciolacustrine silts were responsible for small drag folds seen in the borrow pit just north of the West Bench access road on highway 97 and in the silt sediments at the southeast end of Skaha Lake.

Silt bluffs are presently in an unsaturated state. The glaciolacustrine silt sediments were drained rapidly as the level of glacial Lake Penticton dropped. Klohn Leonoff (1992) suggested that the rate of drop of the level of glacial Lake Penticton was slow enough to allow drainage of silt sediments without causing excess pore pressure generation. It was speculated that generation of excess pore pressure would have caused massive and extensive landslides along the edge of the glaciolacustrine silt sediments which is not consistent with the steep slope angles observed in the silt bluffs. Also, there had been sudden and significant climatic changes in the post glaciation period, which kept the silt bluffs in an unsaturated state.

Evans and Buchanan (1976) described the typical geometry of the silt sediments, These landforms are composed of a gently sloping bench surface, a rounded convex up boundary slope between the bench surface and bluff below, a near vertical bluff face of glaciolacustrine silt, a less steep portion beneath the face covered with colluvial silt derived from glaciolacustrine material above it, a concave colluvial base, a possible vertical gully or lake wall formed by secondary erosion, and the gully or lake bottom consisting of colluvial silt or bedrock.

Glaciolacustrine Penticton silts are varved. The thickness of the varves ranges from 1 m in the deeper parts of the sediments to 2 cm to 3 cm near the top. Shaw (1975) considered seasonal depositional fluctuations and sudden changes in the inflow and outflow of meltwater in the glacial lakes because of changes in the blockages upstream and downstream as the reason for the varved nature of the glaciolacustrine Penticton silts.

Glaciolacustrine Penticton silt sediments are also vertically jointed materials. These joints could be tension cracks due to wetting and drying cycles and stress relief or due to shrinkage and slumping and differential settlements that occurred in these sediments. If jointing is due to shrinkage and differential settlement, it is expected to be present throughout the whole sediment.

2.6 Colluvial Silts

Another feature found in the Okanagan Valley is the colluvial silt deposits. Colluvial silts are derived from glaciolacustrine silts through various erosional mechanisms including slopewash, solifluction, and landslides. Unlike glaciolacustrine silt sediments, the colluvial silt is characterized by its homogeneous appearance and lack of varving and structure; but Lum (1977) reported the presence of lamination but not varving in some colluvial silt deposits. Nyland and Miller (1977) added that these deposits could be found on the slopes that they form below the near vertical glaciolacustrine silt bluffs, depressions, and gully bottoms. V-shaped gullies have been transformed to U-shaped gullies as a result of colluvial silt accumulation on the sides and at the bottom. It is reported that some minor gullies in the area, named paleo-gullies by Nyland and Miller (1977), are completely filled by colluvial silts. Wilson (1985) reported cases of new stages of down cutting in some of these paleo-gullies through colluvial materials in South Thompson Valley. Nyland and Miller (1977) commented that wind blown loess deposits are not present in a significant portion in colluvial deposits.

In his study of the South Thompson Valley, Buchanan (1977) stated that colluvial silt deposits could be very thick in the bottom of some gullies. According to Buchanan (1977), the angle of slopes that colluvial silts form below silt bluffs can be as high as 40 degrees and as low as 4 to 5 degrees.

In a report prepared for Regional District of Okanagan-Similkameen by Klohn Leonoff (1992), it is stated that ravelling, which is the process of erosion of silt bluffs through toppling, small shallow planner slides, and small circular slides, is the source of formation of the colluvial materials. Ravelling stops as soon as colluvial silt reaches the crest of the slope and upon erosion of the colluvial material it continues. It is stated that this process has been active since the drainage of the glacial Lake Penticton. The highest level of colluvial material can be found on slopes, which are located on the banks of rivers or lakes with no active erosion in a long time.

2.7 Geological Hazards

The current geological hazards in the Okanagan Valley include toppling, sinkhole formation and piping, and slides. Slides, in turn, include shallow planar slides and deep-seated rotational slides. These geological hazards are reviewed briefly in the following sections.

2.7.1 Toppling

Both rock and glaciolacustrine silt block toppling occur in the Okanagan Valley. Exposed bedrock in the area is relatively weathered and fractured. Rock toppling can be highly dangerous and the size of the rock blocks can range up to several cubic meters. As mentioned in section 2.5, glaciolacustrine silt sediments are vertically jointed, varved material. Evans and Buchanan (1976) said that glaciolacustine silt sediments from the bluff face could topple in blocks of material ranging from 1 m^3 to 135 m^3. The vertical faces of the blocks follow vertical joints in the glaciolacustrine silt sediments. According to Evans and Buchanan (1976), the blocks, which in most cases are not saturated, disintegrated and fall apart upon hitting the slope beneath. It should be remembered that block toppling is one of the processes involved in the formation of the colluvial silt.

2.7.2 Sinkhole Formation and Piping Processes

The sinkhole formation and piping processes are summarized in a report prepared for the District of Summerland by Golder Associates (1980). Internal erosion in both glaciolacustrine and colluvial silts causes piping and formation of underground tunnels. The trigger for piping processes is the collection of water in surface depressions or penetration of water in more permeable zones such as vertical joints. In a later stage, water penetrates further downward, reaching a more permeable horizontal zone, which allows the horizontal flow of water towards the slope face. A network of underground tunnels can form by further flow of the water and erosion of silt by piping processes. As the process continues, enlargement of the surface depression and collapse of the roof of the underground tunnels result in formation of the sinkholes. It is said that the piping process is not a continuous phenomena, but a sudden process that can occur during a short period of high run off and water infiltration.

Piping processes can also occur in colluvial silts. Evans and Buchanan (1976) stated that formation of secondary gullies in paleo-gullies starts by formation of underground tunnels by piping processes.

Some major sinkholes are reported in an internal memo of the B. C. Ministry of Transportation and Highways (1976). Information presented in this memo was provided by an employee of the regional office who had lived in Penticton for more than 56 years at the time of the memo. The following cases are extracted from the content of above mentioned memo:

- Approximately in 1971, a tractor was lost in a hole, in vicinity of lot 133 in West Bench in Penticton, when ground collapsed.

- Uneven settlement under a recently completed swimming pool in Sage Mesa caused crack formation and damage to the road below the silt bluff because of water flow.

- In Sage Mesa, collapse of a carport foundation occurred into a hole that formed under foundation.

- A major cavity big enough to be filled by several cars was formed under a house in Sage Mesa area.

- A large hole was formed behind an operating D-8 Cat during the construction of Sage Mesa Road. It is said that "when filling this hole, reported seeing material bubbling up just off shore in Okanagan Lake".

- It is reported that "crawling up pipe starting at old motel on Highway 97 and exiting at railroad tracks".

2.7.3 Slides

Slides in silt deposits of the Okanagan Valley can occur in the form of both shallow planar slides and deep-seated rotational slides. These geological hazards are reviewed briefly in the following sub-sections.

2.7.3.1 Sh[illegible] Planar Slides

Shallow planar slides are common feature of the colluvial silt deposits in the Okanagan Valley. According to Evans and Buchanan (1976), shallow planar slides can be result of solifluction processes or, in a larger scale, result of other processes such as undercutting.

Evans and Buchanan (1976) said "the term solifluction has been used in this context to describe the downslope movement of water charged material which follows the thawing of material in previously frozen slopes". This kind of failure is the consequence of flow of thin layer of elongated lobes of soil, saturated by melting water, over the frozen soil beneath.

Flow of soil masses in larger volumes in the form of shallow planar slides can occur as a result of saturation of colluvial silt deposits or undercutting processes. Nyland and Miller (1977) said that the post failure surface is parallel to pre-failure surface. The volume of soil involved in these kind of failures is generally small and the depth of slides is also generally shallow.

2.7.3.2 Deep Seated Rotational Slides

Deep-seated rotational slides in glaciolacustrine silt sediments are reported in the Okanagan Valley and the South Thompson Valley. These landslides are located around Okanagan Lake, Skaha Lake, and Osoyoos Lake in the Okanagan Valley and the South Thompson River Valley.

Many studies have been carried out on historic slides in glaciolacustrine silt sediments including studies by Nasmith (1962), Nyland and Miller (1977), Buchanan (1977), Lum (1977), Wilson (1985), and Klohn Leonoff (1992).

Deep seated rotational slides create the greatest hazard to human life and property. Their size and extent of run out are large and their occurrence is sudden. The slide mechanisms involve removal of the toe of the slope, which can happen by lake or river erosion or by artificial undercutting. The rise of the water table as a result of irrigation, rainfall, and infiltration is another potential mechanism. It has been reported by many investigators (Lum (1977)) that the intact unsaturated strength of glaciolacustrine silt sediments is high enough to avoid deep seated rotational slides and to maintain the integrity of the natural slopes; but it is apparent that the introduction of water decreases the strength of these materials. Based on a report by Klohn Leonoff (1992), many slides have occurred in glaciolacustrine silt sediments adjacent to lands irrigated using the traditional ditch method prior to the use of sprinklers for irrigation.

As part of the screening processes for selecting suitable sites for the current study and in search for deep-seated rotational slides, all major reported landslides were reviewed and visited by author, a team from the Geotechnical Engineering Group of the Department of Civil and Environmental Engineering of the University of Alberta, authorities from local office of B. C. Ministry of Transportation and Highways, and a group of local engineers. Details of the site selection, and sampling are presented in Chapter 3.

2.8 Summary

The main objective of this chapter was to review and investigate the geology of Okanagan Valley. A review of studies carried out on the geology of the valley was presented. Bedrock geology of the valley was reviewed. It was found that the underlying bedrock is dominantly rocks of Shuswap Terrane of Monashee Group from Precambrian Era in the east side of the valley; and acidic and intermediate rocks of Mesozoic Era in the west side.

Late Pleistocene history of the Okanagan Valley was presented. The Okanagan Valley has a north – south trend. As the result, it became a passageway for the flow of glacier ice from mountainous areas to Columbia Plateau, which caused major erosion in the valley. Monashee Mountains were the main source of glacier ice that occupied Okanagan Valley; but there had been contribution from glacier ice from Coast Mountains. Following the maximum advance of the glacier ice, a rapid and extreme climate change caused down melting rather than retreat of the main Okanagan ice lobe. The main glacial lake formed in the valley was Glacial Lake Penticton, which formed on top of the ice sheet rather than its margins because of the ice geometry. Glaciolacustrine Penticton silt sediments were formed in that glacial lake. Glacial Lake Penticton expanded as far north as Enderby and became linked to the drainage system of the Shuswap River in north. End of the late glacial time in this valley was marked by the abandonment of the Shuswap River drainage into Okanagan Valley and its divergence to the Thompson and Fraser Rivers.

Due to the significant impact of the late glacial and deglaciation history on the depositional characteristics of deposits in Okanagan Valley, the surficial geology was reviewed using time and spatial stages of glacial advance and retreat. Surficial geology was presented with emphasize on the formation and distribution of glaciolacustrine silt sediments in the valley. It was found that glaciolacustrine silt sediments exits as far south as the international border at the forty ninth parallel and as far north as Enderby. Maximum elevation of ice surface in Okanagan Valley was about 2150 m; but, glaciolacustrine silt sediments dominantly exist at elevations less than 460 m.

Erosion of glaciolacustrine silt sediments causes formation of colluvial silts. Colluvial silts can be found on the slopes that they form below near vertical glaciolacustrine silt bluffs, depressions, and gully bottoms.

Geological hazards in the area were reviewed. These hazards include rock and silt block toppling, sinkhole formation and piping processes, and shallow and deepseated rotational slides. It is evident that change in the moisture state of silt deposits has a major influence on triggering mechanisms of these natural geological hazards. It was found that deep-seated rotational slides are the most dangerous geological hazard in the area because of the consequences of their occurrence on human life and urban and agricultural developments.

Figure 2.1-A – Locality of the Okanagan Valley Area Relative to Continental North America

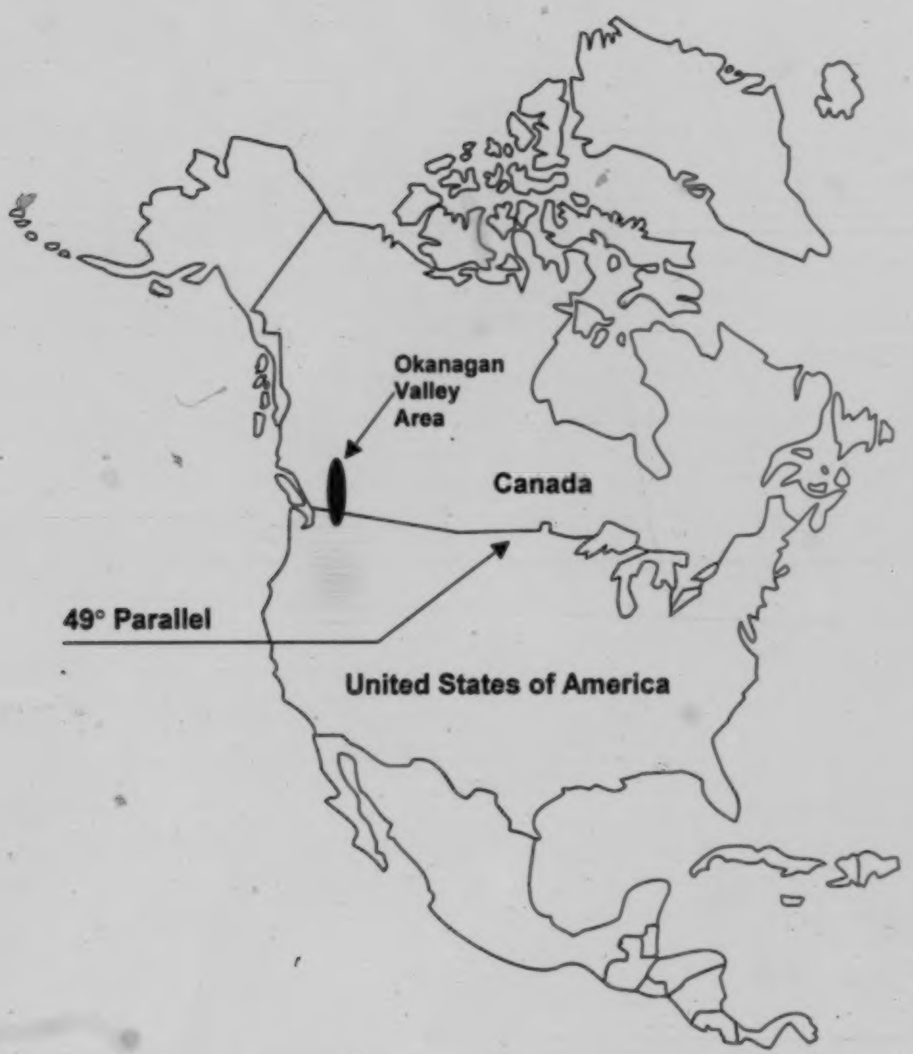
Okanagan
Valley
Area
Canada
49° Parallel
United States of America

Figure 2.1-B – Locality of the Okanagan Lake Area Relative to the Southern Interior of B. C.

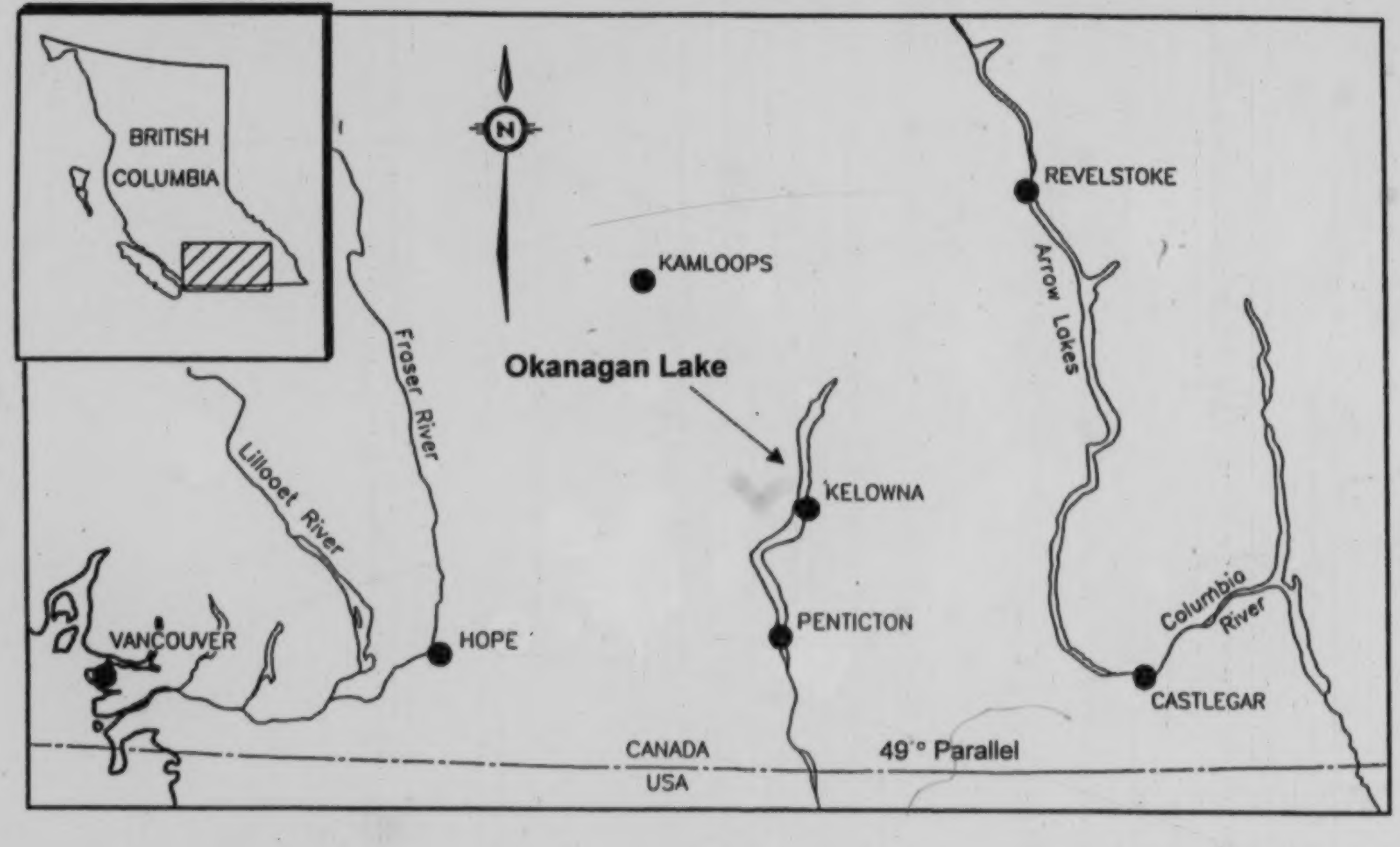
BRITISH
COLUMBIA
N
KAMLOOPS
REVELSTOKE
Arrow Lakes
Okanagan Lake
KELOWNA
PENTICTON
Columbia River
CASTLEGAR
Fraser River
Lillooet River
VANCOUVER
HOPE
CANADA
USA
49° Parallel

Figure 2.1-C – Position of the Okanagan Valley in the Interior System
(after Fulton (1971))

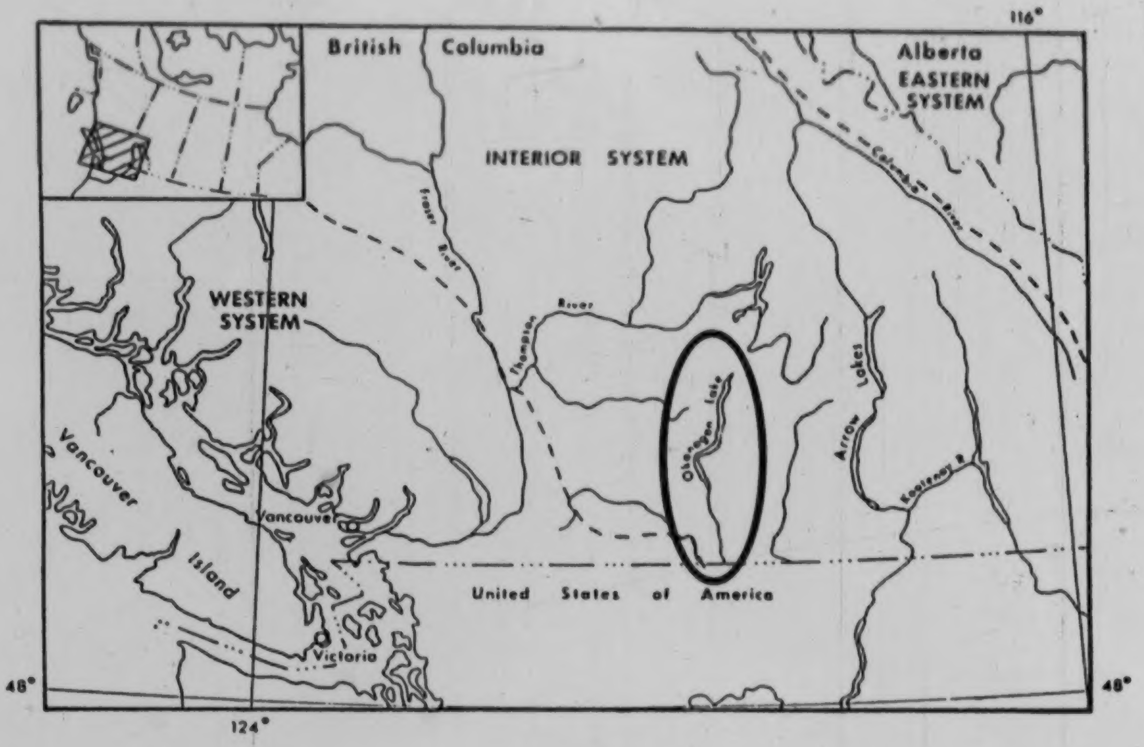
116°
British Columbia
Alberta
EASTERN SYSTEM
INTERIOR SYSTEM
WESTERN SYSTEM
Fraser River
Thompson River
Columbia River
Okanagan Lake
Arrow Lakes
Kootenay R.
Vancouver
Vancouver Island
Victoria
United States of America
48°
124°
48°

CHAPTER THREE

Site Selection and Sampling

3.1 Introduction

In the interior of British Columbia, glaciolacustrine silt sediments can be found in the Okanagan Valley, the South Thompson Valley, and in Nicola Valley area. The silt sediments, chosen as the material to study the behavior of structured soils, are the glaciolacustrine varved laminated silt sediments located in the Okanagan Valley. Nasmith (1962, p. 34) referred to the silt sediments, deposited in glacial Lake Penticton, as "Lake Penticton silt". Previous studies like studies by Nasmith (1962) and Nyland and Miller (1977), indicated that the characteristics of Penticton silt are relatively uniform and independent of the locality.

Glaciolacustrine silt sediments in the interior of British Columbia are susceptible to many geological hazards including block toppling from the face of bluffs, sinkhole formation and piping processes, and deep seated rotational slides. Among these failures, deep-seated rotational slides create the greatest hazard to human life and property. Their size and extent of run out are large and their occurrence is sudden.

The focus of the current study is the behavior and geotechnical response of natural structured soils especially during and after occurrence of deep-seated rotational flow slides. As a result, site selection has been done with emphasis on sites involved in deep seated rotational slides that occurred as a consequence of change of saturation state rather than sites involved in other geological hazards.

There are no records available on possible old slides in the interior of British Columbia. Many studies have been carried out on recent slides in glaciolacustrine silt sediments including studies by Nasmith (1962), Nyland and Miller (1977), Buchanan (1977), Lum (1977), Wilson (1985), and Klohn Leonoff (1992).

Many failures have been reported in these sediments. There are block falls from the vertical silt bluffs, shallow planar slides in sloping colluvial silts, and complex rotational slides. Among those, there are more than twenty major deep seated rotational slides.

As part of the screening processes for selecting suitable sites for this study and in search for deep-seated rotational slides, all reported slides were reviewed by author and visited by a team consisting of author, representatives from the Geotechnical Engineering Group of the Department of Civil and Environmental Engineering of the University of Alberta, authorities from regional office of B. C. Ministry of Transportation and Highways, and a group of local engineers.

In this chapter, major slides are reviewed and details of the site selection and sampling are presented. Taking in to account the size, geometry and documentation, Koosi Creek Slide and Okanagan Lake Park Slide were chosen as the sites for sampling and studying the behavior of this material. Details of the available documentation, engineering geology, and geometry of these sites are presented in this chapter. Also the meteorological records of Okanagan Valley are reviewed.

3.2 Meteorological Records of Okanagan Valley

The climate of Okanagan Valley is mid-latitude and semi-desert in the study area in the southern area of Okanagan Lake. Among the stations of Environment Canada, the station at coordinates latitude 49° 28' and longitude 119° 36' and elevation 344 m in Penticton and the station at coordinates 49° 34' - 119° 39' and elevation 454 m in Summerland are the stations most representative of the locality and elevation of the Penticton silt and also of the Koosi Creek and Okanagan Lake Park Slides.

Meteorological information for Penticton and Summerland Stations are summarized in Tables 3.2-A and B, respectively. This information is based on records of the Atmospheric Environment Service of Environment Canada. Information extracted for Penticton and Summerland Stations are the summary of the records from 1941 to 1990 and 1916 to 1990, respectively. The mean monthly temperature is 9.0° C with maximum and minimum temperatures recorded equal to 40.6° C and –30.0° C, respectively. The mean annual precipitation is approximately 310 mm with an average snowfall of 730 mm. Maximum recorded monthly rainfall, snowfall, and precipitation are 34.4 mm, 261 mm, and 36.3 mm, respectively. Maximum monthly rainfall occurs in June while maximum monthly snowfall and precipitation occur in December. Maximum recorded daily rainfall in the area is 45.5 mm, which happened in October 25th, 1945 in Summerland.

Based on ground-air-water equilibrium analyses and using the meteorological records of the Penticton Station for 1964-1973 period, Nyland and Miller (1977) concluded that the area under study is an undisturbed natural landscape with an annual moisture deficiency of 365.8 mm. Based on the results of the same analysis, they added that monthly analysis showed 120 mm water surplus for the November-February period. Nyland and Miller (1977) speculated that this excess water transforms to surface flow or infiltrates in the soil. Water infiltration causes rise of groundwater table or formation of perched water table on an impervious layer.

Based on results of the ground-air-water equilibrium analyses, Nyland and Miller (1977) concluded that proper practice of irrigation, for example using sprinklers, balances evapotranspiration and does not cause any rise of groundwater table. Traditional irrigation using ditches has been considered as a potential slide and erosion triggering cause. It is also concluded that urban introduction of water can cause a rise of groundwater table.

According to Nyland and Miller (1977), natural vegetation in the area includes sagebrush, bunchgrass, ponderosa pine, rabbitbush, saskatoon bush, and holly bush. Nyland and Miller (1977) added that variety of fruit trees and hygrophytic type plants are present in agricultural and irrigated areas.

3.3 Review of Slides

In a report prepared for the Regional District of Okanagan-Similkameen by Klohn Leonoff (1992), the presence of an old post-glacial slide in the Sage Mesa is mentioned. No further information was provided.

Nasmith (1962) reported occurrence of a slide in the glaciolacustrine silt sediments of the glacial Lake Oliver on the east shore of Osoyoos Lake at the forty nine parallel. According to Nasmith (1962) silt sediments of glacial Lake Oliver are similar to the silt sediments of the glacial Lake Penticton. Based on pictures presented by Nasmith (1962), the slide, which occurred in 1954, appears to be a deep-seated rotational slide. Nasmith (1962) said that the slide occurred in a silt bluff overlain by sandy outwash. According to Nasmith (1962), excess irrigation water caused the saturation of the silts and the rapid flow slide was completed within a few minutes.

In his study of the landforms and observed hazard mapping of the South Thompson Valley, Buchanan (1977) said that slides are not very common in that area. Buchanan (1977) reported two major slides along the north bank of the South Thompson River near Pritchard. The trigger was considered to be undercutting by the river erosion. Buchanan (1977) said that the major portion of the silt bluffs in South Thompson Valley are not in danger of toe erosion by the river.

Buchanan (1977) reported a major slump in the glaciolacustrine silt sediments east of Kamloops and along Harper Ranch Road, above McGregor Creek in north side of the South Thompson River Valley. Review of aerial photographs taken in 1959, 1965/1966, 1986, and 1995, both before and after the study by Buchanan (1977), did not support his opinion regarding the occurrence of a slump. Review of those aerial photograph shows that a small deep-seated rotational slide occurred prior to 1959. In a visit by our team of geotechnical experts in 1996, it was observed that a deep-seated rotational slide has taken place in glaciolacustrine silt sediments. Silt sediments overlay exposed shallow bedrock and the water table appeared to be high.

Buchanan (1977) also reported the occurrence of several smaller slumps along the south side of the South Thompson River Valley between Monte Creek and Neskainlith I.R.No. 2; but he added that those slumps occurred in gravely silty morainal or stream terraces.

Wilson (1985) studied a slide in a gully with natural slope of 40 degrees in the crossing of Trans Canada Highway and Todd Road in Cordillleran region of South Thompson River Valley, near Kamloops. He concluded that the slide was a quasi-rotational failure.

Nyland and Miller (1977) studied ten major failures in the Okanagan Valley. These failures have occurred within the last 70 years. Two more failures are also reported in the report by Klohn Leonoff (1992).

Three failures occurred in silt bluffs of the Marina area of Penticton in east shore of Okanagan Lake. Nyland and Miller (1977) said that North Marina slide occurred in a 55 m high silt bluff with average slope angle of 45 degrees at about 1930. According to Nyland and Miller (1977), Middle Maria and South Maria slides occurred in 55 m and 46 m high silt bluffs with average slope angles of 45 degrees and 51 degrees, respectively. All three slides took place in heavily irrigated areas. There is no available record in the literature regarding the possible triggers for these slides. Nyland and Miller (1977) said that seepage in the lower one third of the Middle Maria slide was noticeable during the post event inspection.

According to Nyland and Miller (1977), three slides occurred north of Marina area and south of Naramata. The slide further north occurred in 1951 in a 48 m high silt bluff with average slope angle of 45 degrees. The slide further south, known as Randolph Creek slide, occurred in 1936 in a 70 m high silt bluff with average slope angle of 59 degrees. The middle slide, known as Johnson Creek slide, occurred in July of 1951 in a 58 m high silt bluff with average slope angle of 30 degrees. All three slides took place in heavily irrigated areas. There is no available record in the literature regarding the possible triggers for these slides. Review of available aerial photographs and pictures show that these slides are deep seated rotational slides with near vertical scarp.

Nyland and Miller (1977) reported occurrence of a failure in a 77 m high silt bluff with average slope angle of 38 degree in north east shore of Skaha Lake. Nyland and Miller (1977) believed that this case was a retrogressive silt block failure; but, based on review of available pictures, it can be concluded that this failure could be a slump type deep-seated rotational slide. Failure took place in silt bluffs of an undeveloped natural area. There is no record available regarding the possible trigger.

Nyland and Miller (1977) reported occurrence of four slides in approximately 40 m high silt bluffs with average 51 degrees slope angle in vicinity of the Summerland Research Station. These slides happened in August 1969 with a smaller slide later in 1969, December 1971, and 1974. In a report by Klohn Leonoff (1992), occurrence of a fifth slide in this area in December of 1987 has been reported. No records are available regarding the triggering mechanisms involved in these cases. It should be reminded that December is the month with maximum monthly snowfall and precipitation. Available pictures do not provide enough information to able us to judge whether the present geometry of the area is the result of silt block failures, deep seated rotational slides, or both.

In a report by Klohn Leonoff (1992), occurrence of a deep seated rotational failure in the silt bluffs facing Lakeshore Drive in Summerland is reported. This slide with approximate volume of 60000 m^3 took place in 1983.

Records of occurrence of five more major slides in Penticton silt sediments were obtained during personal communication with N. Williams, P. Eng. from Interior Testing Services Ltd.. Two relatively old slides, which the date of occurrence is not recorded, took place in South Main Street and Pineview in Penticton. A slide occurred in northern vicinity of Skaha Lake in 1993. Two more slides occurred in Lakeshore Drive area of Summerland and in Highway 97 in Summerland area in 1992 and 1993, respectively. No further information was available regarding these slides. In the visit by our team of experts, all signs necessary for occurrence of a deep-seated rotational slide was evident in the recent

Lakeshore Drive slide site. Bedrock was shallow and exposed. The trigger could have been a combination of over-steeping because of undercutting required for road construction and excess water infiltration.

An internal memo of the B. C. Ministry of Transportation and Highways (1976), provided to the author, revealed more slides in glaciolacustrine Penticton silt sediments. Information presented in this memo was provided by an employee of the regional office that lived in Penticton for more than 56 years at the time of documenting the memo. Based on information recorded in the memo, breakage of water line caused part of Hardman's Orchard, located in vicinity of Naramata, to slide into Okanagan Lake. The slide is visible in Air Photo BC 5654 – 112. Another slide is reported to have taken place immediately north of Naramata in 1960. This slide is recognizable in Air Photo BC 5654 – 107. Occurrence of a large slide in Marina area of Penticton between 1928 and 1930 is also reported. It is reported that a train belonged to C.P. Rail was lost under the slide debris. Based on time proximity, this author believes that it is probable that this slide is the same slide listed as North Marina Slide by Nyland and Miller (1977). It is also mentioned that numerous small slope failures have taken place in east shore of Okanagan Lake between Naramata and Penticton.

A major deep seated rotational slide, known as Chute Creek Slide, occurred north of Naramata and adjacent to Koosi Creek, on east shore of Okanagan Lake. Figure 3.3-A, taken in 1997 and courtesy of the B. C. Ministry of Transportation and Highways, shows the present situation of the slide area. According to Nyland and Miller (1977), this slide, which is named Koosi Creek Slide hereafter, occurred in a 37 m high silt bluff with average slope angle of 40 degrees in 1947. The slope failure occurred suddenly with displacement of at least half a million cubic meters of soil and debris flow of about 50 m in Okanagan Lake. Based on information obtained from local engineers and review of available aerial photographs, a smaller slide occurred inside the first slide sometime after 1967. Bedrock is exposed in the slide scarp and water table appears to be high. Based on results of discussions with local engineers and residents, it appears that the triggering mechanism was a rise of water table due to seepage and intensive irrigation of the bench above the silt bluff.

On March 14th, 1975, a sudden slide removed the access road to the Okanagan Lake Park on Highway 97 south of Peachland and north of Summerland. Figure 3.3-B, taken in 1997 and courtesy of the B. C. Ministry of Transportation and Highways, shows the present situation of the slide area. According to Nyland and Miller (1977), the slide occurred in a 43 m high silt bluff with average slope angle of 45 degrees. Bedrock is high and exposed. The silt bluff was wet near the scarp of the slide and dry at lake level. The toe of slide was located above the lake level. Preliminary studies showed the possible formation of several perched water tables. The possible triggering mechanism is not well known.

One more slide in glaciolacustrine silt bluffs was observed in the area. There is an old slide located less than quarter of kilometer south of the Okanagan Lake Park Slide along the highway 97. The intensity of vegetation and age of trees implied that the slide should be relatively old. The author did not encounter any record regarding this old slide.

Koosi Creek Slide and Okanagan Lake Park Slide are chosen as the suitable sites for the current study, based on results of review of the records, review of technical team, level of documentation, geometry, slide mechanism, and accessibility. The location of these two slides is shown in Figure 3.3-C, relative to Okanagan Lake, Penticton, Summerland, and Naramata. These slides are reviewed and documented in more detail in the following sections.

3.4 Koosi Creek Slide

3.4.1 Documentation of the Records

3.4.1.1 General

Koosi Creek Slide, also known as Chute Creek Slide, is located approximately 9 km north of Naramata, adjacent to the gully of Koosi Creek, on east shore of Okanagan Lake.

It is located between coordinates latitude 49° 39' and longitude 49° 40' and 119° 37' – 119° 38'. Nyland and Miller (1977) said it occurred in 1947; but clips of news reports of the local newspaper, Penticton Herald, indicate that the slide occurred on Monday, August 3rd, 1942 shortly before 9:00 am. Under the headlines of "$900 Property Damage As Three "Tidal" Waves Hit Summerland's Lakefront – Collapse of 400-Foot Cliff North of Chute Creek Hurls Tons of Water Across Lake – Irrigation Seepage May Be A Factor In Causing Huge Slide", "IT LIFTED THE WHARF LIKE MATCHWOOD", and "Two Naramata residents escape mud, clay slide", the local newspaper, Penticton Herald, reported the incident in the issue of Thursday, August 6th, 1942. The following, are extracted from the reports by the Penticton Herald:

"… While the exact cause of the slide has not yet been ascertained, fragmentary reports received at the Herald office would indicate that seepage from irrigation water was a major factor."

"Monday night K. Heales, H. McCutcheon, and Miss G. Moorheart, all of Summerland, visited the scene of the slide and reported that water was pouring out of the exposed cliff, indicating that irrigation seepage had undermined the overhang."

"There appeared to be a pocket from which the earth had slipped off and more was apparently about to fall, was their opinion after survey the site."

"Three small islands each descibed as being "as big as a house," now dot the water where the cliff slid into the lake."

"Another large portion of the undermined clay cliff four miles north of Naramata, at Chute creek, said to be larger than the first slide on Monday, slid quietly into Okanagan lake, late night Wednesday."

"The slide hardly caused a ripple on the lake and had no repercussions on the opposite shore at Summerland."

"It was discovered this morning, Thursday, when residents at Crescent Beach noticed that another large pocket of raw earth had appeared on the cliff on the opposite shore at Chute creek."

"In Summerland the first person to notice the slide was Miss B. Bristow, who, standing atop hospital hill, saw what appeared to be an alfalfa field slide into the lake amid a tremendous splash and a rising cloud of dust."

"After this three different waves struck the community. The second, according to eye-witnesses, was a solid wall of water five feet high."

"This estimate is based on the fact that at the municipal road between Summerland and Crescent Beach, where water is usually two and a half feet below the thoroughfare, wave marks on the cliffs at the roadside are two and a half feet above the road indicating that the second wave had a crest five feet above the water's surface."

"Sailing up to Kelowna on our way to the regatta, we had stopped on the south side of Chute Creek to have breakfast. ... Looking back we saw where a large part of the cliff had fallen into the lake just north of the point. By this time the huge cloud of dust had cleared away and we could see three newly-formed islands, the last one quite far from the shore."

"Stephen Austin, 46, was standing on the road, about six miles north of Naramata, admiring the scenery, when his son, Darryl, 5, spotted the land moving in a gully between the cliffs above them. They jumped into their car and tried to flee. "If my son hadn't yelled and I hadn't stepped on the gas we would have been buried," a shaken Mr. Austin told the Herald. He said he gunned the car for about 30 feet before deciding that it might be best if he and his son bailed out and ran for safety towards the lake. "It seemed as if a whole mountain was coming down. It was like claws trying to grab you.""

During personal communication with Dr. J. Harries, the current owner of the Paradise Ranch on the bench above the slide's scarp, it was mentioned that the grandmother of the ranch owner at the time of slide in 1942 had forgotten to turn off the irrigation over night, which at the time was based on the traditional ditching method.

According to Nyland and Miller (1977), Koosi Creek Slide occurred in a 37 m high silt bluff with average slope angle of 40 degrees. The slope failure occurred sudden with at least half a million cubic meters of soil being displaced and debris flow of about 50 m in Okanagan Lake. Based on information obtained from local engineers, a smaller slide occurred inside the first slide in 1970's. Bedrock is exposed and water table appears to be high. Based on result of discussions with local engineers and residents, it appears that the triggering mechanism was rise of water table due to seepage from Koosi Creek and intensive irrigation of the silt bench above.

3.4.1.2 Topography

Topography of the Koosi Creek Slide area is shown in Figure 3.4.1.2 which is adopted from Topography Map Sheet 82E.062.4.2 on the scale of 1/4000, courtesy of the B. C. Ministry of Environment, Lands, and Parks. This map can be obtained from office of the Geographic Data B. C. in Victoria, B. C..

3.4.1.3 Geology Maps

Geological characteristics of the Koosi Creek Slide area are documented in Surveys and Mapping Branch, Department of Energy, Mines, and Resources (1978) and B. C. Ministry of Environment, Lands, and Parks (1987, 1988, and 1989).

Characteristics of soils and surficial materials of Koosi Creek Slide area and vicinity of Koosi Creek are shown in Figure 3.4.1.3. The following is the description of soils and surficial materials for the 14 zones specified in Figure 3.4.1.3:

Zone Number 1: This zone, locally known as Sunset Acres, covers the area in the toe of the slide in the west side of the Koosi Creek. The debris of the Koosi Creek Slide basically forms this area and unfortunately there have been some permanent residential real estate development and some summer cottage construction in this area. Surface is gently sloped with slope angles ranging from 1 degree to 3 degrees. Soil in the northern part of this zone is stratified glaciolacustrine silt sediments, at least 1 m thick, with thin bands of silty clay and very fine sandy loam. It is mainly covered by colluvial material derived from the slide. Soil in the southern part is colluvial silt. This zone is considered to be well to moderately well drained area. Top 1.0 m can be potentially calcareous and saline phase with electrical conductivity larger than 4 mS/cm. Based on result of some drilling activities carried out by local engineers and mentioned to author during personal communication with Mr. N. William, P.Eng., from Interior Testing Services Ltd., bedrock appears to be only 3 m deep in this zone. As mentioned in section 3.4.2, there are several large boulders in the lakeshore, which seems to be sheared from the bedrock and to be transported to the lakeshore as slide debris.

Zone Number 2: The main body of the slide is part of this zone. Soil in this zone is also stratified glaciolacustrine silt sediments with thin bands of silty clay and very fine sandy loam. This zone has moderate to steep slopes with slope angle ranging from 17 degrees to 35 degrees. Soil in this zone is considered to be well to moderately well drain. Top 1.0 m can be potentially calcareous and saline phase with electrical conductivity larger than 4 mS/cm. As mentioned in section 3.4.2, bedrock is exposed in some areas of this zone, which experienced shearing because of slide occurrence.

Zone Number 3: This zone, which also includes the bench above the slide is a combination of glaciofluvial material and stratified glaciolacustrine silt. Approximately 60% of this zone is covered by 0.5 m to 1.0 m of glaciofluvial sandy loam or loamy sand veneer overlying stratified glaciolacustrine silt sediments. The glaciofluvial material is considered to be well to rapidly drained material. Stratified glaciolacustrine silt sediments with random thin bands of silty clay loam and loamy sand cover the rest of this zone. This zone is gently to moderately sloping area with slope angles ranging from 3 degrees to 8.5 degrees. Slopes are multidirectional with local relief greater than 1 m. Top 1.0 m can be potentially calcareous and saline phase with electrical conductivity larger than 4 mS/cm.

Zone Number 4: Approximately 60% of this zone is covered by 0.5 m to 1.0 m of sandy loam or loamy sand glaciofluvial veneer over moderately sloped stratified glaciolacustrine silt sediments with slope angles ranging from 5 degrees to 8.5 degrees. Moderately sloping fluvial fan deposits cover the rest of this area, which is composed of 0.1 m to 0.5 m of gravelly sandy loam or sandy loam over gravelly loamy sand.

Zone Number 5: This zone is covered by a glaciofluvial veneer of sandy loam or loamy sand over stratified glaciolacustrine silt sediments containing thin bands of silty clay loam and fine sandy loam. The ground is moderately sloped with slope angle ranges between 5 degrees to 8.5 degrees.

Zone Number 6: This zone is a moderately sloping area with slope angles ranging from 8.5 degrees to 24 degrees and local relief greater than 1 m. Soil is stratified glaciolacustrine silt sediment with thin bands of silty clay loam and very fine sandy loam. Occasionally bands of loamy sand have been observed. The area is well to moderately well drain. Top 1.0 m can be potentially calcareous and saline phase with electrical conductivity larger than 4 mS/cm.

Zone Number 7: The geology of this zone can play a significant role in interpreting the slide mechanism for Koosi Creek Slide. This zone consists of moderately steep unidirectional longitudinal slopes of glaciolacustrine silt sediments containing thin bands of silty clay loam and very fine sandy loam and multidirectional exposed bedrock. Slope angle ranges between 17 degrees to 35 degrees. Top 1.0 m of soil deposit can be potentially calcareous and saline phase with electrical conductivity larger than 4 mS/cm.

Zone Number 8 and 9: These zones cover the lake side area and the bench above it, east of Koosi Creek delta. The slopes in these zones are moderately steep ranging from 24 degrees to 35 degrees and 17 degrees to 35 degrees in Zones Number 8 and 9, respectively. Soil is very similar to Zone Number 6 and consists of stratified glaciolacustrine silt sediment with thin bands of silty clay loam and very fine sandy loam. Occasionally bands of loamy sand have been observed. The area is well to moderately well drain. Top 1.0 m can be potentially calcareous and saline phase with electrical conductivity larger than 4 mS/cm.

Zone Number 10: multidirectional slopes of exposed bedrock dominantly cover this zone with slope angles ranging from 17 degrees to 24 degrees. Approximately 20 percent of the surface area of this zone is covered with a thin veneer of colluvial deposits composed of gravelly loamy sand or gravelly sandy loam.

Zone Number 11: This zone is dominantly occupied by moraine (till) material deposited by glacial ice without modification by any other agent of transportation. It is heterogeneous non stratified mix of gravel, sand, silt, and clay. Approximately 30% of the area is covered by a thin eolian veneer of sandy loam or loamy sand. The ground is gently sloped with slope angle ranging from 3 to 5 degrees. This zone is well drained.

Zone Number 12: This area is completely covered by a thin eolian veneer of sandy loam or loamy sand over glacial till same as the one explained in Zone Number 11. Getting closer to the hillside, ground slope is steeper than Zone Number 11 with slopes ranging from 8.5 degrees to 24 degrees. This zone is well drained.

Zone Number 13: This zone mainly representing the gully of the Koosi Creek. The higher elevations of this zone is occupied by 8.5 degrees to 24 degrees slopes of stratified glaciolacustrine silt sediments with thin bands of silty clay loam and very fine sandy loam. The gully bottom is covered with fluvial fan deposits of sandy loam over gravelly loamy sand or gravelly sand.

Zone Number 14: This zone is representing the hillside. The vegetation in this zone is mainly ponderosa pine and bushgrass. The ground is strongly steep with slope angles ranging from 16 degrees to 45 degrees. Approximately 50% of this zone is covered by a thin veneer of sandy loam colluvial material overlying acidic bedrock outcrop. Sandy loam, sand, and loamy sand moraine material cover approximately one third of this zone. The rest is exposed acidic bedrock outcrop.

Information regarding Koosi Creek was obtained through personal communication with Mr. R. Wilson, P. Eng., from Gordon Wilson Associates Inc. in Vernon B. C.. The following information were obtained from his investigations:

"Flow measurements were made at the outlets of the culverts at the Paradise Ranch gates and Sunset Acres access road (creek crossing). The results gave flows of 0.76 gals/sec. (2.877×10^{-3} m^3/sec.) and 0.75 gal/sec. (2.839×10^{-3} m^3/sec.) respectively. An appreciable loss of surface flow was not found between the two culverts. The creek splits its flow immediately above the gates to give 0.25 gals/sec. (0.463×10^{-3} m^3/sec.) in a small channel and 0.51 gals/sec. (1.930×10^{-3} m^3/sec.) in the main channel. Flow at a third culvert on the main channel (some three hundred feet (90 m) above the Paradise Ranch gates) was found to be 0.50 gals/sec. (1.893×10^{-3} m^3/sec.). Another 300 feet (90 m) above the third culvert, the main channel surface flow becomes non-existent. The creek flow reappears some quarter mile (400 m) upstream as a bare trickle and gains strength as you move upstream over the next 100 yards (91 m). Similarly, the smaller channel flows underground several hundred feet (hundreds of meters) above the Paradise Ranch Gates."

"There does not appear to be a buried creek bed that is in the area immediately above Chute Creek slide (referred to as Koosi Creek Slide in current publication), (below the Paradise gate) which takes off of the present channel. There is, however, a significant buried channel well above the creek that runs for a quarter of a mile (400 m). Groundwater that seeps out of the slide face originates from a more regional groundwater flow as a result of deep jointing and fractures in the bedrock. Koosi Creek run-off is definitely a contributing factor, particularly when the creek goes underground."

3.4.1.4 Aerial Photographs

3.4.1.4.1 Pre-Slide Aerial Photographs

Koosi Creek Slide occurred in1942. There is only one set of aerial photographs available prior to the occurrence of the slide. Figure 3.4.1.4.1 shows the pre-slide reconnaissance aerial photograph that is based on Air-Photo BC 109:59, 60, and 61, taken in 1938. Scale of aerial photographs is 1:31680. In order to provide a more detailed presentation of the slide area prior to failure, the desired area of the Air-Photo BC 109:60 is magnified four times and presented in Figure 3.4.1.4.1-B. Following observations can be made from above mentioned aerial photographs:

- Bedrock in the hillside above the future slide area is steep and exposed.
- On the face of the bluff, which the slide occurred later, there is a dark narrow ditch like zone, starting some distance below the top and stretching to the toe of the bluff at the lake level. This darker zone could imply damper soil, which started at the exit of groundwater and follows its flow to the lake level.
- Above the potential groundwater exit zone, the bluff was virtually vertical and less steep below that.
- No major vegetation existed in the face of the bluff.
- Except around the ditch that transformed groundwater to the lake level, no major colluvial or fluvial materials could be observed in the face of the bluff.
- No reworked material existed in the lakeshore.
- Present day sinkholes and piping formations, west of the future slide area, also existed at the time that these photos were taken. It implies that these features occurred long time ago.
- Exposed bedrock exists on the bench above the future slide area.
- Exit of groundwater appears to be at higher elevation compared to present day exit zone.

3.4.1.4.2 Post-Slide Aerial Photographs

The post-slide reconnaissance aerial photograph is based on Air-Photos taken 1963, 1974, and 1985.

The first series of post-slide aerial photographs, reviewed in this study, are Air-Photo BC4195-033 and 034, taken in 1963 (Figure 3.4.1.4.2-A). Scale of aerial photographs is 1:15840. In order to provide a more detailed presentation of the slide area after failure occurrence, the desired area of the Air-Photo BC4195-033 is magnified four times and presented in Figure 3.4.1.4.2-B. Following observations can be made from above mentioned aerial photographs:

- It appears that the elevation of groundwater exit decreased.
- Large fan of silt material from debris of slide formed at the lakeshore.
- In the south east of the bluff, slide created a wall with concave geometry, forming angles larger than 90 degrees.
- Slide formed vertical scarp in the north and northwest part of the bluff.
- Soil on the axis of the slide appears to be damp.
- A bench formed on a notch (Λ) shaped notch on the axis.
- Except the fan formed by debris at lakeshore, the slide surface appears to be formed by intact material.
- The true size of the fan formed by debris of slide is much larger than that appears above lake level.
- At the toe of the slide and north of the debris fan, soil appears to be damper.
- There was a change in vegetation cultivated in the ranch. There was a decrease in the number of trees.
- Koosi Creek delta advanced further into the lake.
- Koosi Creek delta is congested with vegetation, which imply presence of a stable environment and flow regime for the creek.

The second series of post-slide aerial photographs, reviewed in this study, are Air-Photo BC7639 217 and 218, taken in 1974 (Figure 3.4.1.4.2-C). Scale of aerial photographs is 1:15840. Following observations can be made from above mentioned aerial photographs:

- A second slide, in a much smaller scale, occurred inside the 1942 slide. It implies that the second slide occurred sometime between 1963 and 1974.
- A smaller fan formed in the north part of the 1942 slide debris fan by the second slide.
- No major change can be seen in the state of groundwater exit zone.
- The notch on the axis disappeared. It possibly was part of the second slide or it buried under the debris of the second slide.
- No trees can be seen in the ranch.
- Road development in the fan, formed by debris of the 1942 slide, is visible.
- In the bluffs, west of the north west wall, there had been some erosion.
- North and northwest part of scarp of the slide appear to be in a stable condition. No major changes compared to 1963 aerial photographs can be seen.
- The slope of southeast wall decreased to less than 90 degrees.
- Southeast wall has been reworked and its length decreased, possibly by human intervention for land development and expansion of roads to the debris fan area.
- Original debris fan of the 1942 is smaller than what it was in 1963 aerial photographs. There had been erosion by lake.
- One piece of real estate is visible in the debris fan.
- Further erosion of the debris fan exposed some large pieces of rock.
- No major change can be seen in the Koosi Creek gully and delta.

The third series of post-slide aerial photographs reviewed in this study are Air-Photo 30BCC 344 081 and 082, taken in 1985 (Figure 3.4.1.4.2-D). Scale of aerial photographs is 1:15840. Following observations can be made from above mentioned aerial photographs:

- Fan has been eroded and is smaller.

- The length of both northwest wall and southeast wall decreased and toe of slide widened laterally.
- Debris fans of the 1942 slide and the second slide are not distinguishable anymore and formed a uniform gently sloping ground.
- There is more vegetation on both slide slope surface and debris fan, which imply presence of stable environment.
- There is more construction and human use in debris fan.
- Groundwater exit is covered by vegetation and is not as prominent as it was in previous aerial photographs.
- Sinkholes, west of slide area, have been reworked.

More aerial photographs, taken in 1987 and 1993, are available for Koosi Creek Slide area; but the preliminary review did not show any significant changes in the geological state of the slide area. These investigations are not presented in this document.

3.4.2 Field Reconnaissance

A group including representatives from the Geotechnical Group of the Department of Civil and Environmental Engineering of the University of Alberta and local engineers visited the site in May 1996. A site reconnaissance was made and pictures were taken.

The extent of exposure of the bedrock in vicinity of Koosi Creek Slide can be seen in Figure 3.4.2-A. Bedrock forms major portion of the slopes, northwest of the slide area, the southeast slopes of the Koosi Creek gully, and dominantly the hill side north of the slide area and Paradise Ranch. North of the scarp of the slide, on the bench in the cultivated area, there is a piece of exposed bedrock, which imply shallow depth for the bedrock. Also, all along the lakeshore, bedrock is exposed at least half a meter above the lake level.

Figure 3.4.2-B shows the general view of the slide. There is residential development in debris fan, extended into Okanagan Lake. Debris fan is dominantly reworked silt material. Large pieces of transformed rock are visible in the lakeshore, in front of debris fan. During personal inspection of site, exposed bedrock was observed in the northwest scarp, west of the slide axis at mid elevation between top bench and toe of the slide. The horizontal dark strip, along the slide axis, above vegetated area and below vertical scarp, is the groundwater exit zone.

Figures 3.4.2-C and D show a closer look at the groundwater exit zone. Formation of white saline residues on the surface around the groundwater exit zone is visible in Figure 3.4.2-D. The darker color of soil is not only result of higher moisture content of soil; but also it can be due to non-oxidized state of soil material. If the case, the non-oxidized state of the soil around groundwater exit zone can imply longevity in the groundwater regime and continuity in moist state of the strata. Another visible feature in the ground water exit zone was presence of rapidly drained thin bands of very fine sand, as shown in Figures 3.4.2-E and F.

Glaciolacustrine silt bluffs are virtually vertical. Colluvial silt materials are present below the silt bluffs and form very steep slopes, which are expected to improve the stability of the bluffs. Colluvial silt materials also form relatively gentler slopes on the faces of northwest, north, and southeast scarp of the slide. Colluvial slopes are generally between 35 degrees and 45 degrees.

Northwest wall and southeast wall of the slide are shown in Figures 3.4.2-G and H, respectively. Jointed structure is visible on the faces of the top several meters in both figures. Site investigation showed that jointed structure is mainly surface feature; but it should be mentioned that horizontal varving is the inherent of the material. Further investigation showed that, except the top several meters, the main bodies of the cliffs are composed of intact silt sediments.

Presently, Paradise ranch is a vineyard and controlled irrigation using sprinkler system has been practiced. Presence of vegetation in the slide area implies a stable environment.

3.4.3 Geometry of Slide

The plan view of Koosi Creek Slide is shown in Figure 3.4.3-A. The cross section of the axis of slide (section A-A in Figure 3.4.3-A) is shown in Figure 3.4.3-B. The pre-slide cross section is drawn based on assumption of continuity in topography of the area and also interpretation of pre-slide aerial photographs. The soil stratigraphy is based on review of available documents, geological maps, aerial photographs, and field reconnaissance.

3.5 Okanagan Lake Park Slide

3.5.1 Documentation of the Records

3.5.1.1 General

Okanagan Lake Park is located in west shore of the Okanagan Lake along Highway 97, south of Peachland and 29 km north of Summerland. Okanagan Lake Park Slide occurred on March 14th, 1975 and destroyed the access road to the park. It is located between coordinates latitude 49° 41' and longitude 49° 42' and 119° 43' – 119° 44'. According to Nyland and Miller (1977), the slide occurred in a 43 m high silt bluff with average slope angle of 45 degrees.

In a preliminary report on March 25th, 1975, B. Kern, geotechnical engineer of the B. C. Ministry of Transportation and Highways, said that while soil near the lake was dry, soil near highway is slightly damp. As mentioned in the report, three boreholes were drilled by the regional crew of the B. C. Ministry of Transportation and Highways on the shoulders of the Highway 97 on the bench above the slide area. Boreholes did not penetrate more than 3 m and little water was found. It can imply possible formation of several perched water tables. It is also reported that the base of slide was about 13 m above the lake level.

In the above mentioned report, the soil profile is reported to be approximately 3 m of fill for the access road, 6 m of gravelly sand, and stratified gaciolacustrine silt sediment, which overlying the bedrock. Glaciolacustrine silt sediment is reported to be blocky on the top but more homogeneous towards the lake level.

Some information can be obtained from the pictures taken shortly after the slide occurrence and presented in the above mentioned report. Slide slope appears to be very steep. A relatively large fan is formed in the Okanagan Lake by slide debris. Layers composed of fill and granular material formed temporarily near vertical faces. Dampness of the fill and granular material is evident. It appears that highway 97 was constructed in a cut in Colluvial material. Presence of pockets of melting snow in vicinity of slide area both east and west of the highway is evident. There is vegetation present in a ditch located between access road and Highway 97. It was said during personal communication with local people that trees in the Okanagan Lake Park are irrigated during the summer dry season.

Figure 3.5.1.1-A, taken in April 15th, 1975, after Nyland and Miller (1977), shows the post-slide geometry one month after occurrence. Flow of material from fill and gravelly deposit layers is visible. It is evident that slide slip surface sheared the virtually vertical glaciolacustrine silt bluff. Slide debris surface virtually formed a straight line. Debris filled the toe of the bluff and formed a fan in Okanagan Lake.

Figure 3.5.1.1-B, after Nyland and Miller (1977), seems to be the first available picture from the reworked and vegetated shape of the slide area. Lakeshore recreational road was reconstructed in the debris fan. Toe , scarp and bench above the slide were widened.

According to a report entitled "Seismic and Resistivity Survey" of the Okanagan Lake Park Slide, prepared by the B. C. Ministry of Transportation and Highways (1975), slide formed a 6 m scarp within 9 m of Highway 97 and 46 m of access road was initially taken out by the slide. Height of the bluff was estimated to be 53 m. Material towards the west of slide appeared to be distinctly more granular material, deposited in ice contact by glacial melt-water flow. Based on results of seismic wave and resistivity sounding tests, bedrock under Highway 97 in south and north end of the slide area is 18 m to 24 m deep, respectively. Also, bedrock was 3 m to 10 m deep at the lakeshore. It was judged that bedrock was too deep to have any influence on slide mechanism. It was also mentioned that the failure surface intersected undisturbed original ground well above the lake level.

Review of some pictures from reconstruction phase of activities in Okanagan Lake park Slide area, obtained from B. C. Ministry of Transportation and Highways, shows the dampness of soil material towards the scarp of the slope. Spring snowmelt can be involved in failure mechanism in this site.

A copy of an internal report, dated September 16, 1975, on stability of "Okanagan Lake Park Sani-Station and Day Use Area", located at the level of Highway 97 south of Okanagan Lake Park slide, was provided to author for research purpose by B. C. Ministry of Transportation and Highways. It appears that the lawns and trees in Okanagan Lake Park were irrigated. It was mentioned that the igneous intrusive bedrock underlying the glaciolacustrine silt sediments at the Okanagan Lake Park Slide site was at an approximate depth between 18 m to 24 m.

3.5.1.2 Topography

Topography of the Okanagan Lake Park Slide site is shown in Figure 3.5.1.2 which is adopted from Topography Map Sheet 82E.062.4.2 on the scale of 1/5000, courtesy of the B. C. Ministry of Environment, Lands, and Parks. This map can be obtained from office of the Geographic Data B. C. in Victoria, B. C..

3.5.1.3 Geological Maps

Geological characteristics of the Koosi Creek Slide area are documented in Surveys and Mapping Branch, Department of Energy, Mines, and Resources (1978) and B. C. Ministry of Environment, Lands, and Parks (1987, 1988, and 1989).

Characteristics of soils and surficial materials of Okanagan Lake Park and Okanagan Lake Park Slide site area are shown in Figure 3.5.1.3. The following is the description of soils and surficial material for the 13 zones that specified in Figure 3.5.1.3:

Zone Number 1: The main body of Okanagan Lake Park Slide is located in this zone. It should be mentioned that because of safety concerns in a publicly accessed area, the slide has been reshaped. This zone contains moderately steep slopes with slope angles ranging from 17 degrees to 35 degrees. Soil in this zone is stratified glaciolacustrine silt sediments with thin bands of silty clay, very fine sandy loam, and loamy sand. This zone is considered to be well to moderately well drained area. Top 1.0 m can be potentially calcareous and saline phase with electrical conductivity larger than 4 mS/cm. Debris from slide formed a fan in the Oaknagan Lake, which is a part of this zone.

Zone Number 2: This zone includes the scarp and the bench above the slide. Approximately 70% is covered by man-made and man-modified anthropogenic materials. The rest of this zone consists of fluvial fan deposits including 0.1 m to 0.5 m of gravelly sandy loam over very gravelly loamy sand. This zone has a unidirectional longitudinal slope. Slopes in anthropogenic materials range from gentle to steep sloped with slope angles between 1 degree to 35 degrees. Fluvial fan materials form slopes with slope angles ranging between 5 degrees and 17 degrees. Soil in this zone is considered to be rapidly to well drained.

Zone Number 3: Soil in this lakeshore zone is active beach deposits (lacustrine) consisting of loamy sand grading to sand or very gravelly sand. The thickness of the deposit varies between 0.1 m and 1.0 m. This zone is gently sloped with slope angles ranging from 1 degree to 5 degrees. Slopes are unidirectional toward the lake.

Zone Number 4: The characteristics of this zone are completely compatible with those consisting Zone Number 1.

Zone Number 5: This zone consists of fluvial materials, 0.1 m to 0.5 m of gravelly sandy loam grading to very gravelly loamy sand overlying a sandy gravel fan. The ground is moderately sloping with slop angle ranges between 5 degrees to 17 degrees. This zone is considered to be well to rapidly drained area.

Zone Number 6: This zone consists of fluvial fan deposits including 0.1 m to 0.5 m of gravelly sandy loam over very gravelly loamy sand. Ground surface forms gentle slopes with slope angles ranging between 5 degrees and 17 degrees. Soil in this zone is considered to be rapidly to well drain.

Zone Number 7: The characteristics of the soil and surficial material in this zone are compatible with Zone Number 2 but the percentile distribution is different. Approximately 60% of this zone is covered by fluvial fan deposits and only 40% consists of anthropogenic materials.

Zone Number 8: The surface of this zone is covered by moderate slopes of 8.5 degrees to 24 degrees of fluvial fan deposits including 0.1 m to 0.5 m of gravelly sandy loam over very gravelly loamy sand. The surface is relatively stony and approximately 0.1% to 3% of the surface is covered with stones.

Zone Number 9: The characteristics of this zone are the same as those of Zone Number 3.

Zone Number 10: Approximately 80% of this zone is covered by variable slopes of man-made and man-modified anthropogenic materials with gentle to steep slope angles ranging from 1 degree to 35 degree. The rest of this zone consists of gently sloping active beach deposits (lacustrine) consisting of loamy sand grading to sand or very gravelly sand. The slope angles range between 1 degree to 5 degrees. Slopes are unidirectional toward the lake.

Zone Number 11: The ground surface slopes in this zone are moderately steep with slope angles between 17 degrees to 35 degrees. Major portion of this zone, approximately 80%, is covered by glaciofluvial deposits consisting of 0.1 m to 1.0 m of loamy sand or sand over medium to coarse sand. Stratified glaciolacustrine silt sediments containing silty clay loam and very fine sandy loam occupy the rest of this zone. This zone is considered to be rapidly to well drain area.

Zone Number 12: This moderately to gently sloped zone with slope angles between 3 degrees to 8.5 degrees, consists of fluvial fan deposits composed of 0.1 m to 0.5 m of gravelly sandy loam over very gravelly loamy sand. Drainage condition is well to rapidly drained condition.

Zone Number 13: The ground surface slopes in this zone are moderately sloped with slope angles between 8.5 degrees and 17 degrees. Soil materials in approximately 50% of this zone consist of glaciofluvial fan deposits composed of sandy loam over very gravelly loamy sand. A veneer of glaciofluvial gravelly sandy loam occupies approximately one third of this zone over stratified glaciolacustrine silt sediments. Fluvial fan deposits composed of 0.1 m to 0.5 m of gravelly sandy loam over very gravelly loamy sand cover the rest of this zone. Drainage condition is well to rapidly drained condition.

Zone Number 14: moraine deposits and a veneer of colluvial material cover this zone, which represents the hillside west of Highway 97, over bedrock. Vegetation includes ponderosa pine, bunchgrass, and edaphic grassland. The ground surface slope is steep with slope angles ranging from 46 degrees to 70 degrees. Approximately 60% of this zone is covered by a 0.1 m to 1.0 m thick veneer of colluvial deposits composed of sandy loam over acidic bedrock. The rest of this zone is covered by moraine deposits composed of sandy loam, loam, silt loam, and silt. This area is considered to be rapidly to well drain zone.

3.5.1.4 Aerial Photographs

3.5.1.4.1 Pre-Slide Aerial Photographs

Okanagan Lake Park Slide occurred in 1975. Figure 3.5.1.4.1-A shows the pre-slide reconnaissance aerial photograph that is based on Air-Photo BC7644 009 and 010, taken in 1974. Scale of aerial photographs is 1:15000. In order to provide a more detailed presentation of the slide area prior to failure, the desired area of the Air-Photo BC7644 009 is magnified four times and presented in Figure 3.5.1.4.1-B. Following observations can be made from above mentioned aerial photographs:

- The glaciolacustrine silt bluff, which became the site of the slide, appears to be steep.
- Colluvial material exits on the face of the bluff.
- There is a bench between top of the bluff and fill, required for the construction of the access road.
- Bedrock is exposed west of Highway 97 on the hillside and it has steep slopes.
- Extensive vegetation is visible in the ditch between access road and Highway 97 on the bench above the site of the future slide and in a less extent, on the area north of the slide area. Vegetation implies presence of moisture.

3.5.1.4.2 Post-Slide Aerial Photographs

The post-slide reconnaissance aerial photograph is based on Air-Photo 30BCC 360 049 and 050, taken in 1985 (Figure 3.5.1.4.2-A). Scale of aerial photographs is 1:15000. In order to provide a more detailed presentation of the slide area after failure occurrence, the desired area of the Air-Photo 30BCC 360 049 is magnified four times and presented in Figure 3.5.1.4.2-B. Based on records of the B. C. Ministry of Transportation and Highways, the slide area was reworked shortly after the occurrence because of high accessibility of the area and potential dangers to public. As the result, no aerial photographs, taken from site represent the true post failure situation. Following observations can be made from above mentioned aerial photographs:

- Intensity of vegetation in the area decreased.

- Debris of the slide formed a fan in the lake.
- Taking into account passage of approximately ten years time, it appears that slide was in a stable condition.

3.5.2 Field Reconnaissance

A group including author, representatives from the Geotechnical Group of the Department of Civil and Environmental Engineering of the University of Alberta and local engineers visited the site in May 1996. A site reconnaissance was made and pictures were taken.

Figure 3.5.2-A, taken in 1997, courtesy of the B. C. Ministry of Transportation and Highways, shows the present time situation of the slide area. Bedrock is dominant in the hillside, west of Highway 97. Bedrock is also visible at some depth in the lake at lakeshore. No evidence of groundwater level or flow was found in the area. A small slump occurred in the slide zone in the reshaped slope, formed from debris of the slide. This slump also existed during the 1996 visit of author.

The face of reshaped slide slope appears to be dominantly gravelly sand from the gravelly sand layer above the bluff prior to failure. It can imply that failure first occurred in the glaciolacustrine silt bluff and debris of the bluff were buried under flow of material from fill and gravelly sand layer above the bluff.

Glaciolacustrine silt bluffs, north and south of slide area, are virtually vertical. Colluvial silt materials are present below the silt bluffs south of the slide area and in lesser extent below the silt bluffs north of the slide area.

North wall of the slide is covered with reworked material, used to reshape the slide slope. Exposed zone showed presence of dry and relatively intact glaciolacustrine silt sediments. Figure 3.5.2-B, taken in May 1996, shows the face of the south wall. Again, shearing and discontinuity of glaciolacustrine silt bluffs north and south side of the slide area imply passage of slide slip surface through the glaciolacustrine silt sediments.

Figures 3.5.2-C and D, taken in May 1996, show the top and bottom part of the south wall. Presence of a layer of less than 2 m of gravelly sand above the silt deposits is visible. Jointed structure is visible on the face of the top several meters in the glaciolacustrine zone of the bluff. Site investigation and cutting the face of the wall during sampling activities showed that jointed structure is mainly surface feature; but it should be mentioned that horizontal varving is the inherent of the material. As can be seen in Figure 3.5.2-D, except the top several meters, the main body of the cliff is composed of intact rock shape silt deposits.

Presently, introduction of water in Okanagan Lake Park is controlled. Use of the recreational area at the toe of the glaciolacustrine silt bluffs is limited to day-use only to decrease potential hazards to human life.

3.5.3 Geometry of Slide

The plan geometry of the Okanagan Lake Park Slide is shown in Figure 3.5.3-A. The cross section of the axis of slide (section A-A in Figure 3.5.3-A) is shown in Figure 3.5.3-B, adopted from the report on "Seismic and Resistivity Survey" of Okanagan Lake Park Slide by the B. C. Ministry of Transportation and Highways (1975). The pre-slide geometry is drawn based on contours of existing pre-slide topography maps and post-slide geometry is drawn based on surveying of the site. Depth of bedrock is estimated by interpolation using two bedrock profile along Highway 97 and three bedrock profile along the slide area between slide axis and its north end. The soil stratigraphy is based on review of available documents, geological maps, aerial photographs, and field reconnaissance.

3.6 Sampling

3.6.1 General

Undisturbed samples were obtained from Koosi Creek Slide and Okanagan Lake Park Slide sites using high quality block sampling. Sampling was carried out in third week of

July 1996. During this time period, the weather was dominantly sunny with 28° and 15° as the maximum and minimum temperature, respectively.

Due to extreme hardness of the material sampled, a chain saw was used to cut the deposit. Hardness of the material was in such a degree that the chain of the chain saw needed replacement everyday. In case of samples obtained from below the groundwater table, a carving knife was used due to sensitivity of the material. Soil was cut in blocks of approximately 0.35 m x 0.35 m x 0.35 m.

During personal communication with Dr. D. G. Fredlund, Unsaturated Soil Group of the University of Saskatchewan, it became evident that usage of saran wrap is not sufficient and wrapping with aluminum foil is necessary to preserve the moisture in the soil structure. Samples obtained were marked, labeled, and wrapped in two double layers of saran wrap and aluminum foil. Wrapped samples were covered with cotton cloth and waxed in sampling site. Waxed samples were placed in wooden boxes with soft foam in interior faces. Subsequently, boxes containing the samples were filled with wax prior to transporting samples to Edmonton from the sites. Boxes containing block samples were stored in a cold room at an environment of 4°C and 100% relative humidity at the University of Alberta. Some information regarding the sampling at Koosi Creek Slide and Okanagan Lake Park Slide sites is presented in the following sections

3.6.2 Koosi Creek Slide Site

In this site, block samples were obtained from both above and below groundwater table at about elevation 380 m (1250 ft). Figure 3.6.2-A shows the locality of the sampling zone in the Air Photo 30BCC 344 081 (1985) and a general view of the Koosi Creek Slide. Location of sampling was chosen taking into account several criteria including accessibility, safety, and integrity of the intact deposits. The location of the above and below groundwater table samplings are also shown in Figure 3.6.2-B. Sampling was carried out from the groundwater exit zone in the face of the slope. Figure 3.6.2-C shows the location of sampling above groundwater table after sampling. The exposed 0.5 m face was disregarded and samples were obtained from further interior zone. Figure 3.6.2-D shows Gerry Cyre from the University of Alberta while carving a block of soil in the groundwater exit face. A ditch was created to dewater the groundwater exit face and facilitate sampling from below groundwater table. The exposed 0.5 m was disregarded as disturbed material and samples were obtained from material further inside the soil face.

Samples of groundwater were obtained for chemical analyses. Standard half liter water sampling bottles were used. Samples transformed to a double layer dark cooler immediately after sample collection to protect water samples from heat and light. The cooler containing groundwater samples was stored in a cold room at an environment of 4°C and 100% relative humidity at the University of Alberta. Some white precipitates were observed at the area around the groundwater exit. Bag sample of these white precipitates was also obtained for further investigation and chemical analyses.

3.6.3 Okanagan Lake Park Slide Site

Groundwater table could not be located in this site. Block samples were obtained from above groundwater table in the south wall of the slide at about elevation 345 m (1150 ft). Figure 3.6.3-A shows the locality of the sampling zone in the Air Photo 30BCC 360 049 (1985) and a general view of the Okanagan Lake Park Slide. Location of sampling was chosen taking into account several criteria including accessibility, safety, and integrity of the intact deposits. Figure 3.6.3-A shows the location of sampling area at the toe of the south wall, near Okanagan Lake. Samples were obtained from two nearby locations as shown in Figure 3.6.3-B. The exposed 0.5 m face was highly jointed and was disregarded. Samples were obtained from further interior zone. Unlike the exposed desiccated face, which was extremely dry, the interior zone was moist and moisture content increased with distance from the face. Further investigations in the laboratory showed that moisture in the interior zone was between at least 15 % and up to 25%.

3.7 Summary

The main objective of this chapter was review of slides in glaciolacustrine silt sediments in the interior of British Columbia and selection of suitable case histories for further studies. Slides were reviewed. Koosi Creek Slide (also known as Chute Creek Slide) and Okanagan Lake Park Slide were chosen as the sites for further detailed comprehensive geological and geotechnical studies.

Available information about two above mentioned case histories were documented. Topography maps, geological maps, and geometry of these slides were shown. Surficial geology and deposits present in slide areas were discussed. Pre-slide and post-slide aerial photographs were reviewed and discussed. Results of field reconnaissance were documented and presented. From these studies, it is probable that presence of excess water was responsible for triggering both slides.

Details of sampling were presented. Undisturbed samples were obtained from above mentioned sites using high quality block sampling. Samples were obtained from above the groundwater table at both sites and from below the groundwater table at Koosi Creek Slide site.

Also, climatic condition of Okanagan Lake area was presented using meteorological records of the Penticton and Summerland Stations. Okanagan Valley has a semi-arid environment with water deficiency.

Table 3.2-A - Meteorological Records of Penticton Station

(49° 28' - 119° 36' and elevation 344 m) (1941 to 1990)

	Jan.	Feb.	Mar.	Apr.	May	Jun.	Jul.	Aug.	Sep.	Oct.	Nov.	Dec.	Year
Max. Daily Temp. (°C)	0.7	4.4	9.9	15.4	20.4	25.0	28.2	27.6	21.7	14.5	6.5	1.4	14.6
Min. Daily Temp. (°C)	-4.8	-3.0	-1.0	2.0	6.1	10.1	12.3	12.1	7.6	2.8	-0.3	-3.7	3.4
Mean Daily Temp. (°C)	-2.0	0.7	4.5	8.7	13.3	17.6	20.3	19.9	14.7	8.7	3.2	-1.1	9.0
Extreme Max. Temp. (°C)	15.7	16.6	21.7	29.6	33.9	37.7	40.6	38.9	36.6	28.9	19.4	14.4	
Extreme Min. Temp. (°C)	-26.7	-26.7	-17.8	-7.2	-5.6	0.0	2.2	2.9	-3.0	-14.5	-22.3	-27.2	
Rainfall (mm)	8.3	12.0	17.3	25.5	33.0	34.4	23.3	28.4	23.0	15.5	17.6	11.8	250.0
Snowfall (cm)	25.5	11.0	3.3	0.2	0.0	0.0	0.0	0.0	0.0	0.2	7.6	25.2	73
Precipitation (mm)	27.3	20.6	20.4	25.8	33.0	34.4	23.3	28.4	23.0	15.7	24.3	32.1	308.5
Extreme Daily Rainfall (mm)	15.7	18.5	16.3	29.6	38.4	33.5	37.8	23.6	37.6	44.5	19.3	12.4	
Extreme Daily Snowfall (cm)	23.2	23.1	10.0	4.1	0.0	0.0	0.0	0.0	0.0	3.0	20.6	22.1	
Extreme Daily Precipitation (mm)	23.2	18.5	16.3	29.6	38.4	33.5	37.8	23.6	37.6	44.5	19.3	22.1	
Month-end Snow Cover (cm)	5	1	0	0	0	0	0	0	0	0	1	6	
Days with Temp. > 0°C	18	24	31	30	31	30	31	31	30	31	28	20	335
Days with Measurable Rainfall	4	5	7	8	10	9	7	7	7	7	8	5	84
Days with Measurable Snowfall	9	5	2		0	0	0	0	0		3	9	28
Days with Measurable Precipitation	12	9	9	8	10	9	7	7	7	7	9	13	107

Table 3.2-A – Meteorological Records of Penticton Station (Continued)

(49° 28' - 119° 36' and elevation 344 m) (1941 to 1990)

	Jan.	Feb.	Mar.	Apr.	May	Jun.	Jul.	Aug.	Sep.	Oct.	Nov.	Dec.	Year
Pressure (kPa)	97.79	97.69	97.40	97.40	97.35	97.28	97.39	97.34	97.50	97.67	97.62	97.80	97.52
Vapor Pressure (kPa)	0.42	0.50	0.54	0.63	0.85	1.06	1.19	1.21	1.00	0.76	0.58	0.46	0.77
Relative Humidity–0600L (%)	78	79	78	74	71	66	64	69	77	77	77	78	
Relative Humidity–1500L (%)	71	65	50	41	41	39	37	38	44	53	66	72	

Table 3.2-B – Meteorological Records of Summerland Station

(49° 34' - 119° 39' and elevation 454 m) (1916 to 1990)

	Jan.	Feb.	Mar.	Apr.	May	Jun.	Jul.	Aug.	Sep.	Oct.	Nov.	Dec.	Year
Max. Daily Temp. (°C)	0.1	3.6	8.9	14.3	19.3	23.8	27.2	26.6	20.6	13.4	5.6	0.7	13.7
Min. Daily Temp. (°C)	-5.3	-2.9	-0.1	3.3	7.3	11.4	13.9	13.7	9.3	4.4	-0.2	-4.3	4.2
Mean Daily Temp. (°C)	-2.6	0.4	4.4	8.8	13.3	17.6	20.6	20.2	15.0	8.9	2.8	-1.7	9.0
Extreme Max. Temp. (°C)	15.5	16.7	22.2	28.9	33.9	38.3	40.0	37.8	36.0	28.5	19.5	15.6	
Extreme Min. Temp. (°C)	-30.0	-26.7	-21.7	-8.9	-5.0	1.7	4.4	5.6	-3.9	-14.0	-23.0	-29.4	
Rainfall (mm)	6.6	9.5	14.8	23.9	31.8	33.6	26.6	28.9	21.8	16.3	18.5	10.7	243.0
Snowfall (cm)	25.4	10.8	2.3	0.0	0.0	0.0	0.0	0.0	0.0	0.3	8.4	26.1	73.3
Precipitation (mm)	31.9	19.6	17.1	23.9	31.8	33.6	26.6	28.9	21.8	16.6	26.8	36.3	315.0
Extreme Daily Rainfall (mm)	18.4	18.2	13.2	27.2	26.7	34.0	41.7	21.8	27.0	45.5	18.0	22.9	
Extreme Daily Snowfall (cm)	24.3	30.5	33.5	5.1	0.0	0.0	0.0	0.0	0.0	12.7	19.8	45.7	
Extreme Daily Precipitation (mm)	24.3	30.5	33.5	27.2	26.7	34.0	41.7	21.8	27.0	45.5	22.4	45.7	
Month-end Snow Cover (cm)	7	3	0	0	0	0	0	0	0	0	2	6	
Days with Temp. > 0°C	16	22	30	30	31	30	31	31	30	31	27	16	328
Days with Measurable Rainfall	3	4	7	8	10	9	8	8	7	7	9	5	84
Days with Measurable Snowfall	8	4	1		0	0	0	0	0		3	9	25
Days with Measurable Precipitation	11	8	8	8	10	9	8	8	7	7	11	13	107

Figure 3.3-A – Koosi Creek Slide (1942)

(Courtesy of the B. C. Ministry of Transportation and Highways, taken in 1997)

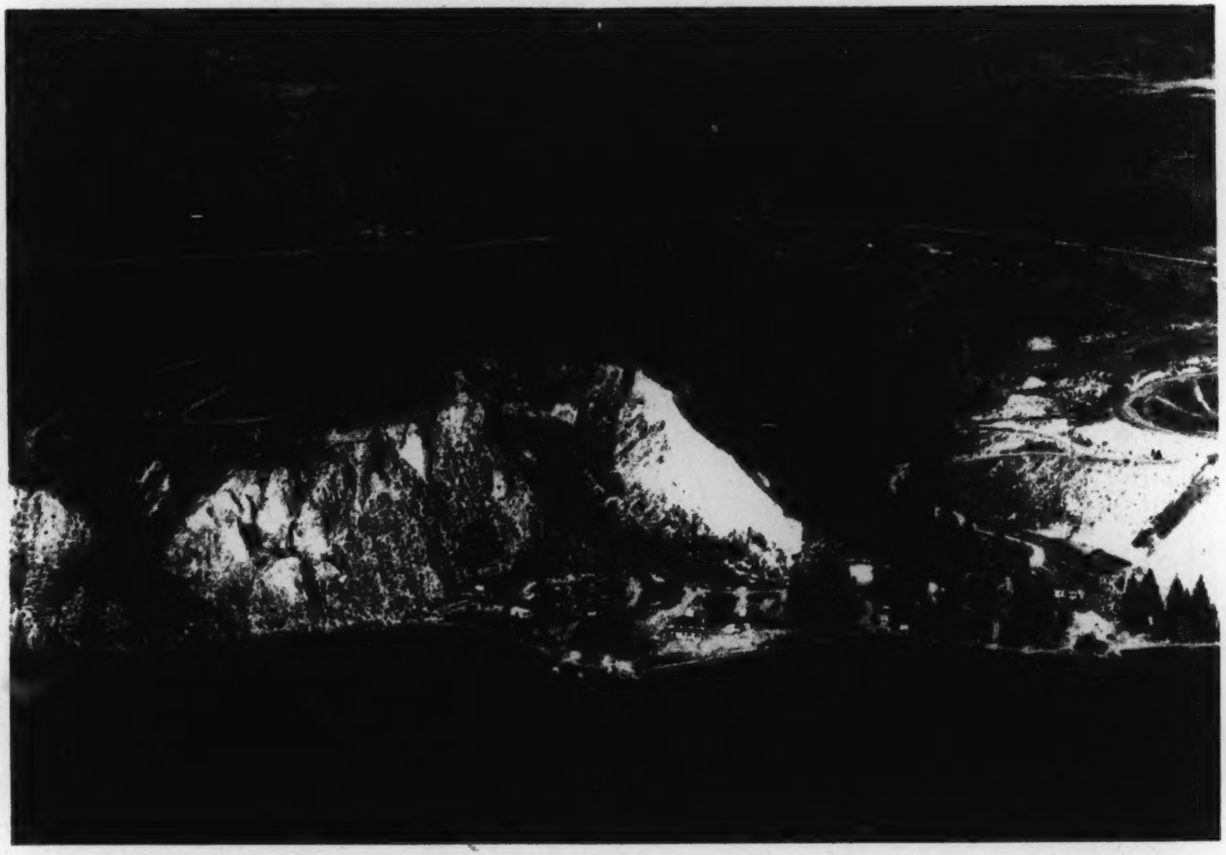

Figure 3.3-B – Okanagan Lake Park Slide (1975)
(Courtesy of the B. C. Ministry of Transportation and Highways, taken in 1997)

Figure 3.3-C – Position of Koosi Creek and Okanagan Lake Park Slides in the Southern Okanagan Lake Area

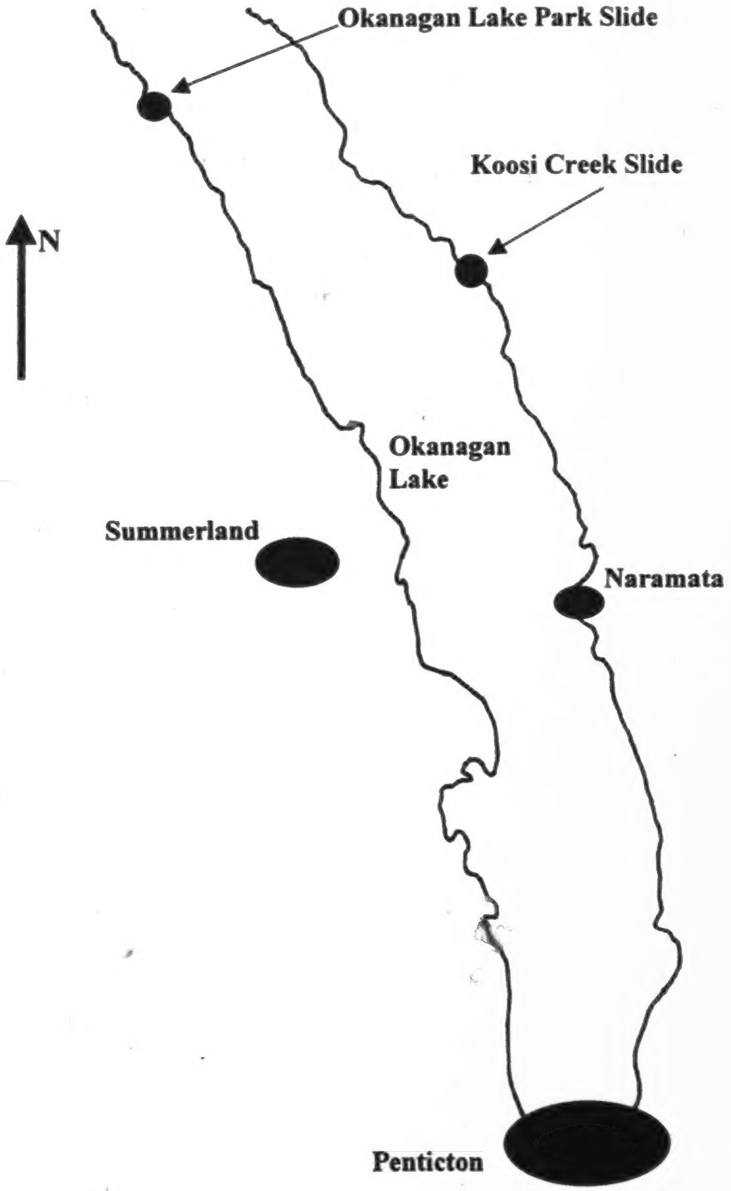
Okanagan Lake Park Slide
Koosi Creek Slide
N
Okanagan Lake
Summerland
Naramata
Penticton

Figure 3.4.1.2 – Topography Map of the Koosi Creek Slide Area

(Scale 1/6250, Contours: 20 feet = 6 m)
(Adopted from Map Sheet 82E.062.4.2, Geographic Data B. C.)

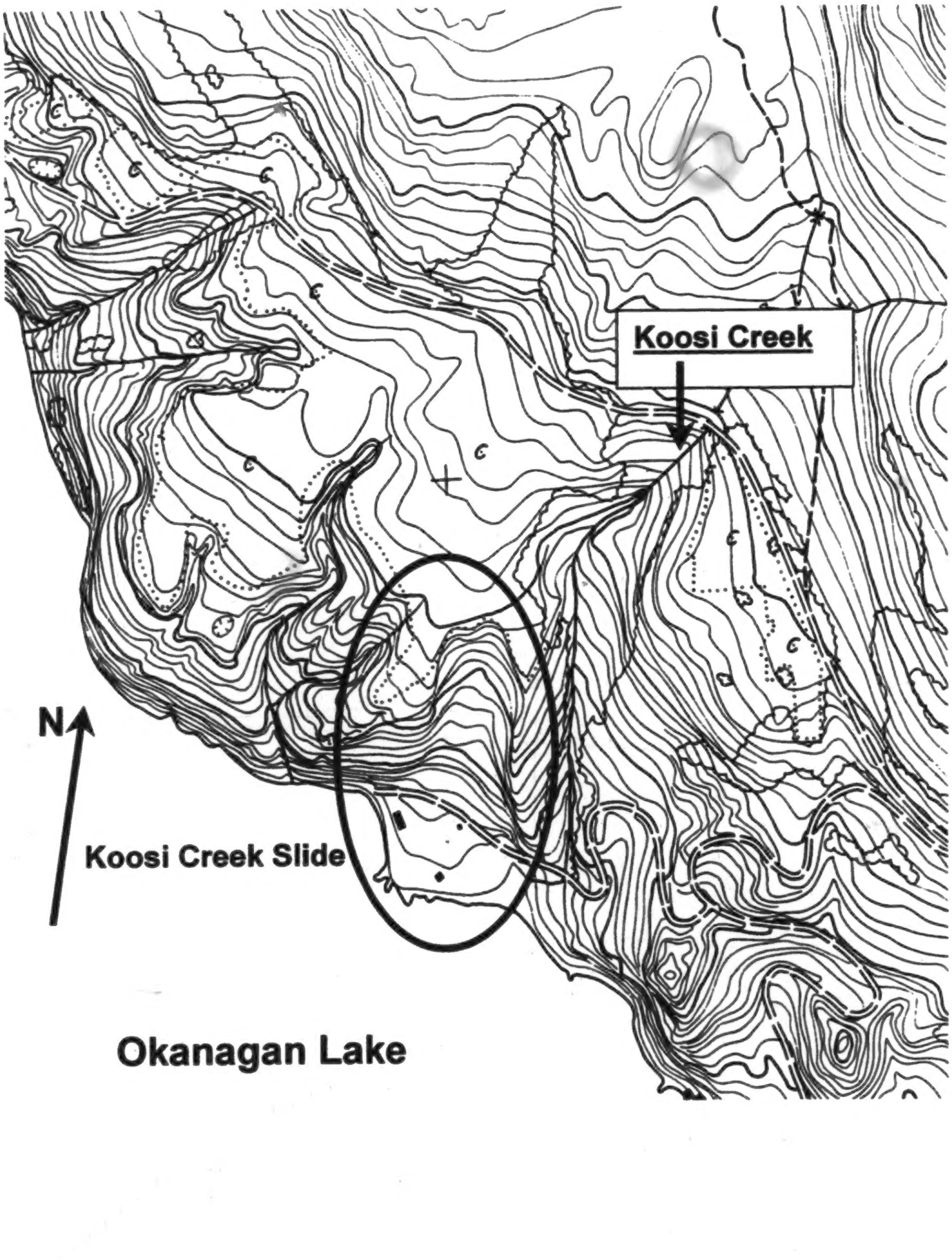
Koosi Creek
N
Koosi Creek Slide
Okanagan Lake

Figure 3.4.1.3 – Surficial Materials of the Vicinity of Koosi Creek

(Note: Zones 1 through 14 are described in section 3.4.1.3)

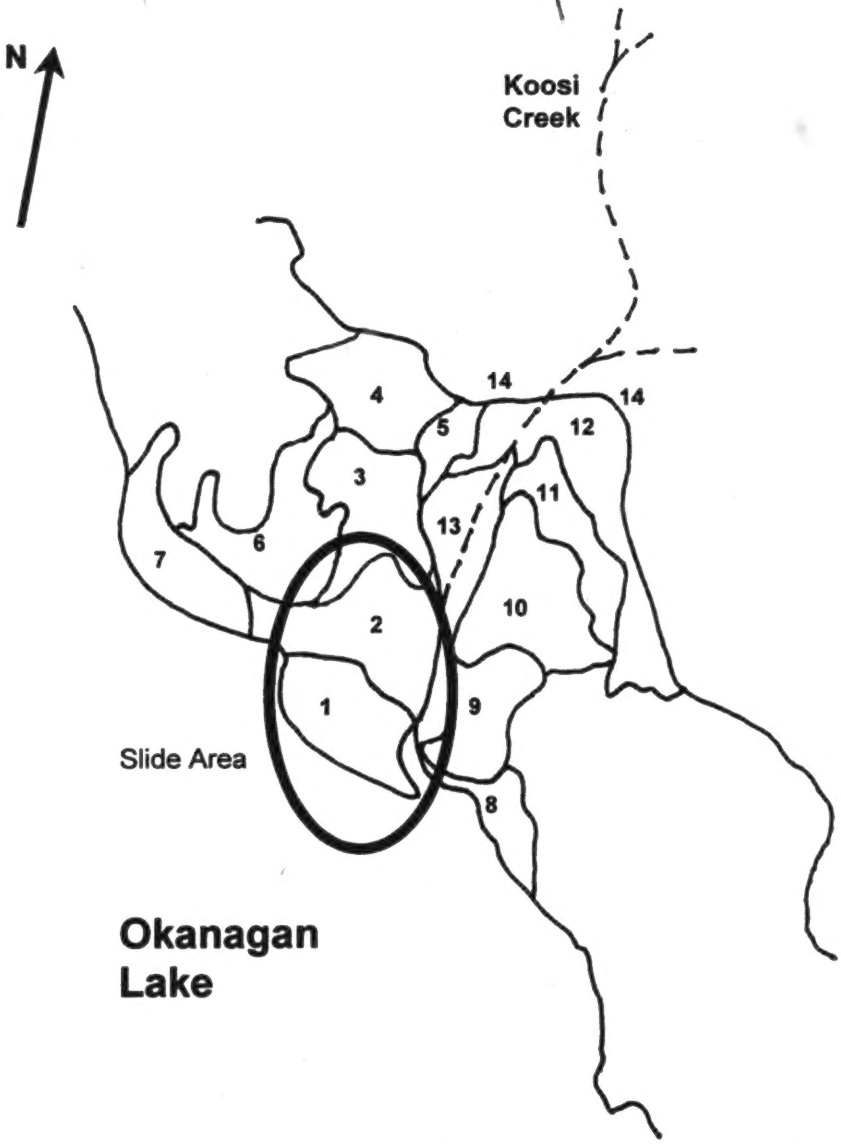
N
Koosi
Creek
14
14
4
5
12
3
11
13
6
7
10
2
1
9
Slide Area
8
Okanagan
Lake

Figure 3.4.1.4.1-A – Pre-Slide Aerial Photograph (1938) (Koosi Creek Slide Area)

(Based on Air-Photo BC 109:59,60, and 61)
(Scale: 1:31680)

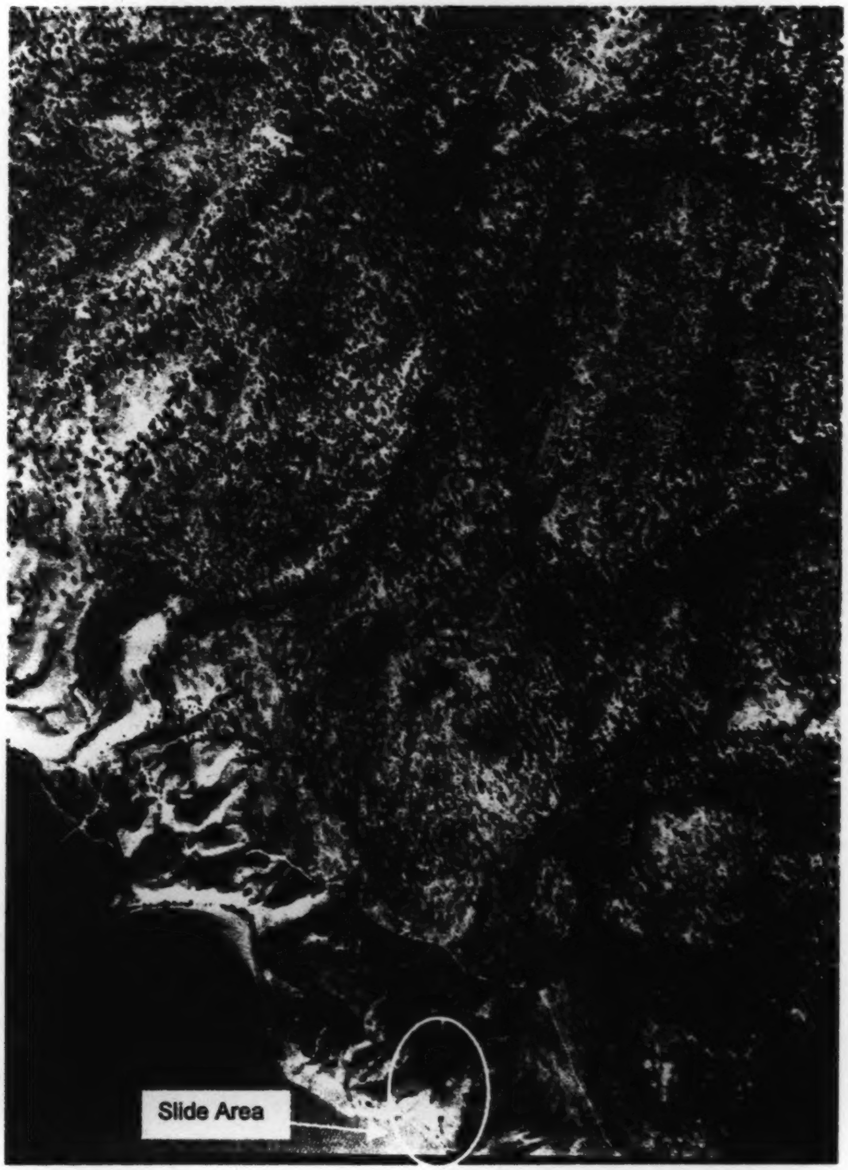

Figure 3.4.1.4.1-B – Magnified Pre-Slide Aerial Photograph of Koosi Creek Slide Area

(Based on Air-Photo BC 109:59,60, and 61 (1938))
(Scale: 1:7920)

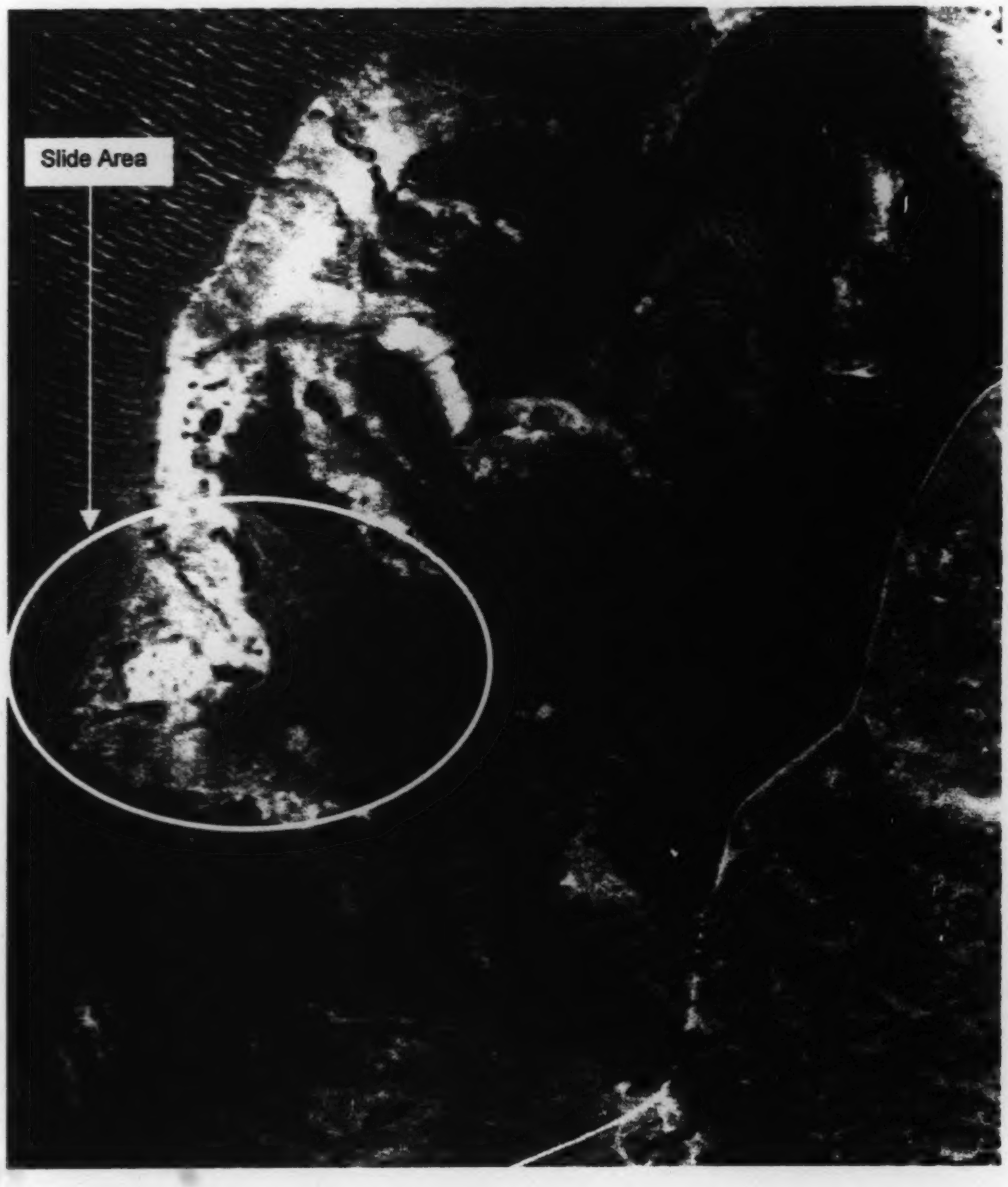

Figure 3.4.1.4.2-A – Post-Slide Aerial Photograph (1963)
(Koosi Creek Slide Area)

(Based on Air-Photo BC4195-033 and 034)
(Scale: 1:15840)

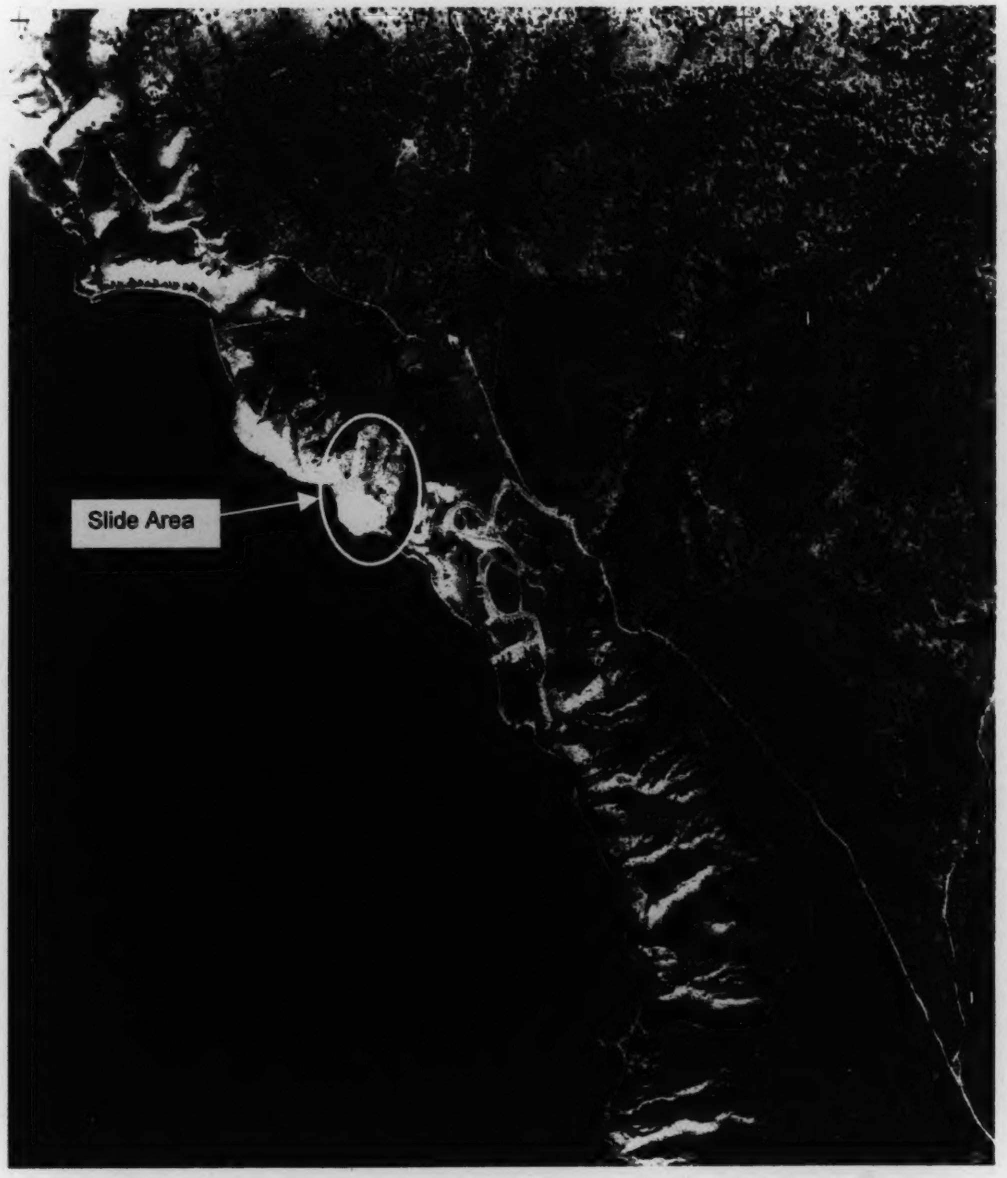

Figure 3.4.1.4.2-B – Magnified Post-Slide Aerial Photograph of Koosi Creek Slide Area

(Based on Air-Photo BC4195-033 and 034 (1963))
(Scale: 1:3960)

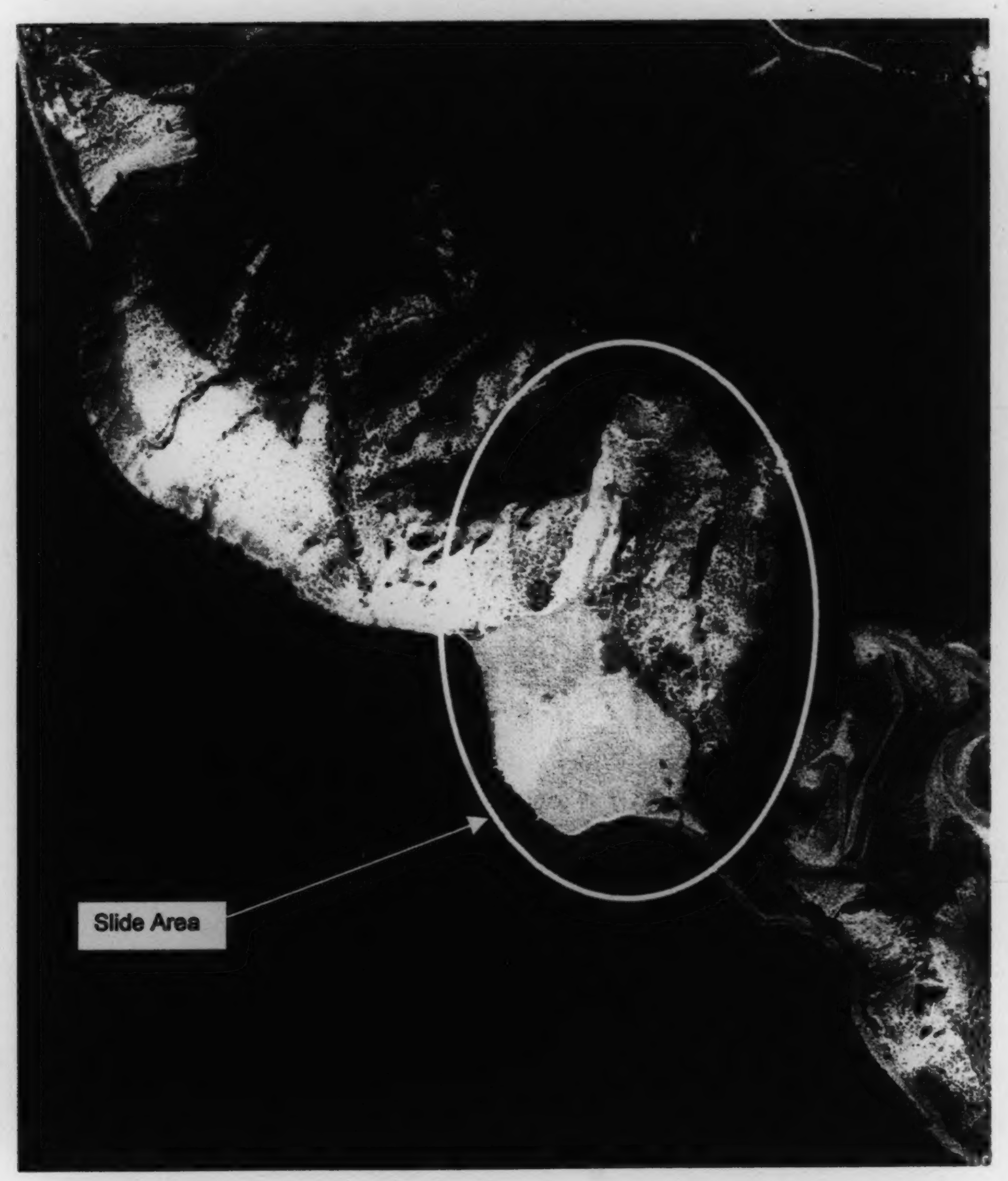

Figure 3.4.1.4.2-C – Post-Slide Aerial Photograph (1974) (Koosi Creek Slide Area)

(Based on Air-Photo BC7639 217 and 218)
(Scale: 1:15840)

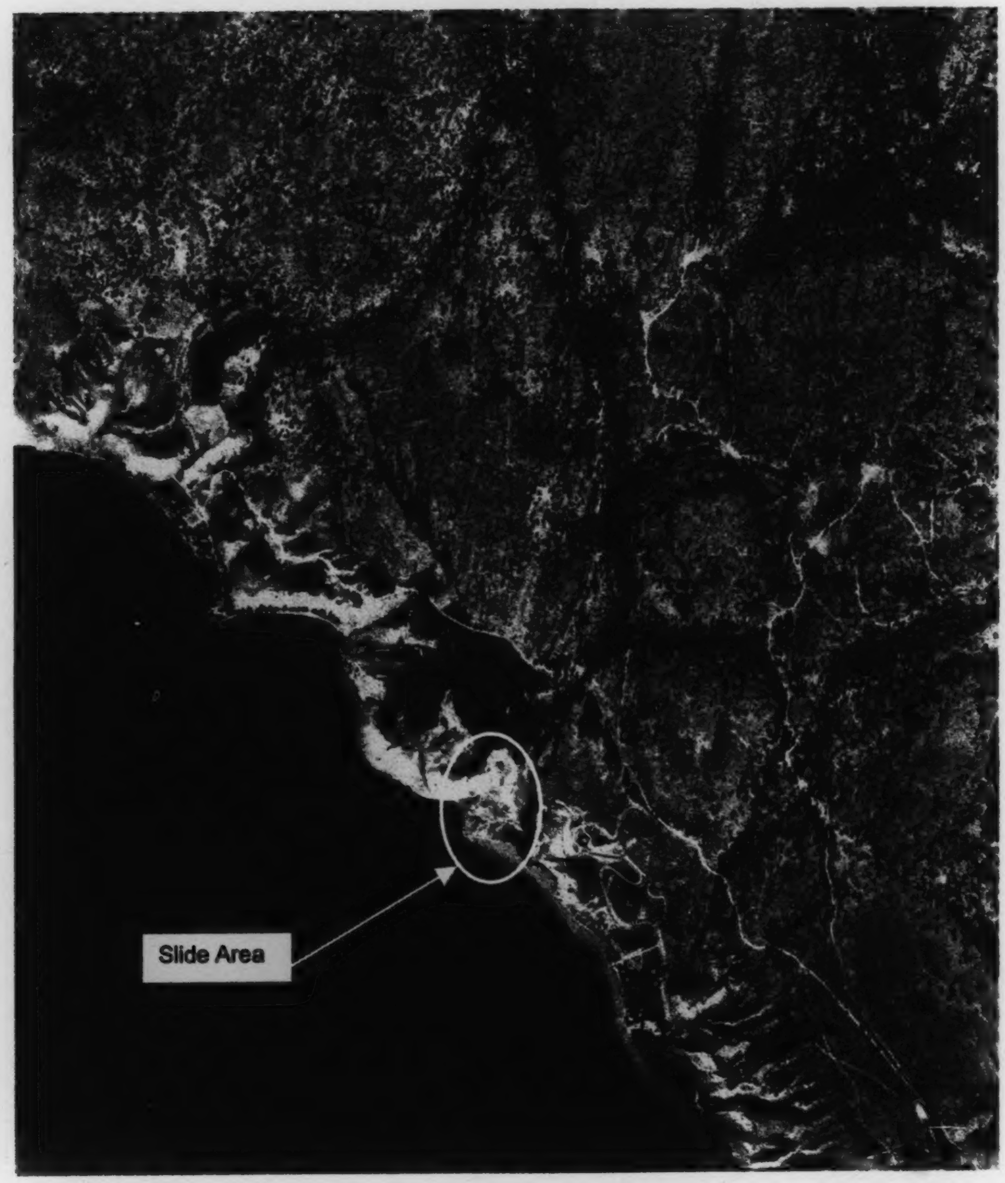

Figure 3.4.1.4.2-D – Post-Slide Aerial Photograph (1985) (Koosi Creek Slide Area)

(Based on Air-Photo 30BCC 344 081 and 082)
(Scale: 1:15840)

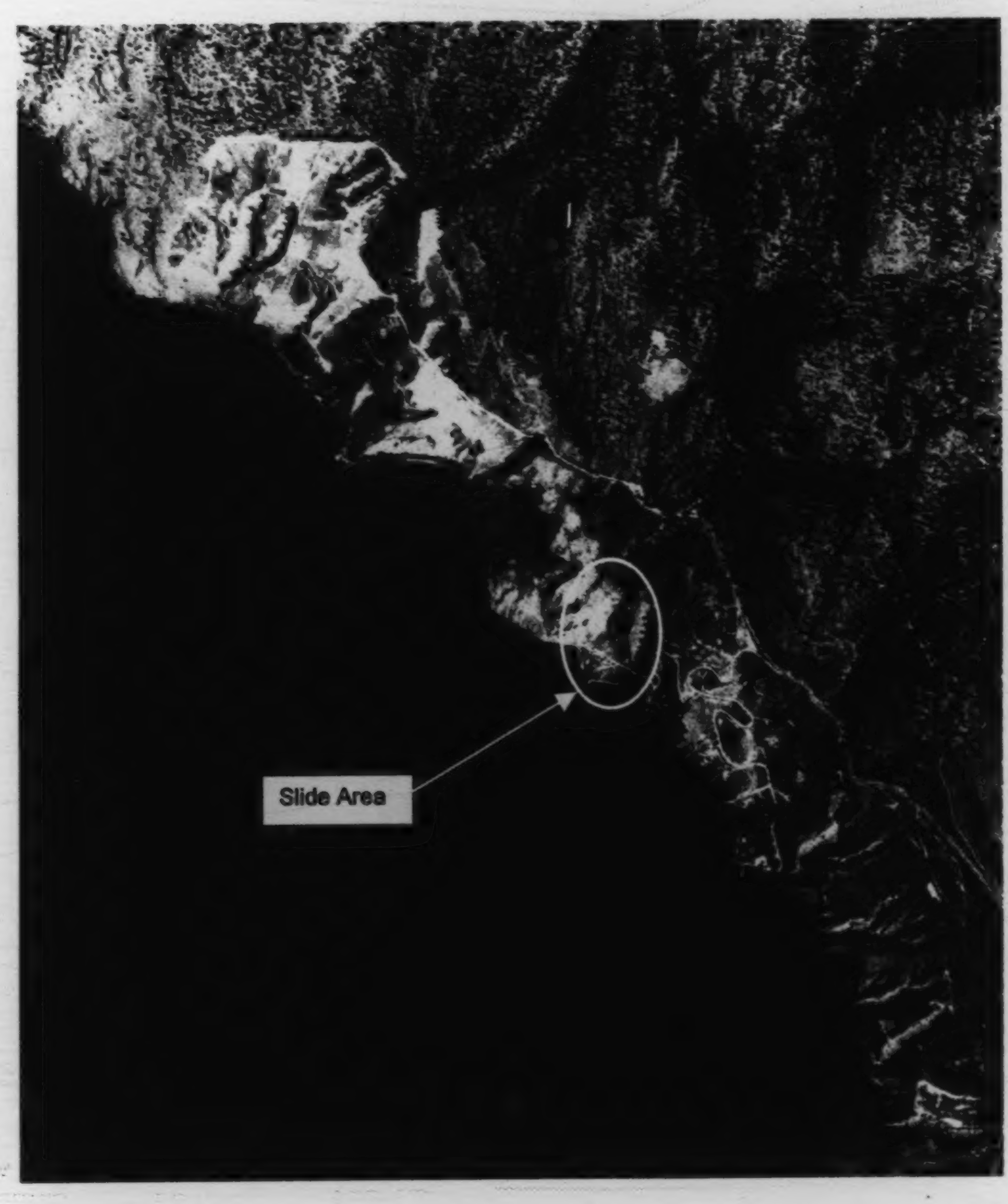

Figure 3.4.2-A – Bedrock Exposure in Koosi Creek Slide Area

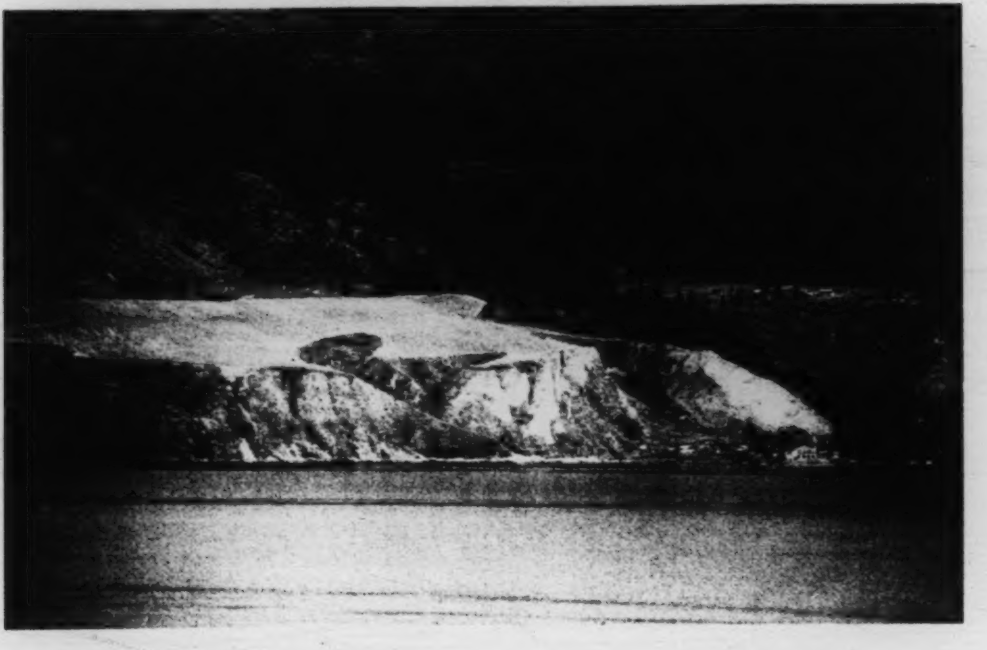

Figure 3.4.2-B – General View of Koosi Creek Slide

Figure 3.4.2-C – Groundwater Discharge Zone (Koosi Creek Slide)

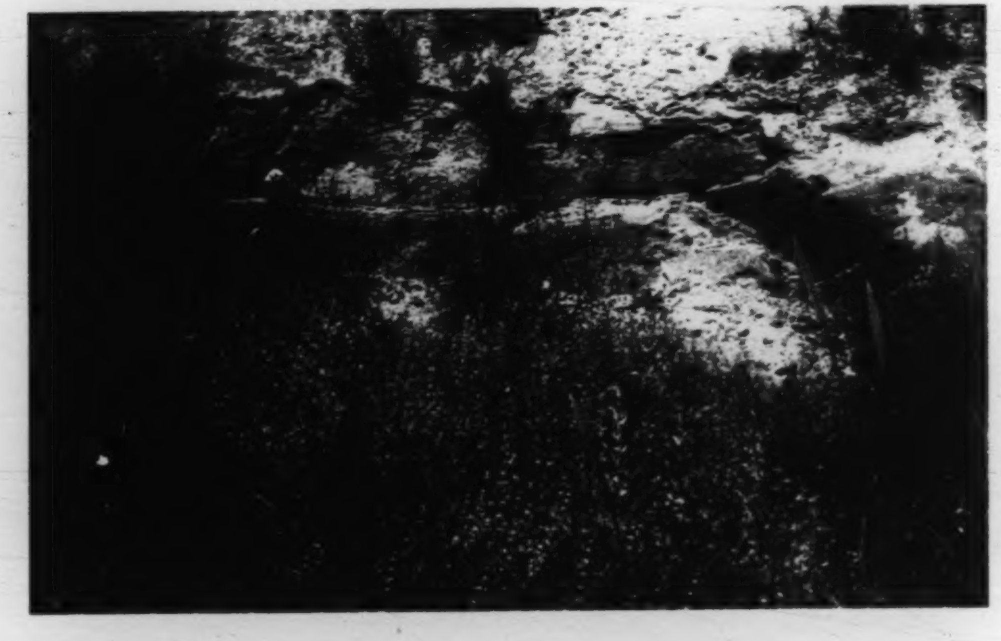

Figure 3.4.2-D – White Precipitates in Groundwater Discharge Zone (Koosi Creek Slide)

Figure 3.4.2-E – Rapidly Draining Strata in Groundwater Exit Zone
(Koosi Creek Slide)

Figure 3.4.2-F – Sand Lenses in Groundwater Exit Zone
(Koosi Creek Slide)

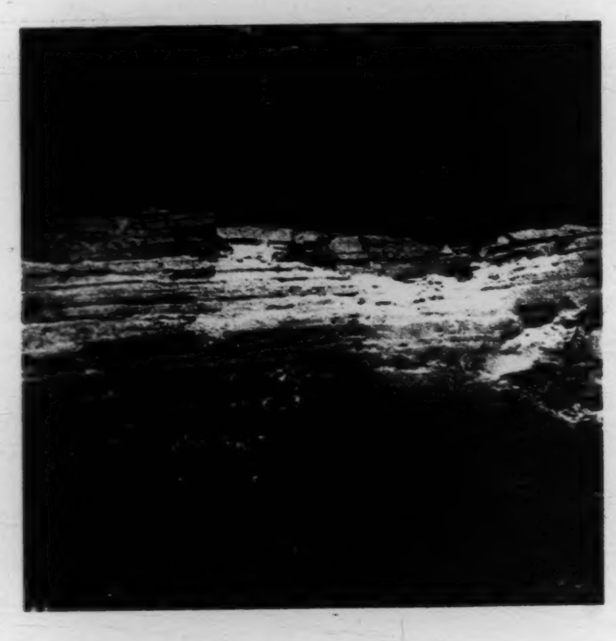

Figure 3.4.2-G – Northwest Wall of Koosi Creek Slide Area

Figure 3.4.2-H – Southeast Wall of Koosi Creek Slide

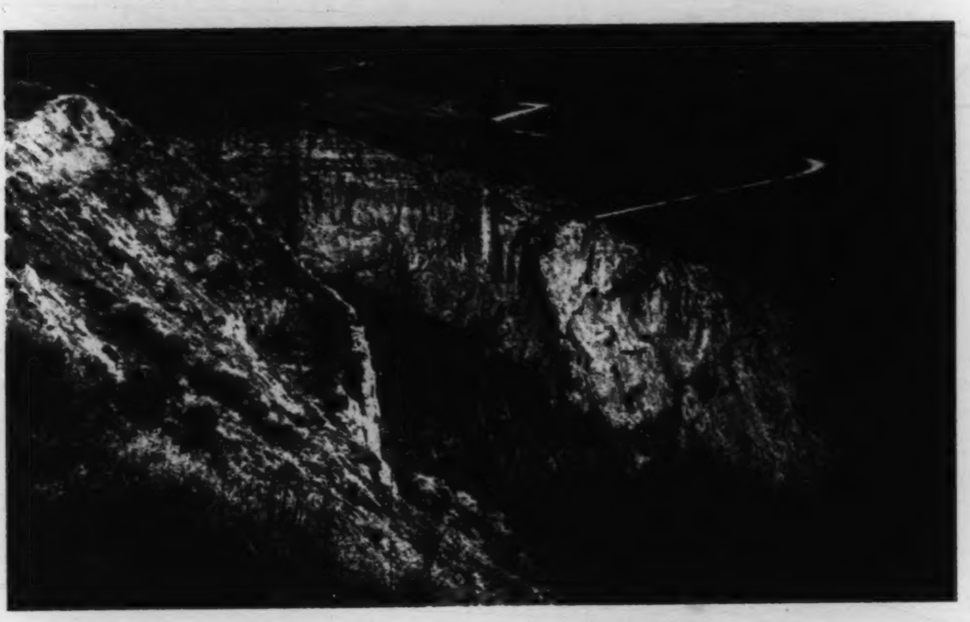

Figure 3.4.3-A – Topography Plan of Koosi Creek Slide

(Scale 1/1667, Contours: 20 feet)
(Adopted from Map Sheet 82E.062.4.2, Geographic Data B. C.)

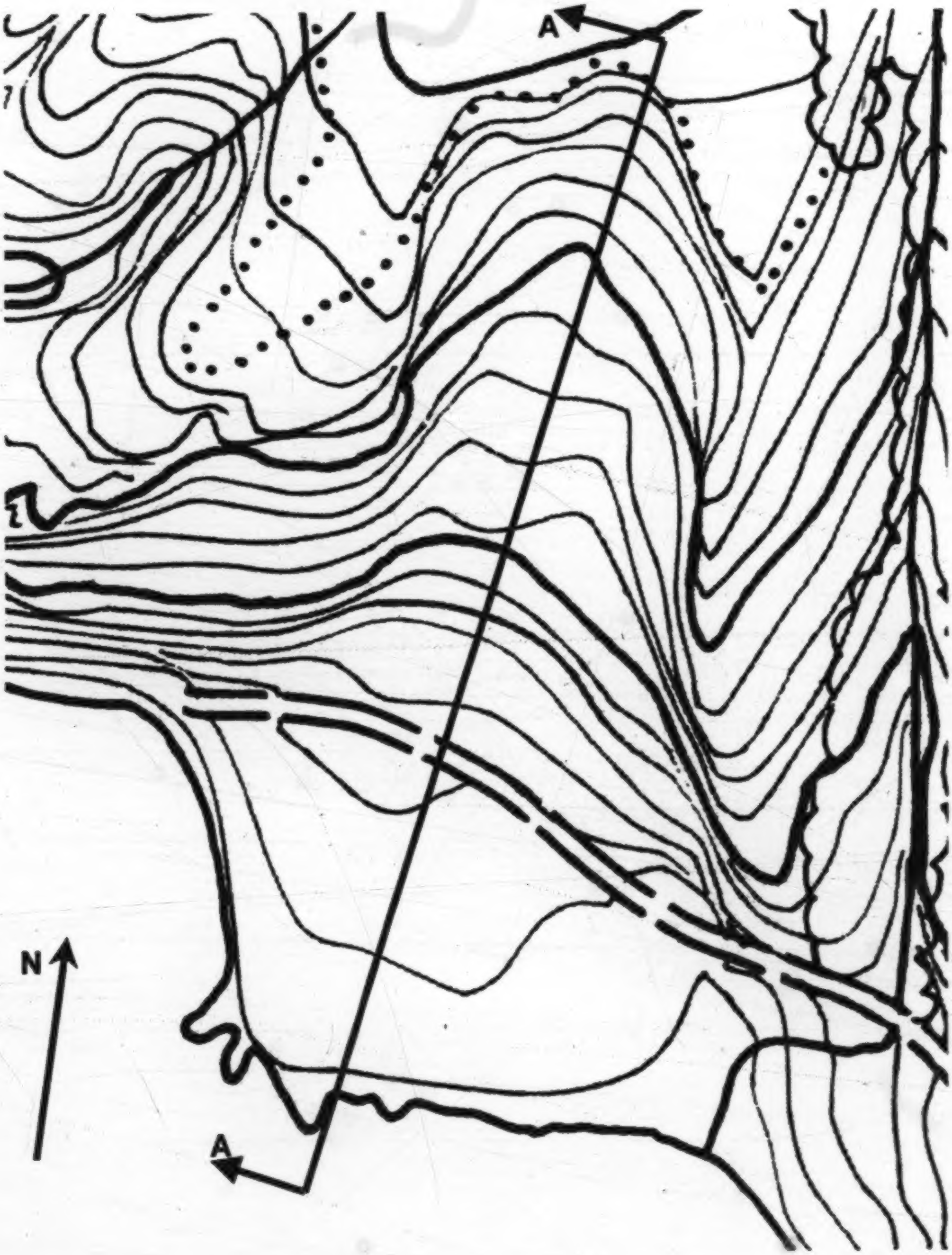

Figure 3.4.3-B – The Cross Section of the Axis of the Koosi Creek Slide

(Section A-A in Figure 3.4.3-A)
(Scale: 17 mm = 100 feet = 30 m)

Notes:

- Pre-slide profile is an approximate estimate based on aerial photograph interpretation.
- Bedrock profile is an approximate estimate based on aerial photograph interpretation.
- Lake level is for typical spring values.

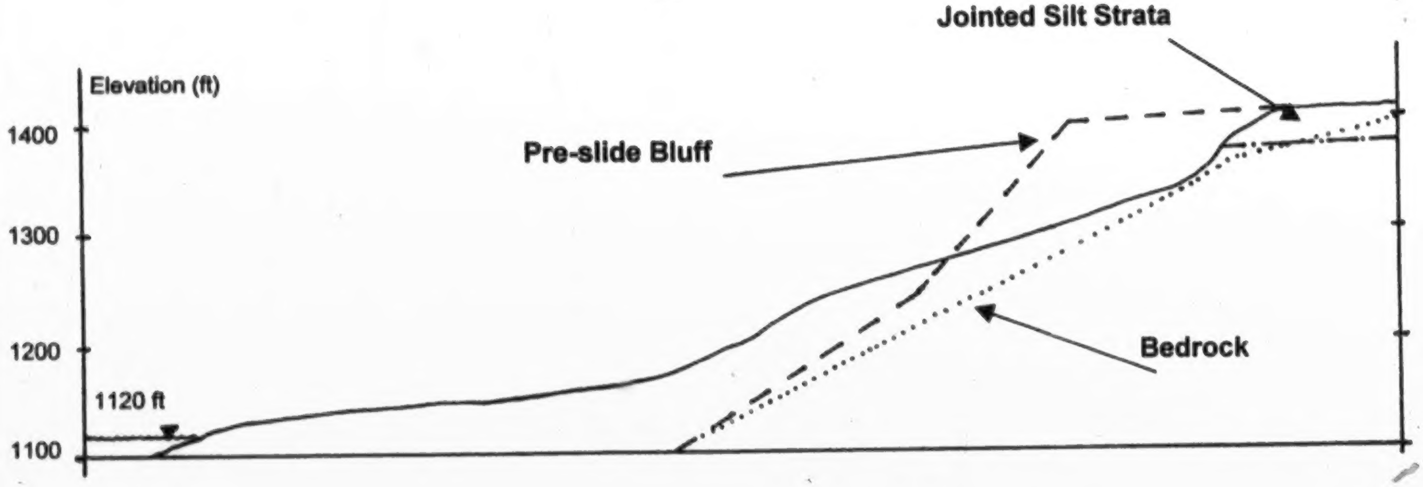
Jointed Silt Strata
Elevation (ft)
1400
Pre-slide Bluff
1300
Bedrock
1200
1120 ft
1100

Figure 3.5.1.1-A – Okanagan Lake Park Slide (May 1975)
(after Nyland and Miller (1977))

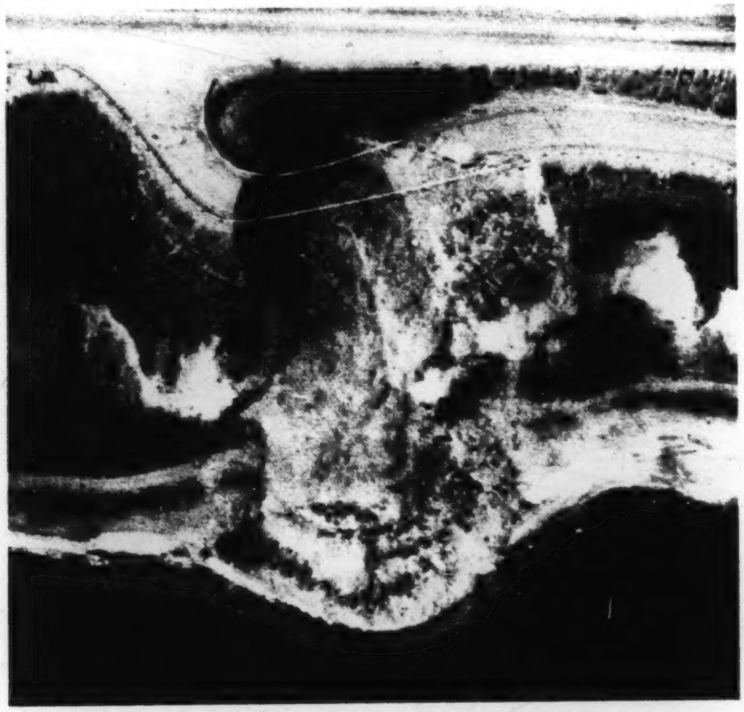

Figure 3.5.1.1-B – Reworked Shape of the Okanagan Lake Park Slide
(after Nyland and Miller (1977))

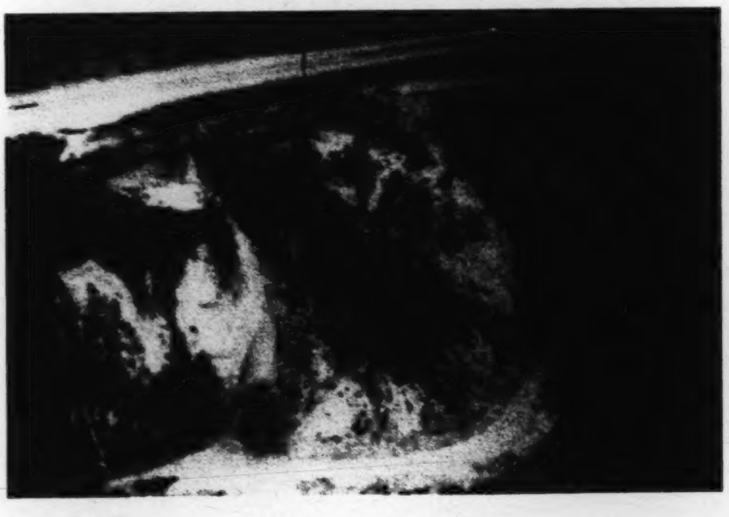

Figure 3.5.1.2 – Topography of the Okanagan Lake Park Slide Area

(Scale: 1/6250, Counters: 20 feet=6 m)
(Adopted from Map Sheet 82E.062.3.4, Geographic Data B. C.)

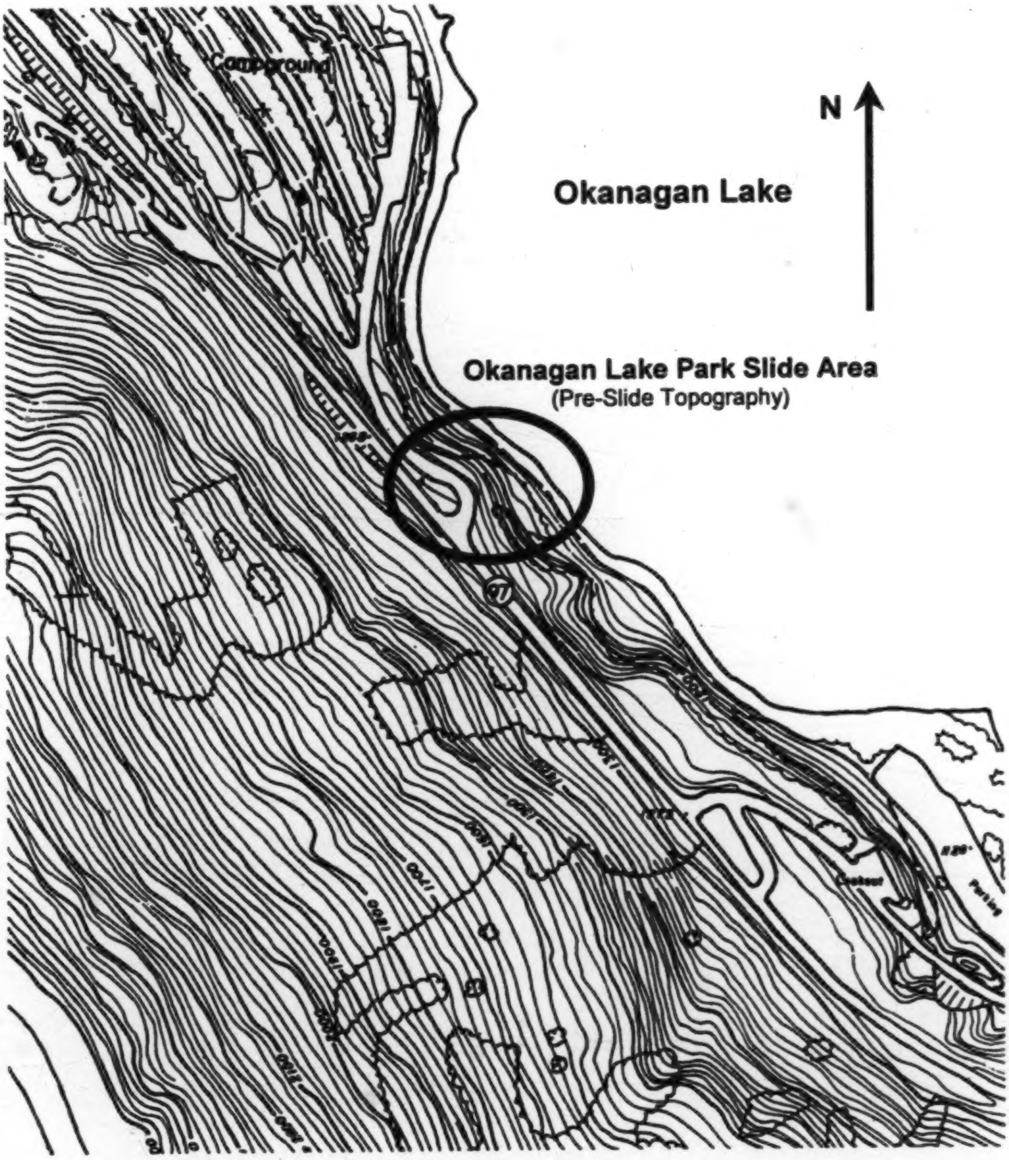
Campground
N
Okanagan Lake
Okanagan Lake Park Slide Area
(Pre-Slide Topography)
97
Lookout
Parking
1700
1800
1900
2000
2100

Figure 3.5.1.3 – Surficial Materials of the Okanagan Lake Park

(Note: Zones 1 through 14 are described in section 3.5.1.3)

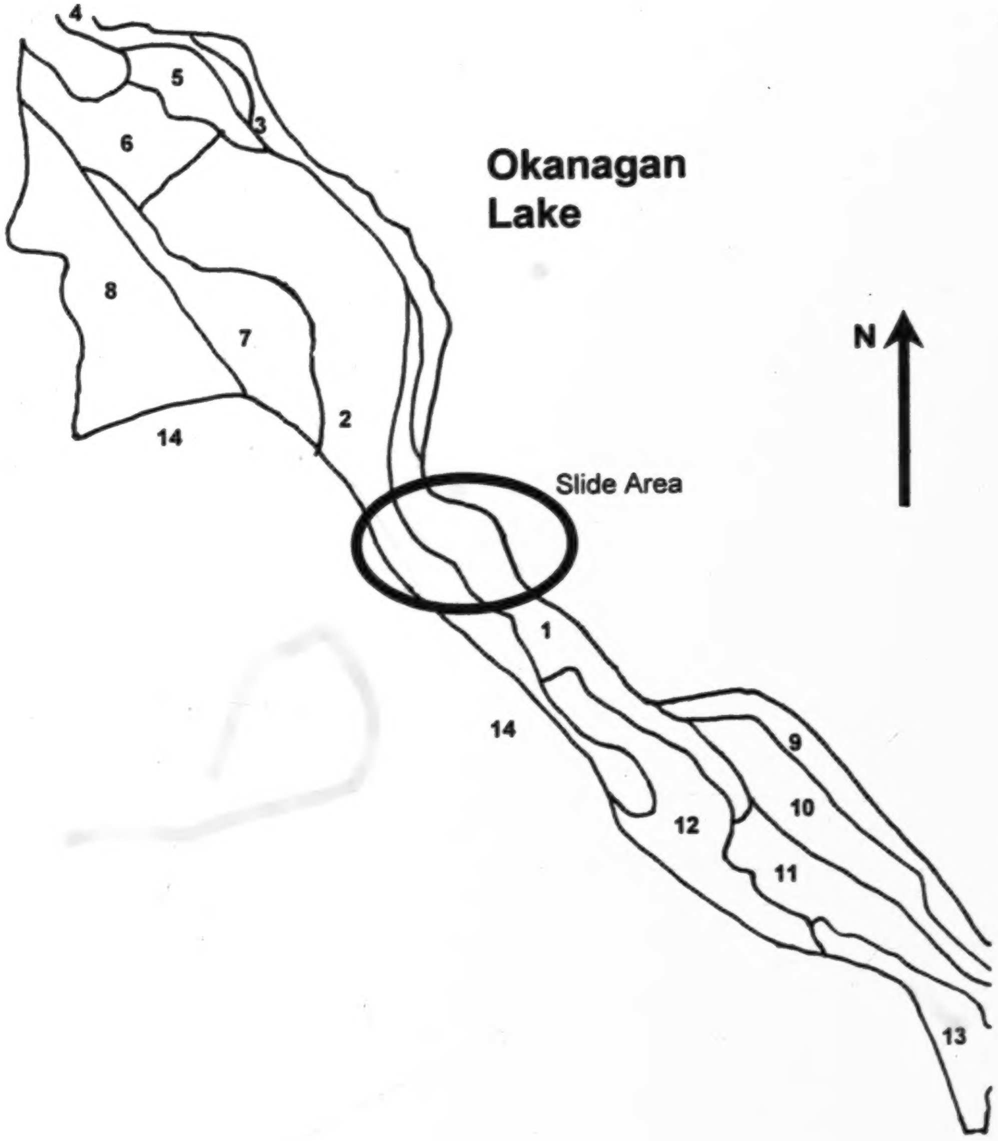
4
5
3
6
Okanagan Lake
8
7
N
2
14
Slide Area
1
14
9
10
12
11
13

Figure 3.5.1.4.1-A – Pre-Slide Aerial Photograph (1974) (Okanagan Lake Park Slide Area)

(Based on Air-Photo BC7644 009 and 010)
(Scale: 1:15000)

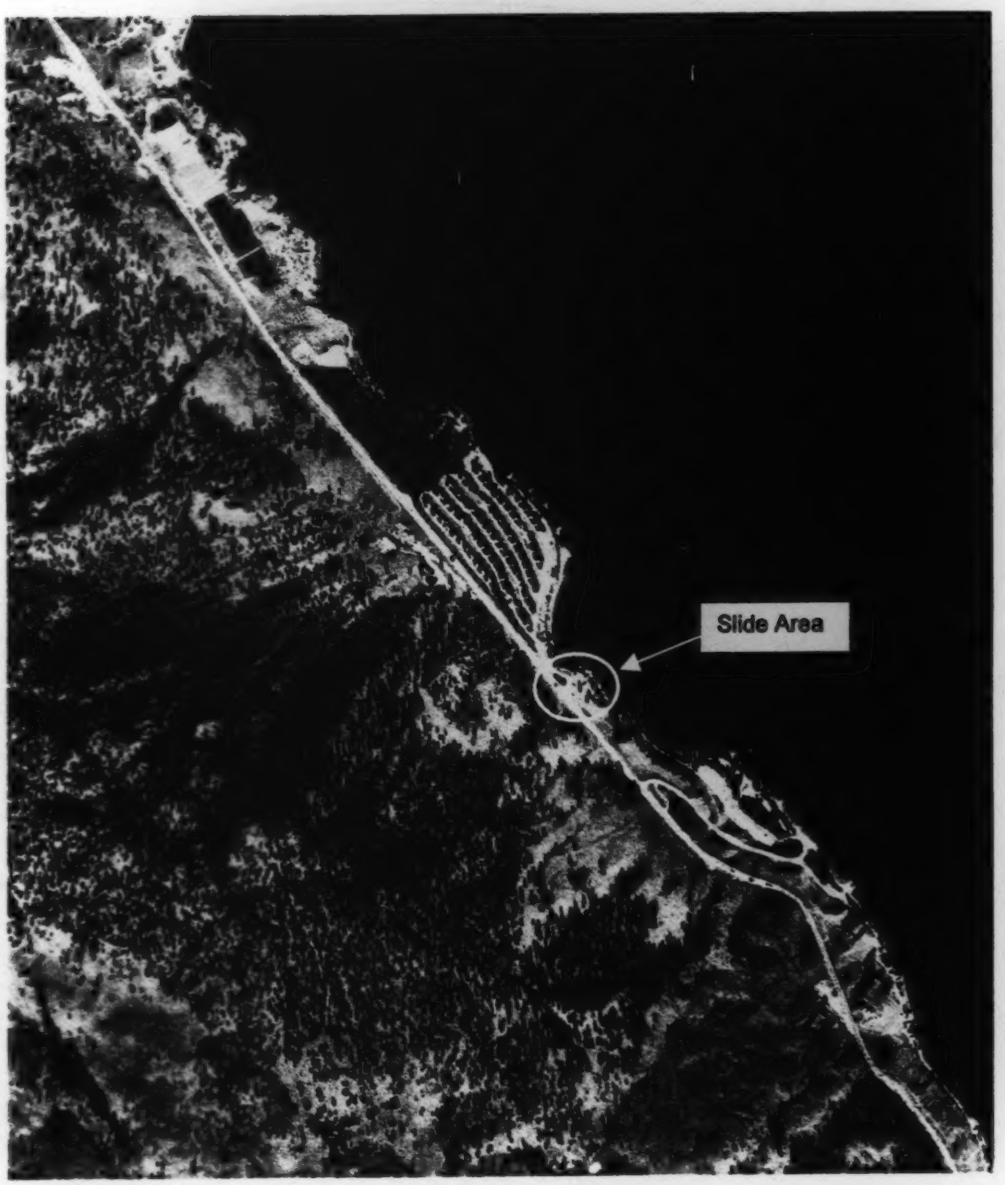

Figure 3.5.1.4.1-B – Magnified Pre-Slide Aerial Photograph of Okanagan Lake Park Slide Area

(Based on Air-Photo BC7644 009 and 010 (1974))
(Scale: 1:3750)

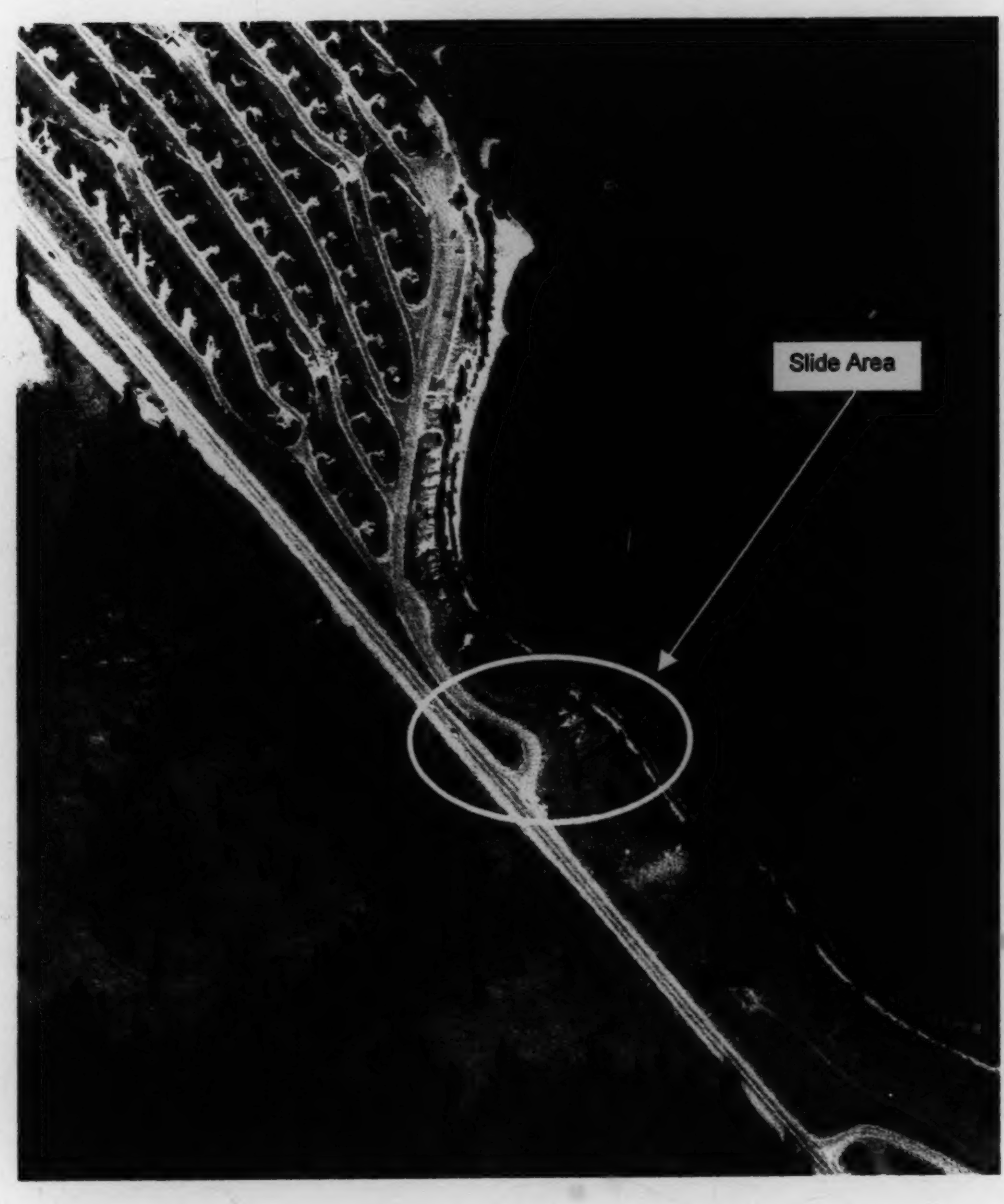

Figure 3.5.1.4.2-A – Post-Slide Aerial Photograph (1985)
(Okanagan Lake Park Slide Area)

(Based on Air-Photo 30BCCC 360 049 and 050)
(Scale: 1:15000)

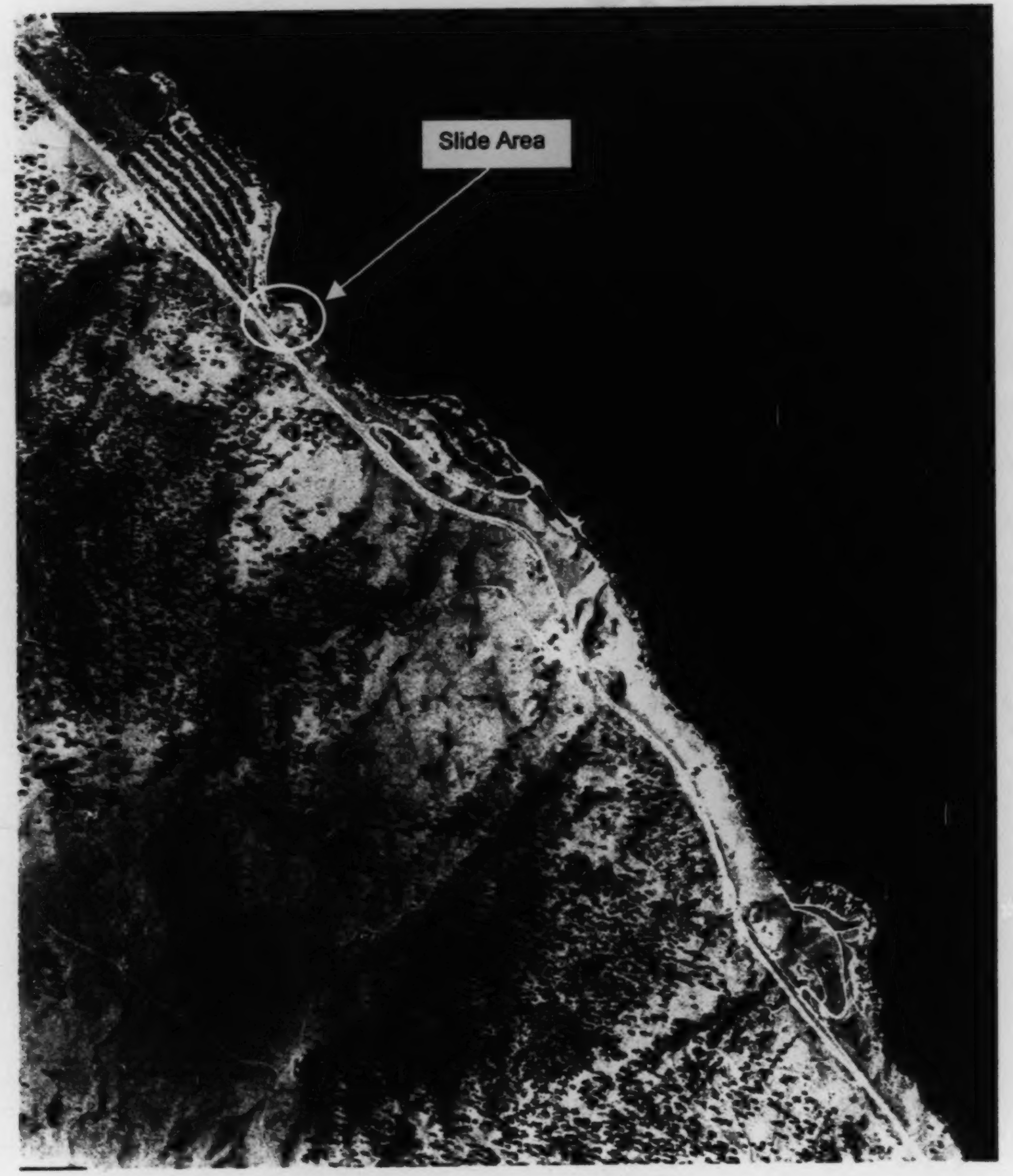

Figure 3.5.1.4.2-B – Magnified Post-Slide Aerial Photograph of Okanagan Lake Park Slide Area

(Based on Air-Photo 30BCCC 360 049 and 050 (1985))
(Scale: 1:3750)

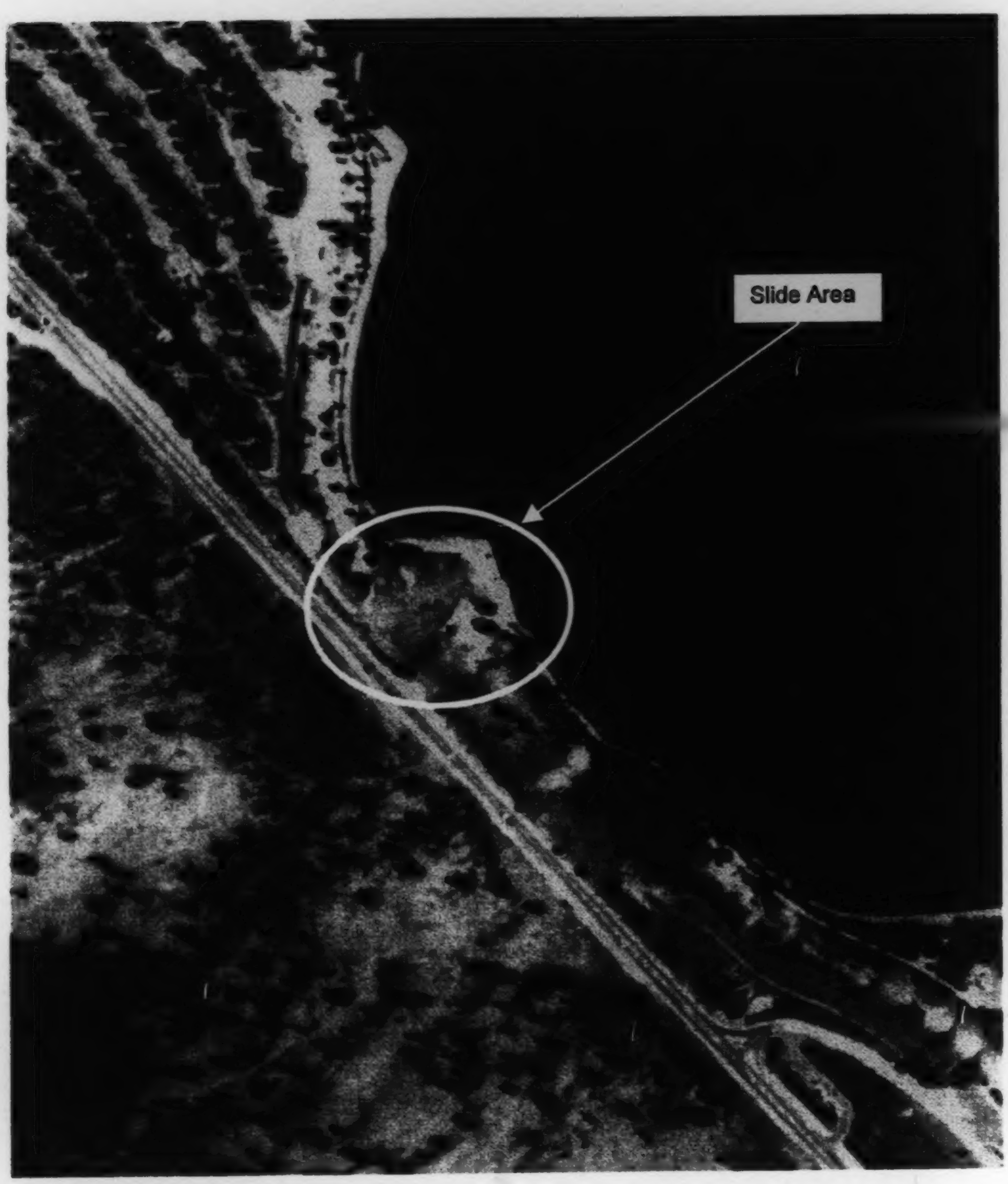

Figure 3.5.2-A – Okanagan Lake Park Slide (1997)
(Courtesy of the B. C. Ministry of Transportation and Highways)

Figure 3.5.2-B – South Wall of the Okanagan Lake Park Slide (1996)

Figure 3.5.2-C – Top Part of the South Wall (Okanagan Lake Park Slide)

Figure 3.5.2-D – Bottom Part of the South Wall (Okanagan Lake Park Slide)

Figure 3.5.3-A –Plan Geometry of Okanagan Lake Park Slide

(Scale: 13 mm = 20 ft = 6 m)

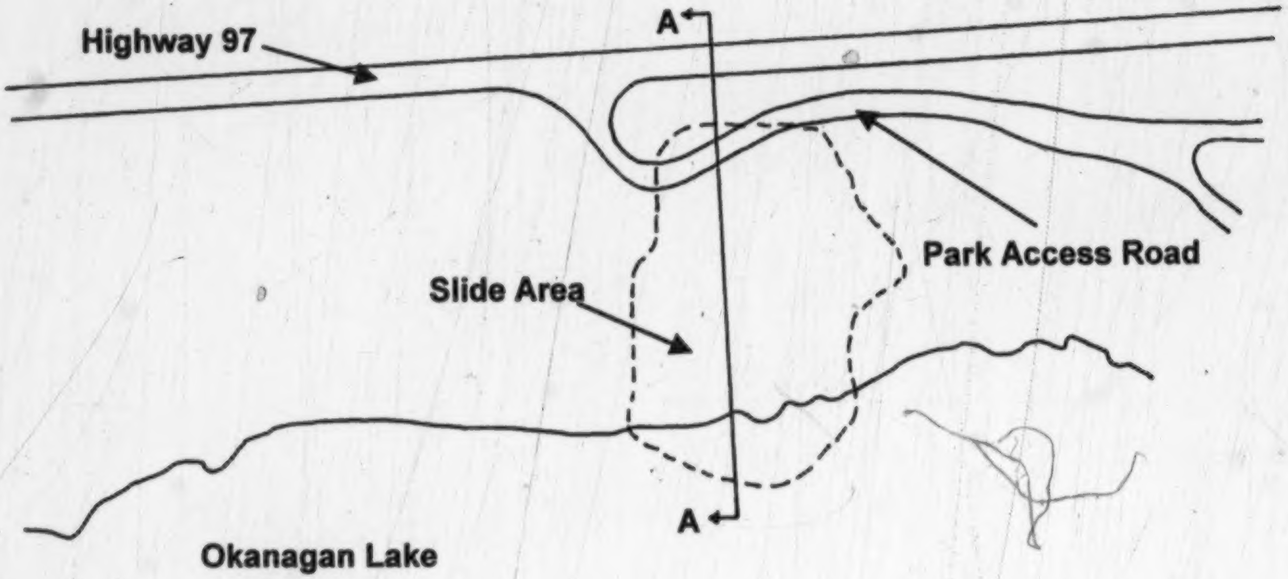
Highway 97
A
Park Access Road
Slide Area
A
Okanagan Lake

Figure 3.5.3-B – The Cross Section of the Axis of the Okanagan Lake Park Slide

(Section A-A in Figure 3.5.3-A)
(Scale: 8 mm = 20 feet = 6 m)

Notes:

- Pre-slide profile is based on pre-slide topography maps.
- Bedrock profile is an approximate estimate based on seismic studies.

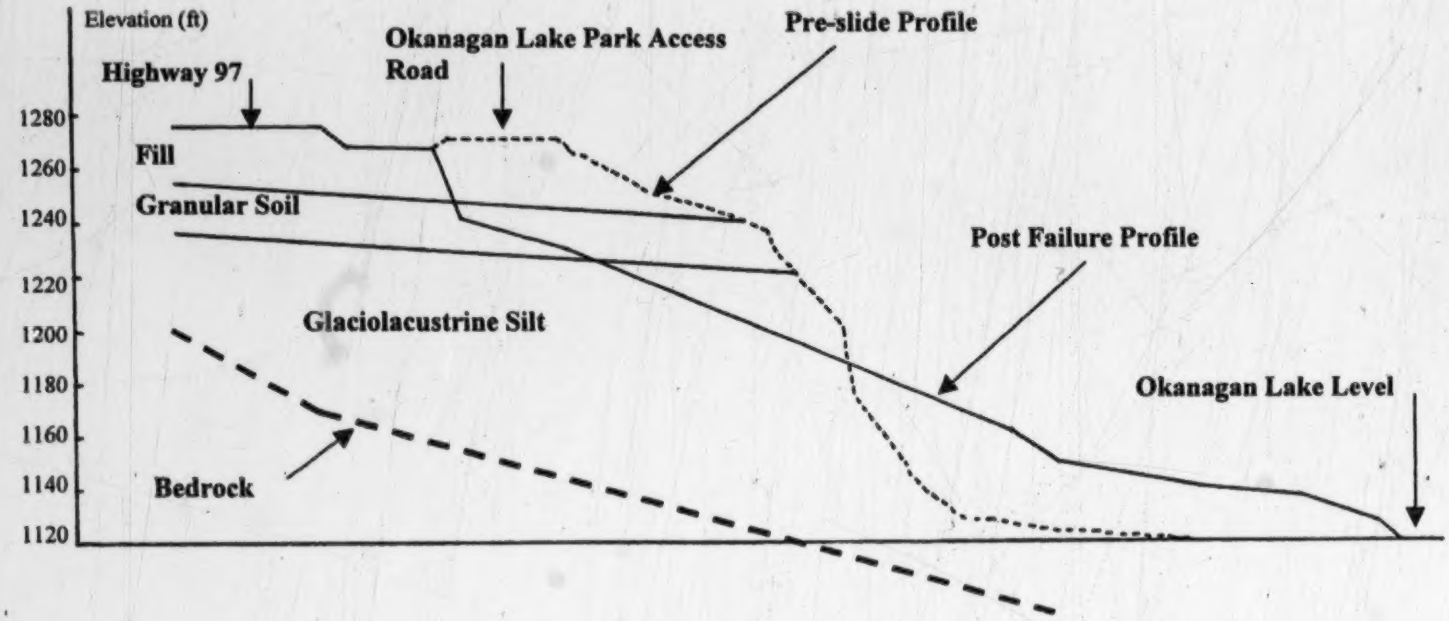
Elevation (ft)
1280
1260
1240
1220
1200
1180
1160
1140
1120
Highway 97
Okanagan Lake Park Access Road
Pre-slide Profile
Fill
Granular Soil
Post Failure Profile
Glaciolacustrine Silt
Okanagan Lake Level
Bedrock

Figure 3.6.2-A – Locality of Sampling Zone in Koosi Creek Slide Site

(Based on Air-Photo 30BCC 344 081)
(Scale: 1:15840)

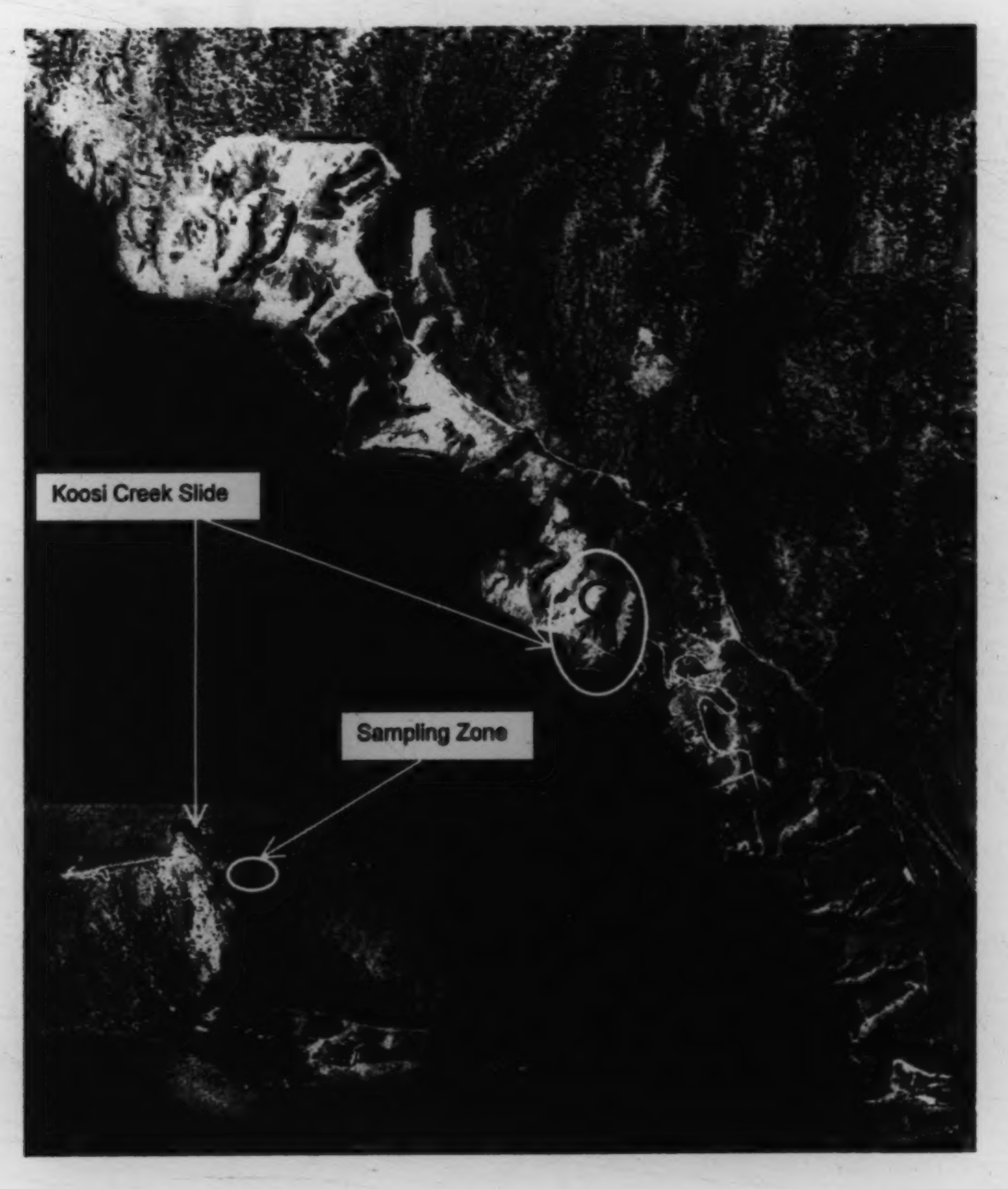
Koosi Creek Slide
Sampling Zone

Figure 3.6.2-B – Closer Look at the Sampling Area
(Koosi Creek Slide Site)

Figure 3.6.2-C – Sampling Area above the Groundwater Exit (Koosi Creek Slide Site)

Figure 3.6.2-D – Sampling Area below Groundwater Exit (Koosi Creek Slide Site)

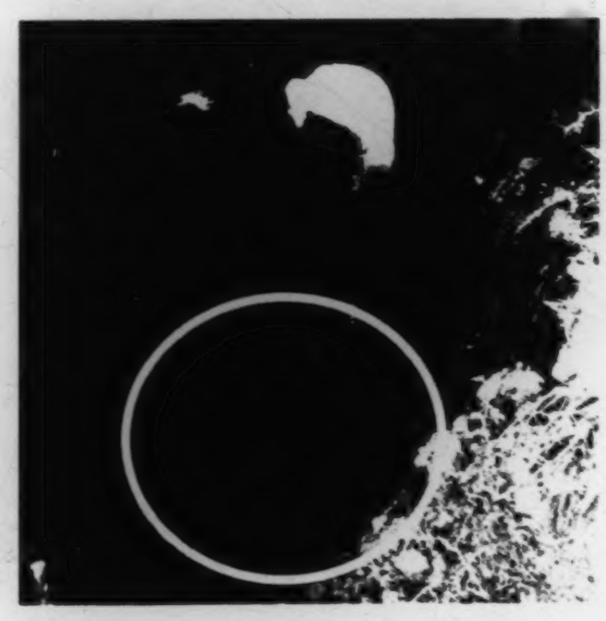

Figure 3.6.3-A – Locality of Sampling Zone in Okanagan Lake Park Slide Site

(Based on Air-Photo 30BCC 360 049)
(Scale: 1:15840)

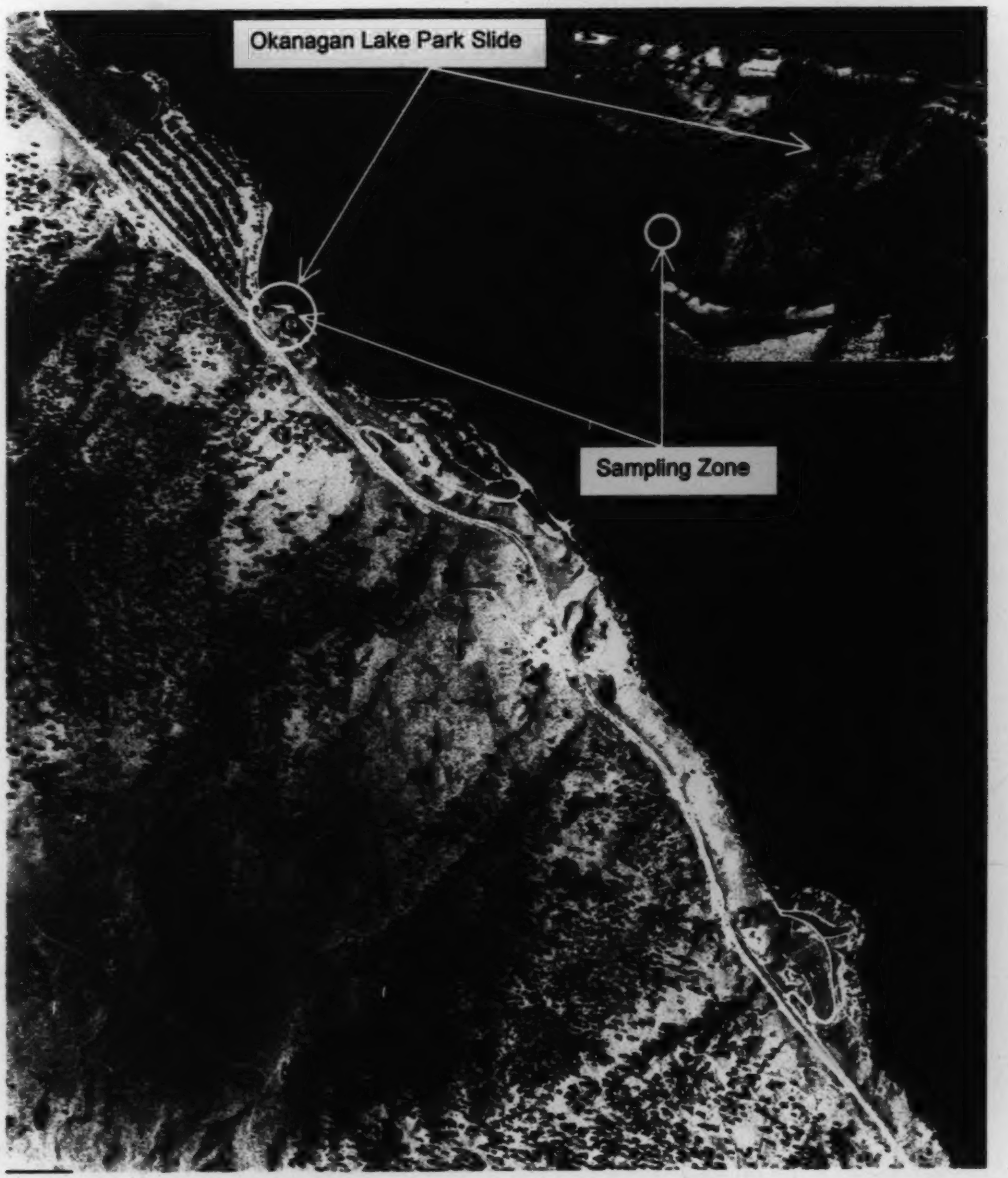
Okanagan Lake Park Slide
Sampling Zone

Figure 3.6.3-B – Sampling Area in the South Wall of Okanagan Lake Park Slide

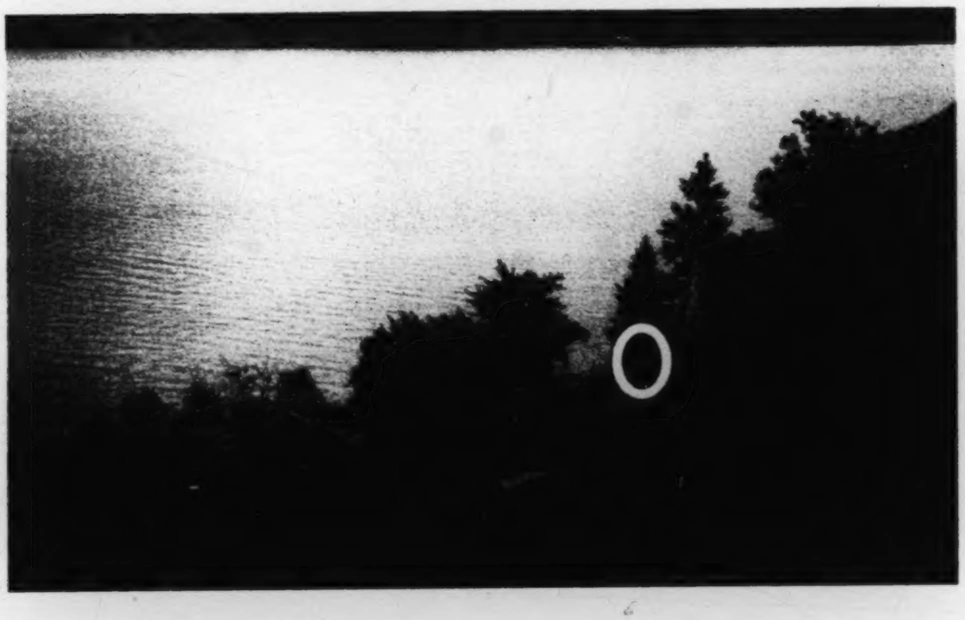

Figure 3.6.3-C – Closer Look at the Sampling Zone (Okanagan Lake Park Slide Site)

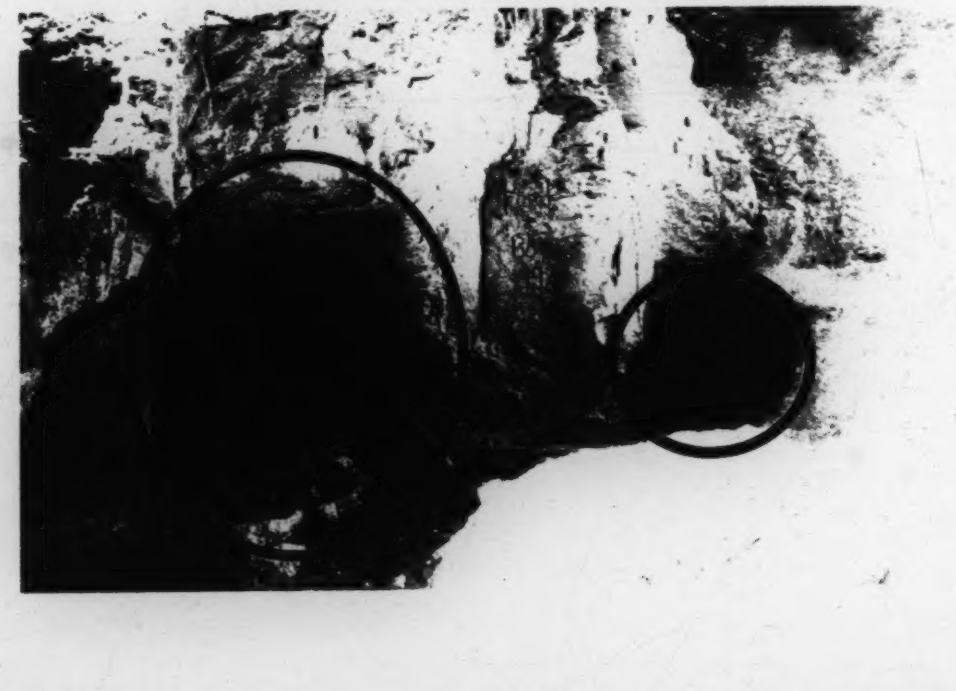

CHAPTER FOUR

Cone Penetration Testing (CPT)

4.1 Introduction

The glaciolacustrine silt sediments in the southern interior of British Columbia, including Penticton silt, are relatively unique geological features and there is limited reliable in-situ test data available. In-situ testing, independently or in conjunction with laboratory testing, can provide significant insight in to the behavior of soils and the determination of their geotechnical properties.

As part of this study, cone penetration testing with pore pressure measurements, in conjunction with seismic down-hole method, (SCPTU) was carried out in bluffs of Penticton silt adjacent to the Okanagan Lake Park Slide. Cone penetration testing (CPT), which is a static penetration test methods, has become one of the most common in-situ tests used by geotechnical engineers because of its simplicity, continuity of recording, and reproducibility of results. Another advantage of the CPT is the rational and reliable theories that have been developed to aid the interpretation processes.

Three seismic piezo cone penetration tests (SCPTU) were carried out. The silt deposits in general and glaciolacustrine silt sediments in the southern interior of B. C. in specific cannot be classified as either of the two main categories of soils (i.e., coarse-grained cohesionless soils (sands) or fine-grained cohesive soils (clays)). The existing empirical relationships between SCPTU test results and soil properties are generally developed using either saturated unaged and uncemented coarse-grained cohesionless soils or saturated fine-grained cohesive soils. Consequently, their applicability is limited to those soils that have been used in establishing the correlation. This study provides an opportunity to examine the validity of existing empirical relationships, developed for saturated coarse-grained cohesionless or saturated fine-grained cohesive soils, to an unsaturated silty deposit.

In this chapter, results of the three SCPTU tests are presented and discussed. These results are used to estimate the soil behavior type, assess structure and cementation, and interpret the soil parameters.

Some empirical equations used in SCPTU interpretation are function of effective vertical stress (σ'_{vo}), which in turn is a function of soil suction in the partially saturated zones. As described in section 5.5, soil suction varies between 100 kPa and 300 kPa for typical values of gravitational water content in Penticton silt sediments (i.e., between 25% and 15%). It was observed during soil sampling that the water content of these sediment increases rapidly with distance from exposed faces. In order to take in to account the effect of partial saturation on the effective vertical stress, values of matric suction equal to 200 kPa and 100 kPa were used in calculation of σ'_{vo} for depths of 2.5-5.0 m and 5.0-29.0 m, respectively.

4.2. General

Three cone penetration testing with pore pressure measurements, in conjunction with seismic down-hole method, (SCPTU) were carried out in the bluffs of Penticton silt adjacent to the Okanagan Lake Park Slide. The location of tests are shown in Figure 4.2-A. Results of the cone bearing resistance (q_c), the sleeve friction (f_s), the friction ratio ($R_f = (f_s/q_c) \times 100$), pore pressure (u), and shear wave velocity are summarized in Figure 4.2-B through D for SCPTU-1 through SCPTU-3, respectively.

A review of the CPT profiles indicates that the groundwater table is at a depth of about 29 m with the possible existence of a perch ground water table between 7 m and 9 m. These sediments are generally uniform but the continuous soil profile by CPT provided the opportunity to detect the stratified nature of these sediments.

4.3 Soil Behavior Type

Robertson (1990) proposed soil classification using normalized cone resistance (Q) and normalized friction ratio (F), defined as follows:

$$Q = \frac{q_c - \sigma_{vo}}{\sigma'_{vo}}$$ (Equation 4.3-A)

$$F = \frac{f_s}{q_c - \sigma_{vo}} \times 100$$ (Equation 4.3-B)

in which,

q_c = cone penetration resistance,

f_s = sleeve friction,

σ_{vo} = vertical overburden stress, and

σ'_{vo} = effective vertical stress.

The soil behavior type classification charts using normalized CPT and CPTU, proposed by Robertson (1990), are shown in Figure 4.3-A. Plots of normalized cone resistance (Q) versus normalized friction ratio (F) for data obtained from SCPT-1 through SCPTU-3 are shown in Figure 4.3-B through D, respectively. These sediments are classified as silt, ranging from silty clay to silty sand. Data corresponding to sediments above the ground water table plot dominantly in the "over-consolidated, aged, cemented" part of Zone 3, 4, and 5. Data corresponding to sediments immediately below the groundwater table plot in the "normally consolidated" to "sensitive" part of the boundary of Zone 3 and 4. The data corresponding to the sediments immediately over bedrock plot in the "normally consolidated" part of Zone 5.

Geological evidences, presented and discussed in Chapter 2 and 3, indicate that the glaciolacustrine silt sediments of glacial Lake Penticton have never been over-consolidated. Consequently, these sediments are normally consolidated soils. As a result, the position of the CPT test data to the right side of the "normally consolidated" zone and in the "over-consolidated, aged, and cemented" zone should be due to physical and chemical processes involved in inter-particle structural bonding rather than mechanical over-consolidation.

Grain size distribution analyses performed as part of several studies including those by Meyer and Yenne (1940), Fulton (1965 and 1975), Quigley (1976), Evans and Buchanan (1976), Lum (1977), and Wilson (1985) generally indicated more than 85% silt size particles. Taking into account the dominant presence of silt size particles in the grain size distribution of these sediments, the position of a significant amount of CPT test data in Zone 5, which is "sand mixture" zone, imply that bonding and structural changes shifted the results of these normally consolidated sediments not only to the right but also upward. It appears that bonding and structural improvements cause a shift in CPT test data relatively towards top right corner of the chart as shown in Figures 4.3-B through D.

Nasmith (1962) stated that if deposits, which belong to geological times prior to the Fraser Glaciation, were present in the Okanagan Valley, they should be in an over-consolidated state due to occupation of the valley by the Okanagan ice lobe during the Fraser Glaciation. Nasmith (1962) reported the presence of a layer of normally consolidated clay that overlying the bedrock and underlying Okanagan Valley. The presence of this normaly consolidated clay is an evidence of complete shearing the Okanagan Valley by the Fraser Glaciation and absence of pre-Fraser Glaciation deposits in the valley. The soil profile obtained using the CPT for sediments below lake level (i.e., 29 m and deeper) is in agreement with the theory elaborated by Nasmith (1962) and detects and confirms the presence of "normally consolidated" and "sensitive" silty sediments overlying the bedrock and underlying Okanagan Lake. Also, based on pore pressure measurements and results of the normalized cone resistance, it appears that there is a tiny layer of sandy silt overlying the bedrock at a depth of approximately 36 m (Figure 4.3-D).

4.4 Assessment of Soil Structure

Mitchell and Solymar (1984) presented results of CPT testing carried out to monitor ground improvement for the foundation of Jebba Hydroelectric Development Project on Niger River in Nigeria. Blast densification and vibro-compaction was used. It was found that cone penetration resistance increased by time. Mitchell and Solymar (1984) speculated that cementation at particle contacts due to dissolution and re-deposition of silica in both quartz and amorphous forms were possible primary factors in the increased cone penetration resistance observed. They also commented that providing reasonably constant environmental conditions, the reaction involving silica might continue for several years.

Eslaamizaad and Robertson (1996(a)) stated that the use of the small strain shear modulus (G_o) in conjunction with cone penetration resistance can improve the evaluation of structural improvements such as cementation and aging in soils. Cone penetration testing in conjunction with seismic down-hole method (SCPTU) allows the measurement of the interval shear wave velocity (V_s). The small strain shear modulus (G_o) can be evaluated from the mass density (ρ) and the interval shear wave velocity (V_s) as follows:

$$G_o = \rho(V_s)^2 \qquad \text{(Equation 4.4-A)}$$

Eslaamizaad and Robertson (1996(a)) proposed a log-log scale presentation of normalized cone resistance ($q_{c1}=(q_c/P_a)/(\sigma'_{vo}/P_a)^{0.5}$) versus G_o/q_c to evaluate compressibility and structural improvements in cohesionless soils. Data obtained from SCPTU-1, 2, and 3 are plotted in Figure 4.4-A on a log q_{c1} versus log G_o/q_c scale. As explained in Chapter 2 and 3, Penticton silt sediments have not been over-consolidated. Consequently, any deviation from the normally consolidated, unaged, and uncemented state should be due to soil structure improvements. As can be seen in Figure 4.4-A, the results of this study plot to the right of the normally consolidated, unaged, and uncemented zone. This implies the presence of bonding in the soil structure of these sediments. Except for the normally consolidated sensitive strata below lake level (29.0 m to 35.0 m), it appears that the compressibility of the deeper sediments decreases and the strength of the bonding in the soil structure increases. Data from deeper sediments plot in an area of the chart typical for cemented sand.

Eslaamizaad and Robertson (1996(b)) proposed the following equation for identifying cemented sands and estimating cementation level in the structure of sands:

$$\frac{G_o}{P_a} = 290.84\left(\frac{q_c}{P_a}\right)^{0.25}\left(\frac{\sigma'_{vo}+a'_p}{P_a}\right)^{0.355}\left(1.0+\frac{a'_p}{P_a}\right)^{2.1695} \qquad \text{(Equation 4.4-B)}$$

in which,

G_o = small strain shear modulus,

P_a = reference pressure of 100 kPa,

q_c = cone penetration resistance in kPa,

σ'_{vo} = effective overburden pressure,

a'_p = attraction intercept, defined as $c'_p / \tan \phi'_p$.

Using Equation 4.4-B, data obtained from SCPTU-1, 2, and 3 are plotted in Figure 4.4-B on a log $(G_o/P_a)(P_a/q_c)^{0.25}$ versus σ'_{vo}/P_a scale. Contours of a'_p/P_a are also shown in the same figure, using Equation 4.4-B. As can be seen in Figure 4.4-B, the proposed equation by Eslaamizaad and Robertson (1996(b)) predicts the existence of some cementing bonds in these sediments.

Based on results presented in Figure 4.4-B, the average value of a'_p is equal to 20 kPa. This value for a'_p corresponds to approximately c'_p of 15 kPa. Lum (1977) reported values of c'_p for glaciolacustrine silt sediments in the southern interior of B. C. larger than 60 kPa. It appears that while the relationship proposed by Eslaamizaad and Robertson (1996(b)) predicts the presence of cementation, it cannot predict the magnitude. It should be mentioned that Equation 4.4-B was developed for sands using data from calibration chamber tests and by manipulation and elimination of relative density from two equations that correlate cone penetration and the small strain shear modulus with relative density. The magnitude of attraction intercept, estimated from data in Figure 4.4-B, cannot be judged because soil in this study is silt rather than sand and also the concept of relative density does not generally apply to silts. Chart of Figure 4.4-B can only be used as a preliminary guideline, taking into account the limited data used in its calibration.

4.5 Soil Parameters Interpretation

Soil parameter interpretation based on CPT can be divided in two main categories: drained and undrained. Drained and undrained interpretations are generally applied to coarse-grained soils of Zones 5, 6, and 7 and fine-grained soils of Zones 3 and 4 in soil behavior type classification, respectively. CPT test data for Penticton silt plot in Zones 3, 4, and 5, but Penticton silt is fine-grained. As it was discussed, Penticton silt conceptually belongs to Zones 3 and 4, but it is transformed to Zone 5 because of cementation. Consequently, the focus of this section is on undrained interpretations. In addition, because of cohesionless nature of Penticton silt, a reference is also made to possible evaluation of friction angle.

4.5.1 Undrained Shear Strength

Robertson and Ghionna (1987) stated the following empirical relationship for estimating undrained shear strength of saturated clays from cone penetration resistance:

$$S_u = \frac{q_c - \sigma_{vo}}{N_K} \qquad \text{(Equation 4.5.1)}$$

in which:

q_c = cone penetration resistance,

σ_{vo} = total overburden pressure, and

N_K = an empirical cone factor with values between 5 and 20 with an average value of 15.

Results of S_u evaluation using data obtained from SCPTU-1, 2, and 3 are presented in Figure 4.5.1. Lum (1977) carried out triaxial testing using samples at saturated, in-situ water content (8%), air-dried (with 2% water content), and oven-dried states. Results of tests carried out by Lum (1977) indicate values of undrained shear strength ranging between 100 kPa for saturated state and up to 700 kPa for oven-dried state. Based on comparison of the results presented in Figure 4.5.1 with test results reported in the literature, it appears that Equation 4.5.1 over-estimates the undrained shear strength of these sediments. It should be reminded that Equation 4.5.1 was developed for saturated clays, but Penticton silt is unsaturated silt. The large values of undrained shear strength obtained using Equation 4.5.1 can be due to unsaturated state of these sediments. On the other hand, as can be seen in Figure 4.5.1, the maximum values of undrained shear strength are at depths 20 m to 25 m. Site reconnaissance showed that the water content at such depths are large enough to prevent any enhanced behavior because of unsaturated state. It appears that using a value larger than typical value of 15 for N_K may be appropriate for predicting undrained shear strength of these sediments.

4.5.2 Sensitivity

Sensitivity (S_t) of clay can be defined as:

$$S_t = \frac{S_u}{S_{u(Remolded)}} \qquad \text{(Equation 4.5.2)}$$

in which:

S_u = undisturbed undrained shear strength and

$S_{u(Remolded)}$ = totally remolded undrained shear strength.

Lunne et al. (1997) proposed that sensitivity could be assessed using CPTU data. According to Lunne et al. (1997), $S_{u(Remolded)}$ can be assumed equal to the sleeve friction (f_s) and S_u can be estimated using Equation 4.5.1.

Results of assessing sensitivity using data from SCPTU-1, 2, and 3 are shown in Figure 4.5.2. Knowing that data from these sediments plot in the "over-consolidated, aged, and cemented" area of the soil behavior type classification chart, it appears that there is a reasonable prediction of sensitivity using recommendations by Lunne et al. (1997). Penticton silt is a cohesionless silt and consequently, the sensitivity observed should be due to interparticle structural bonding. Having the cemented structure, it appears that these sediments are more sensitive than typical cohesionless soils. Also, it can be seen that the strata immediately below lake level is more sensitive.

4.5.3 Estimation of Yield Stress Ratio

Overconsolidation ratio (OCR) is defined as:

$$OCR = \frac{\sigma'_p}{\sigma'_{vo}}$$ (Equation 4.5.3-A)

in which:

σ'_p = maximum past effective consolidation stress and

σ'_{vo} = present effective overburden pressure.

Burland (1990) stated that the term "over-consolidation ratio" should be reserved for describing a known stress history. He proposed the use of the term "yield stress ratio" (YSR) defined as:

$$YSR = \frac{\sigma'_{vy}}{\sigma'_{vo}}$$ (Equation 4.5.3-B)

in which:

σ'_{vy} = vertical yield stress and

σ'_{vo} = effective overburden pressure.

Using this conceptually sound definition, vertical yield stress represents the overall effect of fabric, stress history, chemical processes such as cementation, and physical processes such as aging. In other words, YSR represents the overall state of soil structure and influences of physicochemical bonding.

Lunne et al. (1997) stated that the following equation can be used to assess yield stress ratio using cone penetration resistance (q_c):

$$YSR = k\left(\frac{q_c - \sigma_{vo}}{\sigma'_{vo}}\right) \qquad \text{(Equation 4.5.3-C)}$$

According to Lunne et al. (1997), values of k range between 0.2 to 0.5 with an average value of 0.3.

Equation 4.5.3-C was used to assess the YSR for Penticton silts. Results of this assessment using data from SCPTU-1, 2, and 3 are presented in Figure 4.5.3. Taking into account that as Nasmith (1962) stated, Penticton silt sediments have never been over-consolidated, the values of YSR, plotted in Figure 4.5.3, indicate presence of inter-particle bonding in the structure of these sediments. One may argue that the enhanced YSR observed for these Penticton silt may be due to its unsaturated state. In response, it should be mentioned that as it was observed during soil sampling, the water content of these sediments increases rapidly with distance from exposed faces. Also, CPT interpretation of YSR confirms the normally consolidated state of the strata below lake level, which was also stated by Nasmith (1962).

4.5.4 Friction Angle

Empirical assessment of friction angle using CPT data is generally limited to soils of Zones 5, 6, and 7 in soil behavior type classification chart (i.e. coarse grained soils). There is no reported empirical correlation for predicting friction angle of fine-grained soils like silts. Mineralogical studies such as study by Quigley (1976) indicate that Penticton silt is a cohesionless soil. Consequently, an attempt is made here to assess the friction angle of Penticton silt using the empirical correlations developed for coarse grained cohesionless soils like sands.

Robertson and Campanella (1983) proposed the following equation for evaluating friction angle of uncemented, unaged, moderately compressible, predominantly quartz sands using cone penetration resistance:

$$\tan\phi' = \frac{1}{2.68}\left[\log\left(\frac{q_c}{\sigma'_{vo}}\right) + 0.29\right] \qquad \text{(Equation 4.5.4)}$$

in which:

ϕ' = drained friction angle,

q_c = cone penetration resistance, and

σ'_{vo} = effective overburden pressure.

Friction angle of Penticton silt, using Equation 4.5.4, is approximately 32°. Lum (1977) reported drained friction angle approximately equal to 34°. Wilson (1985) reported values of friction angle between 34° and 42° using borehole shear test. As can be seen, results of prediction based on Equation 4.5.4 are relatively in agreement with above mentioned test results.

4.6 Summary

Three seismic piezo cone penetration tests (SCPTU) were carried out adjacent to Okanagan Lake Park Slide to incorporate the in-situ testing in the evaluation of the behavior of Penticton silt. CPT testing detected the stratified layered nature of these deposits. Interpretation from soil behavior type classification chart indicates that these silt sediments are cemented. Methods of detection of Cementation, proposed by Eslaamizaad and Robertson (1997 (a) and (b)), appear to be applicable to these sediments; but further calibrating data are required for quantitative assessment of magnitude of cementation. It appears that undrained shear strength was overestimated by CPT testing. Upon availability of reliable laboratory test data, empirical cone factor N_K should be modified to suit these bonded sediments. Sensitivity of these sediments was also detected by CPT testing. Reasonable estimates of yield stress ratio (also wrongly known as OCR) were obtained using CPT interpretation. Average friction angle is estimated to be approximately 32°.

Figure 4.2-A – The Location of the SCPTU Tests in the Vicinity of the Okanagan Lake Park Slide

(Picture is the courtesy of the B. C. Ministry of Transportation and Highways (1997))

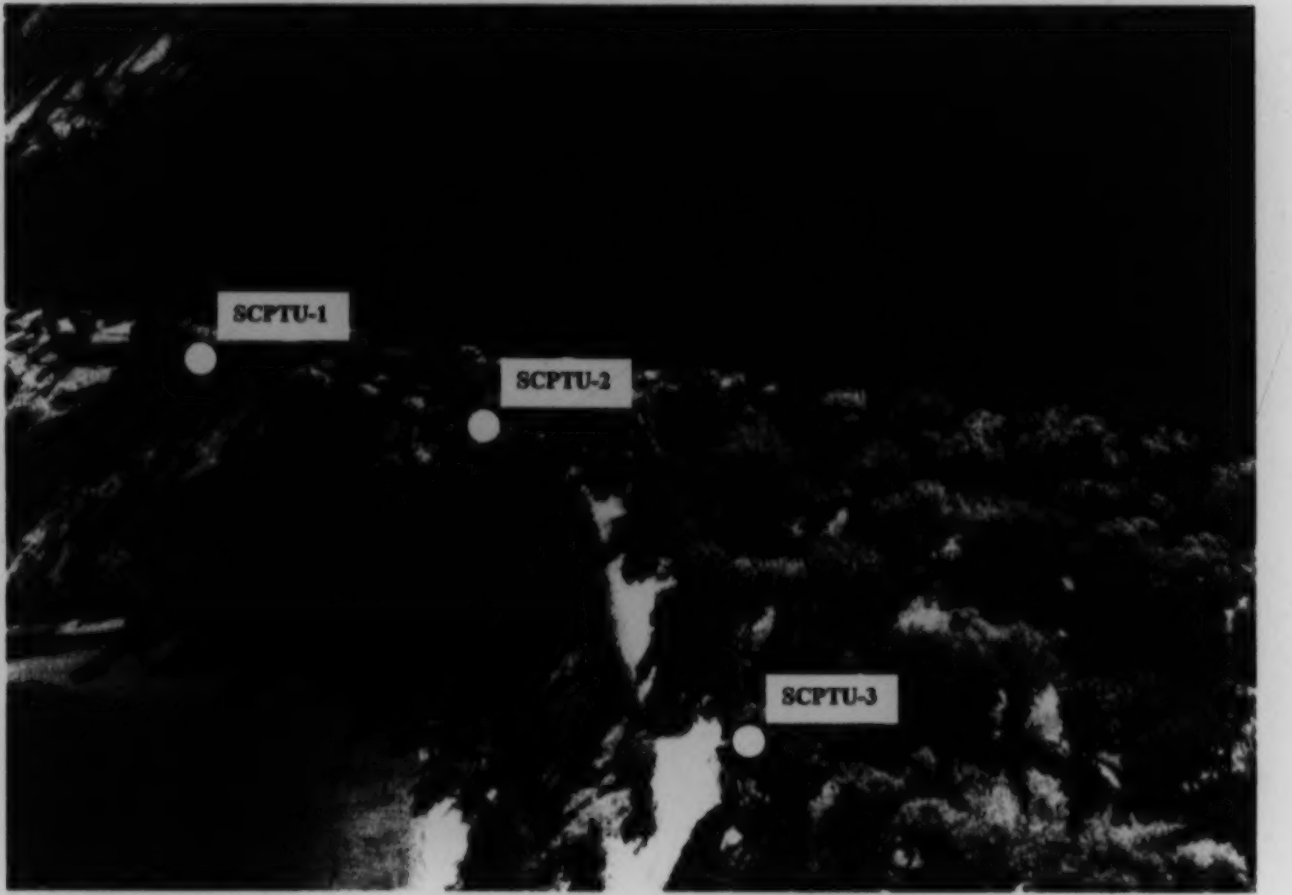
SCPTU-1
SCPTU-2
SCPTU-3

Figure 4.2-B - Summary of the Results for SCPTU-1

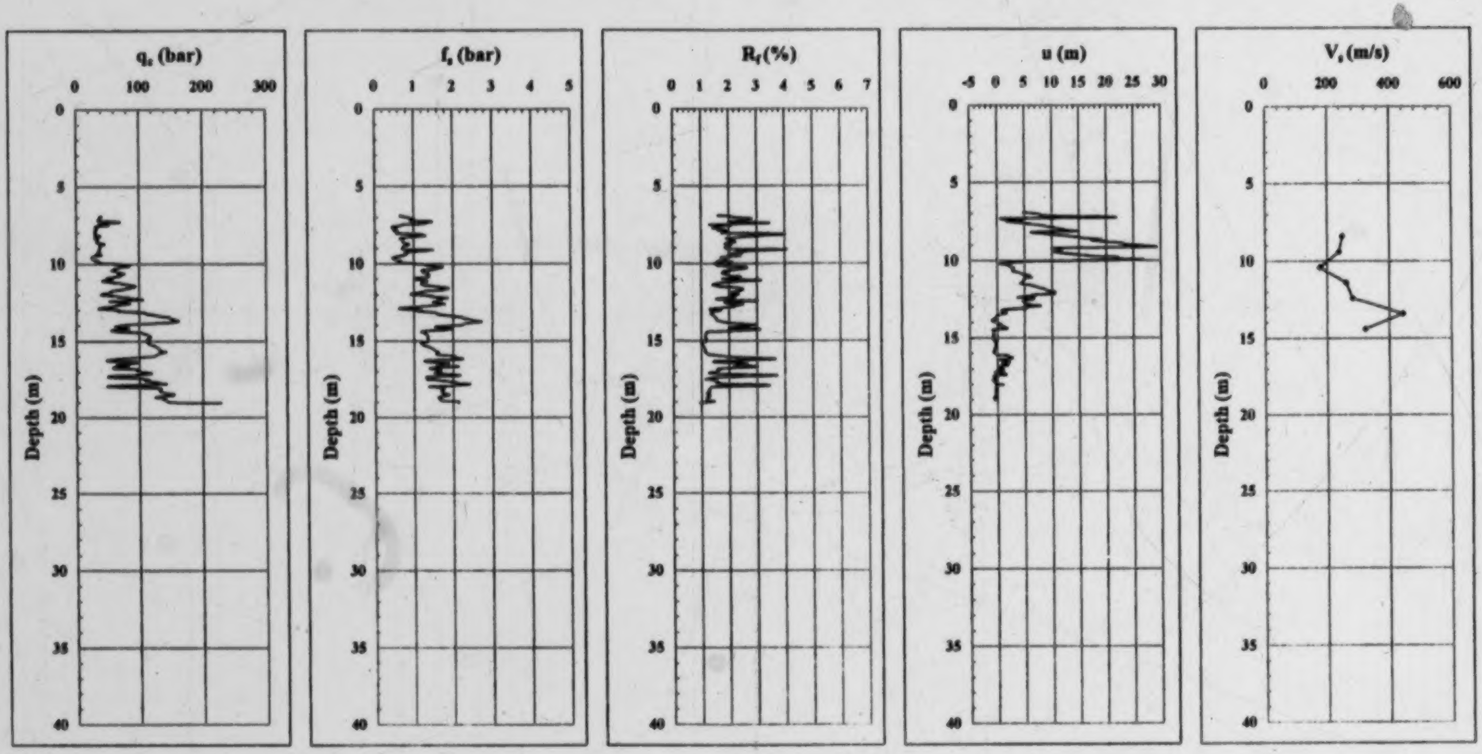

Figure 4.2-C - Summary of the Results for SCPTU-2

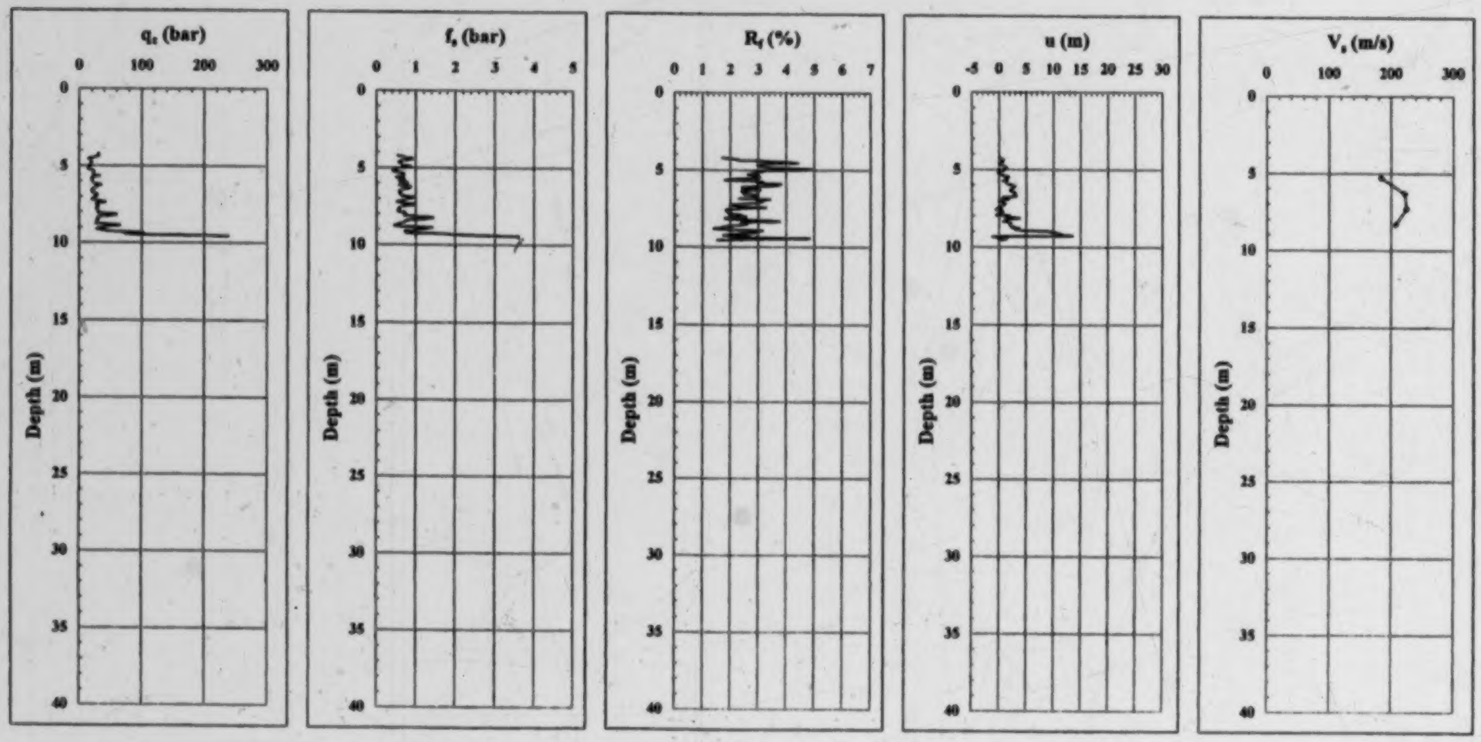

Figure 4.2-D - Summary of the Results for SCPTU-3

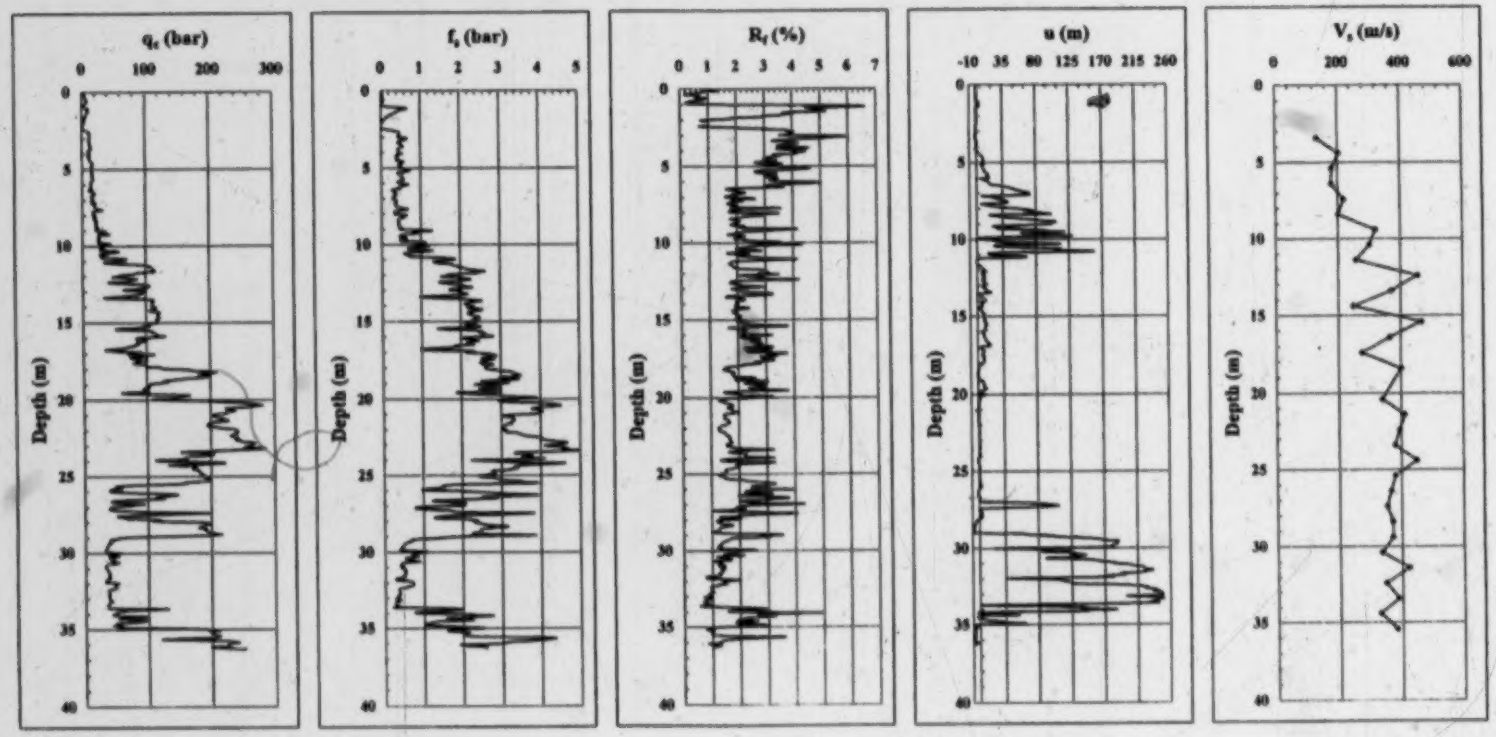

Figure 4.3-A – Soil Behavior Type Classification Chart Based on Normalized CPT and CPTU

(after Robertson (1990))

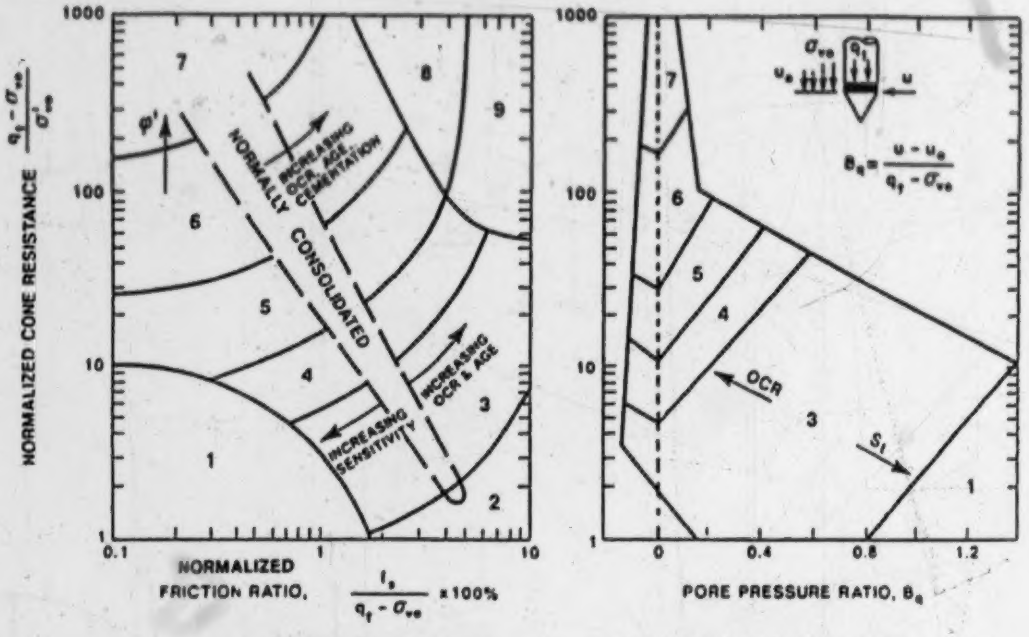

1. SENSITIVE, FINE GRAINED
2. ORGANIC SOILS – PEATS
3. CLAYS – CLAY TO SILTY CLAY
4. SILT MIXTURES – CLAYEY SILT TO SILTY CLAY
5. SAND MIXTURES – SILTY SAND TO SANDY SILT
6. SANDS – CLEAN SAND TO SILTY SAND
7. GRAVELLY SAND TO SAND
8. VERY STIFF SAND TO CLAYEY* SAND
9. VERY STIFF, FINE GRAINED*

(*) HEAVILY OVERCONSOLIDATED OR CEMENTED

Figure 4.3-B - Soil Behavior Type Classification (SCPTU-1)

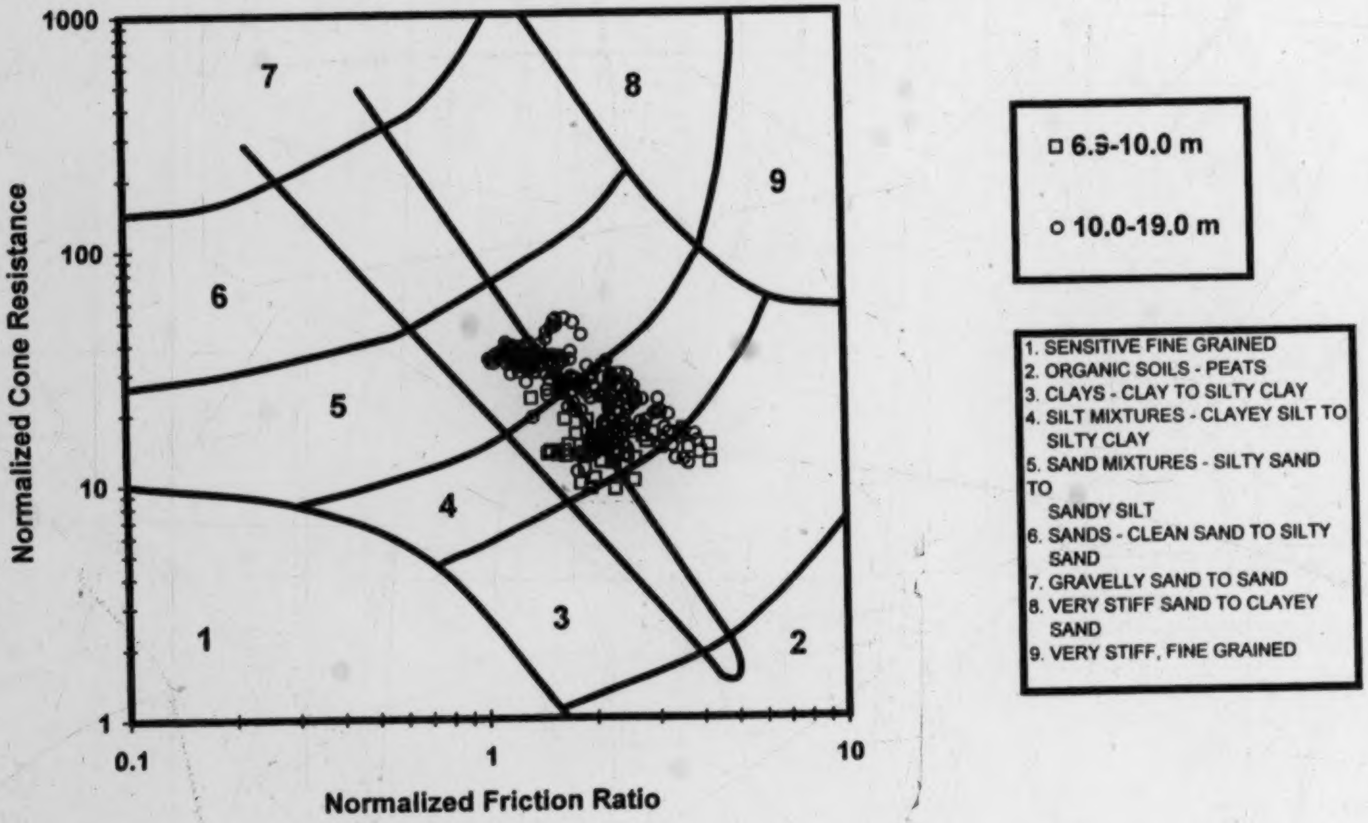

Figure 4.3-C - Soil Behavior Type Classification (SCPTU-2)

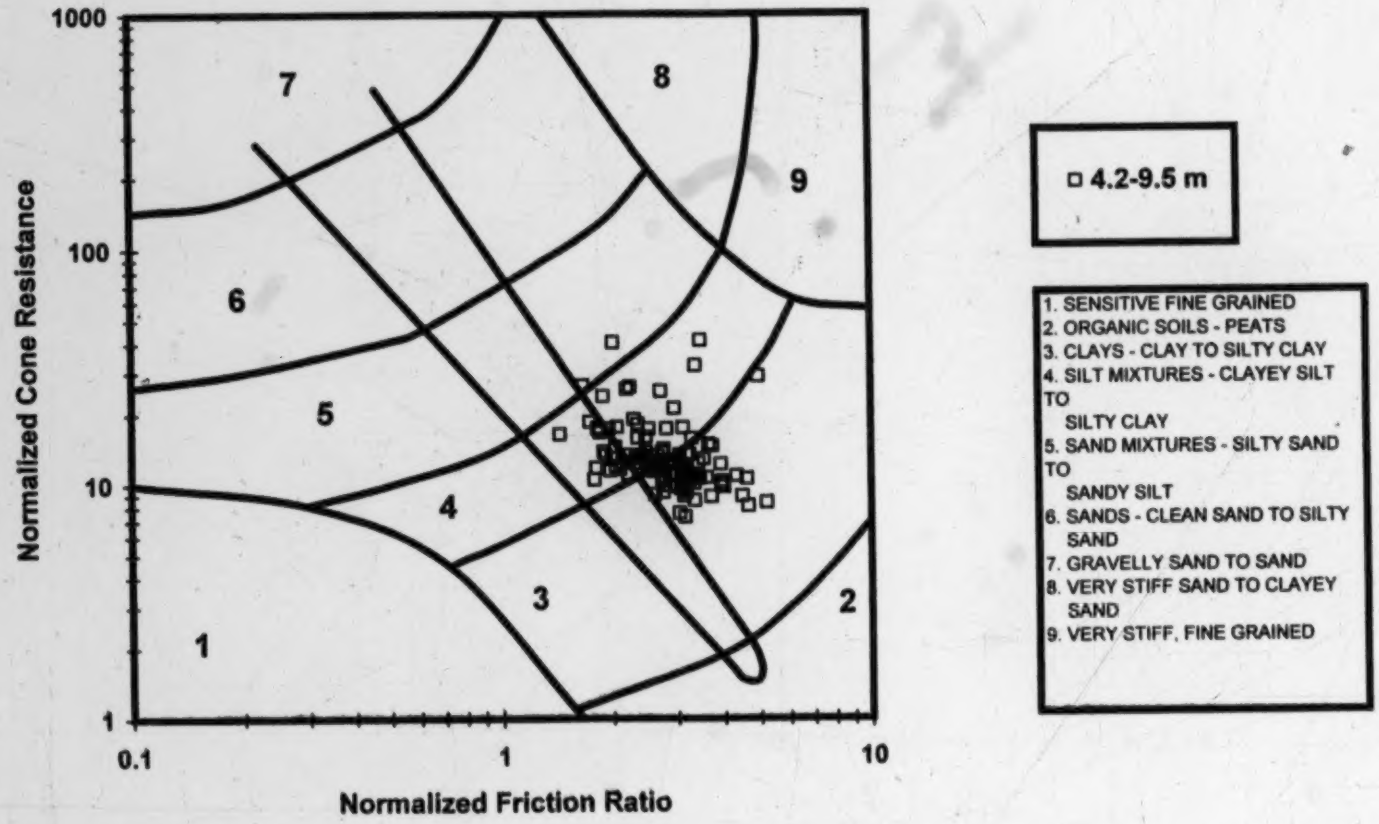

Figure 4.3-D - Soil Behavior Type Classification (SCPTU-3)

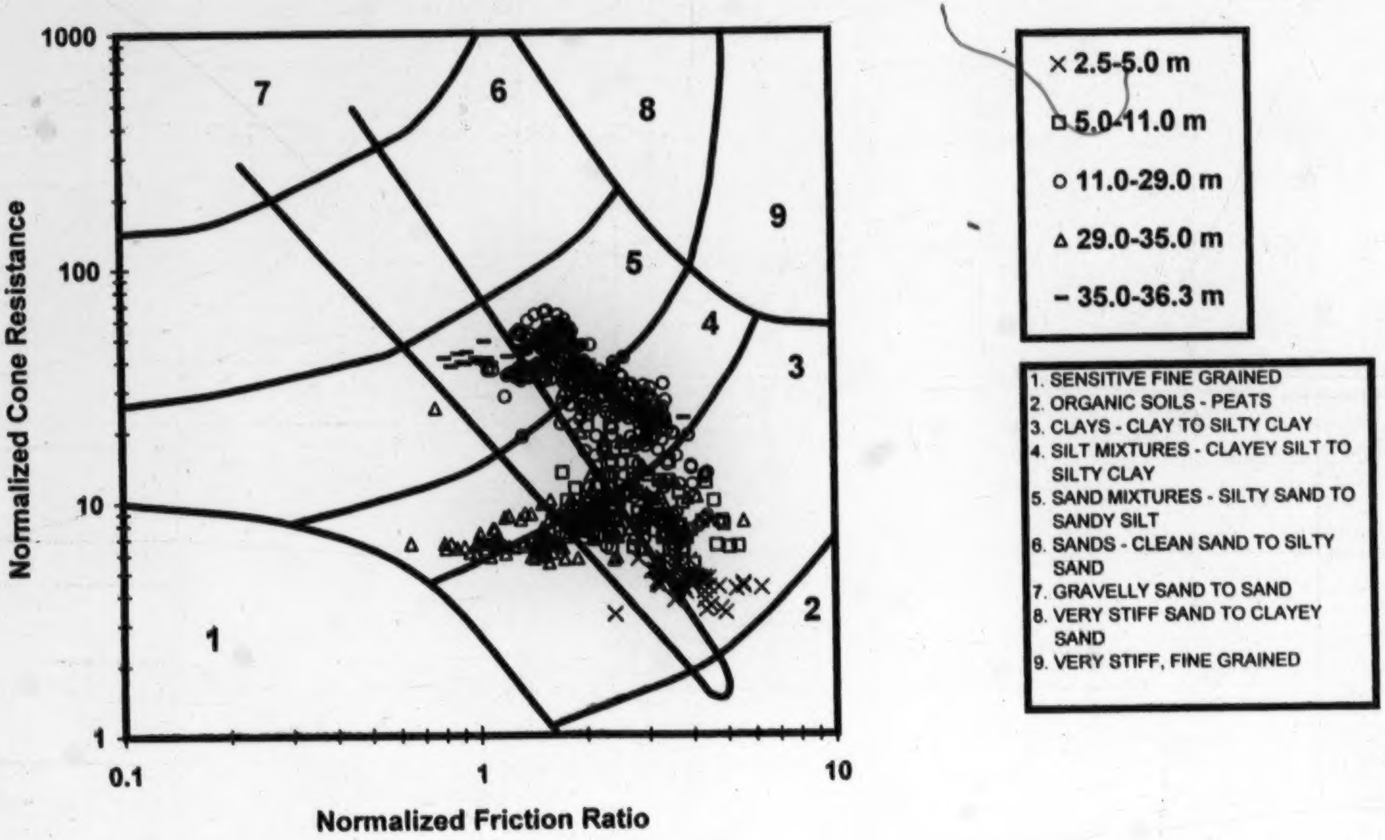

Figure 4.4-A - Use of Unusual Soil Identification Chart for Penticton Silt

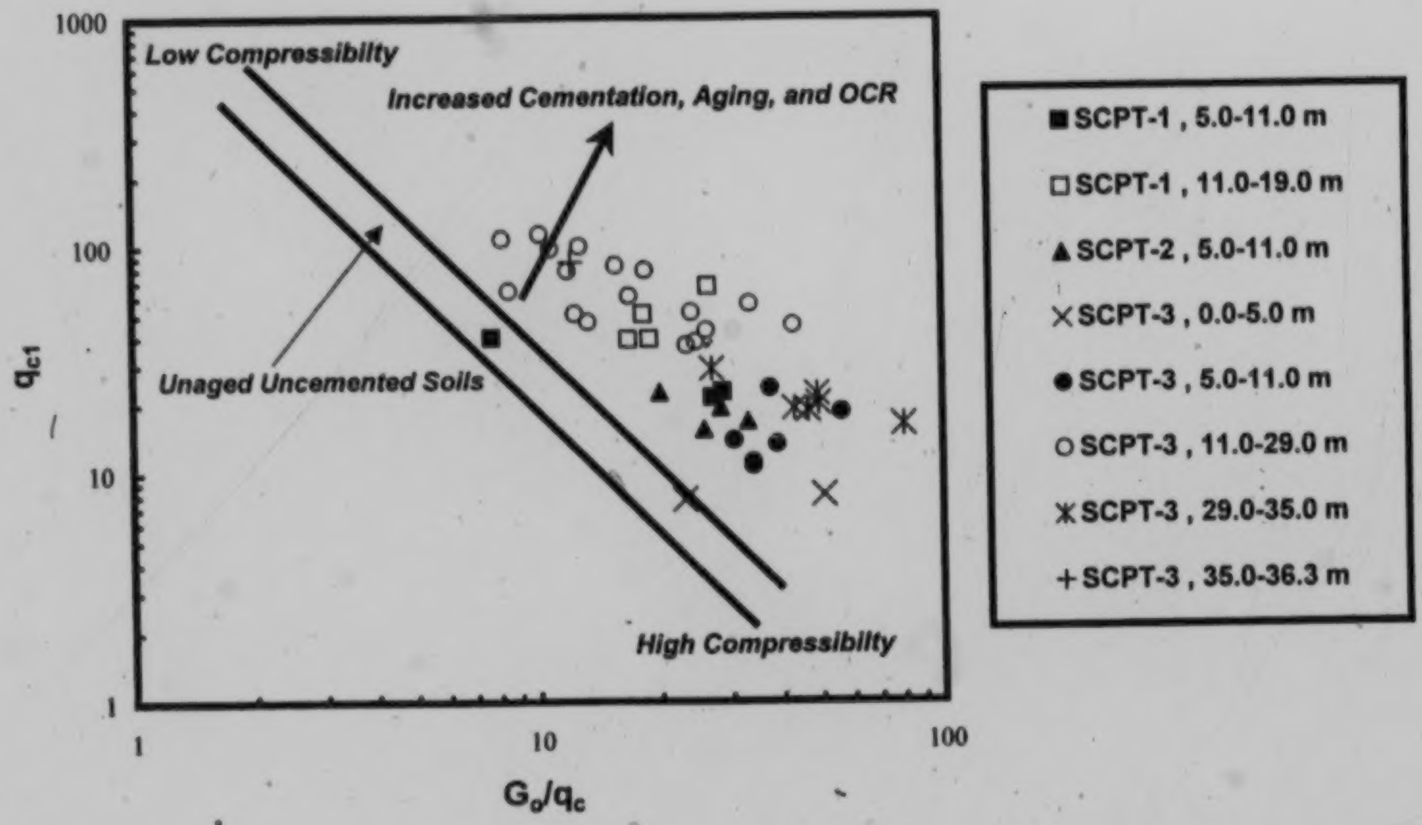

Figure 4.4-B - Use of Cementation Assessment Chart for Penticton Silt

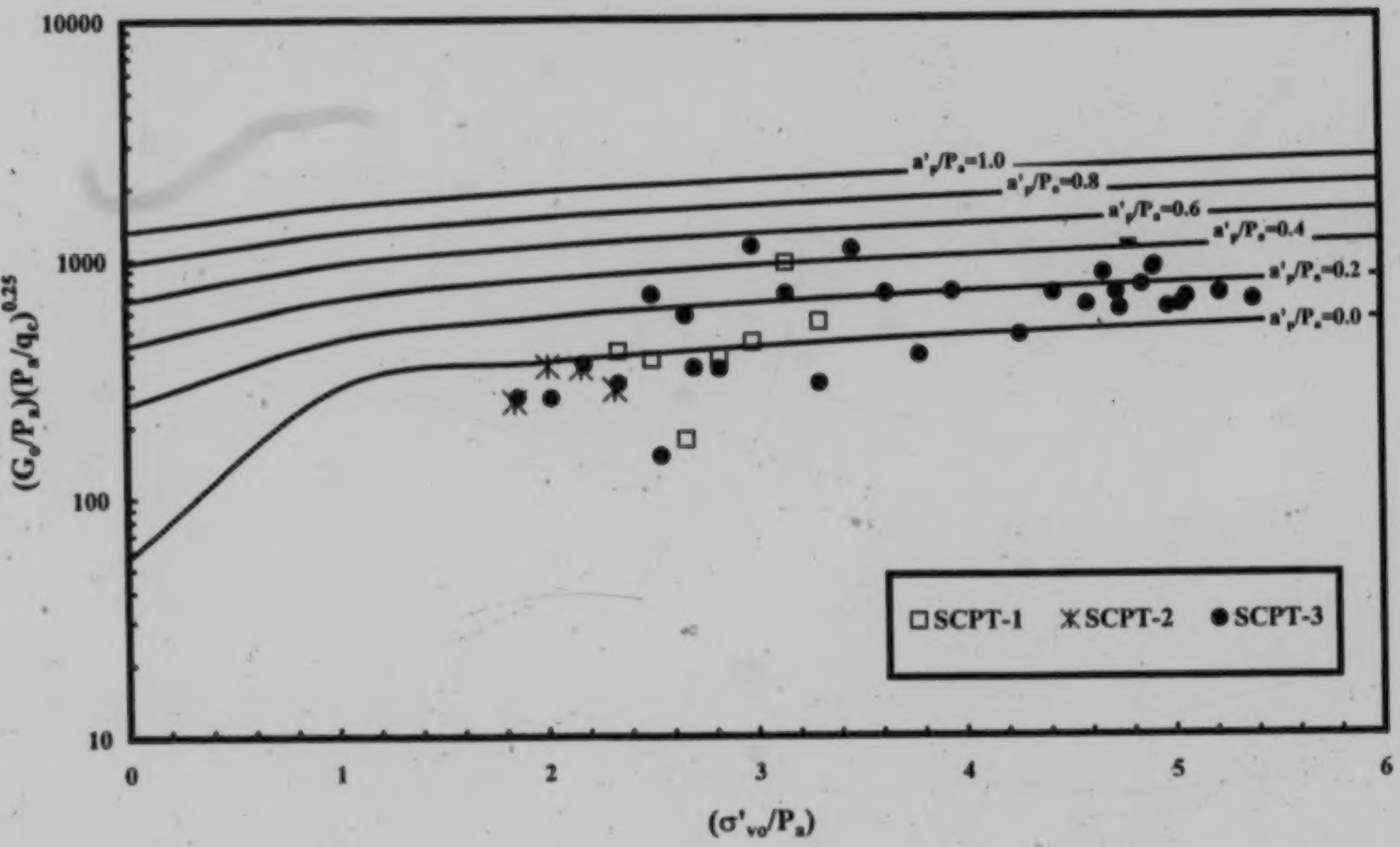

Figure 4.5.1 - CPT Evaluation of S_u for Penticton Silt

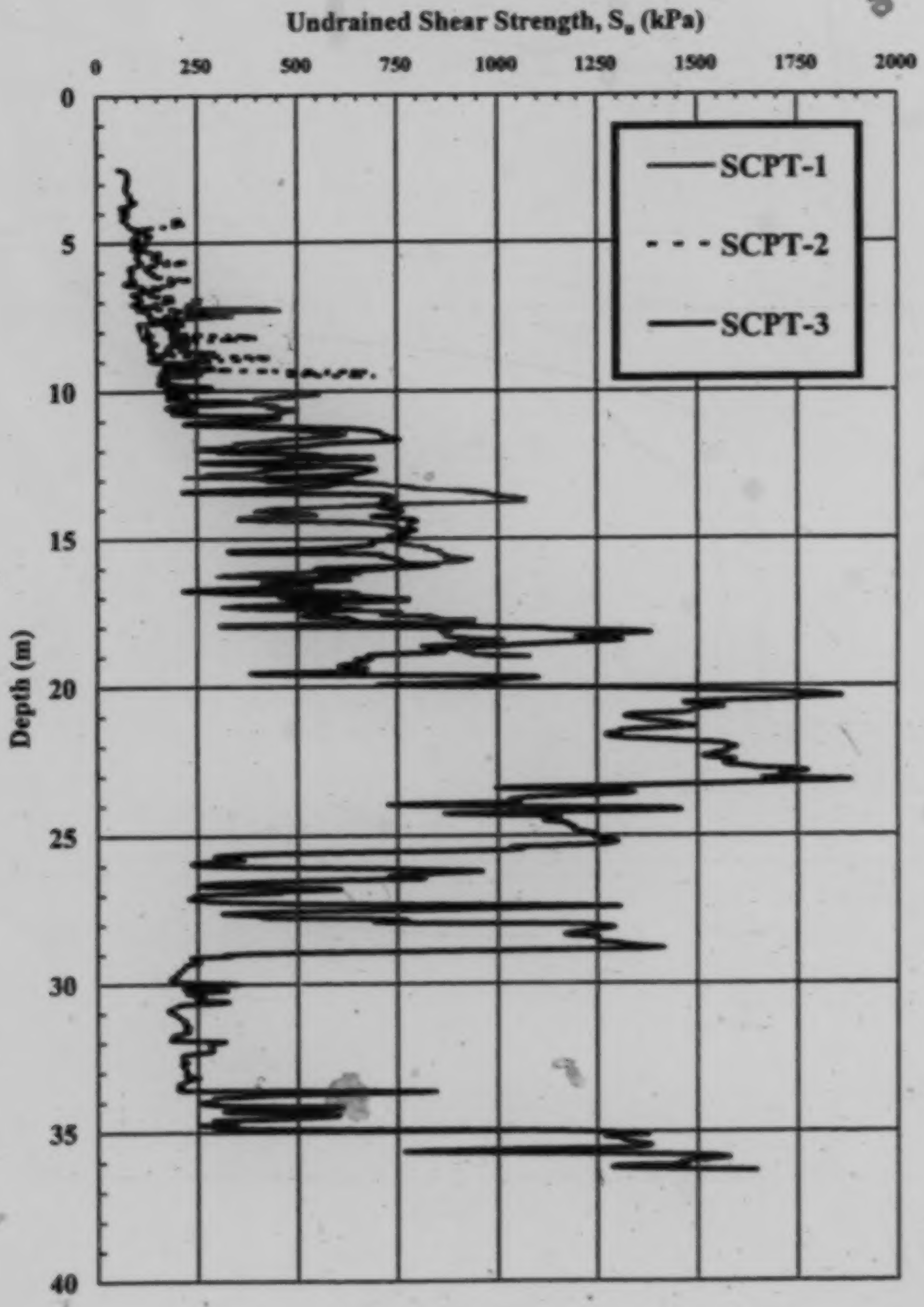

Figure 4.5.2 - CPT Evaluation of S_t for Penticton Silt

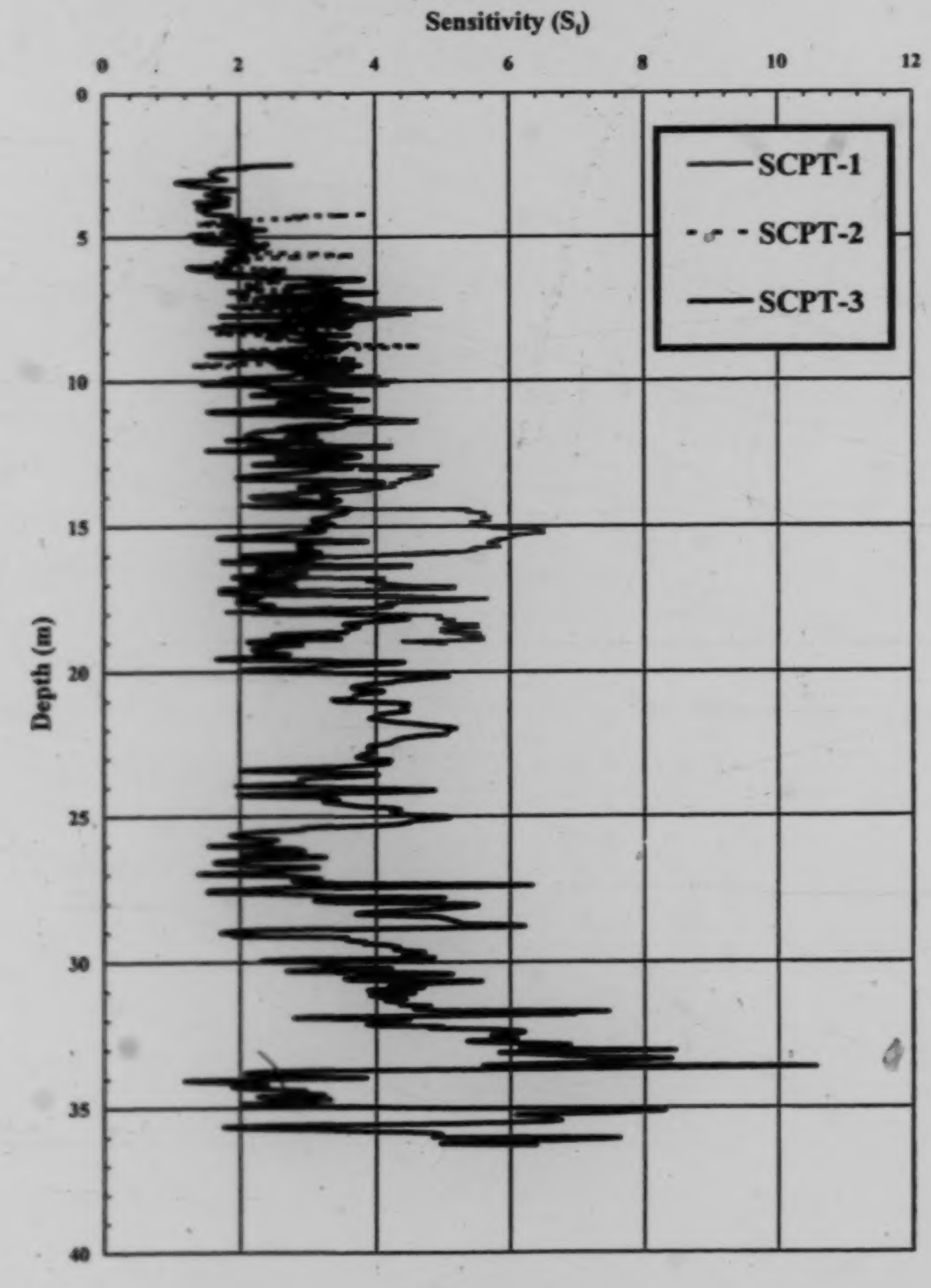

Figure 4.5.3 - CPT Evaluation of YSR (OCR) for Penticton Silt

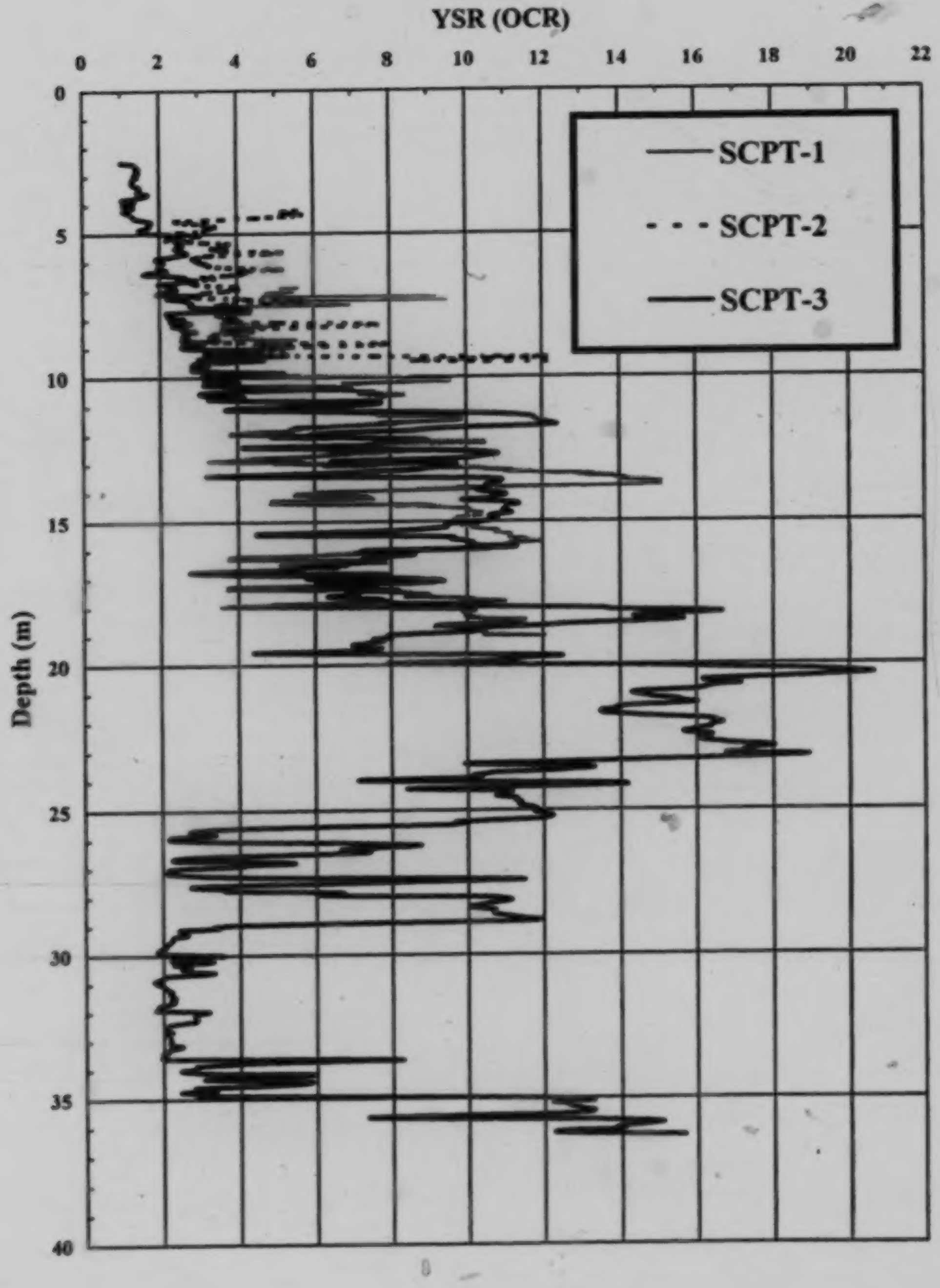

CHAPTER FIVE

Basic Properties of Penticton Silt

5.1 Introduction

Geotechnical engineers use basic soil properties to make preliminary assessments regarding the behavior and response of soils. Basic soil properties are also used to develop empirical relationships. In other areas of science and engineering, a variety of soil properties are considered to be basic properties and are used to estimate preliminary parameters.

As part of this study, it was necessary to determine the basic properties of Penticton silt. The glaciolacustrine silt sediments in the southern interior of British Columbia, including Penticton silt, are relatively unique geological features and there is relatively limited information available about their physical, and chemical properties. An experimental program was carried out to determine and study the basic properties of Penticton silt. Determination of grain size distribution, specific gravity, Atterberg limits, soil-water characteristic curves, mineralogy, soil fabric, and soil and pore fluid chemistry was carried out.

In this chapter, previous studies involving basic properties of glaciolacustrine silt sediments in the southern interior of British Columbia are reviewed and the results from this study are presented and discussed. A summary and concluding remarks from the discussions are also presented.

5.2 Grain Size Distribution

Several researchers have studied the grain size distribution of glaciolacustrine and colluvial deposits in the interior of British Columbia, especially the southern interior. The results of these studies are summarized in Table 5.2.

Three series of grain size analyses were carried out on Penticton silt samples from Koosi Creek Slide and Okanagan Lake Park Slide sites. Tests were performed according to ASTM D421 and D422. Commercially available sodium hexa-metaphosphate $(NaPO_3)_6$, known as Calgon, was used as a dispersion agent. Results of representative grain size analyses are shown in Figure 5.2.

Results of the current study indicate less than 2% sand, 85% to 90% silt, and 8% to 13% clay size portion. These soils are dominantly composed of silt size grains. Sand portion consists of very fine sand grains and the silt size portion is uniform medium silt. These results are in good agreement with the reported grain size distributions in the literature.

The similar grain size distributions of samples obtained from localities on the east and west shores of Okanagan Lake are in support of coments by Evans (1982). He stated that lack of significant difference between grain size distribution of different silt varves, which also implies minor importance of clays in the glaciolacustrine silt sediments in the southern interior of B. C.

In addition, soil sampled at Okanagan Lake Park Slide site is finer grained than soil sampled at Koosi Creek Slide site, which is located at higher elevation. This observation is also in agreement with studies by Fulton (1965 and 1975). He concluded finer grained texture for sediments at the higher elevations of the silt bluffs.

5.3 Specific Gravity, Density, and In-Situ Void Ratio

Several researchers have studied the specific gravity, density, and in-situ void ratio of glaciolacustrine and colluvial deposits in the interior of British Columbia, especially the southern interior. The results of these studies are summarized in Table 5.3.

Specific gravity measurements were carried out on a total of eight samples of Penticton silt from Koosi Creek Slide and Okanagan Lake Park Slide sites. Tests were performed according to ASTM D854. Knowing the presence of mica minerals in these sediments, soil samples were boiled for at least 6 hours. Results were uniform with values from 2.64 to 2.69 with an average of 2.67.

Values of specific gravity measured as part of this study are in agreement with values reported for silty material by Bowles (1986). Results reported by Meyer and Yenne (1940) and Lum (1977) are consistent with values that Bowles (1986) reported for soils containing mica or iron. Results of the current study appear to be small relative to values reported by Bowles (1986) for soils containing mica. Values reported by Bowles (1986) are representative for soils containing biotite mica rather than muscovite mica, which according to X-ray diffraction analyses (section 5.6) is the case for Penticton silt. Also, It should be mentioned that samples were boiled for more than six hours in order to assure the release of possible entrapped air and results were consistent.

5.4 In-Situ Water Content and Atterberg Limits

Several researchers have studied the in-situ water content and Atterberg limits of glaciolacustrine and colluvial deposits in the interior of British Columbia, especially the southern interior. The results of these studies are summarized in Table 5.4.

Three series of tests were carried out to determine liquid, plastic, and shrinkage limits of Penticton silt. Large swelling upon exposure to extra moisture and under no confinement is one of the interesting characteristics of these sediments. During the experimental program, undisturbed samples showed swelling up to 45% by volume. Also to a lesser degree, slurry samples showed some signs of shrinkage and volume decrease upon exposure to drying. Due to sensitive behavior observed, it was also felt appropriate to determine the shrinkage limit. Liquid and plastic limits were determined according to ASTM D4318 specifications and shrinkage limit was determined according to ASTM D427 specifications. Also water content determinations were carried out according to ASTM D2216.

The values of liquid, plastic, and shrinkage limits are 39%, 33%, and 31%, respectively, for samples obtained at Okanagan Lake Park Slide site. The corresponding values for samples from Koosi Creek Slide site are 35%, 30%, and 29%, respectively.

Water content determinations were carried out on undisturbed samples obtained at different depths in Koosi Creek Slide and Okanagan Lake Park Slide sites. The water content at saturation is more than 43%, which is higher than the liquid limit. The in-situ water content in these sediments usually ranges from 15% to 25%, depending on seasonal changes and depth. The water content of exterior one meter generally decreases from 10% to as low as 2% in the desiccated crust.

The reported values of Atterberg limits in the literature vary over a broad range. Results of the current experimental program fall within the reported values in the literature. The range of reported values for liquid limit is so broad that it covers the experimental results of the current study for liquid, plastic, and shrinkage limits. There have been attempts to link the behavior of soils, especially fine-grained soils, to Atterberg limits. Taking into account the diverse results, reported for the Atterberg limits of these uniform sediments, it is improbable to have a reasonable assessment of the response and behavior of these soils by trying to link them to Atterberg limits.

Using values of liquid and plastic limits obtained in this study, plasticity index ranges between 5% and 6%. Combining the results of grain size distribution and Atterberg limits determination, Penticton silt is classified as A-4 silty soil and ML soil in AASHTO and Unified Soil Classification systems, respectively.

5.5 Soil-Water Characteristic Curve

Lum (1977) carried out triaxial testing using unsaturated samples of glaciolacustrine silt from the South Thompson Valley. In an attempt to interpret the extra strength of the unsaturated samples, Lum (1977) presented the minimum values of negative pore pressures that are required to satisfy the equilibrium. These minimum required values of negative pore pressures, which were also referred to as capillary tension, were 400 kPa, 620 kPa, and 1500 kPa for samples at 7.7%, 2.3%, and 0.0% water content, respectively. Knowing that there is no free water present in an oven-dried sample with 0.0% water content, Lum (1977) referred to the 1500 kPa stress as an apparent or effective value.

Wilson (1985) tried to perform in-situ measurements of matric suction using a tensiometer. It was found that the magnitude of in-situ matric suctions were larger than 80 kPa, which was the capacity of the tensiometer at that elevation.

The glaciolacustrine silt sediments in the interior of British Columbia are mainly in an unsaturated state. A soil-water characteristic curve can be an adsorption or a desorption curve. If the volumetric water content versus soil suction relationship is obtained by increments of water content for a dry soil specimen the soil-water characteristic curve is called an adsorption curve. If the relationship is obtained by discrete decrease of water content, the corresponding curve is called a desorption curve. As part of this study, the desorption soil-water characteristic curves were obtained using pressure plate apparatus and the axis-translation technique as explained by Fredlund and Rahardjo (1993). Undisturbed specimens were trimmed from block samples in an environment of +4° C and 100% relative humidity and were saturated under an approximate 1 m head of water. Possible swelling of the specimens was prevented by vertical confinement using an axial mechanical spring. The available porous stones, used in the pressure plate apparatus, had air entry values of 500 kPa or less. As a result, soil-water characteristic curves could be obtained for values of soil suction up to maximum 500 kPa. Results of desorption soil-water characteristic curves for six specimens obtained from the samples of the Penticton silt in Koosi Creek Slide and Okanagan Lake Park Slide sites are shown in Figure 5.5-A.

One of the main features of the glaciolacustrine silt sediments in southern interior of British Columbia is their unsaturated state, but unfortunately and surprisingly there is no record of any previous reliable experimental in-situ or laboratory measurements of soil suction for these sediments. Values presented by Lum (1977) were minimum speculated values require for interpretation of triaxial test results. Attempts by Wilson (1985) at in-situ measurements were unsuccessful due to limited equipment capacity. The results of this study for the desorption soil-water characteristic curves of Penticton silt are the first documented experimental data.

Typical soil-water characteristic curves for a sandy soil, a silty soil, and a clayey soil, adopted from Fredlund and Xing (1994), are shown in Figure 5.5-B. The desorption soil-water characteristic curves for Penticton silt (Figure 5.5-A) are in agreement with expected typical response for the desorption (drying) curves of a silty soil, as discussed by Fredlund and Xing (1994).

Experimental result measured for Specimen OL-1, shown in Figure 5.5-A, is different from the experimental curves of the other specimens. It appears that at a given matric suction, Specimen OL-1 has smaller volumetric water content than other specimens tested. This difference could be due to collapse of the specimen during the saturation as a result of axial vertical stress, induced by the mechanical axial spring on top of the specimen. Taking into account that the possible collapse implies change in fabric and structure of the soil, the author believes that results obtained for this specimen are not reliable and representative of the undisturbed in-situ state of the Penticton silt. As a result, soil-water characteristic curve obtained for Specimen OL-1 is disregarded and is not taken into account in this discussion.

Typical desorption and adsorption soil-water characteristic curves for a silty soil, adopted from Fredlund and Xing (1994), are presented in Figure 5.5-C. Results presented in Figure 5.5-A indicate matric suction ranging from 100 to 300 kPa for values of volumetric water content from 35% to 21%, which correspond to typical gravitational water content in glaciolacustrine silt sediments (i.e., 25% to 15%). Air-entry value appears to be approximately 50 kPa and 100 kPa for soil samples obtained at Okanagan Lake Park Slide and Koosi Creek Slide sites, respectively. The corresponding volumetric and gravitational water contents are 50% and 36%, respectively. The experimental program could not be carried out at values of matric suction higher than 500 kPa because of limiting air-entry value of the pore-stones used in the test set up. Consequently, no reliable value for the residual water content could be obtained. Also no values for residual air content could be obtained, because no adsorption soil-water characteristic curves were obtained during the current experimental program.

The magnitude of suction at values of in-situ water content appears to be significant enough to have a positive contribution to the stability of these silt sediments. Decrease in magnitude of capillary tension (i.e. matric suction) upon increasing water content also appears to be a part of the swelling mechanism in silt sediments. Further investigations during this study indicate that saturating the specimens with an organic fluid and eliminating the matric suction did not cause swelling in these silt sediments. The organic fluid used in these experiments did not have any chemical interaction with the solid phase and did not damage the interparticle structural bonding. Details of the experimental program leading to this conclusion are discussed in Chapter Eight.

5.6 Mineralogy

Flint (1935) stated that the glaciolacustrine silt sediments in the Okanagan Valley consist of fresh feldspathic rock flour, cream-white to pale buff in color. Flint (1935) added that the silt is interbedded with very thin layers of gray to drab clay at low elevations. He did not mentioned what procedure he used to assess the mineralogy of the sediments.

According to Daly (1915), the mineralogical composition of the glaciolacustine silt sediments in the South Thompson Valley is 49% albite (low temperature and low pressure plagioclase feldspar), 15% orthoclase (a kind of K-feldspar), 8.5% anorthite (high temperature and high pressure plagioclase feldspar), and 18% quartz. It should be mentioned that Fulton (1965) stated that Daly (1915) reached this conclusion by means of a chemical analysis and analytical methods applicable only to igneous rocks.

Meyer and Yenne (1940) studied the mineral assemblage of the glaciolacustrine silt sediments in Okanagan Valley. Based on results of quantitative microscopic study on the sand size portion, 90% of the material were composed of equal amounts of quartz and feldspar. In turn, the feldspar portion was composed of 2/3 K-feldspar and 1/3 plagioclase (Ca-feldspar). It was mentioned that many feldspar particles had a "clouded appearance" because of possible kaolinization. The remaining 10% material was reported to be composed of unidentified particles, crystalline rock fragments, and particles of volcanic glass. Meyer and Yenne (1940) said that heavy minerals composed 5% to 10% of the silt size. The composition of heavy minerals is very diverse with hornblende and epidote-zoisite composing three quarters of it. Ferro-magnesian minerals were relatively abundance. Muscovite, brown biotite, and yellow and green volcanic glass were considered to be common.

Fulton (1965) studied the mineralogy of glaciolacustrine silt sediments in the South Thompson Valley. Optical procedure was used to analyze bulk samples. Due to extreme difficulty involved in using optical procedure for silt size particles, only very fine sand grain size portion of the bulk samples was analyzed. Results of the mineralogical analyses of bulk samples are summarized in Table 5.6-A(a). X-ray analysis was used for the clay size fraction. Results of mineralogical analyses of the clay size fraction are summarized in Table 5.6-A(b).

Quigley (1976) carried out x-ray diffraction analysis to study the mineralogy of glaciolacustrine and colluvial silts in Okanagan Valley and South Thompson Valley. It was found that glaciolacustrine and colluvial silts in both valleys had remarkable mineralogical resemblance. Results of the x-ray diffraction analyses are summarized in Table 5.6-A(a) and (b) for the whole soil samples and the clay size fractions, respectively. In contrast to considering clay minerals consisting of mica, illite, chlorite, kaolinite, and smectite as minor constitute of the whole soil sample, Quigley (1976) commented on the significantly strong peaks of the clay minerals on the powder patterns.

The mineralogy of Penticton silt was determined using X-ray diffraction analysis. The clay size fraction was separated from the bulk sample using an ultrasonic bath and then centrifuged. Due to technical set up of the centrifuge, clay size fraction is composed of less than 3 μm particles rather than less than 2 μm particles, which is the traditional boundary in geotechnical engineering. Taking into account the diverse reported mineralogy for these sediments in the literature, X-ray diffraction analyses were carried out in two independent laboratory facilities using undisturbed specimens carved from two different block samples for each site. Weight fractions were measured for both bulk and clay portions of the samples. Sodium metaphosphate was used as a deflocculating agent.

Results of the analyses for the bulk soil samples and the clay size fractions are presented in Table 5.6-B(a) and (b), respectively. Results of the two independent x-ray diffraction analyses were close and consistent. Data presented in these tables reflect overall test results of both independent analyses. Overall results indicate that soil samples from both sites are dominantly composed of mica (muscovite) and chlorite. There are traces of calcite and magnetite. The clay fraction, which is less than 10%, is mainly composed of chlorite, illite / muscovite, and smectite.

In addition, x-ray diffraction analysis was carried out on white precipitates, which were collected at the groundwater exit zone in Koosi Creek Slide site. Results indicate that those white precipitates are bloedite ($Na_2 Mg (SO_4)_2 4H_2O$).

Comparing the results presented in Table 5.6-A(a) and (b) and 5.6-B(a) and (b), it can be concluded that there is an overall agreement between the results obtained in the current study and the studies by Fulton (1965) and Quigley (1976).

Although the study by Quigley suggested only minor amount of mica, he commented on the fact that clay mineral peaks were significantly strong. In another part of his study while carrying out scanning electronic microscopic (SEM) analyses, Quigley (1976) confirmed the abundance of mica particles.

A significant mineralogical feature of these sediments is the abundance of muscovite and relative absence of biotite. This phenomenon can be misinterpreted as the occurrence of very intensive weathering in these sediments. Many soil scientists including Allen and Hajek (1989) suggested that the ratio of muscovite to biotite is an indicator of the degree of weathering in soil environment. Allen and Hajek (1989) said biotite is known to be less stable than muscovite and as the ratio increases (i.e. higher percentage of muscovite and lower percentage of biotite), soil is more weathered. The sharp and distinct mica peaks in the x-ray diffraction analyses indicate well preserved and non-weathered mica particles and reduce the possibility that these sediments were weathered. The high muscovite and low biotite content appears to be the consequence of temperature ranges that the parent rocks in the Monashee Mountains experienced during the past metamorphic activities. Muscovite belongs to lower metamorphic grade shale (greenschist), which occurs at a lower temperature range compared to the temperature range required for biotite formation. During the metamorphic activities in Monashee Mountains apparently the temperature did not get high enough to allow the formation of biotite.

Another major characteristic of these sediments is their large potential swelling behavior when exposed to water under the condition of no or small confining stresses (see Chapter Eight). The expanding clay portion was less than 3% of the total soil mass and such a small mass of expansive clays cannot explain the large observed swelling behavior. The sharp and distinct muscovite peaks in the x-ray diffraction analyses indicate well preserved and non-weathered mica particles and eliminate the possible presence of expandable 2:1 vermiculite particles, generated from weathered mica. The X-ray diffraction peaks for chlorite are compatible with trioctahedral chlorites, which are not expandable rather than pedogenic chlorites (hydroxy-interlayered vermiculite (HIV)), which are expandable. In summary, no expansive minerals at reasonably large mass were detected to be able to explain such a large swelling behavior.

These materials appear to be bonded. Visual inspection and also x-ray diffraction analyses, showed that magnetite is present in these sediments as a minor component. Schwertmann and Taylor (1989) said iron oxides including magnetite can influence the soil structure and create bonding between other major soil components. According to Schwertmann and Taylor (1989), iron oxides including magnetite can cause aggregation or cementation in the soil structure. If they are present in small quantity, they cause aggregation; and if they are present in large quantity, they cause cementation. The bonded and structured state of these sediments can be destroyed by introduction of water while bonds due to iron oxides are not soluble in pore fluids with pH>3. Consequently, while the presence of bonding due to iron oxides is evident, there should be other major sources of bonding for these materials. X-ray diffraction analysis can detect the presence of crystalline forms of the materials and cannot detect amorphous forms. No major crystalline salts, which can act as bonding agent, were detected. As a result, it can be concluded that the main source of soluble bonding cannot be found using x-ray diffraction analyses since it is likely in amorphous forms.

An interesting observation is the similarities between the mineralogy of the Norwegian and Canadian sensitive clays with the glaciolacustrine silt sediments in the interior of British Columbia. Norwegian and Canadian sensitive clays are well known cases of structured soils in which landslides and failures can occur due to structural failure and changes in physicochemical bonding. Karlsrud et al. (1984) and Tavenas (1984) reported the mineralogy of these sensitive clays. Based on results reported by them, both these sensitive clays are rather silty marine deposits and similar to the glaciolacustrine silt sediments in the interior of British Columbia, the dominant minerals are mica and chlorite.

5.7 Fabric and Scanning Electron Microscopy (SEM)

Meyer and Yenne (1940) carried out a macroscopic study using the silt size portion of the glaciolacustrine silt sediment samples from north shore of Skaha Lake and Mission Creek Valley in Okanagan Valley. Results indicated that particles were dominantly angular and lath-shaped with elongation indices larger than 10. Some reworked rounded particles were also observed.

Quigley (1976) carried out binocular and scanning electron microscopic studies on samples of glaciolacustrine and colluvial silts from Okanagan Valley and South Thompson Valley. Based on binocular microscopic observations, Quigley (1976) reported presence of an open porous structure composed of silt size grains of quartz, feldspar, and oriented mica. He added that presence of clay size particles was not apparent. Results of scanning electron microscopy indicated horizontally oriented structure composed of 5 microns to 40 microns silt grains. Large platy particles, which were found to be mica by x-ray analysis, were abundant. Quigley (1976) stated that while some precipitates were observed, presence of salt precipitates was not clear. Quigley (1976) also commented that cementation appeared to be involved in the stability of the soil structure, which consisted of agglomerated clusters.

Lum (1977) studied samples of undisturbed and remolded glaciolacustrine silt sediments from the South Thompson Valley. In both undisturbed and remolded samples, horizontal orientation of platy particles and consequently an anisotropic fabric were observed. Lum (1977) commented that undisturbed and remolded samples had similar fabric, which he referred to it as structure. Lum (1977) reported potential presence of mica, feldspar, and montmorillonite.

A series of scanning electron microscopy (SEM) with energy dispersive x-ray analysis (EDXA) were performed on a variety of undisturbed and reconstituted specimens from Okanagan Lake Park Slide and Koosi Creek Slide sites. The objective of these studies was to investigate the fabric and structure of these materials. These studies were undertaken on both vertical and horizontal fractures.

Undisturbed fractured surfaces were studied. Specimens were gold-coated to create connectivity on the sample surface and avoid charging due to accelerating voltage field. Argon gas in its plasma state was used in a high voltage field as the etcher element for gold coating process. Gold particles, scattered by Argon gas, fall on specimen surface like rainfall and create a coating on it. Due to a high vacuum in the specimen chamber of the SEM setup, moist specimens cannot be tested without any further preparation. In order to test moist and saturated samples, liquid nitrogen slush at –208° C temperature was used to freeze the samples instantaneously. It is stated that due to extreme cold temperature of the liquid nitrogen slush and very small size of the sample, such process freezes the free water in the sample in its locality and does not cause any disturbance to fabric and structure. Frozen specimens were fractured to obtain an undisturbed surface and were transferred to a chamber at –151° C to sublime the surface ice. Subsequently, it was gold coated in a chamber at –172° C.

Fractured surfaces of forty specimens from both sampling sites were studied and more than 250 SEM images were recorded. Selected images are presented in Figure 5.7-A through Q and are discussed in the followings:

Horizontal and vertical fractured surfaces of a silt specimen from Koosi Creek Slide site at its in-situ moisture condition are shown in Figure 5.7-A(a) and (b), respectively. The corresponding fractured surfaces for a silt specimen from Okanagan Lake Park Slide site are shown in Figure 5.7-B(a) and (b), respectively. In-situ water content of these specimens was at about 35% and 15%, respectively. Horizontal and vertical fractured surfaces of an air-dried specimen of a silt specimen from Okanagan Lake Park Slide site are also shown in Figure 5.7-C(a) and (b), respectively. Review of these images indicates that the fabric of the soils from both sites is highly anisotropic with horizontal layering at the level of grain to grain. Platy particles are dominant in the soil fabric and clay size particles are present in a limited quantity.

Figure 5.7-D(a) and (b) show horizontal and vertical fractured surfaces of a slurry specimen with water content of 50%. As can be seen the slurry specimen has a highly anisotropic fabric with horizontal layering at the level of grain to grain, similar to the undisturbed specimens.

A review of the above images is consistent with results of the studies by Quigley (1976) and Lum (1977) and indicates highly anisotropic fabric with preferred horizontal orientation and abundance of platy particles for both undisturbed and reconstituted specimens. Overall results of SEM analyses were also in agreement with results of mineralogical analyses using x-ray diffraction analyses. Also, in contrast with the result of his mineralogical analyses and following SEM analyses, Quigley (1976) concluded that the dominant mineral in the soil structure was 5 to 40 microns platy mica particles.

The effect of one cycle of environmental loading (wetting and drying) can be seen in fractured surfaces of a silt specimen from Okanagan Lake Park Slide site, shown in Figure 5.7-E and F. Horizontal and vertical fractured surfaces of the initially air-dried specimen, after gradual saturation under confined conditions, are shown in Figure 5.7-E(a) and F(a), respectively. The corresponding fractured surfaces of the same saturated specimen after being air-dried again are shown in Figure 5.7-E(b) and F(b), respectively. Comparison of an air-dried specimen such as the one shown in Figure 5.7-C(a) and (b) and images shown for the saturated specimen indicates no major changes in the soil fabric upon gradual saturation under confined condition. Further investigation of these images show that one cycle of environmental loading causes significant change in the soil fabric. Images, presented for the specimen under investigation after air-drying, show changes in soil fabric and formation of a more porous fabric. Formation of collapsible meta-stable voids as large as 20 microns is evident in both horizontal and vertical images.

Change in the soil fabric of these sediments upon slow gradual moistening (damping) and flooding under unconfined conditions are shown in Figure 5.7-G and H. Swelling and formation of micro-cracks with crack widths less than 30 microns in a specimen which was moistened gradually under unconfined condition can be seen in Figure 5.7-G(a). The spider net shape feature in this image is the frozen appearance of the soluble glue, which was used to attach the specimen on the testing stall. As can be seen in Figure 5.7-G(b), swelling and crack formation occurs at the level of grain to grain and no swelling clays are evident. Figure 5.7-H(a) and (b) show formation of cracks with crack widths less than 30 microns in a flooded specimen and disintegration of fabric and structure at the grain to grain level. The black shaded background is frozen water. These observations imply that destructuring due to introduction of moisture, crack formation, and soil swelling occur in the grain to grain and microstructure levels.

Some of the minerals and precipitates, which are present in these soils, are shown in Figure 5.7-I through Q. Energy despersive x-ray analyses along side with reference spectrums and images from Welton (1950) were used to recognize these minerals and precipitates.

Open and flexible muscovite and chlorite particles can be seen in Figure 5.7-I(a) and (b), respectively. According to Mitchell (1993), mica minerals are very flexible. Presence of flexible mica minerals such as muscovite and also open flexible particles similar to those observed in Figures 5.7-I(a) and (b) can imply large deformations and highly flexible behavior for these sediments.

Formation of illite from muscovite and its bonding to a muscovite grain can be seen in Figure 5.7-J(a) and (b). Chemical weathering similar to formation of illite from muscovite can lead to presence of bonding agents in the soil structure; but, such features were not observed in large amounts. Calcite is present in these sediments in limited quantity and a typical calcite particle can be seen in Figure 5.7-K. Calcite can be a source mineral for chemical elements required for carbonate formation in the soil environment. Overgrowth at particle contact and bonding between two muscovite grains can be seen in Figure 5.7-L.

Presence of precipitates that can cause bonding in soils can be seen in Figure 5.7-M through O. Precipitates of $Mg(OH)_2$ on the surface of a quartz grain is shown in Figure 5.7-M(a) while unknown precipitates can be seen on surface of soil grains in Figure 5.7-M(b). A precipitate bridge between two muscovites is shown in Figure 5.7-N(a) and (b). Formation of precipitates of magnesium (Mg) on the surface of a plagioclase can be seen in Figure 5.7-O(a) and (b). Images of aggregated particles from a zone that showed macroscopic evidence of presence of iron oxides are shown in Figure 5.7-P and Q. In addition, Figure 5.7-Q(a) and (b) show not only aggregated particles but also the high degree of flexibility of muscovite particles. The above mentioned observations can imply bonding due to the presence of these soluble precipitates; but, it should be mentioned that these features are not dominant and cannot be the main source of bonding in these sediments. Also, as mentioned in section 5.6, bonding due to iron oxides is not soluble in pore fluids like water, which have pH>3.

5.8 Soil and Pore Fluid Chemistry

Meyer and Yenne (1940) reported approximately 15% weight loss during the acid treatment of a silt soil sample from Okanagan Lake, Skaha Lake, or Mission Creek area. Meyer and Yenne (1940) considered weight loss as an indicator of calcite presence.

Quigley (1976) studied the soil chemistry of the glaciolacustrine and colluvial silts in Okanagan Valley and South Thompson Valley and results are summarized in Table 5.8-A. Values of pH were 8.1 to 9.1, which imply alkaline soil. Values of salinity imply that shallow colluvial silts contained more soluble salts than glaciolacustrine silts. Based on test results, carbonate content was 3.8% to 6.6%. Quigley (1976) commented that presence of x-ray peaks corresponding to calcite implied that these values were reasonable but they might be high because of the presence of sulfates. Based on x-ray diffraction analyses of white residues, produced by drying the supernatant liquids, Quigley (1976) speculated that salt precipitates in silt sediments include gypsum, sodium sulfate, sodium chloride, and calcium sulfate. Using back calculation analyses, Quigley (1976) reported values of soluble evaporites present in silt sediments ranging from 0.06% to 1.06%. He commented these percentages were too small to be detectable during x-ray diffraction analyses, but they are large enough that their occurrence at silt grain contact points can have a significant impact on the behavior of these sediments.

Nyland and Miller (1977) carried out soil chemistry analyses using soil samples obtained from Okanagan Valley and South Thompson Valley. It was concluded that there was no significant difference between chemical properties of glaciolacustrine and colluvial silts and also between Okanagan Valley and South Thompson Valley sediments. Detail of test results are not presented by Nyland and Miller (1977); but the B. C. Ministry of Transportation and Highways provided these test results and a summary is presented in Table 5.8-B. Glaciolacustrine and colluvial silt samples were collected from Magazine Gully and Harper Ranch Road in South Thompson Valley. Samples obtained from Okanagan Valley were from Main and South Gully in Penticton, Falkenberg property, and Chapman-Bauer property.

A full set of chemical analyses was performed on soil samples from Koosi Creek Slide and Okanagan Lake Park Slide sites. In addition, chemical analyses were performed on groundwater samples obtained from Koosi Creek Slide site. Soil and pore fluid chemistry analyses were carried out in a commercial laboratory according to generally accepted methods of analyses presented in Eaton et al. (1995), US EPA (1983 and 1986), and McKeague (1978). Results of these analyses are summarized in Table 5.8-C.

Results of this study for soil chemistry are in agreement with results of studies by Quigley (1976) and B. C. Ministry of Transportation and Highways (1977). Knowing that electric conductivity (E.C.) is related to salinity, values obtained by B. C. Ministry of Transportation and Highways (1977) appear to be large relative to results obtained in this study and the one by Quigley (1976). Similarly, it was found that values of cation exchange capacity (C.E.C.) obtained by B C. Ministry of Transportation and Highways (1977) were relatively large for corresponding exchangeable cations, tabulated in their report.

Values of pH ranges between 8.0 and 8.3 imply that these soils are alkaline. The amount of organic matter is negligible, which dismisses potential theories for instability involving disintegration or volume changes of the organic matter.

Cation exchange capacity ranges between 6.3 and 8.2. According to Fanning et al. (1989), such small values of cation exchange capacity (C.E.C.) imply presence of mica minerals and eliminate possibility of major presence of primary cation exchangers such as expandable 2:1 vermiculite particles, generated from weathered mica, illite, pedogenic chlorites (hydroxy-interlayered vermiculite (HIV)), vermiculite, and smectite. The absence of expandable minerals and exchangeable cations is also supported by the experimental relationship between electric conductivity (E.C.) versus sodium adsorption ratio (S.A.R.), presented by Sposito (1989). For these sediments, the experimental relationship, presented by Sposito (1989), indicates a permeable "good soil structure" as opposed to sodic, expandable, and "poor soil structure".

Base saturation for these sediments ranges between 231% and 265%, which is larger than 100%. Small percentage of clay size particles eliminates possibility of physical weathering; but according to Fanning et al. (1989), base saturation larger than 100% can imply possibility of chemical weathering. Fanning et al. (1989) said chemical weathering can be wedge and layer weathering, which cause the formation of expansible 2:1 minerals by simple transformation; or, it can also occur by complex transformation under acidic conditions. In complex transformation, the 2:1 layer may decompose as rapidly as or even more rapidly than the release of interlayer cations. Other evidence including small values of C.E.C., soil pH that implies alkaline soil, and distinctly sharp and perfect muscovite peaks in x-ray diffraction analyses disregard possibility of chemical weathering in spite of values of base saturation larger than 100%.

The concentrations of soluble Na^+, Ca^{++}, and Mg^{++} in the soil-pore fluid environment are one order of magnitude higher than typical corresponding values in river water and the concentration of sulfate is two orders of magnitude higher than the corresponding value in river water. The concentration of Na^+, K^+, Ca^{++}, Mg^{++}, sulfate, and chloride are below saturation level and can only imply presence of precipitates of soluble salts on particle surfaces or at particle contacts. Presence of these chemicals in such limited concentrations dismisses the formation of crystalline salts.

Carbonate content is 4.6% to 5.9%, which, similar to the concentration of sulfate and chloride precipitates, implies the presence of carbonate precipitates in the soil environment; but these values again are below saturation limit. Taking into account the pH of these soils, carbonate should be present in the form of HCO_3^-.

The concentration of Silicon (Si) in the ground water of Koosi Creek Landslide site is 9.5 ppm, which is at saturation level and is higher than typical value for river water (6.5 ppm). This high concentration of Silicon implies the presence of amorphous silica acid gel in the soil environment. This observation has significant influence in our understanding of the nature of bonding and cementation in these natural structured silt sediments. Many studies including studies by Denisov and Reltov (1961), Henderson et al. (1970), Miura and Yamanouchi (1973 and 1978), Dusseault and Morgenstern (1979), Mitchell and Solymar (1984), and Vigil et al. (1994) not only considered cementation as the source of structural improvements but also speculated that the cementation in soil structure could be due to some mechanisms involving the dissolution and re-precipitation of amorphous or quartz silica and formation of silica acid gel on particle surfaces and at particle contacts. In addition, volcanic origin of Penticton silt and underlying bedrock support a theory implying cementation by silica acid gel; because soils and rocks with volcanic origin are weathering and releasing silica.

Also, the presence of 25000 to 30000 ppm of iron (Fe) in results of soil chemistry analyses and absence of iron (Fe) in results of pore fluid chemistry analyses, indicates possible bonding between soil grains due to aggregation or cementation by iron oxide. Schwertmann and Taylor (1989) said the presence of a very small percentage of Iron oxides could influence the bonding characteristics of soil structure. Iron oxides are known to be cementing agent (in high concentrations) or aggregating agent (in lower concentrations). They can cause cementation in their crystalline form and aggregation in their non-crystalline form. Their aggregation potential is also higher as their oxalate solubility increases. Their high surface area is a potential location for adsorption of H_2O and also attraction of cations (isomorphous substitution). Due to possible release of some iron from mineral structures during inductively coupled plasma (ICP) analyses, it is probable that the observed concentrations of iron (Fe) partially include some structural iron. It should be mentioned that visual investigation, x-ray diffraction analyses, and scanning electronic microscopic (SEM) analyses confirm presence of iron oxides, especially in magnetite form.

Salinity of samples tested as part of the current experimental program is about 0.20 g/L for saturated soil paste. Quigley (1976) reported an average value of approximately 2.9 g/L for salinity of saturated soil paste. The salinity of soils can be important in assessing the stability of soil deposits. Tavenas (1984) commented that marine clays with plasticity less than 20% and salinity less than 3 g/L are susceptible to flow-slide. It should be mentioned that the salinity of Norwegian sensitive clays is reported to be 1 g/L by Karlsrud et al. (1984).

5.9 Summary

The basic properties of Penticton silt were studied. It was found that these sediments are dominantly silt size particles. Specific gravity obtained in the current study is approximately 2.67, which appears to be reasonable for sediment containing muscovite mica. Liquid, plastic and shrinkage limits were approximately 37%, 32%, and 30%, respectively. These sediments are not saturated at liquid limit. Penticton silt can be classified as A-4 silty soil and ML soil in AASSHTO and USC systems, respectively.

At typical in-situ moisture conditions of 15% to 25%, matric suction was found to be 100 kPa to 300 kPa. The soil-water characteristic response was compatible with typical response for silty soils.

Muscovite and chlorite are the dominant minerals present in these sediments, but quartz, K-feldspar, plagioclase are also present. Clay fraction is mainly composed of illite/mica, smectite, and chlorite. Expandable clay content was not found to be large enough to cause destructuring. No major crystalline bonding agent was found; but magnetite and calcite are present in small amount.

Soil fabric of both undisturbed and reconstituted samples was found to be anisotropic with preferred horizontal orientation. Platy particles were found to be abundant. Exposure to moisture caused destructuring at the level of grain to grain of silt particles and formation of micro-cracks with crack widths less than 30 microns. Flexible and compressible particles were observed. Presence of precipitates that can cause bonding and also aggregation due to presence of iron oxides were also observed.

Results of soil and pore water chemistry do not support occurrence of processes leading to significant chemical weathering and presence of major amounts of expansive minerals. These sediments are alkaline and precipitates of main cations are present. The concentrations of these cations are below saturation limit required for formation of crystalline salts. Carbonate content is at a moderate level. Results imply the presence of silica acid gel on the surface of soil particles. Also, concentration of iron implies aggregation of soil particles due to iron oxides.

No unique source of bonding was found. It appears several physical and chemical processes influence the structure of Penticton silt. Bonding agents in the structure of Penticton silt appears to include carbonate and sulfate precipitates, iron oxides, and amorphous silica. This issue will be discussed in more detail in Chapter Eight.

Table 5.2 – Summary of the Grain Size Analyses, Carried out as Part of the Other Studies

Reference	Soil	Location	Sand Size (%)	Silt Size (%)	Clay Size(%)	Comments
Meyer and Yenne (1940)	Glaciolacustrine	Okanagan Lake Skaha Lake Mission Creek Valley	-	more than 99	less than 1	Four samples were tested.
Fulton (1965)	Glaciolacustrine	South Thompson Valley	Less than 10 but usually less than 5	dominant	less than 20	Twenty four samples were tested from individual varves. It was found that a single band can be either coarser or finer than the bands immediately above and below it; but as a general trend, the texture of silt bands at higher elevations of the deposit are significantly finer grained than the texture of those at the lower elevations. Grain size analyses of a single silt band at different localities showed some minor variation.
Fulton (1975)	Glaciolacustrine	Southern Interior	-	-	-	The silt content varies from one site to the adjacent site. It also varies from the bottom to the top of the deposit at the same locality. The veneer sediments, with a maximum thickness less than 2 m, have a finer texture than the thick formations.
Quigley (1976)	Glaciolacustrine	Okanagan Valley South Thompson Valley	-	-	7 to 10	
Quigley (1976)	Colluvial	Okanagan Valley South Thompson Valley	-	-	12 to 19	

Table 5.2 – (Continued)

Reference	Soil	Location	Sand Size (%)	Silt Size (%)	Clay Size(%)	Comments
Evans and Buchanan (1976)	Glaciolacustrine and Colluvial	South Thompson Valley	less than 3	dominant	2 to 12	No major difference was observed between glaciolacustrine and colluvial silts.
Lum (1977)	Glaciolacustrine	South Thompson Valley	4	89	7	Five samples were tested. Sodium hexametaphosphate was used as de-flocculating agent. D_{10}, D_{60}, and C_u were 0.0027 mm, 0.0092 mm, and 3.4, respectively. Using the MIT soil classification, the soils tested were classified as uniform clayey silt.
Evans (1982)	Glaciolacustrine	Northern Interior (Prince George and Quesnel)	-	-	up to 91	
Wilson (1985)	Glaciolacustrine and Colluvial	South Thompson Valley	15 to 20 (fine sand)	70 to 80	less than 3	De-flocculating agent was used. The soil was dominantly uniform medium silt. No major difference was observed between glaciolacustrine and colluvial silts.
Klohn Leonoff (1992)	West Bench/Sege Mesa	Glaciolacustrine	0 to 2	80 to 87	8 to 17	

Table 5.3 – Summary of the Specific Gravity, Density, and In-Situ Void Ratio Determinations, Carried out as Part of the Other Studies

Reference	Soil	Location	Specific Gravity	Density kg/m^3	In-situ Void Ratio	Comments
Meyer and Yenne (1940)	Glaciolacustrine	Okanagan Valley	2.88	-	-	No details were provided.
Quigley (1976)	Glaciolacustrine and Colluvial	Okanagan and South Thompson Valleys	-	-	1.02 to 1.20	These deposits were classified as cemented granular soils and potentially collapsible because of having void ratios greater than 0.8 to 0.9, which was considered as the critical void ratio of granular soils.
Lum (1977)	Glaciolacustrine and Colluvial	South Thompson Valley	2.60 to 2.80	-	-	Nine samples were tested. Average value was 2.77.
Nyland and Miller (1977)	Glaciolacustrine	Okanagan Valley	-	1557 to 1734 (maximum dry)	-	Standard proctor method, ASTM D-698 Method A was used. Optimum water content ranged from 17% to 24% (approximately 85% saturation).
Wilson (1985)	Glaciolacustrine and Colluvial	South Thompson Valley	-	1390 to 1680 (in-situ bulk)	0.68 to 1.02	Specific gravity was assumed to be 2.65.

Table 5.4 – Summary of the In-Situ Water Content and Atterberg Limits Determinations, Carried out as Part of the Other Studies

Reference	Soil	Location	In-Situ Water Content (%)	Plastic Limit W_P (%)	Liquid Limit W_L (%)	Plasticity Index (P.I.)	Comments
Evans and Buchanan (1976)	Glaciolacustrine	South Thompson Valley	2 to 35	-	27 to 37	2 to 12	These sediments can be classified as clayey silt of low plasticity. Four outs of six glaciolacustrine silt samples had in-situ water content above liquid limit.
Evans and Buchanan (1976)	Colluvial	South Thompson Valley	2 to 48 (0.2 to 2 near the surface in summer)	-	25 to 39	4 to 15	These deposits can be classified as clayey silt of low plasticity. There were colluvial silt samples with in-situ water content well above liquid limit.
Nyland and Miller (1977)	Glaciolacustrine	Okanagan Valley	1 to 8	13 to 31	21 to 39	1 to 14	No reference to depth was made for in-situ water content.
Lum (1977)	Glaciolacustrine	South Thompson Valley	7 to 8	-	-	-	Measurement was carried out at the depth of 1.5 m in the month of June.
Evans (1982)	Glaciolacustrine	Northern Interior	-	-	larger than 50	larger than 20	
Wison (1985)	Glaciolacustrine	South Thompson Valley	6 at 5 m depth	-	-	-	Soil was classified as ML, inorganic silt with fine silty sands and slight plasticity.

Table 5.6-A(a) – Summary of the Reported Mineralogical Analyses (Bulk Silt Samples)

Mineral	Fulton (1965)	Quigley (1976)
Quartz	Main	Abundant
Mica	Major	Minor
Feldspar	Major	Moderate
Carbonate	N/A	Minor
Amphibole	N/A	Minor
Ferromagnesian Minerals	Minor	N/A
Clay Minerals (Illite/Mica, Chlorite, Kaolinite, and Smectite)	Minor	Minor

Table 5.6-A(b) – Summary of the Reported Mineralogical Analyses (Clay Fraction Samples)

Mineral	Fulton (1965)	Quigley ((1976)
Smectite	35% - 40%	Abundant
Illite / Mica	28% - 35%	Moderate
Chlorite	27% - 36%	Minor
Kaolinite	N/A	Minor

Table 5.6-B(a) – Results of the X-Ray Diffraction Analyses of the Bulk Sample

Mineral	Okanagan Lake Park Slide Site	Koosi Creek Slide Site
Chlorite	Dominant	Dominant
Mica (Muscovite)	Dominant	Dominant
Quartz	Major	Major
K-Feldspar	Minor	Minor
Plagioclase (Ca-Feldspar)	Minor	Minor
Magnetite	Minor	Trace
Calcite	Minor	Trace
Clay Fraction	Minor	Minor

Table 5.6-B(b) – Results of the X-Ray Diffraction Analyses of the Clay Fraction

Mineral	Okanagan Lake park Site	Koosi Creek Site
Illite	Dominant	Dominant
Smectite	Dominant	Dominant
Chlorite	Major	Major
Vermiculite	Minor	Major
Kaolinite	Minor	Minor
Mica (Muscovite)	Trace	Trace
Mica (Biotite)	Minor	Trace

Table 5.8-A – Summary of Soil Chemistry Analyses by Quigley (1976)

	Okanagan V. (Colluvial)	Okanagan V. (Glacio-lacustrine)	S. Thompson V. (Colluvial)	S. Thompson V. (Glacio-lacustrine)
pH[*]	8.1	9.1	8.8	8.6
Salinity (g/L)	1.4	6.0	14.4	1.4
(M. C. of saturated soil paste)	(M.C.=40%)	(M.C.=41%)	(M.C.=74%)	(M.C.=39%)
Salinity (g/L)[*]	0.22	0.13	2.4	0.14
Soluble Na^+ (ppm)[*]	45	80	1400	52
Soluble K^+ (ppm)[*]	10	9	16	12
Soluble Ca^{++} (ppm)[*]	40	33	143	18
Soluble Mg^{++} (ppm)[*]	11	11	105	12
SO_4^{--} (ppm) [**]	22	116	1587	25
SO_4^{--} (% of dry solid)	0.04	0.23	3.2	0.05
Carbonate (%)[$]	4.6	5.4	3.8	6.6

[*] from liquid extract with ratio of soil/water equal to 1/5.

[**] supernatant liquid with soil to water ratio equal to 1/20.

[$] using Chittick gasometric method of Dreimanis (1965).

Table 5.8-B – Summary of Results of Soil Chemistry Analyses, Courtesy of the B. C. Ministry of Transportation and Highways (1977)

	Okanagan V. (Colluvial)	Okanagan V. (Glacio-lacustrine)	S. Thompson V. (Colluvial)	S. Thompson V. (Glacio-lacustrine)
pH	7.9-8.1	7.7-7.9	8.1-8.5	8.2-8.5
Electric Conductivity (dS/m)	3.6-7.5	3.0-20.8	2.2-5.8	0.4-6.6
C. E. C.** (meq/100 g)	11.9-15.5	12.6-13.9	16.6-18.4	13.1-17.5
SAR$	1.66-8.91	0.86-7.2	1.24-6.34	0.60-12.34
Soluble Na$^+$ (meq/l)*	7.8-47.8	3.9-73.9	4.8-34.4	1.0-56.5
Soluble K$^+$ (ppm)*	0.5-3.6	0.7-1.4	0.4-1.9	0.1-1.3
Soluble Ca^{++} (meq/l)*	29.6-30.7	24.7-164.7	13.9-20.1	4.2-23.2
Soluble Mg^{++} (meq/l)*	14.1-57.6	16.3-46.1	9.8-44.8	1.8-18.8
Total Dissolved Salts (meq/l)	56.2-117.8+	45.6-286.0+	35.1-95.0+	7.2-44.0+

* from soil water paste with water content at liquid limit.

** Cation Exchange Capacity, determined by adding $NaOH_c$ to a mixture with soil/water = 1/5 at pH=8.2.

+ ttal dissolved salts as Na_2SO_4 equivalence.

$ Sodium Adsorption Ratio (SAR)

Table 5.8-C – Summary of Results of Soil and Ground Water Chemistry Analyses

Sample	O.L.P.⁺ (Soil)	K.C.⁺⁺ (Soil)	K.C. (G.W.$)
pH	8.3	8.0	7.61
Electric Conductivity (dS/m)	0.88	1.23	0.85
Sodium Adsorption Ratio (SAR)	1.38	0.91	N/A
Saturation (%)	48	48	N/A
C. E. C.*** (meq/100 g)	8.2	6.3	N/A
Base Saturation (%)	231	265	N/A
Soluble Sodium, Na^+ (ppm)	38.5	48.2	45.6
Soluble Potassium, K^+ (ppm)	3.18	7.85	5.25
Soluble Calcium, Ca^{++} (ppm)	20.6	68.0	112
Soluble Magnesium, Mg^{++} (ppm)	23.7	14.8	35.5
Sulphate-S (ppm)	50.3	82.6	251
Chloride (ppm)	17.3	27.8	5.8
Silicon (ppm)	N/A	1110*	9.5*
Iron (ppm)	30000*	25500*	0.01*
Carbonate (%)	4.6	5.9	N/A
Total Alkalinity (ppm)	109	133	240
TOC** (%)	<0.09	<0.09	N/A

+ Okanagan Lake Park.
++ Koosi Creek.
$ Ground Water.
* Based on results of inductively coupled plasma (ICP) analyses.
** Total Organic Carbon.
*** Cation Exchange Capacity.

Figure 5.2 - Grain Size Distribution for Penticton Silt

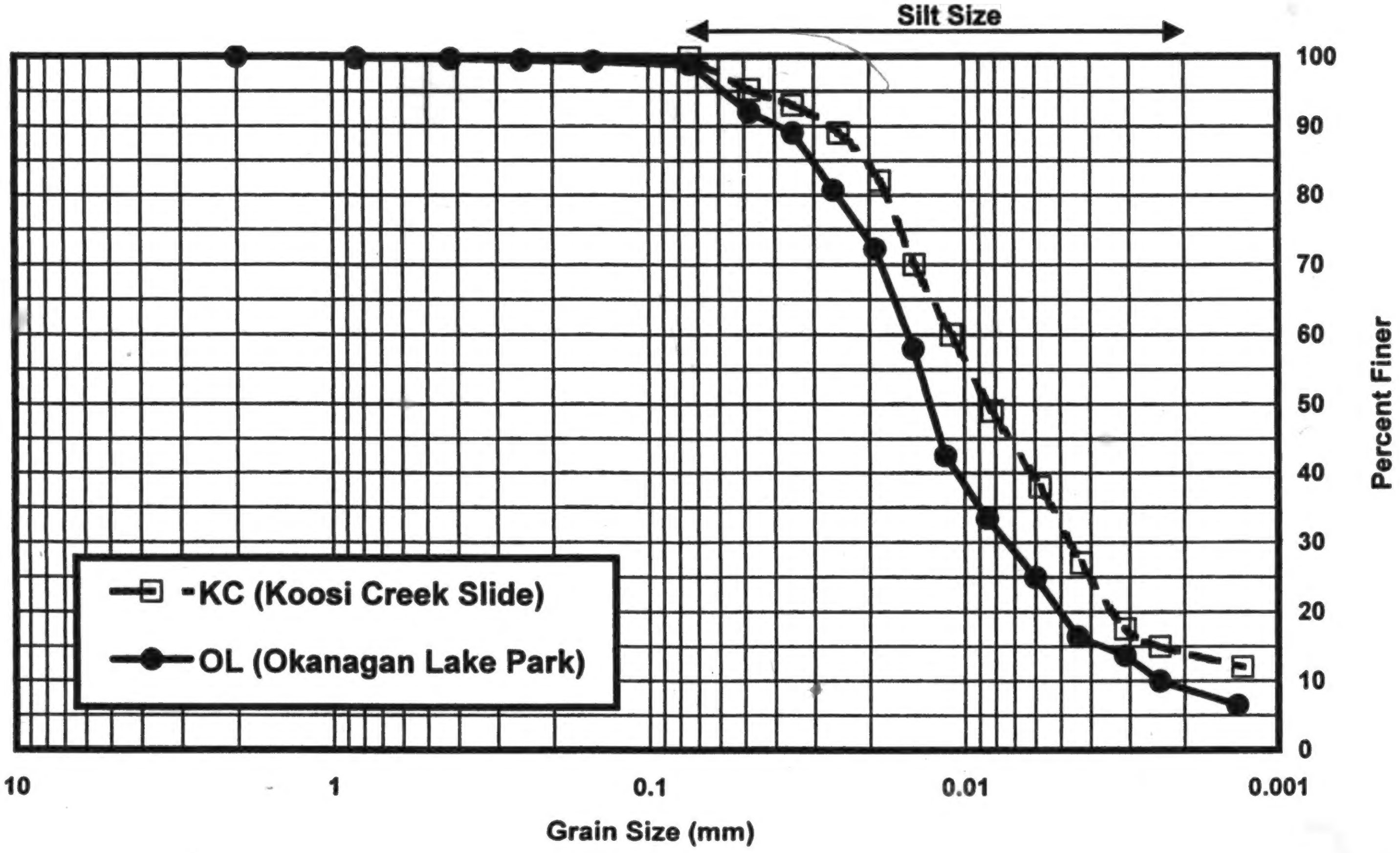

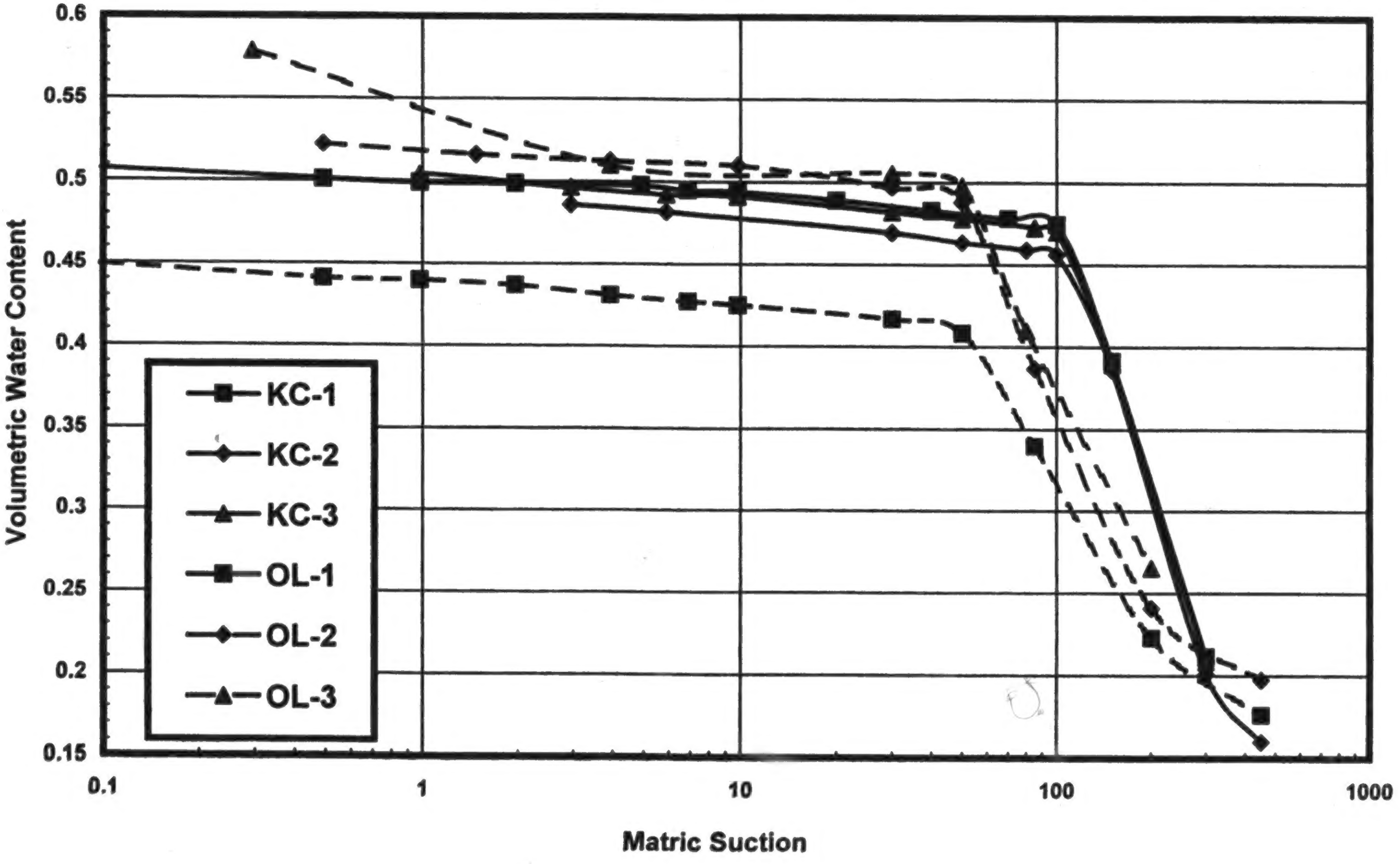

Figure 5.5-A - Soil-Water Characteristic Curve for Penticton Silt

Figure 5.5-B – Typical Soil-Water Characteristic Curves for a Sandy Soil, a Silty Soil, and a Clayey Soil

(after Fredlund and Xing (1994))

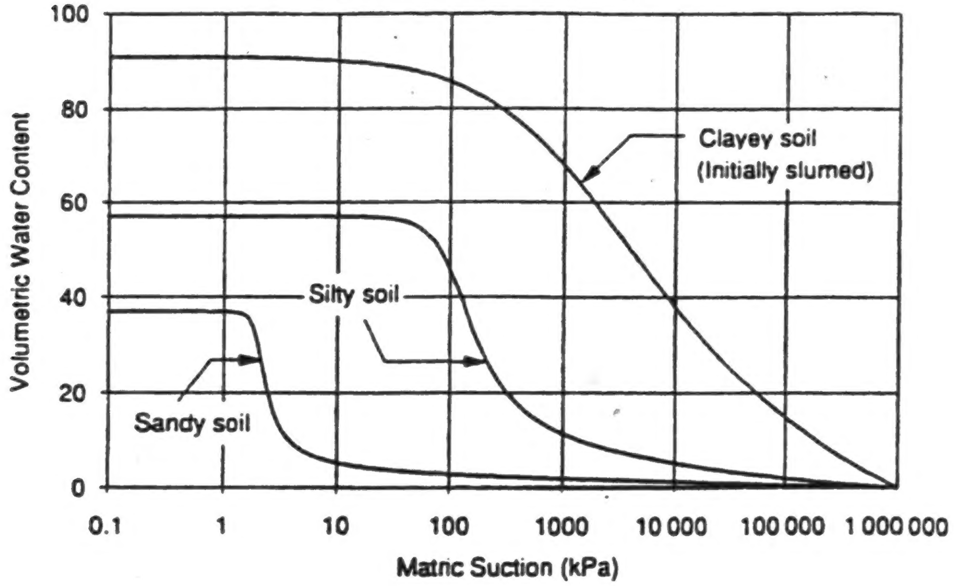

Figure 5.5-C – Typical Desorption and Adsorption Soil-Water Characteristic Curves for a Silty Soil

(after Fredlund and Xing (1994))

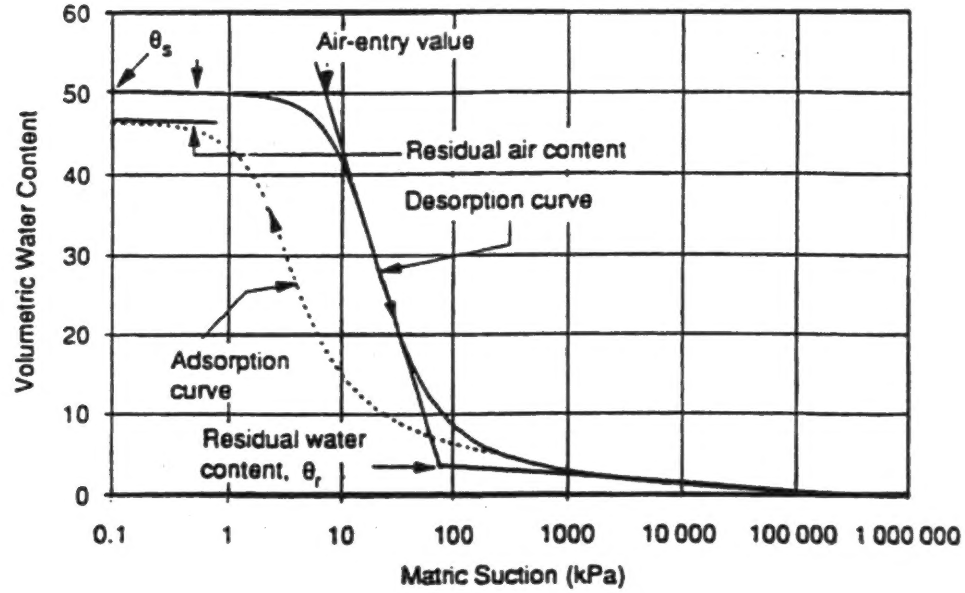

Figure 5.7-A(a) – Horizontal Surface of an Undisturbed Specimen from Koosi Creek Slide Site at its In-Situ Moisture Content

Magnification: 100 Acceleration Voltage: 10 kV

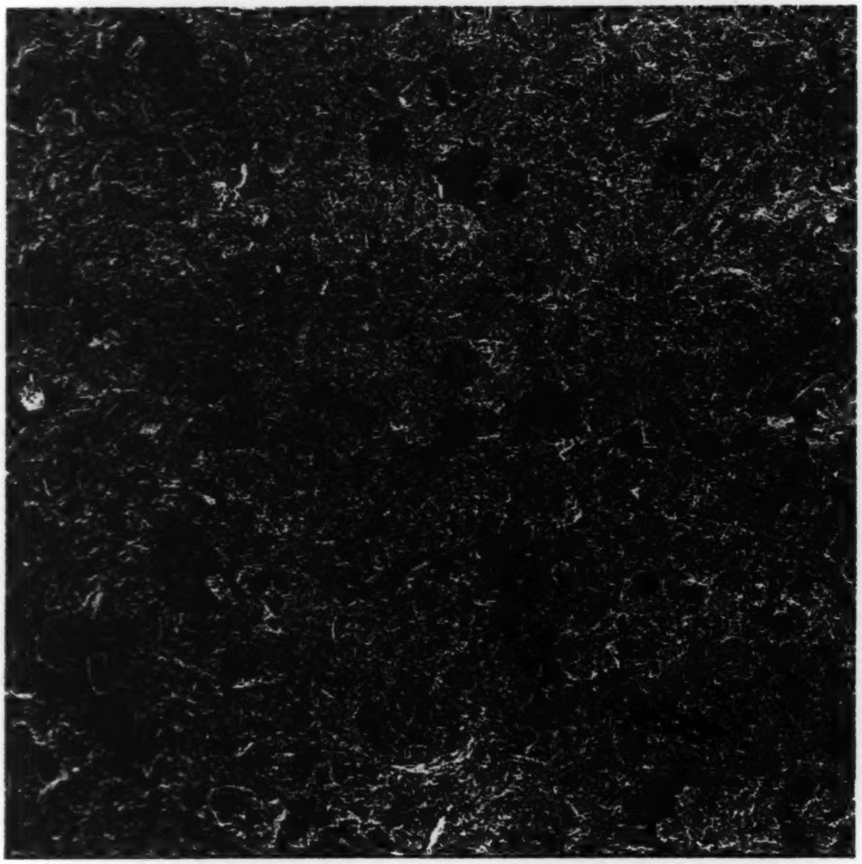

Figure 5.7-A(b) – Vertical Surface of an Undisturbed Specimen from Koosi Creek Slide Site at its In-Situ Moisture Content

Magnification: 100 Acceleration Voltage: 10 kV

Figure 5.7-B(a) – Horizontal Surface of an Undisturbed Specimen from Okanagan Lake Park Slide Site at its In-Situ Moisture Content

Magnification: 100

Acceleration Voltage: 10 kV

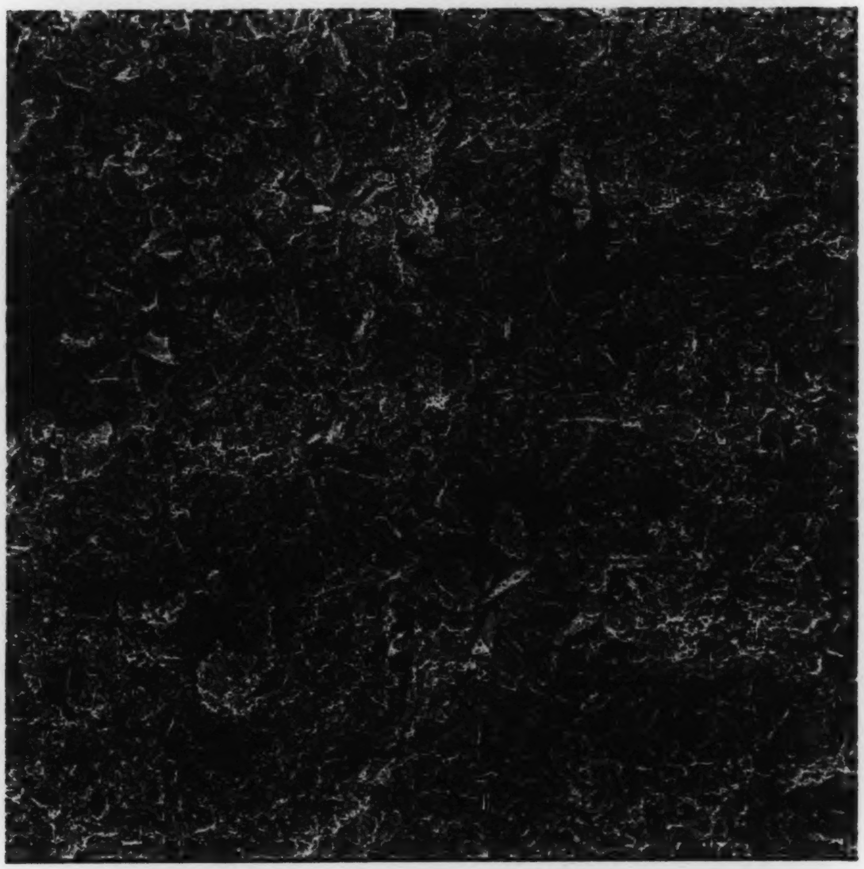

Figure 5.7-B(b) – Vertical Surface of an Undisturbed Specimen from Okanagan Lake Park Slide Site at its In-Situ Moisture Content

Magnification: 100 Acceleration Voltage: 10 kV

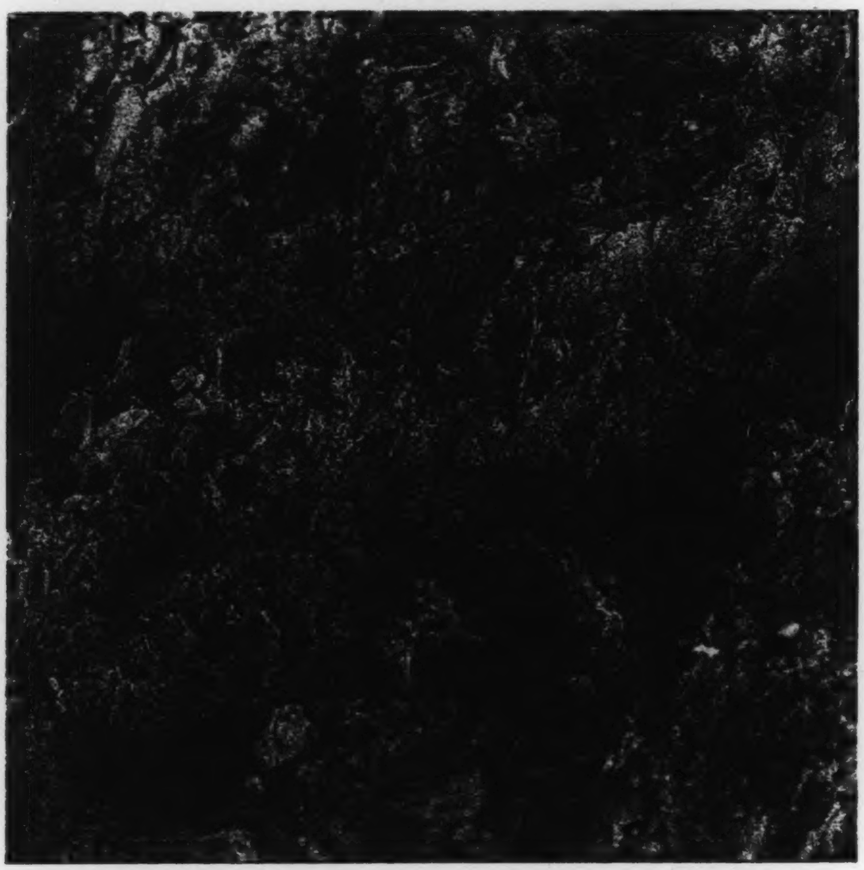

Figure 5.7-C(a) – Horizontal Surface of an Undisturbed Air-Dried Specimen from Okanagan Lake Park Slide Site

Magnification: 100 Acceleration Voltage: 5 kV

Figure 5.7-C(b) – Vertical Surface of an Undisturbed Air-Dried Specimen from Okanagan Lake Park Slide Site

Magnification: 100 Acceleration Voltage: 5 kV

Figure 5.7-D(a) – Horizontal Surface of a Saturated Slurry Specimen of Penticton Silt

Magnification: 100 Acceleration Voltage: 15 kV

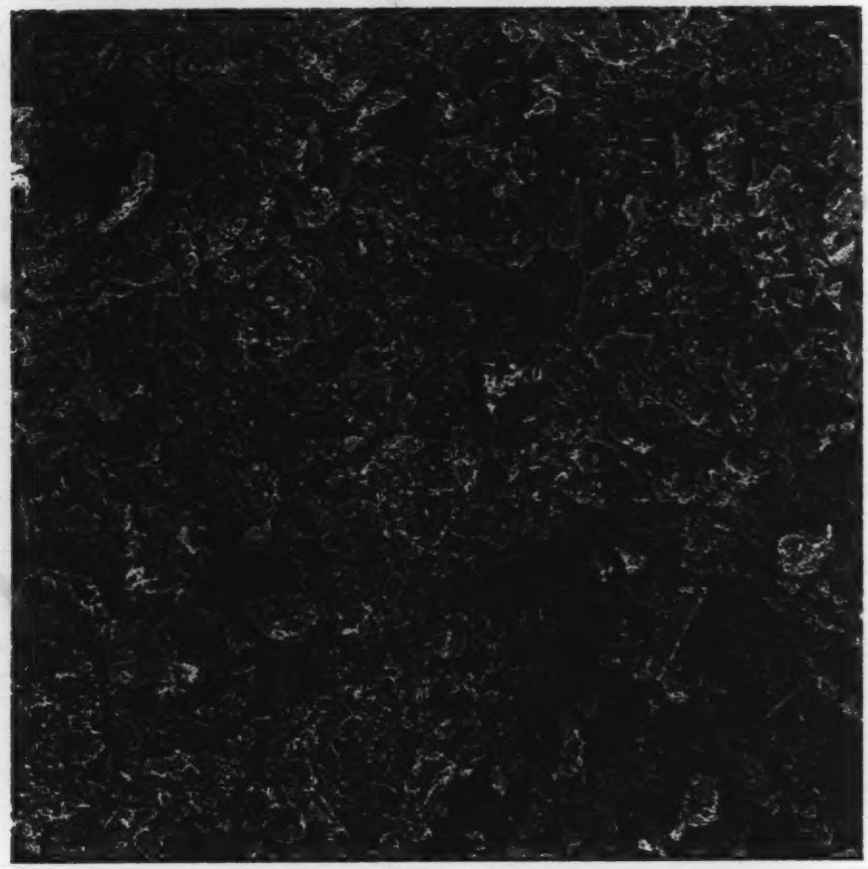

Figure 5.7-D(b) – Vertical Surface of a Saturated Slurry Specimen of Penticton Silt

Magnification: 100 Acceleration Voltage: 5 kV

Figure 5.7-E(a) – Horizontal Surface of an Undisturbed Initially Air-Dried Specimen from Okanagan Lake Park Slide Site after Gradual Saturation

Magnification: 100 Acceleration Voltage: 15 kV

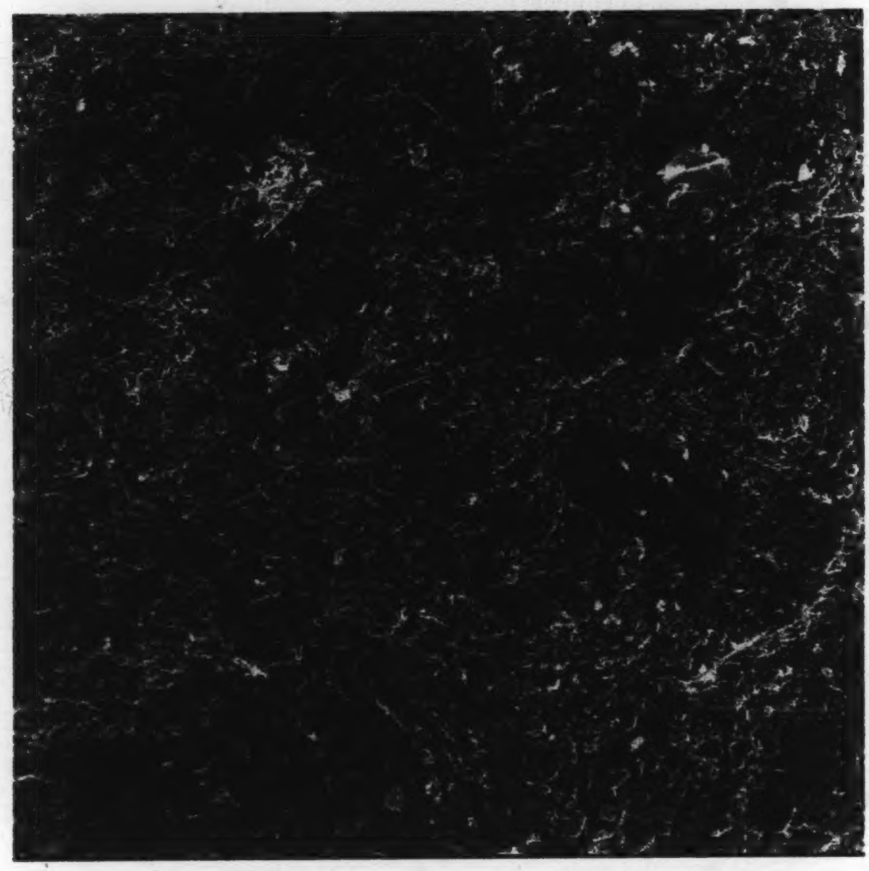

Figure 5.7-E(b) – Horizontal Surface of the Specimen Shown in Figure 5.7-E(a) after Re-Air-Drying

Magnification: 100 Acceleration Voltage: 5 kV

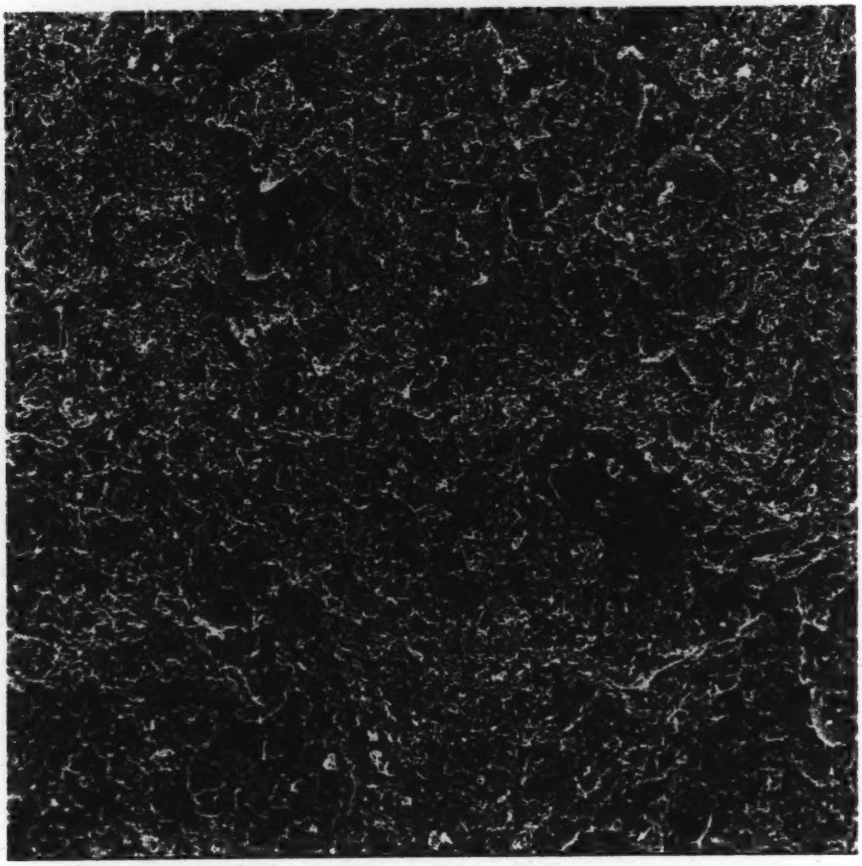

Figure 5.7-F(a) – Vertical Surface of an Undisturbed Initially Air-Dried Specimen from Okanagan Lake Park Slide Site after Gradual Saturation

Magnification: 100 Acceleration Voltage: 15 kV

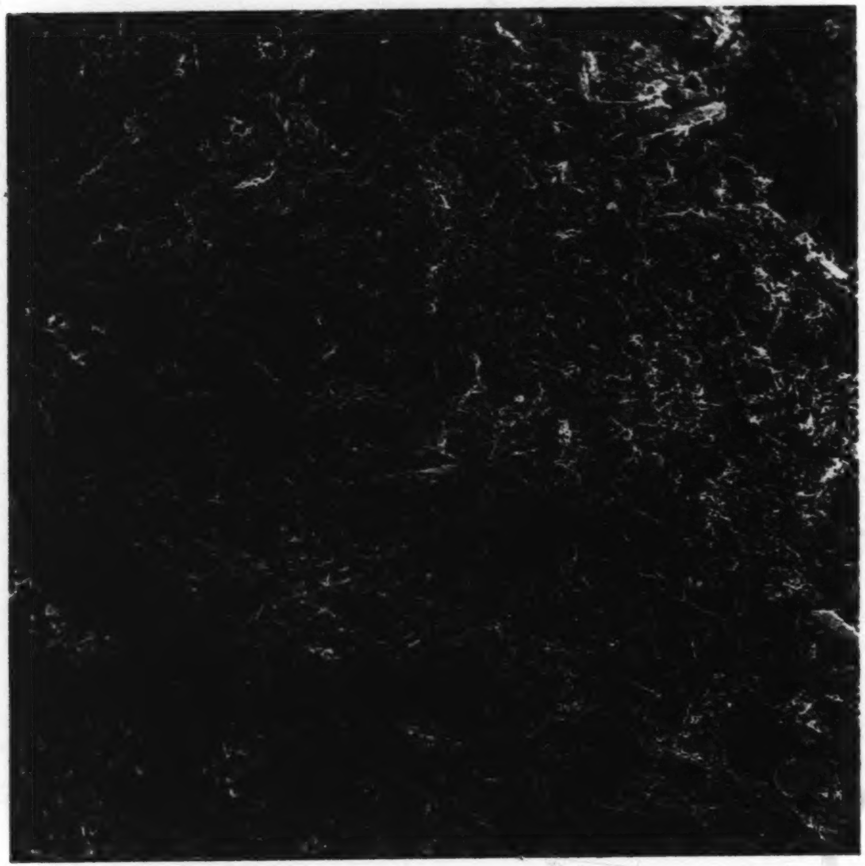

Figure 5.7-F(b) – Vertical Surface of the Specimen Shown in Figure 5.7-F(a) after Re-Air-Drying

Magnification: 100 Acceleration Voltage: 5 kV

Figure 5.7-G – Crack Formation, Swelling, and Destructuring upon Gradual Moistening under Unconfined Condition

(a)

Magnification: 100 Acceleration Voltage: 15 kV

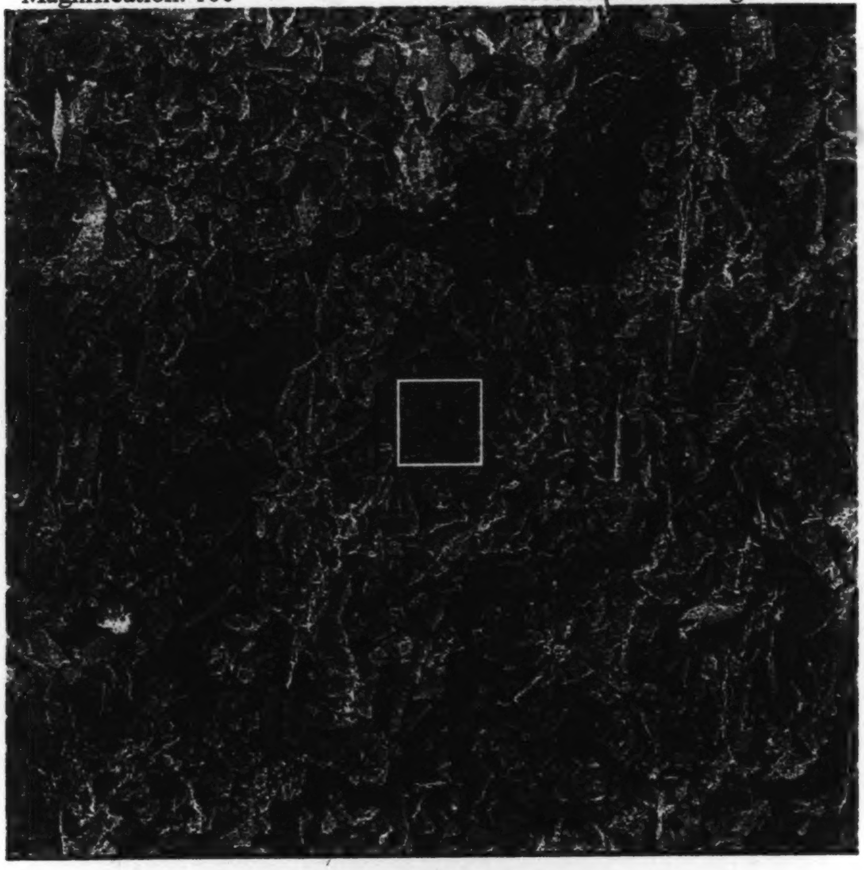

(b)

Magnification: 400 Acceleration Voltage: 15 kV

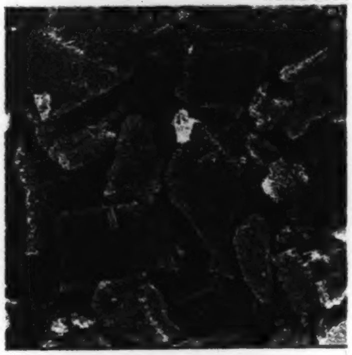

Figure 5.7-H – Crack Formation, Swelling, and Destructuring upon Flooding under Unconfined Condition

(a)

Magnification: 100 Acceleration Voltage: 10 kV

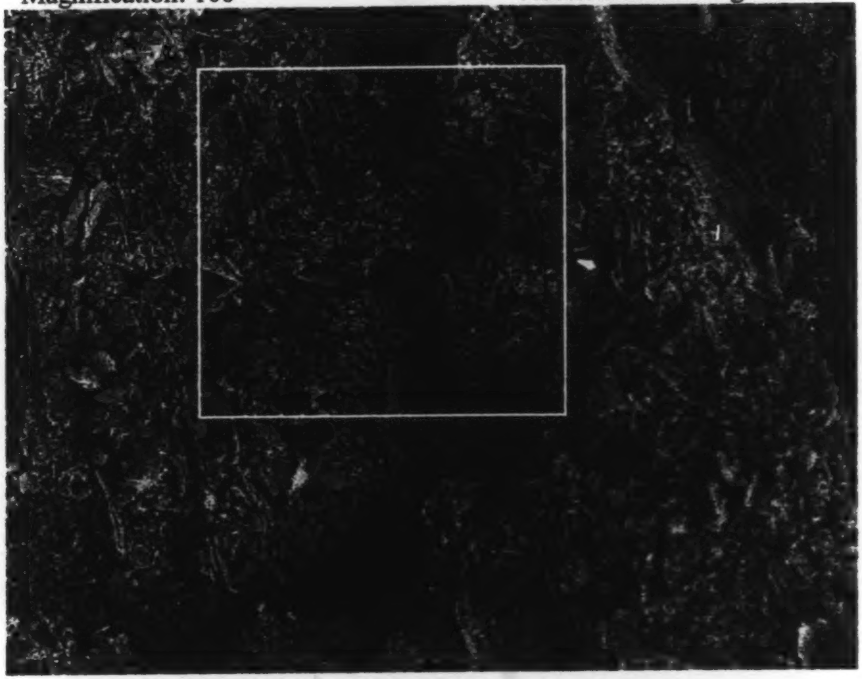

(b)

Magnification: 150 Acceleration Voltage: 10 kV

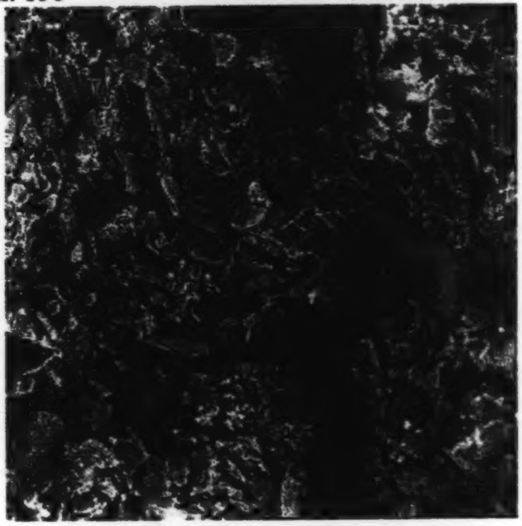

Figure 5.7-I – Open and Flexible Structure of Platy Particles Such as Muscovite and Chlorite in Soil Structure of Penticton Silt

(a)

Magnification: 200 Acceleration Voltage: 5 kV

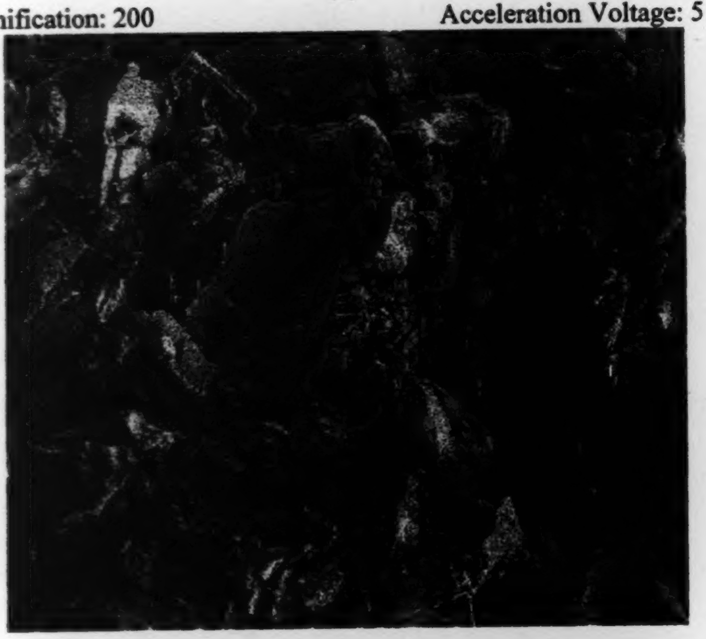

(b)

Magnification: 800 Acceleration Voltage: 2.5 kV

Figure 5.7-J – Illite Formation from Mica (Muscovite) Disintegration

(a)

Magnification: 1000 Acceleration Voltage: 10 kV

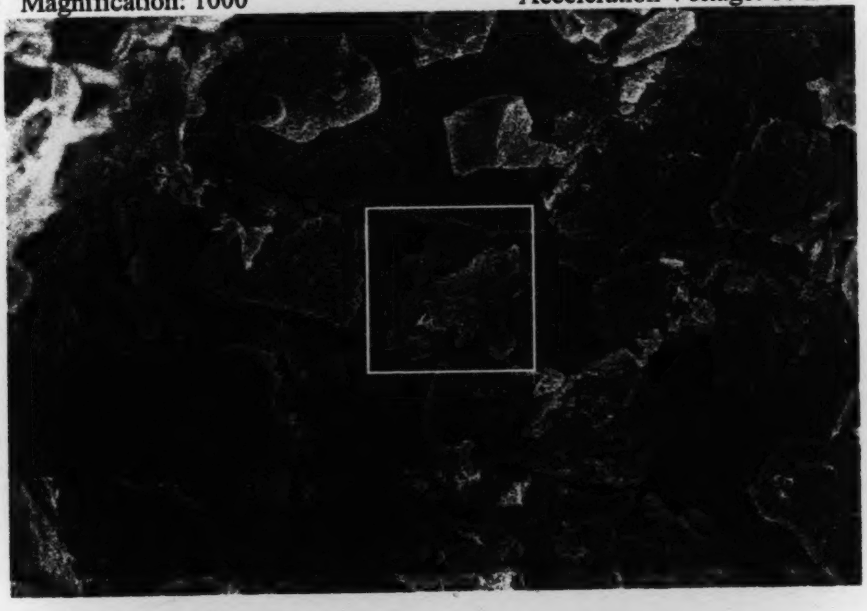

(b)

Magnification: 4000 Acceleration Voltage: 10 kV

Figure 5.7-K – Calcite Particle Present in Penticton Silt Soil Structure

Magnification: 5000 Acceleration Voltage: 2.5 kV

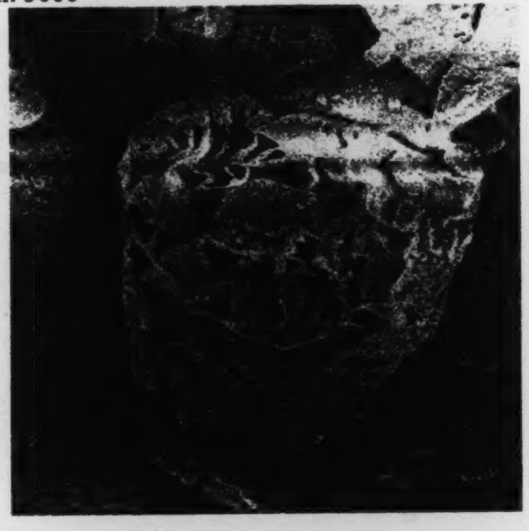

Figure 5.7-L – Silica Over-Growth and Structural Bonding between Two Muscovite Particles

Magnification: 2000 Acceleration Voltage: 15 kV

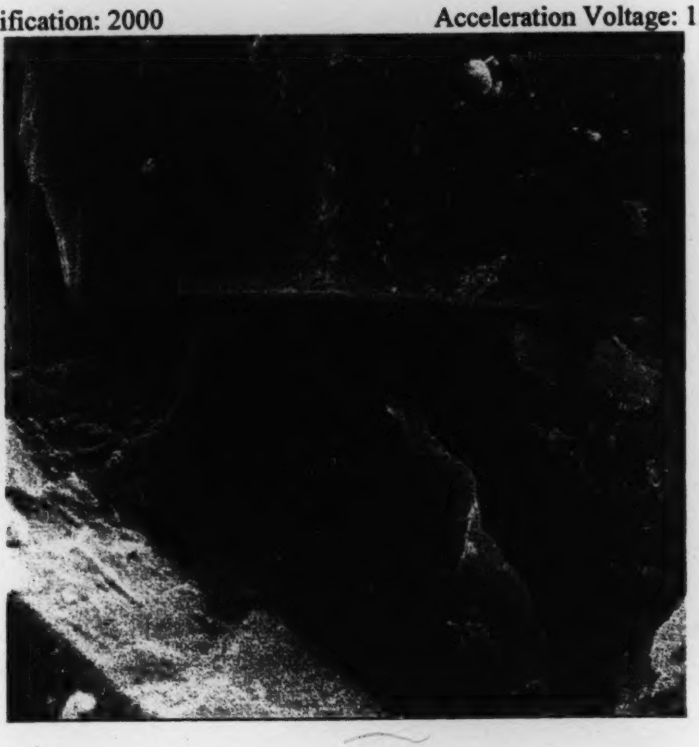

Figure 5.7-M(a) – $Mg(OH)_2$ Precipitates on a Quartz Surface

Magnification: 1500 Acceleration Voltage: 10 kV

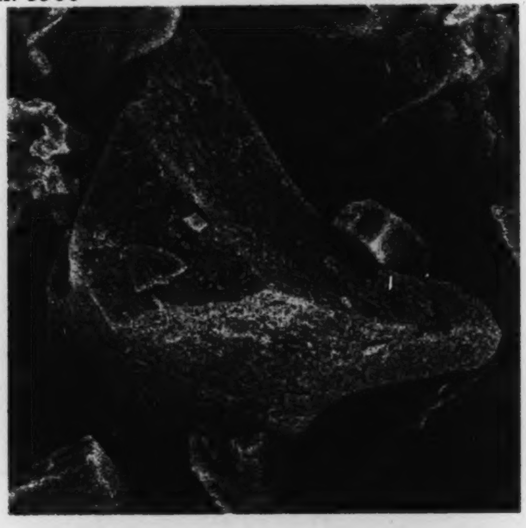

Figure 5.7-M(b) –Unknown Precipitates on the Surface of Particles

Magnification: 2000 Acceleration Voltage: 115 kV

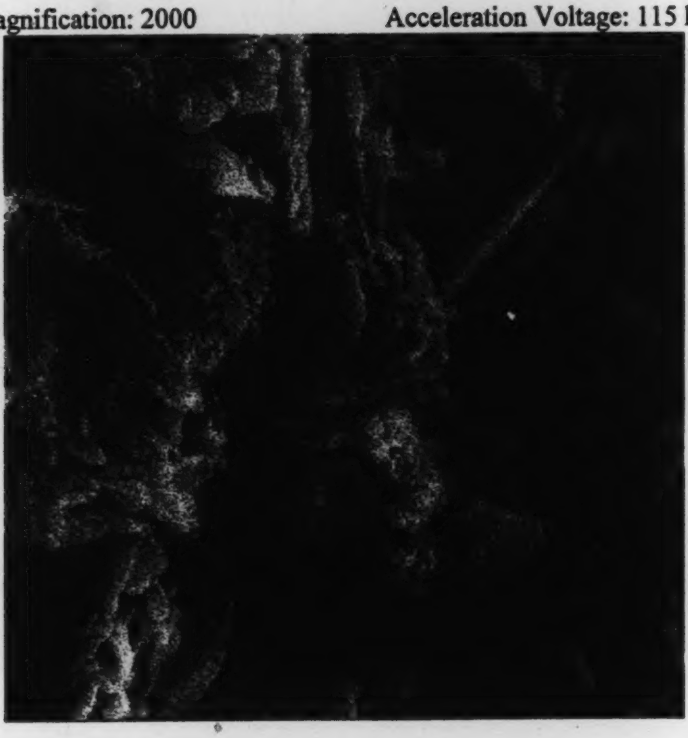

Figure 5.7-N – Precipitate Bridge between Two Muscovite Particles

(a)

Magnification: 1000 Acceleration Voltage: 10 kV

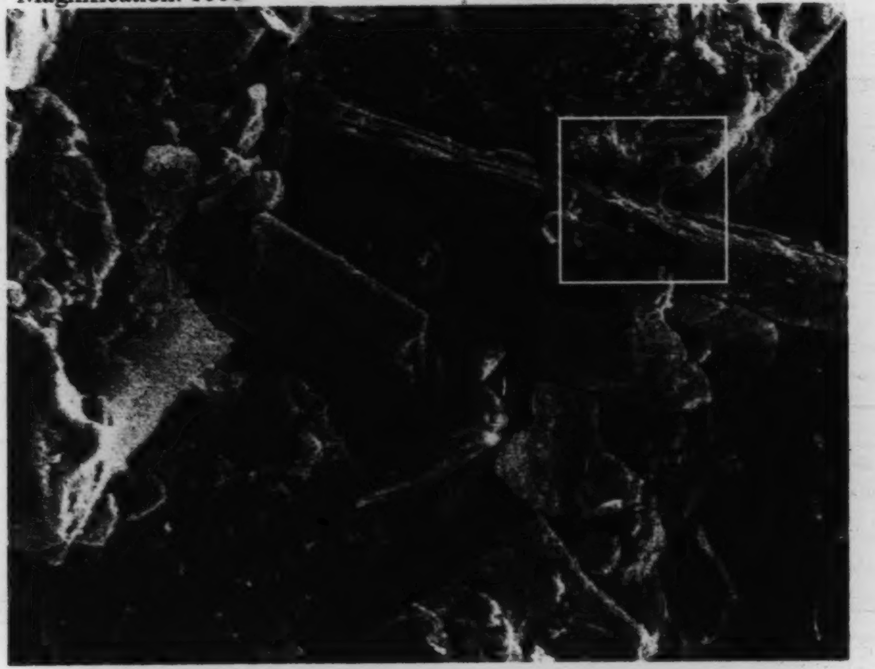

(b)

Magnification: 3500 Acceleration Voltage: 10 kV

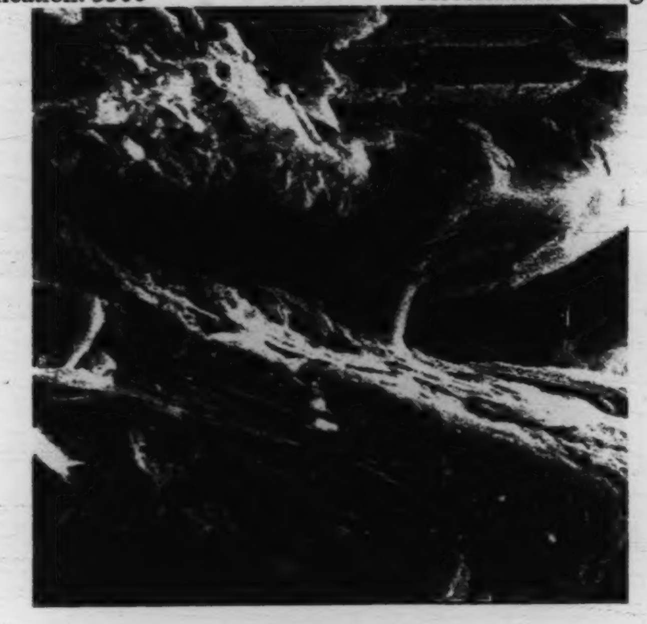

Figure 5.7-O – Formation of Mg Precipitates on Plagioclase Surface

(a)

Magnification: 800 **Acceleration Voltage: 15 kV**

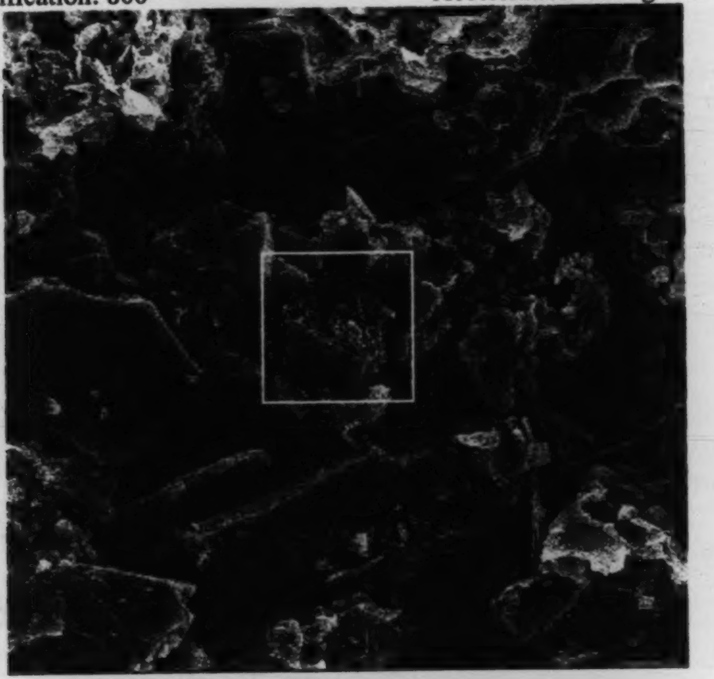

(b)

Magnification: 3500 **Acceleration Voltage: 15 kV**

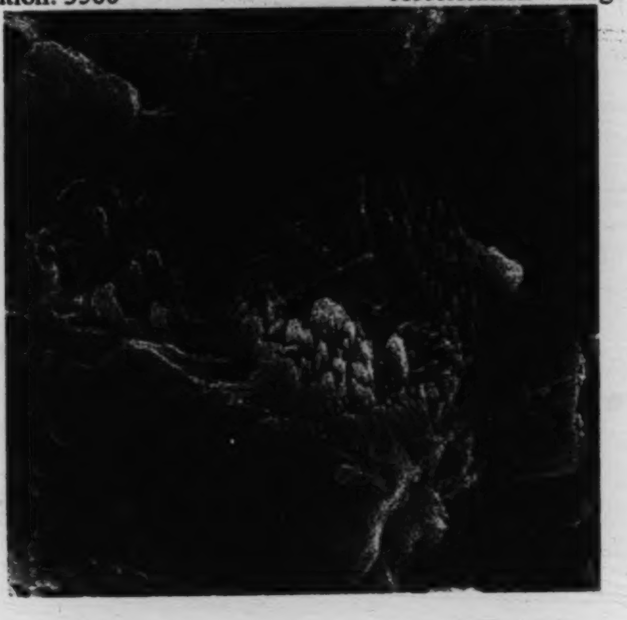

Figure 5.7-P – Aggregation of Particles with Iron Oxides

(a)

Magnification: 400 Acceleration Voltage: 5 kV

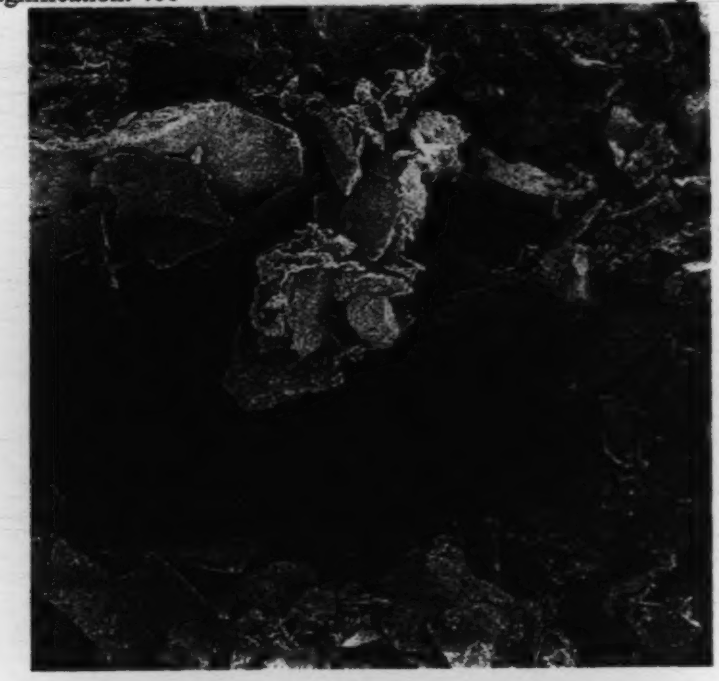

(b)

Magnification: 600 Acceleration Voltage: 5 kV

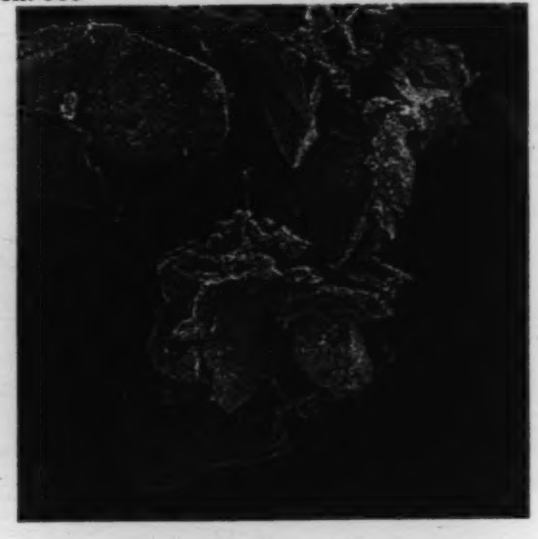

Figure 5.7-Q – Aggregated Deformed Muscovite Particle

(a)

Magnification: 400 Acceleration Voltage: 2.5 kV

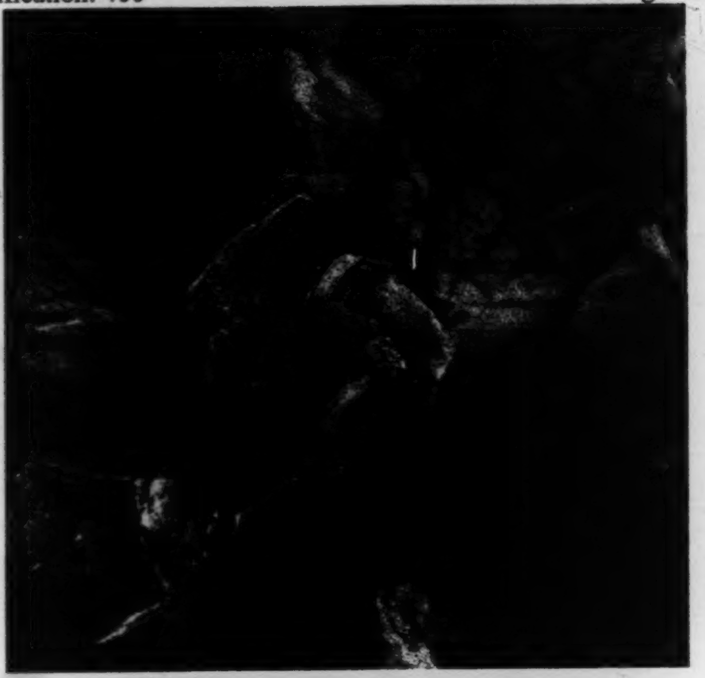

(b)

Magnification: 600 Acceleration Voltage: 2.5 kV

CHAPTER SIX

One-dimensional Consolidation Testing

6.1 Introduction

Compressibility (stiffness) and strength are two of the fundamental mechanical characteristics of soils. In classical soil mechanics, which was developed based on results of studies using reconstituted soil specimens, the behavior and state of a soil is expressed as a function of its void ratio and stress history. The behavior of natural soils can be different from the behavior of reconstituted soil specimens. According to Leroueil and Vaughan (1990), most natural soils have components of stiffness (compressibility) and strength, which cannot be accounted for by the classical principles of soil mechanics. These components of stiffness and strength are the consequence of inter-particle bonding. Natural soils can exist in meta-stable states that are not achievable for reconstituted soils. In sedimentary soils, inter-particle bonding can develop with time and the trend is towards increased stiffness and strength; but, in residual soils, the trend can be the reverse with inter-particle bonding generally breaks down because of weathering processes.

As part of this study of Penticton silt, thirty eight one-dimensional consolidation tests were carried out. In this chapter, the results of the consolidation tests are presented and discussed. Also, a literature review of previous studies on compressibility of structured soils and glaciolacustrine silt sediments in the southern interior of British Columbia are presented.

6.2 Literature Review

6.2.1 Compressibility of Structured Soils

According to Burland (1990), Skempton studied the consolidation of twenty normally consolidated clay deposits under gravitational compaction condition. Skempton used the relationship between the in-situ void ratio (e_o) and the effective overburden pressure (σ_{vo}'); and referred to the resulting curve as the "sedimentation compression curve"

(SCL). As reported by Burland (1990), Skempton concluded that the sedimentation compression curves are essentially linear and converging.

A reconstituted soil specimen can be obtained in many ways. It is necessary to have a standard procedure to make reconstituted specimens in order to be able to compare the behavior of structured soils with a de-structured reference state. Burland (1990) proposed a set of characteristics for a reconstituted clay specimen that can represent the "intrinsic properties" of that soil. A clay specimen should be "reconstituted at a water content of W_L to $1.5W_L$ (preferably $1.25W_L$) without air-drying or oven drying, and then consolidated – preferably under one-dimensional conditions", where W_L is liquid limit. Burland (1990) recommends that the pore fluid chemistry of the slurry should be similar to the chemistry of the pore fluid in the natural state of the clay. The properties of such specimens are independent of the natural and in-situ state of soil; and such properties are representative of its inherent nature. Different soils have different void ratios at their W_L. The consolidation curves of intrinsic state of different soils are different, if they are plotted in e-log σ_v' space; but they have the same shape. In an attempt to have a unique reference line, which represents the intrinsic state of all soils, Burland (1990) normalized the intrinsic compression curves (ICL) using the intrinsic void ratios at effective vertical stresses (σ_v') equal to 100 kPa and 1000 kPa (e^*_{100} and e^*_{1000}). "void index" (I_v) is defined as:

$$I_v = \frac{e - e^*_{100}}{e^*_{100} - e^*_{1000}} \qquad \text{(Equation 6.2.1-A)}$$

Figure 6.2.1-A, adopted from Burland (1990), shows the intrinsic compression curve in e-log σ_v' space and the transformed intrinsic compression line (ICL) in the normalized I_v-log σ_v' space. According to Burland (1990), the intrinsic compression line (ICL) is reasonably unique, which can be represented with the following equation:

$$I_v = 2.45 - 1.285\log\sigma_v' + 0.015\log\sigma_v'^3 \qquad \text{(Equation 6.2.1-B)}$$

Referring to experimental data from the study by Leonards and Ramiah (1959), Burland (1990) said that the compressibility of reconstituted soils are influenced by aging. Burland (1990) presented experimental evidence that the resistance to compression would increase during aging without dependency to volume change due to creep.

Structured soils show increased resistance to compression when compared to the intrinsic state of soils. Burland (1990) criticizes the use of terms "pre-consolidation pressure" and "over-consolidation ratio" when referring to this increased resistance due to the presence of structure. Burland (1990) proposed the term "vertical yield stress" (σ_{vy}') to refer to the critical pressure that represents the increased resistance to compression. He said, "the term pre-consolidation pressure should be reserved for situations in which the magnitude of such pressure can be established by geological means". Burland (1990) also said, "the term over-consolidation ratio should be reserved for describing a known stress history". He proposed the use of the term "yield stress ratio" (YSR), which is defined as the ratio of the vertical yield stress to effective overburden pressure ($YSR=\sigma_{vy}'/\sigma_{vo}'$). The terminology proposed by Burland (1990) has been followed through out this study.

The in-situ natural state of a soil may not be on the ICL. Some of the potential states are summarized in Figure 6.2.1-B. The intrinsic state of soil is presented by the "intrinsic compression line", ICL (line D-I-F). One or several of the following processes may transform the state of a soil from its initial state, i.e. I on ICL Line in Figure 6.2.1-B:

- Partial removal of overburden causes decrease in effective overburden pressure (σ_{vo}') and some increase in void ratio. This process leads the soil to the "over-consolidation" state (transformation along I-O in Figure 6.2.1-B). For a given value of σ_{vo}', soil is at a lower value of void ratio in the over-consolidated state compare to its intrinsic state. In other words, a soil is at a more stable state.

- Drained creep causes a decrease in void ratio at a constant effective overburden pressure (σ_{vo}') (transformation along I-A in Figure 6.2.1-B). Such processes lead the soil to a denser and more stable state.

- If physicochemical bonding develops, the compressibility of soil decreases. Any further increase of the effective overburden pressure (σ_{vo}') smaller than the vertical yield stress (σ_{vy}') causes very little change in void ratio (transformation along I-C in Figure 6.2.1-B). The physicochemical bonding in the soil structure carries extra effective overburden pressure. For a given value of effective overburden pressure (σ_{vo}'), the soil exists at a void ratio higher than those for its intrinsic state. Such processes lead the soil to a "meta-stable" state on the right side of the "intrinsic compression line" (ICL).

- At constant effective overburden pressure (σ_{vo}'), disintegration of solid phase by processes like diagenesis of organic material or dissolution of soluble minerals like calcium carbonate can cause an increase in void ratio (transformation along I-B in Figure 6.2.1-B). Such processes leads the soil to values of void ratio that are higher than those for its intrinsic state and the soil is transferred to a meta-stable state.

Leroueil and Vaughan (1990) and Coop et al. (1995) discussed compressibility and strength characteristics of structured soils, using the framework of critical state soil mechanics. A schematic presentation of the response of an intact structured soil relative to the intrinsic compression line (ICL) is shown in Figure 6.2.1-C. The presence of structure allows the intact specimen to exist in the meta-stable state on the right side of the ICL. Upon reaching the effective yield stress (σ_{vy}'), the compressibility of soil increases and large plastic deformations occur. Finally, at large deformations and after total de-structuring, the soil approaches towards its intrinsic behavior. According to Coop et al. (1995), the distance that an intact structured specimen can travel beyond the intrinsic compression line prior to yielding, is a function of the degree of bonding.

Leroueil and Vaughan (1990) defined yield as a discontinuity in the stress-strain behavior under monotonic stress changes. "An irreversible post yield change in the stiffness and strength of the material" is an indicator of yielding of the soil structure. Bonded structured soils may yield as the result of de-structuring caused by swelling pressure. Swelling yield occurs at low effective stresses.

Kavvadas (1995) studied different states of natural soils and weak rocks using Corinth marl, which is a stiff carbonate silty clay and Ptolemais lignite, which is a weak rock of organic origin. Kavvadas (1995) said several processes could be involved in development of inter-particle bonding in soils. Such processes include thixotropy, aging, drained creep, cold welding caused by the pressure, solution and re-deposition of silicates at particle contacts, coalification caused by the diagenesis of organic sediments through the development of aliphatic chains in molecules, and cementation caused by the deposition of precipitates such as carbonates, gypsum, aluminum oxides, hydroxides or organic matter. He also commented that these processes could cause a gradual increase in stiffness and strength of the structured soils. He also mentioned that the effect of over-consolidation is practically identical to inter-particle bonding processes mentioned; because it can cause significant irreversible modification of the inter-particle attractive forces. Kavvadas (1995) also said that time required for bond development is a function of soil type and type of bonding processes involved.

Coop and Atkinson (1993) said that usage of water as pore fluid in testing such soils is not suitable and can reduce the bonding strength because of solubility of most cementing agents in water. Coop and Atkinson (1993) used light silicon oil of similar viscosity to water as pore fluid.

In a discussion regarding the study by Coop and Atkinson (1993), Huang and Airey (1994) commented on the importance of the pore fluid on the compression behavior. They said particles appear to be weaker in presence of water as pore fluid than in the presence of silicon oil or air.

As a part of an experimental program, Burland et al. (1996) studied the stiffness and compressibility of two lacustrine clays, Todi clay and Pietrafitta clay, and two marine clays, Vallericca clay and Corinth Marl. The state of vertical yield stress (σ'_{vy}) relative to the intrinsic compression line (ICL) was used as the assessment of magnitude of bonding in the soil structure. It was found that as the magnitude of inter-particle bonding in a soil structure is larger, the state of vertical yield stress (σ'_{vy}) is further to the right of the ICL. Burland et al. (1996) also said that the state of vertical yield stress (σ'_{vy}) can be so far to the right of the ICL that it may be even on the right side of the sedimentation compression line (SCL). Vertical yield stress (σ'_{vy}) of all soils, studied by Burland et al. (1996), were in the right side of the ICL. Also, vertical yield stress (σ'_{vy}) of Corinth Marl was in the right side of the SCL, implying presence of significantly large magnitude of inter-particle bonding.

6.2.2 Compressibility of Glaciolacustrine Silts in the Southern Interior of B. C.

Evans and Buchanan (1976) carried out one-dimensional consolidation tests using glaciolacustrine and colluvial silt sediments in the South Thompson River Valley. Glaciolacustrine specimens did not have a significant collapse upon flooding while colluvial specimens experienced major collapse (up to 14%). Collapse was also observed in the slurry specimens upon flooding.

Lum (1977) performed one-dimensional consolidation tests on glaciolacustrine silt sediments in the southern interior of British Columbia. Stress and strain controlled one-dimensional consolidation tests were carried out using specimens obtained from the north shore of the South Thompson River. Results of stress controlled tests are summarized in Figure 6.2.2-A and are explained briefly in the followings:

- Specimen 3-62: It was an undisturbed specimen, tested at its in-situ water content of 7.2%. The specimen was loaded up to 1400 kPa and showed a stiff behavior. Unloading to 670 kPa did not cause significant volume change; but subsequent flooding with water at this stress intensity caused collapse and the specimen experienced a 3.2% volume decrease.

- Specimen 3-64: It was an undisturbed specimen, flooded at a stress intensity of 88 kPa with de-aired water. Flooding at this stress intensity did not cause any volume change. This specimen showed a significantly more compressible behavior than Specimen 3-62 above a stress intensity of 300 kPa.

- Specimen 3-66: It was an undisturbed specimen, flooded at a stress intensity of 88 kPa with simulated septic tank effluent. The effluent used had a pH of 7.8 and contained appropriate concentrations of Ca^{++}, Mg^{++}, K^{+}, and Na^{+}. The specimen experienced a small amount of volume decrease; and the response was more compressible than Specimen 3-64, which was flooded with de-aired water. Also, specimen had a slightly smaller vertical yield stress (σ_{vy}') than Specimen 3-64.

- Specimen 3-33: It was an undisturbed specimen, saturated under 392 kPa cell pressure and 402 kPa back pressure during a period of 30 days. Specimen showed 0.2 % volume increase at the end of saturation. This specimen was more compressible than specimens tested dry or flooded and had a slightly smaller vertical yield stress (σ_{vy}') than the corresponding values for those specimens. The volume increase that occurred during the saturation process can cause changes in fabric and structure of the specimen prior to consolidation testing. Lum (1977) said that 50% of consolidation occurred within the first 15 seconds and the plots of consolidation versus log-time were concave up at the start and practically linear towards the end of each load increment. He also added that pore pressures were dissipated after the first five minutes. Lum (1977) concluded that at saturated state, creep and secondary consolidation should have a major role in the behavior of these materials.

- Specimen 3-71: It was an undisturbed specimen, flooded at a stress level of 88 kPa with 0.01 M HCl. This specimen had not only the most compressible behavior compared to all other undisturbed specimens tested, but also the smallest "vertical yield stress" (σ_{vy}').

- Specimen 3-R1: It was a soil-water slurry specimen, which was air-dried for 30 days in a constant laboratory environment. No details regarding the initial condition of the silt prior to mixing and also the referenced laboratory environment were provided. Lum (1977) concluded that the air-dried reconstituted specimen was more compressible than the undisturbed air-dried specimen (Specimen 3-62) and also had smaller vertical yield stress (σ_{vy}') than Specimen 3-62. As can be seen in Figure 6.2.2-A, both specimens had similar compression, rebound, and collapse behavior upon flooding. Hence, it is difficult to agree with the conclusion drawn by Lum (1977).

- Specimen 3-R2: This reconstituted specimen, which was flooded with water, behaved similar to Specimen 3-71, which was flooded with 0.01 M HCl. Lum (1977) speculated that the same type of bonding that was destroyed by HCl (in his opinion calcium carbonate) was also destroyed by processes involved in making the reconstituted specimens and this bonding was not recovered upon drying. It should be mentioned that bonding agents such as calcium carbonate are not only soluble in acidic pore fluids, but also in water with a pH of 7. The solubility of such soluble bonding agents is a function of their concentration, pH, and concentration of other chemical elements present in the soil environment. The behavior of this specimen implies breakage of aggregation created by bonding agents such as iron oxides, which are only soluble at low acidic pH values.

Lum (1977) also carried out strain controlled one-dimensional consolidation tests. Results of these tests are summarized in Figure 6.2.2-B and are explained briefly in the following:

- Specimen 3-45 and 3-44: They were undisturbed air-dried specimens with 2.44% and 2.97% water content, respectively. Specimen 3-44 was consolidated at 27 times faster strain rate than Specimen 3-45. Lum (1977) stated that the consolidation curves diverged at high stress levels; but he speculated that the difference should be due to difference in water content of two specimens. It is highly unlikely that 0.53% difference in water contents of two specimens causes measurable difference in the soil response. As can be seen in Figure 6.2.2-B, Specimen 3-45, tested under faster strain rate, is slightly more compressible. This behavior can be due to faster rate of loading or error involved in measurements.

- Specimen 3-41 and 3-67: They were undisturbed specimens tested at their in-situ water content of 6.6% and 6.54%, respectively. Both specimens, with approximately 6.5% water content, were significantly more compressible than Specimen 3-45 and 3-44 with approximately 3% water content. Also, both specimens had smaller vertical yield stress (σ_{vy}') than Specimen 3-45 and 3-44.

- Specimen 3-51: It was an undisturbed specimen, which had its water content increased to 23% by being placed between two wetted porous stones for two days. Lum (1977) did not comment on potential disturbance and change in fabric and structure as the result of introducing moisture. The specimen had a smaller vertical yield stress (σ_{vy}') than Specimen 3-41 and 3-67; but its compressibility was comparable.

- Specimen 3-42 and 3-43: These undisturbed specimens were flooded under strain controlled condition. No information was given regarding the initial water content of these specimens; but the final water contents of Specimen 3-42 and 3-43 were 49.7% and 46.3%, respectively. It was found that at 19.6 kPa stress intensity, flooding caused swelling; but at 78.5 kPa stress intensity it caused slight collapse. Lum (1977) recorded swelling pressures at about 17.5 kPa but noted that there was an initial drop in pressure, possibly because of large inward gradient as a result of flooding, followed by pressure built up as a result of elimination of capillary stresses and the swelling of clay minerals.

- Specimen 3-32: It was an undisturbed specimen, saturated under 392 kPa cell pressure and 402 kPa back pressure during a period of 30 days. The compressibility and vertical yield stress (σ_{vy}') of this specimen were comparable with flooded specimens (Specimen 3-42 and 3-43). Lum (1977) commented that the difference observed between compressibility of stress controlled flooded and saturated specimens should be due to structural disturbance as a result of initial swelling of the saturated specimen and also dynamic impact as the result of a sudden change in pore pressure at the start of each load increment.

Lum (1977) concluded that the compressibility of these soils are sensitive to water content and exposure to moisture especially at small values of water content.

Nyland and Miller (1977) carried out one-dimensional consolidation testing on glaciolacustrine silt sediments from the southern interior of B. C. Their results indicated 3% to 11% volume decrease (i.e. collapse) upon flooding. Results also showed that the magnitude of collapse increases as vertical effective stress corresponding to flooding stage increases.

6.3 Experimental Program

6.3.1 General

The glaciolacustrine silt sediments in the southern interior of British Columbia are generally at an unsaturated state. The in-situ water content of block samples obtained from Koosi Creek Slide and Okanagan Lake Park Slide sites was from 30% to 38% and from 10% to 25%, respectively.

One-dimensional consolidation tests were carried out on specimens at different states of moisture. As Coop and Atkinson (1993) also mentioned it, water can interact with cementing agents, precipitates, and minerals in soils and its introduction can change the soil structure. The strength of some cementing agents is a function of the water content. In order to preserve the soil structure and the strength of the cementing agents at a specific moisture condition, it was necessary to use a pore fluid that does not interact chemically with soil but its physical properties are close to those for water. Coop and Atkinson (1993) used light silicon oil as pore fluid. Commercially available Kerosene was chosen as the pore fluid added to unsaturated specimens in this study. The properties of Kerosene used in this experimental program are presented in Table 6.3.1.

6.3.2 Testing Apparatus

Six traditional stress controlled one-dimensional consolidation testing apparatus were used. Specimens were prepared and tested under a variety of moisture conditions. According to Leroueil and Marques (1996), temperature can influence stiffness and strength of soils. A controlled environment room with 80% relative humidity and 23 °C ± 2 °C was used to eliminate temperature as one of the test variables. Use of a controlled environment also prevents structural changes because of water content changes and provides a reference moisture environment for all tests. Deformations were measured using dial gages with 1/100 mm precision.

6.3.3 Test Procedure

Specimens were tested using the traditional incremental stress controlled one-dimensional consolidation testing. Load increments were done every 24 hours. These soils showed a tendency for swelling upon moistening by water under unconfined condition. Hence swelling pressure tests, as described by Head (1982), were carried out on specimens that were saturated by water. Water was gradually introduced to the specimens through filter paper and porous-stone. Any volume increase due to swelling pressure, induced by increasing water content of the specimen, was prevented by adding weights. Response of specimens to water content changes was monitored for 24 hour and swelling pressures observed were measured and recorded. Subsequently, following equilibrium between external stress and internal swelling pressure, standard one-dimensional stress controlled consolidation testing was carried out by incremental loading every 24 hours.

6.3.4 Material, Specimen Preparation, and Test results

Block samples obtained from Penticton silt sediments at Koosi Creek Slide and Okanagan Lake Park Slide sites were used as the material for one-dimensional consolidation testing. Details of geological and basic geotechnical properties of Penticton silt are presented in Chapter 2, 3, and 5.

Specimens were prepared and tested in various ways. The one-dimensional consolidation tests that were carried out during this study can be categorized in six series (Series A through F). Specimens are represented by a three-segment symbol such as "X-YY-ZZ". The first segment refers to the series identification character (i.e. A to F). The second segment refers to the silt that was used, "OL" or "KC", for silts sampled at Okanagan Lake Park Slide site or Koosi Creek Slide site, respectively. The third segment refers to the state of the pores; "D", "W", or "K" for pores filled with air, water, or Kerosene, respectively. The specimen preparation for the six series of one-dimensional consolidation testing is explained in the following:

Series A (Specimens A-OL/KC-W/K): Prior to testing, specimens used in this series were undisturbed specimens at their in-situ water content. Specimens were trimmed in an environment of +4 °C and 100% relative humidity and tested using distilled water (W) or Kerosene (K) as pore fluid. Swelling pressure tests were carried out on specimens that had water as pore fluid. Because of technical limitations in maintaining the initial state of in-situ moisture condition for the duration of testing, no tests were carried out on specimens at the unsaturated in-situ state. Basic properties of the specimens are presented in Table 6.3.4-A.

Series B (Specimens B-OL/KC-D/W/K): Specimens used in this series were undisturbed specimens, air-dried prior to testing at controlled environment of 23 °C ± 2 °C and 80% relative humidity. Subsequently, three specimens of silts from each site were tested using air, water, and Kerosene as pore fluid. Basic properties of these specimens are presented in Table 6.3.4-B.

Series C (Specimens C-OL/KC-D/W/K): Specimens in this series were undisturbed specimens, air-dried prior to testing at controlled environment of 23 °C ± 2 °C and 80% relative humidity. Testing of three specimens of silts from each site were started at air-dried condition. Subsequently, at about 500 kPa, two of the specimens were flooded with water and Kerosene. Basic properties of these specimens are presented in Table 6.3.4-C.

Series D (Specimens D-OL/KC-D/W/K): Specimens in this series were undisturbed specimens, air-dried at controlled environment of 23 °C ± 2 °C and 80% relative humidity. Following air-drying and under the state of zero vertical stress, water was gradually introduced to the specimens in oedometer rings through the base porous-stone and filter paper. Specimens, which were free to have volume change in the vertical direction, swelled. Subsequent to swelling and volume increase, specimens were air-dried at controlled environment of 23 °C ± 2 °C and 80% relative humidity. One-dimensional consolidation testing was carried out following the post swelling air-drying stage. Basic properties of these specimens are presented in Table 6.3.4-D.

Series E (Specimens E-OL/KC-D/W/K): Specimens in this series were trimmed from air-dried soil-water slurry. Soil-water slurry was made in accordance with guidelines proposed by Burland (1990). Air-drying was done at controlled environment of 23 °C ± 2 °C and 80% relative humidity. Subsequently, three specimens of dark and light colored silts were tested using air, water, and Kerosene as pore fluid. Basic properties of these specimens are presented in Table 6.3.4-E.

Series F (Specimens F-OL/KC-FS/W/K/KD/PW): In this series, five more specimens of silts from each site were tested. Among these specimens, there were several slurry specimens. Soil-water and soil-Kerosene slurries were made in accordance with guidelines proposed by Burland (1990). It is suggested by several researchers to re-consolidate the slurry specimens to in-situ state of stress prior to testing. However, re-consolidation to the in-situ state of stress prior to testing can induce structure to soil specimens and can lead to misleading results. Consequently, slurry specimens were cast directly in the oedometer rings and one-dimensional consolidation testing was carried out immediately after casting. Specimen F-OL/KC-W and F-OL/KC-K were made from slurry using water and Kerosene as the mixing fluid, respectively. Specimen F-OL/KC-KD was prepared by air-drying of soil-Kerosene slurry at controlled environment of 23 °C ± 2 °C and 80% relative humidity. Specimen F-OL/QC-PW was prepared by statically compacting air-dried grind soil. Specimen F-OL/KC-FS was an undisturbed specimen, which swelled upon gradual introduction of water through porous stone and filter paper under zero vertical state of stress. Basic properties of these specimens are presented in Table 6.3.4-F.

Thirty eight one-dimensional consolidation tests were carried out using silt sediments sampled at Okanagan Lake Park Slide and Koosi Creek Slide sites. Results, plotted in e-log σ'_v space, are presented in Figure B-6.3-A through F of Appendix B for Series A through F, respectively. Results are also summarized in Figure 6.3-A, B, and C for specimens that had air, water, and Kerosene as pore fluid, respectively.

6.4 Discussion of Results

Results of the one-dimensional consolidation testing, normalized using void ratio at the start of loading (e_o), are presented in Figure 6.4-A through F for Series A through F, respectively. Normalizing the change of void ratios by the void ratio at the start of loading (e_o) makes comparison of the compressibility of Penticton silt at different states of structure and loading easier than the direct comparison.

The state of one-dimensional consolidation curve of soils relative to the intrinsic compression line "ICL" and the sedimentation compression line "SCL" is considered as an assessment of structure and bonding in soils by several researchers including Burland (1990), Burland et al. (1996), Kavadaas (1995), and Leroueil (1997). Figure 6.4-G shows response of Penticton silt relative to the "ICL" and the "SCL" in I_v-log σ_v' space. Theoretical ICL is drawn using Equation 6.2.1-B, proposed by Burland (1990), and experimental intrinsic compression lines, ICL (OL) and ICL (KC) were obtained using the results of F-OL-W and F-KC-W specimens, which were reconstituted slurry specimens made in accordance with guidelines proposed by Burland (1990). As suggested by Burland (1990), there is a reasonable agreement between theoretical and experimental ICL lines for values of effective vertical stress (σ_v') larger than 100 kPa. Burland et al. (1996) said that the ICL is a unique line between values of σ'_v of 10 kPa and 5000 kPa for clays. Within this stress range, a reasonable agreement can be observed between the experimental ICL lines for Penticton silt; but theoretical and experimental curves deviate from each other for values of σ_v' less than 50 kPa or more than 1500 kPa.

In Figure 6.4-G, the natural undisturbed state of Penticton silt is represented by the results of A-OL-W and A-KC-W tests, which were undisturbed specimens at their in-situ water content prior to saturation with water. According to Burland (1990) and Leroueil (1997), the further to the right of the ICL is the vertical yield stress σ_{vy}', the greater is the degree of structure of a soil. As a result, it can be concluded that Penticton silt is structured. Also, Burland et al. (1996) stated that the presence of a vertical yield stress σ_{vy}' to the right of the SCL is an indication of cementation and a sensitive bonded structure. Consequently, it can be implied that Penticton silt is also cemented. In addition, it appears that Specimen A-OL-W (M.C.=10.9%) that was drier at its in-situ state than Specimen A-KC-W (M.C.=36%) has a larger vertical effective yield stress σ_{vy}'. De-structuring of A-KC-W occurs more gradual than the de-structuring of Specimen A-OL-W. Also while A-OL-W appears to be less compressible than A-KC-W prior to yielding, they have similar post-yield compressibility.

The one-dimensional consolidation tests of Series A, shown in Figure 6.4-A, deal with undisturbed specimens that initially were at their in-situ water content. The in-situ water content of OL specimens was at about 10% and those for KC specimens were close to the liquid limit at 36%. It should be mentioned that the water content of these soils at saturated state is at about 45%, which is larger than their liquid limit. The swelling pressure of specimen A-OL-W was 25 kPa. Review of results of Series A indicate that specimens with Kerosene as pore fluid (A-OL-K and A-KC-K) have approximately 200 kPa to 400 kPa larger vertical yield stress σ_{vy}' compared to specimens with water as pore fluid (A-OL-W and A-KC-W). Also, prior to yielding, Kerosene saturated specimens are relatively less compressible than water saturated specimens.

Results for undisturbed specimens of Series B, which were initially air-dried, are shown in Figure 6.4-B. The compressibility of specimens with Kerosene as pore fluid (B-OL-K and B-KC-K) and those with air as pore fluid (B-OL-D and B-KC-D) are essentially the same. The swelling pressure for specimens with water as pore fluid (B-OL-W and B-KC-W) was as high as 90 kPa. Both pre-yield and post-yield behavior of specimens with water as pore fluid was more compressible than specimens with Kerosene or air as pore fluid. The post yield response of specimens with water as pore fluid are significantly more compressible than that for specimens with Kerosene or air as pore fluid. The more compressible response of water saturated specimens and existence of swelling pressure in these specimens imply a significance of water and its interaction with the solid phase in processes involved in de-structuring, swelling, and loss of inter-particle bonding. Also, elimination of capillary tension due to saturation of specimens by Kerosene, which does not have a chemical interaction with the solid phase, did not cause swelling and did not increase the compressibility of the soil specimen.

Results for undisturbed specimens of Series C are shown in Figure 6.4-C. All specimens were initially air-dried and were tested at air-dried state up to the vertical effective stress of 500 kPa. At that stage, Specimen C-OL-K and C-KC-K were flooded with Kerosene. Following flooding, small elastic deformation, approximately 0.01 mm, occurred. The small elastic deformation was probably due to pore pressure generated by flooding. Post-flooding compressibility of specimens flooded with Kerosene were virtually identical to those specimens that were tested air-dried. At the same stage, Specimen C-OL-W and C-KC-W were flooded with water. Flooding with water caused significant volume decrease (i.e., collapse and plastic deformation, and the compressibility of specimens increased significantly). It appears that flooding with water caused yielding. The large volume change and increased compressibility upon flooding by water imply that water and its interaction with the solid phase has a significant influence in processes involved in de-structuring and loss of inter-granular bonding. Comparison of the magnitude of collapse upon flooding by Kerosene and water can imply that collapse phenomena in soils should be mainly due to de-structuring rather than saturation and loss of suction.

Results of specimens of series D, which are shown in Figure 6.4-D, experienced one cycle of environmental loading (wetting and drying) under vertical unconfined condition. Unlike undisturbed specimens of Series A and B, water saturated specimens did not have any significant swelling pressure. All specimens are very compressible with significantly smaller vertical yield stress σ_{vy}' than undisturbed specimens. High compressibility and small values of vertical yield stress σ_{vy}' are indications of de-structuring due to environmental loading. At low to moderate stresses, specimens with Kerosene or air as pore fluid are less compressible than those with water as pore fluid. These differences are an indication of limited existence of structure and inter-particle bonding.

Test results of Series E are shown in Figure 6.4-E. Specimens in this series were initially air-dried specimens, trimmed from soil-water slurry. Similar to undisturbed specimens in Series B, specimens with air or Kerosene as pore fluid have essentially the same response and also are less compressible than specimens with water as pore fluid. The swelling pressure of water saturated specimens is between 30 kPa and 100 kPa. The stiff response of air-dried and Kerosene saturated specimens imply formation of structure and inter-particle bonding in the air-dried slurry. Similar to Series B, the more compressible response of specimens with water as pore fluid and existence of swelling pressure in these specimens imply a significance of water and its interaction with the solid phase in processes involved in de-structuring, swelling, and loss of inter-particle bonding.

Test results for Series F are shown in Figure 6.4-F. Upon first load increment, both soil-water slurry specimens (F-OL-W and F-KC-W) and soil-Kerosene slurry specimens (F-OL-K and F-KC-K) showed some initial collapse, followed by highly compressible behavior. One-dimensional consolidation testing of Specimen F-OL-FS and F-KC-FS were started following the swelling of the specimens upon gradual introduction of water through the base porous stone and filter paper under the condition of no vertical confinement. Similar to slurry specimens, after an initial collapse upon first load increment, specimens had highly compressible behavior. It can be concluded that free swelling and volume increase caused de-structuring of the specimens, which initially were undisturbed and structured. This behavior is in agreement with the study by Leroueil and Vaughan (1990), that predicted yielding as the consequence of swelling at low effective stress levels. Specimen F-OL-PW and F-KC-PW, which were made by statically packing air-dried grind soil in oedometer ring, show some sign of minor structure at low stress levels, followed by highly compressible behavior. The initial behavior can be due to the packing process. Specimen F-OL-KD and F-KC-KD, which were air-dried soil-Kerosene slurry specimens, behaved similar to air-dried packed grind soil specimens and were highly compressible with no indication of structure in their behavior. In summary, regardless of the initial condition, all specimens in Series F behave in a similar manner to un-structured fresh soil slurry and are highly compressible with no indication of structure in their behavior.

Normalized test results are also summarized in Figure 6.4-H, I, and J for specimens that had air, water, and Kerosene as pore fluid, respectively.

Test results for specimens with air as the pore fluid are summarized in Figure 6.4-H. The stiff and also essentially identical response of undisturbed air-dried specimens (B-OL-D and B-KC-D) and air-dried soil-water slurry specimens (E-OL-D and E-KC-D) indicate that the major portion of structure and inter-particle bonding is not due to the natural fabric, particle arrangements, and aging. They should be due to processes that can influence the soil structure in a short period of time. Comparison of stiff behavior of air-dried soil-water slurry specimens (E-OL-D and E-KC-D) with compressible behavior of air-dried soil-Kerosene slurry specimens (F-OL-KD and F-KC-KD) and statically packed air-dried grind soil specimens (F-OL-PW and F-KC-PW) indicates the significance of properties of water and its interaction with the solid phase in the formation of the structure of soil and the inter-particle bonding. Comparison of the behavior of air-dried specimens, which experienced a cycle of environmental loading (D-OL-D and D-KC-D) with the behavior of other specimens in these figures, indicates major de-structuring but limited existence of structure and inter-particle bonding in those specimens.

Test results for specimens with water as the pore fluid are summarized in Figure 6.4-I. Results indicate that the swelling pressure generally increases as the initial water content of specimens decreases. The one-dimensional consolidation curves of specimens that experienced one cycle of environmental loading (D-OL-W and D-KC-W), specimens that experienced free swelling under no vertical confinement (F-OL-FS and F-KC-FS), and specimens of soil-water slurry (F-OL-W and F-KC-W) are highly compressible. Specimens that experienced free swelling under no vertical confinement (F-OL-FS and F-KC-FS), and specimens of soil-water slurry (F-OL-W and F-KC-W) experienced significant initial collapse. In general, results presented and summarized in Figure 6.4-I are in agreement with conclusions drawn based on discussion of specimens with air as pore fluid.

Test results for specimens with Kerosene as pore fluid are summarized in Figure 6.4-J. Results presented in these figures are in complete agreement with conclusions drawn based on discussion of specimens with air or water as pore fluid. Usage of Kerosene, an organic fluid with no chemical interaction with the solid phase of soil, provides the opportunity to saturate soil specimens without causing any damage to fabric and structure. Undisturbed specimens of Series B, which were drier than undisturbed specimens of Series A prior to saturation with Kerosene, were less compressible than specimens of Series A. This observation is an indication of moisture dependency of the degree of structure and inter-particle bonding. In turn, specimens of Series A were much stiffer than specimens of Series D and F. One-dimensional consolidation testing of specimens in Series B, C, and E involved saturating or flooding of air-dried specimens. The stiff and also essentially similar behavior of initially air-dried undisturbed specimens of Series B (B-OL-K and B-KC-K), flooded specimens of Series C (C-OL-K and C-KC-K), and soil-water slurry specimens of Series E (E-OL-K and E-KC-K) indicate that the major portion of structure and inter-particle bonding is not due to the natural fabric, particle arrangements, and aging. They should be due to processes that can influence the soil structure in a short period of time.

Results of some of the one-dimensional consolidation tests of the current study can be compared with similar tests carried out by Lum (1977). Results of both studies are in agreement regarding to increasing compressibility with increasing water content. Results of both studies regarding to collapse due to flooding are also in good agreement.

Lum (1977) concluded that remolded dry specimens were more compressible than dry undisturbed specimen. This conclusion is not in agreement with the results of the current study. Reconstituted Specimen E-OL-D and E-KC-D are as stiff as undisturbed Specimen B-OL-D and B-KC-D. Based on a review of tests carried out by Lum (1977) and presented in Figure 6.2.2-A and B, the difference between the behavior of remolded and undisturbed dry specimens is not as significant as expressed by Lum (1977).

Lum (1977) suggested that destruction of calcium carbonate ($CaCO_3$) bonding occurred upon flooding by 0.01 M HCl. It should be mentioned that calcium carbonate is soluble not only at a pH value corresponding to 0.01 M HCl, but also at values of pH that include distilled water and simulated septic tank effluent used in the study by Lum (1977). The enhanced compressibility of the specimen flooded with 0.01 M HCl compared to specimens flooded with water or simulated septic tank effluent could be the consequence of dissolution of bonding agents such as iron oxides that are soluble at low values of pH. Structural disintegration of some weak soil minerals at low values of pH is also probable.

Lum (1977) suggested that the swelling pressure should be due to the elimination of capillary forces and presence of montmorillonite. The occurrence of a large amount of swelling (up to 45% by volume), relatively small values of swelling pressure, and small percentage of swelling clays present, indicate that elimination of capillary tension and the presence of swelling clays cannot entirely explain the swelling behavior of these sediments. Swelling of these sediments is discussed in Chapter 8 in detail.

6.5 Summary

Based on results of one-dimensional consolidation tests, carried out in this study, and results of studies mentioned in the literature review, the following conclusions can be drawn:

The Glaciolacustrine Penticton silt sediments tested are structured. The improved soil behavior observed in these sediments is mainly due to inter-particle bonding rather than soil fabric and particle arrangement. Recovery of these improved structural behaviors does not need geological times. The elimination of capillary tensions does not cause any significant change in the response of the soil. The strength of inter-particle bonding in these soils appears to be a function of water content. After saturation, undisturbed specimens at drier initial in-situ state were stiffer than undisturbed specimens with higher initial in-situ water content. Environmental loading (wetting and drying) under unconfined condition can cause significant de-structuring; but the presence of a limited amount of inter-particle bonding after exposure to environmental loading was observed. For these silt sediments, swelling pressure was in the range of 15 kPa to 100 kPa when water was used. It was observed that the magnitude of swelling pressure appears to be a function of water content of soil. In these soil sediments, generation of pore pressure can cause elastic deformations; while breakage of inter-particle bonding and occurrence of chemical reaction between water and the solid phase can cause plastic deformations (i.e., collapse).

Table 6.3.1 – Properties of Kerosene Used

Property	Description
Complex Mixture of Petroleum Hydrocarbons (C_9-C_{17})	> 99.9%
Aromatic Content	< 18%
Additives	< 0.1%
Density (at 15 °C)	0.82 kg/L
Viscosity (at 40 °C)	1.0-1.9 cSt
Vapor Pressure (at 25 °C)	< 0.7 kPa
Boiling Point (at 1 atm)	160 °C-290 °C
Flash Point	40 °C (Minimum)
Auto Ignition Temperature	255 °C
Solubility in Water	Insoluble
Appearance	Colorless, oily liquid
Odor	Hydrocarbon Odor

Table 6.3.4-A – Basic Properties of Series A Specimens

Specimen	e_o (Start of Test)	M.C. (%)
A-OL-W	0.883	10.88
A-OL-K	0.885	7.60
A-KC-W	0.923	36.00
A-KC-K	0.927	35.94

Table 6.3.4-B – Basic Properties of Series B Specimens

Specimen	e_o (Start of Test)	M.C. (%)
B-OL-D	0.849	3.48
B-OL-W	0.825	2.68
B-OL-K	0.837	3.39
B-KC-D	0.734	2.57
B-KC-W	0.748	2.69
B-KC-K	0.802	2.64

Table 6.3.4-C – Basic Properties of Series C Specimens

Specimen	e_o (Start of Test)	M.C. (%)
C-OL-D	0.841	3.08
C-OL-W	0.891	3.84
C-OL-K	0.866	3.57
C-KC-D	0.738	3.08
C-KC-W	0.801	2.80
C-KC-K	0.791	2.49

Table 6.3.4-D – Basic Properties of Series D Specimens

Specimen	e_{in} (Initial)	e_{sw} (After Swelling)	e_o (Start of Test)	M.C. (%)
D-OL-D	0.895	1.640	1.049	3.76
D-OL-W	0.869	1.717	1.077	3.55
D-OL-K	0.920	1.750	1.082	3.52
D-KC-D	0.749	1.262	0.826	2.92
D-KC-W	0.793	1.316	0.931	2.54
D-KC-K	0.899	1.609	1.087	3.18

Table 6.3.4-E – Basic Properties of Series E Specimens

Specimen	e_o (Start of Test)	M.C. (%)
E-OL-D	0.657	3.15
E-OL-W	0.657	3.35
E-OL-K	0.672	3.43
E-KC-D	0.628	2.75
E-KC-W	0.758	2.83
E-KC-K	0.645	2.65

Table 6.3.4-F – Basic Properties of Series F Specimens

Specimen	e_{in} (Initial)	e_o (Start of Test)	M.C. (%)
F-OL-FS	0.930	1.851	3.56
F-OL-W	N/A	1.370	49.12
F-OL-K	N/A	1.459	58.5 (by volume)
F-OL-KD	N/A	1.312	3.47
F-OL-PW	N/A	1.564	3.32
F-KC-FS	0.855	1.582	2.77
F-KC-W	N/A	1.242	44.94
F-KC-K	N/A	1.528	52.5 (by volume)
F-KC-KD	N/A	1.286	2.46
F-KC-PW	N/A	1.358	2.58

Figure 6.2.1-A – The Intrinsic Compression Line (ICL) in
(a) e-log σ'_v and (b) I_v-log σ'_v
(after Burland (1990))

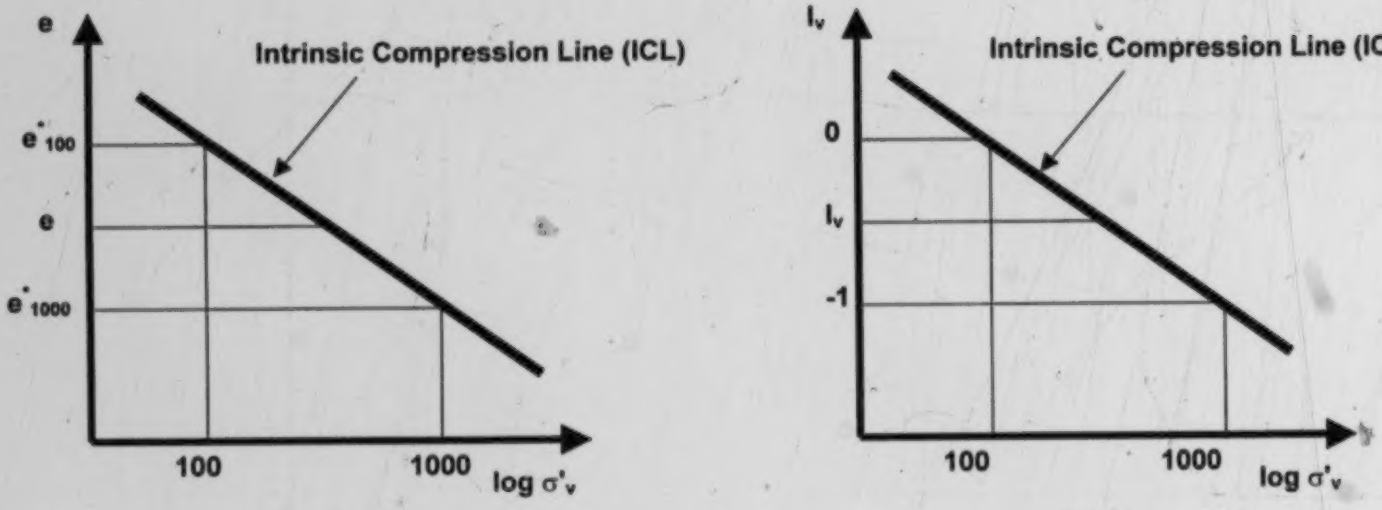

(a) (b)

Figure 6.2.1-B – Summary of State Transformations

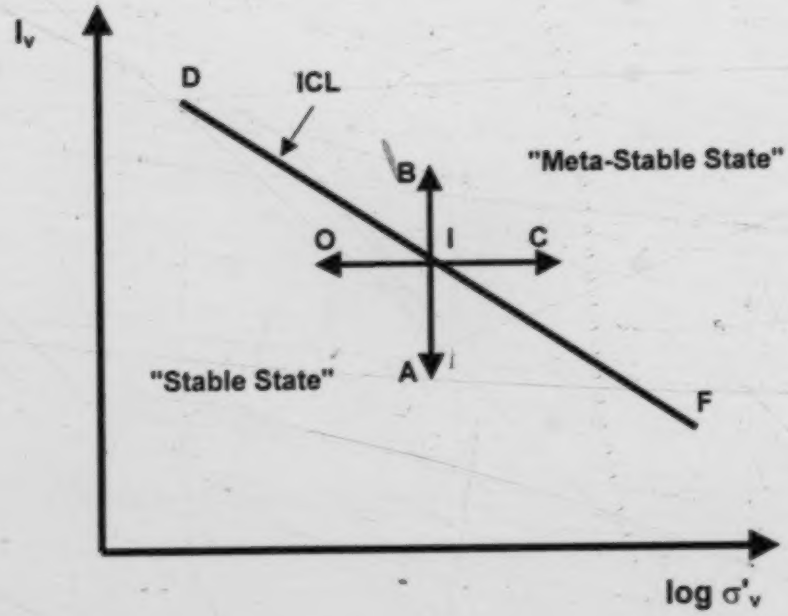
I_v
D
ICL
B
"Meta-Stable State"
O
I
C
"Stable State"
A
F
$\log \sigma'_v$

Figure 6.2.1-C – Compressibilty of an Intact Specimen Relative to the ICL

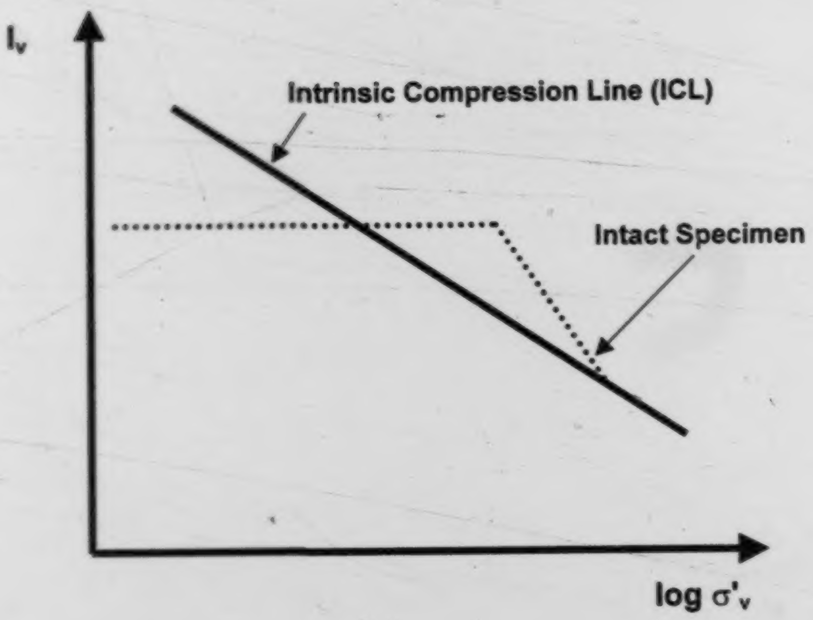

I_v
Intrinsic Compression Line (ICL)
Intact Specimen
$\log \sigma'_v$

Figure 6.2.2-A - Summary of Load Controlled Consolidation Tests

(Carried Out by Lum (1977))

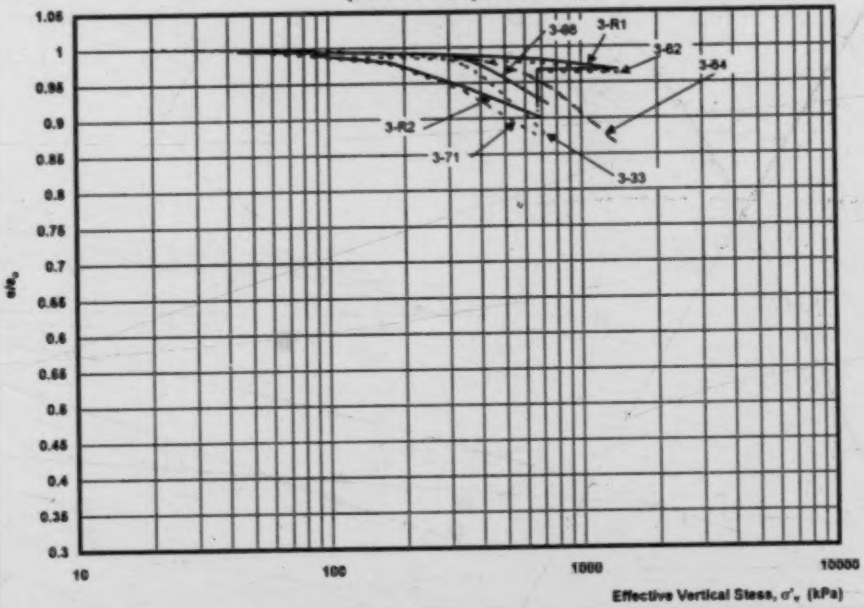

Figure 6.2.2-B - Summary of Strain Controlled Consolidation Tests

(Carried Out by Lum (1977))

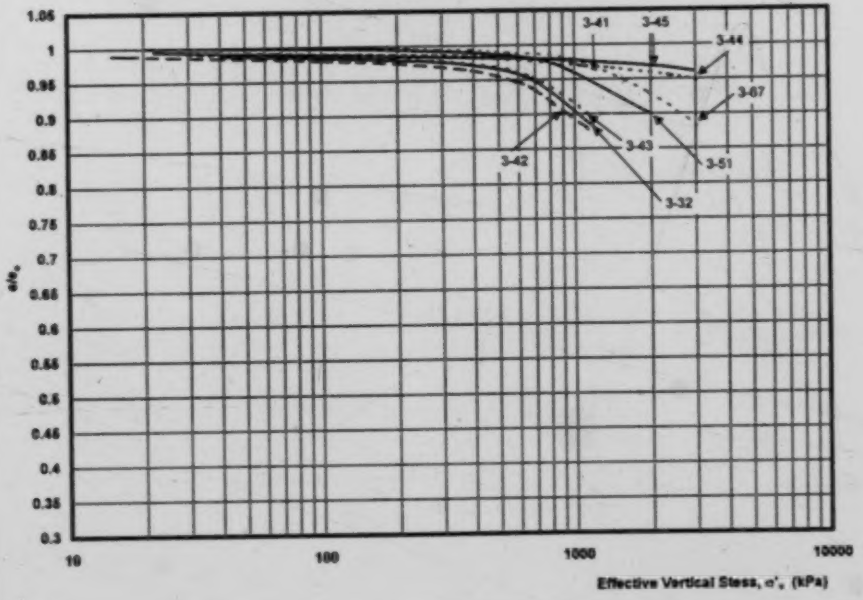

Figure 6.3-A(a) - Summary of One-Dimensional Consolidation Tests for Specimens from Okanagan Lake Park Site with Air as Pore Fluid

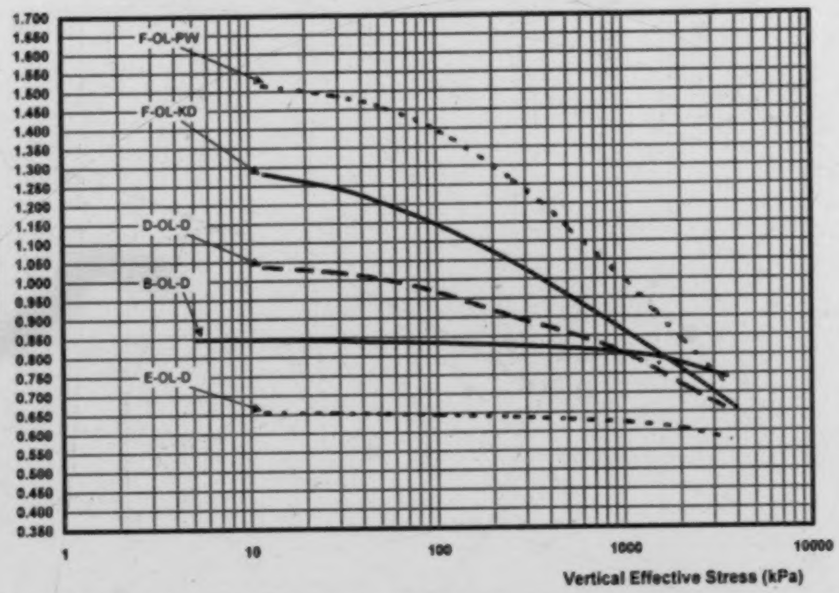

Figure 6.3-A(b) - Summary of One-Dimensional Consolidation Tests for Specimens from Koosi Creek Site with Air as Pore Fluid

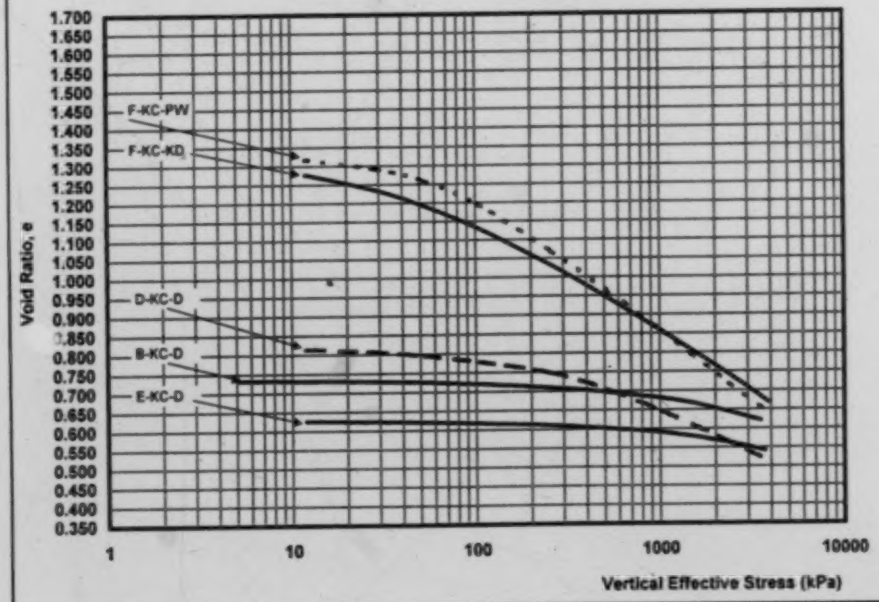

Figure 6.3-B(a) - Summary of One-Dimensional Consolidation Tests for Specimens from Okanagan Lake Park Site with Water as Pore Fluid

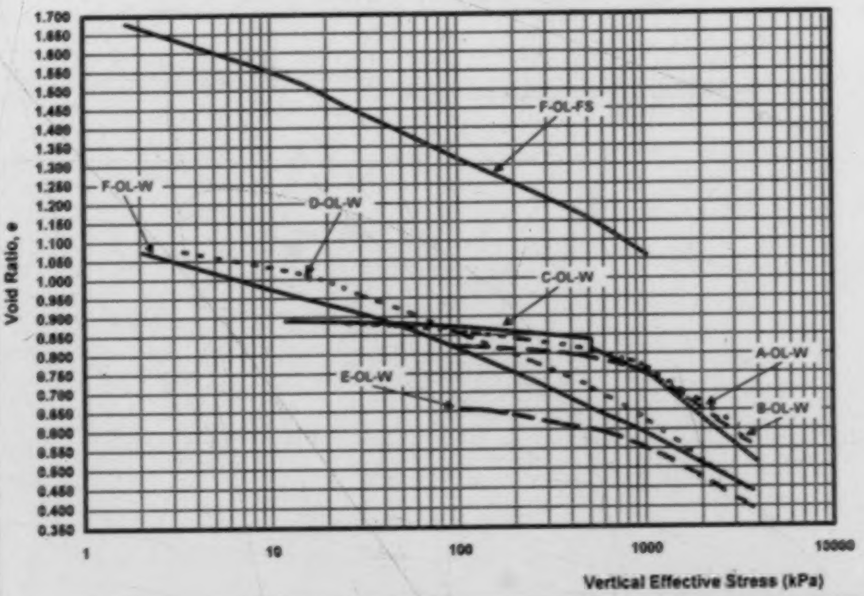

Figure 6.3-B(b) - Summary of One-Dimensional Consolidation Tests for Specimens from Koosi Creek Park Site with Water as Pore Fluid

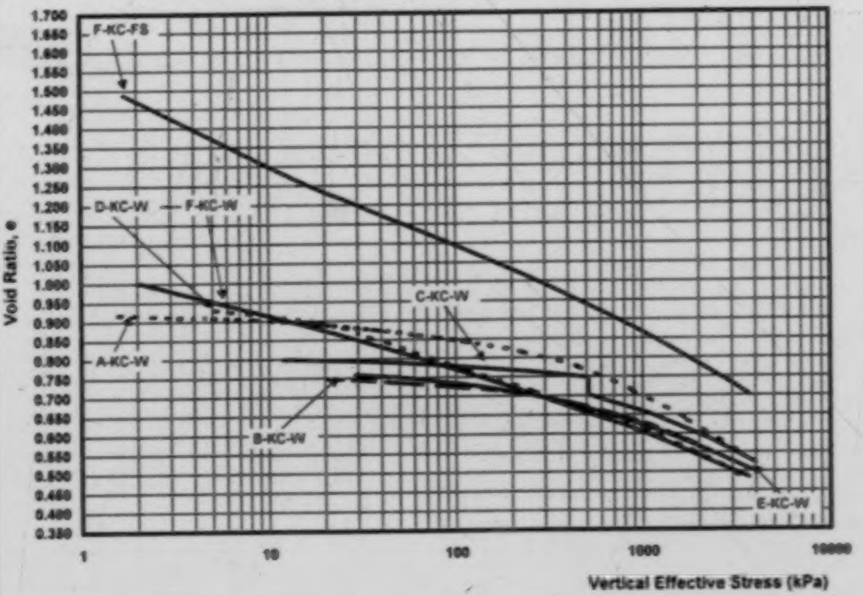

Figure 6.3-C(a) - Summary of One-Dimensional Consolidation Tests for Specimens from Okanagan Lake Park Site with Kerosene as Pore Fluid

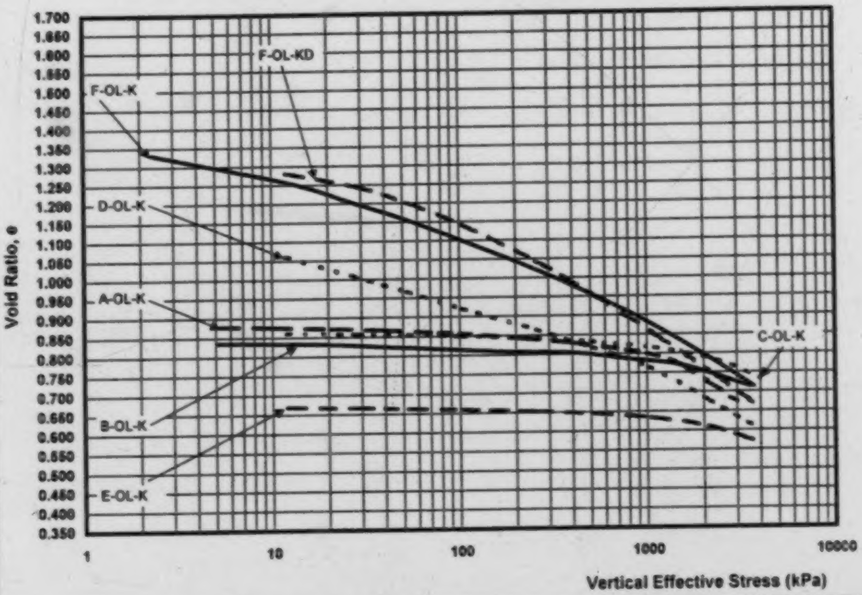

Figure 6.3-C(b) - Summary of One-Dimensional Consolidation Tests for Specimens from Koosi Creek Site with Kerosene as Pore Fluid

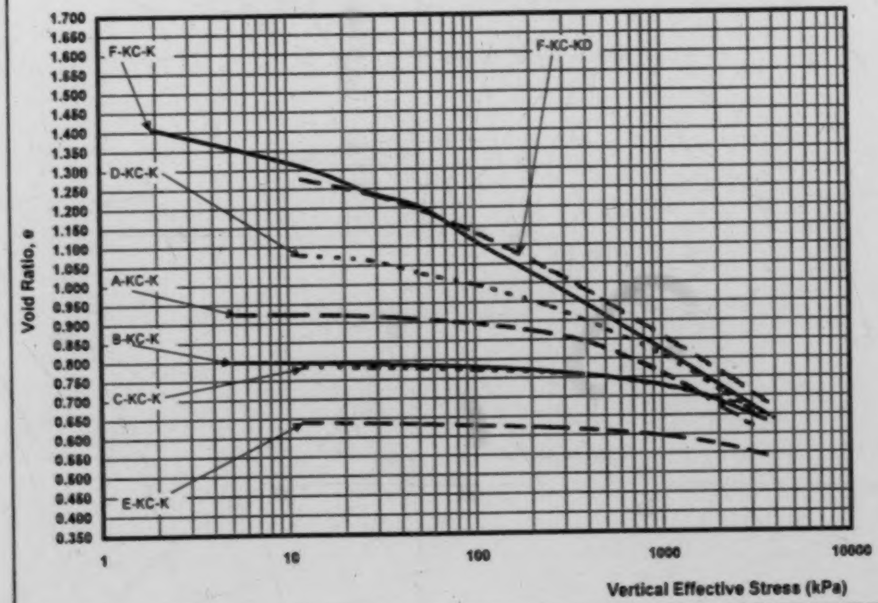

Figure 6.4-A(a) - Normalized One Dimensional Consolidation Test Results
Series A, Okanagan Lake Park Slide Site Specimens

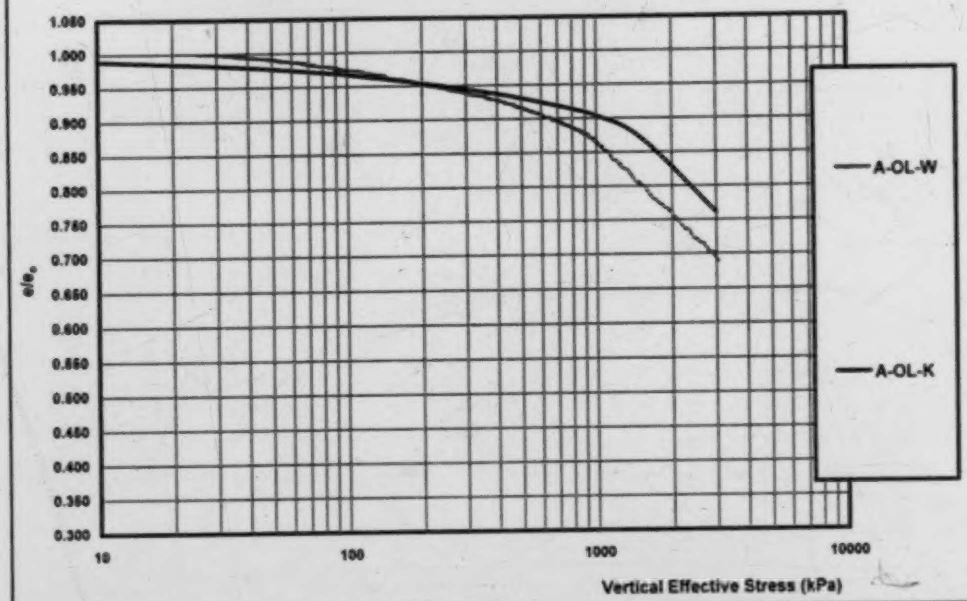

Figure 6.4-A(b) - Normalized One Dimensional Consolidation Test Results
Series A, Koosi Creek Slide Site Specimens

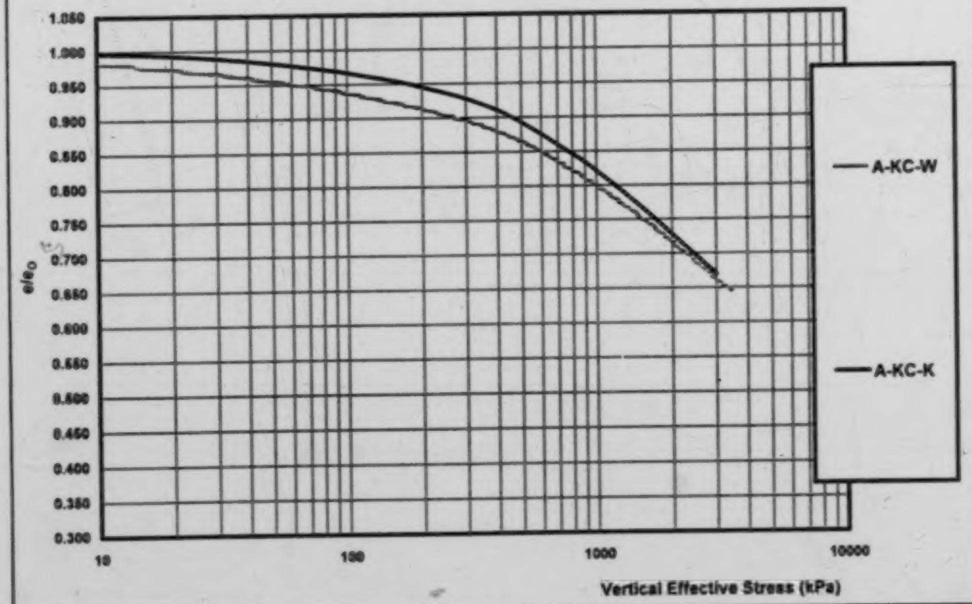

Figure 6.4-B(a) - Normalized One Dimensional Consolidation Test Results
Series B, Okanagan Lake Park Slide Site Specimens

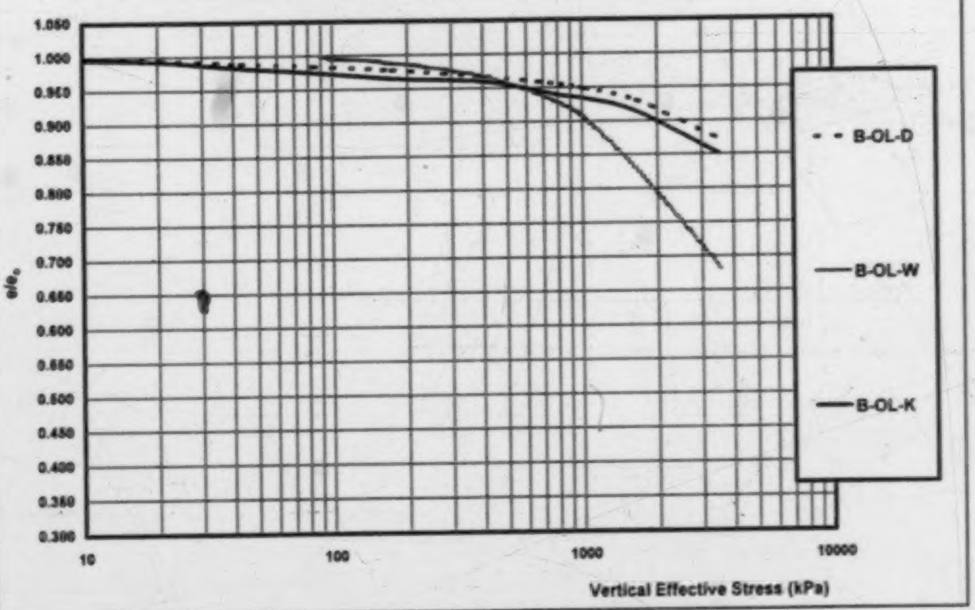

Figure 6.4-B(b) - Normalized One Dimensional Consolidation Test Results
Series B, Koosi Creek Slide Site Specimens

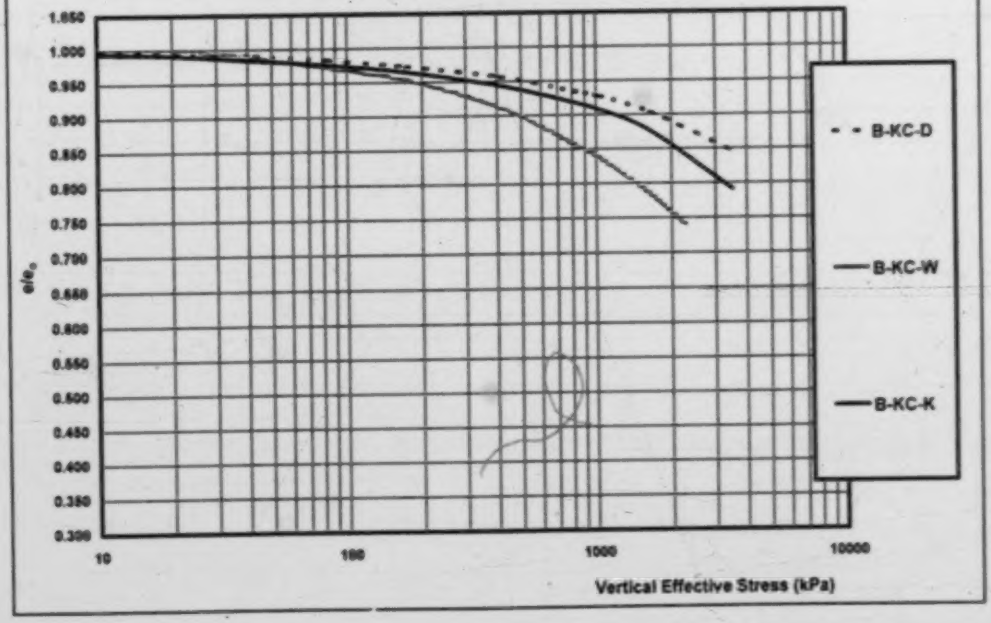

Figure 6.4-C(a) - Normalized One Dimensional Consolidation Test Results
Series C, Okanagan Lake Park Slide Site Specimens

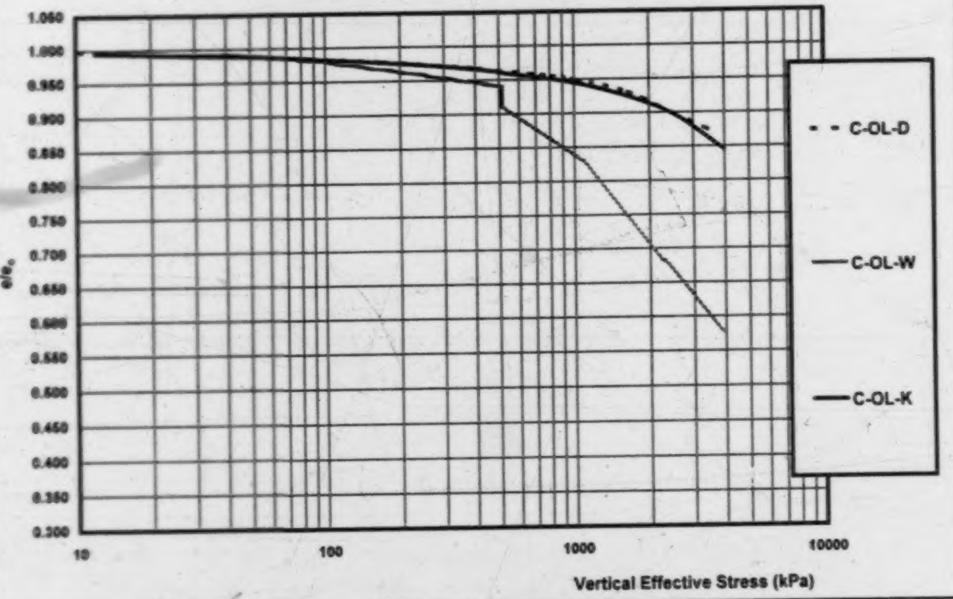

Figure 6.4-C(b) - Normalized One Dimensional Consolidation Test Results
Series C, Koosi Creek Slide Site Specimens

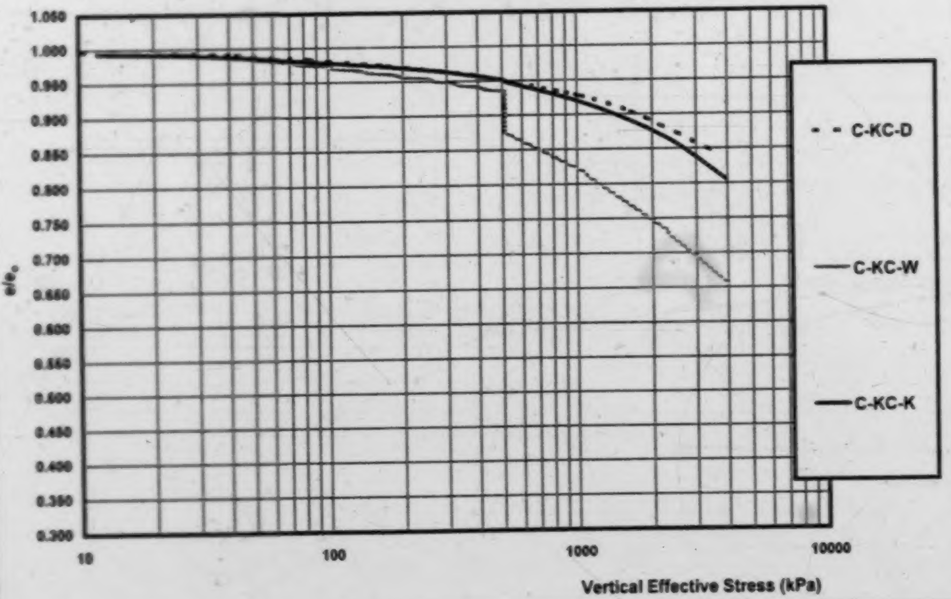

Figure 6.4-D(a) - Normalized One Dimensional Consolidation Test Results Series D, Okanagan Lake Park Slide Site Specimens

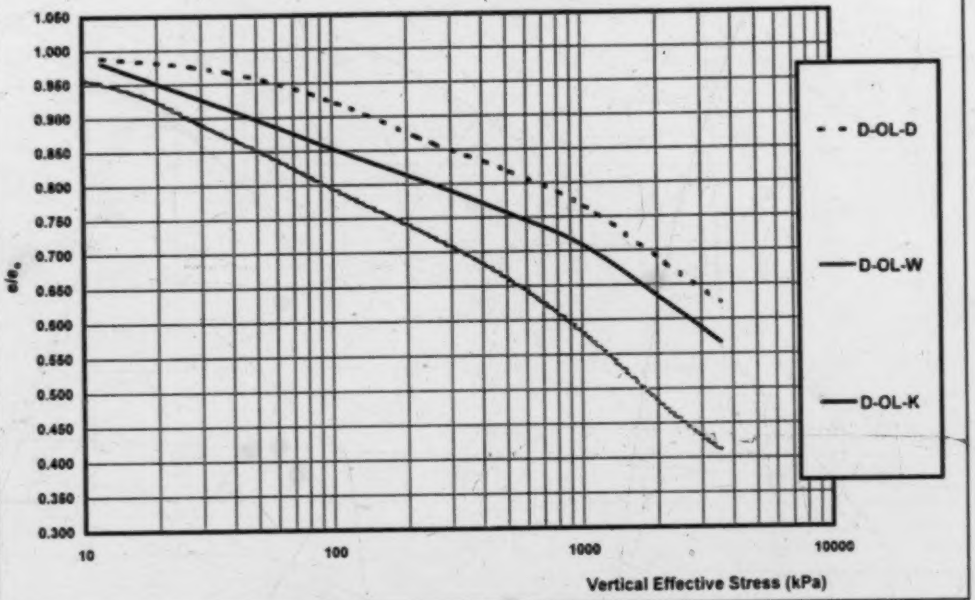

Figure 6.4-D(b) - Normalized One Dimensional Consolidation Test Results Series D, Koosi Creek Slide Site Specimens

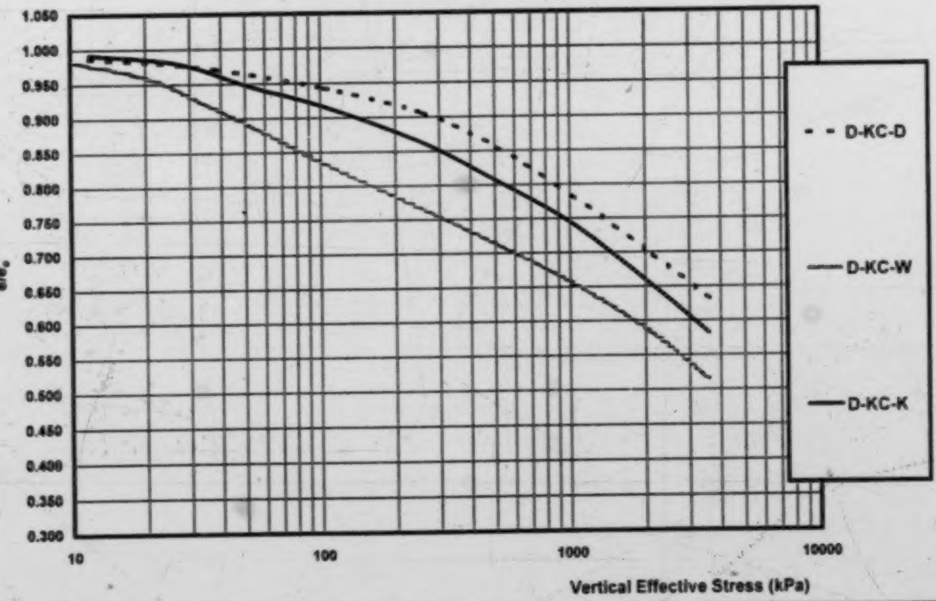

Figure 6.4-E(a) - Normalized One Dimensional Consolidation Test Results
Series E, Okanagan Lake Park Slide Site Specimens

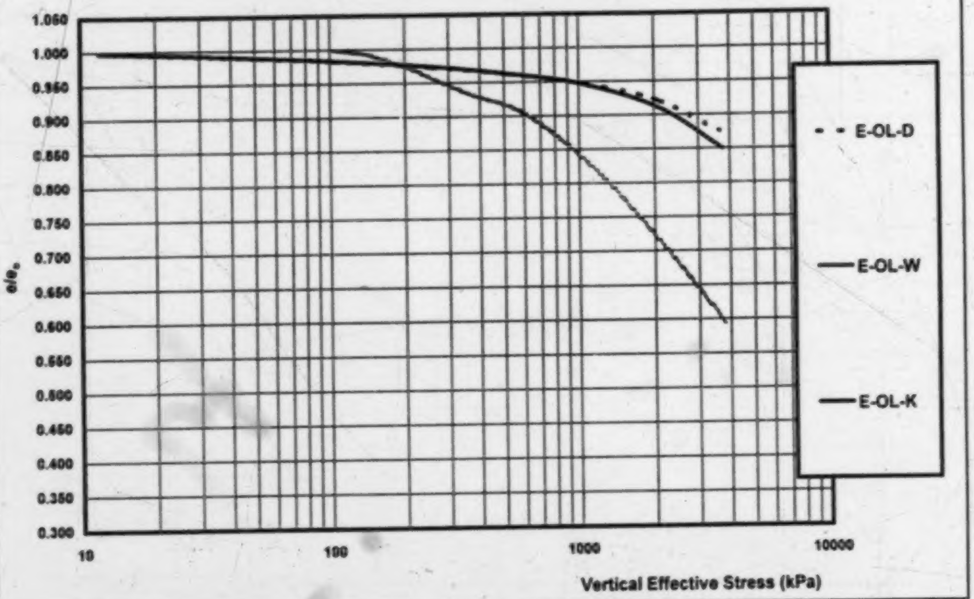

Figure 6.4-E(b) - Normalized One Dimensional Consolidation Test Results
Series E, Koosi Creek Slide Site Specimens

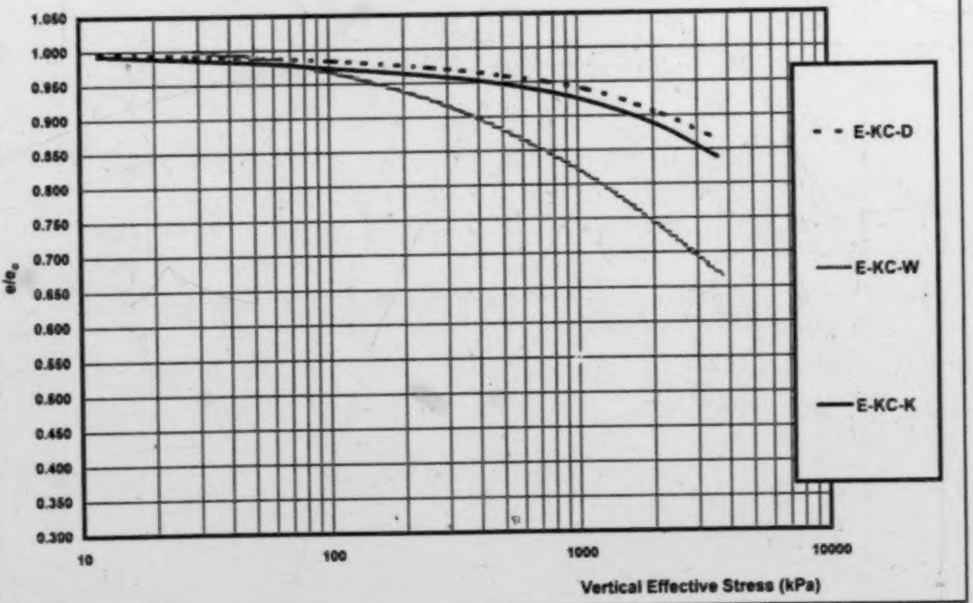

Figure 6.4-F(a) - Normalized One Dimensional Consolidation Test Results
Series F, Okanagan Lake Park Slide Site Specimens

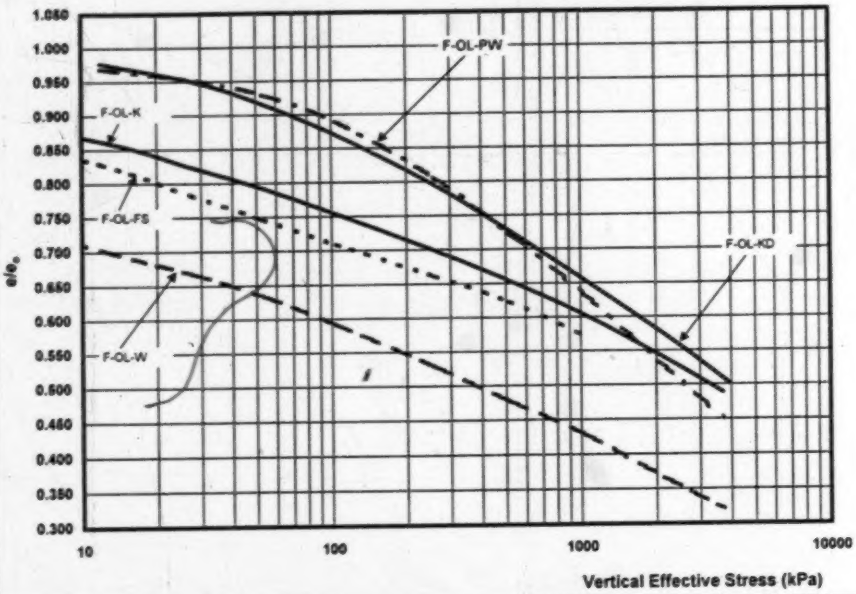

Figure 6.4-F(b) - Normalized One Dimensional Consolidation Test Results
Series F, Koosi Creek Slide Site Specimens

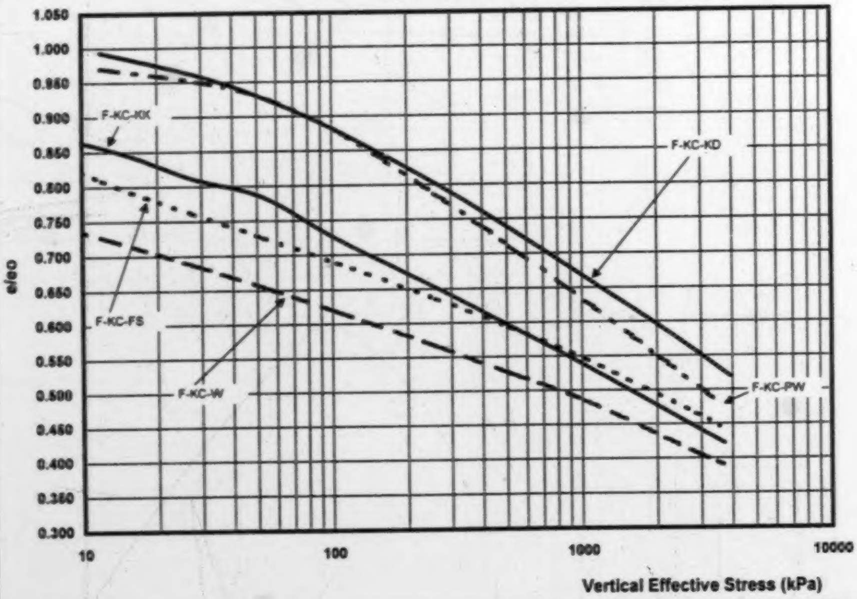

Figure 6.4-G - State of OL and KC Relative to the ICL and the SCL

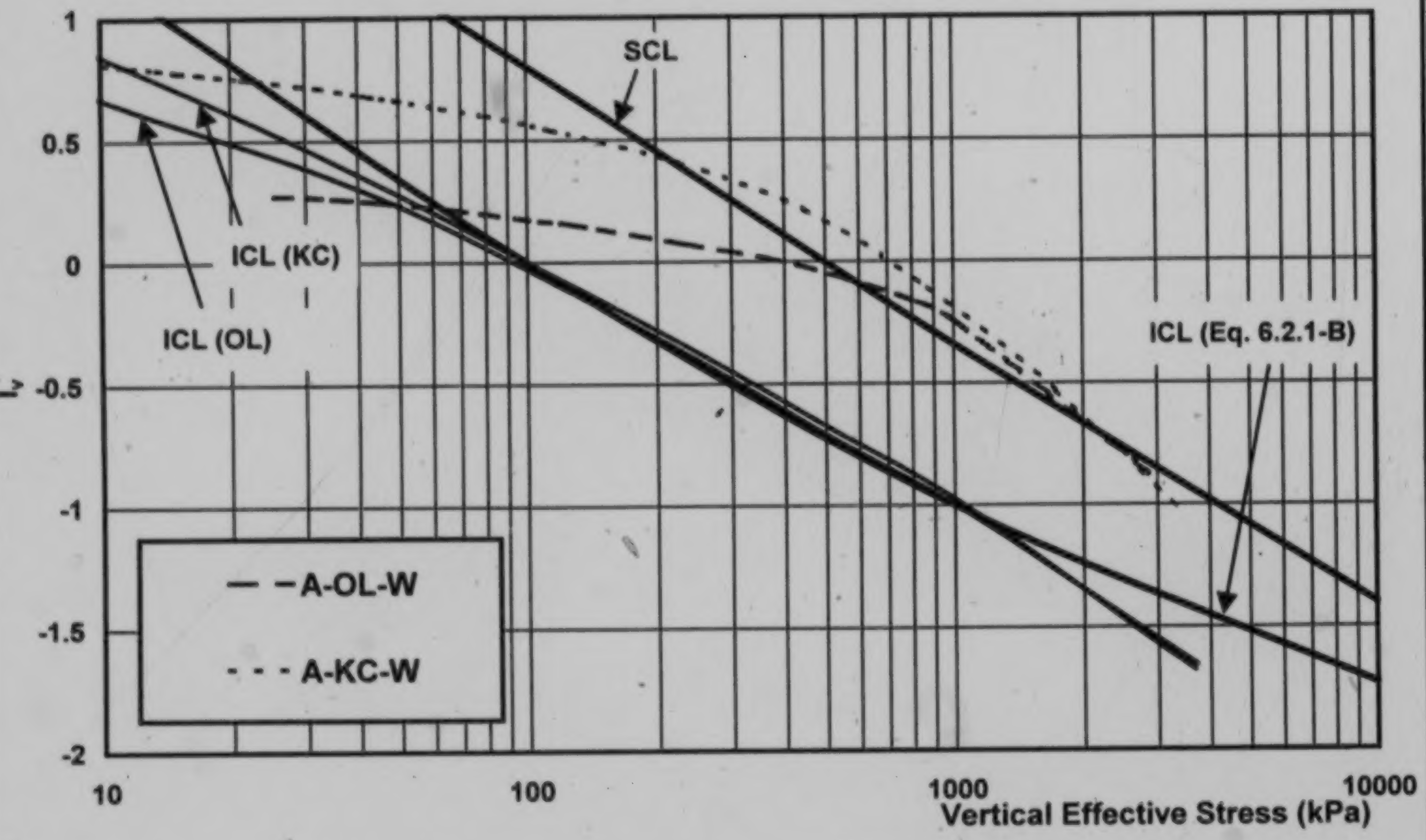

Figure 6.4-H(a) - Summary of Normalized 1-Dimensional Consolidation Tests for Specimens from Okanagan Lake Park Site with Air as Pore Fluid

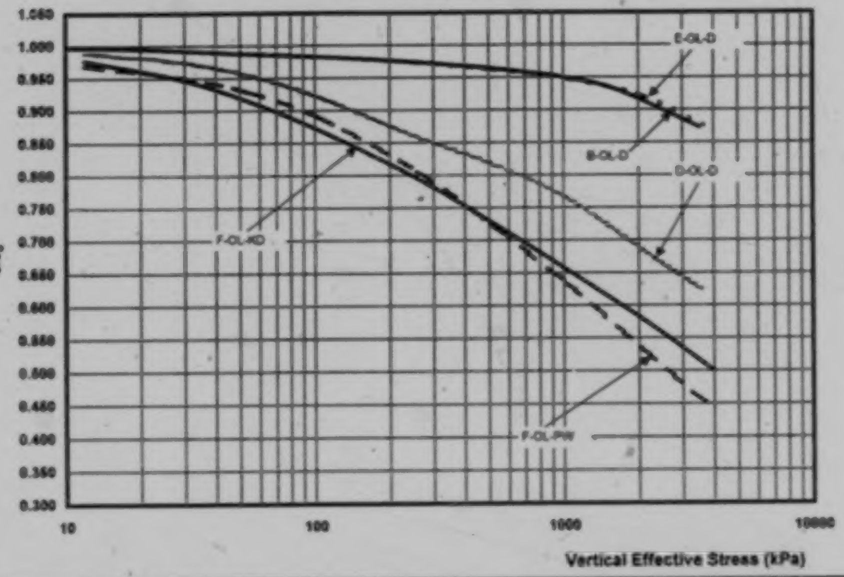

Figure 6.4-H(b) - Summary of Normalized 1-Dimensional Consolidation Tests for Specimens from Koosi Creek Site with Air as Pore Fluid

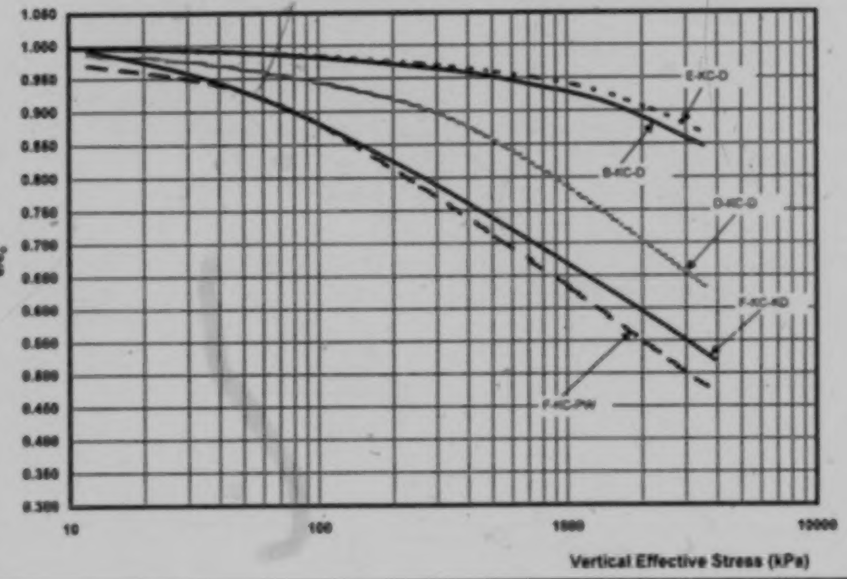

Figure 6.4-I(a) - Summary of Normalized 1-Dimensional Consolidation Tests for Specimens from Okanagan Lake Park Site with Water as Pore Fluid

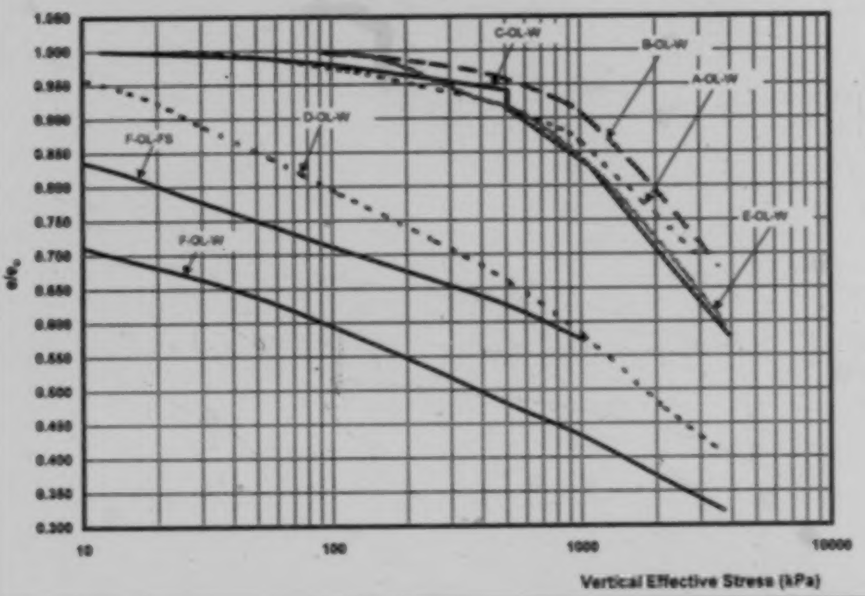

Figure 6.4-I(b) - Summary of Normalized 1-Dimensional Consolidation Tests for Specimens from Koosi Creek Site with Water as Pore Fluid

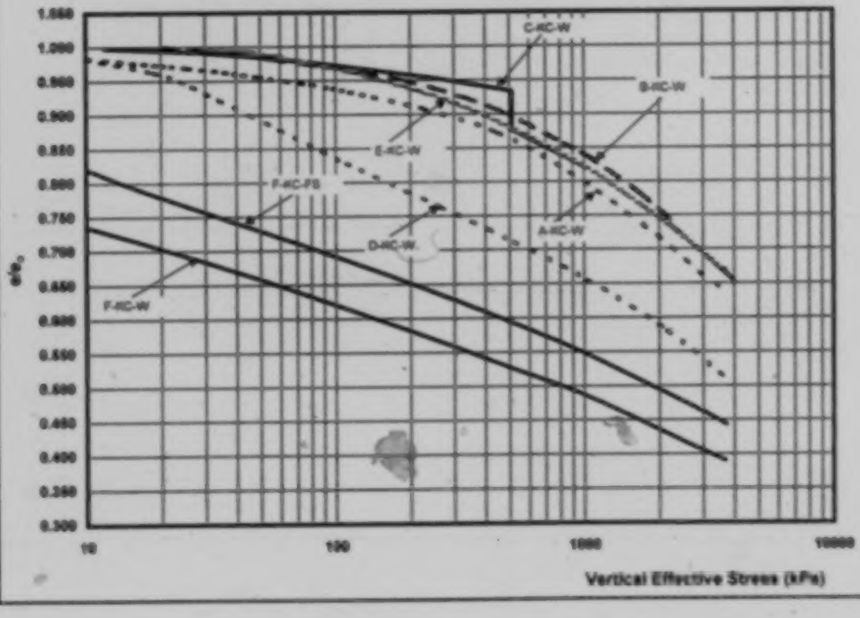

Figure 6.4-J(a) - Summary of Normalized 1-Dimensional Consolidation Tests for Specimens from Okanagan Lake Park Site with Kerosene as Pore Fluid

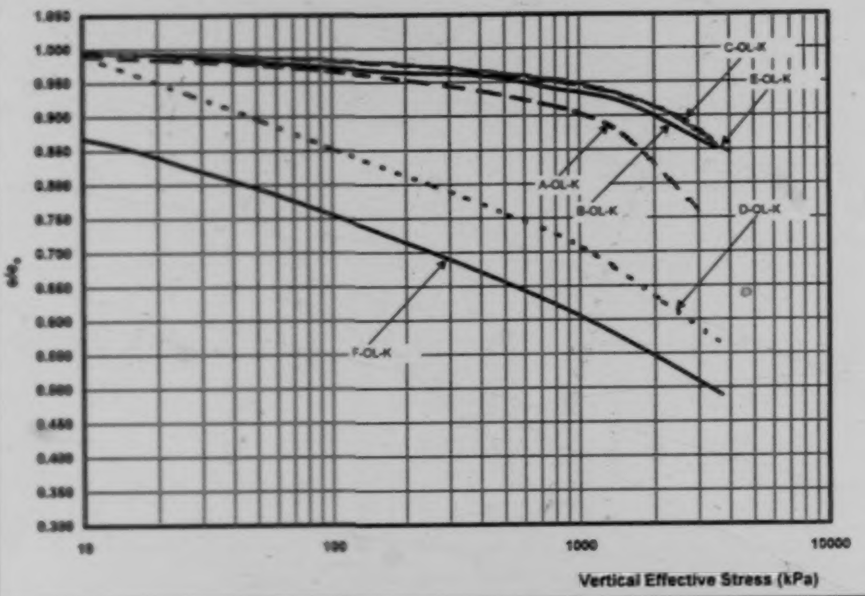

Figure 6.4-J(b) - Summary of Normalized 1-Dimensional Consolidation Tests for Specimens from Koosi Creek Site with Kerosene as Pore Fluid

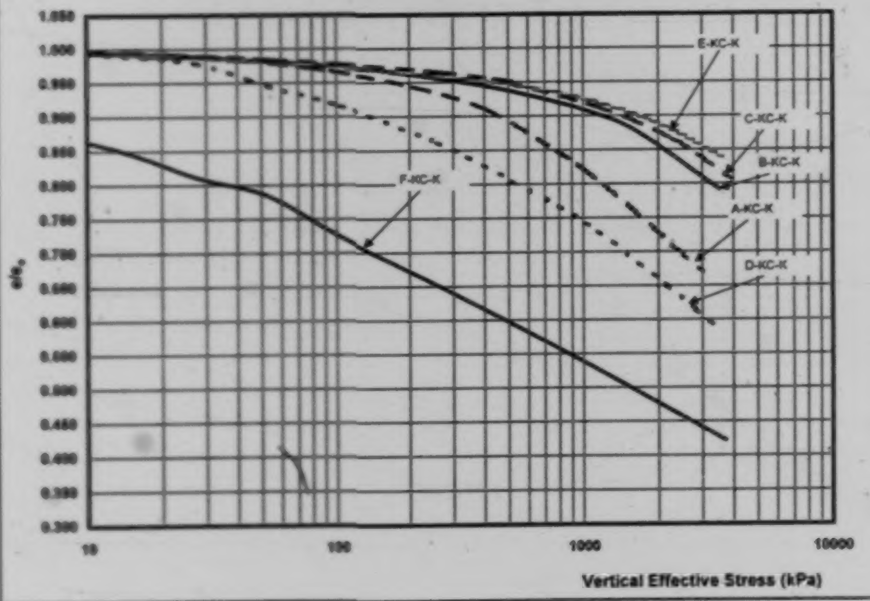

CHAPTER SEVEN

Triaxial Testing

7.1 Introduction

According to critical state soil mechanics the behavior and state of an ideal saturated soil can be uniquely expressed in terms of the void ratio and the state of stress. The behavior of structured soils can be influenced by many parameters. Due to the influence of their structure and at a given state of stress and void ratio, their behavior can be different from the behavior of ideal soils.

The triaxial test is the most common shear strength test for soils and can be used for testing all types of soils. As part of this study, triaxial tests were carried out to determine the influence of soil structure on the shear strength parameters of Penticton silt. Five series of triaxial tests were carried out using reconstituted and undisturbed specimens of Penticton silt. Specimens at different initial water content were tested using either water or Kerosene as the pore fluid.

In this chapter, previous studies involving the shear strength of structured soils and also glaciolacustrine silt sediments in the southern interior of British Columbia are reviewed and results from this study are presented and discussed.

7.2. Literature Review

7.2.1 Shear Strength of Structured Soils

Critical state soil mechanics, developed using reconstituted isotropically consolidated saturated clayey soils, is proven to be a strong framework for studying the behavior of ideal soils. According to Leroueil (1997), its fundamentals are based on works of Terzaghi, Casagrande, and Hvorslev. Roscoe et al. (1958) unified the works by Rendulic (1937) and Hvorslev (1937) and developed the basic framework for critical state soil mechanics using reconstituted isotropically consolidated saturated clay specimens. Figure

7.2.[illegible]matically illustrates the failure envelope for reconstituted saturated soils in the space formed by the deviator stress (q), effective mean normal stress (p'), and void ratio (e). Ideal soils, which are unstructured or de-structured, cannot exist outside this intrinsic failure envelope. The failure envelope in triaxial space consists of the Roscoe-Rendulic surface, the Hvorslev surface, and a no-tension cut-off line. The Roscoe-Rendulic surface is also known as a limit state, yield, or state boundary surface. The boundaries of the Roscoe-Rendulic surface are the normal compression line (NCL) and the critical state line (CSL). The normal compression line (NCL) is defined as the line formed by isotropic consolidation of a reconstituted clayey soil with initial water content close to its liquid limit. At large strains, an ideal saturated soil moves towards a unique state in the e-q-p' space. The assembly of these ultimate states forms the "critical state line" (CSL). The projection of critical state line (CSL) in the q-p' plane is a straight line, defined as:

$$q = M\,p' \qquad \text{(Equation 7.2.1)}$$

in which:

$q = \sigma'_1 - \sigma'_3$,

$p' = \dfrac{\sigma'_1 + \sigma'_2 + \sigma'_3}{3}$, and

M is the strength parameter at the critical state, which is equal to $\dfrac{6 \sin\phi'}{3 - \sin\phi'}$ in triaxial compression.

Interested readers are referred to Atkinson and Bransby (1978) for detailed study of concepts of the critical states soil mechanics.

Many researchers including Airey (1993), Burland (1990), Burland et al. (1996), Coop (1990), Coop and Atkinson (1993), Coop and Lee (1993 and 1995), Coop et al. (1995), Cuccovillo and Coop (1993), Kavvadas (1995), Lee and Coop (1995), Leroueil and Vaughan (1990), and Leroueil (1992 and 1997) have studied the behavior and response of structured soils and weak rocks utilizing the concepts of yielding and critical state soil mechanics. These studies showed that structured soils can exist in a meta-stable state beyond the boundaries of the unstructured failure envelope. Using the framework of critical state soil mechanics, the influence of soil structure on the mechanical behavior of a natural soil can be addressed by comparing the behavior of the structured and de-structured soil. Some of these studies are briefly reviewed in the following.

Leroueil and Vaughan (1990) defined yield as a discontinuity in the stress-strain behavior under monotonic stress changes. They also mentioned that an irreversible post yield change in the stiffness and strength of the material is an indicator of yielding of the structure. Three different types of yield for structured soils are swelling, shearing, and compression yield and shown in Figure 7.2.1-B, adopted from Leroueil and Vaughan (1990). According to Leroueil and Vaughan (1990), bonded structured soils may yield as the result of de-structuring caused by swelling pressure. Swelling yield, which occurs at low effective stresses, is due to the inability of the structure to retain stored strain energy. At low effective stresses, structured soils may also yield in tension. Leroueil and Vaughan (1990) stated that if the structure were strong enough to resist the swelling pressure, the soil would yield in tension rather than compression.

According to Leroueil and Vaughan (1990) and Coop et al. (1995), yielding of the structure may also occur in either compression or shear. A schematic presentation of compression and shear yield of structured soils is shown in Figure 7.2.1-C(a) and (b), respectively. The intrinsic state boundary surface (SBS), obtained using reconstituted specimen is also shown. Structured soils can exist in states outside the intrinsic state boundary. If a structured soil specimen is isotropically consolidated to a stress level beyond its effective yield stress, de-structuring occurs. For structured soil that is loaded in shear, three stages can be recognized. During the first stage of shearing, no significant change in mean effective normal stress (p') occurs. The induced external forces are balanced with internal structural forces. The second stage is characterized by yielding of the structure. At this stage, the de-structuring of the soil occurs. Finally, at third stage, the state of soil travels towards the critical state for reconstituted specimen.

Coop et al. (1995) studied the influence of soil structure using a marine clay, a calcarenite, and a boulder clay (till). Coop et al. (1995) observed that layered (stratified) structured soils do not approach the critical state of the reconstituted specimen. Figure 7.2.1-D shows the test results, reported by Coop et al. (1995), for a calcarenite. Coop et al. (1995) described several observations about structured soils using these test results. Review of test results in Figure 7.2.1-D(a) indicates that intact specimens reached states outside the normal compression line (NCL); but at elevated stresses, both intact and reconstituted specimens approached the same NCL line. The stress paths for specimens of calcarenite, yielded in compression (prior to shearing) and shearing, are shown in Figure 7.2.1-D(b) and (c), respectively. Data were normalized using effective mean normal stress at critical state (p'_{cs}). Reconstituted state boundary is also shown in both figures. Stress paths, presented in Figure 7.2.1-D(b), belong to the specimens that were compressed beyond their effective yield stress and are similar to the reconstituted stress path. The normalized stress paths were shifted towards the reconstituted state boundary as the magnitude of the isotropic compression increased. Results, presented in Figure 7.2-D(c), belong to specimens that yield in shear. The stress paths for these specimens reached states beyond the reconstituted state boundary and had well defined yield points. The stress paths for specimens that yielded in shear also traveled towards the reconstituted critical state.

Coop and Lee (1995) carried out a series of tests using saturated, flooded, and dry specimens of a decomposed granite, a carbonate sand, and a silica (quartz) sand. Results indicate that in a dry condition, these materials can exist at states beyond the saturated state boundary. However, the ultimate friction angle was not influenced by absence of water in the pores. Results also showed that the critical state for dry soil is closer to the state boundary's apex (peak value) than the one for saturated soil.

Coop (1990) and Coop and Atkinson (1993) compared the mechanical behavior of cemented and uncemented carbonate sands. They stated that the main effects of cementing agents were filling pores (i.e., reducing the void ratio, and causing a well defined yield point in compression or shearing yield). Cemented specimens reached states beyond the state boundary of uncemented specimens; but at large strains, all specimens traveled towards the same critical state.

Coop and Atkinson (1993) said that usage of water as a pore fluid in testing structured soils is not suitable and can reduce the bonding strength because of solubility of most cementing agents in water. Coop and Atkinson (1993) used a light silicon oil of similar viscosity to water as a pore fluid.

In a discussion regarding the study by Coop and Atkinson (1993), Huang and Airey (1994) commented on the importance of the pore fluid on the compression behavior. They said particles appear to be weaker in the presence of water as pore fluid than in the presence of silicon oil or air.

Based on a study using naturally cemented carbonate soils, Airey (1993) concluded that cementation increases the size of the yield surface and magnitude of the shear modulus. The influence of cementation on the bulk modulus was found to be insignificant.

Huang and Airey (1993) used artificially cemented carbonate sand to study the effect of cement content and density. Results indicate that the influence of cementation decreases as the density increases. It was also found that the shape of yield surface changes with the cement content.

Clough et al. (1981 and 1989) studied the influence of cementation on static and dynamic behavior of sands. Results showed that cementation causes a more brittle response; but it has little influence on friction angle. It was concluded that cementation, similar to density, increases the resistance to liquefaction and its effect is more pronounced than density.

As a part of an experimental program, Burland et al. (1996) studied the shear strength of two lacustrine clays, Todi clay and Pietrafitta clay, and two marine clays, Vallericca clay and Corinth Marl. It was found that due to structural effects, peak strength envelopes were curved and lay well above the intrinsic strength envelopes. For all intact clays studied by Burland et al. (1996), failure points formed relatively linear Hvorslev failure surfaces, which lay above the intrinsic Hvorslev failure surfaces and extended well to the right of the intrinsic critical state line (CSL). It was concluded that due to structural effects, these natural clays are more resistant to compression and shear. Results indicated that the source of structural improvements is mainly cohesive rather than frictional. Burland et al. (1996) said that slip surfaces were formed during undrained testing of reconstituted Pietrafitta clay specimens and not the other clay specimens. Referring to the study by Morgenstern and Tchalenko (1967), they stated that slip surface formation was triggered by mica particles. It was also concluded that the post rupture strength envelope of the Pietrafitta clay lay below the corresponding intrinsic envelope because of formation of this slip surfaces by mica particles. Regarding operational strength, Burland et al. (1996) recommended the use of the intrinsic critical state friction angle (ϕ'_{cs}) and a small cohesion intercept. This conclusion was made because of the close coincidence of the post rupture friction angle (ϕ'_{pr}) and the intrinsic critical state friction angle (ϕ'_{cs}). For highly fissured soils, use of the residual friction angle (ϕ'_r) was recommended.

The effect of structure on soil behavior is as important as void ratio and stress history. Norwegian and Canadian sensitive clays are well known cases of structured soils in which landslides and failures can occur due to soil structure failure and changes in physicochemical bonding. Karlsrud et al. (1984) and Tavenas (1984) reviewed the behavior of these deposits. Both of these deposits are silty marine deposits, with mica and chlorite as the dominant minerals. According to Karlsrud et al. (1984), leaching of the salt water pore fluid caused the structural changes in Norwegian marine clays and increased their sensitivity from 3-6 to values larger than 20. Karlsrud et al. (1984) showed that Norwegian sensitive clays have extremely brittle behavior in undrained triaxial tests. These soils reach their peak strength at very small axial strains of 0.3% and their post peak strength is about 50% of the peak strength. Karlsrud et al. (1984) also state that the post peak strength loss in undrained triaxial testing of Norwegian sensitive clays is entirely due to pore pressure increase and hence, decrease in effective stress.

They also concluded that the undrained shear strength of Norwegian sensitive clays is highly anisotropic.

Karlsrud et al. (1984) reported an important observation involving the behavior of Norwegian sensitive clays in combined drained and undrained loading. Three kinds of tests were conducted. The first kind of tests was traditional undrained shear tests. The second kind of tests involved undrained shearing of specimens, which had gone through drained shear loading with maximum drained shear stress less than the peak undrained shear strength of the soil. The results of these kind of tests showed that the drained shear loading caused a slight increase in peak undrained strength and decrease in post peak strain softening. In the third kind of tests, specimens were given drained shear loading in excess of the undrained shear strength of the soil prior to undrained shearing. Results of the third series of the experiment showed that those specimens could not carry any extra load upon starting the undrained shearing. These specimens also showed significant sudden strain softening response and a drop of shear stress to the level of undrained shear strength.

Karlsrud et al. (1984) also commented about the behavior of Eastern Canadian sensitive clays. The Canadian structured clay deposits showed strain softening behavior in undrained shearing and had effective stress envelope and post peak effective shear strength, which were above the envelope for the un-structured soil. Karlsrud et al. (1984) also mentioned that the post peak strain softening for these materials during undrained shearing occurred as the consequence of breakage of cementation bonds with small pore pressure generation. According to Karlsrud et al. (1984), the stress-strain curve of the undrained shearing tests of Eastern Canadian sensitive clays showed a post peak plateau with a distinct value for post peak shear strength. This behavior is in contrast with the post peak behavior for tests done on Norwegian sensitive clays.

There are structured soils that have a de-structured state stronger than their structured state. Cicolella and Picarelli (1990) presented test results obtained about the behavior of Bisaccia Clay, which is a homogeneous intensely fissured clay shale. Results indicated that the shear strength of the undisturbed specimen is significantly smaller than the peak strength of the reconstituted over-consolidated specimen. It was also smaller than the shear strength at the critical state for the reconstituted over-consolidated specimen. The shear strength of the structured soil was approximately the same as the residual value. The behavior observed by Cicolella and Picarelli (1990) can be due to the influence of fissures. Guerriero (1995) presented experimental data obtained on Masseria Marino Clay, which is a weathered and softened clay shale. It was found that the mechanical behavior of the softened clay shale depends on the interaction between the de-structured matrix and the intact lithorelicts and can be controlled by the de-structured matrix. Due to softening and weathering influences, the shear strength of the structured soil was close to the critical state value and the structured yield surface was inside the intrinsic yield surface.

7.2.2 Shear Strength of Glaciolacustrine Silts in the Southern Interior of B.C.

Evans and Buchanan (1976) carried out drained direct shear tests using silt sediments in the South Thompson River Valley. Residual drained friction angle (ϕ'_r) was found to be between 24.0° and 30.5°.

Lum (1977) studied the shear strength of glaciolacustrine silt sediments in the South Thompson River Valley using unconfined compression and consolidated drained triaxial tests. In unconfined compression testes, specimens with initial average water content of 7% were subjected to uniaxial load perpendicular and parallel to the bedding. The average shear strength was found to be 210 kPa and 180 kPa for specimens loaded perpendicular and parallel to the bedding, respectively. Drained consolidated triaxial tests were carried out at various effective confining stresses ranging between 5 kPa and 300 kPa. Specimens, tested at effective confining stresses less than 100 kPa, strain softened. The behavior of specimens was contractive up to the peak deviator and dilative afterwards. Values of strain at failure were less than 1.1%. Peak values of deviator stress ranged from 130 kPa to 240 kPa. Specimens, tested at effective confining stresses higher than 100 kPa, did not strain softened. Drained friction angle (ϕ') was found to be 33.7°, using results of tests at high effective confining stresses. Based on results of tests at low effective confining stresses, cohesion intercept (c') and drained friction angle (ϕ') were found to be 60 kPa and 17.8°, respectively.

Lum (1977) also carried out triaxial tests using specimens at saturated, in-situ, air-died, and oven-dried states. The water content of specimens at in-situ and air-dried states was 8% and 2%, respectively. Results showed that shear strength increases as water content decreases.

Wilson (1985) carried out borehole shear and direct shear tests. Based on borehole shear tests, friction angle was between 34° and 42°. Direct shear tests were carried out using unsaturated reconstituted specimens at water content of 4.4%. Friction angle and cohesion intercept was found to be 38° and 2 kPa.

Sobkowicz and Coulter (1992) carried out undrained direct shear tests using specimens at their in-situ water content. For specimens at values of water content significantly lower than plastic limit, friction angle and cohesion intercept were 35° and 30 kPa, respectively. The corresponding values for specimens with values of water content at about plastic limit were 30° and 30 kPa. Residual values of friction angle and cohesion intercept were 10° and 10 kPa.

7.3 Experimental Program

7.3.1 General

The glaciolacustrine silt sediments in the southern interior of British Columbia are generally in an unsaturated state. The in-situ water content of block samples obtained from Koosi Creek Slide and Okanagan Lake Park Slide sites was from 30% to 35% and from 15% to 25%, respectively.

Triaxial tests were carried out using specimens at different states of moisture. As Coop and Atkinson (1993) also mentioned water can interact with cementing agents, precipitates, and minerals in soils and its introduction can change the soil structure. Also, the strength of some cementing agents is a function of the water content. In order to preserve the soil structure and the strength of the cementing agents at a specific moisture condition, it was necessary to use a pore fluid that does not interact chemically with soil but its physical properties are close to those for water. Coop and Atkinson (1993) used a light silicon oil as pore fluid. Commercially available Kerosene was chosen as the pore fluid added to unsaturated specimens in this study. The properties of Kerosene used in this experimental program were presented in Chapter Six, Table 6.3.1.

7.3.2 Testing Apparatus

An automated triaxial testing system, modified and extended version of the CKCe/p cyclic triaxial testing system, was used. Figure 7.3.2 shows the automated triaxial testing system. This triaxial testing equipment is a closed-loop feedback computer controlled system. Back pressure saturation, isotropic or anisotropic consolidation, drained or undrained shear, stress or strain controlled test, and arbitrary stress path test are among automatic features of this system. Five sensors are used in this system: a load cell to monitor the axial load, a LVDT to measure the vertical displacement, three pressure transducers to detect the chamber pressure, the effective pressure, and the volume change.

7.3.3 Material and Specimen Preparation

Block samples obtained from glaciolacustrine Penticton silt sediments at Koosi Creek Slide and Okanagan Lake Park Slide sites were used as the material for the triaxial testing. Details of geological and basic geotechnical properties of Penticton silt are presented in Chapter 2, 3, and 5.

Undisturbed and reconstituted specimens, approximately 65 mm in diameter and 125 mm in length, were used. All undisturbed specimens were trimmed at their natural water contents in an environment of +4 °C and 100% relative humidity. Undisturbed specimens at water content of about 20% were trimmed using a sharp straight edge and those at water content of about 35% were trimmed using a wire saw. Reconstituted specimens were made using Penticton silt, which were grind from block samples and passed through ASTM sieve #100 (Opening Diameter = 0.150 mm). Reconstituted specimens were prepared by static compaction of moist soil in seven layers. Grind soil was mixed with the mixing fluid thoroughly using an electric industrial mixer at water content of approximately 15%.

Also, undisturbed specimens were tested using either water or Kerosene as pore fluid to study the influence of chemical interaction between liquid and solid phases on shear strength and its parameters. Undisturbed specimens used for this part of the study were air-dried upon trimming to have a reference initial condition. An environment of 23 °C ± 2 °C and 80% relative humidity were used for air-drying to maintain a slow rate of moisture loss and prevent any potential damage to the soil structure.

7.3.4 Test Procedure

All specimens were saturated using either distilled water, Koosi Creek ground water, or Kerosene. The pore fluid was introduced through the bottom drainage while the top drainage was open to atmosphere to allow airflow out of the specimen. Cell and back pressure were maintained approximately equal to avoid change in specimen dimensions. Upon continuous flow of liquid from top drainage, top and bottom drainage valves were closed and specimen were put under back pressure saturation by applying at least 400 kPa cell and back pressures. Pore pressure parameter (B value) was monitored and specimen were assumed to be saturated for B values greater than 0.98.

Both isotropically and anisotropically consolidated specimens were used in this study. Specimens were consolidated in forty incremental segments over a time period ranging from 24 hours to 48 hours. True evaluation of K_o for natural structured sediments is a difficult, if not an impossible task. Horizontal to vertical effective stress ratio ($K = \sigma'_3/\sigma'_1$) equal to 0.5 was chosen as a reasonable approximation for anisotropic consolidation.

Initial void ratio was calculated from dry density and initial water content. Initial void ratio was also calculated using specimen dimensions. Results of these calculations were in agreement for at least up to two decimal digits. Possible volume changes during saturation were monitored. Void ratio after saturation, consolidation, and shearing were calculated using measured volume changes.

The following stress paths were used in triaxial testing:

- Monotonic conventional undrained strain controlled compression triaxial testing at 0.1%/min strain rate: This stress path was followed by keeping the effective lateral stress constant and increasing the deviator stress.

- Monotonic conventional drained strain controlled compression triaxial testing at 0.05%/min strain rate: This stress path was followed by keeping the effective lateral stress constant and increasing the deviator stress.

- Monotonic drained stress controlled constant deviator stress (q-constant) triaxial testing at 1 kPa/min stress rate: This stress path was followed by keeping the deviator stress constant and decreasing the effective lateral stress. The triaxial testing system was not capable of performing strain controlled q-constant test; therefore, the post peak behavior could not be studied.

- Monotonic undrained stress controlled extension triaxial testing at 1 kPa/min stress rate: This stress path was followed by keeping the effective lateral stress constant and decreasing the deviator stress at 1 kPa/min stress rate. The post peak behavior in extension could not be studied because the test was carried out stress controlled.

7.4 Test Results and discussions

7.4.1 General

Specimens are represented by a three segment symbol such as XX(VV)-Y-ZZZNNN. The first character of the first segment stands for reconstituted (R) or undisturbed (U) while the second character of this segment refers to the initial condition of the specimen (i.e., air-dried (A) or in-situ moisture state (I)). A possible parentheses in this segment stands for the site that the specimen was obtained (i.e., Okanagan Lake Park (OL) or Koosi Creek (KC)). The second segment stands for the pore fluid used (i.e. water (W) or Kerosene (K)). The third segment stands for the consolidation condition and the stress path (i.e., CIU, CAU, CAD, EAU, and q-constant). The number in front of the third segment refers to the vertical effective stress (σ'_v) component of the consolidation stress.

Triaxial test results are presented, explained, and discussed in this section and the following one.

7.4.2 Reconstituted Specimens

Isotropically and anisotropically consolidated triaxial tests were carried out using reconstituted specimens. Kerosene was used as the pore fluid to avoid any possible chemical reaction between solid and liquid phases and make truly unstructured specimens.

Isotropically consolidated undrained compression tests were carried out. A summary of the test results for specimens consolidated to 300 kPa, 400 kPa, and 500 kPa are presented in Figure 7.4.2-A through C, respectively. Results of these tests are normalized using the mean effective normal stress at critical state (p'_{cs}) and are presented in Figure 7.4.2-D. As can be seen, results form a unique state boundary surface.

The stress path of Specimen RA-K-CIU400, was chosen as the base yield surface (i.e., state boundary) for this study. Figure 7.4.2-E and F show the summary of test results for Specimen RA-K-CAU372 and RA-K-CAD372. These specimens were sheared after anisotropic consolidation to the yield surface of the Specimen RA-K-CIU400. The peak undrained deviator stress of the anisotropically consolidated specimen is slightly larger than the corresponding value for the isotropically consolidated specimen. Several studies including study by Karlsrud et al. (1984) showed a segment of drained shear loading increases the peak undrained shear strength. It can be concluded that anisotropic consolidation, which induces drained shear loading, is the reason for larger peak undrained deviator stress of Specimen RA-K-CAU372, compared to Specimen RA-K-CIU400.

Soil failure in extension can occur in the toe region of slopes at shallow depths. An anisotropically consolidated stress controlled undrained extension test was carried out to have an assessment of strength parameters in extension. A summary of the test results for Specimen RA-K-EAU190 are presented in Figure 7.4.2-G. This specimen was sheared after anisotropic consolidation to the vertical effective yield stress (σ'_v) equals to 190 kPa (p' = 127 kPa).

7.4.3 Undisturbed Specimens

7.4.3.1 Specimens at 36% to 38% In-Situ Water content

Three triaxial tests were carried out using undisturbed specimens obtained from Koosi Creek Slide site. Stress paths, in q-p' space, are shown in Figure 7.4.3.1-A. The in-situ water content of these specimens was between 36% and 38%. Groundwater, also obtained from Koosi Creek Slide site, was used as the pore fluid. The objective of this section of the experimental program was to study the strength behavior of these sediments at a naturally saturated state. Studying the behavior at a naturally saturated state was achieved using these soil specimens, which had their in-situ state close to saturation, and also specimens of ground water as the pore fluid. These specimens were sheared after being consolidated anisotropically to the yield surface of the Specimen RA-K-CIU400.

A summary of the results for the specimen that was sheared undrained is presented in Figure 7.4.3.1-B. Four key observations and conclusions can be made using this test: First, pore pressure generation influenced, but did not govern the initial behavior of the specimen during the shearing. Excess pore pressure increased gradually and reached a peak at about 0.5% strain. Then, it dropped gradually until it reached a plateau. This conclusion can be better described using Figure 7.2.1-C(b) and stress paths for reconstituted (de-structured) and structured intact specimens. For a de-structured specimen, the behavior is completely controlled by pore pressure generation and the stress path follows a semi-circular shape in q-p' space by continuous decrease of p'. In contrast for a strongly structured soil, the behavior is controlled by the soil structure rather than by pore pressure generation. Consequently, stress path follows a vertical line in q-p' space. The stress path for Specimen UI(KC)-W-CAU372 in q-p' space was close to vertical with some minor decrease of p'. Second, deviator stress continued to increase even though pore pressure dropped. Third, the post pore pressure peak stress path in q-p' space approximately followed the 3:1 drained stress path slope towards the peak strength. Fourth, the stress-strain curve and the stress path indicate a ductile behavior and failure. Fourth observation can be supported with the fact that no sudden and sharp changes in the stress-strain curve or the stress path in the q-p' space can be observed. These observations indicate that stress path and specimen's response was controlled by soil structure and structural bonding rather than pore pressure generation.

A summary of the results for specimen that was sheared drained is presented in Figure 7.4.3.1-C. The peak deviator stress is only 50 kPa greater than the corresponding value for the undrained test. As it was mentioned, it appears that the behavior is controlled by soil structure and structural bonding rather than pore pressure generation. Close values of peak deviator stress of drained and undrained triaxial test confirms lack of significance of pore pressure generation on the response of these materials.

A drained stress controlled constant deviator stress triaxial test was also carried out to study the effect of pore pressure generation under the condition of constant overburden pressure. Such condition can happen by rise of groundwater table. A summary of test results is shown in Figure 7.4.3.1-D. Specimen's volume continuously increased throughout the shearing; but it was not the case for axial deformation. Specimen experienced axial expansion prior to failure. A distinct peak in axial deformation marked the failure. Upon failure, axial strain continuously decreased at a constant rate; but the post failure behavior could not be reliable because the test was carried out stress controlled.

7.4.3.2 Specimens at 23% to 28% In-Situ Water content

Test results presented in Chapter 5 and 6 indicate that Penticton silt is structurally bonded and bonding agents and their magnitude appear to be moisture sensitive. The objective of this section of the experimental program was to study the influence of the structural bonding present at these water content levels on the strength behavior. Undrained and drained triaxial tests were carried out using undisturbed specimens obtained from Okanagan Lake Park Slide site. Specimens with water contents at the upper bound of the in-situ values (23% to 28%) were chosen in order to be in the lower bound of structural bonding influences. Kerosene was used as the pore fluid to saturate the specimens in order to preserve the structure of the specimens as it is in their in-situ state. These specimens were sheared after being consolidated anisotropically to the yield surface of the Specimen RA-K-CIU400. Stress paths in q-p' space are shown in Figure 7.4.3.2-A.

A summary of the results for specimen that was sheared undrained is presented in Figure 7.4.3.2-B. Several observations can be made from this test. Excess pore pressure increased and reached a peak at about 0.5% strain. Then, it dropped gradually until it reached a plateau; and it increased again. Deviator stress continued to increase even though pore pressure dropped and it reached a plateau. Deviator stress dropped sharply and reached another plateau. This drop in deviator stress and formation of the second plateau coincided with the second stage of pore pressure rise. The stress path in q-p' space was virtually a p' constant path up to the peak deviator stress, followed by a plateau at peak and sharp drop. The pre-failure behavior was essentially elastic, followed by a brittle failure. As can be seen in q-p' space, the stress path for pre-peak and peak segments were completely independent of pore pressure response. These observations indicate that stress path and specimen's response was controlled completely by soil structure and structural bonding rather than pore pressure generation.

A summary of the results for specimen that was sheared drained is presented in Figure 7.4.3.2-C. The peak deviator stress was close to the corresponding value under the undrained condition. As it was mentioned, it appears that the behavior is controlled by soil structure and structural bonding rather than pore pressure generation. As a result, a major difference between peak drained and undrained deviator stress is not expected. The peak deviator stress was approximately 50 kPa smaller than the corresponding value for the undrained test. Such response can possibly be due to easier slippage and movement of flaky mica particles under the condition of free drainage and volume change compared to the zero volume change condition in undrained test.

7.4.3.3 Air-Dried Water Saturated Specimens

Two undrained and two drained triaxial tests were carried out using air-dried water saturated specimens. The objective of this section of the current study was to investigate the behavior of these sediments upon extreme moisture changes (i.e., air-dried to saturated state). Also the failure envelope for this extreme case of moisture changes can be obtained. The air-dried water content was less than 6.5%. Triaxial tests were carried out using undisturbed specimens obtained from Okanagan Lake Park Slide site. Distilled de-aired water was used as the pore fluid to saturate the specimens. These specimens were sheared after being consolidated anisotropically to the yield surface of the Specimen RA-K-CIU400. Stress paths, in q-p' space, are shown in Figure 7.4.3.3-A.

A summary of the results for Specimen UA-W-CAU372(a) and (b) that were sheared undrained are presented in Figure 7.4.3.3-B and C, respectively. In the case of Specimen UA-W-CAU372(a), approximately 70 kPa excess pore pressure was generated upon closure of drainage valve. This response implies that specimen was undergoing creep at the end of anisotropic consolidation. Following this stage of pore pressure generation under virtually constant deviator stress condition, pore pressure and deviator stress increased approximately 50 kPa, which caused the failure of the specimen. The overall stress path looks more like a semi-constant deviator stress than an undrained stress path. The specimen's response showed only minor signs of soil structure and structural bonding. Investigating void ratio changes shows that during saturation process, the specimen experienced a cycle of swelling-consolidation. It appears that de-structuring occurred during saturation-consolidation process.

A summary of test results of the second undrained test, Specimen UA-W-CAU372(b), showed that this specimen experienced only 20 kPa excess pore pressure generation upon closure of the drainage valve. Both pore pressure and deviator stress increased up to 1% axial stress. The deviator stress increased at a rate approximately three times higher than that of pore pressure, created relatively sharp rising stress path. This stage was followed by a stage of small and gradual decrease of excess pore pressure, simultaneous with small and gradual increase of deviator stress. In q-p' space, stress path followed the 3:1 drained stress path slope during this stage and failed. It appears that the specimen's response was influenced by excess pore pressure generation; but the sharp rising stress path is an indication of the major influence of soil structure in the behavior and increase in the magnitude of deviator stress. Based on available information, it cannot be judged whether the structural influences is due to structural bonding or due to fabric improvement. It is possible that soil fabric and particle arrangements improved because of the consolidation and also collapse during saturation process.

A summary of the results for Specimen UA-W-CAD372(a) and (b) that were sheared drained are presented in Figure 7.4.3.3-D and E, respectively. Saturation process was the main difference between these two drained triaxial tests. Specimen UA-W-CAD372(a) was saturated and then consolidated while Specimen UA-W-CAD372(b) was consolidated before saturating. Specimen UA-W-CAD372(a) collapsed upon saturation and experienced major void ratio decrease during consolidation. Void ratio decrease during drained shearing was insignificant. Based on the stress-strain curve, the behavior of the specimen was ductile and stress-strain curve formed a plateau at peak deviator stress of 330 kPa. Formation of the plateau implies the tendency of these sediments for creep and possible failure under sustained stresses. The void ratio variation was different for Specimen UA-W-CAD372(b). This specimen did not experience significant void ratio changes during consolidation; but upon saturation void ratio decreased slightly. The behavior of the specimen was elastic and brittle and strain softened; but it showed a dilative behavior during drained shearing. Such behavior is contradictory to the behavior observed for reconstituted, de-structured, or ideal soil. In this case, strain softening behavior could be due to destruction of the bonds in the soil structure rather than contractive behavior.

The peak deviator stress of Specimen UA-W-CAD372(a) was significantly smaller than the corresponding value for UA-W-CAD372(b). It appears that the soil structure of specimen that was saturated prior to consolidation was changed to a greater extend than the other specimen. Such speculation can also be supported by ductile and brittle response of Specimen UA-W-CAD372(a) and (b), respectively. The brittle response of Specimen UA-W-CAD372(b) could be an indication of the resistance of the bonds in the soil structure; and the ductile response of Specimen UA-W-CAD372(a) could be an indication of frictional behavior.

Several studies including the study by Nagaraj et al. (1998) suggested the idea of no changes in soil fabric under isotropic state of stress and changes in soil fabric in presence of shear stresses. Consequently, it is probable that the soil fabric of Specimen UA-W-CAD372(a) and UA-W-CAD372(b) changed differently because of saturation under isotropic and anisotropic conditions, respectively. The larger peak deviator stress of Specimen UA-W-CAD372(b) compared to Specimen UA-W-CAD372(a) may be due to major improvements in soil fabric because of saturation and collapse after anisotropic consolidation, which is in presence of shear stresses.

For a purely frictional de-structured soil and under the drained condition, the peak deviator stress should be larger than the corresponding value under the undrained condition. The peak deviator stress for Specimen UA-W-CAD372(a) was approximately equal to the corresponding value for the undrained specimen (UA-W-CAU372(b)). Such response signifies the importance and role of the soil structure in the strength behavior of these sediments and down plays the role of the excess pore pressure generation.

7.4.3.4 Air-Dried Kerosene Saturated Specimens

Experimental evidences presented in previous chapters indicate that Penticton silt is structured and the structural bonding agent is moisture sensitive. It also appears that the magnitude of structural bonding in the soil system increases as the water content decreases.

Three undrained and drained triaxial tests were carried out using air-dried Kerosene saturated specimens. Specimens were trimmed from block specimens obtained from Okanagan Lake Park Slide site. The objective of this section was to assess the magnitude of structural bonding present in Penticton silt at its extreme values (i.e., air-dried state). Also, the test results could lead to defining the yield surface for this condition. Kerosene was used as pore fluid to saturate the specimens. Use of Kerosene as pore fluid made it possible to eliminate matric suction as one of the variables while preserving the moisture sensitive soil structure.

Summary of test results for Specimen UA-K-CAU372 that was sheared undrained after anisotropic consolidation are presented in Figure 7.3.4.3-A and B. Loading continued until the limits of the testing system was reached and the specimen failed under the sustained load. The peak deviator stress is significantly larger than the corresponding value for all other tests, presented in previous sections of this chapter. Review of Figure 7.4.3.4-A and B shows that specimen's response was not influenced by excess pore pressure generation. The stress path in the q-p' space rises essentially vertical and subsequently followed the drained 3:1 slope in the p'-q space. The specimen's response indicates that the load was carried by the soil structure. In fact, the excess pore pressure increased until it reached its maximum value (i.e., equal to the effective cell pressure). In other words, the deviator stress increased up to 2700 kPa while the specimen was under zero effective lateral stress, which is similar to the unconfined uniaxial test. This phenomenon is not compatible with the behavior of a granular material and the extra strength observed should have a non frictional origin. This behavior is similar to rocks or cement based materials such as concrete. These results are significant evidences of strong bonding in the soil structure.

Two specimens, anisotropically consolidated to vertical effective stresses of 372 kPa and 1680 kPa, were tested under drained condition. A summary results is shown in Figure 7.4.3.4-B and C for Specimen UA-K-CAD372 and UA-K-CAD1680, respectively. In both cases, tests were continued until the loading limit of the testing system was reached. Specimens did not fail and experienced some creep under sustained loads. The magnitude of the maximum deviator stress, reached during these tests, was in agreement with the corresponding value for the undrained test.

7.4.4 General Discussion

Stress paths of the reconstituted specimens in q-p' space are summarized in Figure 7.4.4-A. The critical state lines in compression and extension for the saturated reconstituted unstructured state are also shown in this figure. Based on these results, the critical state strength parameter is 1.48 and 0.95 in compression (M_C) and extension (M_E), respectively. The critical state strength parameter in compression is expected to be 1.5 times its value in extension, which is approximately the case in this study. The relationship between friction angle and M_C is as follows:

$$\phi' = \sin^{-1}\left(\frac{3M_C}{6+M_C}\right)$$ Equation (7.4.4-A)

Using measured M_C from Figure 7.4.4-A, friction angle is approximately 36.5°, which is a reasonable value for silty soils and is consistent with previous literature on these soils.

Stress-strain curves of undrained tests are shown in Figure 7.4.4-B. Stress paths for triaxial tests are summarized and presented in q-p' space in Figure 7.4.4-C and D. Some general discussions are presented here using the results presented in above mentioned figures.

The pre-yield undrained response of Specimen UI(OL)-K-CAU372 was conceptually different from the corresponding response of Specimen UI(KC)-W-CAU372 that had higher in-situ water content. The specimen at the lower in-situ water content had a pre-yield elastic behavior with a brittle yielding while specimen at higher in-situ water content had a ductile and plastic behavior with some influence from pore pressure generation.

The in-situ water content of Specimen UI(KC)-W-CAD372 and Specimen UI(OL)-K-CAD372 were 36% (at about L.L.) and 27% (at about P.L.), respectively. Because of stronger structural bonding at lower value of in-situ water content, it was expected that the peak deviator stress of Specimen UI(OL)-K-CAD372 be larger than the corresponding value for Specimen UI(KC)-W-CAD372; surprisingly, the results are opposite. This phenomenon can be explained using the behavior of these two specimens. The response of Specimen UI(OL)-K-CAD372 was elastic and brittle while the response of Specimen UI(KC)-W-CAD372 was ductile with large deformations. It appears that large plastic deformations allow Specimen UI(KC)-W-CAD372 releases energy better than Specimen UI(OL)-K-CAD372. Consequently and under the free volume change condition, the specimen with a ductile behavior reached higher values of peak deviator stress than the specimen with elastic and brittle behavior.

The undrained peak deviator stress of air-dried water-saturated specimen, UA-W-CAU372(b), was significantly lower than the corresponding values for Specimen UI(OL)-K-CAU372 and Specimen UI(KC)-W-CAU372. Specimen UA-W-CAU372(b) experienced extreme change in its water content. Such response for this specimen can be due to major de-structuring because of such extreme change in the state of specimen (i.e., from air-dried condition to water-saturated condition).

Test results show that undrained triaxial stress paths of Penticton silt are generally not controlled by excess pore pressure generation. These stress paths are generally controlled by soil structure; but there are signs of some pore pressure generations. Mitchell (1993) reported results of studies by Gilboy (1927) and Terzaghi (1931) about compressibility of soils with high mica content. Those results showed that presence of mica minerals cause large elastic deformations. Generation of some pore pressure during undrained shearing of the structured Penticton silt can be due to elastic deformation of mica particles under zero overall volume change.

The peak drained deviator stress for undisturbed specimens is smaller than the corresponding value for the reconstituted specimen. As it was mentioned in Chapter two, these sediments are stratified. This response can be due to formation of shear bands, failure along fissures, or slippage involving flaky particles.

Experimental evidence, presented in previous chapters, indicate that these sediments are structurally bonded and magnitude of bonding is moisture sensitive. The estimated state boundary for Penticton silt at de-structured state, structured at in-situ state, and structured air-dried state are shown in Figure 7.4.4-C and D. As can be seen in these figures, the size of the state boundary increases as the magnitude of the moisture sensitive structural bonding increases. Figure 7.4.4-E, adopted from Cui and Delage (1996), shows contours of the state boundary for compacted Jossigny silt at various matric suctions (u_a-u_w). It appears that there is some resemblance between the contours of the state boundary for Penticton silt at various moisture sensitive structural bonding and compacted Jossigny silt at various matric suctions. Comparison of these contours can imply that increase in structural bonding and increase in matric suction conceptually has the same effect on soil behavior.

Critical state line (CSL) for de-structured reconstituted state is shown in Figure 7.4.4-C and D. critical state strength parameter is defined as:

$$M_C = \frac{6\sin\phi'}{3-\sin\phi'}$$ Equation (7.4.4-B)

Assuming no frictional contribution to the structural bonding, proposed contours of the peak strength envelope for structured undisturbed Penticton silt at in-situ and air-dried states are also drawn in these figures. The peak strength envelopes for the structured states of Penticton silt do not pass through the origin and intercept with the deviator stress axis. The author proposes a parameter ω, defined as the intercept of the peak strength envelope with the deviator stress axis, to be used as an assessment of soil structure and structural bonding. Using this definition, ω can be calculated as follows:

$$\omega = \frac{(6\cos\phi')(c')}{3-\sin\phi'} \qquad \text{Equation (7.4.4-C)}$$

Using matric suction (s) as a variable, Alonso et al. (1990) proposed a constitutive model for unsaturated soils using q-p-s space. Figure 7.4.4-F, adopted from Leroueil (1997), show the state boundary surface in q-p-s, proposed by Alonso et al. (1990), and contours of state boundary and critical state line (CSL) at various matric suctions. The contours presented for Penticton silt at various structured states and the contours proposed by Alonso et al. (1990) at various matric suctions appear to be similar. Comparison of these contours can imply that the effect of structural bonding and matric suction are conceptually the same on soil behavior.

7.5 Summary

A variety of triaxial tests were carried out to study the shear strength behavior of glaciolacustrine Penticton silt. Concepts of the critical state soil mechanics (CSL) were utilized. Using test results and discussions, presented in this chapter, the following conclusions can be drawn:

Glaciolacustrine Penticton silt sediments are strongly structured. The soil structure is moisture sensitive. The magnitude of structural bonding increases as the soil water content decreases.

Undrained stress paths are strongly controlled by the soil structure. It appears that pore pressure generation does not have significant influence on the undrained response of structured Penticton silt.

Due to lack of influence by pore pressure generation, the peak deviator stress in drained and undrained tests were close to each other.

At typical in-situ water contents, it appears that the deformational characteristics and failure modes are more influenced by the interaction between the liquid and solid phases than the peak deviator stress.

The extremely strong response of these materials at air-dried state and under unconfined condition shows that the material's behavior is not frictional and the source of enhanced strength should be cohesive.

It was found that the state boundary surface of Penticton silt expands as the magnitude of the moisture sensitive structural bonds increases. It also appears that the effect of structural bonding on state boundary and peak strength envelope is conceptually the same as matric suction.

Use of structural bonding parameter, ω, in conjunction with critical state strength parameter, M, is proposed in order to interpret and model the response of structured soils using the framework of critical state soil mechanics.

Figure 7.2.1-A – Failure Envelope for Reconstituted Saturated Soils

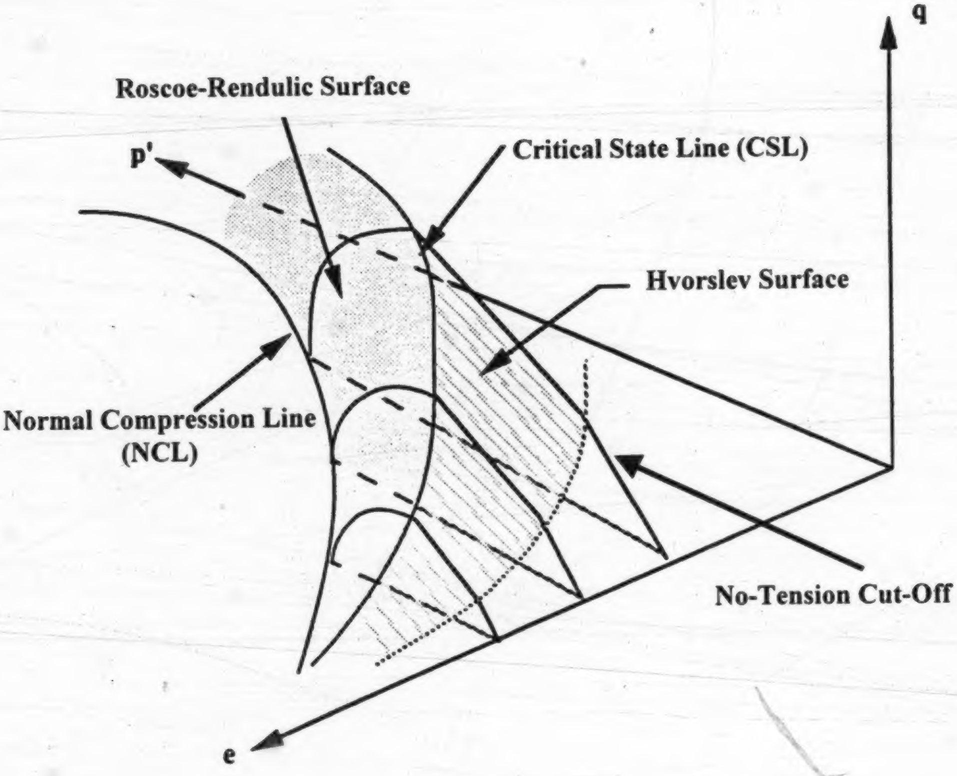
q
Roscoe-Rendulic Surface
p'
Critical State Line (CSL)
Hvorslev Surface
Normal Compression Line
(NCL)
No-Tension Cut-Off
e

Figure 7.2.1-B – Different Types of Yielding
(after Leroueil and Vaughan (1990))

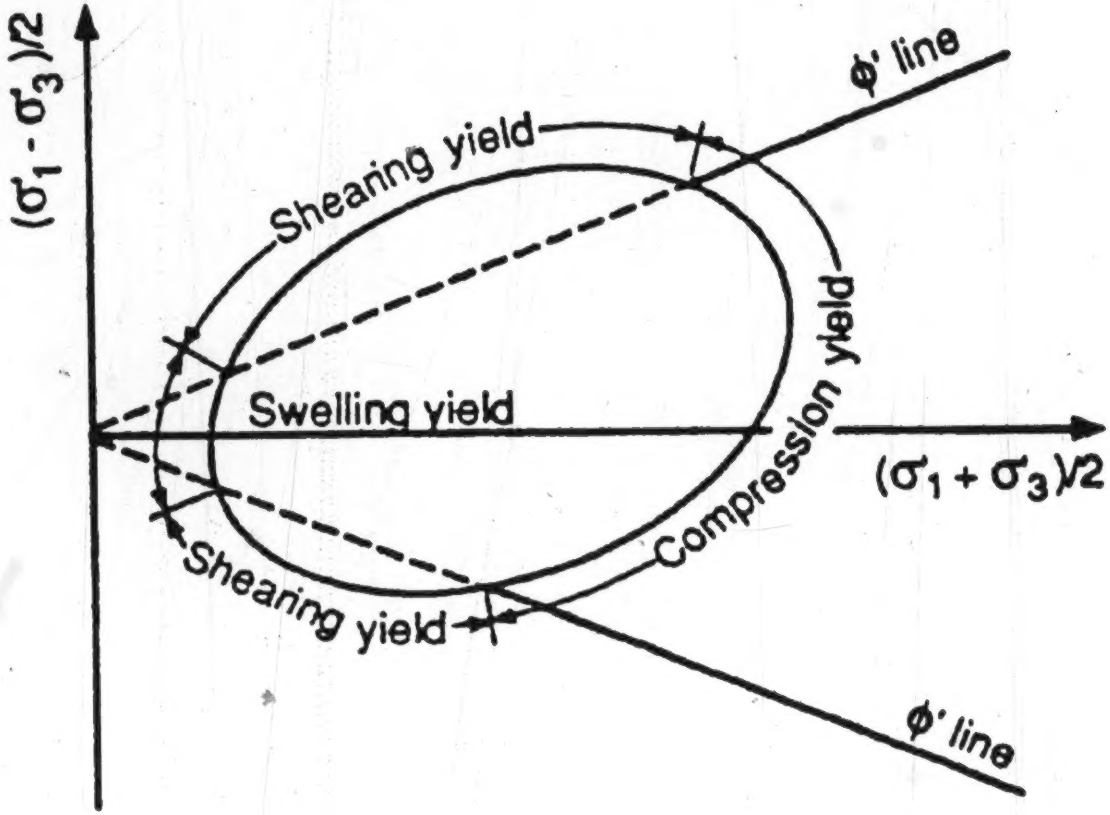
$(\sigma'_1 - \sigma'_3)/2$
ϕ' line
Shearing yield
Swelling yield
Compression yield
$(\sigma'_1 + \sigma'_3)/2$
Shearing yield
ϕ' line

Figure 7.2.1-C – Compression and Shear Yield of Structured Soils

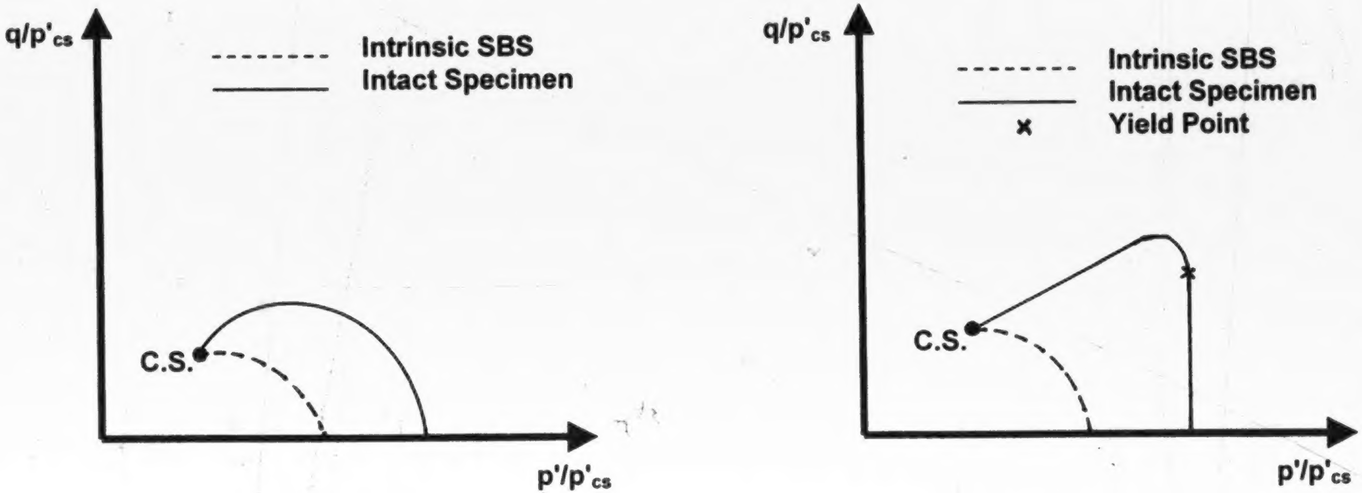
q/p'cs
Intrinsic SBS
Intact Specimen
C.S.
p'/p'cs
q/p'cs
Intrinsic SBS
Intact Specimen
x
Yield Point
C.S.
p'/p'cs

(a) Compression Yield

(b) Shear Yield

Figure 7.2.1-D - Typical Test Results for Structured Intact Calcarenite

(after Cuccovillo and Coop (1993))

(a) Isotropic Compression

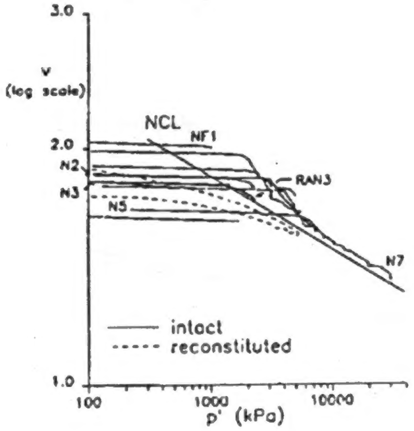

(b) Compression Yield

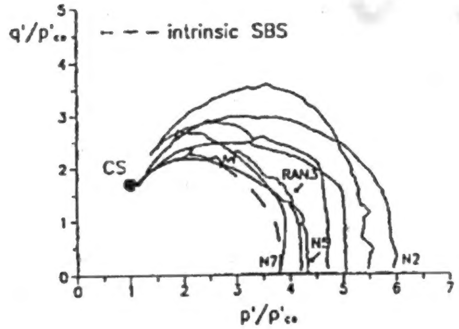

(c) Shearing Yield

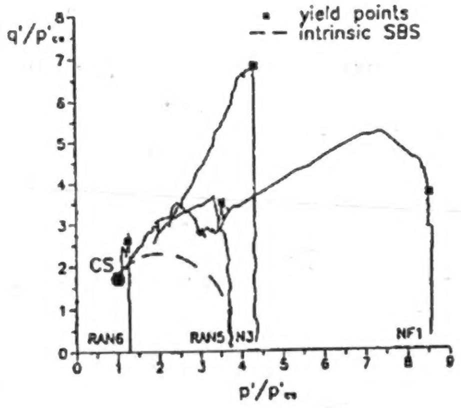

Figure 7.3.2 – Automated Triaxial Testing System

(a) View of the Overall Testing Apparatus

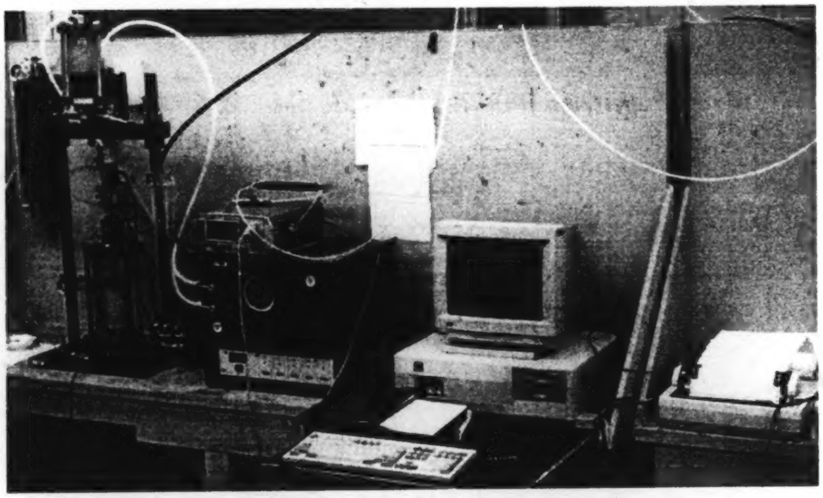

(b) A Close up of the Loading Frame

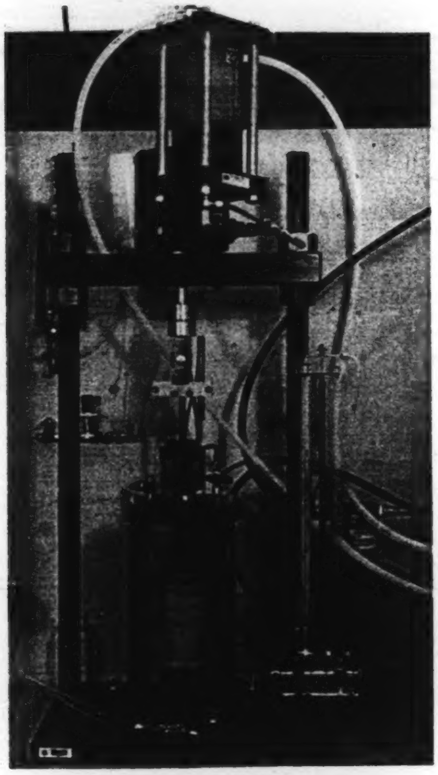

Figure 7.4.2-A - Summary of Test Results (Specimen RA-K-CIU300)

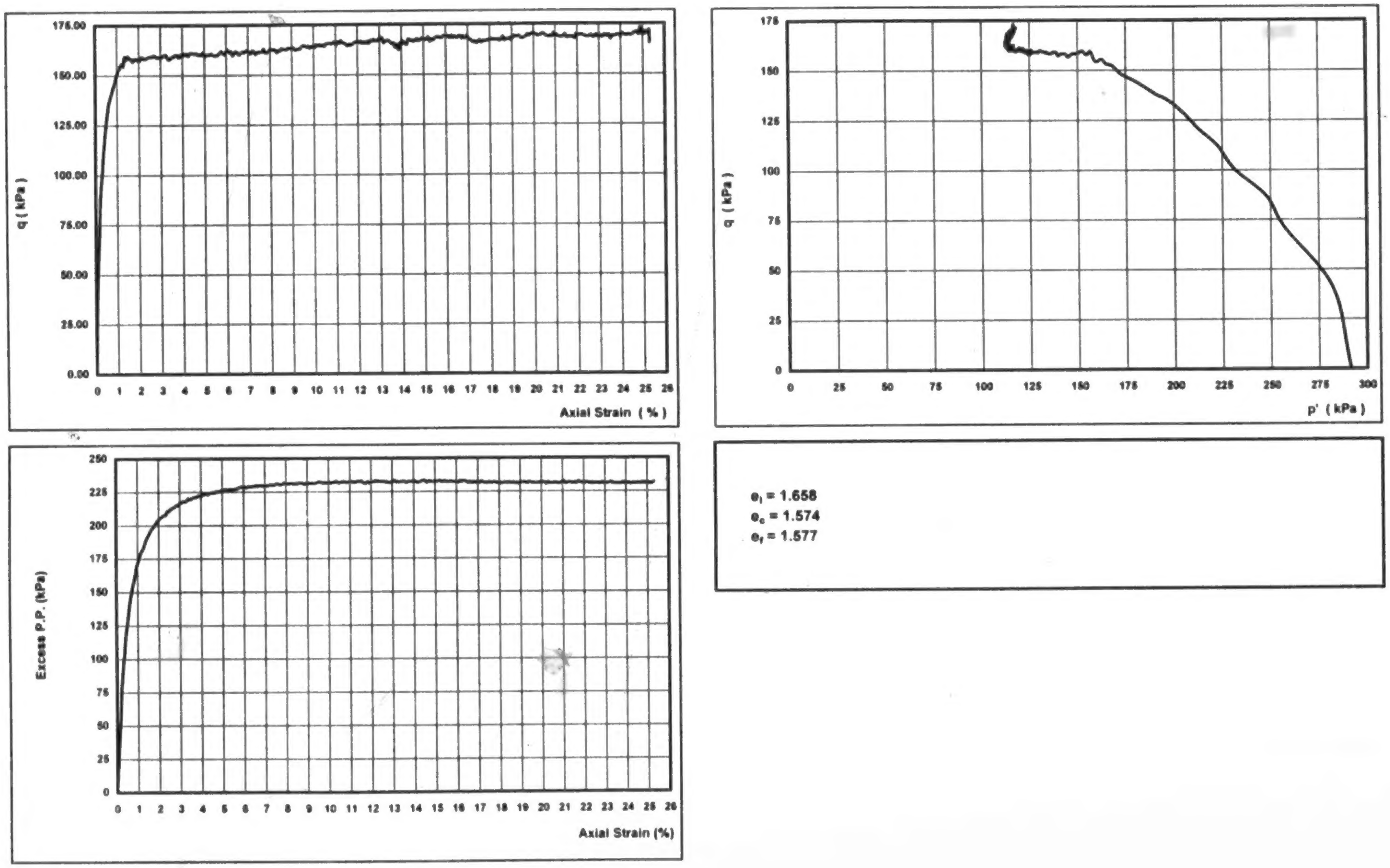

e_i = 1.658
e_c = 1.574
e_f = 1.577

Figure 7.4.2-B - Summary of Test Results (Specimen RA-K-CIU400)

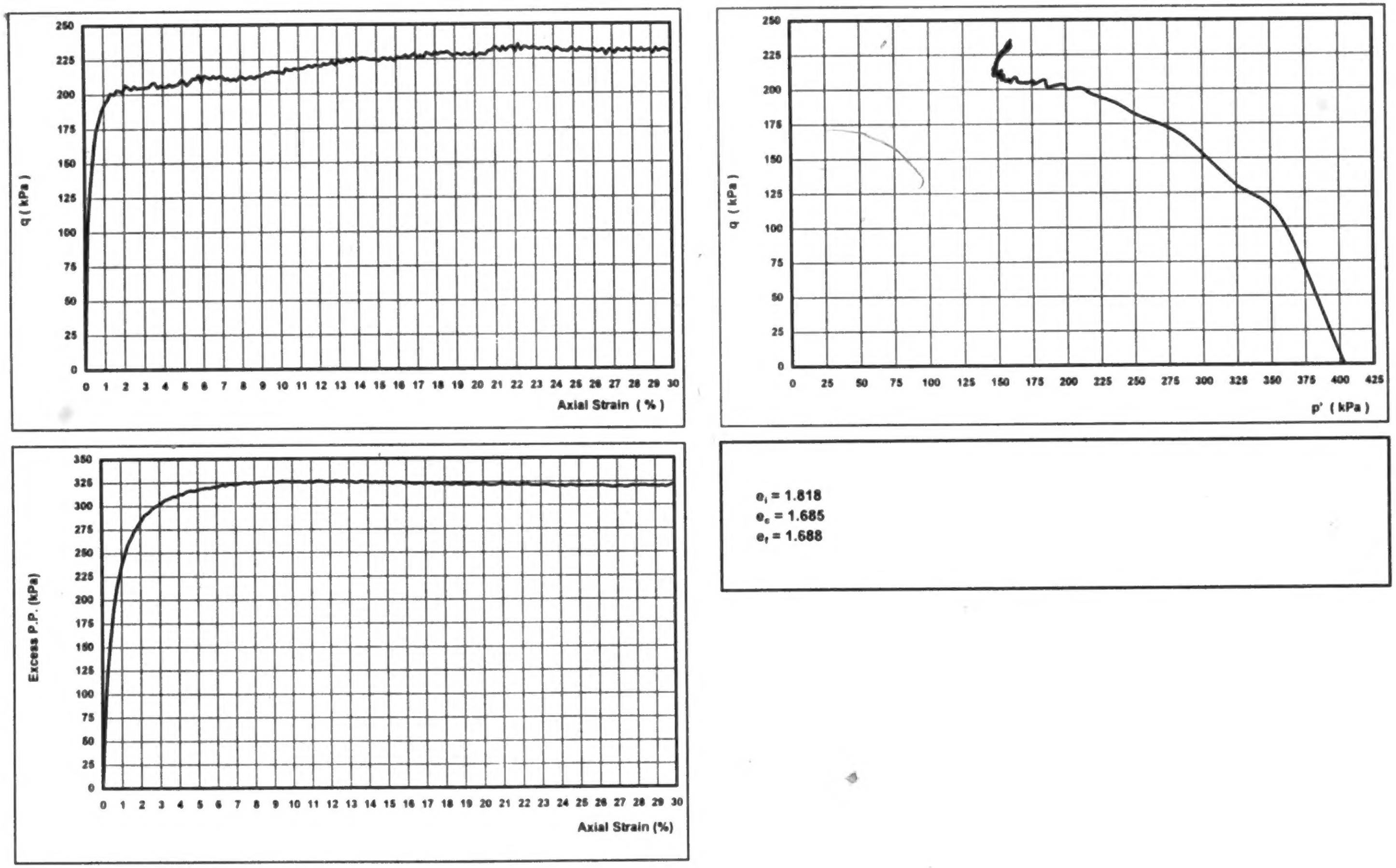

$e_i = 1.818$
$e_c = 1.685$
$e_f = 1.688$

Figure 7.4.2-C - Summary of Test Results (Specimen RA-K-CIU500)

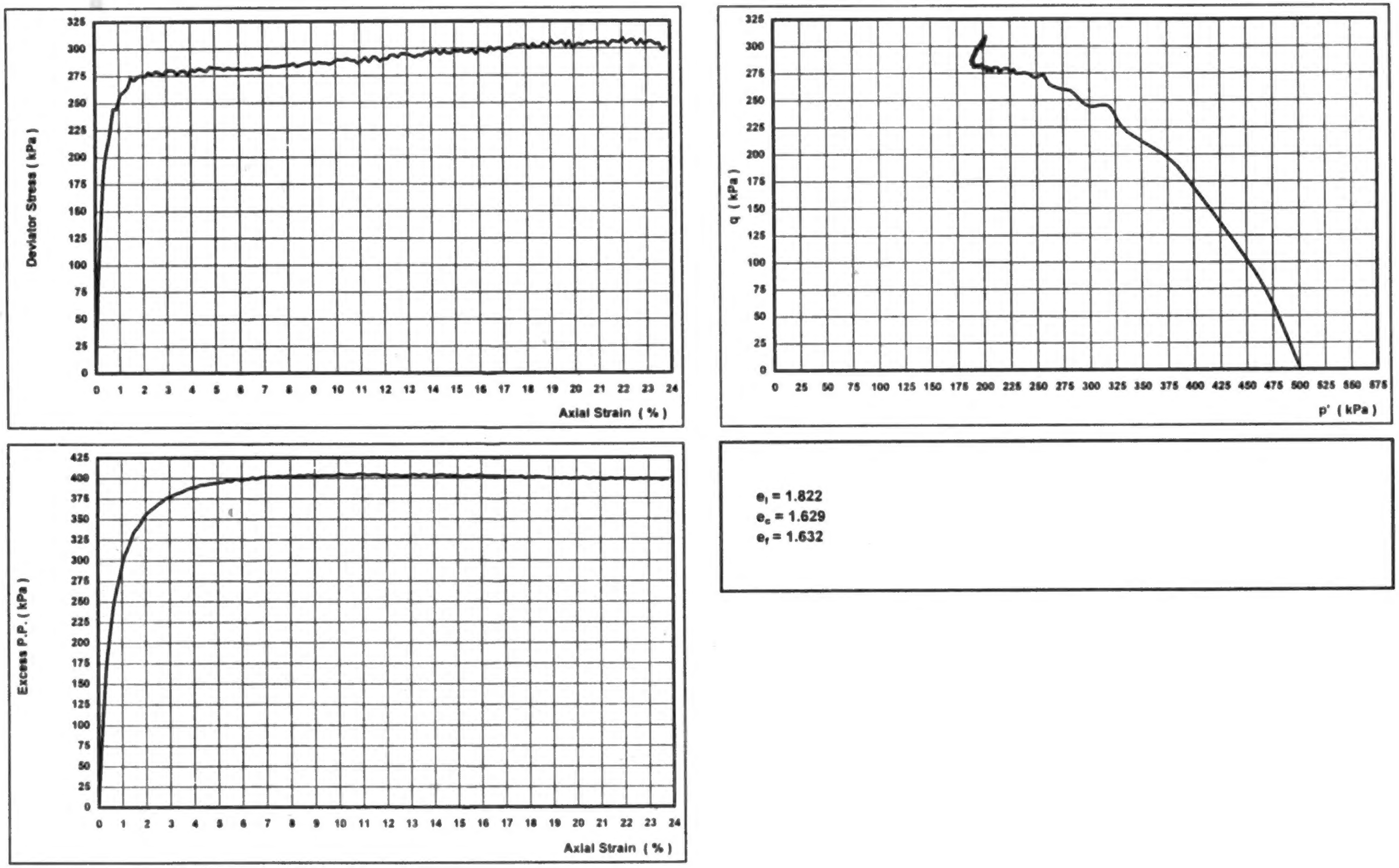

$e_i = 1.822$
$e_c = 1.629$
$e_f = 1.632$

Figure 7.4.2-D - Normalized Summary Results for Reconstituted CIU Tests

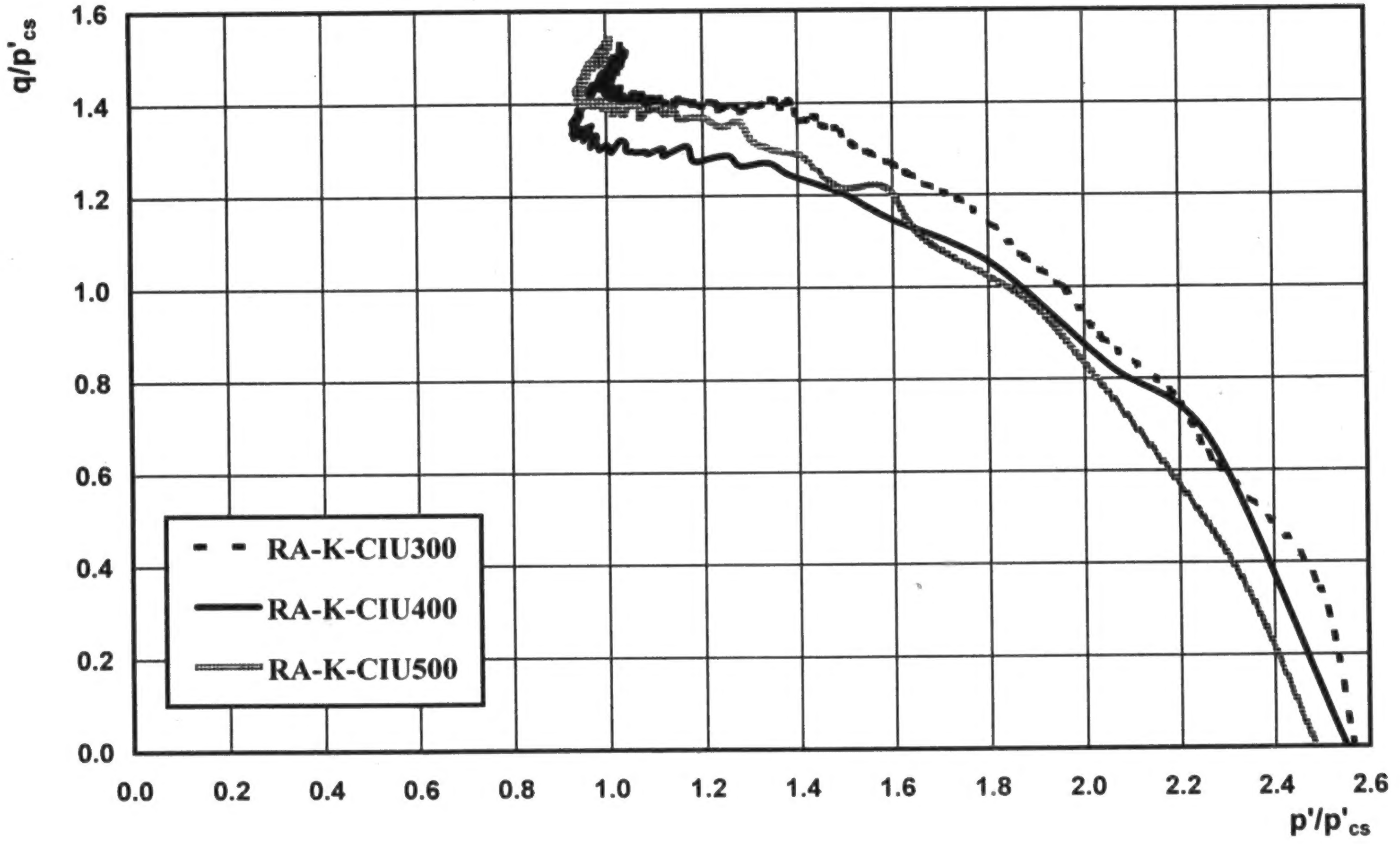

Figure 7.4.2-E - Summary of Test Results (Specimen RA-K-CAU372)

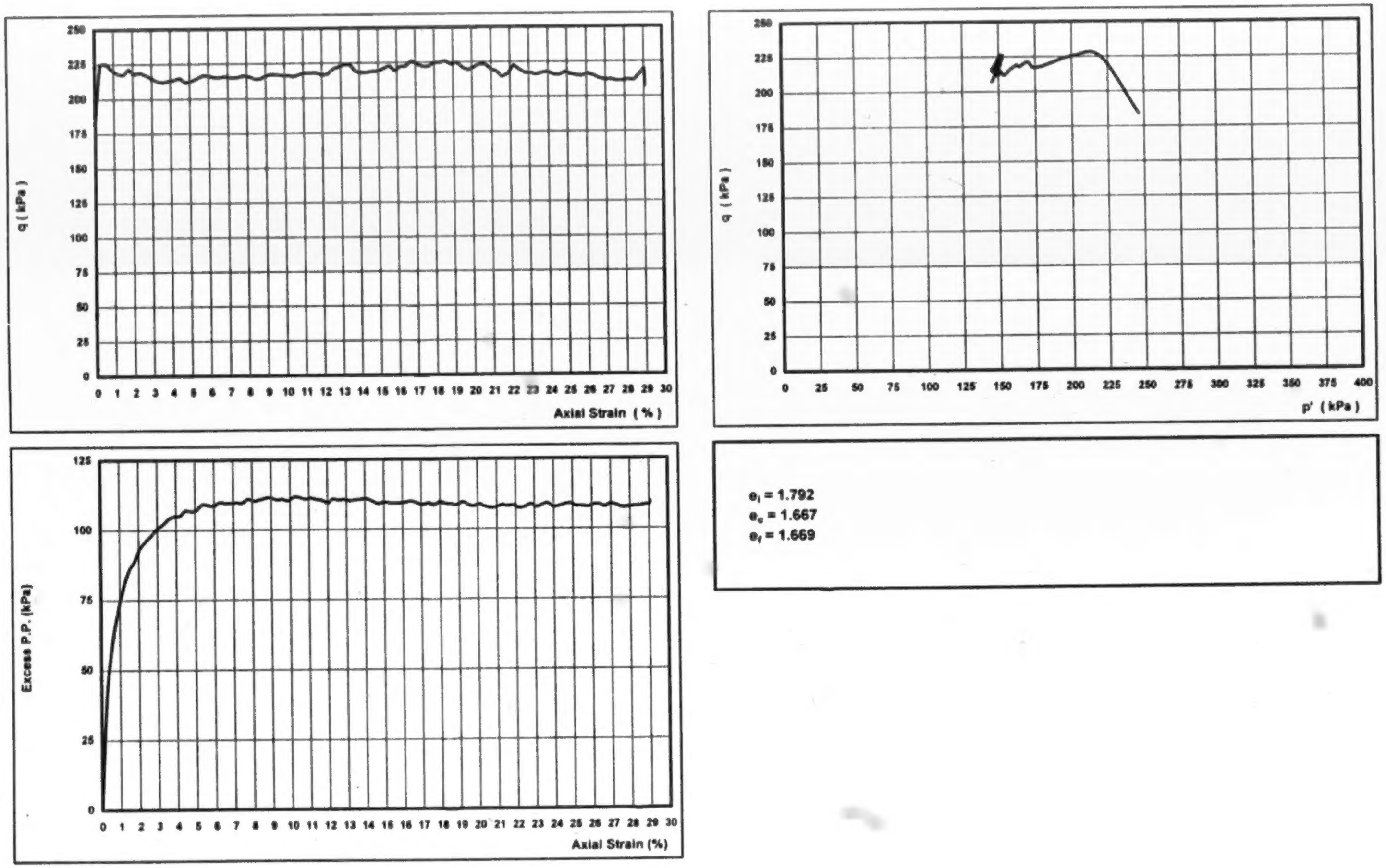

$e_i = 1.792$
$e_c = 1.667$
$e_f = 1.669$

Figure 7.4.2-F - Summary of Test Results (Specimen RA-K-CAD372)

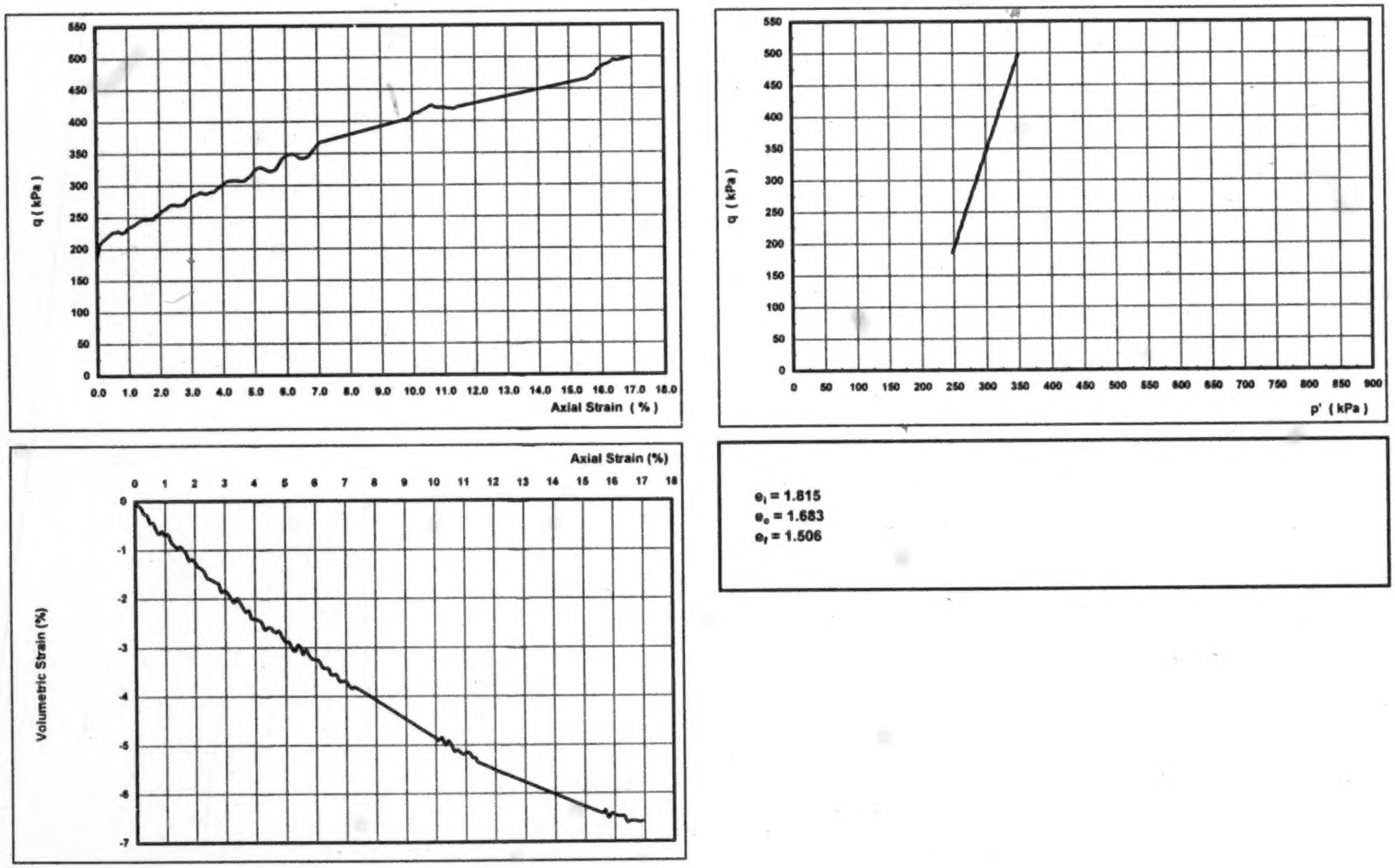

$e_i = 1.815$
$e_c = 1.683$
$e_f = 1.506$

Figure 7.4.2-G - Summary of Test Results (Specimen RA-K-EAU190)

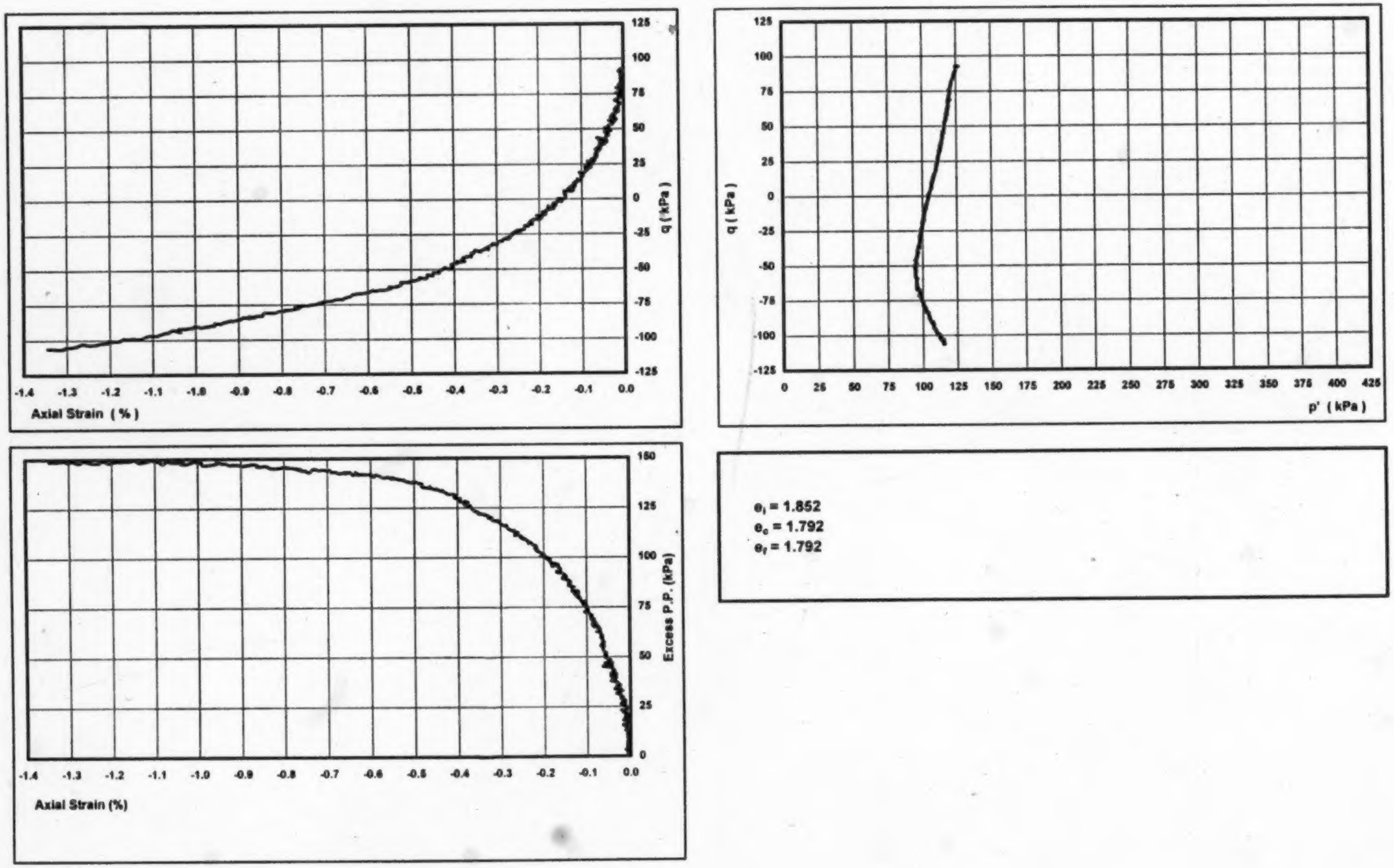

$e_i = 1.852$
$e_c = 1.792$
$e_f = 1.792$

Figure 7.4.3.1-A - Summary Results for Specimens from Koosi Creek Slide Site with In-Situ Water Content of 36%-38%

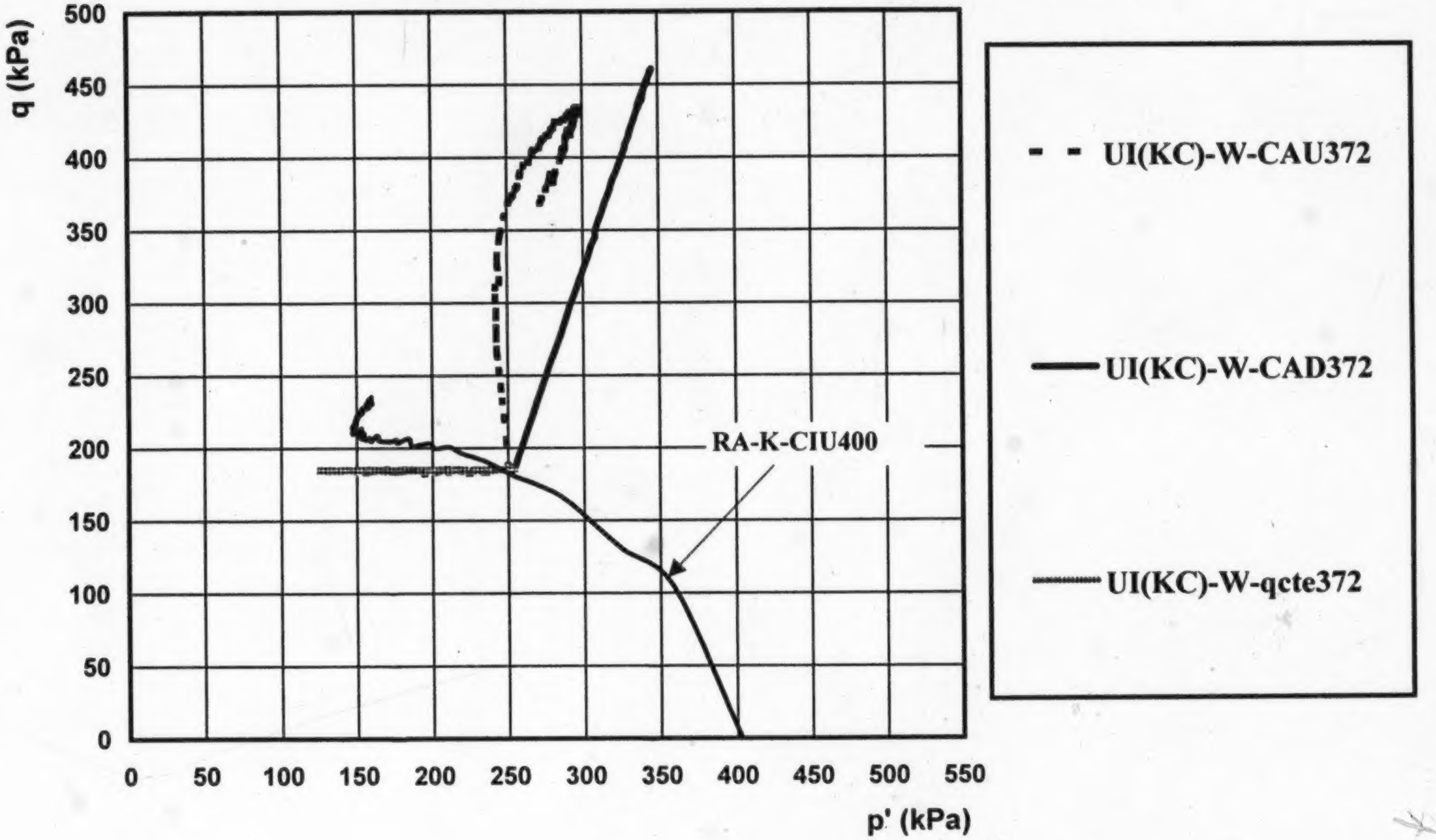

Figure 7.4.3.1-B - Summary of Test Results (Specimen UI(KC)-W-CAU372)

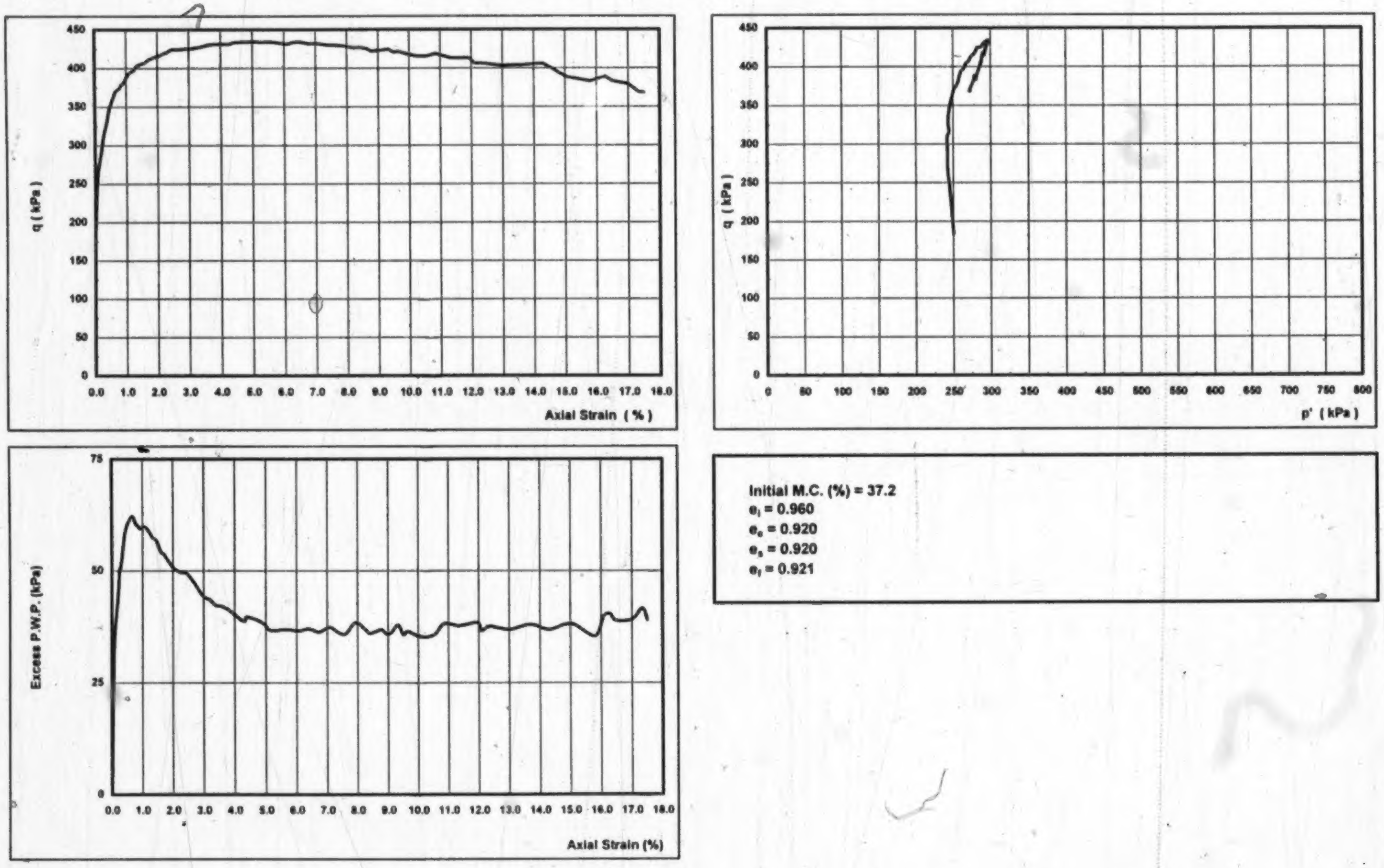

Initial M.C. (%) = 37.2
$e_i = 0.960$
$e_c = 0.920$
$e_s = 0.920$
$e_f = 0.921$

Figure 7.4.3.1-C - Summary of Test Results (Specimen UI(KC)-W-CAD372)

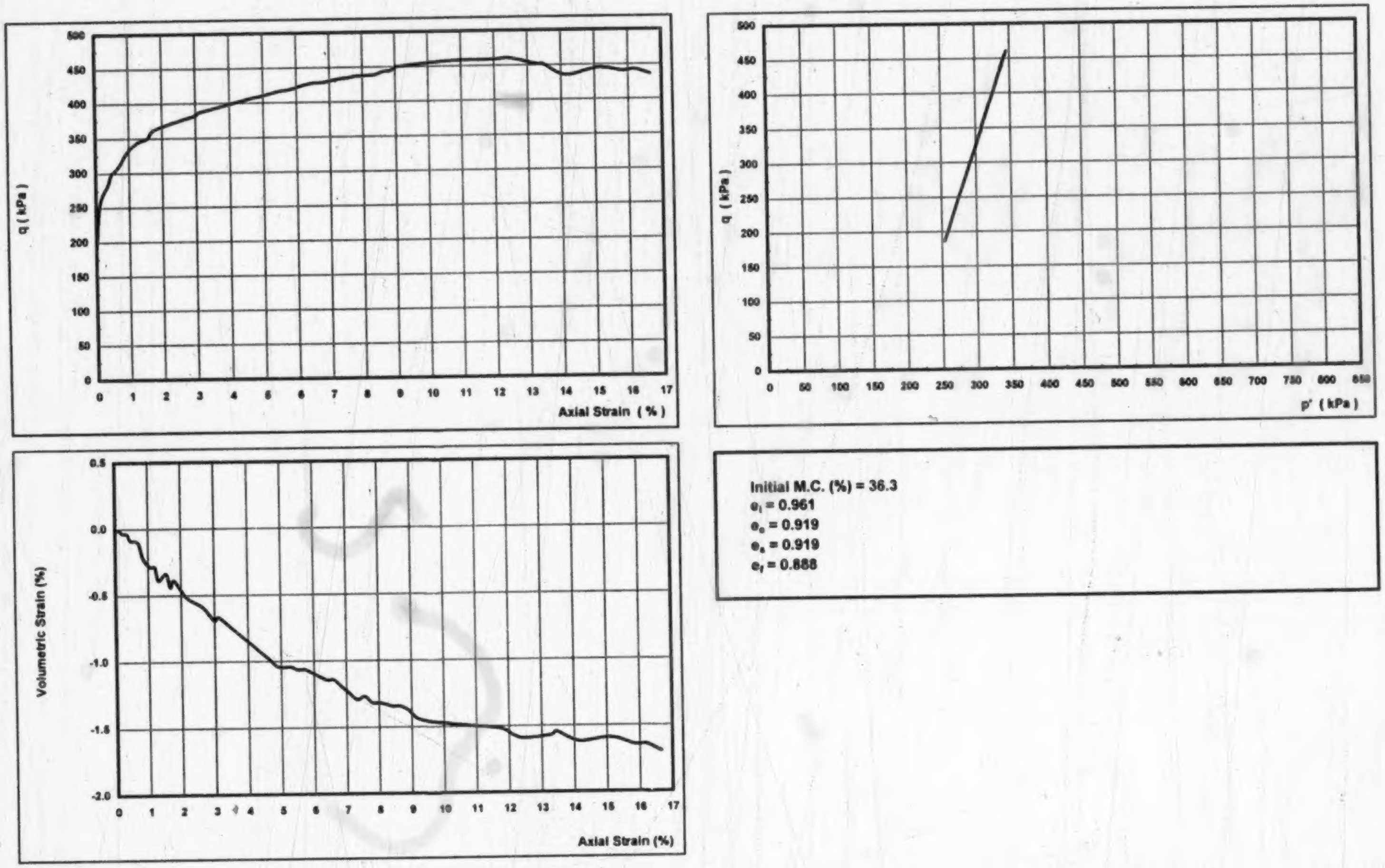

Initial M.C. (%) = 36.3
$e_i = 0.961$
$e_c = 0.919$
$e_s = 0.919$
$e_f = 0.888$

Figure 7.4.3.1-D - Summary of Test Results (Specimen UI(KC)-W-qcte372)

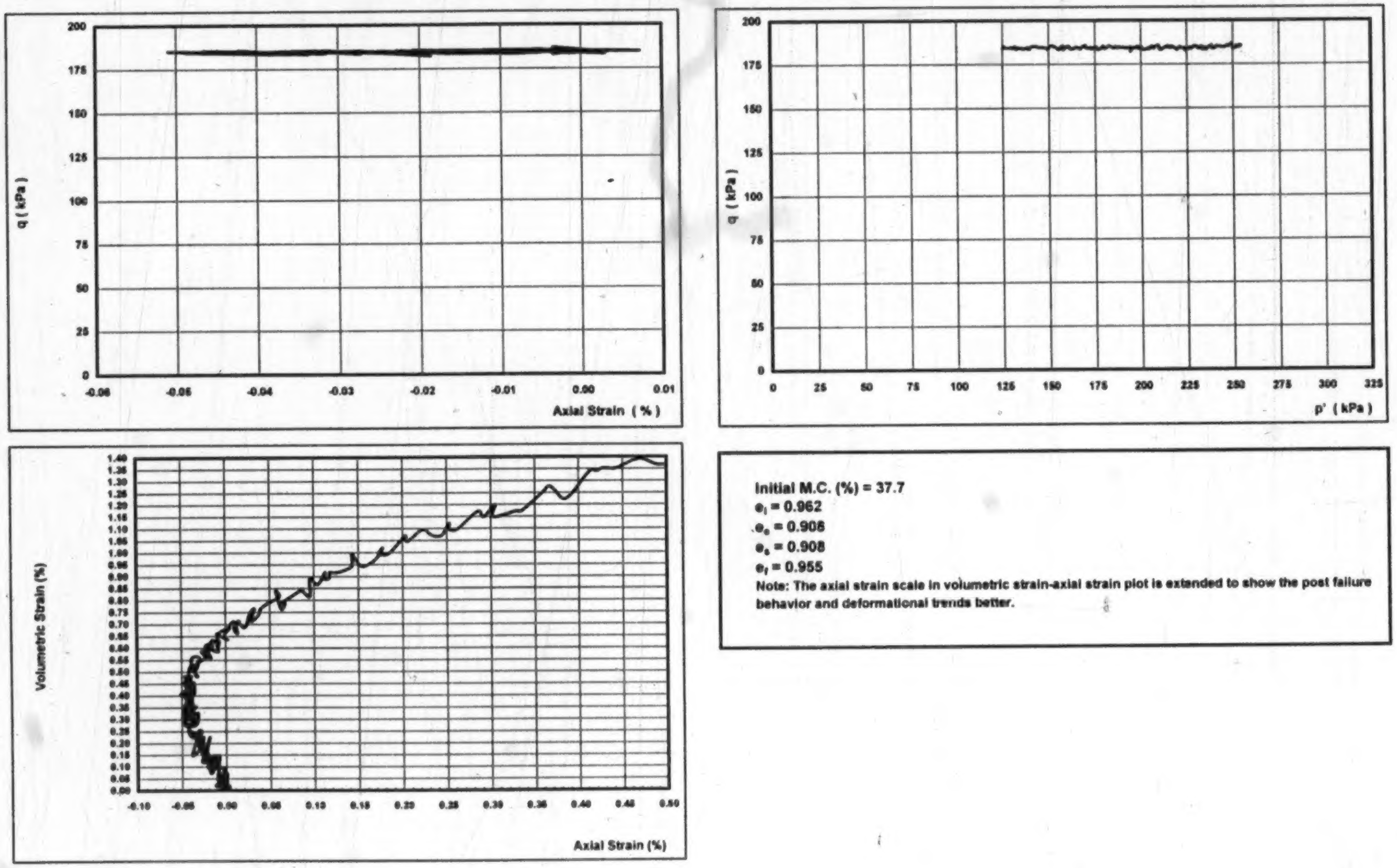

Initial M.C. (%) = 37.7
e_i = 0.962
e_c = 0.908
e_s = 0.908
e_f = 0.955
Note: The axial strain scale in volumetric strain-axial strain plot is extended to show the post failure behavior and deformational trends better.

Figure 7.4.3.2-A - Summary Results for Specimens from Okanagan Lake Park Slide Site with In-Situ Water Content of 23%-28%

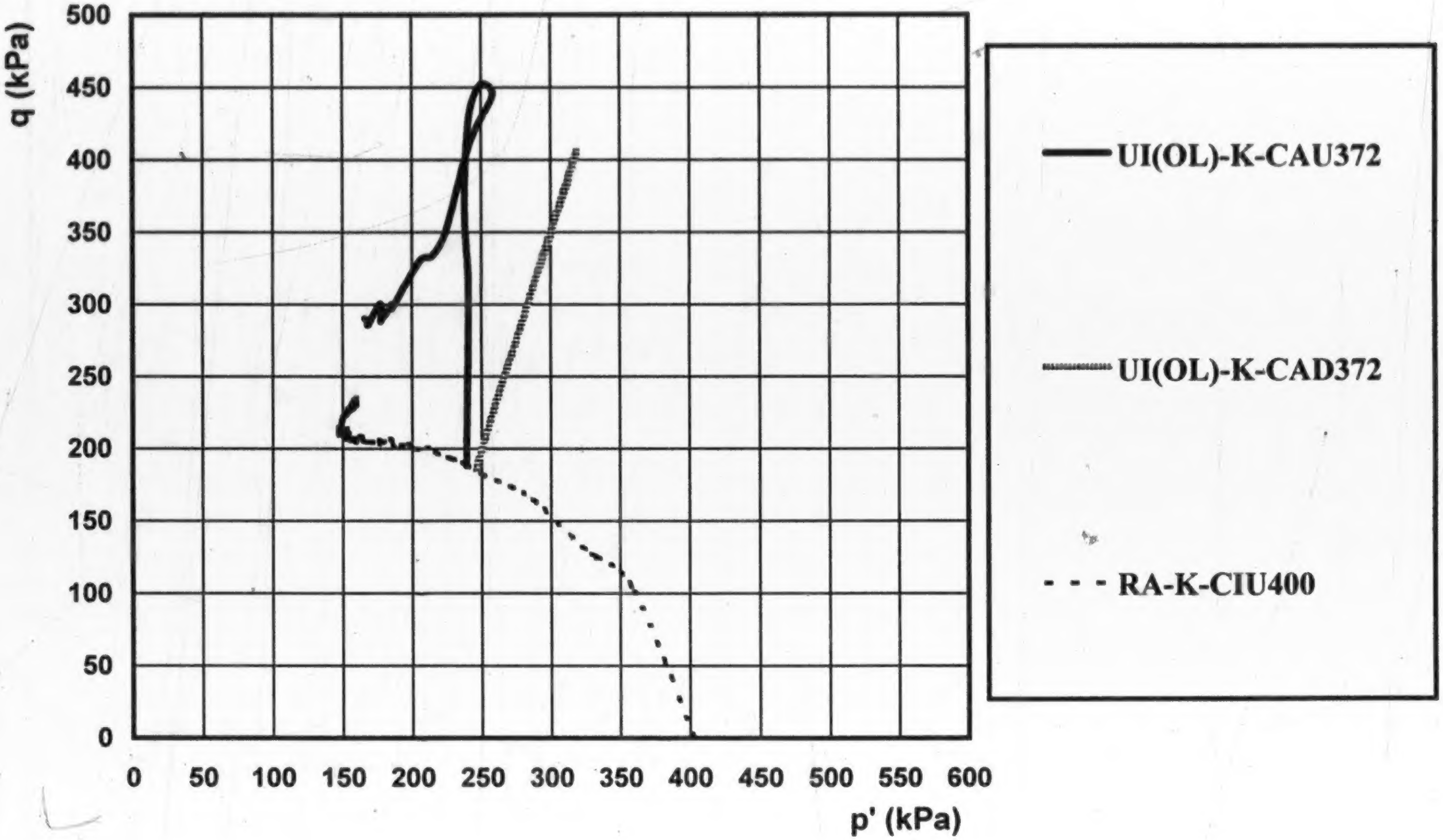

Figure 7.4.3.2-B - Summary of Test Results (Specimen UI(OL)-K-CAU372)

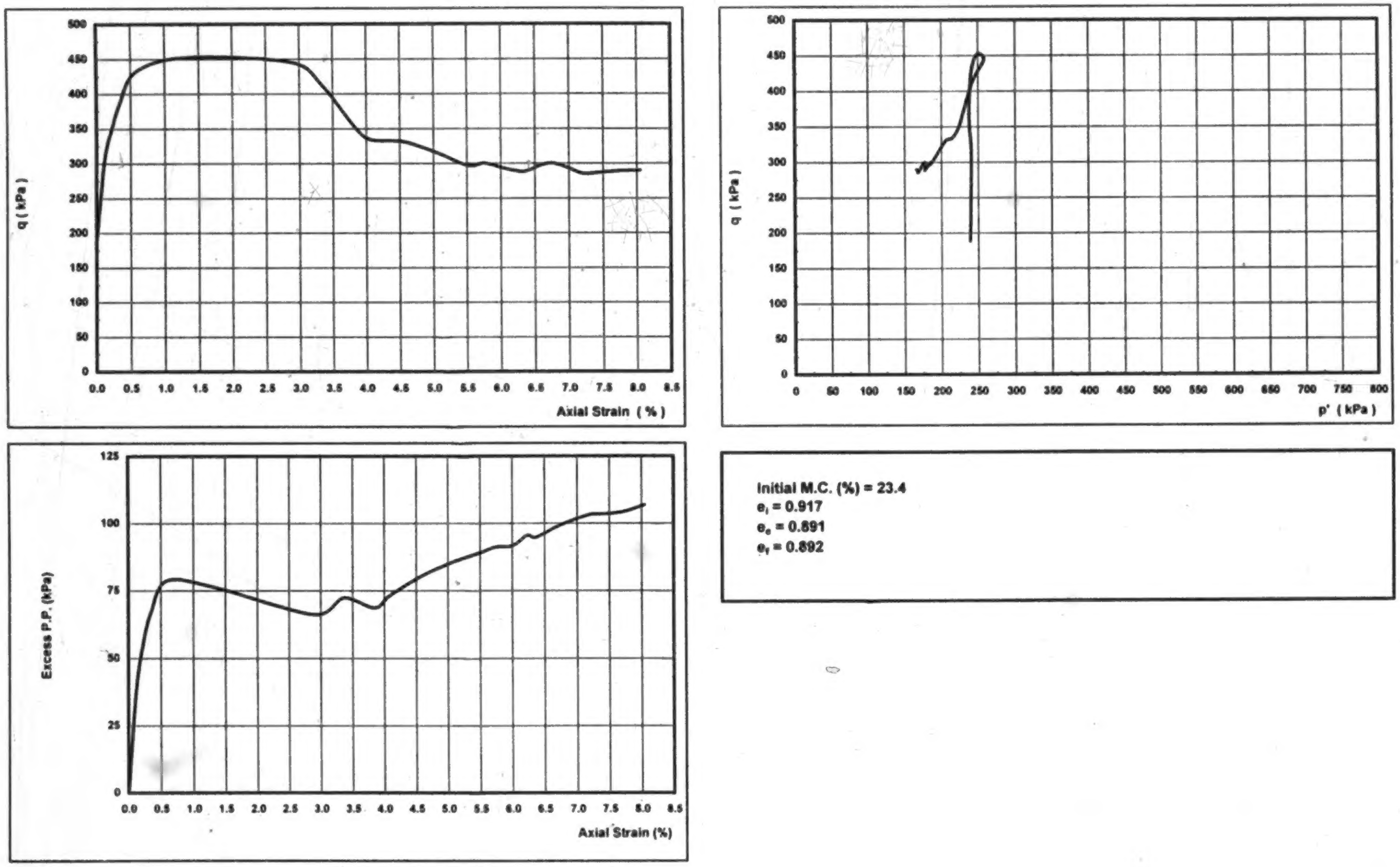

Initial M.C. (%) = 23.4
$e_i = 0.917$
$e_c = 0.891$
$e_f = 0.892$

Figure 7.4.3.2-C - Summary of Test Results (Specimen UI(OL)-K-CAD372)

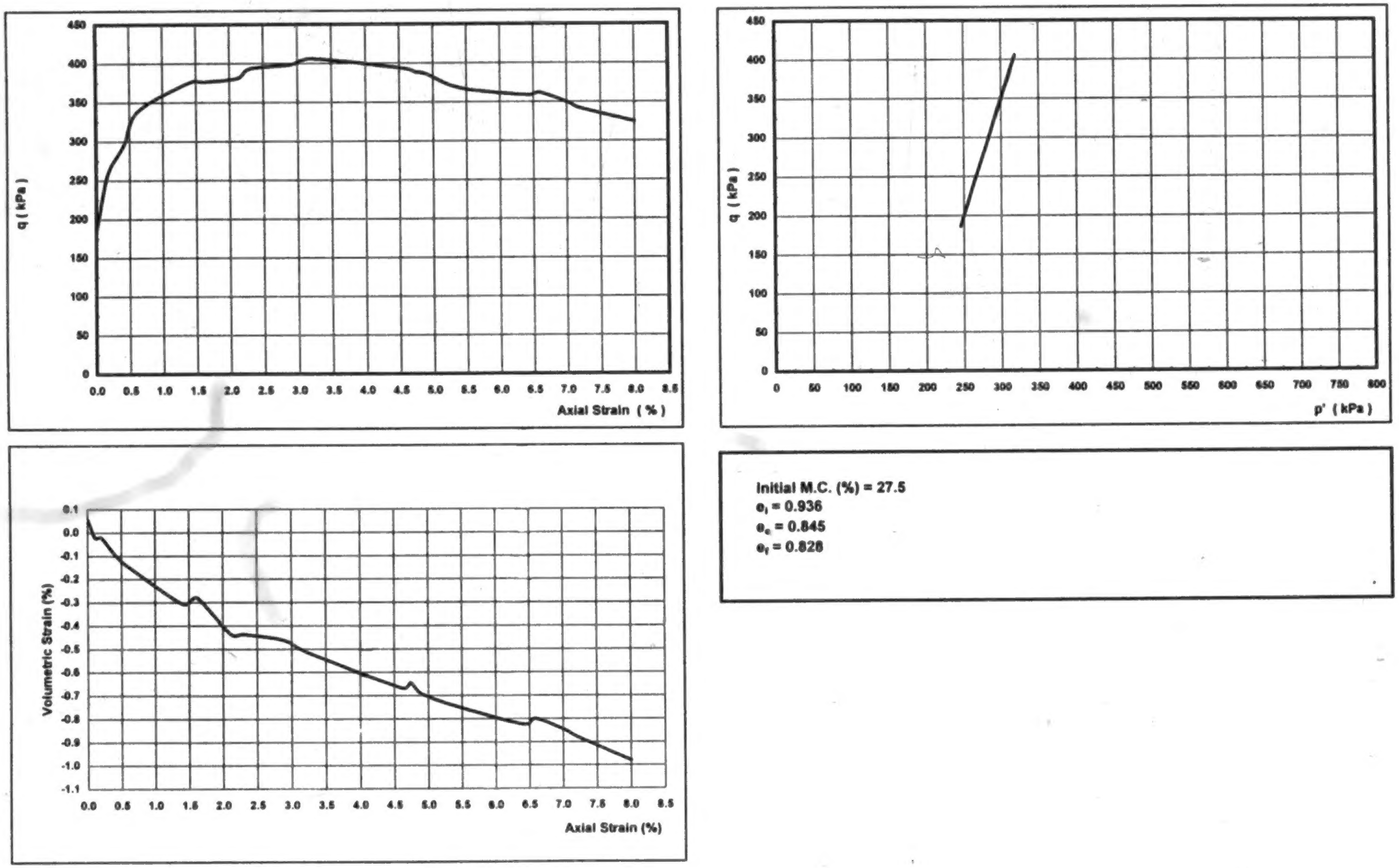

Initial M.C. (%) = 27.5
$e_i = 0.936$
$e_c = 0.845$
$e_f = 0.828$

Figure 7.4.3.3-A - Summary Results for Air-Dried Water Saturated Specimens

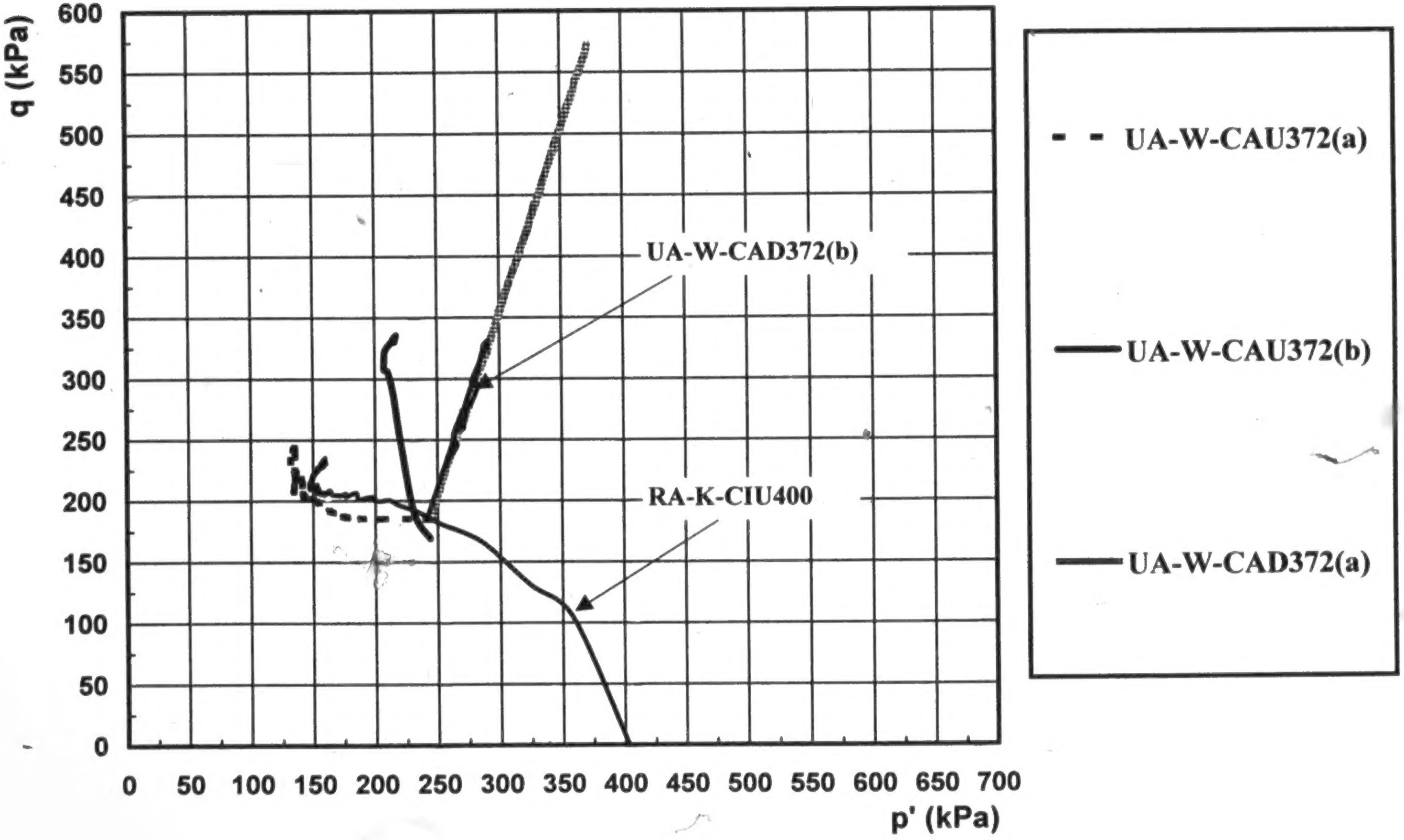

Figure 7.4.3.3-B - Summary of Test Results (Specimen UA-W-CAU372(a))

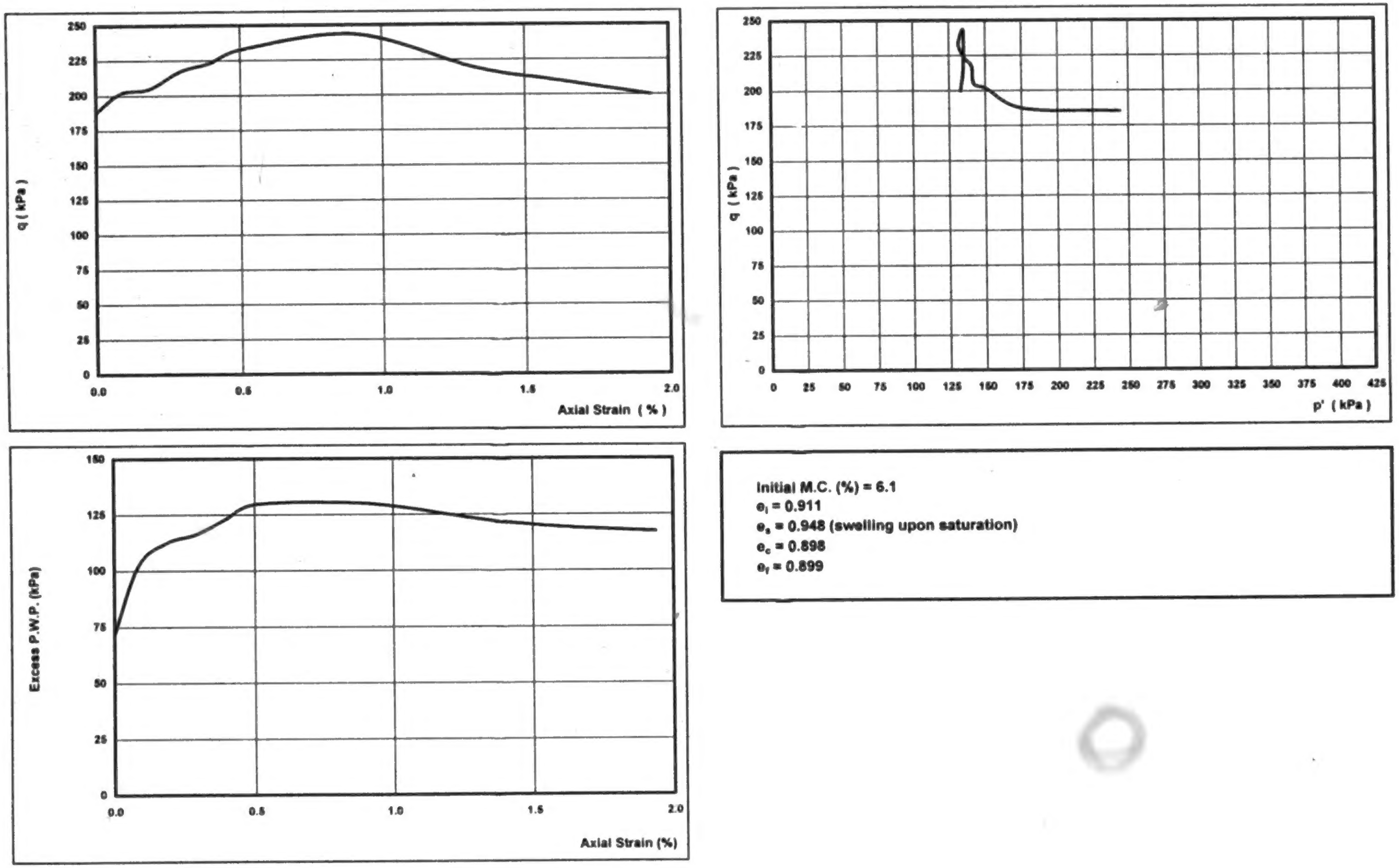

Initial M.C. (%) = 6.1
e_i = 0.911
e_s = 0.948 (swelling upon saturation)
e_c = 0.898
e_f = 0.899

Figure 7.4.3.3-C - Summary of Test Results (Specimen UA-W-CAU372(b))

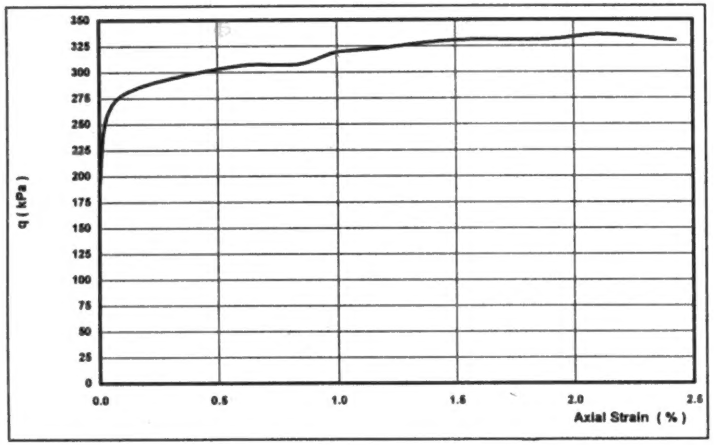

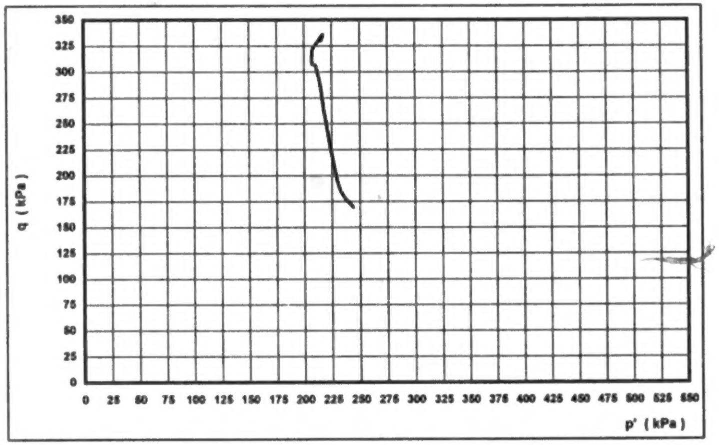

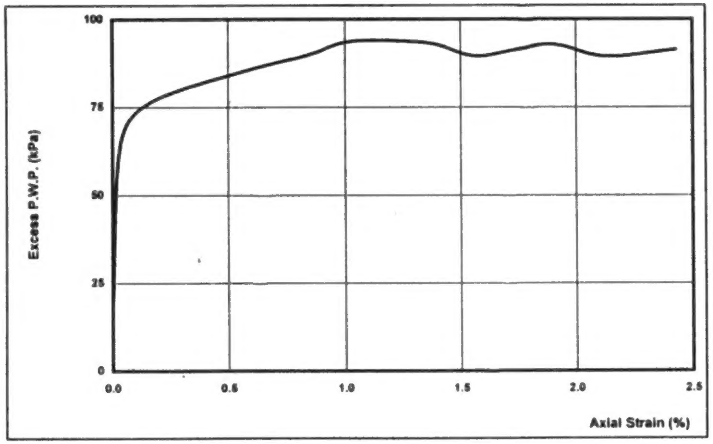

Initial M.C. (%) = 3.7
$e_i = 0.928$
$e_s = 0.866$
$e_c = 0.785$
$e_f = 0.781$

Figure 7.4.3.3-D - Summary of Test Results (Specimen UA-W-CAD372(a))

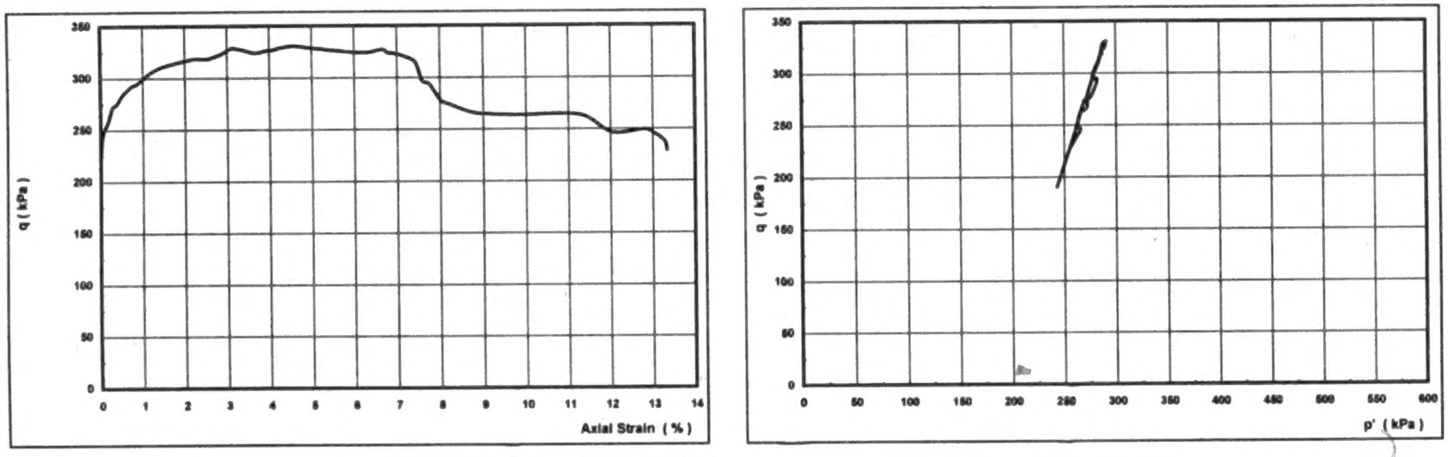

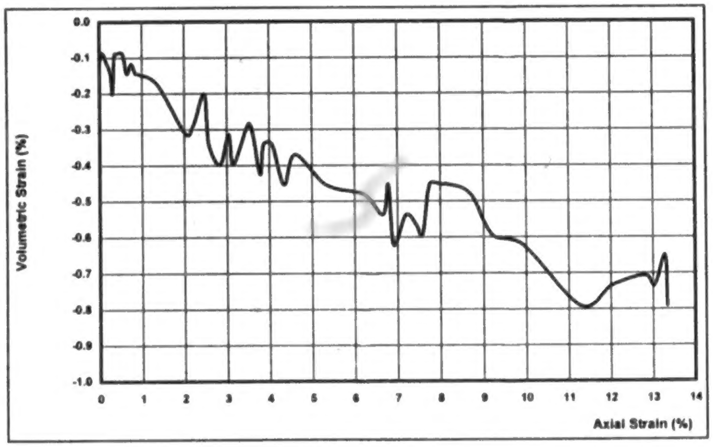

Initial M.C. (%) = 1.9
$e_i = 0.825$
$e_s = 0.772$
$e_c = 0.708$
$e_f = 0.700$

Figure 7.4.3.3-E - Summary of Test Results (Specimen UA-W-CAD372(b))

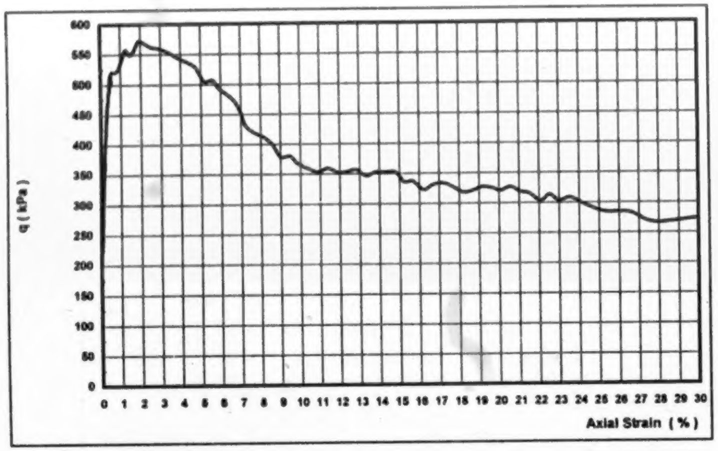

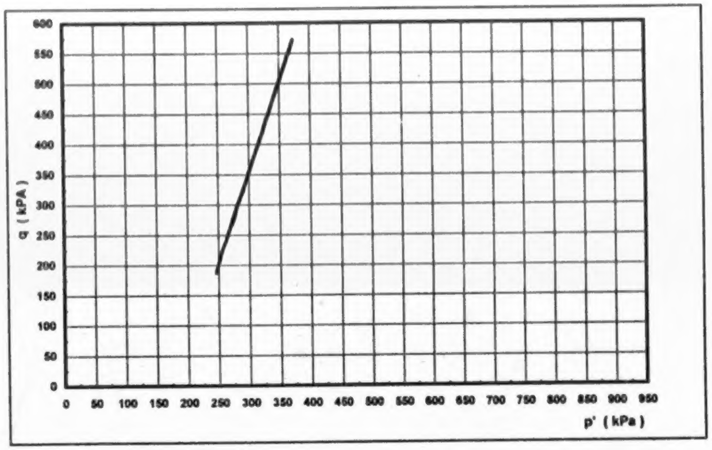

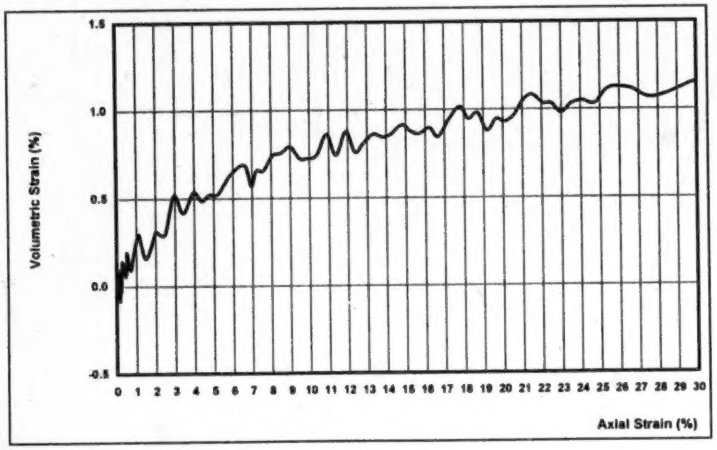

Initial M.C. (%) = 6.2
e_i = 0.885
ec = 0.883
e_s = 0.871 (saturation after consolidation)
e_f = 0.892

Figure 7.4.3.4-A - Summary of Test Results (Specimen UA-K-CAU372)

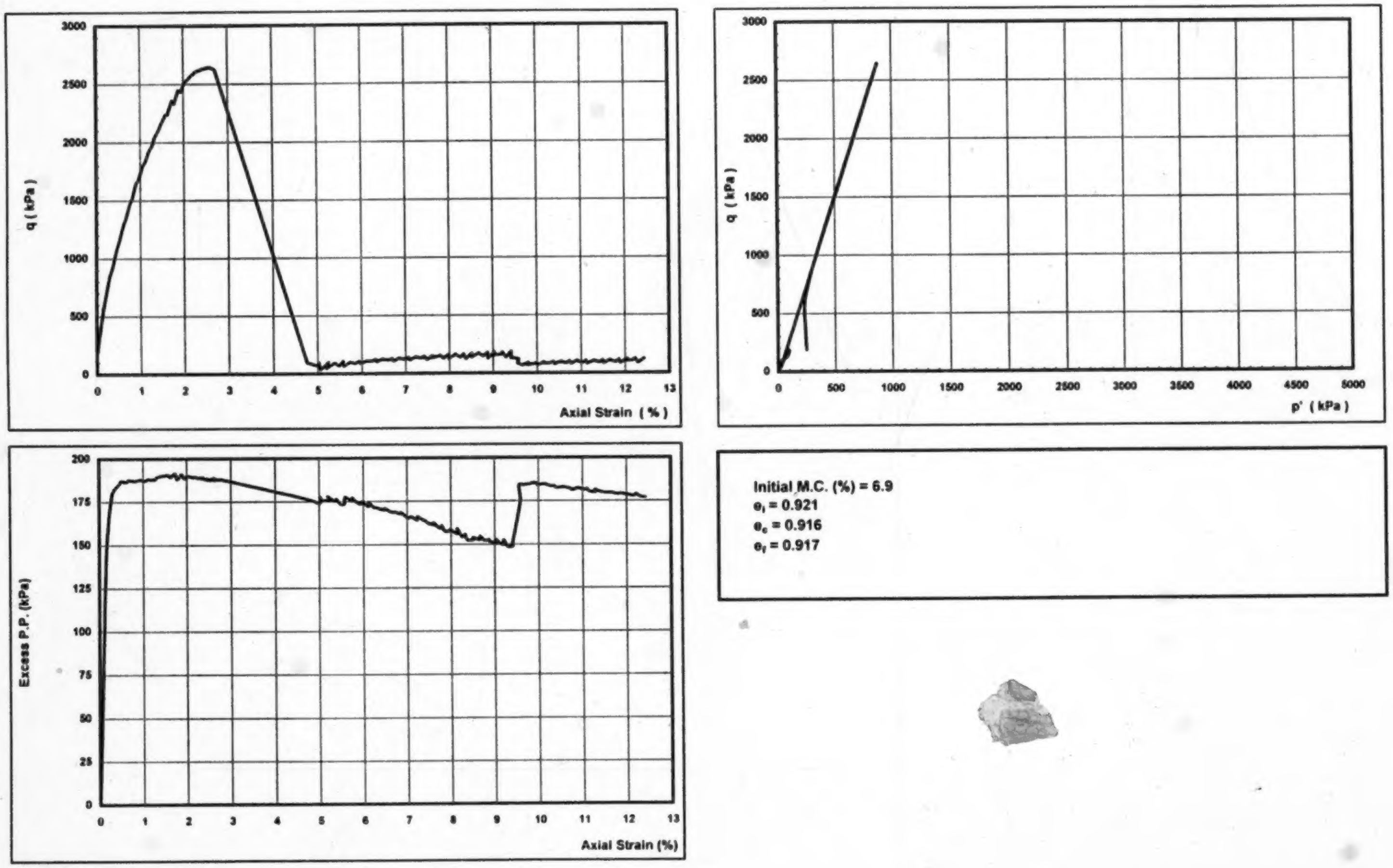

Initial M.C. (%) = 6.9
e_i = 0.921
e_c = 0.916
e_f = 0.917

Figure 7.4.3.4-B - Pore Pressure Generation in Specimen UA-K-CAU372

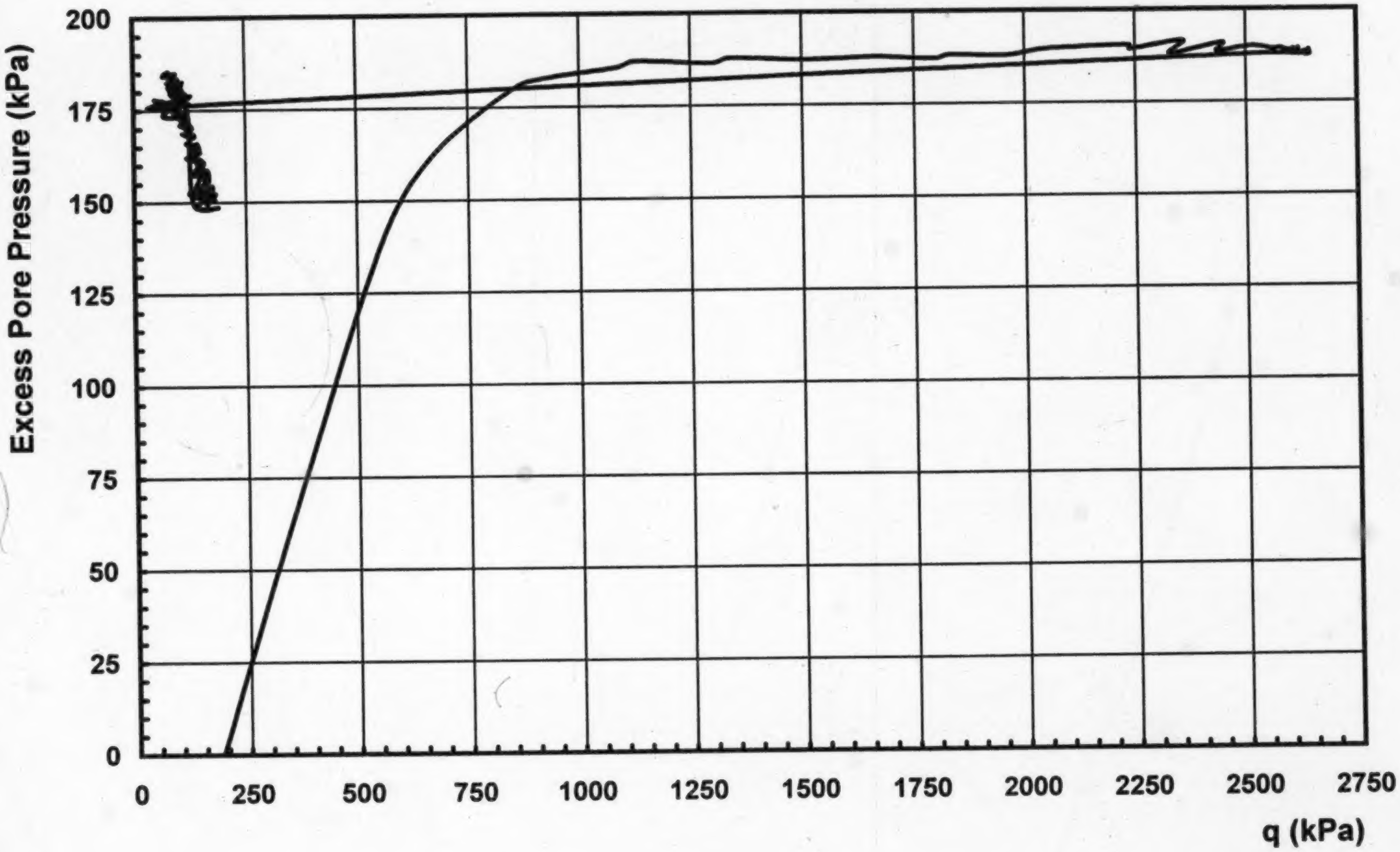

Figure 7.4.3.4-C - Summary of Test Results (Specimen UA-K-CAD372)

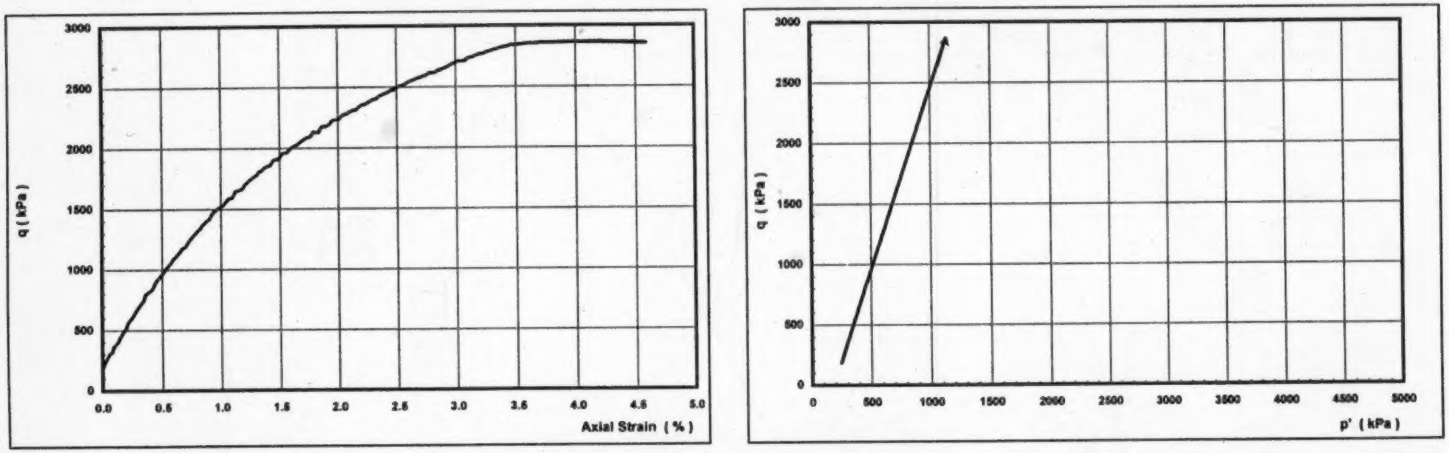

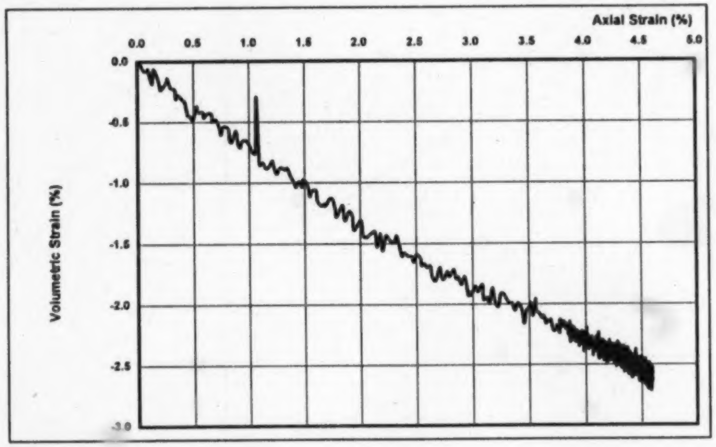

Initial M.C. (%) = 1
$e_i = 0.904$
$e_c = 0.898$
$e_f = 0.846$
Note: Test was continued up to the maximum capacity of the apparatus; but the specimen did not fail.

Figure 7.4.3.4-D - Summary of Test Results (Specimen UA-K-CAD1680)

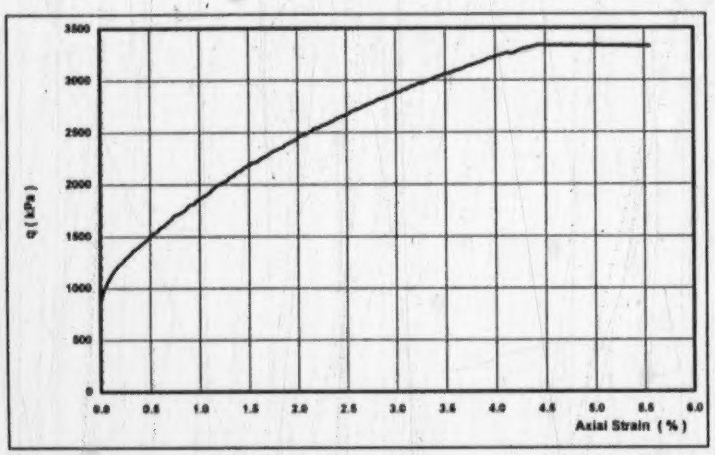

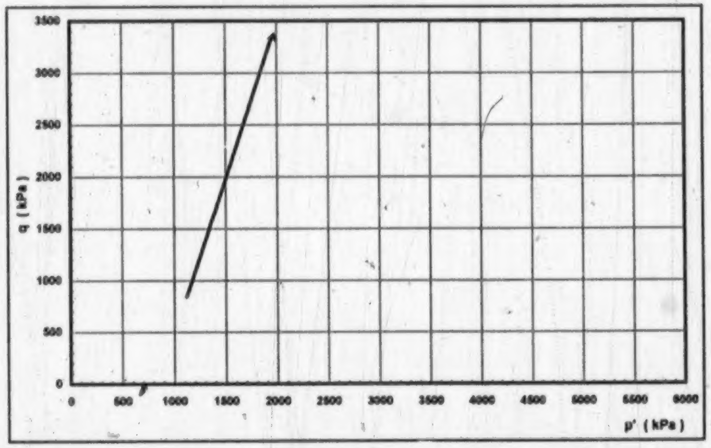

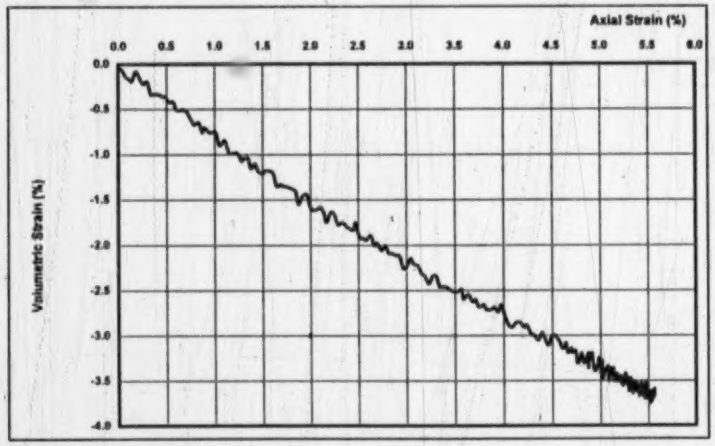

Initial M.C. (%) = 1
e_i = 1.064
ec = 1.030
e_f = 0.958
Note: Test was continued up to the maximum capacity of the apparatus; but the specimen did not fail.

Figure 7.4.4-A - Stress Paths of Reconstituted Specimens

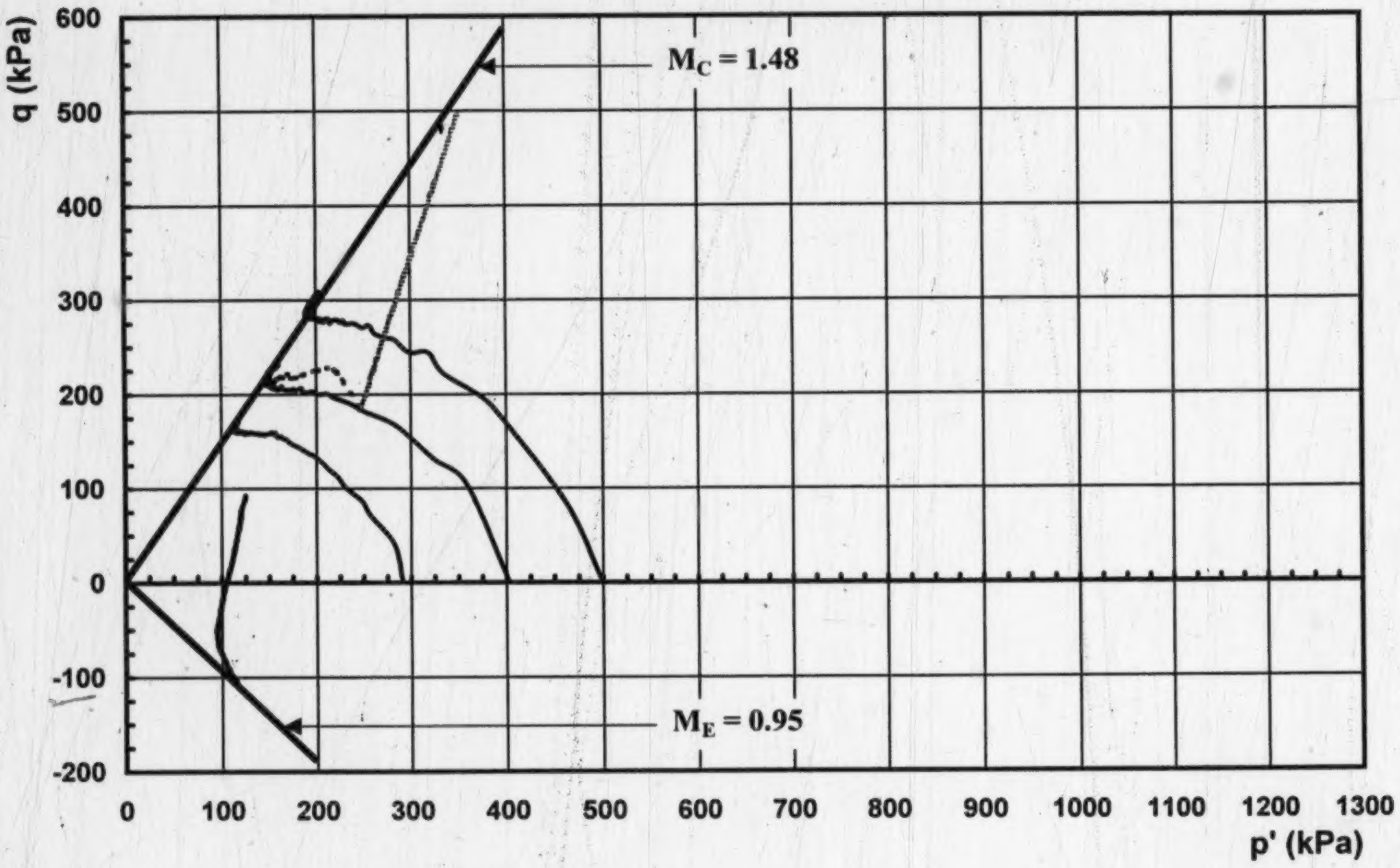

Figure 7.4.4-B - Stress - Strain Curves of Undrained Compression Tests

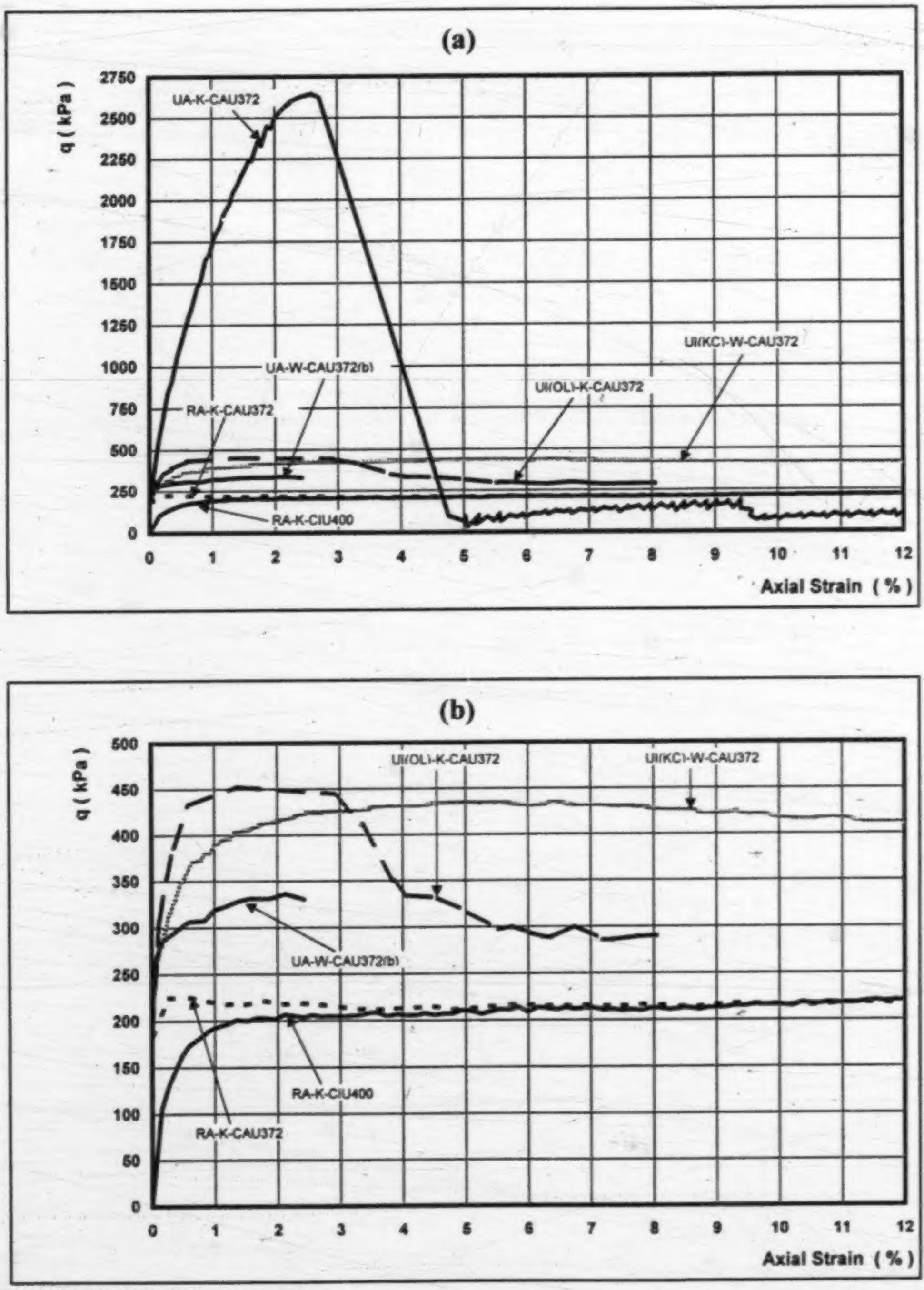

Figure 7.4.4-C – Stress Paths of Undisturbed Specimens
(Series UI(KC)-W, UI(OL)-K, and UA-W)

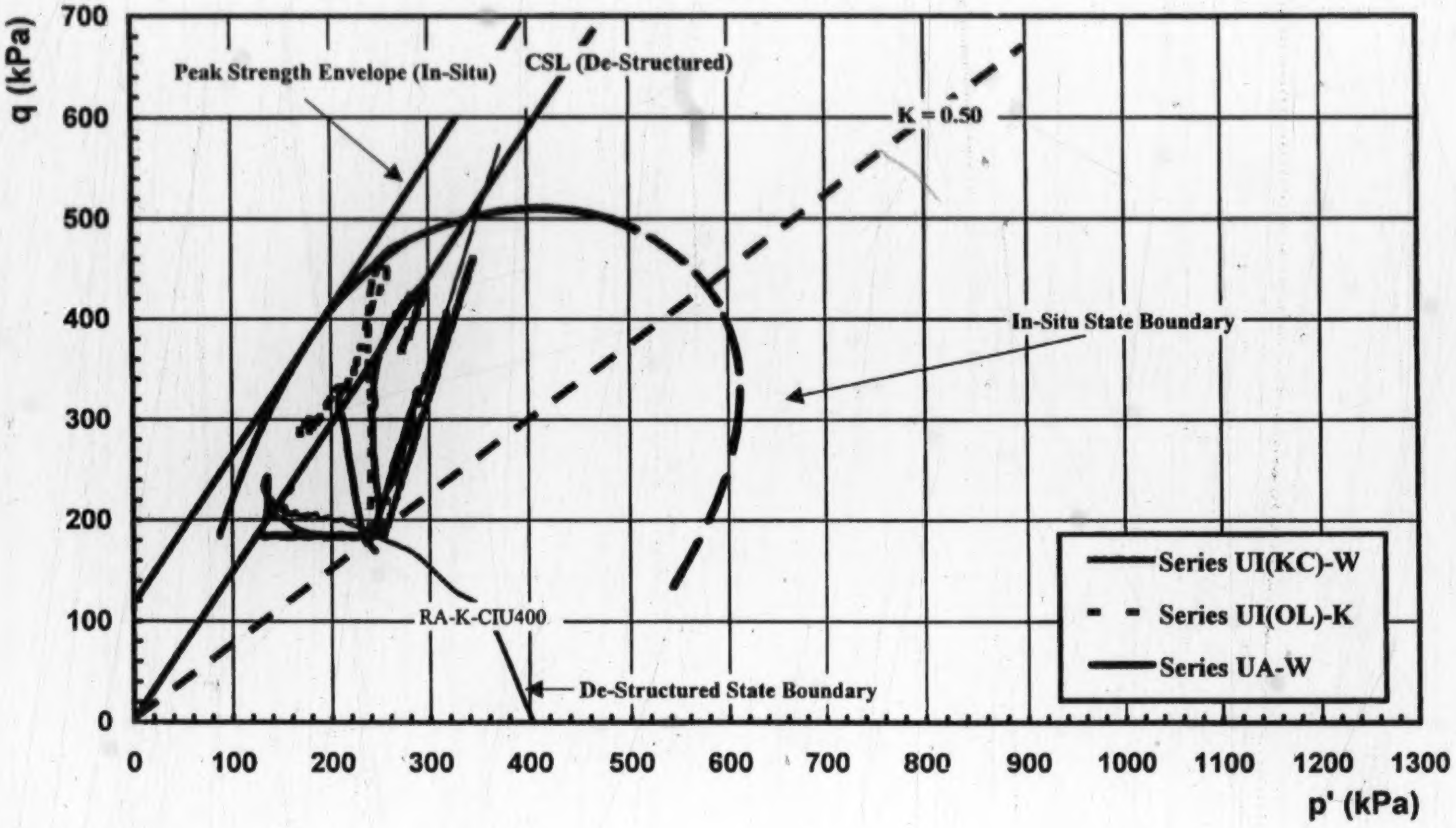

Figure 7.4.4-D – Stress Paths of Undisturbed Specimens (Series UA-K)

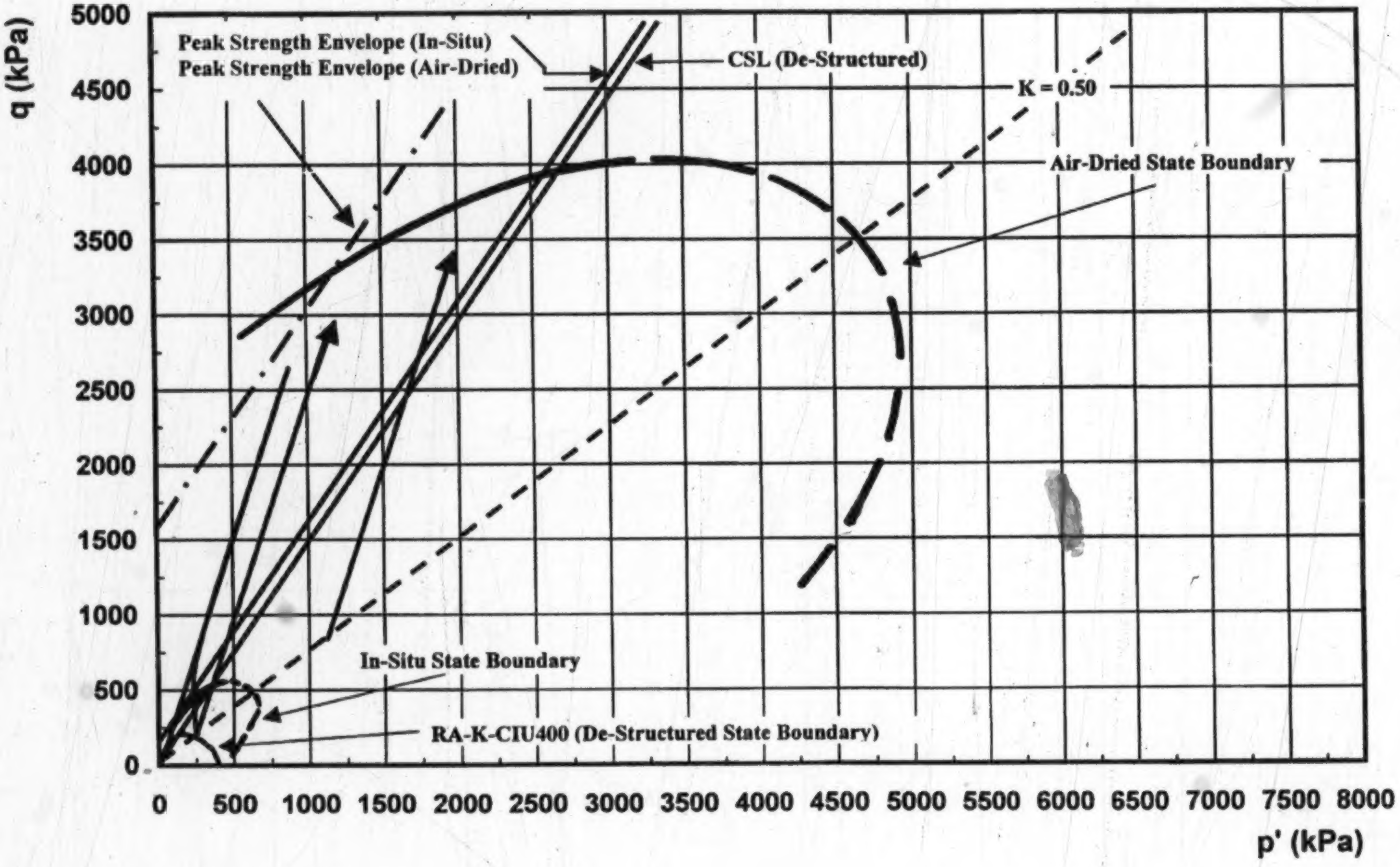

Figure 7.4.4-E – Contours of the State Boundary for Compacted Jossigny Silt at Various Suctions

(after Cui and Delage (1996))

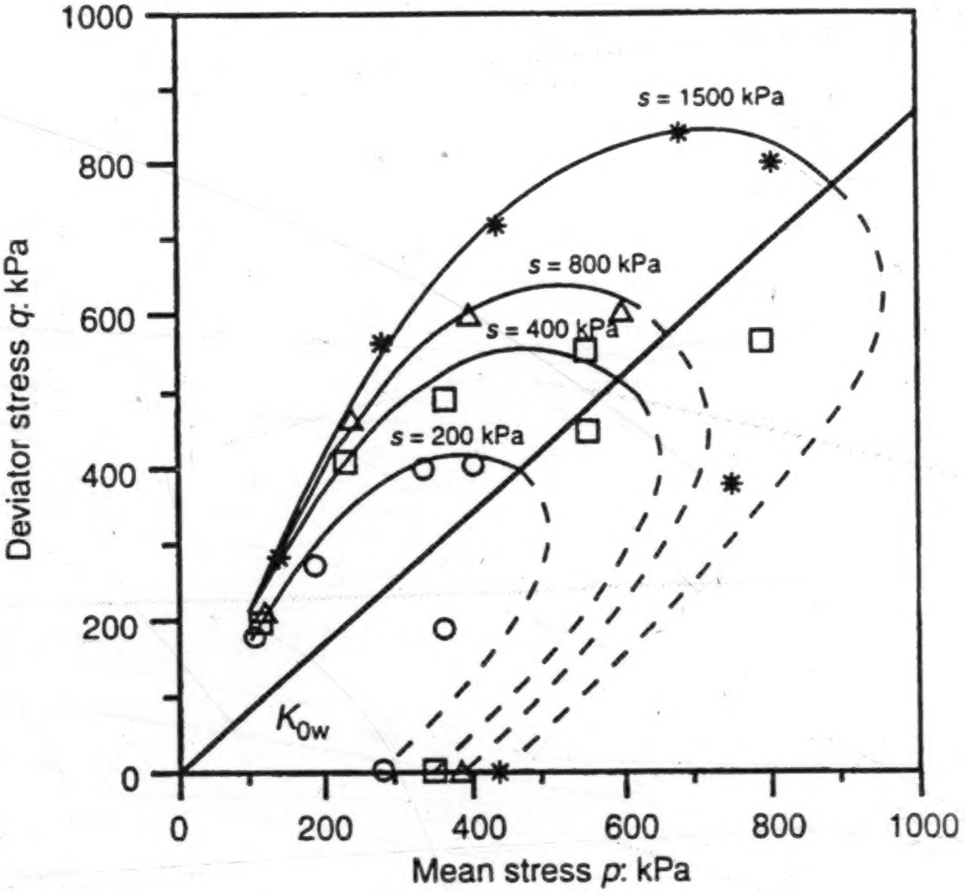

Figure 7.4.4-F – State Boundary Surface in q-(p-u_a)-s Space

(after Alonso et al. (1990))

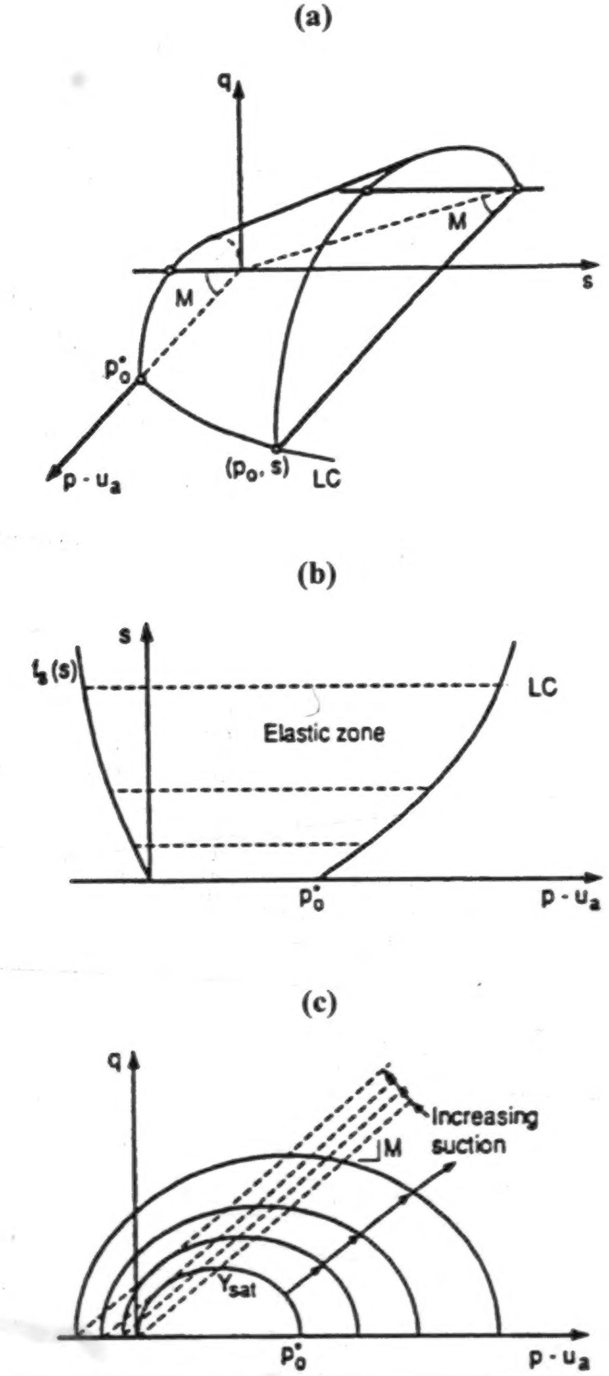
(a)
q
M
M
s
p_0^*
p - u_a
(p_0, s)
LC
(b)
s
$f_s(s)$
LC
Elastic zone
p_0^*
p - u_a
(c)
q
Increasing suction
M
Y_{sat}
p_0^*
p - u_a

CHAPTER EIGHT

Soil Structure of Penticton Silt

8.1 Introduction

Both classical and critical state soil mechanics were developed using reconstituted saturated specimens and both can describe the behavior of ideal soils. Many studies have been carried out to address the issues involved in implementing the concepts of soil mechanics to structured soils.

At a given state of stress and void ratio (e), the behavior of structured soils can be different from the behavior of ideal soils. Soils, natural or processed, are different from ideal soils because of being structured and / or unsaturated.

Soils are generally structured. The behavior of structured soils can be influenced by many parameters. The structure of a soil is a function of fabric, chemical processes such as cementation, and physical processes such as aging. Structured soils may also be unsaturated and their behavior be influenced by degree of saturation and presence of capillary stresses.

Geological and geotechnical properties of deposits known as Penticton silt have been studied and described in previous chapters of this study. The following are some of the key observations:

- These deposits are glaciolacustrine sediments of glacial Lake Penticton.
- They have never experienced any mechanical over-consolidation.
- These sediments are mainly composed of silt size mica (muscovite) and chlorite particles. Their plasticity is low and they are non-active soils.

- They are unsaturated with values of matric suction ranging between 100 kPa and 300 kPa for typical values of in-situ water contents.

- These sediments are structured and it appears that they are structurally bonded.

- Structural bonding and its magnitude is moisture sensitive.

- Bonding agents include silica acid gel, sulfate and carbonate precipitates, and iron oxides.

- At low water contents, the behavior of these sediments is purely non-frictional and non-granular similar to cemented materials such as concrete.

- As the water content increases and the state of these sediments changes from air-dried towards water-saturated, the following phenomenological changes occur simultaneously:

  ⇒ The magnitude of matric suction decreases.

  ⇒ The nature of these materials transforms from a non-frictional cemented material to a granular frictional material.

  ⇒ De-structuring and crack formation occurs.

  ⇒ Water-soluble precipitates, present in the bonded soil structure, dissolve.

  ⇒ At low values of confining stresses, significant swelling occurs; but at higher values of confining stresses, major collapse occurs.

As can be concluded from the above mentioned observations, several fundamentally different physical and chemical phenomenon occur simultaneously upon change in soil water content. Based on the above mentioned observations, it was necessary to carry out some experiments to separate the simultaneous physical and chemical phenomenon and address the following issues:

- role of soil suction in changes of soil structure,
- phenomenon involved in de-structuring and also transformation of soil from a purely non-granular and non-frictional material to a frictional granular material, and
- significant swelling observed in spite of absence of significant amount of active clay minerals.

As part of this study, some laboratory testing was carried out to determine and separate the simultaneous physical and chemical processes involved in the soil structure changes observed.

In this chapter, some of the previous studies involving soil structure, physical and chemical processes involved in the soil structure, and unsaturated soils are reviewed and results from this study are presented and discussed.

8.2. Literature Review

8.2.1 Soil Structure

Mitchell (1993) discussed the structure of soils and defined the structure of a soil as a composition of its fabric and inter-particle force system. He also defines fabric as "the arrangement of particles, particle groups, and pore spaces in a soil". Figure 8.2.1-A, adopted from Mitchell (1993) summarizes the factors and processes controlling soil structure. This inter-particle force system is the result of factors such as soil composition, history, present state, and environment. In structured soils, the present state is generally different from the initial state because of chemical and physical processes, which have altered the state and have caused changes in the fabric and inter-particle force system.

These processes can be both physical and chemical and can influence the structure of both cohesive and cohesionless soils.

Many studies have been carried out to investigate the physical processes that influence soil structure. According to Mitchell (1993), consolidation, especially under pressure, causes structural improvement, which increases the strength of the soil by decreasing the porosity and forming stronger inter-particle contacts. Confining pressure, especially as a function of time, is considered to induce structural improvements to soil as mentioned by Afifi and Richart (1973), Lee (1977), Anderson and Stokoe (1978), Dusseault and Morgenstern (1979), and Mesri et al. (1990). Schmertmann (1991) and Mesri et al. (1990) reported that structural improvements could occur because of particle rearrangements. Structural improvements are also considered to cause an increase in horizontal stresses by Whitman et al. (1964) and Schmertmann (1987 and 1991). Based on a comparison of undisturbed and reconstituted specimens, an increase in the cyclic strength of the soils as a result of over-consolidation was reported by Ishihara et al. (1978). They also mentioned that the degree of improvement is a function of fines content. Temperature can also influence physical processes that can change the soil structure. According to Mitchell (1993), changes in structure as a result of pressure increase occur faster at high temperatures than at low temperatures. As can be seen in Figure 8.2.1-A, wetting and drying, as well as freezing and thawing, can lead to structural changes in soil through physical processes. Wetting leads to elimination of mechanical forces in the form of capillary tension. Mitchell (1993) said that cycles of wetting and drying or freezing and thawing can change the particle assemblages. Drying can cause shrinkage, which leads to structural collapse and tension cracks in some soils. Mitchell (1993) said that drying can transfer clay particles to the contact points of adjacent silt and sand particles. Concentration of clay particles at contact points of silt and sand grains can cause structural improvements. According to Mitchell (1993), shearing and unloading are among the physical processes that can change soil structure. Shearing can cause structural collapse in homogeneous isotropic normally consolidated soils or formation of shear bands and structural changes in the vicinity of the shear bands in over-consolidated soils. Mitchell (1993) said that seepage could cause erosion through particle movements and consolidation as the result of seepage forces. Physical weathering can be in the form of mechanical disintegration resulting in reduction of particle size. Fanning et al. (1989) reported cases of the formation of clay minerals like illitic clays correspond quantitatively to mechanical disintegration of mica minerals in the sand and silt grain sizes.

Athabasca oil sands, which are also referred to as locked sands, are considered to be the extreme case of physical structure determining processes. According to Mossop (1980), Athabasca oil sands are composed of 95% quartz, 2% feldspar, and 3% mica flakes and clay minerals (predominantly illite and kaolinite). Dusseault and Morgenstern (1979) said that the enhanced stiffness and strength of these deposits is purely due to their physical interlocked fabric and they do not have a cemented structure. However, Dusseault and Morgenstern (1979) acknowledged the possibility of involvement of dissolution and re-deposition of silica in formation of the deformed interlocked shape of the particles.

Chemical processes, as summarized in Figure 8.2.1-A, are also involved in processes that change and influence the structure of soils. According to Mitchell (1993), diffusional processes and chemical reactions are time, temperature, and pressure dependent. According to Mitchell (1993), seepage can remove or introduce chemicals, colloids, and microorganisms. Cementation and aggregation can occur as the result of precipitation of materials onto particle surfaces or at particle contacts. Several researchers including Dupas and Pecker (1979), Clough et al. (1981), Rad (1982 and 1984), Rad and Tumay (1986), Acar and El-Tahir (1986), and Acar (1987) considered cementation or some kind of welding at the particle contacts as a source of structural improvements in soil. Seed (1979) stated that improvement in the cyclic resistance of sand can be due to cementation or welding at particle contact points. Many other studies including Denisov and Reltov (1961), Henderson et al. (1970), Miura and Yamanouchi (1973 and 1978), Lee (1977), Dusseault and Morgenstern (1979), Mitchell and Solymar (1984), and Mitchell (1986) not only considered cementation as the source of structural improvements but also speculated that cementation in some soils was due to mechanisms involving the dissolution and re-precipitation of amorphous or quartz silica and formation of silica acid gel on particle surfaces. According to Mitchell (1993) and Fanning et al. (1989), chemical weathering and mineralogical transformations are processes that can change the soil structure. For example, chemical weathering can cause mineral transformation of a potassium (K) bearing mica like biotite to an expansible 2:1 mineral like Vermiculite by replacement of potassium (K) with hydrated cations or water (H_2O). Structural changes due to chemical processes involving inter-particle forces can happen in the soil environment as the result of changes in the pore fluid chemistry. Hight et al. (1994) also mentioned that clay content, mineralogy of clay, and chemistry of pore fluid can influence the structure of the soil.

Marine sediments known as Norwegian and Eastern Canadian sensitive clays, several glacial sediments in the New York state and southern Ontario, and glaciolacustrine sediments in the southern and northern interior of British Columbia are all reported to be structured and sensitive. A reasonable percentages of mica and chlorite in the composition of these sediments are interesting features, as reported by Karlsrud et al. (1984), Boone and Lutenegger (1997), Geertsema and Schwab (1997), Quigley (1976 and 1980), and this study.

As mentioned earlier, mica minerals are involved in many physical and chemical structural determining processes such as mechanical disintegration resulting in reduction of particle size, mineral transformation of a mica to an expansible 2:1 mineral. Mica minerals can be partially responsible for some behaviors of structured soils such as high compressibility, formation of slippage surfaces, and high elastic swelling.

Gilboy (1927) studied the elastic compression and swelling of sand-mica mixtures with different percentages of mica content. Gilboy (1927) found that presence of flaky shaped particles could transform a sand from a dense low compressible material to a loose soil that can even be more compressible than the most active clays. According to Gilboy (1927), coarse mixtures made with an appropriate content of mica had swelling capacities identical with those of highly active, water saturated clays. Gilboy (1927) said the initial void ratio, the compressibility, and the elastic swelling of cohesionless granular soils increases as the percentage of the flaky mica particles increases. He concluded that the percentage of flaky shaped particles in soils has a significant effect on soil properties and behavior.

Terzaghi (1931) studied the swelling of two phase soil systems. A two phase system was defined as a solid-water system with water contents above the air entry value. Terzaghi (1931) said every two phase system, which is capable of swelling, contains a solid phase, which is under a pressure equal to the tension in the liquid phase. Terzaghi (1931) stated that the presence of this pressure is the essential condition for swelling. Terzaghi (1931) said water penetrates into a soil because of a difference in hydrostatic pressure in the external and internal water, and physicochemical activity is possible only after water has entered the system due to mechanical causes. Terzaghi (1931) commented that part of the water entering a swelling system forms an adsorption compound with the solid phase and its physical properties changes. Commenting on the characteristics of the elastic swelling of the saturated Norwegian quick clays, Terzaghi (1931) said their maximum amount of flaky mineral constituents (chlorite, talc, muscovite, and biotite) is consistent with the amount of mica content of a dry sand-mica mixture with similar elastic swelling characteristics. Terzaghi (1931) concluded that the swelling capacity of fine disperse two phase systems is dependent on the elastic properties of the solid phase and the physicochemical reactions between the solid and the liquid phase in the water-solid interface can only be a minor role. Terzaghi (1931) claimed that cohesion observed for a two phase soil system is in fact an apparent cohesion due to capillary pressure. While soil systems under study had water contents between saturation and air entry value, Terzaghi (1931) repeatedly referred to the significance of meniscus water, interstitial water, and capillary tensions in the elastic swelling. Terzaghi (1931) said that the surface tension of water could influence only the exterior surface of a two phase system. Using this argument and considering a two phase system as a special case of three phase system and without any experimental or analytical evidence, Terzaghi (1931) extrapolated the extent of his opinions about the characteristics of the elastic swelling of the two phase systems to three phase systems.

Figure 8.2.1-B, adopted from Mitchell (1993) based on studies by Gilboy (1927) and Terzaghi (1931), shows the relationship between swelling index (C_s) and mica content for coarse-grained mixtures. According to Mitchell (1993), the sheets of mica particles are held together by moderate strength electrostatic bonds, provided by potassium ions in between the sheets. Mitchell (1993) added that these in-between layer potassium bonds are weaker than the bonds within the layers. Mitchell (1993) concluded that both high compressibility and large elastic swelling of sand and silts containing mica minerals are due to the thin plate morphology of mica flakes.

The electrochemical state of the solid-aqueous interface can influence the de-structuring and to some extent the swelling of some soils. Lamb (1956) said that the repulsive forces between two colloid particles increase as the dielectric constant of the aqueous phase increases. Lamb (1956) carried out an observational test to study the flocculation of kaolinite using benzene, alcohol, and water as the pore fluid. Among these three pore fluids, benzene and water have the lowest and the highest dielectric constant, respectively. It was found that the degree and rate of flocculation increase as the dielectric constant of the pore fluid decreases. Chanturiya et al. (1996) also showed that electrochemical polarization of the solid/aqueous phases influences the surface tension in fluid meniscus and separation of air bubbles from the solid's surface.

McKyes et al. (1974) said that amorphous material such as iron oxides, aluminum oxides, and silicates can coat the particle surfaces and make soils cemented and sensitive. Among these, special attention is paid to silica surfaces in the following paragraphs. Formation of amorphous cementing agents such as silica and aluminia from crystalline minerals in soils has been recognized in many studies by soil scientists including the studies by Hashimoto and Jackson (1960) and Dudas and Harward (1971). These studies also showed that these amorphous materials can be removed from soil structure by using NaOH solution. Different forms of silica surfaces have different physical and chemical properties. The colloidal interactions, adhesion, and friction of silica surfaces are more complex than those for chemically inert surfaces.

Vigil et al. (1994) studied interactions of silica surfaces. Results of the study by Vigil et al. (1994) indicate significant structural and chemical changes at the solid-liquid and solid-solid interfaces during silica surface interactions. Such interactions can have major influences on the soil structure and chemical structure determining processes. Figure 8.2.1-C, adopted from Vigil et al. (1994), shows the three main chemical groups of the silica surface, which can be reversibly interchanged by addition or removal of water and protons. Silica in soils can exist in crystalline form such as crystalline quartz or amorphous form such as fused silica. The silica surface is in hydrophobic or hydrophilic state if the surface chemical groups are mainly siloxane (i.e., Si-O-Si) or silanol (Si-OH) groups, respectively. The states of silica surface can change from hydrophobic to hydrophilic and vice versa. Transformation of hydrophobic silica to hydrophilic silica occurs by hydroxylation; and the reverse reaction occurs by de-hydroxylation. Hydrophobic-hydrophilic transformations can also occur by silanation reactions or by etching in acids or bases. Vigil et al. (1994) said hydroxylation of silica groups at a silica-vapor surface or silica-water interface produces short protruding hairs of silica gel composed of polymeric chains of $-Si(OH)_2-O-Si(OH)_2-OH$, which can turn to "short protruding silica acid gel hairs" upon loosing one or more protons. Vigil et al. (1994) said silica particles could chemically bond (sinter) to each other. Also, silica cracks can re-heal with time; but under different conditions, the cracks can swell and grow.

Commenting on the colloidal interactions, Vigil et al. (1994) mentioned that it has been said "in contrast to the surface chemistry of silica, the colloidal interactions of silica surfaces are generally considered in terms of the attractive van der Waals and repulsive double layer force (the DLVO theory) together with an additional short-range monotonic repulsion that is generally stated to be due to a layer of structured water residing at the silica-water interface." This repulsive force is also called structural or hydration force.

Among interactions of silica surfaces, Vigil et al. (1994) also studied the swelling of silica surfaces. It was found that hydrophilic silica surfaces, exposed to humid air, swell approximately 10 A° to 20 A°; and they remain swollen even after being fully immersed in water or aqueous electrolyte solutions. Vigil et al. (1994) presented evidence that shows such phenomena are not due to an exponentially decaying repulsive force and hydration effects. Vigil et al. (1994) showed that the force holding two swollen silica surfaces together after remaining in water saturated air was larger than that from condensed water meniscus capillary force. Vigil et al. (1994) said that both swelling and enhanced adhesion can be explained by some slow chemical reaction which is taking place across the water film. Using Figure 8.2.1-D and E, adopted from Vigil et al. (1994), this process was described by them as follows:

"When water adsorbs on a hydrophilic silica surface, a 10 to 20 A° thick silica gel layer of silanol and silicilic acid groups grows on that surface. This would also be consistent with the ease of formation of silica gels in water. The swelling would be enhanced by the electrostatic repulsion between the negatively charged acidic groups on hairs and surfaces, and the resulting gel-layer would thus resemble a very short polymer or polyelectrolyte brush (or polymer stub). The short-range (20 to 40 A°) stabilizing repulsion between two such surfaces in humid air or immersed in water would then be due to the "steric" repulsion between these protruding groups as they overlap, rather than to any water-structuring effect. Further, when allowed to remain in contact for longer times, some of the protruding groups from opposite surfaces would be expected to react chemically and combine, ultimately growing (sintering) into one continuous network. Such sintering processes would account for the swelling and the enhanced adhesion".

Vigil et al. (1994) continued "no swelling or high adhesion was observed for the hydrophobic silica surfaces exposed to water vapor, suggesting that the predominantly unchanged hydrophobic siloxane groups on these surfaces do not swell or react, as expected. However, a small time dependent increase in the adhesion energy was noted, which suggests that some sintering could be taking place even in the absence of water."

Vigil et al. (1994) added that the water adjacent to the silica surfaces and present within the surface gel layer is found to be normal without any structural or hydrated characteristics beyond the water molecules directly bound to the silica groups. This finding is not in support of presence of repulsive forces due to hydration effects. Vigil et al. (1994) also commented that the high adhesion forces are not entirely due to formation of silica bonds; but there is significant contribution from capillary forces.

The behavior of a cohesive or cemented soil may be similar to the non-granular non-frictional bonded behavior of cement based materials such as concrete. The strength envelope of concrete under combined bi-axial and triaxial stresses were studied by several researcher including Newman and Newman (1972), Tasuji et al. (1978), Richart et al. (1928), Lew and Reichard (1978), and MacGregor (1992). Figure 8.2.1-F, adopted from Tasuji et al. (1978), shows the strength envelope of concrete under bi-axial stress state, normalized by uniaxial compressive strength. Unlike the egg-shaped strength envelope of natural soils, the strength envelope is relatively square shaped in the compression-compression zone. Figure 8.2.1-G, adopted from MacGregor (1992), shows the results of triaxial compression tests on concrete. MacGregor (1992) suggested the following relationship for the axial stress of concrete under triaxial stress state at failure:

$$\sigma_{1f} = f_c' + \alpha\sigma_3 \qquad \text{(Equation 8.2.1)}$$

in which, α is an empirical constant depending on different kind of concrete.

8.2.2 Soils at the Unsaturated State

Structured soils may also be unsaturated. As shown in Figure 8.2.2-A, adopted from Fredlund and Rahardjo (1993), soil mechanics can be categorized into saturated and unsaturated soil mechanics. Fredlund and Rahardjo (1993) said that the terms "saturated soil mechanics" and "unsaturated soil mechanics" is used to distinguish the zones that positive and negative pore water pressures exit, respectively. A change in the degree of saturation is considered to be responsible for expansion of swelling clays and collapse of loose silty soils.

Fredlund and Rahardjo (1993) considered an unsaturated soil as a four phase system. According to Fredlund and Rahardjo (1993), a portion of a mixture is considered as an independent phase if it has differing properties from the contiguous materials and definite bounding surfaces. The phases of an unsaturated soil are solid, water, air, and air-water interface or contractile skin. Air and water mixtures can be im-miscible or miscible. In an im-miscible mixture, there is no interaction between air and water. It is a mixture of free water and air, separated by the contractile skin. The miscible mixture of air and water can be in the form of dissolved air in water or water vapor in the air.

Surface tension is the distinct property of the contractile skin of the meniscus water Existence of surface tension is due to pressure differences in air-water interface (i.e., suction induced by air and water pressure differences (u_a-u_w)). Also, the existence of capillary phenomenon and capillary height in an unsaturated soil is due to the surface tension induced by contractile skin. In unsaturated soil mechanics, soil suction has been used by many researchers including Fredlund and Morgenstern (1977) as one of the stress variables to represent mechanical influences of surface tension and capillary phenomenon in soil behavior. Surface tension, which is the distinct property of the contractile skin meniscus water, is nothing but one of the physical structure determining process. As a result, the influence of surface tension and consequently capillary pressure, suction, and negative pore pressure on soil behavior can be considered as a special case of structural influences on the behavior of structured soils.

Total suction is a function of relative humidity and consists of matric and osmotic suction. According to Fredlund and Rahardjo (1993), Aitchison (1965) defined total, matric, and osmotic suctions as follows:

"Matric or capillary component of free energy- In suction terms, it is the equivalent suction derived from the measurement of the partial pressure of the water vapor in equilibrium with the soil water, relative to the partial pressure of the water vapor in equilibrium with a solution identical in composition with the soil water."

"Osmotic (or solute) component of free energy- In suction terms, it is the equivalent suction derived from the measurement of the partial pressure of the water vapor in equilibrium with free pure water."

"Total suction or free energy of the soil water - In suction terms, it is the equivalent suction derived from the measurement of the partial pressure of the water vapor in equilibrium with a solution identical in composition with the soil water, relative to partial pressure of water vapor in equilibrium with free pure water."

The relationship between total, matric, and osmotic suction can be formulated as follows:

$$\psi = (u_a - u_w) + \pi \qquad \text{Equation (8.2.2-A)}$$

in which:
ψ = total suction,
$(u_a - u_w)$ = matric suction,
u_a = pore air pressure,
u_w = pore water pressure,
π = osmotic suction.

According to Fredlund and Rahardjo (1993), the capillary phenomena is associated with matric suction. Maximum capillary height for air-water system ($h_{c(a-w)}$) can be calculated from the following equation:

$$h_{c(a-w)} = \frac{2T_{S(a-w)} \cos \alpha_w}{\rho_w g r} \qquad \text{(Equation 8.2.2-B)}$$

in which:
$T_{S(a-w)}$ = surface tension of air-water interface,
r = pore radius,
α_w = contact angle of water,

ρ_w = density of water,

g = gravitational acceleration.

Similarly, The maximum capillary height for Kerosene-water ($h_{c(K\text{-}w)}$) and air-Kerosene ($h_{c(a\text{-}K)}$) systems, can be written, respectively, as follows:

$$h_{c(K-w)} = \frac{2T_{S(K-w)}\cos\alpha_w}{\rho_w g r} \qquad \text{(Equation 8.2.2-C)}$$

$$h_{c(a-K)} = \frac{2T_{S(a-K)}\cos\alpha_K}{\rho_K g r} \qquad \text{(Equation 8.2.2-D)}$$

in which:

$T_{S(K\text{-}w)}$ = surface tension of Kerosene-water interface,

$T_{S(a\text{-}K)}$ = surface tension of air-Kerosene interface,

α_K = contact angle of Kerosene,

ρ_K = density of Kerosene.

Lamb (1956) carried out capillary tests using water, oil, and air. The following conclusions were drawn for $h_{c(a\text{-}w)}$, $h_{c(o\text{-}w)}$, and $h_{c(a\text{-}o)}$:

$$\frac{h_{c(a-w)}}{h_{c(a-o)}} \approx 2 \qquad \text{(Equation 8.2.2-E)}$$

$$h_{c(a-w)} \approx h_{c(a-o)} + h_{c(o-w)} \qquad \text{(Equation 8.2.2-F)}$$

Using Equation 8.2.2-B, the capillary pressure for air-water interface ($u_{c(a\text{-}w)}$) can be written as follows:

$$u_{c(a-w)} = (u_a - u_w) = \frac{2T_{S(a-w)}\cos\alpha_w}{r} \qquad \text{(Equation 8.2.2-G)}$$

Fredlund and Rahardjo (1993) added that the capillary height and the radius of the curvature of the water surface (r/cos α) are directly related to the soil–water characteristic curve. Fredlund and Rahardjo (1993) also commented about the limitations that the use capillary phenomena has in describing the mechanical behavior of soils at the unsaturated state. Fredlund and Rahardjo (1993) acknowledged the existence of other parameters in soil structure that can significantly increase the magnitude of negative pore water pressure in soils. The adsorptive forces between clay particles was mentioned as an example of such parameters.

In saturated soil mechanics, the behavior of a soil can be expressed in terms of the total stress, σ, and the pore water pressure, u_w. The behavior of saturated soils, which are composed of two phases, can be described using effective stress (σ-u_w) as the stress state variable. The equilibrium of soil structure and contractile skin in unsaturated soils cannot be expressed entirely by the effective stress as the stress state variable. In unsaturated soil mechanics, the behavior of a soil is expressed in terms of the total stress, σ, the pore water pressure, u_w, and the pore air pressure, u_a. Fredlund and Rahardjo (1993) said that (σ-u_a) and matric suction (u_a-u_w) are the suitable stress state variables for unsaturated soils that control the equilibrium of soil structure and contractile skin.

The shear strength is one of the main mechanical characteristics of a soil. Mohr-Coulomb failure criteria can be used to express the shear strength of a saturated or an unsaturated soil. The shear strength of a saturated soil can be expressed in terms of effective stress parameters as follows:

$$\tau_{ff} = c' + (\sigma_f - u_w)_f \tan\phi' \qquad \text{(Equation 8.2.2-H)}$$

in which:

τ_{ff} = shear stress on the failure plane at failure,

c' = effective cohesion,

$(\sigma_f - u_w)_f = \sigma'_f$ = effective normal stress on the failure plane at failure,

ϕ' = effective angle of internal friction.

In an attempt to determine the shear strength of soils at unsaturated state, Bishop (1959) proposed the following relationship for the effective stress in an unsaturated state:

$$\sigma'_f = (\sigma - u_a) + \chi(u_a - u_w) \qquad \text{(Equation 8.2.2-I)}$$

in which:

u_a = pore air pressure,

u_w = pore water pressure, and

χ = a parameter with values between 0 and 1, depending on soil type and degree of saturation.

According to Fredlund and Rahardjo (1993), stress variables (σ-u_a) and (u_a-u_w) can be used to express the shear strength of an unsaturated soil as follows:

$$\tau_{ff} = c' + (\sigma_f - u_a)_f \tan\phi' + (u_a - u_w)_f \tan\phi^b \qquad \text{(Equation 8.2.2-J)}$$

in which:

τ_{ff} = shear stress on the failure plane at failure,

c' = effective cohesion,

$(\sigma_f - u_a)_f$ = net normal stress state on the failure plane at failure,

ϕ' = angle of internal friction associated with the net normal stress state variable, $(\sigma_f$-$u_a)_f$,

$(u_a - u_w)_f$ = matric suction on the failure plane at failure, and

ϕ^b = angle indicating the rate of increase in shear strength relative to matric suction, $(u_a - u_w)_f$.

Oberg and Sallfors (1995) said that for many silts and sands and for practical engineering purposes, the enhanced shear strength of soils at an unsaturated state is a function of the degree of saturation (S_r). Based on this speculation and using soil – water characteristic curve, Oberg and Sallfors (1995) proposed the following equation for the shear strength of such soils at the unsaturated state:

$$\tau_{ff} = c' + (\sigma_f - u_a)_f \tan\phi' + (u_a - u_w)_f S_r \tan\phi' \qquad \text{(Equation 8.2.2-K)}$$

Resembling the effective stress phenomena for saturated soils, Oberg (1997) proposed the concept of effective matric suction and the following equation for effective stress of soils at an unsaturated state:

$$\sigma' = \sigma - u_{eff} \qquad \text{(Equation 8.2.2-L)}$$

in which:

$$u_{eff} = (u_a - u_w)S_r, \text{ if } u_a = u_{atm}, \text{ or} \qquad \text{(Equation 8.2.2-M)}$$

$$u_{eff} = u_a(1 - S_r) + u_w S_r, \text{ if } u_a \neq u_{atm}. \qquad \text{(Equation 8.2.2-O)}$$

Vanapalli et al. (1996) also proposed a similar equation for the shear strength of soils at an unsaturated state as follows:

$$\tau_{ff} = c' + (\sigma_f - u_a)_f \tan\phi' + (u_a - u_w)_f \left[(\tan\phi') \left(\frac{S_r - S_{residual}}{100 - S_{residual}} \right) \right] \qquad \text{(Equation 8.2.2-P)}$$

in which $S_{residual}$ is the residual degree of saturation in percent.

Many attempts have been made to describe the state of an unsaturated soil using the concepts of the critical state soil mechanics. The strength envelope of a saturated soil can be expressed as follow:

$$q = M p' \qquad \text{(Equation 8.2.2-Q)}$$

in which:

$q = \sigma'_1 - \sigma'_3$,

$p' = \dfrac{\sigma'_1 + \sigma'_2 + \sigma'_3}{3}$, and

M is the strength parameter at the critical state in the saturated conditions.

Different relationships have been proposed for unsaturated soils by several researchers including Fredlund et al. (1978), Escario and Saez (1986), Toll (1990), Wheeler and Sivakumar (1993), Maatouk et al. (1995). Conceptually, all these relationships try to introduce strength parameters at the critical state in unsaturated condition, using net mean normal stress ($p-u_a$) and matric suction (u_a-u_w). While some researchers like Fredlund et al. (1978) stated that these two stress state variables are independent, others like Maatouk et al. (1995) stated that they might be dependent.

Fredlund et al. (1978) said that the relationship between τ and ($\sigma-u_a$) are linear and contours of matric suction (u_a-u_w) in τ-($\sigma-u_a$) space are parallel. Fredlund et al. (1978) also assumed a constant value for ϕ^b. Fredlund et al. (1978) stated that the net mean normal stress ($p-u_a$) and matric suction (u_a-u_w) are independent variables and proposed the following relationship for the strength envelope of unsaturated soils:

$$q = M(p - u_a) + M_b(u_a - u_w) \qquad \text{(Equation 8.2.2-R)}$$

in which M_b is assumed to be independent from the net mean normal stress ($p-u_a$).

Escario and Saez (1986) carried out direct shear tests using unsaturated specimens of Madrid grey clay, Guadalix de la sierra red clay, and Madrid clayey sand. Results indicated linear relationships between τ and ($\sigma-u_a$); but contours of matric suction (u_a-u_w)

in τ-(σ-u_a) space diverged as (σ-u_a) increased. Results also showed a non-linear relationship between τ and (u_a-u_w) (i.e., variable ϕ^b value).

Toll (1990) proposed a framework for unsaturated soil behavior. Toll (1990) said both stress variables, (p-u_a) and (u_a-u_w), were function of degree of saturation. He proposed the following equation for the strength envelope of unsaturated soils:

$$q = M_a(p-u_a) + M_w(u_a-u_w) \qquad \text{(Equation 8.2.2-S)}$$

in which:

M_a = total stress ratio at the critical state, and

M_w = suction ratio at the critical state.

Toll (1990) concluded that the critical state can be characterized using five state variables which are: net mean normal stress (p-u_a), matric suction (u_a-u_w), deviator stress (q), specific volume (v) or void ratio (e), and degree of saturation (S_r). Toll (1990) also concluded that for an unsaturated soil, the void ratio at the critical state is not unique because shearing would not entirely destroy the initial fabric.

Alonso et al. (1990) presented a constitutive model for soils at the unsaturated state using net mean normal stress (p-u_a), deviator stress (q), void ratio (e), and suction (s). Details of the numerical model are beyond the scope of this study but some key elements of the model are relevant to the current study. Alonso et al. (1990) said that the volumetric response of partially saturated soil depends not only on the initial and final stress and suction values but also on the stress path. The proposed constitutive model is based on state boundary surfaces in q-p-s space as shown in Figure 8.2.2-B. In this model and as can be seen in Figure 8.2.2-B(b), the state boundary surface of soils at the unsaturated state expands as suction increases. An interesting feature of the model is the introduction of the critical state line (CSL) for the condition of non-zero suction. The critical state line (CSL) for unsaturated state has been introduced by modeling the influence of suction as an intercept with deviator stress (q) axis. It was assumed that M, the slope of the critical state line (CSL), is independent of the unsaturated state and suction. In this model the magnitude of the intercept of the CSL with deviator stress (q) axis increases as suction increases.

Wheeler and Sivakumar (1993) carried out triaxial testing using unsaturated reconstituted specimens of speswhite kaolin. They proposed that the behavior of soils at unsaturated state is a function of five state variables, which are: net mean normal stress ($p-u_a$), matric suction (u_a-u_w), deviator stress (q), specific volume (v) or void ratio (e), and degree of saturation (S_r) or water content (w). Contours of normal compression line (NCL) in specific volume (v) – net mean normal stress ($p' = p-u_a$) space are presented in Figure 8.2.2-C(a) for various values of suction. Contours of critical state line (CSL) in specific volume (v) – net mean normal stress ($p' = p-u_a$) and deviator stress (q) net mean normal stress ($p' = p-u_a$) spaces are presented in Figure 8.2.2-C(b) and (c), respectively, for various values of suction. Investigating the experimental results presented by Wheeler and Sivakumar (1993) can make an important observation. It can be seen that the normal compression line (NCL) and the critical state line (CSL) are not the same for saturated specimens and specimens under zero suction condition. According to Wheeler and Sivakumar (1993), these experimental results are an indicator of a heterogeneous soil structure and retained soil structure even after shearing for unsaturated soil. It can also be speculated that the elimination of suction does not necessarily transfer the soil to a saturated state. Results presented in Figure 8.2.2-C(b) show that contours of the critical state line (CSL) in specific volume (v) – net mean normal stress ($p' = p-u_a$) space for various suction values converge at high values of net mean normal stress ($p' = p-u_a$). Using results presented in Figure 8.2.2-C(c), Wheeler and Sivalumar (1993) concluded that the projections of the critical state line (CSL) for different values of suction in q-($p-u_a$) space are parallel straight lines. Based on test results presented in Figure 8.2.2-C(c), Wheeler and Sivakumar (1993) proposed the following equation for the strength envelope:

$$q = Mp' + \mu(s) \qquad \text{(Equation 8.2.2-T)}$$

in which μ(s) is the intercept of the critical state line (CSL) at a given suction value with the deviator stress (q) axis. The slope of the critical state line, M, is assumed to be independent of suction. Later, Wheeler and Sivakumar (1995) suggested that both the slope of the critical state line (CSL), M, and its intercept with the deviator stress (q) axis, μ, are function of the soil suction and proposed the following equation for the strength envelope of soils at unsaturated state:

$$q = M(s)(p - u_a) + \mu(s) \qquad \text{(Equation 8.2.2-U)}$$

Maatouk et al. (1995) carried out an experimental program to extend the concepts of yielding and critical state to unsaturated state. Reconstituted specimens of collapsible silty soil from the Trois-Rivieres in Quebec, which has low plasticity and low activity, was used. Contours of the critical state line (CSL) in e-(p-u_a) and q-(p-u_a) spaces are shown in Figure 8.2.2-D(a) and (b), respectively, for various suction values. As can be seen in Figure 8.2.2-D(a), contours of the critical state line (CSL) in e-(p-u_a) space are straight lines and converge. Results indicate that the size of the yield surface increases as the magnitude of suction increases. Maatouk et al. (1995) said that the shape of the yield surfaces for various suction values are similar to those reported for natural clays with high friction angles. As shown in Figure 8.2.2-D(b), contours of the critical state line in q-(p-u_a) space for various suction values are straight lines; but in contrast with results presented by Wheeler and Sivakumar (1993), they converge. Maatouk et al. (1995) proposed the following equation for the strength envelope of the material tested at an unsaturated state:

$$q = C^{*} + M^{*}(p - u_a) \qquad \text{(Equation 8.2.2-V)}$$

in which:

C^{*} is strength parameter at unsaturated state, and

M^{*} is strength parameter at the critical state in unsaturated state.

Cui and Delage (1996) carried out triaxial tests using reconstituted specimens of compacted Jossigny silt at unsaturated state. Figure 8.2.2-E shows contours of the yield surfaces for compacted Jossigny silt with different magnitudes of suction. As can be seen, the yield surface expands as the magnitude of the suction increases. Cui and Delage (1996) said that the elliptical inclined shape of the yield surfaces at various values of suction is similar to the general shape of yield surfaces reported for natural soils (i.e., structured soils).

Commenting on the application of the critical state soil mechanics for unsaturated state of soils, Leroueil (1997) said:

> "The concepts of limit and critical states apply well to unsaturated soils. It has been shown, in particular, that the limit state curve increases in size when the matric suction increases. It must be recognized, however, that a tremendous research effort is still needed to get a good understanding of these materials."

8.3 Experimental Program

8.3.1 Relevant Test Results Presented from the Previous Chapters

A soil-water characteristic curve was obtained for Penticton Silt. Results obtained indicate matric suction ranged from 100 to 300 kPa for typical in-situ gravitational water content values from 25% to 15%.

The mineralogy of these sediments was studied using X-ray diffraction analyses. Results of these analyses did not indicate the presence of crystalline salts; but some magnetite was detected. Results indicate that less than 3% of the total soil mass consists of active expandable clays. Muscovite minerals were found to be non-weathered and chlorite minerals are not expandable chlorite.

Fabric and composition of these sediments were studied using scanning electron microscopy (SEM) in conjunction with elemental dispersive x-ray analysis (EDXA).

Results indicate an anisotropic fabric with preferred horizontal orientation and abundance of platy particles. Results confirm that active expandable clays were not present in significant percentage. It was found that de-structuring and crack formation occur in the level of grain to grain. The grain surfaces do not appear to be clay coated. Open and flexible flaky structure of muscovite and chlorite particles was observed. Iron oxides and sulfate and carbonate precipitates of typical cations (especially Na^+, Mg^{++}, and Ca^{++}) are detected.

Soil and pore fluid chemical analyses were carried out. Results indicate these sediments are alkaline. Small values of cation exchange capacity (CEC) indicate presence of mica particles and absence of active expandable clays. Oxides of iron were detected. Soluble precipitates of sulfate and carbonate in ground water have concentrations larger than typical values for river water, which confirms the presence of such chemicals in the soil structure. Results also support the presence of significant amounts of silica acid gel in the soil structure.

One dimensional consolidation tests were carried out as part of this study. Some relevant test results for undisturbed and reconstituted specimens are presented in Figure 8.3.1-A and B, respectively.

An undisturbed specimen tested air-dried (B-OL-D) had a very stiff response; but an undisturbed specimen saturated with water (B-OL-W) showed a tendency for swelling (90kPa swelling pressure) and became highly compressible. Another undisturbed specimen (B-OL-K) was saturated with Kerosene, which is chemically inert. The behavior of this specimen was not similar to water saturated undisturbed specimen but similar to the air-dried undisturbed one. Two undisturbed air-dried specimens, C-OL-W and C-OL-K, were flooded at 500 kPa with water and Kerosene, respectively. While flooding with water caused collapse and increase of compressibility, flooding with Kerosene only caused elastic deformation and no change in compressibility.

Slurry specimens F-OL-W and F-OL-K, which were prepared using water and Kerosene, respectively, had a similar highly compressible behavior; but it was not the case for the corresponding air-dried slurry specimens. While the air-dried water slurry specimen (E-OL-D) was very stiff, similar to undisturbed air-dried specimen (B-OL-D), the air-dried Kerosene slurry specimen (F-OL-KD) was highly compressible and behaved similar to a specimen, which was prepared by static compaction of grind soil (F-OL-PW).

Triaxial tests were also carried out in this study. Some relevant test results are presented in Figure 8.3.1-C. The Kerosene saturated air-dried undisturbed specimen (UA-K-CAU372) was, by an order of magnitude, stronger than the water saturated air-dried undisturbed specimen (UA-W-CAU372(b)). The kerosene saturated specimen reached the condition of zero lateral stress long before failure which implies a non-frictional purely bonded behavior similar to rock or cement based materials such as concrete.

8.3.2 Observational Experiments

A series of qualitative and quantitative observational tests were carried out to further study the soil structure of Penticton silt. Water can interact with cementing agents, precipitates, and minerals in soils and its introduction can change the physicochemical state of the soil structure. Also, the strength of some cementing agents can be a function of the water content. In order to study the physicochemical state and nature of the bonding in the soil structure, it was necessary to use a reference liquid that does not interact chemically with soil but its physical properties are close to those for water. Commercially available Kerosene was chosen as the reference liquid in this part of this study. The properties of Kerosene used in this experimental program were presented in Chapter Six, Table 6.3.1. These observational tests are explained briefly here:

- ***Observational Test One (OT-1):*** Two air-dried undisturbed specimens of Penticton silt were put in two beakers and consequently were flooded with distilled water and Kerosene, respectively, and remained flooded for 24 hours. For the specimen flooded with distilled water (Specimen OT-1-W), complete crack development and de-structuring occurred almost spontaneously; and the specimen collapsed and turned into a small pile of soil at the bottom of the beaker. In contrast, the specimen flooded with Kerosene (Specimen OT-1-K) remained intact. After 24 hours of submergence, further manual inspection of the specimen OT-1-K showed that specimen maintained its initial integrity and remained as stiff and strong as it was before flooding with Kerosene. Identical experience using undisturbed specimens at their in-situ water content (15% to 25%) produced virtually identical results, except that the rate of de-structuring was slower for the specimen at in-situ water content than the air-dried one.

- ***Observational Test Two (OT-2):*** This test (OT-2) was similar to OT-1 with a slight difference in method of liquid introduction to the specimens. Two air-dried undisturbed specimens of Penticton silt were put on two glass plates. Consequently, distilled water and Kerosene were introduced to the bottom of Specimen OT-2-W and OT-2-K, respectively. For the specimen exposed to distilled water (Specimen OT-2-W), water was mimicked by the specimen, cracks developed, and collapse occurred. After a few minutes, the specimen turned into a cone shaped pile of soil at the bottom of the glass plate. In contrast, Specimen OT-2-K mimicked Kerosene with a slower rate and became wet; but remained intact. After 24 hours of exposure, further manual inspection of the specimen OT-2-K showed that the specimen maintained its initial integrity and remained as stiff and strong as it was before exposure to Kerosene. Identical experience using specimens at their in-situ water content (15% to 25%) produced similar results, except the rate of de-structuring was slower for the specimen at in-situ water content than the air-dried one.

- ***Observational Test Three (OT-3):*** Two undisturbed specimens of the Penticton silt at their in-situ water content were trimmed and placed into oedometer rings. The thickness of the specimens was chosen to be not more than ¾ of the height of the rings. Under the state of zero vertical stress, distilled water and Kerosene were gradually introduced to Specimen OT-3-W and OT-3-K, respectively, through the base pore-stone and filter paper. The introduction of the liquids was done very slowly in order to prevent any possible heave. Photographs of Specimen OT-3-W and OT-3-K, approximately 18 hours after starting the experiment, are shown in Figure 8.3.2-A(a) and (b), respectively. For water saturated specimen (OT-3-W) crack formation, de-structuring, and swelling occurred. Specimen swelled approximately 40% by volume and overflowed the edge of the oedometer ring. In contrast, the Kerosene saturated specimen (OT-3-K) remained intact and further manual inspections indicate preservation of specimen's strength and stiffness.

- ***Observational Test Four (OT-4):*** Two slurry reconstituted specimens, OT-4-W and OT-4-K, were made using Penticton silt and distilled water and Kerosene, respectively. The liquid content of the specimens was chosen between liquid limit and 1.5 times liquid limit. The slurry specimens were cast directly in the oedometer rings; and subsequently, they were air-dried in a controlled environment of 23 °C ± 2 °C and 80% ± 5% relative humidity. Following completion of air-drying, the oedometers were removed and the specimens were examined manually. Manual inspection showed that the air-dried water slurry specimen, OT-4-W was similar to a bonded material, brick, or rock. It was very stiff and strong. In contrast, the air-dried Kerosene specimen had no cohesion, little stiffness, and no strength. The specimen crumbled to a pile of dry powder.

- ***Observational Test Five (OT-5):*** Six undisturbed specimens of Penticton silt were trimmed and placed into oedometer rings. The thickness of the specimens was chosen to be not more than 1/2 of the height of the rings. Under a state of zero vertical stress, distilled water, methanol (99.9%), ethanol (95%), buthanol, decanol, and Kerosene were gradually introduced to Specimen OT-5-W, OT-5-M, OT-5-E, OT-5-B, OT-5-D, and OT-5-K, respectively, through the base porous-stone and filter paper. The introduction of the liquids was done slowly in order to prevent any possible heave. The response and behavior of these specimens are presented in Table 8.3.2. In summary, it can be stated that the level of destructuring and swelling decreases as the chemical activity of pore fluid decreases.

- ***Observational Test Six (OT-6):*** Two slurry reconstituted specimens, OT-6-M and OT-6-E, were made using Penticton silt and methanol and ethanol as the saturating fluid, respectively. The liquid content of the specimens was chosen between the liquid limit and 1.5 times the liquid limit. Slurry specimens were cast directly in the oedometer rings; and subsequently, they were air-dried in a controlled environment of 23 °C ± 2 °C and 80% ± 5% relative humidity. Following completion of air-drying, the oedometers were removed and specimens were examined manually. Manual inspection showed that the air-dried methanol slurry specimen (OT-6-M) had a stronger soil structure and was stiffer and stronger than the air-dried ethanol slurry specimen (OT-6-E).

Combining observational tests 4 and 6, it can be stated that the magnitude of stiffness and strength of specimens decreases in the following order:

OT-4-W, OT-6-M, OT-6-E, and OT-4-K

- ***Observational Test Seven (OT-7):*** In this experiment, Observational Test One was repeated and extended to include some other structured soils, available in the Geotechnical Engineering Laboratory of the Department of Civil and Environmental Engineering of the University of Alberta. Undisturbed specimens of Penticton silt, Whitehorse silt, Morkill River silt, Norwegian Quick clay, and naturally bitumen free air-dried Athabasca locked sand were used. Results were similar to the results of Observational Test One, except for the specimen of bitumen free air-dried Athabasca locked sand. For all other soils tested, complete crack developments, de-structuring, and spontaneous collapse of the specimens flooded with distilled water occurred and the specimens flooded with Kerosene remained intact. For specimens of the bitumen free air-dried Athabasca locked sand and after 24 hours of submergence, both specimens appeared to remain intact; but upon a slight touch with a pencil, the sand specimen flooded with distilled water fell apart and collapsed. The Kerosene flooded specimen resisted manual disturbance but the level of resistance to any disturbance was not as strong as the other Kerosene flooded specimens. Upon abrasion with a sharp object, grains of sands could be separated from the surface.

- ***Observational Test Eight (OT-8):*** In this experiment, Observational Test Two was repeated and extended to include the same undisturbed soil specimens used in Observational Test Seven. Results were in complete agreement with Observational Test Two, except for specimens of the bitumen free air-dried Athabasca locked sand. Results for the sand was similar to the results of the Observational Test Seven.

- ***Observational Test Nine (OT-9):*** An attempt was made to carry out a series of scanning electron microscopy (SEM) using air-dried Kerosene slurry specimens of Penticton silt. This attempt failed because of intense charging that occurred even with accelerating voltages as low as 1.5 kV. Referring to the test results described in section 5.7 of Chapter 5, it should be mentioned that charging phenomena did not occur during the SEM analyses of air-dried water slurry Penticton silt specimens. In SEM, charging phenomena is a function of non-connectivity of the specimen. Due to the weak connection between the grains the gold coating could not provide adequate connection from grain to grain to achieve conductivity. This observational study implies that there was not bonding between the silt grains when using air-dried Kerosene slurry specimen.

- ***Observational Test Ten (OT-10):*** The bitumen free air-dried Athabasca locked sand flooded with water did not disintegrate spontaneously and the Kerosene flooded specimen did not behave like a fully bonded material. Maintaining its integrity in water upon saturation and the associated elimination of suction indicates a presence of structure; but a lack of resistance to abrasion in Kerosene implies that the source of structural bonding is not dominantly chemical. A series of scanning electron microscopy (SEM) analyses, carried out by Touhidi-Baghini (1998), are used to further investigate the soil structure of the bitumen free air-dried Athabasca locked sand. Figure 8.3.2-B shows the soil fabric of the Athabasca locked sand. As can be seen, the fabric appears to be clean and locked. Further magnification, shown in Figure 8.3.2-C, shows that there are some fine grain soils at the contact point of some sand grains. Figure 8.3.2-D shows fractured contact points which indicate that for the dry state of the bitumen free Athabasca locked sand, fine grain materials are gathered around the contact point of sand grains like a weld ring. Figure 8.3.2-E shows the texture of the fine grain materials at the contact points, which elemental dispersive x-ray analysis (EDXA) identified as kaolinite and mica.

8.4 Discussion

As mentioned in the introduction, several simultaneous physicochemical phenomenons can occur in a soil structure as the state of soil moisture changes. Using experimental results presented in section 8.3, some phenomenons are discussed in the following sections. An attempt is made to separate simultaneous physicochemical changes in the soil structure in order to have a better understanding of the behavior of Penticton silt and the nature of its soil structure.

In these discussions, referenced is made to surface tension and relative permittivity (dielectric constant) of pore fluids used in this study. These values were obtained from the Chemical Rubber Co. (CRC) publications and summarized in Table 8.4.

8.4.1 Role of Suction

Suction is generally modeled and represented by capillary tension. The behavior of the soil specimens upon saturation with Kerosene implies that soil suction does not play a major role in the behavior of Penticton silt. It appears that water sensitive soil structure plays a more significant role than soil suction.

Knowing that Kerosene and water are immiscible, one can argue that saturating a specimen of soil by Kerosene does not eliminate soil suction entirely because a meniscus interface will still exist following such a process. The answer to such argument can be divided in to the following discussions:

A series of observational studies similar to the Observational Test One but using oven-dried specimens, which do not have any free (non-structured) water, were carried out. Results were similar to results of OT-1 in spite of the absence of any free water capable of forming an air-water or Kerosene-water interface meniscus.

Based on such a theory and using Equation 8.2.2-B, C, D, E, F, and G and knowing that $T_{S(a\text{-}w)} = 72$ mN/m, $T_{S(K\text{-}W)} = 40$ mN/m, $T_{S(a\text{-}K)} = 26$ mN/m, $\alpha_w = 0$ °C, and $\alpha_K = 42$ °C, it is indisputable that a Kerosene saturated soil must be significantly more flexible and weaker than an air-dried soil ($h_{c(K\text{-}w)}$ is only 55% of $h_{c(a\text{-}w)}$). Its behavior should be closer to the behavior of a water saturated soil rather than the behavior of an air-dried soil. However, all experimental evidence, presented in section 8.3.1 and 8.3.2, indicate the opposite.

Methanol and ethanol are liquids that are miscible with water. Response of soil specimens submerged in these liquids did not show complete disintegration while it is apparent that no water-methanol/ethanol interface meniscus exists. The level of de-structuring of the Specimen OT-5-M and OT-5-E were significantly less than Specimen OT-5-W. This supports the idea that the elimination of the interface meniscus and consequently soil suction is not the fundamental source of soil de-structuring for Penticton silt.

The level of de-structuring of alcohol saturated specimens in Observational Test Five (OT-5) were significantly different while as can be seen in Table 8.4, the values of surface tension are close for these liquids. Again, this experiment confirms the fact that elimination of suction is not the main source of de-structuring for Penticton silt.

Air-dried slurry specimens in Observational Test Four (OT-4) behaved absolutely different, water slurry specimen was a highly bonded material similar to concrete, where as Kerosene slurry specimen was unbonded powdered soil. The contrast observed indicates that soil suction is not the main source of enhanced stiffness and strength of these sediments in the unsaturated state. One could argue that the difference in the behavior observed could be due to differences in soil fabric because of the use of different liquids in making the slurries. However, differences in soil fabric should lead to friction angle differences rather than an absolute contrast in the nature of the material, i.e. bonded and frictional. It should be mentioned that the air-dried Kerosene saturated specimen (UA-K-CAU372) reached the zero lateral effective stress state during undrained triaxial testing. This response supports the purely bonding nature of the soil specimen tested.

8.4.2 Nature of Bonding and Destructuring

The previous discussion indicates that the elimination of soil suction is not the main de-structuring mechanism for Penticton silt. It is apparent from the results of this study that the behavior of these sediments is not purely frictional. In order to discuss de-structuring for a material with some form of bonding, it is appropriate to first discuss the possible source and nature of the bonding.

A theory implying a structurally bonded soil system with crystalline salts cannot be supported by results of X-ray diffraction analyses, soil and pore fluid chemistry analyses, and scanning electron microscopy (SEM). No major crystalline salts were detected in X-ray diffraction analyses and scanning electron microscopy (SEM). Also, the concentration of cations and sulfate were not large enough to indicate any crystalline salt formation. Carbonate content was also less than 6%.

Iron oxides were amongst the detected bonding agents in the soil structure of Penticton silt. It can be argued that iron oxides are not the main source of bonding. The structurally bonded nature of these sediments alters and weakens upon exposure to distilled water (pH = 7); but iron oxides are only soluble in pH values below approximately 3. Hence, iron oxides can contribute to the bonded soil structure in Penticton silt; but they are not the main source of bonding.

Sulfate and carbonate precipitates of Na^+, Mg^{++}, and Ca^{++} were detected; but again, they cannot be the main source of bonding. First, the concentration of these precipitates is not significant enough to justify the enhanced stiff and strong behavior of these sediments. Second, these precipitates are not soluble in methanol and ethanol but specimens saturated with these alcohols, OT-5-M and OT-5-E, were de-structured. Third, while these precipitates are not soluble in methanol, ethanol, and Kerosene, the stiffness and strength of air-dried methanol, ethanol, and Kerosene slurry specimens were not the same. These arguments support the fact that sulfates and carbonates are not the main source of bonding in Penticton silt.

Silica acid gel was another potential bonding agent, investigated during soil and pore fluid chemical analyses. It is apparent that all other potential sources of bonding such as carbonates, which are generally referred to as the main sources of bonding by others, are not the key bonding element. Silica acid gel is an amorphous material and cannot be detected by X-ray diffraction analyses and scanning electron microscopy. Special attention to the results obtained in OT-5 and OT-6 helps to confirm the significance of the bonding due to the silica acid gel in the soil structure. Water and Kerosene belong to two completely different families of chemicals. The role of silica acid gel can be better understood by focussing on the test results for alcohol saturated specimens in OT-5. As can be seen in Table 8.4, the values of surface tension for these alcohols are very similar; and hence, capillary stress cannot be the main reason for the different level of de-structuring and behavior observed. Taking into account the variation of dielectric constant of these alcohols, one may assume that the difference in the de-structuring level could be due to the level of electrochemical forces in the soil structure. This argument should be rejected because electrochemical forces are small and cannot justify the magnitude of the swelling observed.

Close attention should be paid to the decreasing level of de-structuring with increasing size of the alcohol molecule. As the size of the alcohol molecule increases, the level of de-structuring decreases. As the size of the alcohol molecule increases, the number of $-OH^-$ arms per unit volume of voids in the soil structure decreases. This observation is in complete agreement with the results obtained in the study by Vigil et al. (1994). The results from this study on Penticton silt supports the theory indicating the importance of active silica surfaces as oppose to inert mineral particles. As was mentioned in section 8.2.1, the surface of silica minerals is not an inert surface. Taking into account the age of the soil particles and variety of physical and chemical processes that can convert an inert silica surface to an active one, it can be claimed that the majority of silica surfaces of soil minerals are active silica surfaces. Natural silica mineral surfaces are likely covered by "short protruding silica acid gel hairs", which as Vigil et al. (1994) stated, can interact with the aqueous phase in soils. At a given state of moisture, if the water content decreases, liquid is extracted from the soil structure and siloxane (Si-O-Si) groups can form between the "short protruding silica acid gel hairs" of the silica surfaces of two particles. Such process is shown in Figure 8.2.1-D(b). On the other hand, if the water content increases liquid is introduced to the soil structure and silanol (Si-OH) groups can form from the breakage of inter-particle bonds that are in the form of siloxane (Si-O-Si) groups of two "short protruding silica acid gel hairs" of the two adjacent silica surfaces of two particles. Upon this bond breakage, particles are free from each other and they can have stationary and non-stationary movements and rotations. The macroscopic outcome of these movements will appear in the form of crack formations, de-structuring, and swelling. Swelling will be discussed in detail in the following section.

Without any experimental measurements, it is a common practice to extend the soil-water characteristic curve to about 1,000,000 kPa matric suction for values of water content corresponding to air-dried state. As the results of this study indicate, the magnitude of matric suction cannot be so large. Generally, at such values of water content, fine-grain soils are bonded and do not behave like frictional granular materials. On the other hand and at low values of relative humidity and water content such as air-dried condition, the magnitude of silica acid gel bonding increases. It appears that these enhanced values of stress could be due to significant bond formation between the "short protruding silica acid gel hairs" of the surface of the adjacent grains by transformation of hydrophilic groups to hydrophobic groups. Also at low values of water content, sulfates and carbonates form precipitates.

The author does not deny the involvement, contribution, and role of the other bonding agents in the structurally bonded response and behavior of Penticton silt; but it appears that the only bonding agent, being present in Penticton silt, being sensitive to moisture, and being able to justify the responses observed in this study is silica acid gel. It is likely that the other forms of bonding agents mentioned in literature and this study also contribute to some degree to the stiffness and strength of the structurally bonded response of Penticton silt.

It should be mentioned that the chemical activity of silica acid gel is a surface chemistry phenomenon; and consequently, its magnitude is a function of specific surface of the soil. Hence, its influence can only become important for soils with large specific surface similar to silts and clays.

8.4.3 Swelling

Upon exposure to water, the Penticton silt specimens swell approximately 40% by volume. Possible contributing processes are listed and discussed in this section.

Elimination of soil suction and capillary stresses is known to be responsible for expansion of soils. All test results presented in section 8.3 are in contradiction with a swelling theory based on elimination of soil suction. Special attention should be paid to outcomes of Observational Test Five (OT-5). The alcohols used in these tests were miscible with water. As a result, while soil suction was eliminated in all alcohol saturated specimens, the amount of swelling varied significantly. Also it should be reminded that Kerosene saturated specimen did not swell at all. Hence, observations presented in section 8.3 indicate that the elimination of soil suction is not a key process in swelling for Penticton silt.

Results of X-ray diffraction analyses indicate the presence of a limited quantity of expandable clays (less than 3% of the total mass). The expandable clay present has some contribution to the overall swelling; but it is evident that such a small amount of swelling clays cannot be responsible for the large amount of volume increase observed.

Electrochemical forces, colloidal interactions, and the polarity of the pore fluid can also cause swelling; but such forces and the consequent repulsion are not big enough to justify such large amount of volume increase. Also values of electric conductivity obtained for these sediments and reported in Chapter 5 does not support the presence of any large electrochemical forces in these soils.

Gilboy (1927), Terzaghi (1931), and Mitchell (1993) discussed the high compressibility and elastic swelling of sand-mica mixtures. Before any further discussion and knowing the state of the technology in 20's and 30's, it should be mentioned that Gilboy (1927) and Terzaghi (1931) used the term "mica" in a rather loose manner. X-ray diffraction analysis was not invented at that time and their judgment was based purely on observational methods. This author believes the relationship between elastic swelling and mica content, discussed by Mitchell (1993), should be revised to refer to all platy particles. A swelling theory based on spring style elastic deformation of platy particles cannot directly apply to the behavior observed for Penticton silt. Elastic swelling, proposed by Gilboy (1927) and Terzaghi (1931) and presented in Figure 8.2.1-B, is based on tests using sand-mica mixture, which were mixed and tested dry. Also, this relationship is for the rebound curve of the compression-swelling test. In contrast to the Gilboy (1927) and Terzaghi (1931) experiments, the swelling phenomena observed in testing Penticton silt specimens occurs in correlation with a change in the soil moisture. It is apparent that the spring style elastic swelling of platy particles is not the controlling process for the swelling of Penticton silt; but this author believes that the swelling is influenced by the elasticity of platy particles such as mica and chlorite.

Regardless of the swelling mechanisms involved, there should be an independent triggering mechanism to first transfer a bonded non-frictional material to a frictional granular material. As was discussed in section 8.4.2, as the soil moisture increases the bonds formed between hydrophobic "short protruding silica acid gel hairs" of adjacent particles breaks and "short protruding silica acid gel hairs" transform to the hydrophilic groups. The consequence of this process is the formation of a granular mass from a bonded material.

This author believes that in the case of swelling, again, the transformation of "short protruding silica acid gel hairs" from hydrophobic to hydrophilic is the fundamental key mechanism involved. As shown in Figure 8.2.1-E, during such transformation the "short protruding silica acid gel hairs" swell and push the soil particles apart. Reviewing the results in Observational Test Five (OT-5) supports this theory. As can be seen in Table 8.4, as the number of available –OH$^-$ arms in pore fluid decreases, the amount of swelling decreases.

Supporting the swelling of the "short protruding silica acid gel hairs" theory does not imply that this author disregards the involvement of the above mentioned other mechanisms. At this stage, it is clear that transformation of a bonded Penticton silt specimen to a frictional granular material and its swelling should involve the silica surface elements of the "short protruding silica acid gel hairs" and their phase transformation; but the overall magnitude of the swelling is the result of elimination of soil suction, electrochemical forces, expansion of active clays, elastic swelling of the platy particles, and phase transformations of the "short protruding silica acid gel hairs" in the silica surfaces.

8.4.4 General Discussion

Carrying out a full scale experimental program using a variety of soils to validate the conclusions presented in this chapter and also previous chapters is beyond the scope of the current study. Limited experiments, carried out during in Observational Test Seven (OT-7), Eight (OT-8), and Ten (OT-10), can imply the following conceptual conclusions:

Results of this study and a review of the literature about sensitive soils, indicate that many sensitive soils contain reasonable amounts of mica and chlorite. This observation shows that the key issue is not the presence or absence of clay size particles but the activity of the minerals defined by the state of silica surface and grain size rather than plasticity and clay content.

It appears that the elimination of soil suction is not the main process in the behavior of the soil mass. Believing in such a theory does not practically disregard and invalidate the experimental results presented in the extensive existing literature on the behavior of soils, which links an unsaturated state to soil suction. The macroscopic mechanical behaviors and responses observed are definitely valid experimental results; but the discussions of those studies that tend to introduce soil suction as the sole source of enhanced stiffness and strength and improved behavior and response in unsaturated state may be questionable. While there is disagreement between this study and the literature on unsaturated soils regarding the origin of improved behavior, macroscopic mechanical results presented appear to resemble the corresponding results reported in the literature on unsaturated soils.

From the practical perspective and knowing the influence of pore fluid and degree of saturation on structural bonding, a structure contributing parameter can replace the soil suction parameter in equations such as the ones proposed by Fredlund and Rahardjo (1993) (Equation 8.2.2-J), Oberg (1997) (Equation 8.2.2-L), and Vanapalli et al. (1996) (Equation 8.2.2-P).

Experimental results of this study show that a structurally bonded soil could behave similar to a bonded material as oppose to frictional granular material. Such results suggest that another approach towards practical implication of the soil structure can be the use of unconfined compressive strength in an equation similar to the one proposed by MacGregor (1992) for concrete.

Figure 8.2.1-A and 8.2.2-A, adopted from Mitchell (1993) and Fredlund and Rahardjo (1993) respectively, show some sort of soil classification based on structure and state of saturation, respectively. It is relevant that surface tension is a special case of a physical structure determining process. Conceptually these two soil classification charts can be combined into a unified soil classification chart similar to the one proposed in Figure 8.4.4-A. Amongst soil classification charts, the one presented in Figure 8.4.4-B which is adopted from Morgenstern (1992), is of special interest. This chart combines the unsaturated and structured state of the soil in a problem oriented soil classification chart. Until development of a more comprehensive soil classification chart, the chart proposed by Morgenstern (1992) is recommended.

In Chapter 7, it was indicated that conceptually, the contours of the state boundary for structured Penticton silt are similar to the ones reported for unsaturated soils at various soil suctions. It is relevant that surface tension is a special case of a physical structure determining process. Taking into account these facts and the results of discussions presented here and in previous sections, it can be conceptually proposed that except for the case of an ideally reconstituted laboratory soil specimen, all other soils are generally structured. In other words, it appears that the only soils without any structural influences are soils such as young, normally consolidated, saturated cohesionless soils. In this regard, even over-consolidation can be a special case of structure; and the Hvorslev surface can be a structured state boundary. Results imply that the literature developed for implication of the soil suction at an unsaturated state can be implemented to introduce a unified conceptual critical state soil mechanics for studying soil behavior. Also, the results of some studies indicate that physical and chemical structural determining processes not only influence the cohesion intercept but also the friction angle.

Equation 8.2.2-U was proposed by Wheeler and Sivakumar (1995) to introduce the concept of soil suction to the critical state soil mechanics (CSSM). Taking into account results presented in this study and the literature discussed in section 8.2, the author conceptually proposes that for structured soils, the following equation, which is a modified version of Equation 8.2.2-U, should be used to represent the unified critical state soil mechanics:

$$q = M_S \, p' + \Omega \qquad \text{(Equation 8.4.4)}$$

in which:

M_S is the structured strength parameter, and

Ω is the intercept of the peak strength envelope with the deviator stress axis, which is an indicator of the magnitude of the soil structure.

The proposed critical state model is shown in Figure 8.4.4-C. Ω is a parameter which represents the accumulative effect of all physical and chemical structural determining processes such as ω (see Chapter 7), $\mu(s)$ (for soil suction proposed by Wheeler and Sivakumar (1995)), c (cohesion), apparent cohesion due to over-consolidation, etc. It should be mentioned that M_S and Ω are strain dependent; and therefore, they will be mobilized at different strains. Generally, most components of Ω are small strain phenomena. Consequently, in shear strength calculations, we cannot count on simultaneous existence of maximum values of both.

8.5 Summary

Based on results of experiments, carried out in this study, and results of studies mentioned in the literature about structured and/or unsaturated soils, the followings can be proposed:

Results of this study imply that soil suction (surface tension) is not a key structure determining parameter for Penticton silt. Results showed that decrease or elimination of soil suction did not cause major changes in the response and behavior of Penticton silt.

Penticton silt, which is a dominantly silt size low plasticity non-active soil, is structured. The soil structure of Penticton silt is structurally bonded; and inter-particle bonding and its magnitude are moisture sensitive. Bonding agents, present in soil structure of Penticton silt, includes amorphous silica acid gel, iron oxides, sulfate and carbonate precipitates of Na^+, Mg^{++}, and Ca^{++}; but results of this study imply that the key bonding agent is amorphous silica acid gel.

In spite of being a low plasticity non-active soil, specimens of Penticton silt swell up to 40% by volume upon exposure to water. Elimination of soil suction, swelling of clay particles, interaction of electrochemical forces, elastic deformation of platy particles such as mica particles, and chemical transformation of silica surfaces groups are considered to cause soil swelling for Penticton silt. Results of this study imply that while all these mechanism could be involved in the swelling of specimens of Penticton silt, the chemical transformation of silica surfaces groups is the key mechanism involved. Results imply that a swelling theory without involvement of chemical transformation of silica surfaces cannot support the observed magnitude of swelling. Results also imply that the triggering mechanism for the phenomena of transformation of Penticton silt from a bonded material to a frictional granular material depends heavily on chemical transformation of silica surfaces groups.

Results of this study conceptually imply that the state of silica surfaces groups combined with a small grain size could be the key issue regarding the sensitive behavior of sensitive and/or collapsible soils rather than plasticity and clay content. Chemical activity of silica acid gel is a surface chemistry phenomenon; and consequently, its magnitude is a function of specific surface of soil. Hence, its influence can only become important for soils with large specific surface similar to silts and clays.

Knowing that surface tension and consequently soil suction is a special case of this physical structure determining processes, it is proposed to use soil classification based on state of soil structure rather than saturation state of soil.

Results and discussions presented in this study imply that the effect of soil structure on peak strength envelope and state boundary is similar to the effect of soil suction.

The following equation is conceptually proposed for structured soils to represent unified critical state soil mechanics:

$$q = M_S \, p' + \Omega \qquad \text{(Equation 8.4.4)}$$

Coefficient Ω represents the overall accumulative effect of physical and chemical structure determining processes.

Table 8.3.2 – Summary of Results (Observational Test Five (OT-5))

Specimen	Liquid	Description of the Response
OT-5-W	Distilled Water (H_2O)	Crack formation, de-structuring, and swelling occurred. Specimen swelled approximately 42% by volume. Manual inspection of the specimen indicate loss of stiffness and strength.
OT-5-M	Methanol (99.9%) (CH_3OH)	Crack formation, de-structuring, and swelling occurred. Specimen swelled approximately 15% by volume (i.e. approximately 1/3 of OT-5-W). Manual inspection of the specimen indicate loss of stiffness and strength. The level of disintegration was not as severe as for the OT-5-W.
OT-5-E	Ethanol (95%) (C_2H_5OH)	Crack formation, limited de-structuring, and minor swelling occurred. Specimen swelled approximately 4% by volume. Manual inspection of the specimen indicate limited loss of stiffness and strength. The level of disintegration was very limited.
OT-5-B	Buthanol (C_4H_9OH)	Limited crack formation occurred. Slight swelling (approximately 1% to 2%) occurred. Manual inspection of the specimen showed transformation to a flexible and soft soil specimen; but overall, it was sound specimen with some cracks.
OT-5-D	Decanol ($C_{10}H_{21}OH$)	No crack formation, de-structuring, or swelling occurred; but manual inspection using a sharp object showed some softness. Specimen did not remain like a piece of rock; but maintained its integrity completely.
OT-5-K	Kerosene (C_9H_{12} to $C_{17}H_{36}$)	No crack formation, de-structuring, or swelling occurred. Manual inspection showed that specimen remained as stiff and strong as before saturation. It maintained its integrity and it was still like a stiff piece of rock.

Table 8.4 – Characteristics of Pore Fluids Used in Observational Tests

Pore Fluid	Surface Tension (at 1 atm & 25 °C) (mN/m)	Relative Permittivity (Dielectric Constant) (at 1 atm)
Water (H_2O)	71.99	80 at 20 °C
Methanol (CH_3OH)	22.07	33 at 20 °C
Ethanol (C_2H_5OH)	21.97	25 at 20 °C
Buthanol (C_4H_9OH)	24.93-22.54	17-18 at 20 °C
Decanol ($C_{10}H_{21}OH$)	28.51	3-7 at 25 °C
Kerosene (C_9H_{12} to $C_{17}H_{36}$)	22.38 to 27.05	2 at 20 °C

Figure 8.2.1-A – Structure Determining Factors and Processes
(after Mitchell (1993))

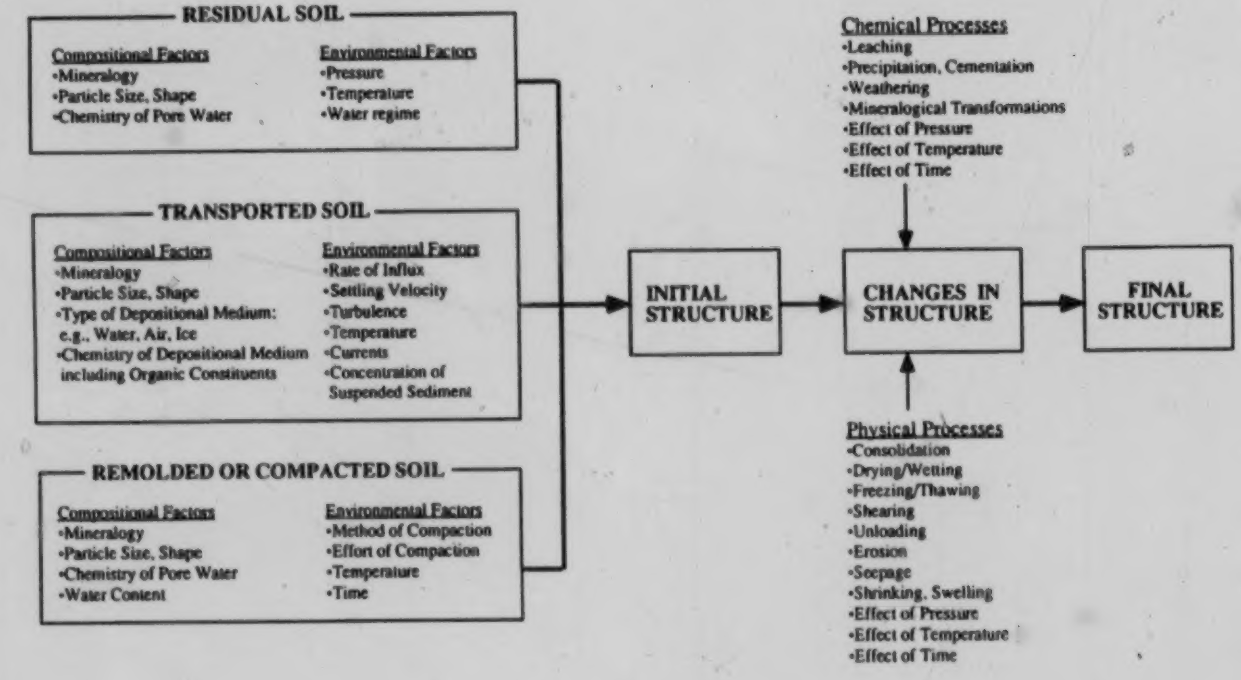
RESIDUAL SOIL
Compositional Factors
•Mineralogy
•Particle Size, Shape
•Chemistry of Pore Water
Environmental Factors
•Pressure
•Temperature
•Water regime
TRANSPORTED SOIL
Compositional Factors
•Mineralogy
•Particle Size, Shape
•Type of Depositional Medium: e.g., Water, Air, Ice
•Chemistry of Depositional Medium including Organic Constituents
Environmental Factors
•Rate of Influx
•Settling Velocity
•Turbulence
•Temperature
•Currents
•Concentration of Suspended Sediment
REMOLDED OR COMPACTED SOIL
Compositional Factors
•Mineralogy
•Particle Size, Shape
•Chemistry of Pore Water
•Water Content
Environmental Factors
•Method of Compaction
•Effort of Compaction
•Temperature
•Time
INITIAL STRUCTURE
CHANGES IN STRUCTURE
FINAL STRUCTURE
Chemical Processes
•Leaching
•Precipitation, Cementation
•Weathering
•Mineralogical Transformations
•Effect of Pressure
•Effect of Temperature
•Effect of Time
Physical Processes
•Consolidation
•Drying/Wetting
•Freezing/Thawing
•Shearing
•Unloading
•Erosion
•Seepage
•Shrinking, Swelling
•Effect of Pressure
•Effect of Temperature
•Effect of Time

Figure 8.2.1-B – Relationship between Swelling Index and Mica Content for Coarse-Grained Mixtures

(after Mitchell (1993))

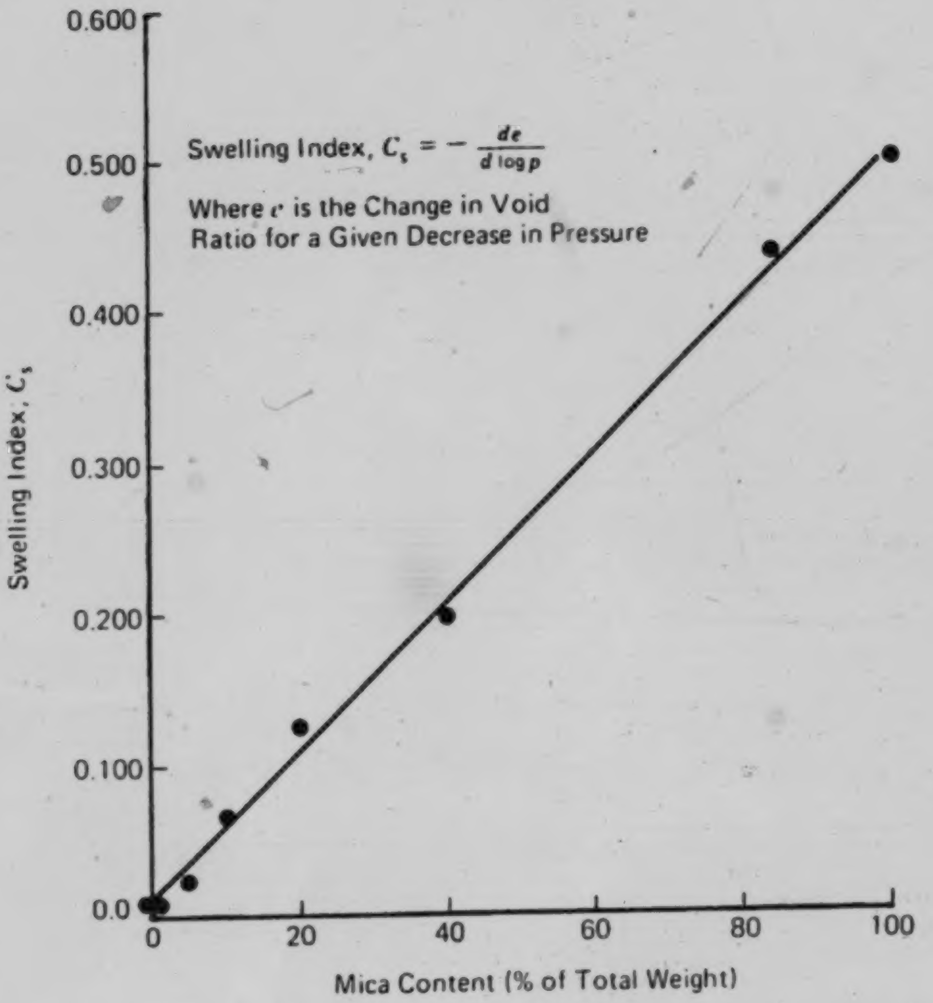

Figure 8.2.1-C – Main Chemical Groups of Silica Surface

(a) Siloxane Groups (Si-O-Si) (Hydrophobic)
(b) Silanol Groups (Si-OH) (Uncharged Hydrophilic)
(c) Silicic Acid Groups (Si-O$^-$) (Charged Hydrophilic)
(d) Typical Chemical Structure for Silica Acid Gel
(after Vigil et al. (1994))

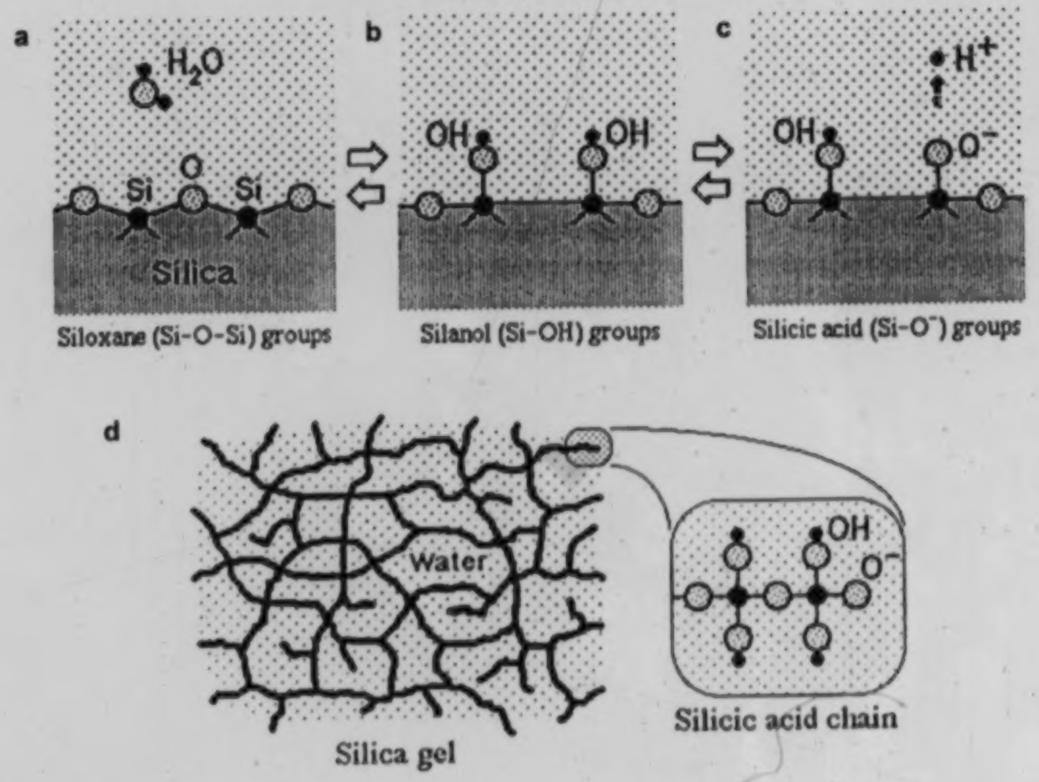
a
H_2O
Si
O
Si
Silica
Siloxane (Si-O-Si) groups
b
OH
OH
Silanol (Si-OH) groups
c
H^+
OH
O^-
Silicic acid (Si-O$^-$) groups
d
Water
Silica gel
OH
O^-
Silicic acid chain

Figure 8.2.1-D – Bonding (Sintering) of Silica Groups

(a) Sintering reaction of two hydrophobic silica surfaces by a water condensation reaction.
(b) Sintering of two hydrophilic silica surfaces by dehydration.
(c) Sintering of two hydrophobic silica surfaces without involving water.

(after Vigil et al. (1994))

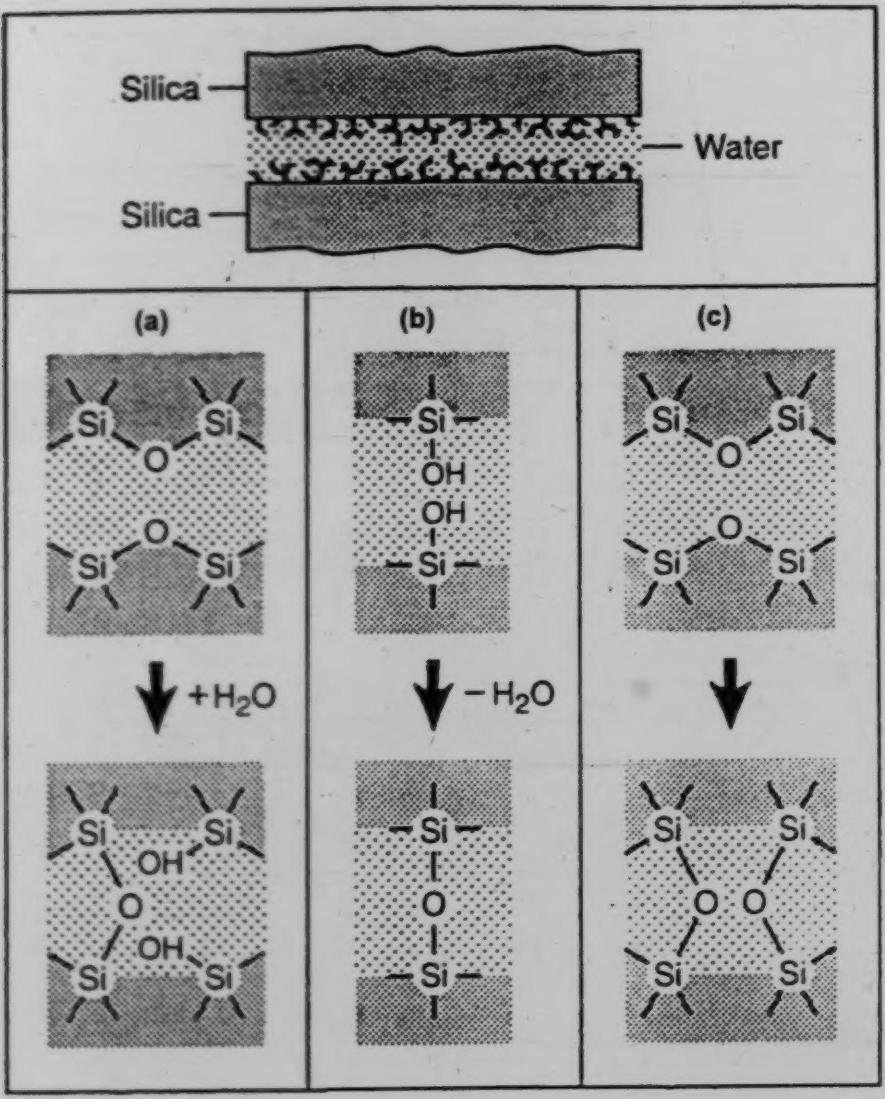
Silica
Water
Silica
(a)
(b)
(c)
Si
O
OH
+H₂O
−H₂O

Figure 8.2.1-E – Swelling of the Silica Surfaces

(a) Un-Swollen Structure of Hydrophobic Surface
(b) Un-Swollen Structure of Hydrophilic Surface
(c) Swollen Structure Hydrophilic Surface

(after Vigil et al. (1994))

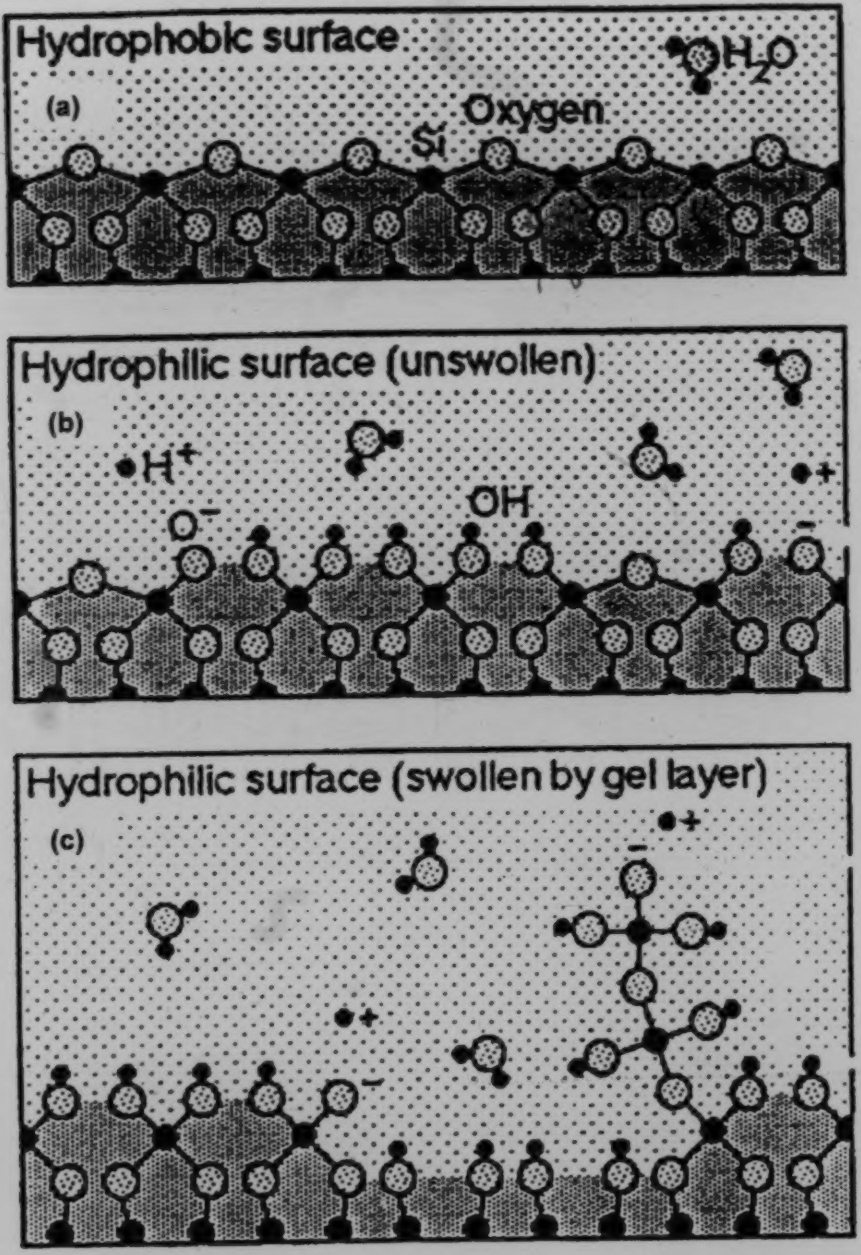
Hydrophobic surface
(a)
H_2O
Oxygen
Si
Hydrophilic surface (unswollen)
(b)
H^+
O^-
OH
+
−
Hydrophilic surface (swollen by gel layer)
(c)
+
−
+
O^-

J

Figure 8.2.1-F – Bi-Axial Ultimate Strength Envelope of Concrete

(after Tasuji et al. (1978))

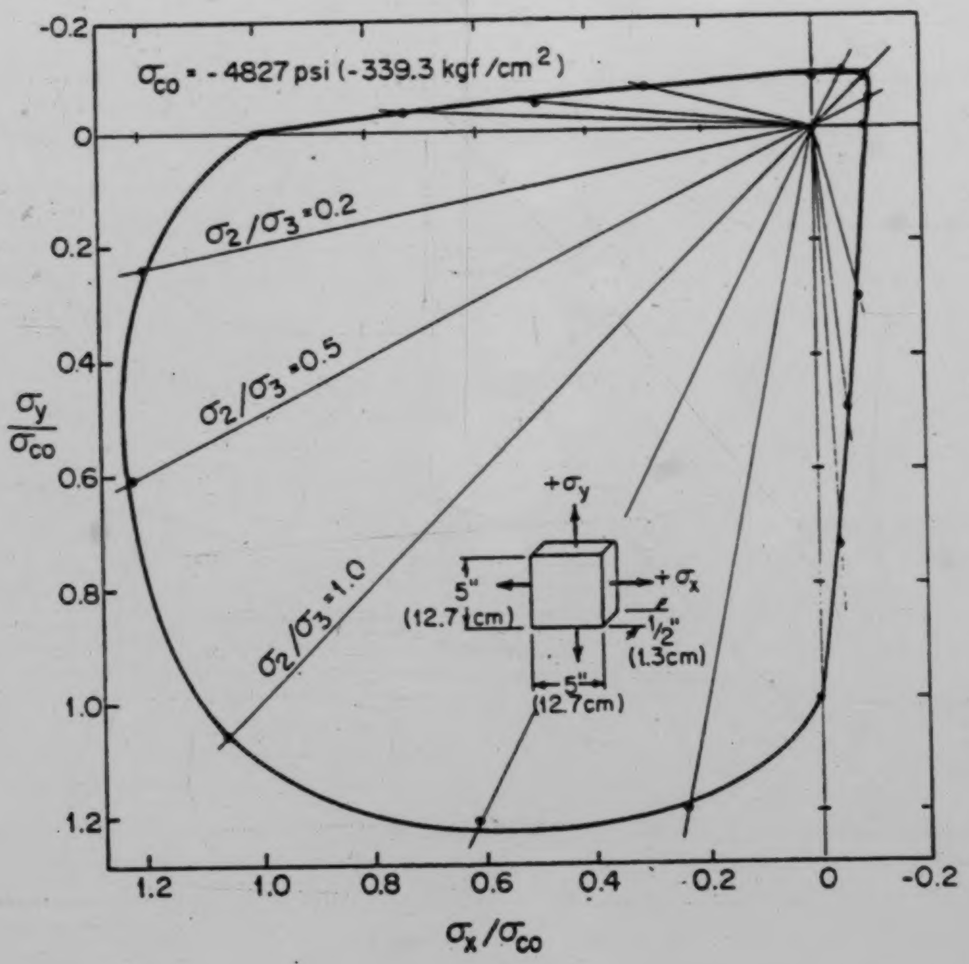

Figure 8.2.1-G – Results of Triaxial Tests on Concrete

(after MacGregor (1992))

(a) Axial Stress-Strain Curves

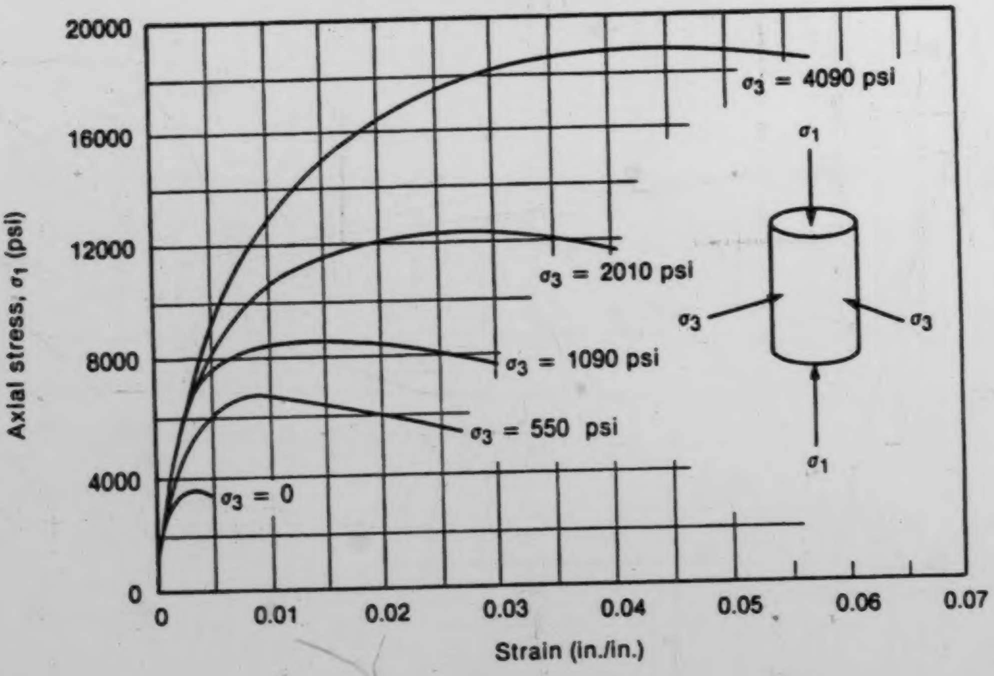

(b) Mohr Rupture Envelope

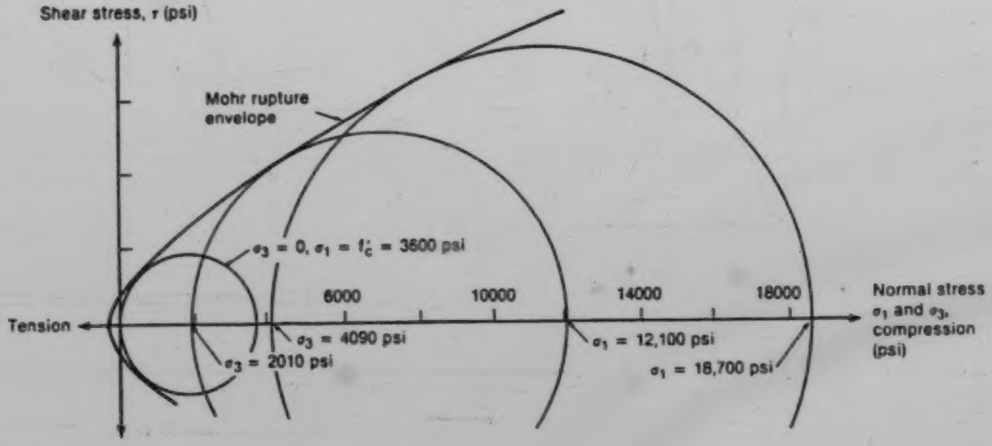

Figure 8.2.2-A – Soil Mechanics Categorization Using Pore Water Pressure (u_w)
(after Fredlund and Rahardjo (1993))

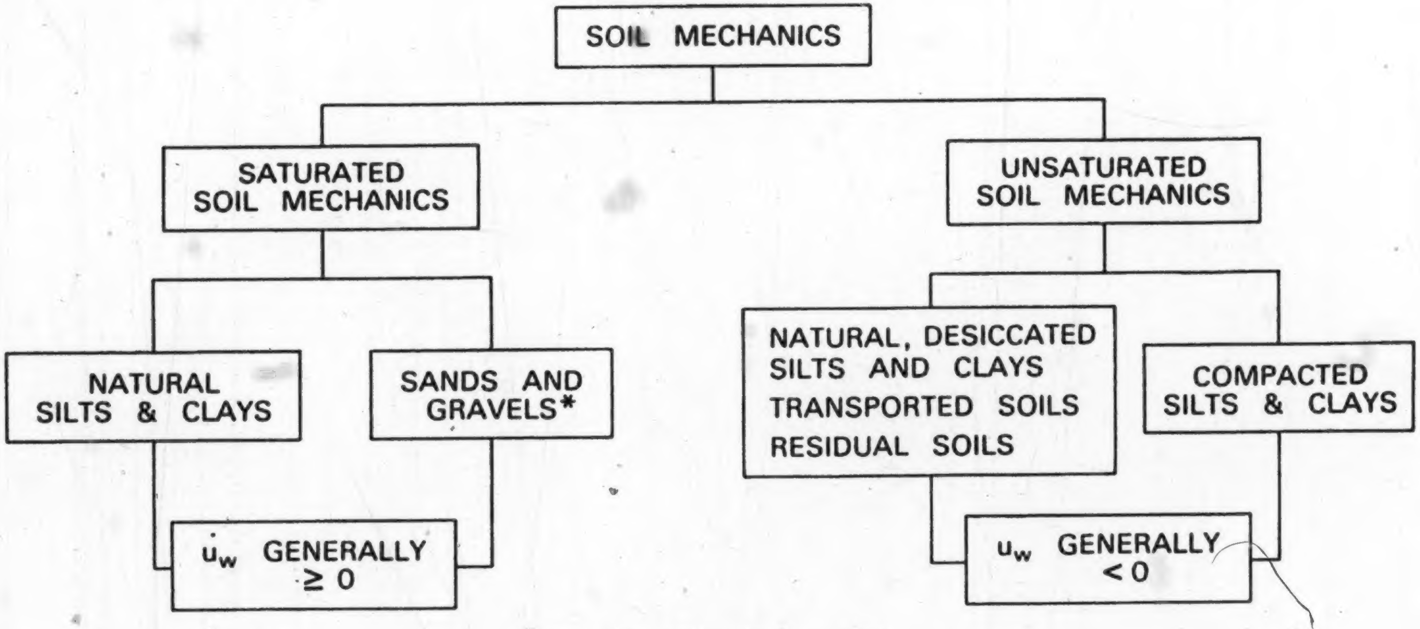
SOIL MECHANICS
SATURATED SOIL MECHANICS
UNSATURATED SOIL MECHANICS
NATURAL SILTS & CLAYS
SANDS AND GRAVELS*
NATURAL, DESICCATED SILTS AND CLAYS
TRANSPORTED SOILS
RESIDUAL SOILS
COMPACTED SILTS & CLAYS
u_w GENERALLY ≥ 0
u_w GENERALLY < 0

* may be saturated or dry

Figure 8.2.2-B – State Boundary Surface in q-(p-u_a)-s Space
(after Alonso et al. (1990))

(a)

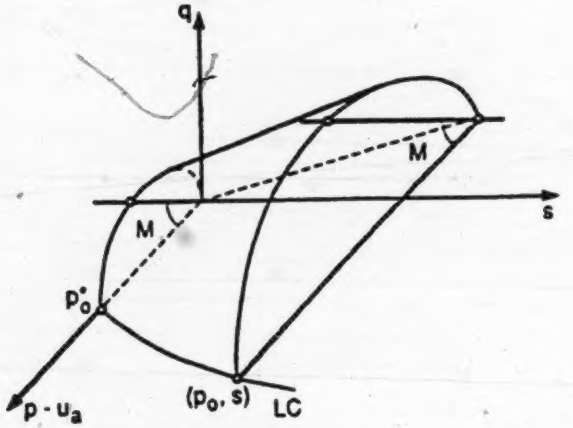
q
M
M
s
p_o^*
$p - u_a$
(p_o, s)
LC

(b)

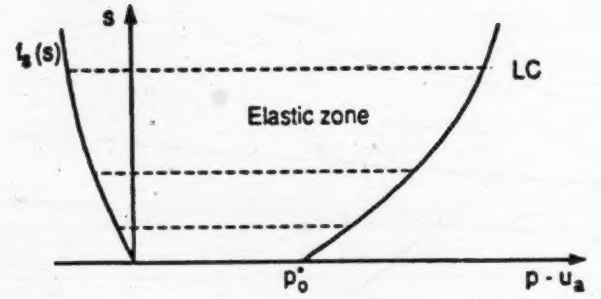
s
$f_s(s)$
LC
Elastic zone
p_o^*
$p - u_a$

(c)

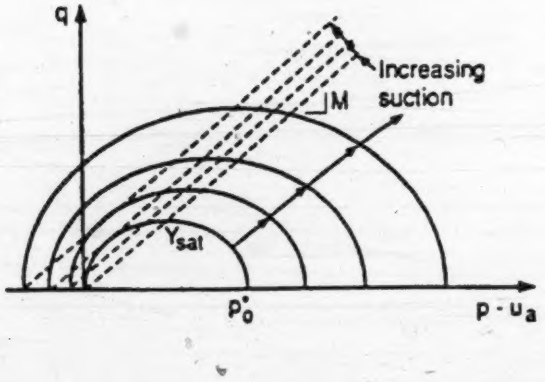
q
Increasing suction
M
Y_{sat}
p_o^*
$p - u_a$

Figure 8.2.2-C – Triaxial Test Results at Various Suctions

(after Wheeler and Sivakumar (1993))

(a) The Contours of the Normal Compression Line (NCL)

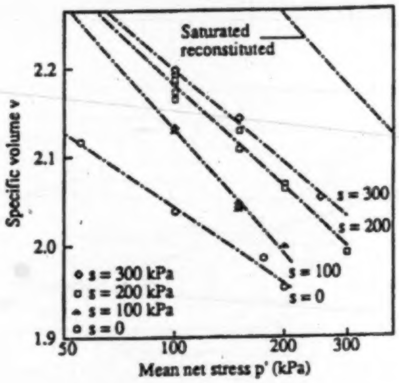

(b) The Contours of the Critical State Line (CSL) in v-(p-u_a) Space

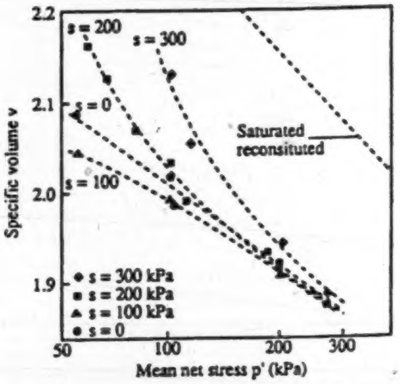

(c) The Contours of the Critical State Line (CSL) in q-(p-u_a) Space

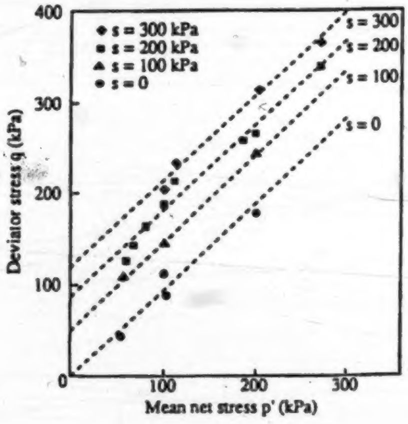

Figure 8.2.2-D – Critical State Line (CSL) at Various Suctions
(after Maatouk et al. (1995))

(a) The Contours of the Critical State Line (CSL) in e-(p-u$_a$) Space

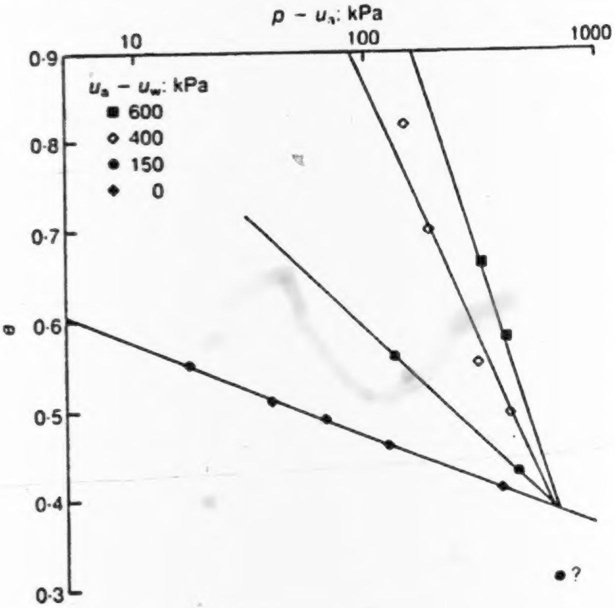

(b) The Contours of the Critical State Line (CSL) in q-(p-u$_a$) Space

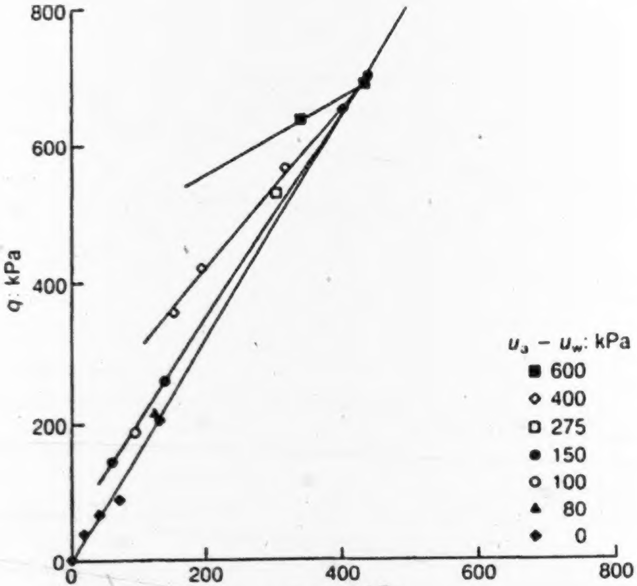

Figure 8.2.2-E – Contours of the State Boundary for Compacted Jossigny Silt at Various Suctions

(after Cui and Delage (1996))

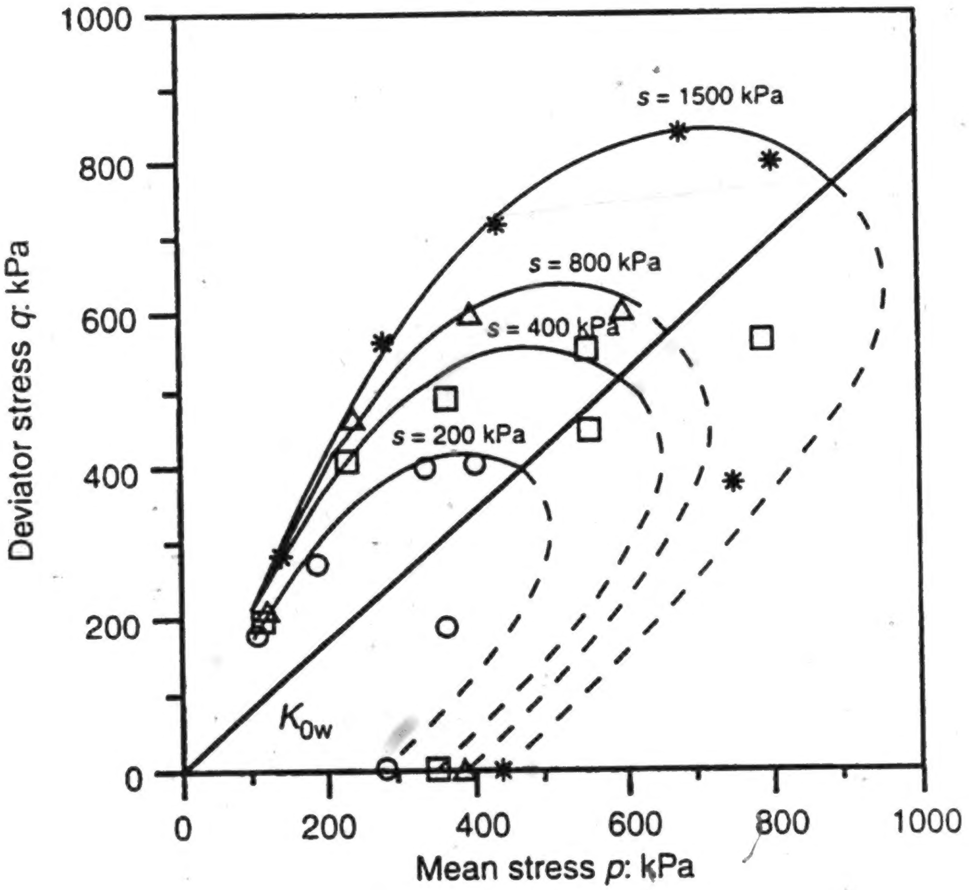

Figure 8.3.1-A - One Dimensional Consolidation Testing for Structure Determination (Results of Undisturbed Specimens)

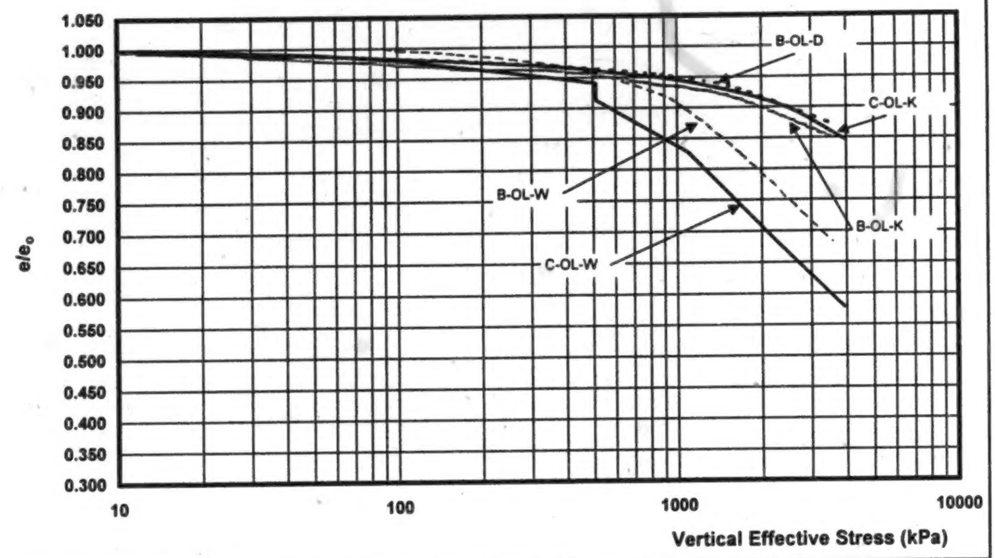

Figure 8.3.1-B - One Dimensional Consolidation Testing for Structure Determination (Results of Reconstituted Specimens)

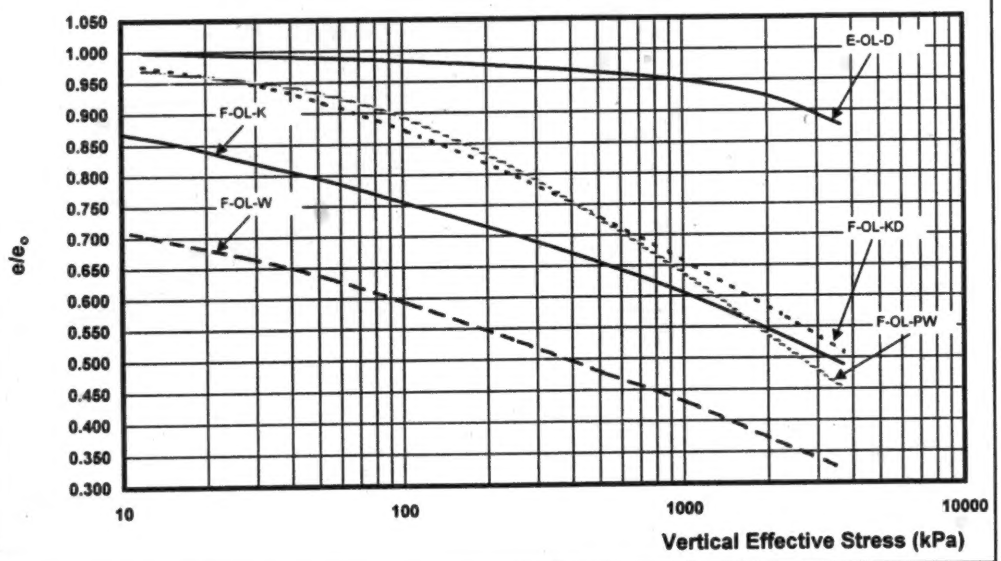

Figure 8.3.1-C - Summary of Triaxial Test Results for Structure Determination

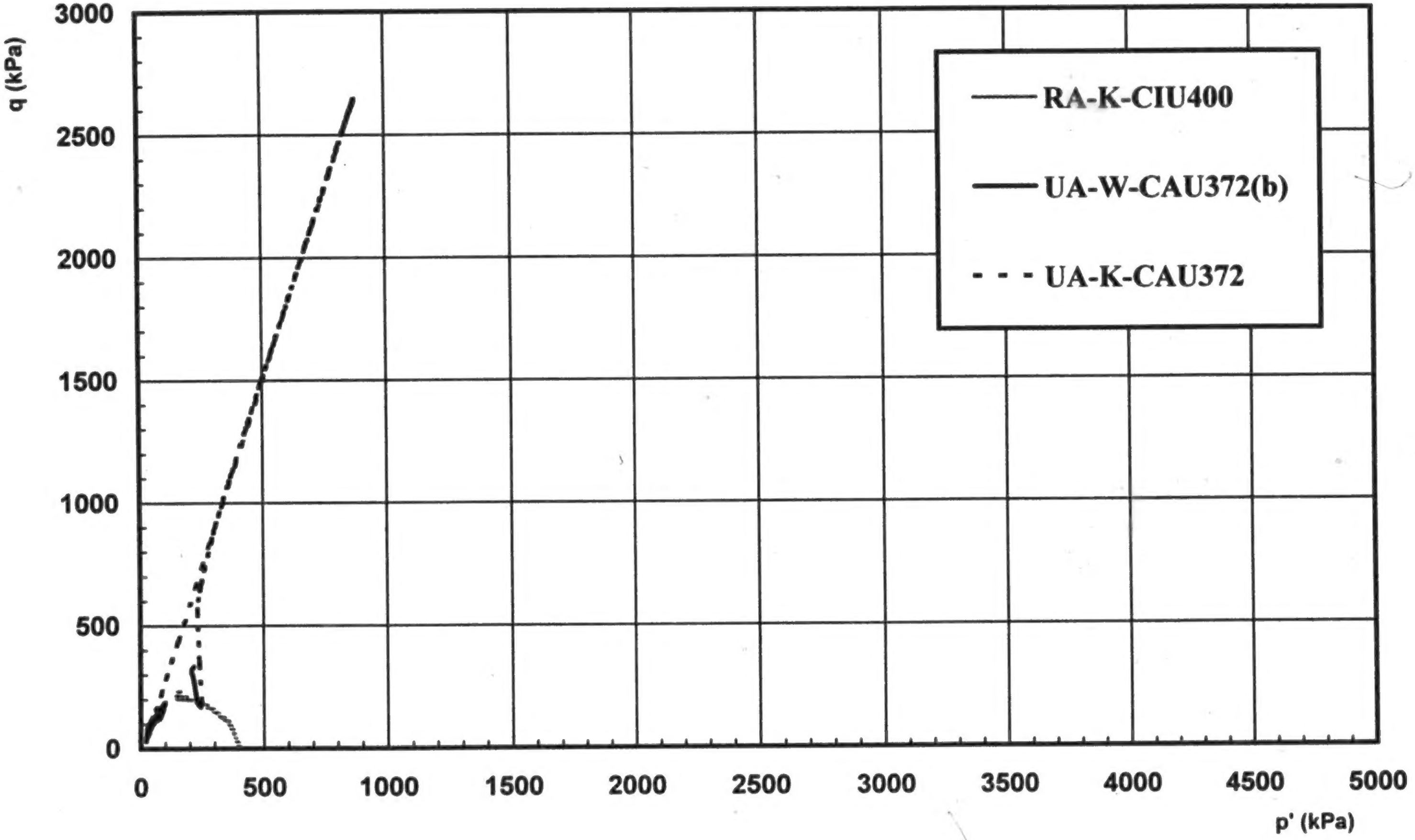

Figure 8.3.2-A – Response of Penticton Silt to Moistening

(a) Specimen OT-3-W (after 18 Hours of Exposure to Water)

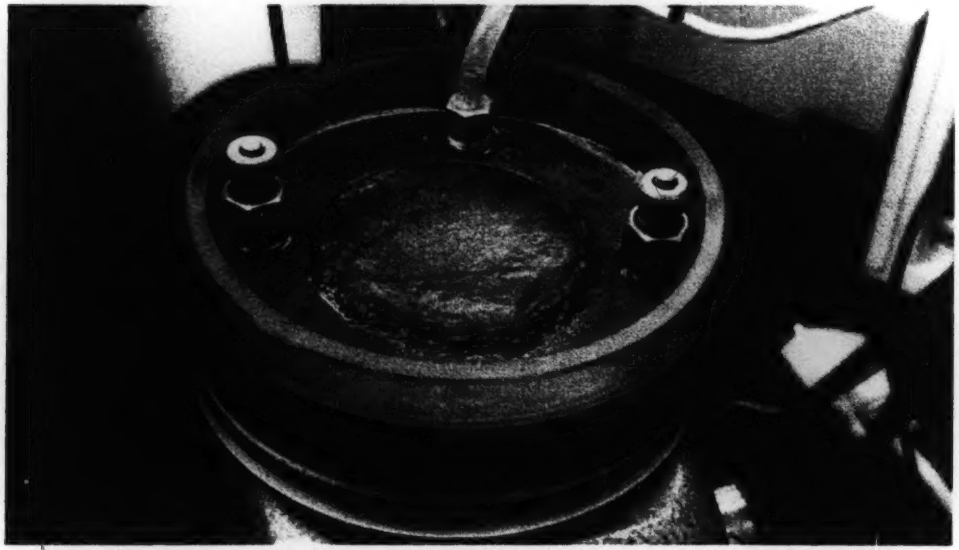

(b) Specimen OT-3-K (after 18 Hours of Exposure to Kerosene)

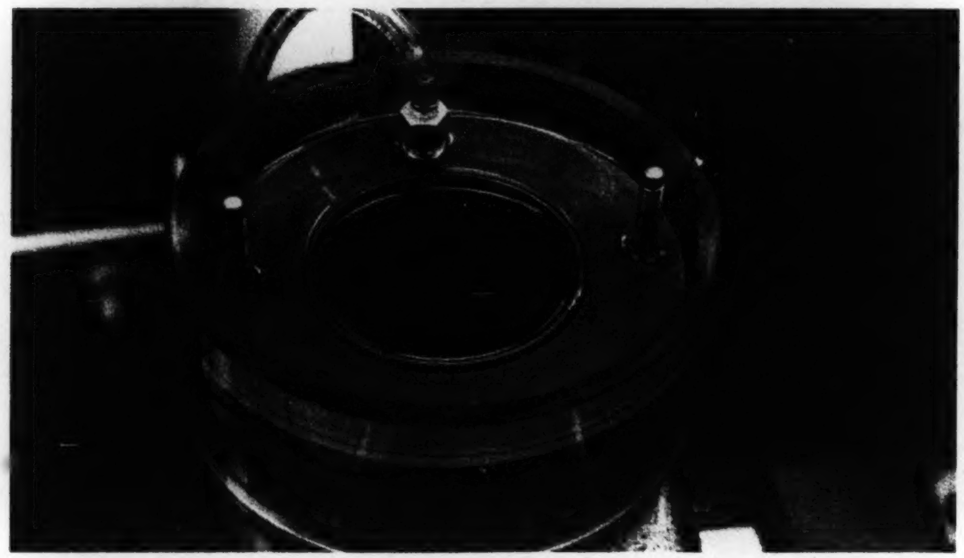

Figure 8.3.2-B – Soil Fabric of the Athabasca Locked Sand
(Courtesy of Touhidi-Baghini (1998))

Magnification: 10 Acceleration Voltage: 2.5 kV

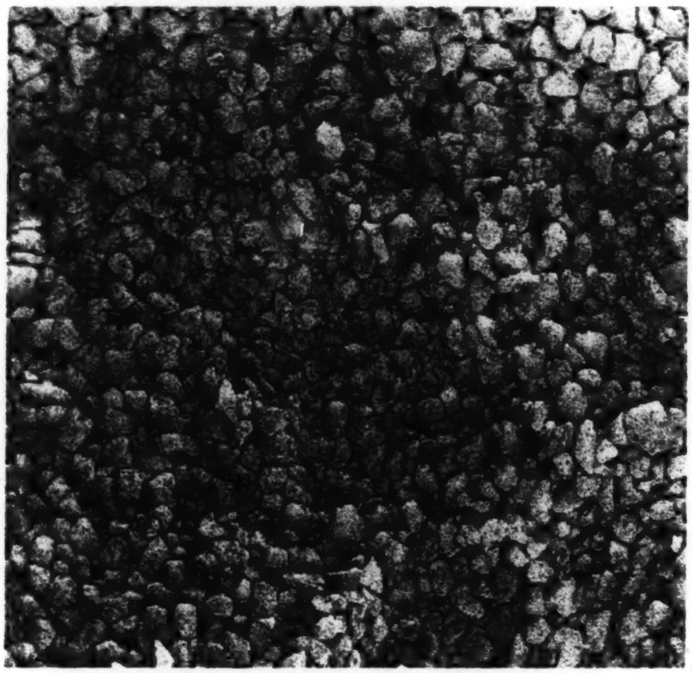

Figure 8.3.2-C – Contact Point of Two Sand Grains
(Courtesy of Touhidi-Baghini (1998))

Magnification: 300 Acceleration Voltage: 2.5 kV

Figure 8.3.2-D – Presence of Fine Grains Around the Contact Points

(Courtesy of Touhidi-Baghini (1998))

Magnification: 150 Acceleration Voltage: 2.5 kV

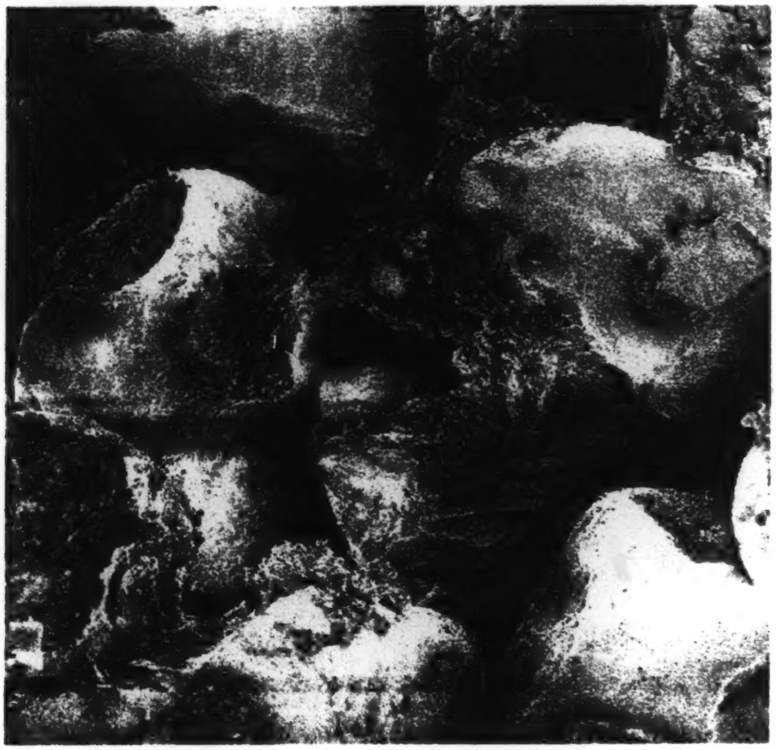

Figure 8.3.2-E – Texture of the Fine Grains Around the Contact Points

(Courtesy of Touhidi-Baghini (1998))

Magnification: 2000 Acceleration Voltage: 2.5 kV

Figure 8.4.4-A – Structure and Saturation State Oriented Soil Classification

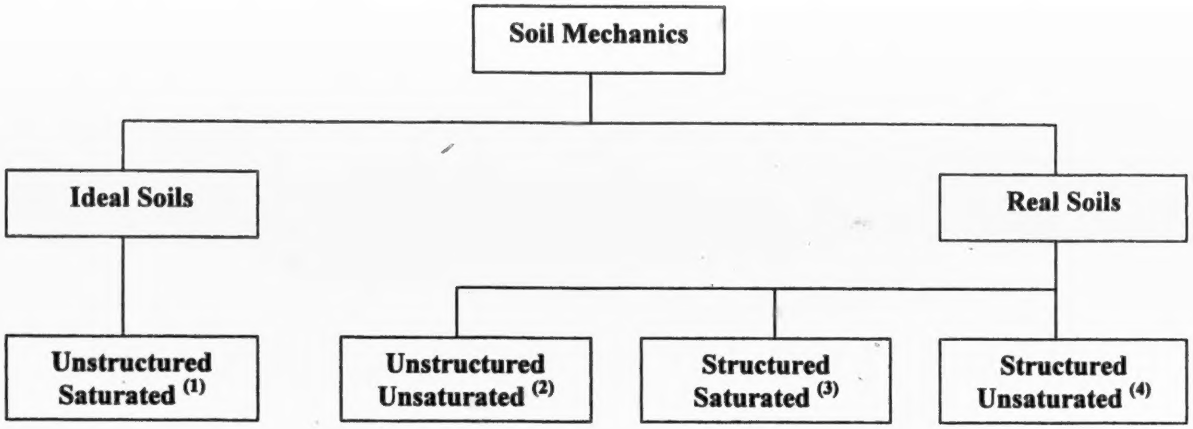
Soil Mechanics
Ideal Soils
Real Soils
Unstructured Saturated (1)
Unstructured Unsaturated (2)
Structured Saturated (3)
Structured Unsaturated (4)

(1) Examples: reconstituted saturated soils and normally consolidated cohesionless soils

(2) Examples: unaged uncemented quartz cohesionless soils

(3) Examples: cemented saturated cohesionless soils and saturated clayey soils

(4) Examples: cemented unsaturated cohesionless soils, natural unsaturated clayey soils, and compacted clayey soils

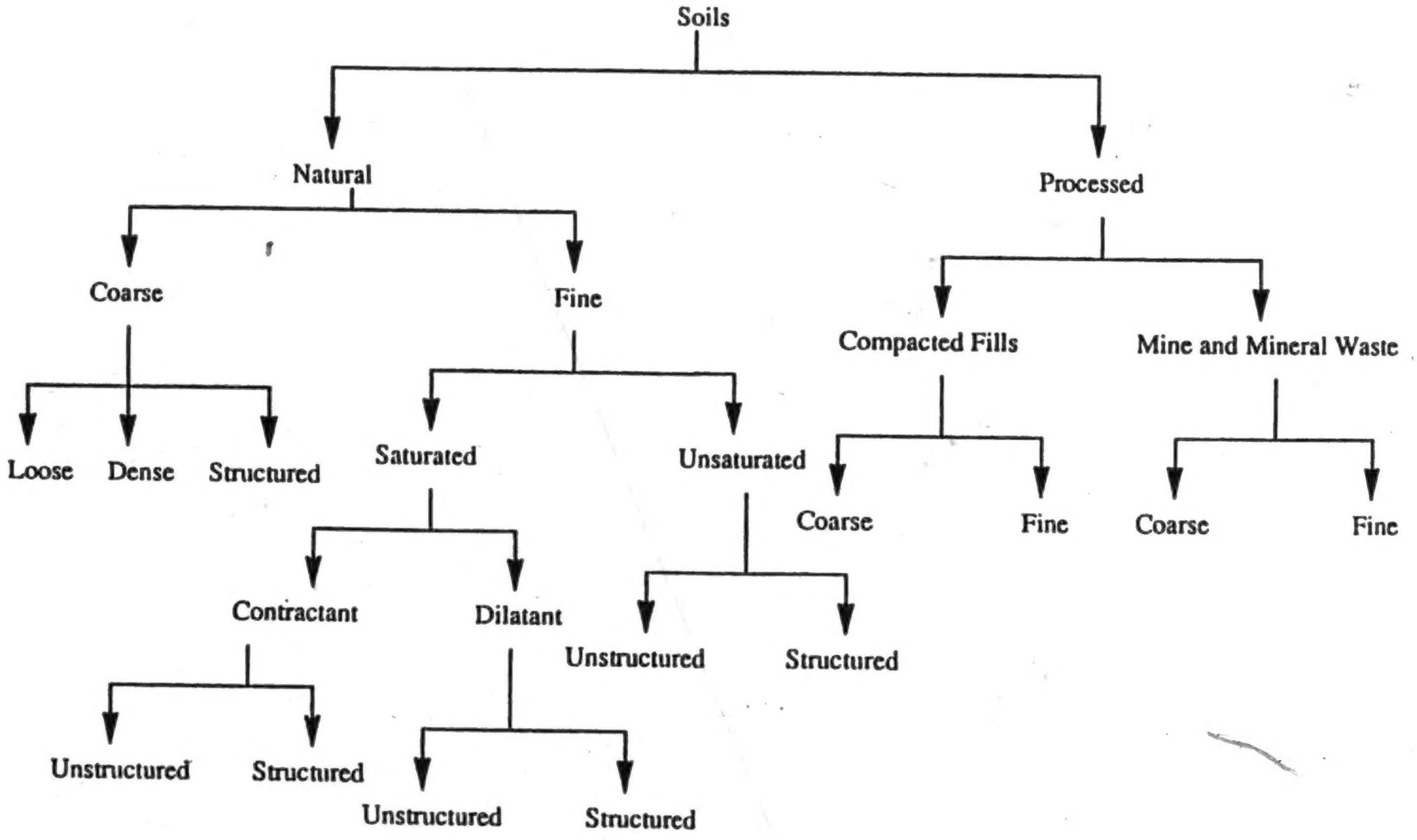

Figure 8.4.4-B – Problem Oriented Soil Classification
(after Morgenstern (1992))

Soils
Natural
Processed
Coarse
Fine
Compacted Fills
Mine and Mineral Waste
Loose
Dense
Structured
Saturated
Unsaturated
Coarse
Fine
Coarse
Fine
Contractant
Dilatant
Unstructured
Structured
Unstructured
Structured
Unstructured
Structured

Figure 8.4.4-C – Proposed Structure and/or Unsaturated Peak Strength Envelope

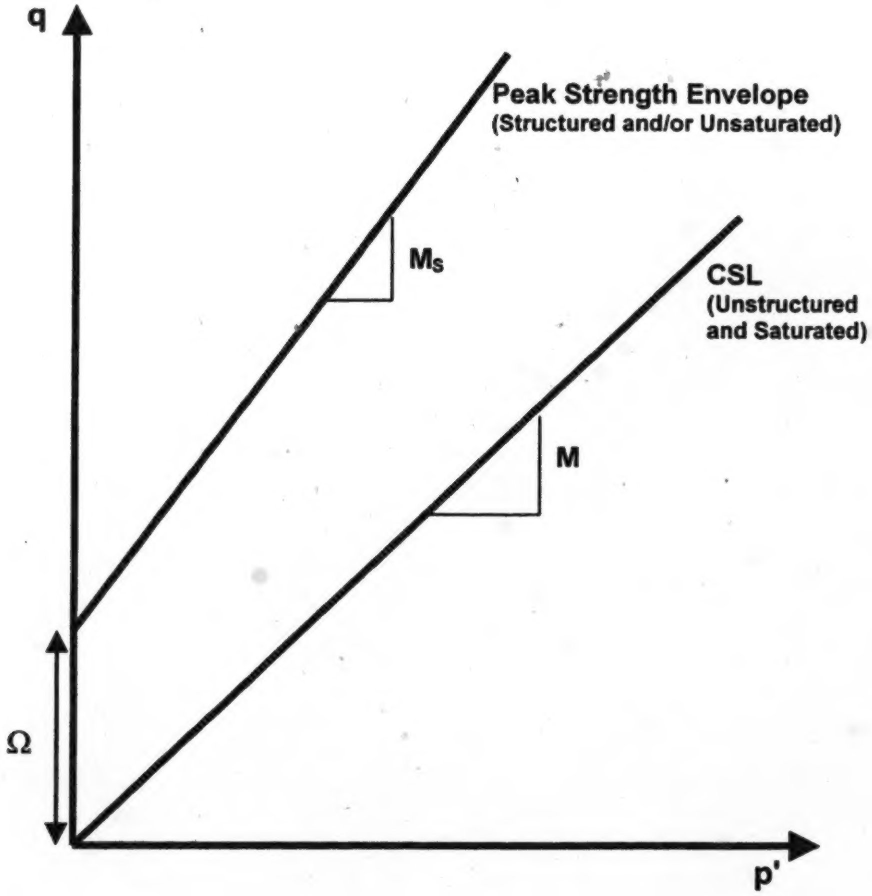
q
Peak Strength Envelope
(Structured and/or Unsaturated)
M_S
CSL
(Unstructured
and Saturated)
M
Ω
p'

CHAPTER NINE

Summary, Conclusions, Practical Implications, and Recommendations

9.1 Summary

The main objective of this study was to investigate the nature and behavior of glaciolacustrine silt sediments in the Okanagan Valley in the southern interior of British Columbia. These sediments are known as Penticton silt by geologists. Depositional history, geology, and geological hazards in the Okanagan Valley were reviewed in Chapter 2. Site selection and sampling were described in Chapter 3. Koosi Creek Slide and Okanagan Lake Park Slide were chosen as the study area. The following experiments were carried out:

- seismic cone penetration testing with pore pressure measurements (SCPTU),
- grain size analysis,
- specific gravity determination,
- Atterberg limits,
- soil water characteristic curve,
- X-ray diffraction analysis,
- scanning electron microscopy (SEM),
- soil and pore fluid chemistry,
- one dimensional consolidation testing,
- triaxial testing, and
- structure determining observational tests.

Undisturbed and reconstituted specimens of Penticton silt were used at saturated, in-situ, and air-dried states. Microscopic and macroscopic response and behaviors were investigated. These experiments were presented and discussed in Chapter 4, 5, 6, 7, and 8. Physical and chemical processes involved in soil structure of Penticton silt was established. Mechanical behavior and characteristics of Penticton silt, especially compressibility and strength, was studied under variety of conditions.

Stability of glaciolacustrine silt sediments in the southern interior of British Columbia and possible failure mechanisms involved in the Koosi Creek Slide and the Okanagan Lake Park Slide failures are discussed in the following section as part of general conclusions.

9.2 General Conclusions and Practical Implications

9.2.1 General Conclusions

Based on results of this study and previous studies mentioned in the literature, the following conclusions can be drawn for Penticton silt:

Monashee Mountains were the main source of glacier ice that occupied Okanagan Valley. Glaciolacustrine silt sediments exists as far south as the international border at the forty nine parallel and as far north as Enderby. Glaciolacustrine silt sediments under study were the sediments of glacial Lake Penticton.

Comprehensive review of the geological history of Penticton silt indicates that glaciolacustrine Penticton silt sediments have never been exposed to any mechanical over-consolidation due to any overburden removal.

It was found that presence of excess water was responsible in occurrence of most geological hazards in the area including Koosi Creek Slide and Okanagan Lake Park Slide.

Seismic cone penetration testing with pore pressure measurements (SCPTU) was found promising in determining soil behavior type and detecting the stratified unusual cemented nature of Penticton silt. It should be reminded that these predictions were correct because they have been used in conjunction with geological history.

Penticton silt is a silt size low plasticity non-active soil with specific gravity of 2.67 and is mainly composed of mica (muscovite) and chlorite particles. The fabric of Penticton silt is highly an-isotropic with preferred horizontal layering.

Penticton silt is a structured soil with inter-particle physicochemical bonding. Major portions of Penticton silt sediments are at an unsaturated state; but results of this study indicate that surface tension (i.e. soil suction or capillary tension), does not play a major role in the enhanced response and behavior of Penticton silt.

The inter-particle physicochemical bonding present in the soil structure of Penticton silt and its magnitude are moisture sensitive. Bonding agents include amorphous silica acid gel, carbonate and sulfate precipitates of Na^+, Mg^{++}, and Ca^{++}, and iron oxides. Among bonding agents, silica acid gel present in the silica surfaces was found to be the key bonding agent. It was also found that transformation of these sediments from a bonded material in the air-dried state to a frictional granular material involves changes in the state of silica surfaces groups.

Penticton silt has potential for swelling and collapse at low and high confining stresses, respectively. It was found that pore pressure generation can only cause elastic deformation; but breakage of physicochemical bonds can cause plastic deformation (i.e. collapse). Swelling pressures measured ranged from 15 kPa to 100 kPa. The magnitude of swelling increased as the initial state of soil specimen was drier. Swelling mechanism involved elimination of soil suction (i.e. surface tension), expansion of active clays, electrochemical repulsion, and expansion of silica acid gel on the silica surfaces. Among these, expansion of silica acid gel was found to be the trigger and the key mechanism involved.

Parameter ω, which is the intercept of the peak strength envelope with q axis in q-p' space, was proposed as the assessment of soil structure. Parameter ω can be calculated using Equation (7.4.4-C).

The friction angle for Penticton silt was approximately 37°. Using measured friction angle and Equation 7.4.4-C, the cohesion intercept is approximately 60 kPa and 800 kPa for in-situ and air-dried states, respectively.

The peak deviator stresses in drained and undrained tests were very close. Consequently, it can be concluded that the response of Penticton silt specimens were controlled by structural bonding present in their soil structure rather than pore pressure generation.

The size of the state boundary (i.e., yield surface) increases as water content of Penticton silt decreases and consequently, the magnitude of moisture sensitive structural bonding increases.

Also, based on results of this study and previous studies mentioned in the literature, the followings can be implied for many structured soils:

Results of this study conceptually imply that the state of silica surfaces groups combined with a small grain size could be the key issue regarding the sensitive behavior of sensitive and/or collapsible soils rather than plasticity and clay content. Chemical activity of silica acid gel is a surface chemistry phenomenon; and consequently, its magnitude is a function of specific surface of soil. Hence, its influence can only become important for soils with large specific surface similar to silts and clays.

It appears that the effect of structural bonding on the state boundary and peak strength envelope is phenomenologically similar to the effect of soil suction. Such observation is not surprising because soil suction (surface tension) is a special case of physical and chemical structure determining processes.

Discussions present in the literature on unsaturated soils consider soil suction (i.e., surface tension), as the source of improved behavior. While the results of this study confirm the improved behavior of Penticton silt in an unsaturated state, it disregards a major contribution from soil suction (i.e. surface tension). Such observation and the fact that discussions in the literature on unsaturated soils are based on valid test results imply that the mechanical relationships developed for unsaturated soils are valid. However, the discussions involved in the source and nature of enhanced behavior of unsaturated soils may be questionable for some soils.

Taking into account the resemblance between the effect of structural bonding and soil suction on soil behavior, the following equation (originally Equation 8.4.4) is conceptually proposed for structured soils to represent a unified peak strength envelope:

$$q = M_S\, p' + \Omega \qquad \text{(Equation 9.2.1)}$$

As stated by several investigators including Wheeler and Sivakumar (1993) M_S may not be equal to M due to influences of soil structure. The coefficient Ω represents the overall accumulative effect of physical and chemical structure determining processes such as cementation, aging, over-consolidation, and soil suction. Both M_S and Ω are strain dependent. Parameter Ω mobilizes at small strains while M_S mobilizes at larger strains. Consequently their maximum values should not be taken into consideration in shear strength calculations simultaneously.

9.2.2 Practical Implications

At early stages of this study, a series of sensitivity slope stability analyses were carried out for Koosi Creek Slide and Okanagan Lake Park Slide. These sensitivity analyses were carried out using Slope/W (1995) and soil parameters reported by Sobkowicz and Coulter (1992), Wilson (1985), and Lum (1977). The sensitivity analysis also included a variety of assumed values of ϕ^b. Results showed more sensitivity to assumed values of cohesion intercept rather than ϕ^b. However and in general, a reliable and comprehensive trend was not observed in the results.

The outcome of the sensitivity analysis is in agreement with experiences with other unusual structured soils such as Norwegian and Canadian "quick clays", mentioned by

Karlsrud et al. (1984) and Tavenas (1984). Karlsrud et al. (1984) stated that the stability analysis for sensitive clays of Norway requires careful consideration of geologic processes such as leaching, weathering and erosion and mechanical characteristics (compressibility, moduli, and strength) of the clays within the slope. They also commented that a simple limiting equilibrium effective stress analysis could not give a correct assessment of the possibility for massive landslide in quick clays.

The effect of structure on the mechanical behavior of structured soils can be as important as the state of stress, stress history, and pore pressure generation. Also and as it was found in this study the soil structure influence may vary with changes in the water content. It appears that a semi-empirical method similar to common practice for Norwegian and Canadian quick clays is suitable for stability analysis of silt bluffs composed of Penticton silt.

Approximately all cases of geological hazards, reported for Penticton silt sediments, involve the presence of excess water. Results of this study showed that Penticton silt specimens might regain their integrity, stiffness, and strength upon removal of excess water. In other words, improvement of soil structure of Penticton silt does not need geological time. In practical terms, this observation is promising. If silt bluffs can be retained, no major damage occurs during periods of presence of excess water and sediments gain their stiffness upon expulsion of excess water.

In cases of shallow planar slides, it is common to presume elimination of soil suction is the cause. Based on results of this study, it appears that the failure mechanism for these shallow slides is similar to the response of Penticton silt specimens upon exposure to water under the condition of zero vertical confinement. It appears that the top portion of silt slopes swells upon exposure to excess water and looses the integrity of its soil structure. Upon exposure to excess water and swelling, breakage of water sensitive bonds, elimination of soil suction, and change in fabric occur. Consequently, silt deposits at shallow depth strain soften and flow. This interpretation can be further supported by the fact that swelling pressures observed in this study were small and specimens exposed to water under confined conditions maintained their integrity.

Using the results of this study and information documented and presented in Chapter 3, the followings can be stated for the failure mechanism involved in Koosi Creek Slide:

A series of limit equilibrium back analyses of the slope were carried out using Slope/W (1995) and results of this study. For a factor of safety of 1 and a purely bonded behavior (i.e., $\phi = 0.0$), the soil parameter "c" should be in the range of 125 kPa to 150 kPa. Using reasonable values of soil suction and ϕ^b for these sediments, it was found that the contribution of soil suction is in the range of 35 kPa to 50 kPa. Consequently, there should be other mechanisms and processes involved in the soil structure of these sediments. The geometry of slide could not be matched using $c = 0.0$ and friction angle of 37°, obtained from triaxial testing of reconstituted specimens. However, it is apparent that the steeper portion of the bluff (i.e., steeper than 37°) would have failed under the condition of zero cohesion. Factor of safety was 2.0 using the least recorded values of "c" for these sediments (i.e., 60 kPa) and friction angle of 37°. Consequently, it appears that the stability and failure mechanisms involved should be more complicated than what can be achieved by limit equilibrium analyses. In addition, this slide may be a case of progressive failure.

A tributary branch of Koosi Creek passes through the scarp of the slide. Inspection of pre-slide aerial photograph shows that the groundwater from this tributary branch exited the face of the silt bluff at about the mid-height. Consequently some part of the glaciolacustrine silt sediments involved in the slide were at saturated condition. Also, the current owner of Paradise Ranch stated that the grandmother of the ranch owner at the time of slide had forgotten to turn off the irrigation over night, which at the time was based on traditional ditching method. Bedrock is high and exposed. Field reconnaissance showed that the failure plane also passed close to the bedrock. The top portion of the slide scarp is part of the desiccated fissured zone of the glaciolacustrine silt sediment and has a close to vertical slope.

The author believes that the Koosi Creek Slide occurred as a result of a combined mechanism involving the flow of water through fissures at or on the top portion, disintegration of soil structure and breakage of bonds, and excess pore water generation because of excessive irrigation and seepage. Shearing of the bedrock implies that the whole slide mass flowed at once and suddenly.

Using the results of this study and information documented and presented in Chapter 3, the following can be stated for the failure mechanism involved in Okanagan Lake Park Slide:

The glaciolacustrine silt sediments at the lake level were dry while the materials involved in the slide were wet. The top portion of the slide was composed of fill and granular deposits, overlying intact glaciolacustrine silt sediments. Everyday in the month of March experiences temperatures above 0 °C. Also, the presence of a small ditch between Highway 97 and the access road appears to play a role in the failure. This ditch could have acted as a collection for runoff water from melting snow uphill, where rock crops out and has little infiltration. The runoff collected in the ditch appears to flow downward to the glaciolacustrine silt sediments through well drained fill and granular soil layers. Taking into account the dry condition of the silt sediments at the lake level, it is apparent that there was not enough water to saturate the slope and generate excess pore pressure. Pictures, taken after slide occurrence, show that debris on the surface of the post slide geometry are mainly fill and granular materials.

The author believes that this failure occurred in two stages. In the first stage, the glaciolacustrine silt sediments underlying the fill and granular layer strain softened and flowed because of disintegration of soil structure. Upon increase of water content, breakage of inter-particle physicochemical bonds and elimination of soil suction occurred and led the glaciolacustrine silt sediment part of the slide to flow. In the second stage, fill and granular material, which are in a undercut condition, moved.

9.3 Recommendations for Further Studies

Based on results of this study and previous studies mentioned in the literature, the following recommendations are suggested for further studies:

More seismic cone penetration testing with pore pressure measurement (SCPTU) in soils known to be structured should be carried out to establish structure determining relationships for CPT. Due to poor literature about silty soils, special attention should be paid to these kind of deposits.

Specific gravity determination should be improved. Using the current practice, dissolution of soluble material from the solid phase causes possible errors in measurements.

Test procedure for soil water-characteristic curve determination should be modified. External volume change during the test is one of the shortcomings of the current practice.

Quantitative experiments should be carried out to further establish the role of the amorphous silica in soil structure.

Taking into account the bonded nature of structured soils and lack of significance of excess pore pressure generation in their behavior, there is need for comprehensive study on the creep behavior of structured soils.

Further one-dimensional consolidation tests at elevated stresses are required to better establish the deformational characteristics of structured soils.

Extensive triaxial testing using Penticton silt and other structured soils is necessary to better establish the contours of the state boundary and the peak strength envelope. Such experimental programs should include various levels of bonding, water content, and soil suction. Extensive test results is needed to establish values of soil structure parameter, Ω, for various structured soils.

Results of this study can have some significant implications for the emerging area of geo-environmental engineering and further studies is required to establish proper guidelines. From the mechanical stability point of view, as it was found in this study, saturation by organic fluids is not as critical as saturation with water. However, replacement of an organic contamination such as hydrocarbon contamination by water during environmental cleaning may cause mechanical instability in some soils.

References

Acar, Y. B. 1987. Discussion of "Time-dependent strength gain in freshly deposited or densified sand". American Society of Civil Engineers, ASCE, Journal of the Geotechnical Engineering Division, Volume 113, No. 2, pp. 171-173.

Acar, Y. B., and El-Tahir, E. A. 1986. Low strain dynamic properties of artificially cemented sand. American Society of Civil Engineers, ASCE, Journal of Geotechnical Engineering Division, Volume 112, No. 11, pp. 1001-1015.

Afifi, S. S., and Richart, F. E. ,Jr. 1973. Stress-history effects on shear modulus of soils. Japanese Society of Soil Mechanics and Foundation Engineering, Soils and Foundations, Volume 13, No. 1, pp. 77-95.

Airey, D. W. 1993. Triaxial testing of naturally cemented carbonate Soil. American Society of Civil Engineers, ASCE, Journal of Geotechnical Engineering Division, Volume 119, No. 9, pp. 1379-1398.

Aitchison, G. D. 1965. Moisture equilibria and moisture changes in soils beneath covered areas, A Synposium in Print, Butterworths, Australia, 278 p.

Allen, B. L. and Hajek, B. F. 1989. Chapter 5, Minerals in soil environments. Second Edition, Editors: Dixson, J. B. and Weed, S. B., The Soil Science Society of America, Madison, Wisconsin, U.S.A., pp. 199-278.

Alonso, E. E., Gens, A., and Josa, A., 1990. A constitutive model for partially saturated soils. Geotechnique, Volume 40, No. 3, pp. 405-430.

Anderson, D.G., and Stokoe, K. H. ,II 1978. Shear modulus, a time-dependent soil property. American Society for Testing and Materials, Dynamic Geotechnical Testing, ASTM STP 654, pp. 66-90.

Atkinson, J. H., and Bransby P. L. 1978. The mechanics of soils, an introduction to critical state soil mechanics. McGraw-Hill, 375 p.

B. C. Ministry of Environment, Lands, and Parks. 1979. Topographic map, Summerland-Salmon Arm. Map E82.062.3.4 (scale: 1/5000). Geographic Data B. C.

B. C. Ministry of Environment, Lands, and Parks. 1979. Topographic map, Summerland-Salmon Arm. Map E82.062.4.2 (scale: 1/5000). Geographic Data B. C.

B. C. Ministry of Environment, Lands, and Parks. 1987. Soils of the Okanagan and Similkameen Valleys. Map E82.062 (scale: 1/20000).

B. C. Ministry of Environment, Lands, and Parks. 1988. Soil drainage. Map E82.062 (scale: 1/20000).

B. C. Ministry of Environment, Lands, and Parks. 1989. Surficial material. Map E82.062 (scale: 1/20000).

B. C. Ministry of Transportation and Highways. 1975(a). Internal preliminary report regarding Okanagan Lake Park Slide. March 25th, 1975. Prepared by: B. Kern, Geotechnical and Materials Engineering, Thompson-Okanagan Regional Office, B. C. Ministry of Transportation and Highways.

B. C. Ministry of Transportation and Highways. 1975(b). Okanagan Lake Park Slide, seismic and resistivity survey. May 1975. Geotechnical and Materials Engineering, Thompson-Okanagan Regional Office, B. C. Ministry of Transportation and Highways.

B. C. Ministry of Transportation and Highways. 1975(c). Internal memo regarding Okanagan Lake Park sani-station and day use area. September 16, 1975. Geotechnical and Materials Engineering, Thompson-Okanagan Regional Office, B. C. Ministry of Transportation and Highways.

B. C. Ministry of Transportation and Highways. 1976. Internal memo regarding silt bluffs in Penticton, dated August 18, 1976. Geotechnical and Materials Engineering, Thompson-Okanagan Regional Office, B. C. Ministry of Transportation and Highways.

B. C. Ministry of Transportation and Highways. 1977. Internal memo regarding soil chemistry analyses of glaciolacustrine and colluvial silt deposits in Penticton area. Geotechnical and Materials Engineering, Thompson-Okanagan Regional Office, B. C. Ministry of Transportation and Highways.

Bishop, A. W. 1959. The principle of effective stress. Norwegian Geotechnical Institute, Oslo, Publication No. 32, pp. 1-4.

Boone, S. J. and Lutenegger, A. J. 1997. Carbonates and cementation of glacially derived cohesive soils in New York State and southern Ontario. Canadian Geotechnical Journal, Volume 34, pp. 534-550.

Bowles, J. E. 1986. Engineering properties of soils and their measurement. 3rd Edition. McGraw-Hill, 218 p.

Buchanan, R. G. 1977. Landforms and observed hazard mapping, South Thompson Valley, British Columbia. Geotechnical and Materials Branch, B. C. Ministry of Highways and Public Works, Victoria, British Columbia, 18 p.

Burland, J. B. 1990. On the compressibility and shear strength of natural clays. Geotechnique, Volume 40, No. 3, pp. 329-378.

Burland, J. B., Rampello, S., Georgiannou, V. N., and Calabresi, G. 1996. A laboratory study of the strength of four stiff clays. Geotechnique, Volume 46, No. 3, pp. 491-514.

Chanturiya, V. A., Vigdergauz, V. E., and Nedosekina T. V. 1996. Physical and chemical principles of oredressing. Journal of Mining Science, Volume 32, No. 1. pp. 63-69.

Church , B. N., 1980. Geology of the Kelowna Tertiary outlier (west half) (NTS 82E). B. C. Ministry of Energy, Mines, and Petroleum Resources, Preliminary Map 39.

Church , B. N., 1981. Geology of the Kelowna Tertiary outlier (east half) (NTS 82E). B. C. Ministry of Energy, Mines, and Petroleum Resources, Preliminary Map 45.

Cicolella, A., and Picarelli, L. 1990. Decadimento meccanico di una tipica argilla a scaglie di elevata plasticita. Rivista Italiana di Geotecnica, 24: 5-23.

Clough, G. W., Sitar, N., Bachus, C., and Rad, N. S. 1981. Cemented sands under static loading. American Society of Civil Engineers, ASCE, Journal of Geotechnical Engineering Division, Volume 107, No. GT6, pp. 799-817.

Clough, G. W., Iwabuchi, J., Rad, N. S., and Kuppusamy, T. 1989. Influence of Cementation on Liquefaction of Sands. American Society of Civil Engineers, ASCE, Journal of Geotechnical Engineering Division, Volume 115, No. 8, pp. 1102-1117.

Coop, M. R. 1990. The mechanics of uncemented Carbonate Sands. Geotechnique, Volume 40, No. 4, pp. 607-626.

Coop, M. R., and Atkinson, J. H. 1993. The mechanics of cemented carbonate sands. Geotechnique, Volume 43, No. 1, pp. 53-67.

Coop, M. R., and Lee, I. K. 1993. The behavior of granular soils at elevated stresses. Predictive Soils Mechanics, Editors: Houlsby, G. T. and Schofield, A. N., Thomas Telford, London, pp. 186-198.

Coop, M. R., Atkinson, J. H., and Taylor, R. N. 1995. Strength and stiffness of structured and unstructured soils. Proceedings of the 11th European Conference on Soil Mechanics and Foundation Engineering, Copenhagen, Volume 1, pp. 1.55-1.62.

Coop, M. R., and Lee J. K. 1995. The influence of pore water on the mechanics of granular soils. Proceedings of the 11th European Conference on Soil Mechanics and Foundation Engineering, Copenhagen, Volume 1, pp. 1.63-1.72.

Cuccovillo, T., and Coop, M. R. 1993. The influence of bond strength on the mechanics of carbonate soft rocks. Geotechnical Engineering of Hard Soils-Soft Rocks, Athens, Balkema, Rotterdam, pp. 447-455.

Cui, Y. J. and Delage, P. 1996. Yielding and plastic behaviour of an unsaturated compacted silt. Geotechnique, Volume 46, No. 2, pp. 291-311.

Daly, R. A. 1915. A geological reconnaissance between Golden and Kamloops, British Columbia, along the Canadian Pacific Railway: Canada Geological Survey Memo No. 68, 260 p.

Dawson, G M., 1878. On the surficial geology of British Columbia. Geological Society of London. Quarterly Journals, Volume 34, pp. 89-123.

Dawson, G M., 1879. Preliminary report on the physical and geological features of the southern portion of the interior of British Columbia. Geological Society of Canada. Rept. of Prog. 1877-1878, pp. B 1-173.

Dawson, G M., 1891. On the later physiographical geology of the Rocky Mountain region in Canada, with special reference to changes in elevation and to the history of the glacial period. Proceedings and Transactions of the Royal Society of Canada. Volume 8. Section 4 pp. 3-74.

Denisov, N. Y., and Reltov, B. F. 1961. The influence of certain processes on the strength of soils. Proceedings of the 5th ICSMFE, Volume 1, pp. 75-78.

Department of Energy, Mines, and Resources. 1978. Soils of the Penticton map area (NTS 82E), Map E82/12 (scale: 1/50000). Surveys and Mapping Branch, Department of Energy, Mines, and Resources.

Dudas, M. J. and Harward, M. E. 1971. Effect of dissolution treatment on standard and soil clays. Proceedings, Soil Science Society of America, Volume 35, No. 1, pp. 134-140.

Dupas, J. M., and Pecker A. 1979. Static and dynamic properties of sand-cement. American Society of Civil Engineers, ASCE, Journal of the Geotechnical Engineering Division, Volume 105, No. 3, pp. 419-436.

Dusseault, M. B., and Morgenstern, N. R. 1979. Locked sands. Q. J. Eng. Geol., 12, pp. 117-131.

Eaton, A. D., Clesceri, L. S., and Greenberg, A. E. 1995. Standard methods for the examination of water and wastewater. 19th edition. American Public Health Association. pp. 3-33-3-39.

Environment Canada. 1991. Canadian Climate Normals. Temperature and Precipitation, 1941-1990, Penticton A Station, British Columbia. Atmospheric Environment Services, Ottawa, Canada.

Environment Canada. 1991. Canadian Climate Normals. Temperature and Precipitation, 1916-1990, Summerland CDA Station, British Columbia. Atmospheric Environment Services, Ottawa, Canada.

Escario, V., and Saez, J. 1986. The shear strength of partly saturated soils. Geotechnique, Volume 36, No. 3, pp. 453-456.

Eslaamizaad, S. and Robertson, P. K. 1996(a). A framework for in-situ determination of sand compressibility. Proceedings of the 49th Canadian Geotechnical Conference, St. John's, Newfoundland, Canada.

Eslaamizaad, S. and Robertson, P. K. 1996(b). Seismic cone penetration test to identify cemented sands. Proceedings of the 49th Canadian Geotechnical Conference, St. John's, Newfoundland, Canada.

Evans, S. G., and Buchanan, R. G. 1976. Some aspects of natural slope stability in the silt deposits near Kamloops. B. C. Proceedings, 29th Canadian Geotechnical Conference, Vancouver, B. C., 57 p.

Evans, S. G. 1982. Landslides and surficial deposits in urban areas of British Columbia: a review. Canadian Geotechnical Journal, Volume 19, pp. 269-288.

Fanning, D. S., Keramidas, V. Z., El-Desoky, M. A. 1989. Chapter 12, Minerals in soil environments. Second Edition, Editors: Dixson, J. B. and Weed, S. B., The Soil Science Society of America, Madison, Wisconsin, U.S.A., pp. 551-634.

Flint , R. F. 1935. White silt deposits in the Okanagan Valley, B. C. Transcripts of the Royal Society of Canada, Section IV, p. 107.

Fredlund, D. G. and Morgenstern, N. R. 1977. Stress state variables for unsaturated soils. Journal of Geotechnical Engineering Division, American Society of Civil Engineers, ASCE, Volume 107 (GT5), pp. 447-466.

Fredlund, D. G., Morgenstern, N. R., and Widger, R. S. 1978. The shear strength of unsaturated soils. Canadian Geotechnical Journal, Volume 15, No. 3, pp. 313-321.

Fredlund, D. G., and Rahardjo, H. 1993. Soil mechanics for unsaturated soils. John Wiley and Sons Inc., New York, USA, 517 p.

Fredlund, D. G., and Xing, A. 1994. Equation for the soil-water characteristic curve. Canadian Geotechnical Journal, Volume 31, pp. 521-532.

Fulton, R. J. 1965. Silt deposition in late-glacial lakes of southern British Columbia. American Journal of Science, Volume 263, pp. 553-570.

Fulton, R. J. 1969. Glacial lake history, southern Interior Plateau, British Columbia. Geological survey of Canada, Paper # 69-37, 14 p.

Fulton, R. J. 1971. Radiocarbon geochronology of southern British Columbia. Geological Survey of Canada, Paper # 71-37, 28 p.

Fulton, R. J. 1975. Quaternary geology and geomorphology, Nicola-Vernon area, British Columbia. Geological Survey of Canada, Memoir 380.

Fulton, R. J., and Smith, G. W. 1978. Late Pleistocene stratigraphy of south-central British Columbia. Canadian Journal of Earth Science, Volume 15, pp. 971-980.

Geertsema, M. and Schwab, J. W. 1997. Retrogressive flowslides in the Terrace-Kitimat area, British Columbia: from early post-deglaciation to present and implications for future slides. Proceedings, 11th Vancouver Geotechnical Society Symposium, Foresty Geotechnique and Resource Engineering, pp. 115-133.

Geological Survey of Canada. 1982. Geological map of British Columbia, Map 932A, 2nd Edition. Department of Mines and Technical Services.

Geo-Slope International Ltd. 1995. Computer program SLOPE/W for stability analysis. User's Giude, Version 3, Calgary, Alberta, Canada.

Gilboy, G. 1927. The compressibility of sand-mica mixtures. Proceedings, American Society of Civil Engineers, ASCE, pp. 555-568.

Golder Associates Consulting Geotechnical Engineers. 1980. Report to the corporation of the district of Summerland on stage II and III program to assist the development of municipal policy for subdivision and building construction in areas of potentially unstable soils. Golder Associates, Consulting Geotechnical Engineers, 6 p.

Guerriero, G. 1995. Modellazione sperimentale del comportamento meccanico di terreni in colata. Ph.D. Thesis, Universita di Napoli "Federico II".

Hashimoto, I. and Jackson, M. L. 1960. Rapid dissolution of allophane and kalinite-halloysite after dehydration. Clays and Clay Minerals, Volume 7, pp. 102-113.

Head, K. H. 1982. Manual of soil laboratory testing, volume 2, permeability, shear strength, and compressibility. ELE International Limited, Great Britain, 747 p.

Henderson, J. H., Syers, J. K., and Jackson, M. L. 1970. Quartz dissolution as influenced by pH and the presence of a disturbed surface layer." Isr. J. Chemistry, 8, pp. 357-372.

Hight, D. W., Georgiannou, V. N., and Ford, C. J. 1994. Characterization of clayey sands. Behavior of Offshore Structures, Volume 1: Geotechnics, Edited by Chryssostomidis, C., Triantafyllou, M. S., Whittle, A. J., and Hoo Fatt, M. S., Massachusetts Institute of Technology, Pergamon, pp. 321-340.

Holland, S. S. 1976. Landforms of British Columbia, a physiographic outline. B. C. Department of Mines and Petroleum Resources. Bulletin 48, 138 p.

Huang, J. T., and Airey, D. W. 1993. Effects of cement and density on an artificially cemented sand. Geotechnical Engineering of Hard Soils - Soft Rocks, Athens, Balkema, Rotterdam, pp. 553-560.

Huang, J. T., and Airey D. W. 1994. Discussion of "The mechanics of cemented carbonate sands" by Coop, M. R., and Atkinson, J. H.. Geotechnique, Volume 44, No. 3, pp. 533-537.

Hvorslev, M. J. 1937. Uber die Festigkeitseigenschaften gestorter bindiger Boden Ingeniorvidenskabelige Skrifter A No. 45.

Ishihara, K., Sodekawa, M., and Tanaka Y. 1978. Effects of overconsolidation on liquefaction characteristics of sands containing fines. American Society for Testing and Materials, Dynamic Geotechnical Testing, ASTM STP 654, pp. 246-264.

Karlsrud, K., Aas, G., Gregersen, O. 1984. Can we predict landslide hazards in soft sensitive clays? Summary of Norwegian practice and experiences. 4th International Symposium on Landslides in Conjunction with 37th Canadian Geotechnical Conference, Toronto, Ontario, Canada, pp. 107-130.

Kavvadas, M. 1995. A framework for the mechanical behavior of bonded soils. Proceedings of the 11th European Conference on Soil Mechanics and Foundation Engineering, Copenhagen, Volume 3, pp. 3.113-3.118.

Kelowna Geology Committee. 1995. Geology of the Kelowna area and origin of the Okanagan Valley British Columbia. Kelowna Geology Committee, 181 p.

Klohn Leonoff. 1992. West bench/Sage Mesa area geotechnical hazards review. 80 p.

Lamb, T. W. 1956. The storage of oil in an earth reservoir. Journal of the Boston Society of Civil Engineers, Volume 43, No. 3, pp. 111-173.

Lee, I. K., and Coop, M. R. 1995. The intrinsic behavior of a decomposed granite soil." Geothechnique, Volume 45, No. 1, pp. 117-130.

Lee, K. L. 1977. Adhesion bonds in sands at high pressures. American Society of Civil Engineers, ASCE, Journal of the Geotechnical Engineering Division, Volume 103, No. 8, pp. 908-913.

Leonards, G. A., and Ramiah, B. K. 1959. Time effects in the consolidation of clay. ASTM Special Technical Publication, No. 254, pp. 116-130.

Leroueil, S., and Vaughan, P. R. 1990. The general and congruent effects of structure in natural soils and weak rocks. Geotechnique, Volume 40, No. 3, pp. 467-488.

Leroueil, S. 1992. A framework for the mechanical behavior of structured soils, from soft clays to weak rocks. Proceedings of US-Brazil NSF Geotechnical Workshop on Applicability of Classical Soil Mechanics Principles to Structured Soils, Belo Horizonte, pp. 107-128.

Leroueil, S., and Marques, M. E. S. 1996. Importance of strain rate and temperature effects in geotechnical engineering. Session on Measuring and Modelling Time Dependent Soil Behavior, ASCE Convension, Washington D.C., Geotechnical Special Publication 61, 60 p.

Leroueil, S. 1997. Critical state soil mechanics and the behavior of real soils. Symposium on Recent Developments in Soil and Pavement Mechanics, Rio de Janeiro, Brazil, pp. 41–80.

Lew, H. S. and Reichard, T. W. 1978. Prediction of strength of concrete from maturity. Accelerated Strength Testing, ACI Publication SP-56, American Concrete Institute, Detroit, pp. 229-248.

Lum, K. K. Y. 1977. Stability of the Kamploops silt bluffs. M.A.Sc. Thesis, The University of British Columbia, Vancouver, Canada, 114 p.

Lunne, T., Robertson P. K., and Powell, J. J. M. 1997. Cone penetration testing in geotechnical practice. E & FN Spon, an imprint of Routledge, London, U. K., 312 p.

Maatouk, A., Leroueil, S., and La Rochelle, P. 1995. Yielding and critical state of a collapsible unsaturated silty soil. Geotechnique, Volume 45, No. 3, pp. 465-477.

MacGregor, J. G. 1992. Reinforced concrete, mechanics and design. 2nd Edition, Prentice Hall, New Jersey, 848 p.

Mathews, W. H. 1944. Glacial lakes and ice retreat of south-central British Columbia. Royal Society of Canada Transactions, 3rd Series, Volume 38, Section 4, pp. 39-57.

Matyas, E. L., and Radhakrishna, H. S. 1968. Volume change characteristics of partially saturated soils. Geotechnique, Volume 18, No. 4, pp. 432-448.

McKyes, E., Sethi, A., and Yong, R. N. 1974. Amorphous coatings on particles of sensitive clay soils. Clays and Clay Minerals, Volume 22, pp. 427-433.

McKeague, J. A. 1978. Manual on soil sampling and methods of analysis. 2nd Edition. Canadian Society of Soil Science, 212 p.

Mesri, G., Feng, T. W., and Benak, J. M. 1990. Postdensification penetration resistance of clean sands. American Society of Civil Engineers, ASCE, Journal of the Geotechnical Engineering Division, Volume 116, No. 7, pp. 1095-1115.

Meyer, C., and Yenne, K. A. 1940. Notes on mineral assemblage of the "white silt" terracesin the Okanagan Valley, British Columbia. Journal of Sedimentary Petrology, Volume 10, No. 1, pp. 8-11.

Mitchell, J. K. 1993. Fundamentals of soil behavior. John Wiley & Sons, Inc., New York, N. Y., 437 p.

Mitchell, J. K., and Solymar, Z. V. 1984. Time-dependent strength gain in freshly deposited or densified sand. American Society of Civil Engineers, ASCE, Journal of the Geotechnical Engineering Division, Volume 110, No. 11, pp. 1559-1576.

Mitchell, J. K. 1986. Practical problems from surprising soil behavior. American Society of Civil Engineers, ASCE, Journal of the Geotechnical Engineering Division, Volume 112, No. 3, pp. 259-289.

Miura, N., and Yamanouchi, T. 1973. Compressibility and drained shear characteristics of a sand under high confining pressures. Technology Reports of the Yamaguchi University, Volume 1, No. 2, PP. 271-290.

Miura, N., and Yamanouchi, T. 1978. Discussion on "Adhesion bonds in sands at high pressure". American Society of Civil Engineers, ASCE, Journal of the Geotechnical Engineering Division, Volume 104, No. 12, pp. 1523-1525.

Morgenstern, N. R., and Tchalenko, J. S. 1967. Microscopic structures in kaolin subjected to direct shear. Geotechnique, Volume 17, pp. 309-328.

Morgenstern, N. R. 1992. The evaluation of slope stability: A 25 year perspective. in Stability and Performance of slopes and Embankments – II, American Society of Civil Engineers, ASCE, Geotechnical Special Publication, No. 31, pp. 1-26.

Mossop, G. D. 1980. Geology of the Athabasca oil sands. AAAS, Science, Volume 207, pp. 145-152.

Nagaraj, T. S., Pandian, N. S., and Narasimha Raju, P. S. R. 1998. Compressibility behavior of soft cemented soils. Geotechnique, Volume 48, No. 2, pp. 281-287.

Nasmith, H. 1962. Late glacial history and surficial deposits of the Okanagan Valley, B. C. B. C. Department of Mines and Petroleum Resources, Queen's Printer, B. C., Bulletin No. 46.

Newman, K. and Newman, J. B. 1972. Failure theories and design criteria for plain concrete. Part 2 in M. Te'eni, (ed.), Solid Mechanics and Engineering Design, Wiley-Interscience, New York, pp. 83/1-83/33.

Nyland, D., and Miller G. E. 1977. Geotechnical hazards and urban development of silt deposits in the Penticton area. B. C. Ministry of Highways and Public Works, Geotechnical and Materials Branch, Victoria, British Columbia, 35 p.

Oberg, A-L. and Sallfors, G. 1995. A rational approach to the determination of shear strength parameters of unsaturated soils. Proceedings, 1st International Conference on Unsaturated Soils, Paris, Volume 1, pp. 151-158.

Oberg, A-L. 1997. Matrix suction in silt and sand slopes, significance and practical use in stability analysis, Ph.D. Dissertation, Department of Geotechnical Engineering, Chalmers University of Technology, Goteborg, Sweden, 160 p.

Penticton Herald. 1942. $900 property damage as three "tidal" waves hit Summerland's lakefront. Penticton Herald, Thursday August 6th, 1942.

Penticton Herald. 1942. It lifted the wharf like matchwood. Penticton Herald, Thursday August 6th, 1942.

Penticton Herald. 1942. Two Naramata residents escape mud, clay slide. Penticton Herald, Thursday August 6th, 1942.

Quigley, R. M. 1976. Mineralogy, chemistry and structure, Penticton and South Thompson silt deposits. Faculty of Engineering Science, The University of Western Ontario, London, Canada, 17 p.

Quigley, R. M. 1980. Geology, mineralogy and geochemistry of Canadian soft soils: a geotechnical perspective. Canadian Geotechnical Journal, Volume 17. No. 2, pp. 261-285.

Rad, N. S. 1982. Static and dynamic behavior of cemented sands. Ph.D. Dissertation. Stanford University, Stanford, California.

Rad, N. S. 1984. Effect of cementation on penetration resistance of sand. Fugro Postdoctoral Report No. GE-84-01, Louisiana State University, Baton Rouge, La., 222 pp.

Rad, N. S., and Tumay M. T. 1986. Effect of cementation on the cone penetration resistance of sand: a model study. ASTM, Geotechnical Testing Journal, Volume 9, No. 3, pp. 117-125.

Rendulic, L. (1937) Ein Grundgesetz der Tonmechanikund sein Experementeller Beweis. Der Bauingeneur 18.

Richart, F. E., Brandtzaeg, A., and Brown R. L. 1928. A study of the failure of concrete under combined compressive stresses. Bulletin 185, University of Illinois Engineering Experiment Station, Urbana, Ill., 104 p.

Robertson, P. K. 1990. Soil classification using the cone penetration test. Canadian Geotechnical Journal, Volume 27, pp. 151-158.

Robertson, P. K. and Campanella, R. G. 1983. Interpretation of cone penetration tests: Part I: Sand. Canadian Geotechnical Journal, Volume 20, No. 4, pp. 718-733.

Robertson, P. K. and Ghionna, V. N. 1987. Capability of in-situ testing. Conferenze di Geotecnica di Torino, XIII CICLO, 105 p.

Roscoe, K. H., Schofield, A. N., and Wroth, C. P. 1958. On yielding of soils. Geotechnique, Volume 8, No. 1, pp. 22-53.

Schmertmann, J. H. 1987. Discussion of "Time-dependent strength gain in freshly deposited or densified sand". American Society of Civil Engineers, ASCE, Journal of the Geotechnical Engineering Division, Volume 113, No. 2, pp. 173-175.

Schmertmann, J. H. 1991. The mechanical aging of soils. American Society of Civil Engineers, ASCE, Journal of the Geotechnical Engineering Division, ASCE, Volume 117, No. 9, pp. 1288-1330.

Schwertmann, U., and Taylor, R M. 1989. Chapter 8, Minerals in soil environments. Second Edition, Editors: Dixson, J. B. and Weed, S. B., The Soil Science Society of America, Madison, Wisconsin, U.S.A., pp. 379-438.

Seed, H. B. 1979. Soil liquefaction and cyclic mobility evaluation for level ground during earthquakes. American Society of Civil Engineers, ASCE, Journal of the Geotechnical Engineering Division, Volume 105, No. 2, pp. 201-255.

Shaw, J. 1975. Sedimentary succession in Pleistocene ice-marginal lakes. Society of Econ. Paleo. and Min., Special Publication No. 23, Editors: Jopling, A. V., and MacDonald, B. C.

Sobkowicz, J., and Coulter. 1992. Highway 97 – Bentley road to Okanagan Lake Park, functional design – geotechnical considerations. Draft Document, Thurber Engineering Limited, Victoria, B. C., Canada.

Sposito, G. 1989. The chemistry of soils. Oxford University Press, New York, 277 p.

Tasuji, M. E. Slate, F. O., and Nilson A. H. 1978. Stress-strain response and fracture of concrete in biaxial loading. Journal of the American Concrete Institute, Volume 75, pp 306-312.

Tavenas, F. 1984, Landslides in Canadian sensitive clays – a state-of-the-art. 4th International Symposium on Landslides in Conjunction with 37th Canadian Geotechnical Conference, Toronto, Ontario, Canada, pp. 141-153.

Templemann-Kluit, D. J., 1989. Geological map with mineral occurrences, fossil localitities, radiometric ages and gravity field for Penticton map area (NTS 82E), southern British Columbia. Geological Survey of Canada, O. F. 1969.

Terzaghi, K. 1931. The influence of elasticity and permeability on the swelling of two-phase systems. In: Alexander J. (Editor), Colloid Chemistry, Volume III, Chemical Cataloge Co., New York, pp. 65-88.

Toll, D. G. 1990. A framework for unsaturated soil behavior, Geotechnique, Volume 40, No. 1, pp. 31-44.

Touhidi-Baghini, A. 1998. Absolute permeability of McMurray formation oil sands at low confining stresses. Ph.D. Dissertation, Geotechnical Engineering Group, Department of Civil and Environmental Engineering, University of Alberta, Edmonton, AB, Canada.

U. S. EPA. 1983. Methods for chemical analysis of water and wastewater. United States Environmental Protection Agency.

U. S. EPA. 1986. Test methods for evaluating solid waste, physical/chemical methods. 3rd Edition. United States Environmental Protection Agency.

Vanapalli, S. K., Fredlund, D. G., Pufhal, D. E., and Clifton, A. W. 1996. Model for prediction of the shear strength with respect to soil suction. Canadian Geotechnical Journal, Volume 33, No. 3, pp. 379-392.

Vigil, G., Xu, Zhenghe, Steinberg, S., and Israelachvili, J. 1994. Interactions of silica surfaces. Journal of Colloid and Interface Science, 165, pp. 367-385.

Welton, J. E. 1950. SEM petrology atlas. The American Association of Petroleum Geologists, Tulsa, Oklahoma, U. S. A., 237 p.

Wheeler, S. J., and Sivakumar, V. 1993. Development and application of a critical state model for unsaturated soil. Predictive Soil Mechanics, Editors: Houlsby, G. T. and Schofield, A. N., Thomas Telford, London, U. K., pp. 709-728.

Wheeler, S. J., and Sivakumar, V. 1995. An elasto-plastic critical state framework for unsaturated soil. Geotechnique, Volume 45, No. 1, pp. 35-53.

Whitman, R. V., Miller, E. T., and Moore, P. J. 1964. Yielding and locking of confined sand. American Society of Civil Engineers, ASCE, Journal of Soil Mechanic and Foundation Engineering Division, Volume 90, No. 4, pp. 57-84.

Wilson, R. G. 1985. A stability analysis of a glaciolacustrine silt bluff slope, Kamploops, British Columbia. B.A.Sc. Thesis, The University of British Columbia, Vancouver, Canada, 39 p.

APPENDIX A

Maps of the Surficial Deposits of Late Glacial and Recent Age of the Okanagan Valley

Note:

Surficial deposits of late glacial and Recent age for southern and northern Okanagan Valley, adapted from Nasmith (1962), are shown in Map A-2.5-A and B, respectively. These maps can be found in the pocket on the inside back cover of the thesis.

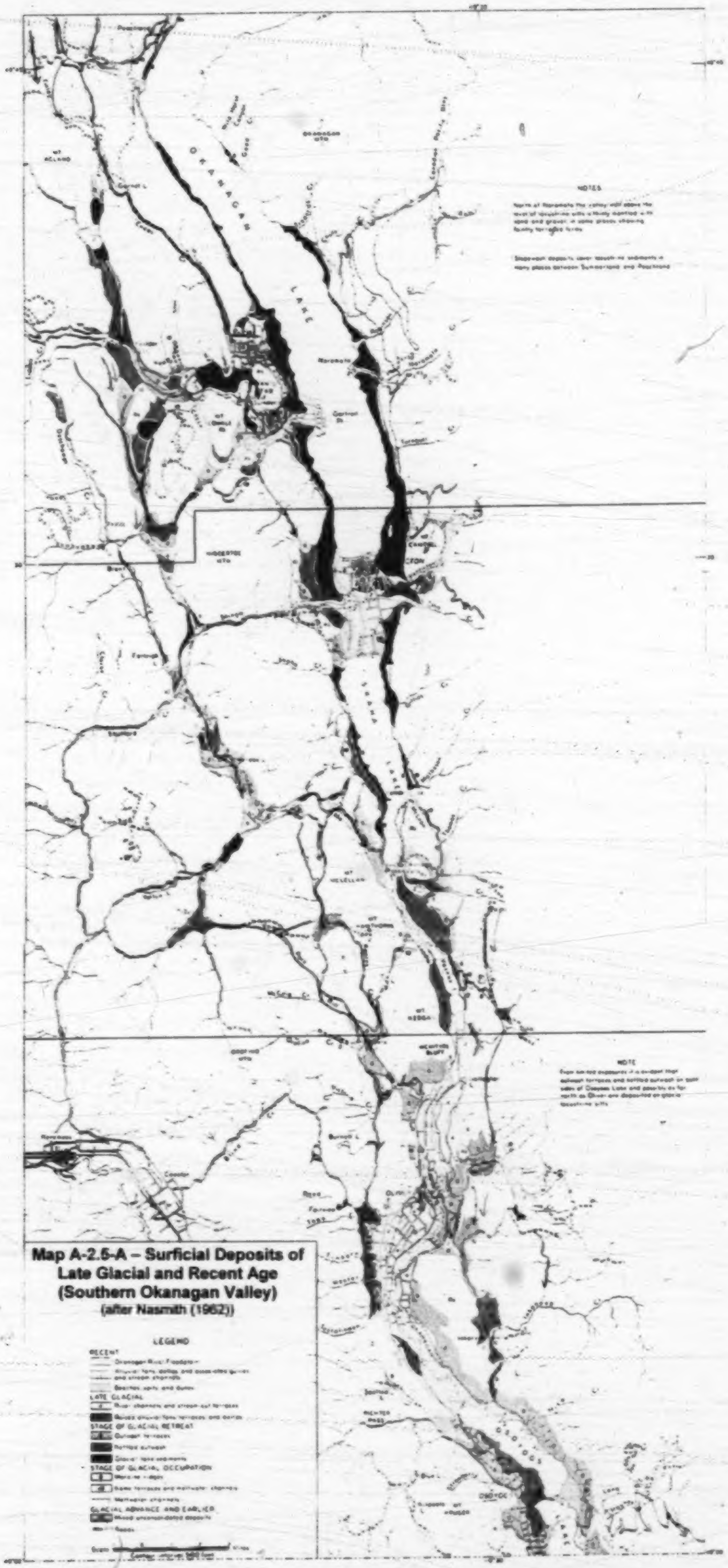

Map A-2.5-A – Surficial Deposits of Late Glacial and Recent Age (Southern Okanagan Valley)

(after Nasmith (1962))

LEGEND

RECENT

Okanagan River floodplain

Alluvial fans, deltas, and associated gullies and stream channels

Beaches, spits and dunes

LATE GLACIAL

River channels and stream-cut terraces

Raised alluvial fans, terraces and deltas

STAGE OF GLACIAL RETREAT

Outwash terraces

Pitted outwash

Glacial lake sediments

STAGE OF GLACIAL OCCUPATION

Moraine ridges

Kame terraces and meltwater channels

Meltwater channels

GLACIAL ADVANCE AND EARLIER

Mixed unconsolidated deposits

Roads

Scale Miles

Contour interval 500 feet

NOTES

North of Naramata the valley wall above the level of lacustrine silts is thinly mantled with sand and gravel in some places showing faintly terraced forms.

Slopewash deposits cover lacustrine sediments in many places between Summerland and Peachland.

NOTE

From exposed sections it is evident that outwash terraces and kettled outwash on both sides of Osoyoos Lake and possibly as far north as Oliver are deposited on glacial lacustrine silts.

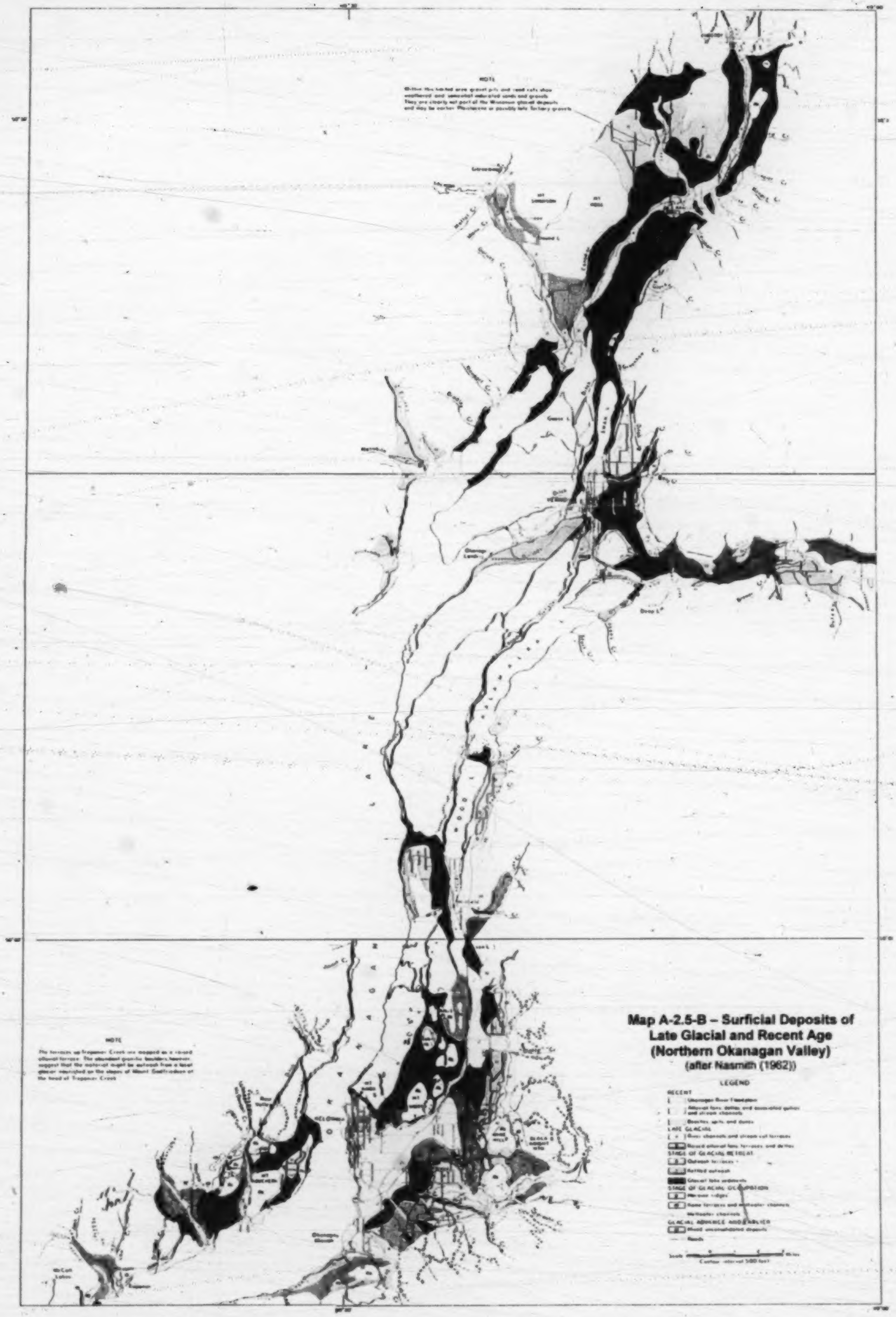

Map A-2.5-B – Surficial Deposits of Late Glacial and Recent Age (Northern Okanagan Valley)

(after Nasmith (1962))

NOTE
Within the hatched area gravel pits and road cuts show weathered and somewhat indurated sands and gravels. They are clearly not part of the Wisconsin glacial deposits and may be earlier Pleistocene or possibly late Tertiary gravels.
NOTE
The terraces up Trepanier Creek are mapped as a raised alluvial terrace. The abundant granite boulders, however, suggest that the material might be outwash from a local glacier nourished on the slopes of Mount Gottfriedsen at the head of Trepanier Creek.
OKANAGAN
KELOWNA
LEGEND
RECENT
Okanagan River Floodplain
Alluvial fans, deltas and associated gullies and stream channels
Beaches, spits and dunes
LATE GLACIAL
River channels and stream cut terraces
Raised alluvial fans, terraces and deltas
STAGE OF GLACIAL RETREAT
Outwash terraces
Pitted outwash
Glacial lake sediments
STAGE OF GLACIAL OCCUPATION
Moraine ridges
Kame terraces and meltwater channels
Meltwater channels
GLACIAL ADVANCE AND EARLIER
Mixed unconsolidated deposits
Roads
Scale
Miles
Contour interval 500 feet

APPENDIX B

One Dimensional Consolidation Test Results

Note:

Details of the one dimensional consolidation tests can be found in Chapter Six.

Figure B-6.3-A(a) - One Dimensional Consolidation Test Results
Series A, Okanagan Lake Park Slide Site Specimens

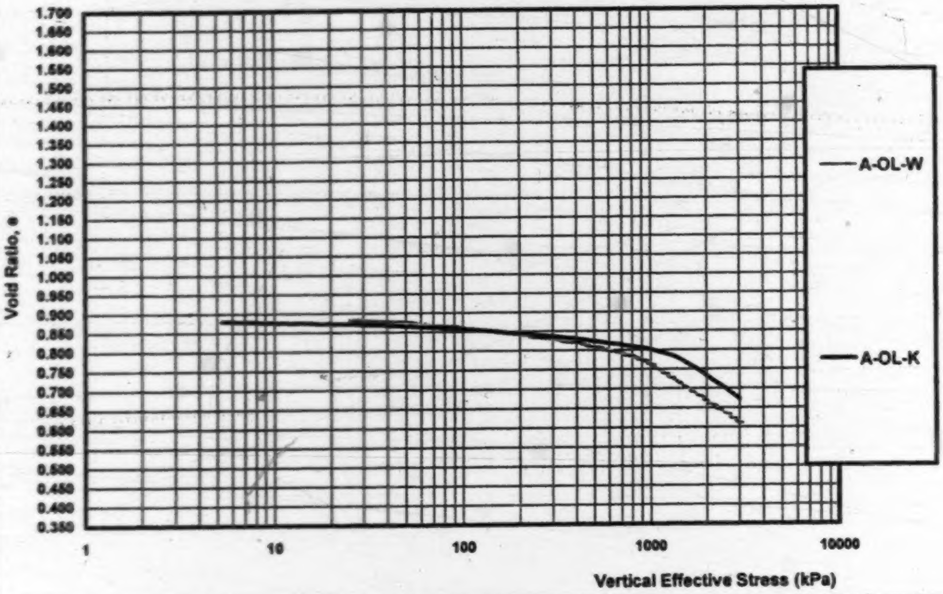

Figure B-6.3-A(b) - One Dimensional Consolidation Test Results
Series A, Koosi Creek Slide Site Specimens

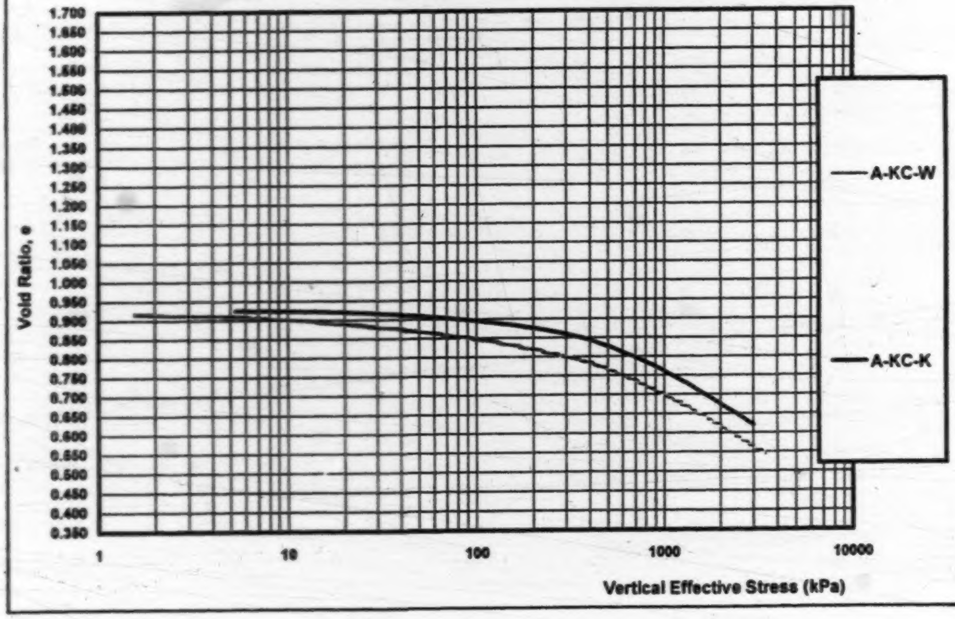

Figure B-6.3-B(a) - One Dimensional Consolidation Test Results
Series B, Okanagan Lake Park Slide Site Specimens

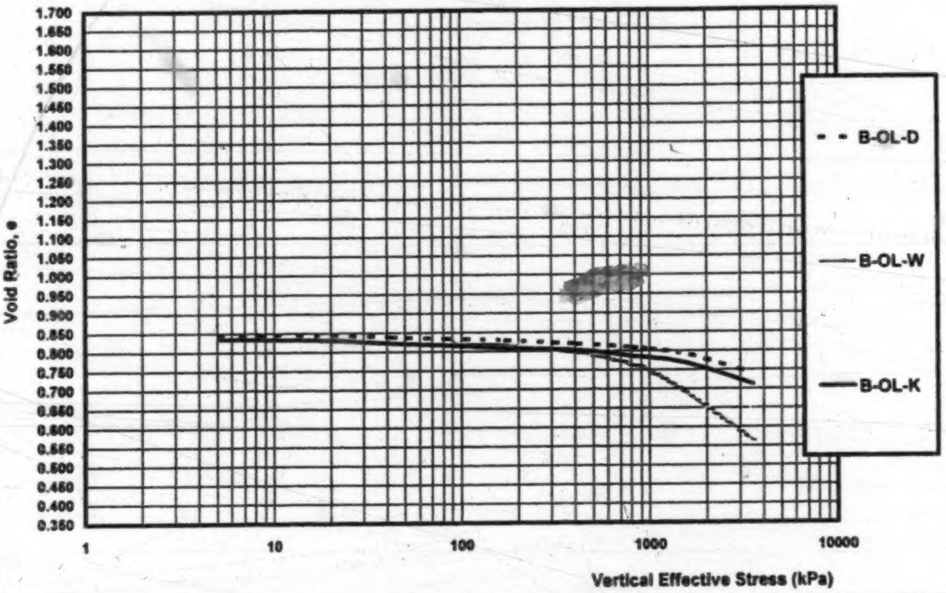

Figure B-6.3-B(b) - One Dimensional Consolidation Test Results
Series B, Koosi Creek Slide Site Specimens

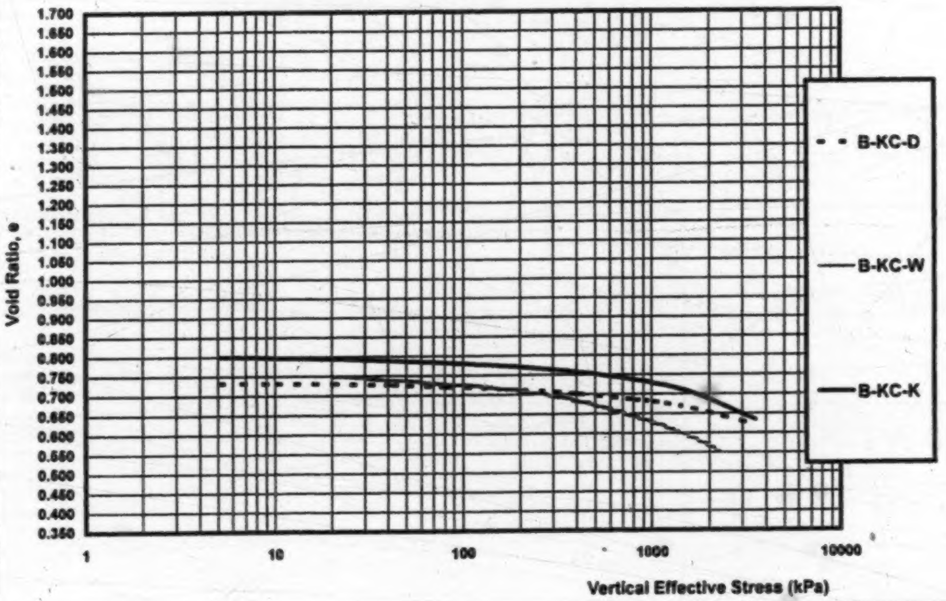

Figure B-6.3-C(a) - One Dimensional Consolidation Test Results
Series C, Okanagan Lake Park Slide Site Specimens

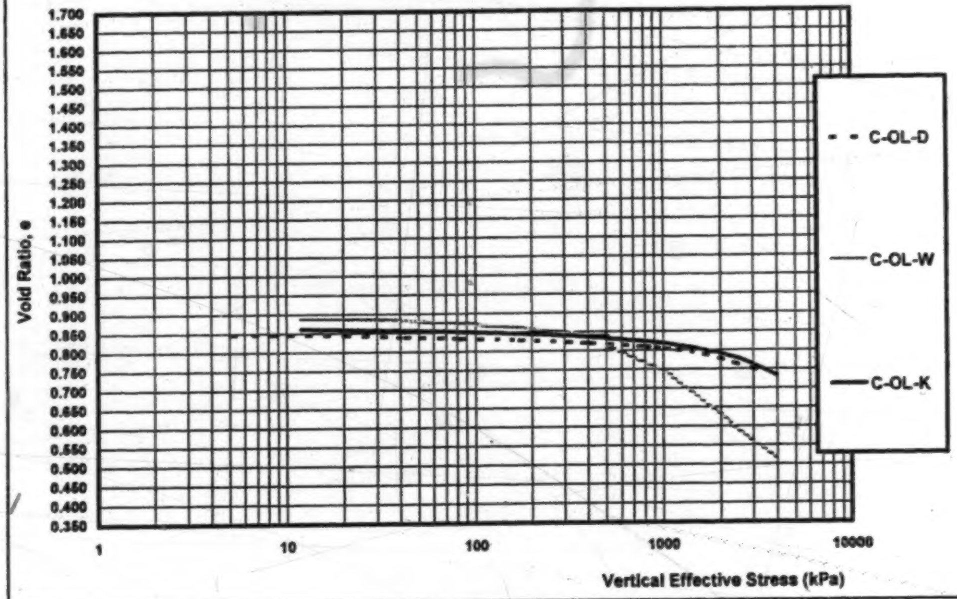

Figure B-6.3-C(b) - One Dimensional Consolidation Test Results
Series C, Koosi Creek Slide Site Specimens

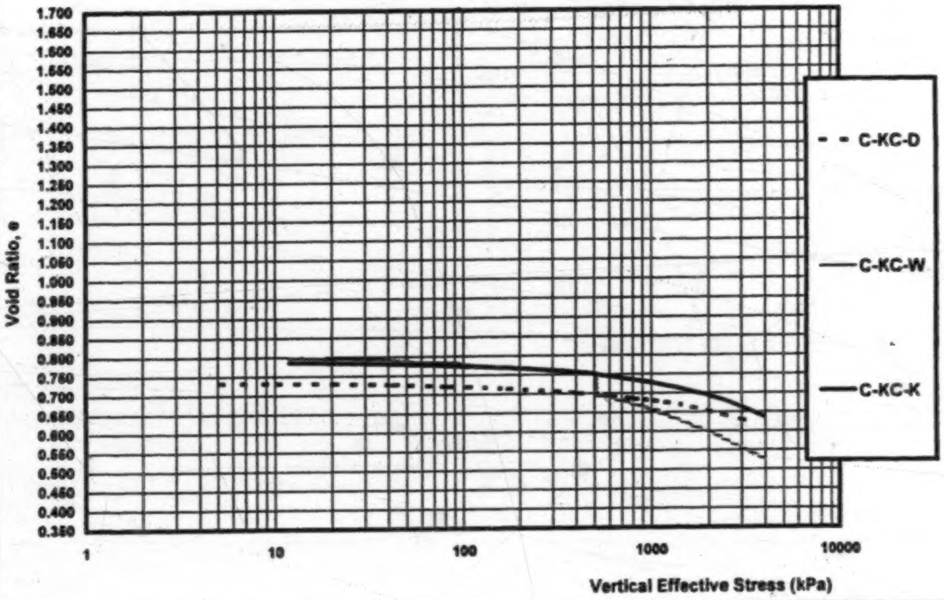

Figure B-6.3-D(a) - One Dimensional Consolidation Test Results
Series D, Okanagan Lake Park Slide Site Specimens

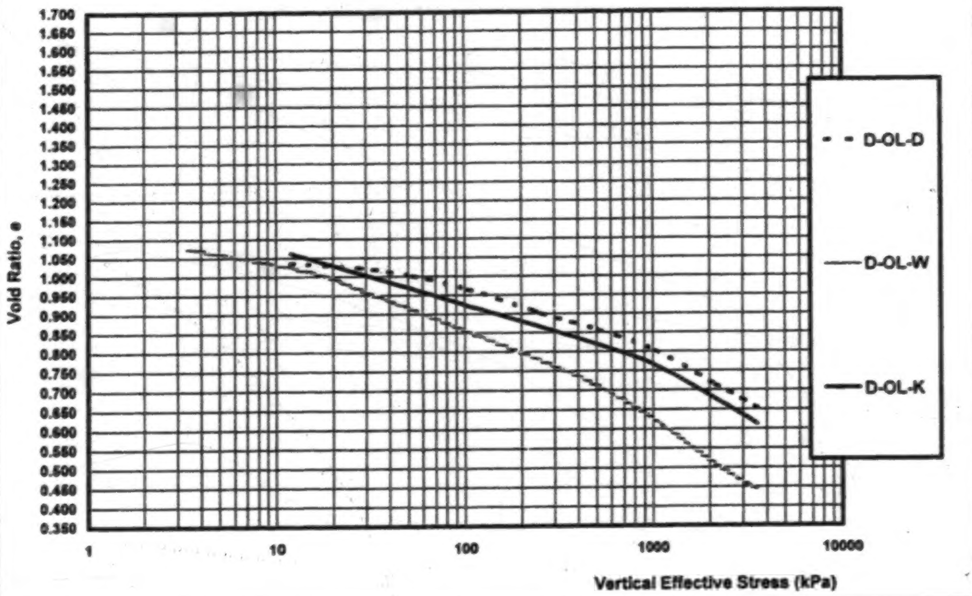

Figure B-6.3-D(b) - One Dimensional Consolidation Test Results
Series D, Koosi Creek Slide Site Specimens

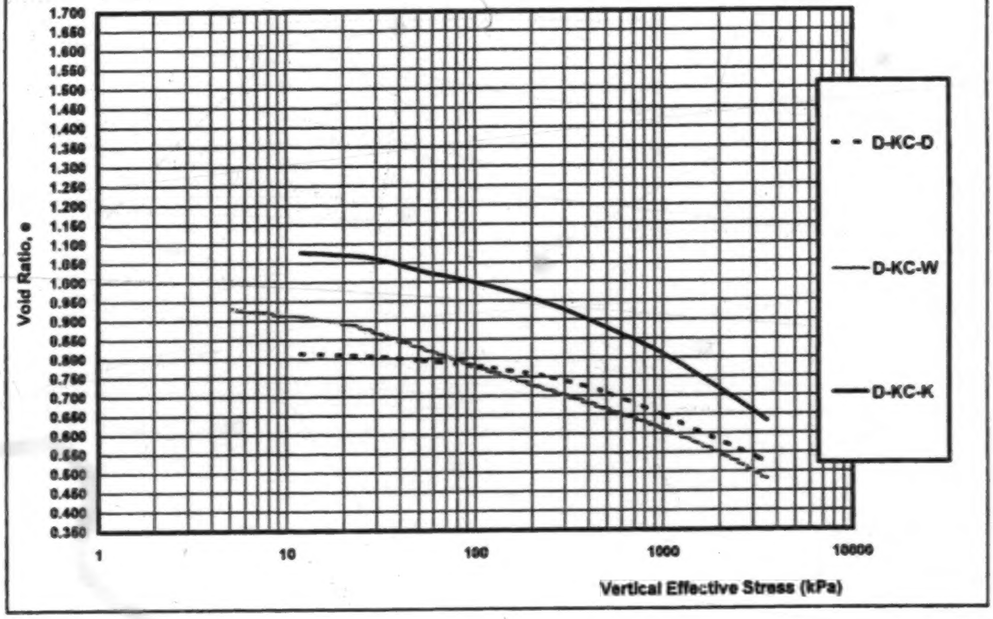

Figure B-6.3-E(a) - One Dimensional Consolidation Test Results
Series E, Okanagan Lake Park Slide Site Specimens

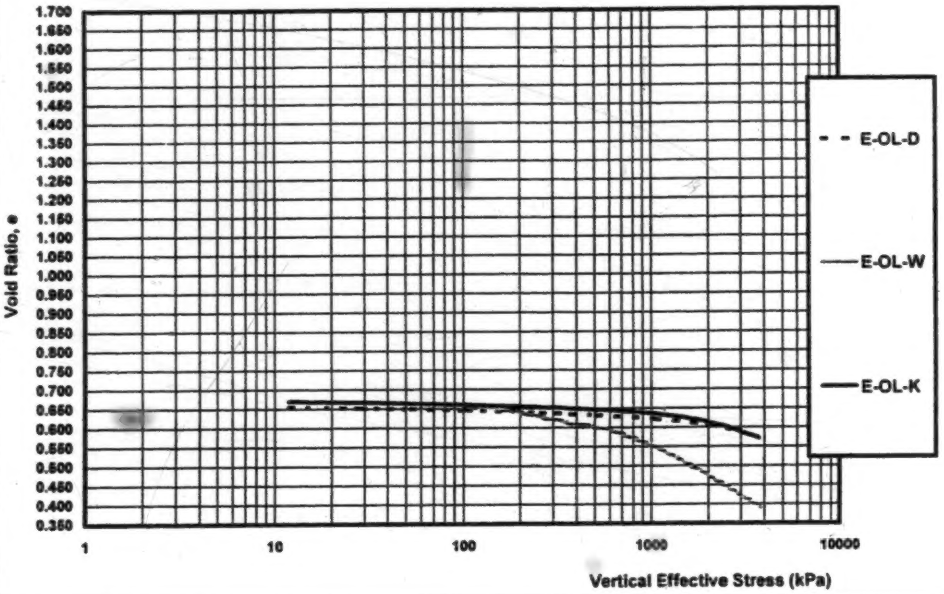

Figure B-6.3-E(b) - One Dimensional Consolidation Test Results
Series E, Koosi Creek Slide Site Specimens

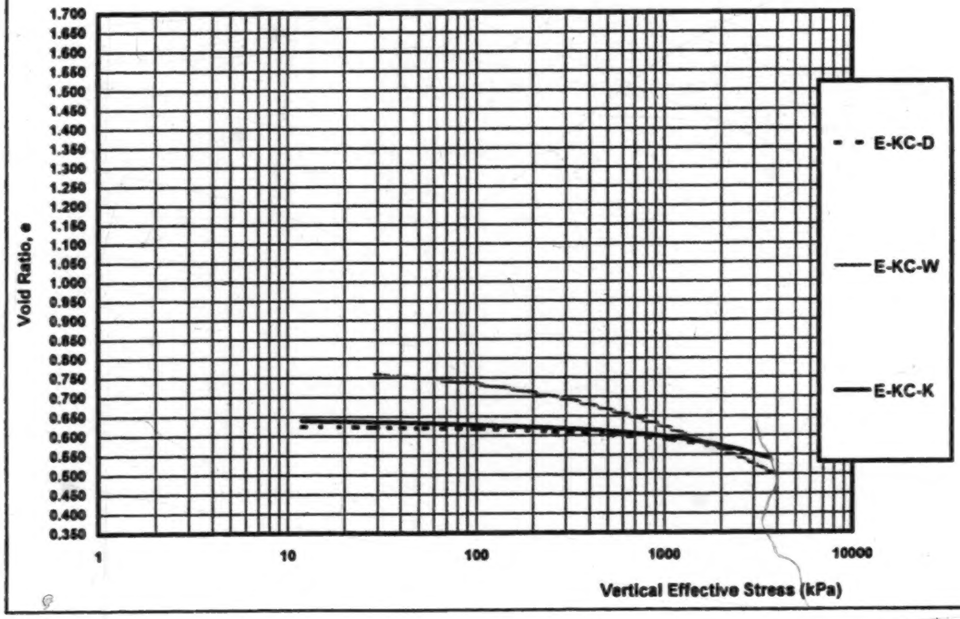

Figure B-6.3-F(a) - One Dimensional Consolidation Test Results
Series F, Okanagan Lake Park Slide Site Specimens

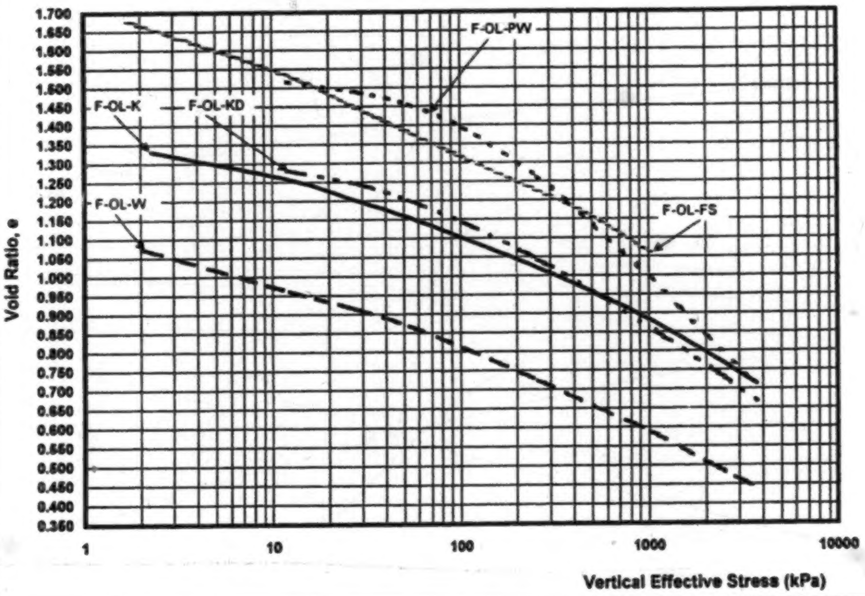

Figure B-6.3-F(b) - One Dimensional Consolidation Test Results
Series F, Koosi Creek Slide Site Specimens